Halophilic responses to a range of salts and their relevance to Mars

Thesis

Halophilic responses to a range of salts and their relevance to Mars

Peter Frederick Woolman Morwool

B.Sc. Molecular Biology and Genetics (Hons)

M.Sc (Res)

A thesis submitted for the degree of Doctor of Philosophy

Astrobiology

November 2018

School of Environment, Earth & Ecosystems

The Open University

UK

Declaration

The research described herein was funded by the Open University, where the majority of the research was carried out. It is all my original research and the experiments and data analysis were carried out by me, with the following exceptions:

- Thin sections (Chapter 2) were prepared by Michelle Higgins of the Open University Thin Section Laboratory. I carried out analysis of these thin sections.
- I carried out sample preparation and target site selection for EMPA analysis (Chapter 2), but the instrument was calibrated and programmed by Sam Hammond of the Open University.
- I powdered samples for XRD analysis (Chapter 2), but further processing, operation of the instrument and comparison of spectra with library data was carried out by Paul Schofield of the Natural History Museum, UK.
- I carried out sample and standard preparation for ICP-MS analysis (Chapter 2), but the instrument was operated by Sam Hammond of the Open University. I analysed the data.
- I prepared and dehydrated samples for Total Organic Carbon (Chapter 2) measurement, but the instrument was operated by Patrick Rafferty of the Open University. I carried out all further data analysis.
- I carried out sample preparation for Total Gravimetric Analyses (Chapter 2), but the instrument was operated by Pete Landsberg of the Open University. I carried out all further data analysis.
- For tRFLP analysis (Chapter 3), I carried out DNA extraction, amplification and fragmentation as well as the data analyses, but tRF profiles were generated by the bioinformatics company Macrogen in Seoul, South Korea.

- For MiSeq analyses (Chapter 3), I carried out DNA extraction, but the sequencing process was carried out by the bioinformatics company Research and Testing Laboratory, Texas. I carried out all subsequent analyses of these sequences.
- I carried out growth of the mixed cultures on a variety of agar compositions for isolation purposes, but at DLR, Cologne with the assistance of Dr Stefan Leuko as part of a COST funded Short Term Scientific Mission (STSM)
- For sequencing of isolates (Chapter 4), I carried out DNA extraction and amplification. The sequencing was carried out by the bioinformatics company Macrogen in Seoul, South Korea. I carried out further analyses of this data.
- In order to generate the growth curves in Chapter 4, I established approximately 500 cell cultures in batches of 60-80, each of which would undergo 10 optical density measurements over the course of the next 30 days. I unfortunately broke my arm midway through one of these experiments. In order to not have wasted the work that had already been put into this batch of cultures, the final five optical density measurements for each member of this batch of cultures were made by Ben Stephens and Dr Ceri Gwyther of the Open University.

Abstract

This Thesis investigated the survival of salt-tolerant microorganisms in environments where salts other than NaCl are present, with the aim being to shed new light on the martian astrobiological potential of halophiles.

Salt tolerant microorganisms, "halophiles", are often proposed as analogues for potential martian life because, for water to exist on, or near, the present-day martian surface requires it to be highly saline. Furthermore, martian salt deposits are often proposed as locations in which to find evidence of ancient martian life; halophiles can undergo "entombment" within salt crystals for indeterminately long periods of time, and there is evidence that this provides protection from the extremes of the martian environment. Both of these proposals, however, are based upon studies of halophiles in terrestrial environments where NaCl is the dominant salt, whereas the martian environment is dominated by a wide range of salt compositions

In this Thesis, Boulby Mine in Yorkshire was studied as its deposits feature a gradual transition from halite (NaCl) to potash (NaCl and KCl in equal concentrations) that might influence the microbial community present. Despite using both culture-independent and culture-dependent techniques, no difference was found in the microbial community across this transition in salt chemistry. It was shown that the NaCl requirement of obligate halophiles, isolated from these deposits, could be lowered by the presence of many other salts (KCl, K_2SO_4, $MgCl_2$, $MgSO_4$, Na_2SO_4, $CaSO_4$). Furthermore, with the exception of $MgCl_2$, the presence of these dissolved salts facilitated the entombment of viable cells and improved the UV tolerance of entombed microorganisms. This Thesis, therefore, suggests that the presence of non-NaCl salts in a martian environment could support the growth, entombment and survival of organisms analogous to halophiles.

Acknowledgements

I would like to start by thanking my supervisors: Karen Olsson-Francis and Victoria Pearson. I am immensely grateful for all they have taught me, giving me this wonderful opportunity and guiding me throughout the PhD process. In fact, the entire lab group was a constant source of support and advice and I am indebted by their assistance in maintaining my cell cultures and growth curve experiments when a broken arm left me unable to operate a pipette for two months. Special attention must also be made to Michael Macey and Stephen Summers, who taught me the bioinformatics techniques and theories utilised in this project. I must also thank Thomas Edwards, lead exploration geologist of Boulby Mine, for going out of his way to help provide samples for this project. I need to thank the community within the department. Coffee breaks and Friday drinks were a much-needed emotional crutch, and I'm also incredibly grateful for the geologists who put up with many basic questions from a microbiologist with no prior experience of rocks. Outside the department, I must also thank the PhD Students who took part in our weekly roleplaying games. Words cannot state how much I benefited from quickly establishing a circle of friends in Milton Keynes.

I must also thank my family: they made me the man I am today and encouraged me to follow my childhood dreams to become a "space scientist". They also provided financial support once my funding ran out, and I would not have been able to complete the project without them. Finally, more than anyone else, I would like to thank my wife, Florence. She has put up with a lot over the course of this project (including moving to Milton Keynes!) and I could not have made it to the end without her constant emotional support.

Table of contents

Abbreviations and acronyms

Al - Aluminium

ANOSIM – Analysis of similarities, statistical test

ANOVA – Analysis of variance, statistical test

Ba - Barium

BLAST - Basic local alignment search tool

bp – Base pairs

C - Carbon

Ca – Calcium

$CaCl_2$ - Calcium chloride

$CaSO_4$ – Calcium sulfate

CHNOPS – Carbon, Hydrogen, Nitrogen, Oxygen, Phosphorus & Sulfur – the elements essential for life

Cl – Chlorine

CO_2 – Carbon Dioxide

CTAB - Cetrimonium bromide

ddH_2O – Double distilled water

DNA - Deoxyribonucleic acid

dNTP - Deoxynucleotide triphosphate

DPX – Dibutyl phthalate xylene

EDTA - Ethylenediaminetetraacetic acid

EMPA - Electron microprobe analysis

Fe - Iron

FEG-SEM - Field electron gun – Scanning Electron Microscopy

GDB – Gentle dissolution buffer

GYP – Glucose yeast peptone media

H – Elemental hydrogen

H_2 – Molecular hydrogen

HiRISE - High Resolution Imaging Science Experiment

ICP-MS - Inductively coupled plasma mass spectrometry

JPL – Jet Propulsion Laboratory

K – Pottasium

K_2SO_4 – Pottasium sulfate

KCl – Pottasium chloride

MAVEN - Mars atmosphere and volatile evolution obiter

Mg – Magneium

$MgSO_4$ – Magnesium sulfate

Mg_2Cl_2 – Magneium chloride

Mn - Manganese

MPM – Modified Payne's media

mRNA – Messenger ribonucleic acid

N – Elemental nitrogen

N_2 – Molecular nitrogen

Na – Sodium

Na_2SO_4 – Sodium sulfate

NaCl – Sodium chloride

$NaClO_4$ – Sodium perchlorate

NO_3^- - Nitate ion

NASA - National Aeronautics and Space Association

NCBI - National Centre for Biotechnology Information

O – Elemental oxygen

O_2 – Molecular oxygen

Si – Silicon

Sr – Strontium

P - Phosphorus

PCR - Polymerase chain reaction

ppm – Parts per million

rRNA - Ribosomal ribonucleic acid

RSL – Recurring Slope Lineaea

S – Sulfur

SO_4^- – Sulfate ion

SDS - Sodium dodecyl sulfate

SEM - Scanning electron microscope

SIMPER - Analysis of dissimilarity, statistical test

TOC – Total organic carbon

tRF – Terminal restriction fragment

tRFLP - Terminal restriction fragment length polymorphism

UV - Ultraviolet

XRD - X-Ray diffraction

XRF - X-Ray fluorescence

List of tables

List of figures

Chapter 1: Introduction

1.1 - Astrobiology

1.1.1 - General overview

Humanity has long been captivated by the idea of life beyond the Earth. Whilst the term "astrobiology" does not appear to have been used prior to 1953 (by the Soviet astronomer, Gavriil Tikhov, (Cockell, 2001)), the scientific concept is centuries old. Certainly it has existed since 1600 when the Italian monk Giordano Bruno was burned at the stake for the idea that intelligent life existed elsewhere in the universe (Cockell, 2001). Bruno based his ideas on the, then highly controversial, work of Copernicus. These days the "Copernican Principle" is a fundamental keystone of modern astronomical science: "*there is nothing special about local [terrestrial] conditions in both the spatial and temporal sense*" (Ćirković, 2004). The Copernican Principal implies the existence of life on other worlds (Whitmire and Matese, 2009).

Even prior to the invention of space flight, the public's imagination had been captured by authors such as Jules Verne and Herbert George Wells, who speculated about how the vastly different environmental conditions on the Moon and Mars would cause life to develop along different lines to on the Earth. This was, in part, fuelled by work of scientists, chief among them Percival Lowell, who suggested that features visible on the martian surface were vast irrigation projects built by an intelligent martian civilization (Lowell, 1908).

As ground-based observational techniques advanced, and the space-age began, the data accumulated regarding our nearest planetary neighbours quashed some of this fervour for astrobiology (Jones, 2008, Gronstal, 2013). It became increasingly clear that the

environmental conditions on the Moon (Cockell, 2010), Mars (Gross, 2014) and Venus (Grinspoon and Bullock, 2007) were considerably less habitable than on the Earth. For example, liquid water (Grotzinger, 2009), essential to all terrestrial life, was not observed on the surface of any other planets within our Solar System.

Of the rocky planets within our Solar System, Mercury's proximity to the Sun means that it is too warm for life akin to that found on Earth (Helbert, 2014). Venus is a comparable size and composition to the Earth and is located within the habitable zone (Moore et al., 2017, Way et al., 2017, Cockell, 2001), but the extreme temperatures, pressures and acid rain (Voosen, 2017) render the surface hostile to all known life. Like the Earth, Mars has seasons and ice caps (Herschel, 1784) and the work of Lowell had popularised the idea of a planetary-wide network of canals. The arrival of the Mariner probes in the 1970s, however, showed that the planet lacked any surface water (Sagan and Fox, 1975, Leighton et al., 1965), and, although the results are still debated (Levin and Straat, 2016, Levin and Straat, 1981, Biemann and Bada, 2011, Biemann, 2007, Navarro-González et al., 2006), the Viking landers did not find unequivocal proof of life's existence, or absence, on the martian surface. In the following decades, however, the independent advancement of planetary science (see Section 1.2) and microbiology began to re-open the question of life within our Solar System (Gronstal, 2013).

a) Microbiology

At the time of the Viking missions, biologists had typically considered the terrestrial habitable environment to be a relative narrow window (Rampelotto, 2010), even though some microbes - extremophiles - were known to survive in environments considerably more extreme than those in which humans could survive. At the time, however, extremophiles were believed to be low in diversity (Cavicchioli, 2011). It was

believed that they required complex, non-extremophilic, life to already exist before they could develop (Cavicchioli, 2011), and thus could never arise in the hostile environments in our Solar System. As a result, they were considered of limited use to astrobiology.

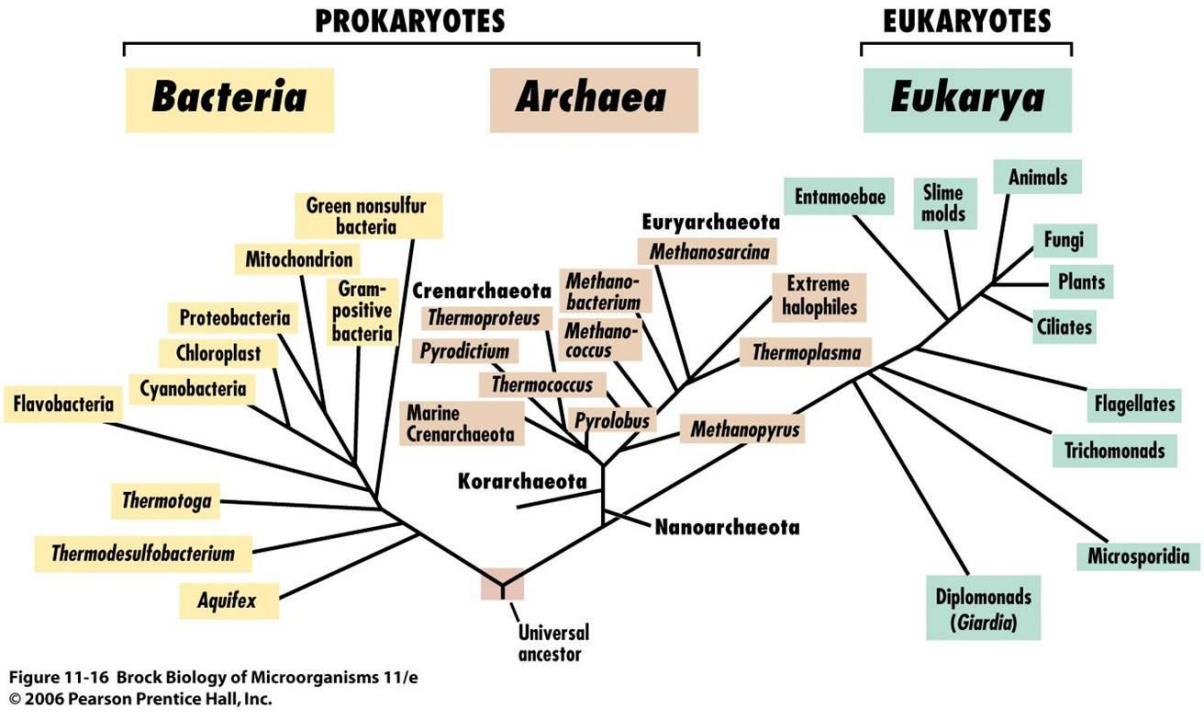

Figure 1.1 - Simplified view of the three domains of life (Madigan et al., 2006)

The gradual acceptance of the ideas proposed by Carl Woese in his studies of molecular phylogeny changed the view that extremophiles were highly specialised bacteria (Moreira and López-García, 1998). Many of the most extremophilic microbes were shown not to be specialised bacteria, but instead represented an entirely separate branch of the tree of life, far more closely related to each other and to the eukaryotes than to bacteria (Cavicchioli, 2011). The tree of life had to be redrawn (Figure 1.1) to take these findings into account. Under the current structure, the tree of life is split into three "domains": the eukaryotes, the bacteria and the archaea (Moreira and López-García, 1998). The majority of extremophilic microbes belong to the domain Archaea

(Castro-Fernandez et al., 2017). The archaea, and by extension the majority of extremophiles, are an incredibly ancient lineage (Castro-Fernandez et al., 2017) that did not require complex non-extremophilic bacteria to exist before they could evolve. This meant that organisms analogous to terrestrial extremophiles could potentially arise in extra-terrestrial environments that were never suitable for the vast majority of terrestrial organisms (Des Marais et al., 2008).

The discovery of the domain Archaea roughly coincided with the advent of culture-independent community sequencing (Barns et al., 1996). Prior to this, microorganisms could only be detected and identified in an environment by growing samples in the laboratory. As DNA extraction techniques became more advanced, it became possible to sequence and identify microorganisms without growing them (Harper-Owen et al., 1999). While archaea had initially been discovered in extreme environments, culture-independent studies detected them in low concentrations in practically all terrestrial environments (Hugenholtz and Tyson, 2008), and in a wider range of environments than the bacteria. These discoveries increased the range of terrestrial environments that were considered habitable and, as such, widened the range of potentially habitable extra-terrestrial locations, including those within otherwise hostile environments (Gómez et al., 2012, Cockell, 2014).

b) Planetary science

On Earth, the presence of liquid water (and its chemistry) is almost always the factor that predicts the presence, or absence, of life (Knoll and Grotzinger, 2006). In the late 1990s, NASA adopted its current strategy to “follow the water”, which attempts to identify habitable environments before attempting to directly detect evidence of life (Graf et al., 2005, Grotzinger, 2009).

There is now abundant evidence that the martian surface once possessed large bodies of liquid water (Grotzinger, 2009, Rosenberg and Head III, 2015, Seybold et al., 2017, Carr and Head, 2010a, Bost et al., 2010, Frydenvang et al., 2017, Hansen, 2009, Cassanelli et al., 2015, Hynek et al., 2015, Osterloo and Hynek, 2015, Carr and Head Iii, 2010). As a result, it has been suggested that, even if the present-day surface is inhospitable, Mars might once have been habitable (Westall et al., 2015, Cockell, 2014).

The aim of this Thesis is to investigate one such potentially habitable environment on Mars: the brines which comprised the final macroscopic bodies of water on the martian surface. This Thesis investigates the response of terrestrial halophiles (salt tolerant microorganisms) to brines and salt deposits consisting of salts other than terrestrially abundant NaCl. Section 1.2 of this introduction outlines what is known about Mars. The sections that follow here, however, provide an introduction to the origin of life studies and the factors that must be considered when evaluating the potential habitability of Mars.

1.1.2 - Origins of life in our Solar System

The existence of life in an extra-terrestrial environment requires both an origin or source and a habitable environment in which it can persist. What is known about the origin of terrestrial life and the limits of terrestrial habitable environments can be used to attempt to interpret the astrobiological potential of other worlds.

a) Abiogenesis

For life to exist on a body in our Solar System, it needs to have had an origin from an abiological source – a process known as abiogenesis. Studies of the origins of life and its

ability to arise from abiotic environments are stymied by the fact that there is only one known example of it occurring, i.e., on Earth (Walker, 2017, Hazen, 2017).

The mechanism behind the origin of terrestrial life remains uncertain, as any geological or geochemical evidence for it has been lost through tectonics and planetary resurfacing (Abramov and Mojzsis, 2009, Ohmoto et al., 2008). The oldest remaining evidence for the presence of life and biological processes can be dated to approximately 3.7 Ga (Dong et al., 2016, Nutman et al., 2016, Dodd et al., 2017), but life may have originated before this date.

There are two main theories for the origins of life on Earth: RNA world or vesical first (Kauffman, 2007), because a self-replicating molecule (such as DNA or RNA) and a means of concentration and containing compounds for chemical reactions (a role played in the modern-day by the cell membrane) are the only two definite requirements for early life (Dzieciol and Mann, 2012).

Many theories for the origin of terrestrial life suggest that it initially occurred in deep sea hydrothermal vents where the proton gradient could drive chemical reactions inside pores of the rock (Sojo et al., 2016, Herschy et al., 2014). Another theory suggests the origin of life occurred in shallow shorelines (Pasteris et al., 2006) where the evaporation of salt water during low-tide would concentrate primitive biomolecules inside the fluid inclusions of salt crystals for chemical reactions to occur. These could then be released to intermingle following dissolution of the crystals at high-tide before re-crystallising at low-tide, re-concentrating the molecules in different ratios for further reactions (Pasteris et al., 2006). A similar theory proposes that the origin of life occurred between the platy crystals of clay minerals in aqueous environments (Bernal, 1951), where simple organic molecules could be absorbed and synthesised to more

complex biomolecules *via* the catalytic properties of the clay surfaces (Rossi et al., 2014, Subramaniam et al., 2011).

It is unlikely that early life was photosynthetic. Prior to the generation of the ozone layer by photosynthetic organisms (Bekker, 2014), the Earth's surface was exposed to solar radiation, as Mars is today (Fendrihan et al., 2009a). This implies life originated away from the sunlight, and, as such, primary production must have been driven by a process other than photosynthesis (Judson, 2017). Primary production was therefore likely driven by chemolithoautotrophic or chemoheterotrophic energy acquisition mechanisms. This is one of the reasons why hydrothermal vents, with their large naturally occurring proton gradients, are often proposed as the location of life (Lane, 2017).

b) Origins of potential martian life

If life were to be discovered on Mars this would not necessarily indicate a second, independent origin of life. There are two scenarios which could explain the presence of potential martian life: independent abiogenesis and lithopanspermia.

Independent abiogenesis

The independent abiogenesis scenario is one in which an origin of life event occurred on Mars separate from the origin of terrestrial life. The probability of such an event occurring cannot be determined statistically since only one origin of life (Earth) can be studied (Walker, 2017). As will be outlined in Section 1.2.2b, the martian surface environment 4.1 to 3.7 Ga (the Noachian period) appears to have been similar to the terrestrial Archaean environment (Anguita et al., 2006, Bost et al., 2010), when life is believed to have first arisen (Allen, 2016, Schwartzman, 2014, Cavalazzi and Barbieri,

2016). There is, however, no evidence of martian deep-sea hydrothermal vents, but similar systems could have been induced within Noachian impact craters (Chatterjee, 2016). Many of the conditions required for alternative models for the terrestrial origin of life, for example in transient salt-crusts (Pasteris et al., 2006) or clays (Rossi et al., 2014, Subramaniam et al., 2011), seem as plausible for Mars as they do for the Earth, because there is abundant evidence of equivalent environmental conditions (Hynek et al., 2015, Osterloo and Hynek, 2015, Grotzinger et al., 2014).

Earth features large interconnected global oceans, which allowed life to colonise the planet (Westall et al., 2015). It is uncertain whether Mars ever possessed a large global ocean, and if it did, it disappeared relatively early in martian history (Parker et al., 1993, Rodriguez et al., 2016a, Wordsworth, 2016). This, therefore, means that if life emerged in a martian impact-induced hydrothermal system (Chatterjee, 2016), it is plausible that it would not be able to leave its local area before the impact-induced heat dissipated. This could potentially mean that if life had arisen on Mars, it might have been spatially limited and became extinct relatively quickly (Westall et al., 2015). On the other hand, depending on how common the abiotic origins of life are, Mars might have featured many spatially and temporally diverse origins of life. On Earth it is believed that the rapid and wide spread of microbial life quickly precluded prebiotic molecules ever building up again in concentrations suitable for further abiogenesis (Lane et al., 2010, Enay, 1993).

Lithopanspermia

The second scenario to explain the potential presence of microorganisms on Mars is that it shares an origin with terrestrial life and became transported from one planet to

another inside meteorites (Horneck et al., 2008, Davies, 2003). This theory is called lithopanspermia.

It is known that rocks have been transferred between the inner planets (Gladman et al., 1996), since large impact events eject debris (ejecta) into space (Worth et al., 2013). This can fall onto other planets as meteorites (Worth et al., 2013). Martian meteorites have been positively identified on Earth (Gladman et al., 1996), and, while venusian meteorites have not been identified, it is theoretically possible that they exist (Jourdan and Eroglu, 2017).

There is also evidence to suggest that microbes could survive ejection from the Earth, the harsh conditions of transit in space, and delivery onto another planetary body provided they are encased within ejecta (Horneck et al., 2008). If this ejecta landed in a habitable environment, the microbes could migrate into the new environment, spread and colonise (Davies, 2003).

The high density of life on the terrestrial surface ensures that ejecta containing terrestrial microorganisms will have been transferred into space (Worth et al., 2013). Although transfer of materials from Mars to Earth is more dynamically favourable than the opposite direction, in the billions of years since life arose it is statistically likely that some terrestrial microbes have been delivered to the surface of our nearest planetary neighbours (Jourdan and Eroglu, 2017, Worth et al., 2013).

If this scenario were true, it means that, if martian life is ever discovered, it could potentially share a common origin with life on Earth. However, it should not be automatically assumed that this origin is terrestrial – it may originate on Mars or even Venus (Walker, 2017, Davies, 2003).

Proving whether a potential organism discovered on Mars came from an independent origin or shared ancestry with terrestrial life would be difficult. The vastly different membrane composition between archaea and prokaryotes suggests that these organisms diverged even before the cell boundary was formed (Peretó et al., 2004). Depending on how early potential martian life diverged from terrestrial life, it may not have even needed to use DNA; early terrestrial life used RNA instead (Forterre et al., 2004), and synthetic biology experiments show that there is no inherent value in the four nucleotides used in terrestrial DNA compared to other potential nucleotides (Pinheiro and Holliger, 2012). Potential martian life could therefore be very different to any terrestrial life, yet still share a distant common origin

1.1.3 - Habitability

Regardless of its origin, life needs a habitable environment in which to survive. The boundaries of a habitable environment are less stringent than those required for an origin of life, but the conditions would need to persist for life to remain (Westall et al., 2015).

A habitable environment has three components: a solvent, bioessential elements and a source of energy (Cockell et al., 2016). A solvent is required because life undertakes a wide variety of chemical reactions to survive (Brack, 2002, Westall and Brack, 2018); chemical reactions between dissolved substances are considerably more energetically favourable than chemical reactions between solids (Pryor, 2018, Westall and Brack, 2018). All terrestrial life uses water as a solvent, and this is the basis for NASA's "follow the water" strategy (Graf et al., 2005, Grotzinger, 2009).

Theoretically, the solvent does not necessarily have to be water. Astrobiological investigations into Saturn's moon Titan focus on the theoretical utilisation of methane as a solvent (McKay, 2016). Despite the cold temperatures of the martian surface (-60 °C, Section 1.2.1d, McKay,1999), liquid methane is unlikely to form (its boiling point is -161.5 °C Kim et al., 2015) and, therefore, (as will be described in Section 1.2.1b), water is the only viable candidate for a martian solvent. In order for it to remain stable under martian conditions, however, a high salt concentration is required (Catling et al., 2010).

In order for life to survive, it also requires the so-called "CHNOPS" elements (carbon, hydrogen, nitrogen, oxygen, phosphorus and sulfur, Cockell et al., 2016). These elements need to be available in a form exploitable by microorganisms for an environment to be considered habitable. Carbon is an essential component of all biomolecules because of the wide range of possible bonding configurations (Kupriyanova et al., 2017, Westall and Brack, 2018). Sources of carbon for potential martian organisms include the CO_2 in the atmosphere (Murukesan et al., 2016) or delivery from space in the form of micrometeorites (Westall et al., 2015), which would allow autotrophy (the biotic fixation of abiotic carbon) to occur. Meanwhile, already (abiotically) fixed nitrogen is found within the sediments investigated by the Curiosity rover (Stern et al., 2015). The remaining CHNOPS elements have, likewise, been detected in minerals in Mars' Gale Crater, which has led to its classification as a habitable environment in the Noachian and (potentially) Hesperian periods (Grotzinger et al., 2014) when water was present.

In addition, life requires an energy source in order to fuel its many chemical reactions (Stelmach et al., 2018). On Earth most biological energy comes from photosynthesis, generating energy from sunlight (Nelson and Junge, 2015). On Mars, photosynthesis

seems unlikely, since exposure to sunlight would also require exposure to the extreme solar radiation (see Section 1.2.1c and Cockell, 1998). Photosynthesis is, however, a complex form of energy generation that appeared relatively late in terrestrial evolution (Bekker, 2014, Fischer et al., 2016). An alternative is chemotrophy, which involves energy being generated from chemical concentration gradients rather than from sunlight (Payler et al., 2016, Hays et al., 2017, Emerson et al., 2016). A wide variety of different molecules can be utilised as electron donors and electron acceptors for this process, many of which are present on Mars even in the present day (for example, organic molecules and hydrogen as potential donors, with iron and sulfates as acceptors, Westall et al., 2015) implying that chemotrophy could occur. A detailed review of martian environments - past and present - is given in the following sections.

1.2 - Mars

1.2.1 - Present-day Mars

The martian surface was initially characterised by the orbiting Mariner missions in the 1960s and 70s (Leighton et al., 1965, Sagan and Fox, 1975, Collins Jr, 1971), and then by the Viking landers in the late 1970s (Margulis et al., 1979). The Viking landers had life detection as their primary goal but produced negative (and still debated) results (Levin and Straat, 2016, Levin and Straat, 1981, Biemann and Bada, 2011, Biemann, 2007, Navarro-González et al., 2006). The landers did, however, analyse the composition of the martian atmosphere and regolith (McSween Jr, 1984), which, in turn, enabled the identification of meteorites from Mars within collections on Earth (Wasson and Wetherill, 1979, Wood and Ashwal, 1982). This determination of provenance meant that these meteorites could be used to further determine environmental conditions and processes on Mars (Burbine et al., 2002).

In 1997, the Mars Global Surveyor (MGS) orbiter began comprehensively mapping the martian surface (Smith et al., 2001). Since then, six orbiting spacecraft have (successfully) arrived in Mars' orbit to map and characterise the geomorphology, atmosphere and polar regions (Edwards et al., 2014) while seven landers and/or rovers have (successfully) landed on the martian surface to further characterise specific geographical locations (Carr and Bell, 2014). At the time of writing, Mars continues to be a target for astrobiological investigation, with the InSight, ExoMars 2020 and Mars 2020 landers being the most prominent upcoming missions.

As a result of this attention, the present-day surface and atmospheric conditions have been extensively characterised. They are described below.

a) Atmosphere

Mars has a relatively thin atmosphere, having been stripped by solar winds (Dehant et al., 2007); the current surface air pressure is 6.1mbar (Korablev et al., 2018), less than 1% of that found on Earth and it is still falling (Hassler et al., 2014). The Curiosity rover measured daily fluctuations in the mean atmospheric pressure on the order of a couple of percent when Mars is furthest from the Sun and tens of percent when it is at its closest (Martínez et al., 2017).

The composition of the martian atmosphere, as recorded by the Curiosity Rover in its first 105 days in Gale Crater, is displayed in Table 1.1. This data differs slightly from historic data from Viking and ground-based observations (Nier et al., 1976), which is believed to be a result of seasonal and geographic variation as well as improvement in the accuracy of analytical instruments over time (Martínez et al., 2017). As a result, this

data is believed to represent typical conditions on the martian surface in the present day.

Table 1.1 - Percentage composition of the martian atmosphere as measured by Curiosity in its first 105 sols. Data from Mahaffy et al., (2013)

Gas	Percentage abundance
CO_2	96 (±0.7)
Ar	1.93 (±0.03)
N_2	1.89 (±0.03)
O_2	0.145 (±0.009)
CO	< 0.1

b) Temperature

Mars is considerably colder than the Earth, with an average global temperature of -60 °C (McKay, 1999, Ferguson and Lucchitta, 1984). On Earth, the thick atmosphere (Haberle et al., 2017) and extensive oceans (Sleep and Zahnle, 1998) provide heat-sinks to buffer global temperatures and keep them reasonably stable. Without these, temperatures on Mars can vary significantly by geography, season and even time of day. In equatorial regions, air temperatures near the surface can briefly reach as high as 26 °C, but can drop by more than 100 °C at night (Pierrehumbert, 2010).

c) Radiation at the martian surface

Although Mars only receives 43 % as much solar radiation as the Earth (owing to the increased distance from the sun) the surface UV dose rate is three orders of magnitude higher (Schuerger et al., 2006). This is owing to a combination of atmospheric factors: its relative thinness and the lack of any significant ozone layer (Cockell, 1998). This results in a radiation environment similar to that of space; high-energy, low-wavelength (> 300 nm) UV radiation can penetrate to the martian surface (Schuerger et al., 2006), which receives approximately 1,500 kJ/m^2 of UV irradiance each day (Cockell et al.,

2000). The subsurface is better shielded from this radiation; the depth it can penetrate varies with wavelength, but it is typically on the order of 1 mm (Ertem et al., 2017).

Furthermore, the absence of a global scale magnetic field (Dehant et al., 2007) means that Mars receives significantly more cosmic rays (ionising particles from deep space) than the Earth (Matthiä et al., 2016). Although cosmic rays provide less than 10,000 times the energy to the martian surface than solar UV (Pavlov et al., 2012) they are still important as they can penetrate several meters of regolith (Sheshpari et al., 2017), which is much deeper than the few millimetres that UV can reach (Pavlov et al., 2012, Musilova et al., 2015).

d) Water

Surface/near surface water

The temperature and pressure regime on the martian surface (described above) is such that water can exist as atmospheric vapour or as ice, but never as a liquid (Allen, 2016). This is illustrated using the phase diagram of water in Figure 1.2.

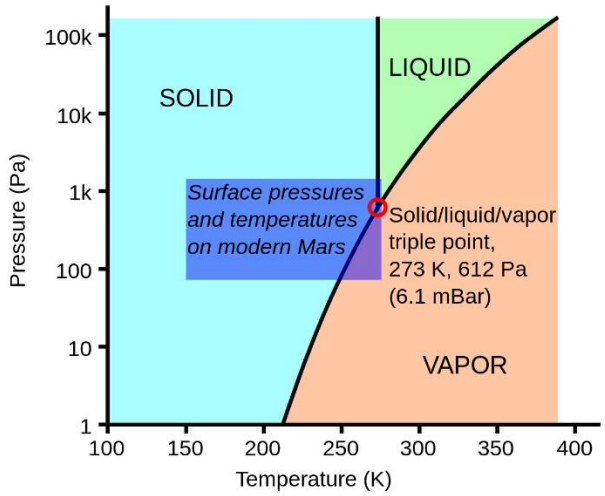

Figure 1.2 - Phase diagram for water showing how temperature and pressure affect the phase of water, with typical values for the martian environment shown as a dark blue box. Image from Whittet (2017)

Water vapour has been detected in the martian atmosphere, with levels of between 5-70 pr.μm depending on seasonal variation (Trokhimovskiy et al., 2015). The majority of the water on the martian surface and near sub-surface, however, is frozen as ice (Christensen, 2006). It has been estimated that there is enough water-ice in the surface and near sub-surface to cover the entire planet to a depth of 30 m (Clifford and McCubbin, 2016). While much of this ice can be found in the polar ice-caps, particularly the northern one (Brown et al., 2015), the majority of the water-ice is located in a layer of permafrost underneath the surface regolith across most of the planet. The thickness of this permafrost is undetermined (Mitrofanov et al., 2007), but the abundance of water in the near subsurface correlates with distance from the equator (Figure 1.3, Christensen, 2006).

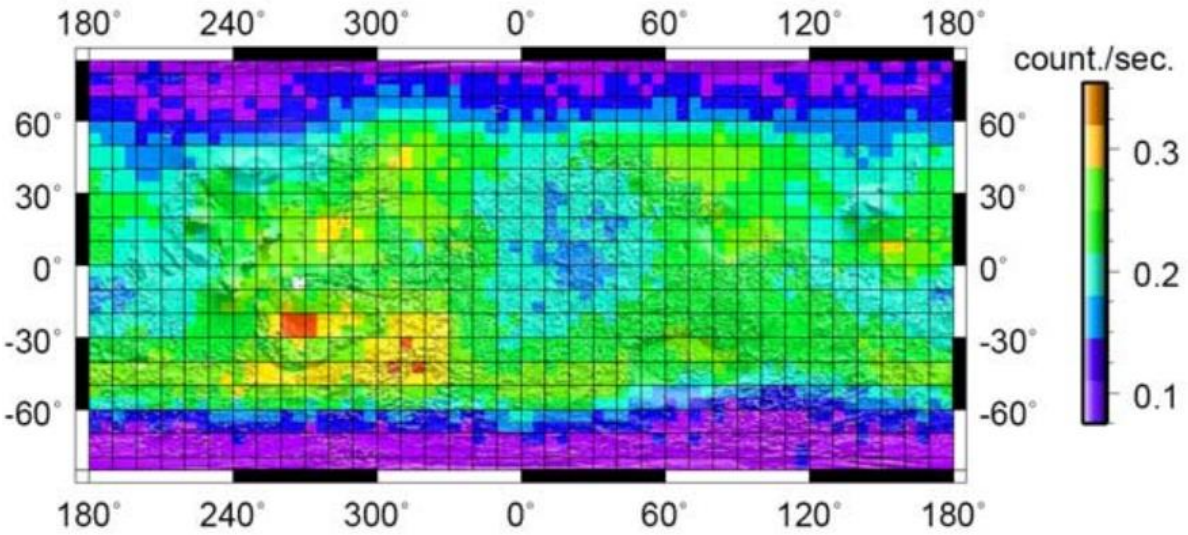

Figure 1.3 - Distribution of neutron counts across the martian surface according to High Energy Neutron Detector data from Mars Odyssey. Neutron counts negatively correlate with hydrogen ions, which are believed to represent water-ice. Image adapted from Christensen 2006.

In the summer months, some of the permafrost melts and sublimes directly into the atmosphere and in the winter it deposits as ice again without ever entering the liquid

phase (Richardson and Wilson, 2002); the triple point of water in relation to martian conditions (as shown in Figure 1.2) means that pure liquid water is never stable.

However, a high concentration of dissolved salt depresses the freezing point of water (Catling, 2014, Oakes et al., 1990) such that the liquid phase could be possible (Figure 1.4), at least for short periods of time (Massé et al., 2016).

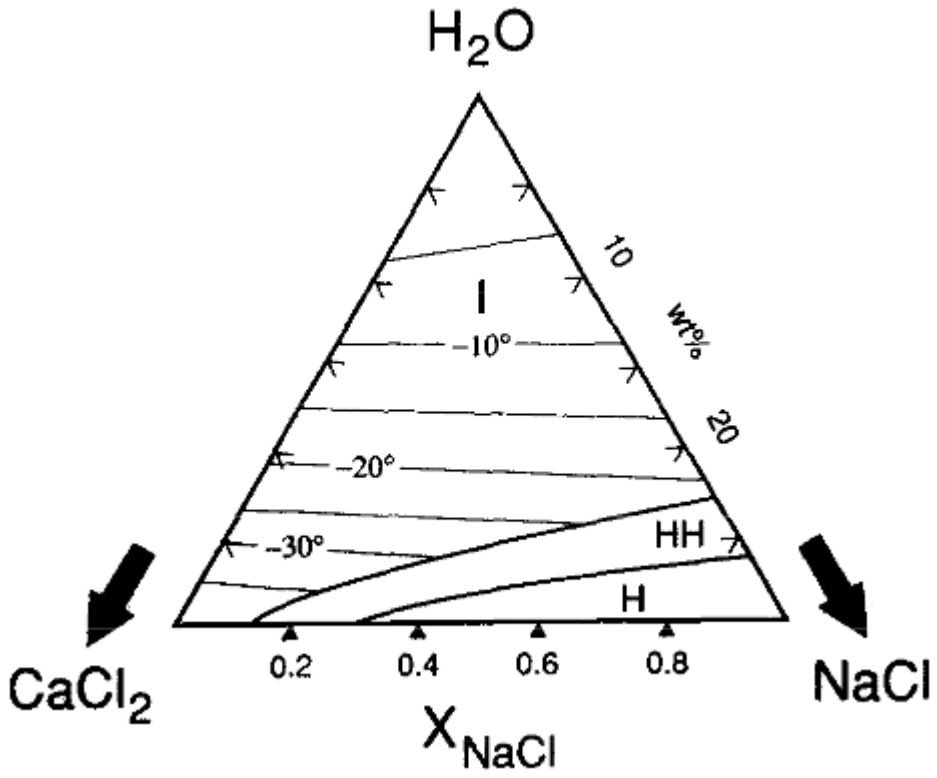

Figure 1.4 - Freezing point of brines (in °C) of increasing concentrations of NaCl and $CaCl_2$ (in a terrestrial atmosphere). Image from Oakes, C. S., et al. (1990)

Surface brines

The Mars Reconnaissance Orbiter (MRO) observed thin, dark streaks (Figure 1.5) on the slopes of the Southern Highlands of Mars (McEwen et al., 2011) during the summer months (McEwen et al., 2013) when the martian temperatures can exceed 0 °C (Stillman and Grimm, 2018). These have been named Recurring Slope Lineae (RSL) and they form branching pathways which head downhill in a manner reminiscent of terrestrial

streams. This led to the hypothesis that they are formed from liquid water dampening the regolith (McEwen et al., 2013). “Dry” theories have also been proposed that do not invoke water, where the RSL are instead formed of avalanches of dust induced by seasonal changes in surface pressure (Schmidt et al., 2017). These avalanche-based theories are supported by the fact that the downwards spread of RSL is halted when they reach slopes shallower than 27 °, a feature observed in terrestrial avalanches (Dundas et al., 2017). Areas with RSLs, however, correspond with areas of elevated humidity (Bhardwaj et al., 2017), indicating localised inputs of water vapour to the atmosphere.

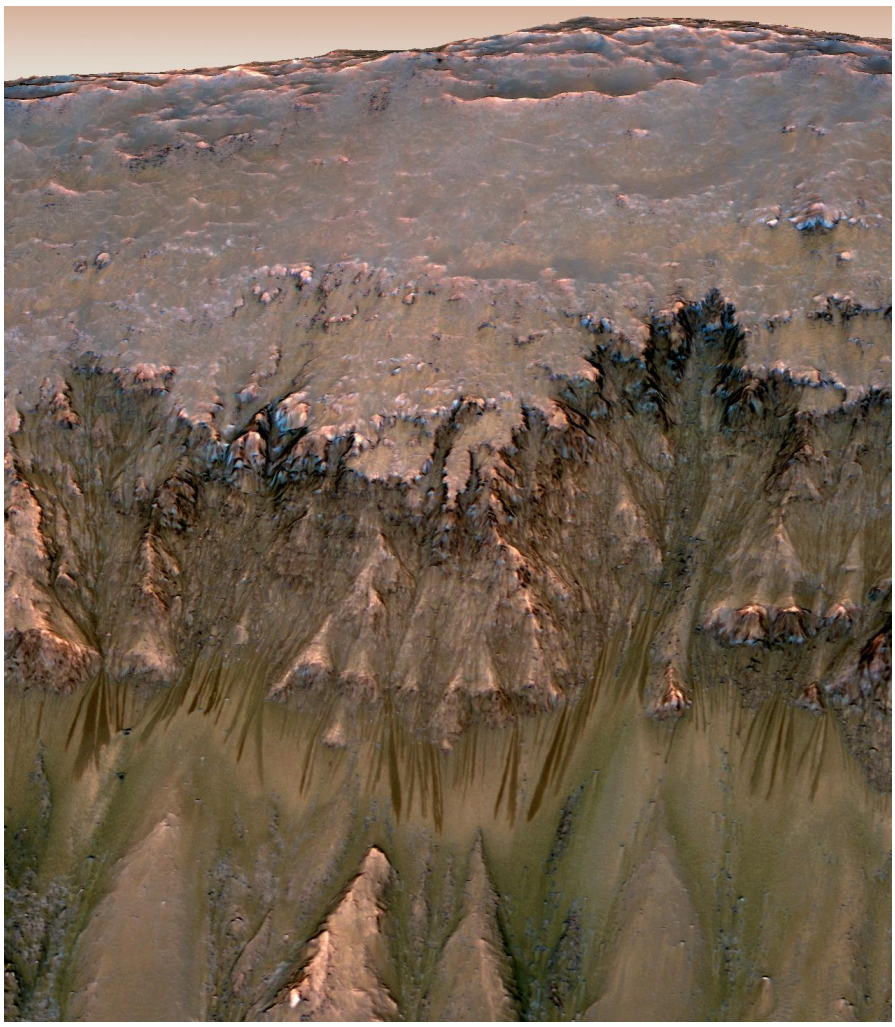

Figure 1.5 - Re-projected view of HiRISE images obtained on May 30, 2011 showing RSL flowing down a slope. Image credit: NASA/JPL-Caltech/Univ. of Arizona

The implication that the RSL may represent brines has not resulted in any direct detection of liquid water (although the spectra were obtained in mid-afternoon, the warmest part of the day, when the water might not be present, Dundas et al., 2017), but has led to the search for evidence of evaporite deposits. Hydrated salt crystals (mainly consisting of $MgSO_4$ and magnesium perchlorate) have been found where RSL have previously been observed (Ojha et al., 2015). While the spectra of RSL imply that potential martian brines would be likely to contain a high $MgSO_4$ concentration, $MgSO_4$ has a relatively small impact upon the phase diagram of water, and thus other salts are required to provide stability to potential brines (Massé et al., 2014). Hydrated Na and Mg perchlorates have also been detected in the aftermath of RSL disappearance (Ojha et al., 2015), as well as at every lander site (Davila et al., 2013b, Kerr, 2013), implying their abundance across the martian surface (Kerr, 2013). Perchlorates can have a very strong effect on the freezing point of water, and are thus likely to be a major component of any potential martian brine (Massé et al., 2014).

While the composition of RSL (if they are indeed brines) remains uncertain (Stillman et al., 2017), the water activity (see Section 1.3.1) of most modelled martian brines tend to fall in the range of 0.4 - 0.6 (Dundas et al., 2017). The lowest water activity at which terrestrial growth has been detected is 0.64 (Stevenson et al., 2015b) and planetary protection guidelines consider an extra-terrestrial environment uninhabitable if the water activity is below 0.5 (Rettberg et al., 2016). This would imply that even if RSL are brines, they would be uninhabitable. They are, however, still of astrobiological importance, because they are the best evidence of liquid water, an essential requirement of life (Jones, 2018), on the martian surface in the present day.

Discovering the source of the water, if RSL are water, is, therefore, essential. Water-based theories of RSL formation have two primary hypotheses:

1) It has been suggested that RSL are fuelled by the over pressurisation of subsurface aquifers (Stillman and Grimm, 2018), implying the existence of relatively large bodies of water in the martian near-subsurface. The regular appearance of RSL in similar locations years after year, would imply that aquifers must become recharged over the winter months (Stillman et al., 2016). The mechanism behind such recharging remains uncertain and there are no convincing models to do so (Stillman et al., 2016).
2) RSL could also be fuelled by deliquescence onto salt crystals from both the atmospheric water (Nikolakakos and Whiteway, 2015) and/or the cryosphere (Pavlov et al., 2010). It has been shown, *via* modelling, that atmospheric water vapour is capable of condensing directly onto salt crystals to form small pockets of brine (Nikolakakos and Whiteway, 2015). In this theory, the salts detected following RSL disappearance (Ojha et al., 2015) might predate RSL formation. Salts are found across the present day surface of Mars. The cations consist mainly of Mg and Fe, with smaller amounts of Na and K, while the anions consist mainly of sulfate and perchlorate with smaller amounts of chlorides (Massé et al., 2014, Clark and Van Hart, 1981, Kounaves et al., 2010, Hecht et al., 2009). These may originate from aqueous alteration of rocks during ancient wetter conditions (Clark and Van Hart, 1981) and reactions between volcanic gases (Catling et al., 2010), and provide surfaces for deliquescence.

Deliquescence could theoretically happen across the planet, not just at sloped surfaces where RSL are visible. For example, there is evidence (a correlation between surface

temperature, atmospheric humidity, and changes in the hydration states of salts) to suggest that it occurs in Gale Crater in the present day, but water has yet to be detected (Martín-Torres et al., 2015). The ESA ExoMars 2020 rover will carry the HABIT (HabitAbility, Brine Irradiation and Temperature) instrument, which will attempt to generate brines on the martian surface from deliquescence of atmospheric water in order to prove that it is possible (Rodionov et al., 2017).

Potential liquid water in the deep subsurface

In the deep subsurface (on the order of kilometres), temperature and pressure increases. This could potentially put conditions into the area of the phase diagram where pure liquid water is stable (Mancinelli, 2000), though it is currently unfeasible to either detect or sample it. On Earth, water is found wherever the pressure and temperature regimes allow it. Models suggest that the colder martian core and lower gravity mean that the region of the martian subsurface conducive to liquid water has a larger volume than that of the Earth (Michalski et al., 2013).

There is also radar evidence from the Mars Express orbiter to suggest the presence of a large body of water (several km diameter, and tens of cm deep) 1.5 km beneath the South Polar glaciers (Orosei et al., 2018). The temperature of this water is estimated to be approximately -68 ℃, implying, as with the potential near-surface brines, high concentrations of perchlorate in order to maintain this liquid state (Orosei et al., 2018); the pressure of the overlying ice is unlikely to be able to induce the melting needed for such a body to exist.

1.2.2 - Early Mars

In the absence of field geologists on the martian surface, or extensive subsurface excavations, Mars' geological history and stratigraphic relationships have been determined mainly though orbital observation (Carr and Head Iii, 2010, Wordsworth, 2016, Rogers et al., 2018). These observations have been primarily of surface outcrops (Squyres et al., 2004, Sautter et al., 2016, Viviano-Beck et al., 2017), volcanic plains (Brož et al., 2015), cliff faces (Treiman, 2003) and crater density, distribution and preservation state (Hartmann and Neukum, 2001, Kreslavsky and Head, 2018, Irwin et al., 2018, Tanaka et al., 2014, Day et al., 2016). The lack of precipitation-induced erosion, tectonic movement or (recent) volcanism means that such geomorphological features survive on the martian surface considerably longer than they do on Earth.

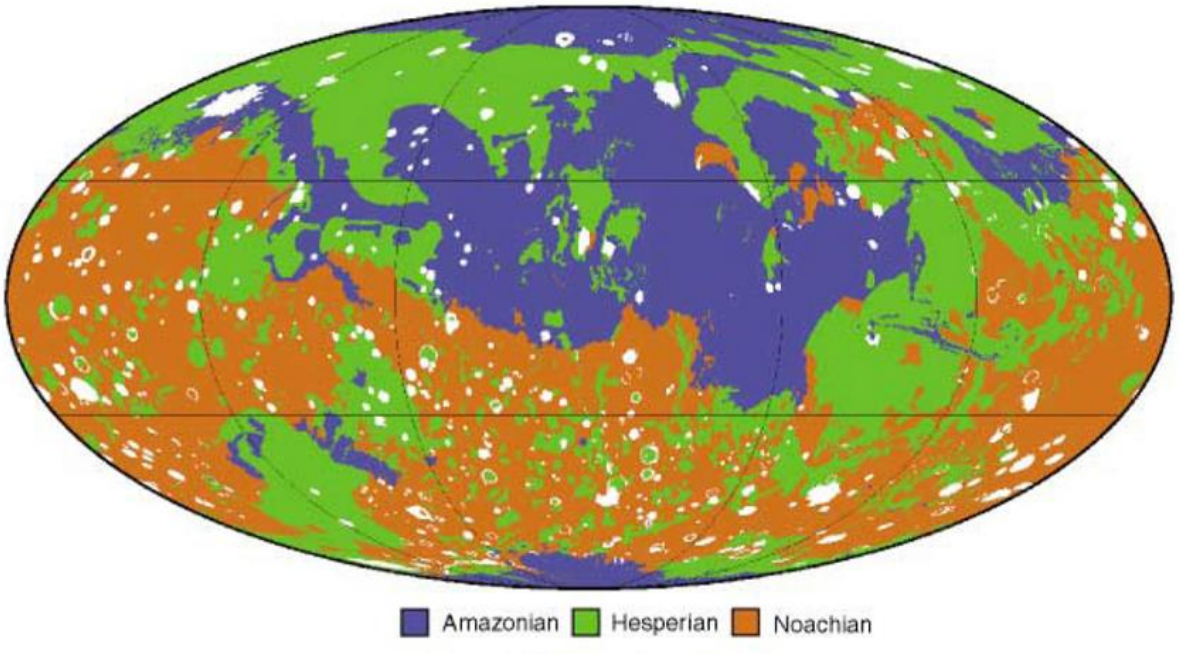

Figure 1.6 - Global distribution of Amazonian, Hesperian and Noachian terrain. Adapted from (Solomon et al., 2005)

Orbital observations have divided the martian terrain into three categories (Tanaka, 1986), as shown in Figure 1.6, and thus three geological periods: Amazonian, Hesperian

and Noachian. A fourth period (Pre-Noachian) is in the early stages of being defined and characterised, although it's timings and environmental conditions remain poorly constrained in comparison to the other periods (Carr and Head Iii, 2010, Bouley et al., 2018). The preservation of these terrains and the features upon them can reveal much about the environmental conditions, both of the time when they formed and the time since (Carr and Head Iii, 2010).

a) Pre-Noachian

The Pre-Noachian is defined as the geological period from 4.5 - 4.1 Ga (Andrews-Hanna and Bottke, 2017). Mars formed around the same period of time as the Earth (Fitoussi et al., 2016, Izidoro et al., 2014), but no terrain remains that formed between the accretion of the planet and the start of the Noachian period 4.1 Ga (Carr and Head Iii, 2010). There is, however evidence of a catastrophic event that occurred around 4.5 Gya and this is defined as the start of the Pre-Noachian period. The exact nature of this catastrophic event is uncertain (the two main theories are an impact or sudden violent tectonics (Citron and Zhong, 2012)), but evidence for its occurrence exists in the fact that it caused a marked dichotomy between the Northern and Southern hemispheres of Mars (Carr and Head Iii, 2010). To this day, there remains an average of 3 km difference in height (Wilhelms and Squyres, 1984) between the "Southern Highlands" and the "Northern Lowlands" (Figure 1.7).

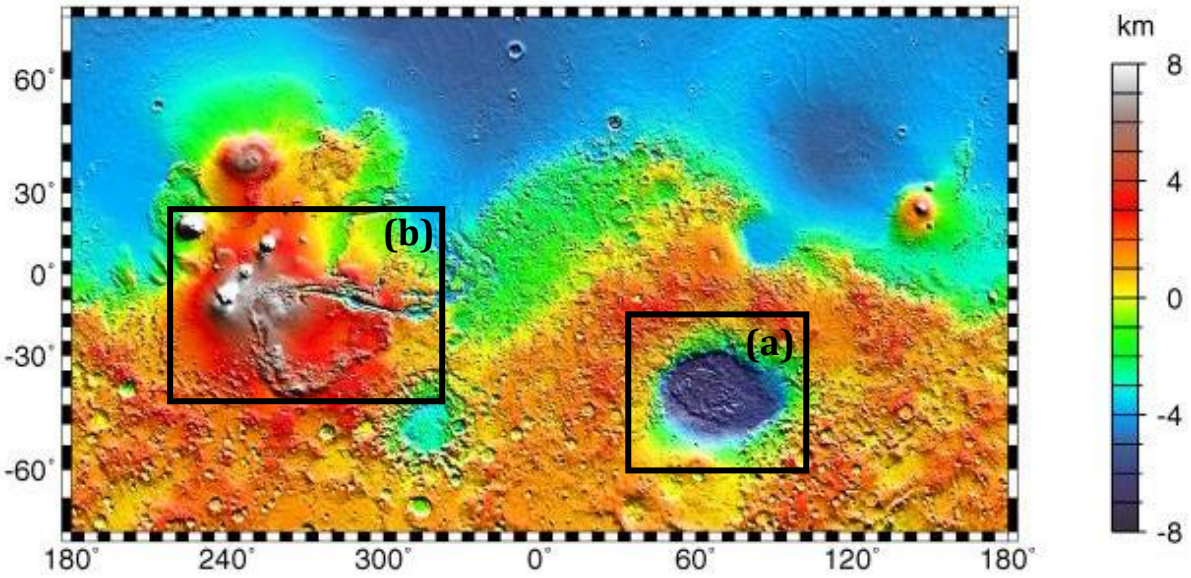

Figure 1.7 - Topographic map of Mars, based on Mars Global Surveyor Orbiter data. The Hellas Basin (a) and Tharsis Regions (b) are marked (PIA02031, 1999)

The end of the Pre-Noachian period (the start of the Noachian) is generally accepted as the impact event, that formed the Hellas Basin, and the start of the Late Heavy Bombardment (LHB) approximately 4.1 Ga (Andrews-Hanna and Bottke, 2017).

Despite the absence of Pre-Noachian terrain (Carr and Head Iii, 2010), preservation of the boundary region between the highlands and the lowlands allows some general conclusions about this period to be drawn. All evidence of volcanism and lava in this boundary region is younger than the Tharsis volcanic plateau, implying very little volcanic activity occurred between the formation of the boundary and the early Noachian (Andrews-Hanna and Bottke, 2017). This also implies that, even in this early stage of martian history, there was no plate tectonics (Andrews-Hanna and Bottke, 2017). In addition, martian surfaces older than 3.9 Ga preserve evidence of an ancient global magnetic field similar to the one on Earth today (Weiss et al., 2008), which implies that, during the Pre-Noachian, the surface would have been better protected from the solar radiation environment.

The pre-Noachian boundary region displays evidence of fluvial erosion, but this erosion can be dated to much later in Mars' geological history (Andrews-Hanna and Bottke, 2017), implying that little aqueous alteration occurred during the Pre-Noachian period. There is, however, evidence to indicate that the Pre-Noachian period featured episodic impact events (Palumbo and Head, 2017). These would have raised local temperatures by hundreds of kelvin and transferred enough surface water (either as liquid or ice) to the atmosphere that the basin and its surroundings might experience rainfall rates typical of a terrestrial tropical rainforest (2 m/year) for hundreds of years afterwards (Palumbo and Head, 2017). Rock debris from these impact events would also persist in the atmosphere for comparable periods of time. Depending upon the frequency of these large impacts, as well as smaller ones to maintain the conditions, it is feasible that this could have provided a greenhouse effect to raise global temperatures sufficiently to allow liquid water to persist long-term on the surface (Carr and Head, 2010a).

b) Noachian

The Noachian period lasted from 4.1 - 3.7 Ga, and its terrain is mainly found in the Southern Highlands (Figure 1.6). Noachian surfaces possess complicated networks of valleys and the main hypothesis for their formation is aqueous erosion induced by rivers and streams (Wordsworth, 2016, Rosenberg and Head III, 2015, Davis et al., 2016, Cassanelli et al., 2015, Andrews-Hanna and Lewis, 2011, Carr and Head Iii, 2010, Parsons et al., 2013, Wordsworth et al., 2013). Noachian terrains also possess inverted channels, which are presumed to have been formed by sedimentation in these streams (Davis et al., 2016, Mirino et al., 2018, Balme et al., 2016). Erosion models and drainage basin morphology both imply that the Noachian featured common and wide-spread precipitation, though it remains uncertain whether it was mainly rain or snow (Seybold

et al., 2017). There is geochemical evidence for surface liquid water in this period; clays and soils that have undergone aqueous alteration are found in abundance on Noachian terrain (Loizeau et al., 2018, Tirsch et al., 2015, Michalski et al., 2010). There is also geomorphological evidence to suggest that this time period would have seen the presence of long term lakes and seas within impact craters such as Hellas (Moore and Wilhelms, 2001) and Gale Crater (Frydenvang et al., 2017). It has even been suggested that a large ocean could have covered most of the northern hemisphere during at least the early Noachian (Parker et al., 1993, Rodriguez et al., 2016a, Fawdon et al., 2018).

The Noachian period is marked by intense volcanism, but it was focused in the Tharsis Region (Figure 1.7b); across the rest of the planet, the rate of resurfacing of Noachian terrain by impacts is significantly higher than the rate of resurfacing by volcanic activity (Carr and Head, 2010b). The Tharsis volcanism would have pumped large volumes of CO_2 and water vapour into the atmosphere, creating a greenhouse effect (Jakosky and Phillips, 2001) that would raise global temperatures (Westall et al., 2013).

Surfaces formed in the early Noachian contain magnetic anomalies consistent with formation under a global magnetic field, which is not observed today (Connerney et al., 2001). The failure of the internal dynamo generating this field is dated to between 4.0-3.8 Ga (Arkani-Hamed and Olson, 2010, Weiss et al., 2008), although it is uncertain how gradual a process this failure was (Kuang et al., 2008). Following failure of the dynamo, the planet would have been exposed to the cosmic radiation of space and the atmosphere would have become exposed to solar winds (Section 1.2.1a) causing its loss to space, and the gradual development of the the modern radiation environment (see Section 1.2.1c).

It is now hypothesised, thanks to the data gathered by the Curiosity Rover, that Gale Crater was a habitable lake during the late-Noachian period (Grotzinger et al., 2014). It is highly likely that it was not the only habitable environment on the martian surface during this time and Noachian Mawrth Vallis has also been identified as a potential habitable environment (Michalski et al., 2010). The general picture that has been built up of the martian environment during the Noachian, is one of a warmer, wetter world than the one today. The conditions were, perhaps, comparable to those of the Archaean Earth (Anguita et al., 2006, Bost et al., 2010).

It is uncertain how this warmer, wetter environment was maintained over the course of the Noachian, and whether it featured transient periods of warmth in an otherwise cold system (Wordsworth et al., 2015). Even taking into account the volcanism-generated greenhouse effect (Jakosky and Phillips, 2001) and the high rate of impact events (Segura et al., 2002), all climate models indicate there would be insufficient heat to allow water to remain stable at the martian surface for the period of time required for the observed valley networks to form (Wordsworth, 2016). This disparity between the models and the observed Noachian fluvial features is heightened further when one takes into account the fact that the younger Sun was considerably colder than it is today and thus would have provided much less heat to the martian surface (Wordsworth, 2016).

Owing to the uncertainties in likely temperatures and pressures in the Noachian, it cannot be determined whether stable freshwater was ever present on the martian surface or if it was mainly brines. It can, however, be assumed that warmer temperatures and pressures would mean that liquid water could be stable with lower

salinities than postulated modern brines, though by how much lower is uncertain (Hansen, 2009).

As the Noachian ended, most bodies of water dried up (Osterloo and Hynek, 2015), with the salts within them precipitating out to form large chloride deposits (Hynek et al., 2015). These can be found in the bases of craters on Noachian terrains across the Southern Highlands (Osterloo et al., 2008). Similar terrestrial deposits contain fluid-inclusions, tiny pockets of the brines that formed them (Natalicchio et al., 2014, Shen et al., 2017). Microorganisms from these inclusions can be detected and grown much later (Lowenstein et al., 2011, Schubert et al., 2009, Schubert et al., 2010, Norton and Grant, 1988, McGenity et al., 2000, Gramain et al., 2011), as will be discussed in greater detail later in this Chapter (Section 1.3.3).

c) Hesperian

The Hesperian period extended from the end of the Late Heavy Bombardment (approximately 3.7 Ga) to approximately 3.0 Ga (Carr and Head Iii, 2010), which means it overlaps with the terrestrial Archaean period. The Hesperian environment differed significantly from the Noachian environment that proceeded it. It is unknown whether this transition was sudden or gradual (Warner et al., 2010), but there are several explanations for why it occurred.

The end of the LHB meant that there was significantly fewer impact events (Segura et al., 2002). The atmosphere also thinned significantly around the same time, possibly because of the failure of the magnetic field exposing the atmosphere to solar winds (Dehant et al., 2007) or because of a sudden and large-scale precipitation of carbonates

in the late Noachian, which removed large volumes of CO_2 from the atmosphere and altered its composition (Fernandez-Remolar et al., 2011, Hu et al., 2015).

The Hesperian featured considerably more volcanism than the Noachian, with the surviving surface terrain comprised mainly of large lava plains (Carr and Head, 2010b). Increased volcanism would have produced greenhouse gases which would make global temperatures relatively warm in comparison to those found in the present day. The absence of large valley networks (Carr and Head, 2010b) and the distribution of Hesperian-aged circumpolar ice deposits (Fastook et al., 2012), however, indicate that the lack of impact-induced heat (Segura et al., 2002) made global temperatures colder than in the Noachian. They were likely below the freezing point of water (Fastook et al., 2012) with polar temperatures estimated to be between -50 and -70 ℃ (Kress and Head, 2015), and local temperatures within craters such as Gale to be -43 ℃ (Kling et al., 2017).

There is little aqueous erosion of Hesperian features, implying both a drier environment than the Noachian and that this dry environment has persisted ever since (Carr and Head, 2010b). Despite these arid conditions, there is still widespread evidence of localised liquid water, though not to the extent seen in the Noachian. Valley networks are found on the sides of several Hesperian volcanoes (Fassett and Head Iii, 2006), as well as across the plains (Anguita et al., 2006, Parsons et al., 2013, Warner et al., 2010, Andrews-Hanna and Lewis, 2011). The morphology of these valleys implies that they were not formed by the constant presence of liquid water, but instead represent catastrophic flooding events (Warner et al., 2010, Andrews-Hanna and Lewis, 2011, Carr and Head Iii, 2010). These flooding events resulted from overflow of subsurface

aquifers (Rodriguez et al., 2016b, Marra et al., 2015) and lakes (Lapotre et al., 2016, Goudge and Fassett, 2018).

It has long been thought that lakes were rare and transient during this period, but there is contradictory evidence from Curiosity. The fluvial deposits (including mudstones and conglomerates; Williams et al., 2013, Vaniman et al., 2014) uncovered in Gale Crater indicate water with a depth of at least 100 m may have persisted for thousands to hundreds of thousands of years (Grotzinger et al., 2015). This has given rise to the hypothesis that Hesperian Mars featured long-lived crater lakes (Moore and Wilhelms, 2001, Frydenvang et al., 2017). Given the pressure and temperature regime on Mars at that time, these lakes should have been lost to evaporation in a few thousand years. Hence, it has been proposed that these Hesperian crater lakes may have been covered by ice sheets similar to terrestrial Antarctic lakes, thin enough to still allow sediment deposition but sufficient to retain water for longer periods of time (Kling et al., 2017). The theory is supported by an apparent absence of wind-induced waves during this period, as evidenced by the morphology of lake deltas in Gale Crater (Palucis et al., 2016). While, as yet unproven, this hypothesis would significantly extend the lifetime of bodies of liquid water under martian conditions (Moore and Wilhelms, 2001, Frydenvang et al., 2017).

d) Amazonian

The longest martian geological period is the Amazonian, which has lasted two thirds of martian history: from 3 Ga to the present day (Carr and Head, 2010b). This period is the most well defined and characterised. The environmental conditions that have prevailed during this period (described above in Section 1.2.1) have been relatively stable, with significantly less large-scale alteration of surface morphology than previous periods

(Ehlmann and Edwards, 2014) and slower rates of erosion and volcanism (Carr and Head Iii, 2010).

Although active volcanism has never been observed on Mars, there is some evidence to suggest that it might still occur (Hauber et al., 2011). This limited volcanism and the lack of large-scale liquid water movement or impact events means that the majority of the surface morphological changes during this period appears to be the result of the movement of water-ice glaciers (Carr and Head, 2010b).

1.2.3 - Martian habitability

While it is difficult to draw definitive conclusions about the environment of Mars in the ancient past, it seems certain that Mars and Earth once resembled each other more than they do today (Anguita et al., 2006, Bost et al., 2010, Westall, 2005). There is strong evidence that, during the Noachian, Mars was more habitable, potentially to the extent that life could have developed and spread (see Section 1.1.2). Determining the habitability of Mars in the present day, however, remains problematic; Section 1.2.1 describes environmental factors that that make the present-day surface inhospitable to life and it remains uncertain whether life is capable of overcoming them. The following sections discuss the potential habitability of Mars today, focusing on the environments in which potential life may be found.

a) Deep subsurface habitability

Studies of the terrestrial deep subsurface, >100 m in depth (Probst et al., 2018), have repeatedly detected life in all environments that meet the three criteria of habitability outlined in Section 1.1.3 (Onstott et al., 2014). In fact, subsurface prokaryotes are estimated to comprise near 50 % of the Earth's total biomass (Whitman et al., 1998) and

there does not appear to be any limits to the depth or pressure at which life can be found, so long as water is stable (Onstott et al., 2014). Microbes have been detected and isolated in coal beds as deep as 2.4 km below sea-level (Inagaki et al., 2015), but there is indirect evidence for microbial activity occurring as deep as 10 km (Plümper et al., 2017).

The higher temperatures and pressures within the martian subsurface, compared to the surface, would support the stability of liquid water (Michalski et al., 2018). Microorganisms in the terrestrial deep subsurface can survive chemolithotrophically: generating the energy required for organic life *via* the oxidation of naturally occurring reduced compounds within the rocks (Payler et al., 2016, Hays et al., 2017, Emerson et al., 2016). This implies that the subsurface of Mars (at a depth of up to 6 km, Michalski et al. 2016) could potentially be a habitable environment. Exactly how large a volume, and how deep this water would be, remains uncertain due to the limited available knowledge about the martian subsurface (Michalski et al., 2013).

More recently, a large body of liquid water has been detected below the martian South Polar ice caps (Eigenbrode et al., 2018). This is postulated to contain high concentrations of dissolved salts (See Section 1.2.1d and Eigenbrode et al., 2018). Terrestrial sub-glacial lakes with temperatures below 0 °C (such as Lake Vostok), are believed to contain viable bacterial species (Sapp et al., 2018, Bulat, 2016), which raises the possiblity that the martian subsurface lake might be habitable. However, this martian lake is proposed to be -68 °C, below the lowest temperature at which metabolic activity of terrestrial microbes has been reported (-50 °C, Clarke et al., 2013, see Section 1.2.1c). Furthermore, as will be discussed within Section 1.4.2, assumptions about the habitability of saline environments are based around terrestrial studies in NaCl-rich

environments and do not consider the other salts dominant in the martian environment (Ojha et al., 2015, Massé et al., 2014, Kerr, 2013); this newly proposed martian environment may contain perchlorates (Orosei et al., 2018).

b) Near subsurface habitability

Even depths as shallow as a meter below the martian surface could be protected from many of the features that would render the surface uninhabitable (Ivarsson and Lindgren, 2010). UV can only penetrate a few mm into the martian soil (Ertem et al., 2017), and even cosmic rays can only penetrate as deep as 5 cm (Pavlov et al., 2012, Musilova et al., 2015). Water is also believed to be able to exist as small pockets of brine condensed onto the surface of salt crystals (Nikolakakos and Whiteway, 2015, Fischer et al., 2014), with indirect evidence for this detected by Curiosity in Gale Crater (Martín-Torres et al., 2015). On Earth similar near surface deliquesced brines in the Atacama desert contain microorganisms (Davila et al., 2013a, Davila et al., 2015) indicating that they can be a habitable environment.

Periodic releases of methane have been detected in the martian atmosphere that may originate from the subsurface (Oehler and Etiope, 2017, Fries et al., 2015, Webster et al., 2014). This methane could be formed *via* abiotic process such as photo-degradation of meteoritic organic molecules or ongoing serpentinization (Hu et al., 2016), but it could also be biotic; in the absence of sunlight, methanogenesis (generation of CH_4 from CO_2 and H_2) is a commonly suggested mechanism for energy generation by martian analogue organisms (Sinha and Kral, 2015, Schirmack et al., 2015). Curiosity has also detected CHNOPS elements, large organic molecules (Eigenbrode et al., 2018), and potential electron donors and acceptors in Gale Crater (Grotzinger et al., 2014), which

could imply that a relatively habitable environment persists in the relatively shallow subsurface of Gale Crater to this day.

Potential survival in the near subsurface, however, is complicated by the heavy ion form of cosmic radiation. Heavy ions can potentially trigger secondary radiation cascades in the martian regolith. While not lethal over short time periods (years or decades) these would kill dormant organisms that were incapable of active DNA-repair over the course of millions of years, even at depths as deep as 5 m (Dartnell et al., 2007). The near martian subsurface will be investigated for its habitability by the ExoMars 2020 rover. This will contain a radar system for mapping the subsurface within 2 m of the rover (Ciarletti et al., 2017). It will also possess the largest drill yet taken to Mars (also 2 m) in order to retrieve, and analyse, samples of interest identified by the radar (Ciarletti et al., 2017). One of the key aims of the mission is to characterise habitability in the present-day near subsurface (Josset et al., 2017),

c) Surface habitability

When considering the martian surface, both in the present day and the distant past, in terms of the three factors used to define habitability (CHNOPS elements, liquid water and an energy source, Section 1.1.3), it would theoretically be considered habitable. CHNOPS elements have been detected in Gale Crater (Grotzinger et al., 2014) and the environmental conditions wold potentially allow autotrophy (Murukesan et al., 2016, Westall et al., 2015). As discussed above (Section 1.2.1d) there is the potential for salt-rich liquid water to exist both now and in the distant past, potentially creating a habitat for salt tolerant organisms. The present-day martian surface, however, is exposed to a variety of environmental extremes (Section 12.1) that the subsurface is not. From a practical perspective, the martian subsurface, therefore, appears to be more habitable

but there is an absence of firm data on its conditions. This will change with the arrival of the InSight and ExoMars 2020 missions, but for now the surface conditions are considerably better characterised.

Many terrestrial organisms, known as extremophiles, are known to be able to tolerate some of the extreme environmental factors, such as the temperatures, atmosphere, radiation (at least in small amounts) and desiccation, on the martian surface, at least in small amounts (De Vera et al., 2014). As such, terrestrial extremophiles are often used as analogues in astrobiology experiments (Gómez et al., 2012, Mancinelli et al., 2004) and their ability to survive under Mars relevant conditions are considered below.

Temperature

The mean martian temperature is -60 ℃ (McKay, 1999). While the lower limit of metabolic activity of microorganisms is believed to be around -50 ℃ (Clarke et al., 2013) this is not the limit for survival and there are reports of cells being revived following exposure to temperatures as low as -196 ℃ (Mazur, 1980, Bakermans, 2017a). Dormant terrestrial cells could theoretically withstand the mean martian global temperature and be successfully revived later under warmer conditions (Bakermans, 2017b). The martian surface temperature is highly variable depending upon geographic location, season of the year and time of day. At the equator, the temperature can vary as much as 100 ℃ across a day-night cycle (from approximately 20 to approximately -150 ℃, Pierrehumbert, 2010). This, at least temporarily, puts the surface within the temperature range where metabolic activity and reproduction is possible.

Terrestrial microorganisms, however, even extremophilic ones, require a stable thermal environment to survive (Schumann, 2016). This range of temperatures includes the

melting point of water, thus the inhospitable temperature variation is further complicated by freeze-thaw effects, generated by the formation of sharp, microscopic ice crystals (Kong et al., 2017, Sleep and Zahnle, 1998). Despite this, there is evidence to suggest that terrestrial microorganisms, even non extremophilic ones, can survive simulated exposure to the martian diurnal temperature cycle, although this has only been tested over the course of weeks rather than years (Mickol et al., 2018a, Mickol et al., 2018b). Alternatively, as dormant cells contain considerably less water (Ulanowski et al., 1987) microorganisms on today's martian surface might be able to withstand this temperature cycling by remaining continually dormant, instead of reviving in the periodic warmer temperatures.

Atmospheric pressure

There are no naturally occurring terrestrial surface environments where pressure is as low as it is on the present-day martian surface (6.1 mbar, Korablev et al. 2018), although microorganisms have been successfully cultured from clouds and the terrestrial troposphere where the pressure was presumed to be much lower than the surface (Schuerger and Nicholson, 2016). A variety of terrestrial microorganisms used for Mars analogue experiments, however, have shown an ability to withstand simulated martian pressures (Mastascusa et al., 2014, Nicholson et al., 2013, Mickol and Kral, 2017).

Screening of environmental samples from a wide variety of terrestrial sources in artificially generated martian-pressure environments has shown that, despite the survival of common microorganisms in these environments, they do exert a selection pressure. Some microorganisms tolerate these conditions better than others (Schuerger and Nicholson, 2016). These so-called hypobarophiles were primarily isolated from cold

environments, such as the Alps and Canadian mountains, implying that low-pressure stress resistance might use similar pathways to cold resistance (Schuerger and Nicholson, 2016). While the study of the low-pressure tolerances of microorganisms is still in its early days, there is no evidence to suggest that the low pressures found on the present-day martian surface would render it uninhabitable (Schulze-Makuch et al., 2017)

Atmospheric composition

The martian atmosphere is anaerobic - it contains little to no oxygen (Table 1.1). While, by modern standards, an anaerobic environment is considered extreme, the origin of terrestrial life likely occurred in an anaerobic environment (Michalski et al., 2018). The vast majority of the Earth's atmospheric oxygen is produced by photosynthesis and, prior to the Great Oxygenation Event (Blaustein, 2016), oxygen was toxic to terrestrial life (Michalski et al., 2018). All terrestrial aerobes are descendants of extremophilic oxygen tolerant microorganisms (Fischer et al., 2016). The Earth's high oxygen content is therefore one factor with which it might be stated that Earth is a more extreme environment than present-day Mars.

Earth still retains many organisms capable of operating in anaerobic environments (Cockell et al., 2017, Ollivier et al., 1994). Many of these have adapted to tolerate the widespread aerobic environment, but obligate anaerobes can still be found in environments which oxygen cannot reach, such as the seafloor and hydrothermal vents (Miroshnichenko and Bonch-Osmolovskaya, 2006). Experiments with anaerobic organisms have shown that many are capable of growth under simulated martian atmospheric conditions (Beblo-Vranesevic et al., 2017, Rettberg et al., 2017, Bauermeister et al., 2014). While the vast majority of terrestrial organisms could not

survive the martian atmosphere, the lack of oxygen does not render the present-day martian surface uninhabitable.

Radiation

The radiation environment on the surface of Mars is comparable to that of space (Schuerger et al., 2006), with heavy bombardment from both solar UV and cosmic ionizing radiation (Section 1.2.1c). UV radiation can cause adjacent pyramidine bases on the same strand of DNA to form covalent bonds (Goosen and Moolenaar, 2008), whereas ionising radiation can cause single strand or double strand breaks in the DNA sequence (Shibata and Jeggo, 2019). Terrestrial microorganisms are known to exist which can withstand radiation at dosages significantly higher than any that naturally occur in terrestrial environments (Musilova et al., 2015). So called "radiation resistant organisms" achieve this survival by a combination of two mechanisms: 1) the existence of multiple copies of the genome per cell to act as a "backup" and 2) highly efficient DNA-repair machinery (Soppa, 2013). Both of these mechanisms are already present in "radiation-resistant organisms" because they initially evolved as a response to desiccation stress (Musilova et al., 2015).

Despite the existence of many radiation resistant microorganisms on Earth, there are none known to be able to withstand equivalent doses of radiation to the values found on the martian surface (Musilova et al., 2015). This, therefore, renders the majority of the martian surface uninhabitable to known terrestrial organisms, at least in terms of long-term survival over a period of years. As mentioned earlier, the UV radiation can be blocked by a relatively small amount of regolith (Ertem et al., 2017, Pavlov et al., 2012, Musilova et al., 2015) or by salt crystals (Stan-Lotter et al., 2002b, Leuko et al., 2015), but the cosmic radiation, while lower in intensity, can cause damage to cells at much

lower depths (Dartnell and Patel, 2014). Terrestrial microorganisms, however, have not developed radiation-resistance as such, but have instead gained it as a side effect of desiccation resistance (Dartnell et al., 2010). It, therefore, does not seem unreasonable to suggest that long-term gradual exposure to the martian radiation environment could cause evolution of resistance mechanisms not needed by terrestrial life (Dartnell et al., 2007).

While Mars is unlikely to have ever had an ozone layer generated by photosynthesis (Cockell et al., 2000), the Earth also did not have one when life first emerged (Fendrihan et al., 2009a). On the early Earth, life must have relied on the magnetic field (Fendrihan et al., 2009a) and the radiation absorbing properties of water (Westall et al., 2006) to protect it from radiation. It seems reasonable to suggest that on Noachian Mars, both of these factors could have provided protection to potential martian organisms (Fendrihan et al., 2009a) although neither of these factors remain to the present day. If Mars ever possessed life on the surface, it appears that the radiation environment is the most extreme environmental condition that it would have had to adapt to. The radiation is, therefore, one of the key environmental conditions on the martian surface that will be investigated in this thesis.

Desiccation

On present-day Mars, the majority of the surface is dry - there are no seas, lakes or oceans (Zahnle, 2001). This severely limits the number of potential habitable environments. If water does exist on the martian surface it is likely to be transient (Bhardwaj et al., 2017, Jones, 2018, Martín-Torres et al., 2015) and organisms would have to cope with extended periods of dryness. Terrestrial desert environments also only possess transient water, but microorganisms are still able to survive (Paulino-Lima

et al., 2016, Azua-Bustos et al., 2014, Yu et al., 2015). "Xerotolerant" microorganisms have developed a wide range of responses to desiccation stress including the formation of biofilms and secretion of exopolysaccharides (Lebre et al., 2017). The ability to become dormant and form spores also provides protection against desiccation for long periods of time (Jones and Lennon, 2010, Lebre et al., 2017). Any potential martian microorganism would, therefore, require adaptations to periods of dryness and an absence of water.

Salt

Salts (of the compositions outlined in Section 1.2.1d) are found across the present-day surface of Mars (Massé et al., 2014, Clark and Van Hart, 1981, Kounaves et al., 2010, Hecht et al., 2009). This implies saline bodies of water once existed, some of which may persist into the present day (Ojha et al., 2015).

High concentrations of salt create an extreme environment. Terrestrial salt tolerant microorganisms - "halophiles" - have been discovered (McGenity and Oren, 2012, Mancinelli, 2005) that can grow even in saturated brines (Madigan et al., 2006). These salt-tolerant organisms have primarily been studied in NaCl dominated brines, and relatively little is known about their tolerance to other salts. This is the main topic of this Thesis and will be discussed in greater detail later (Section 1.4.2).

Adapting to surface extremes

The present-day martian surface environment is unlikely to be habitable to any known terrestrial extremophile, with the most extreme environmental factor being the radiation environment. There is evidence, however, to suggest that all of these environmental conditions were less extreme in the distant past (Section 1.2.1b) and it is

believed that life could have survived on the martian surface during the Noachian period. For life to survive into the Hesperian it would have had to adapt to these environmental stresses, but it seems likely that some could have developed physiological adaptations to the worsening environmental conditions (De Vera et al., 2014).

There has never been an extinction event capable of eradicating all forms of terrestrial microbial life and models suggest that it is too diverse and widespread for one to ever happen (Sloan et al., 2017). It, therefore, seems reasonable to suggest that even if the Noachian-Hesperian transition was sudden and catastrophic, potential Noachian life might have been able to survive into the Hesperian where habitable environments, if they existed, were smaller scale and considerably more transient (Cockell, 2014). As the last bodies of water, and thus potentially the last habitable environments, on the martian surface would contain a high salt content (Davila and Schulze-Makuch, 2016, Osterloo and Hynek, 2015), in this Thesis, halophiles are investigated as a model for terrestrial organisms that would, theoretically, be best suited for such a transition.

1.3 - Halophiles

Halophiles are salt tolerant microorganisms. They were amongst the earliest extremophiles to be discovered, since many of the extremely halophilic archaea possess a distinctive pink colour induced by a photosynthetic pigment which was known of even in the time of Pliny the Elder (79 AD) (Bostock, 1855). Halophiles are found in all three domains of life, and representatives are known from archaea (Hou and Cui, 2017), bacteria (Kindzierski et al., 2017), fungi (Zhang and Wei, 2017) and even plants (Chakradhar et al., 2017). The most extreme salt tolerances tend to be found in one

specific family of archaea, the *Halobacteriaceae*. Halophiles are found in highly saline areas from around the globe, such as salterns (Viver et al., 2015), the dead sea (Mullakhanbhai and Larsen, 1975, Oren, 1983) or salt flats (Vogt et al., 2018).

Extremophiles, such as halophiles, are often difficult to work with in the laboratory. The extremes of their environments mean that they are often present in only low diversity communities (Twing et al., 2017) with very low biomass (Direito et al., 2012). Extremophilic microbes are often "obligate extremophiles", that have adapted for survival in extreme conditions, but are unable to grow in less extreme conditions (Rasuk et al., 2016). These extreme conditions are often difficult to replicate in the laboratory, for example many anaerobes are highly susceptible to oxygen stress (Miroshnichenko and Bonch-Osmolovskaya, 2006). Extremophiles also tend to grow very slowly (Corkrey et al., 2018), over the course of months and years, which can lead to studies using extremophiles to be lengthy. For these reasons, many studies of extremophiles tend to be culture-independent, based upon the activity of unculturable extremophiles in the field rather than cell cultures in the lab (Alain and Querellou, 2009). Analysis of DNA can identify which microorganisms are present in a community (Clark et al., 2017), while mRNA can show which microbes are active and their responses to variable environmental conditions (Tripathy et al., 2016).

Fortunately, halophiles are amongst the easiest extremophiles to culture since their environmental extreme is one that can be easily generated and maintained in the laboratory (Ma et al., 2010). As such there is decades of research, which has investigated the adaptation mechanisms that halophiles have developed (Grant et al., 1998b, DasSarma and DasSarma, 2006, Ma et al., 2010, McGenity, 2017) to cope with the most abundant terrestrial salt: NaCl (Fox-Powell et al., 2016). The following sections,

therefore, present an overview of what is currently known about the mechanisms that halophiles employ to survive in terrestrial, NaCl-rich brines.

1.3.1 - Osmosis and water activity

As discussed earlier (Section 1.1.3), water is considered essential for life, because of its use as a solvent (Brack, 2002, Westall and Brack, 2018). Cells need to have a precisely balanced internal water concentration (Beckett, 1986). This is controlled by osmosis, a passive, energy-free process (Kramer and Myers, 2012) that cells exploit to take in from, or release water to, the environment (Figure 1.8). Osmosis involves the movement of water through a membrane from an area of low solute concentration to one of high solute concentration, in an attempt to equalise solute concentrations (Figure 1.8). When a cell is removed from its normal environment and immersed in one rich in salt, water leaves the cells and enters the saline environment in order to equalise solute concentrations on either side of the cell membrane. As a result, the cells dry out and die (Grant et al., 1998b).

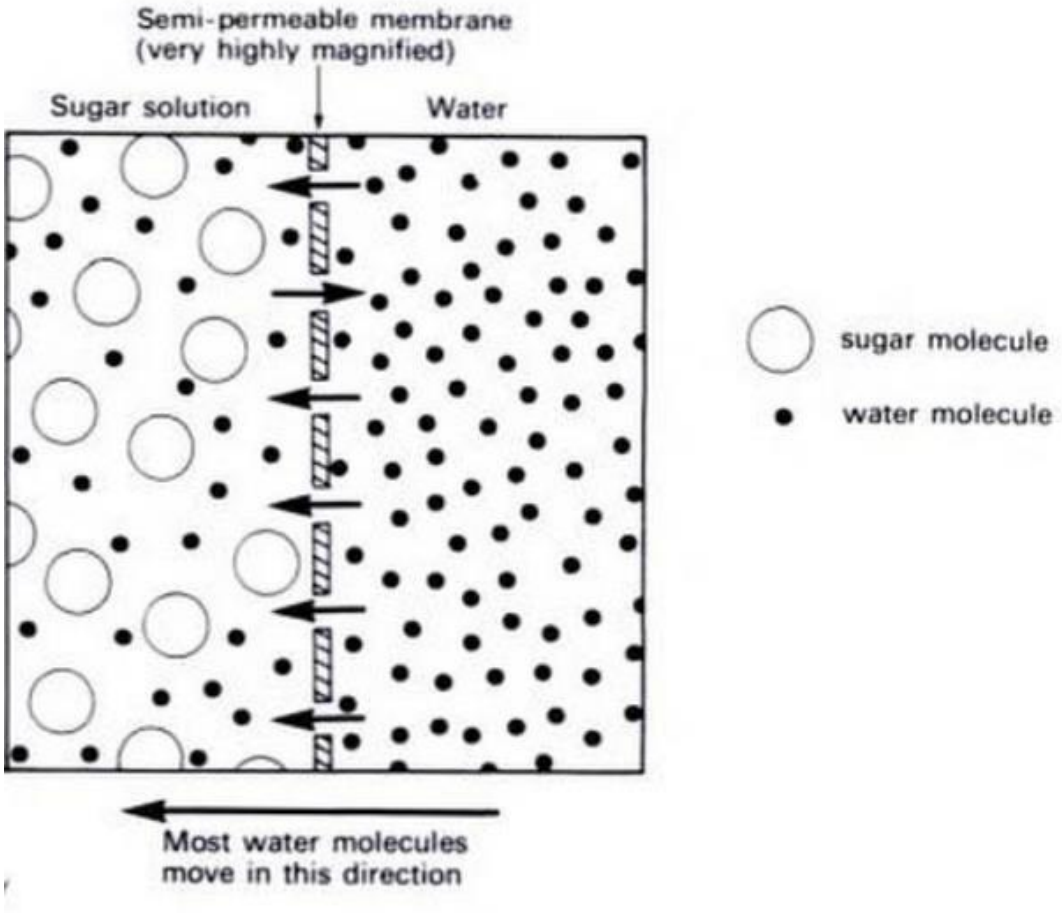

Figure 1.8 - The process of osmosis. Water moves in both directions through the semi-permeable membrane, but the net movement of water is always towards the greater concentration of dissolved compounds. Adapted from Beckett, B.S. (1986)

Terrestrial organisms are adapted to exist in osmotic equilibrium with their surroundings (Kramer and Myers, 2012). In conditions of high NaCl, non-halophilic microorganisms have this osmotic equilibrium disrupted resulting in the water moving out of their cells, causing them to dry out and die. As a result, many terrestrial halophiles have their internal osmotic potential adapted to high solute concentrations, as will be described in more detail in section 1.3.2 (Gunde-Cimerman et al., 2018). In an extra-terrestrial environment where the solute may not be NaCl, it is important to have a thorough understanding of the osmotic gradient between the cell and its surroundings as this may impact on how habitable that brine might be.

A wide variety of terms are used to describe the osmotic potential of solutions (Griffin, 1996). The two most frequently used are water activity (a_w) and water potential (ψ). The terms tend to be used interchangeable in the literature (Van Long et al., 2017, Chirife and Resnik, 1984, Vandeputte et al., 2017, Labuza, 1980, Grant, 2004, Stevenson et al., 2015a, Ciancio et al., 2016, Da Silva et al., 2016, Aujla and Paulitz, 2017, Yan et al., 2015) as they measure the same parameter, but use different techniques and units (Griffin, 1996). For the purposes of this Thesis, water activity is the measure used, but it can be converted into water potential for comparison with other studies using Equation 1, where T is the temperature in kelvin and V_w is the molar volume of water (Mueller et al., 2011). By monitoring the water activity of solutions of different salts and determining whether these solutions can allow growth, it can be investigated whether these changes in water activity are responsible for whether these environments are, or are not, habitable to halophiles.

Equation 1 - Conversion between water activity and water potential

$$\psi = 8.314\mathrm{T} \ln a_w/V_w$$

1.3.2 - Halophilic tolerance to salts

Halophiles can be divided into the moderate halophiles, which can survive salinities of 0 M to roughly 3.4 M, and the obligate, or extreme, halophiles (Figure 1.9), which can survive from roughly 3.4 M NaCl to saturated solutions (Madigan et al., 2000). As a general rule, the moderate halophiles and the extreme halophiles use separate methods (Bell, 2012) to survive high salt concentrations (Figure 1.10) which are described below

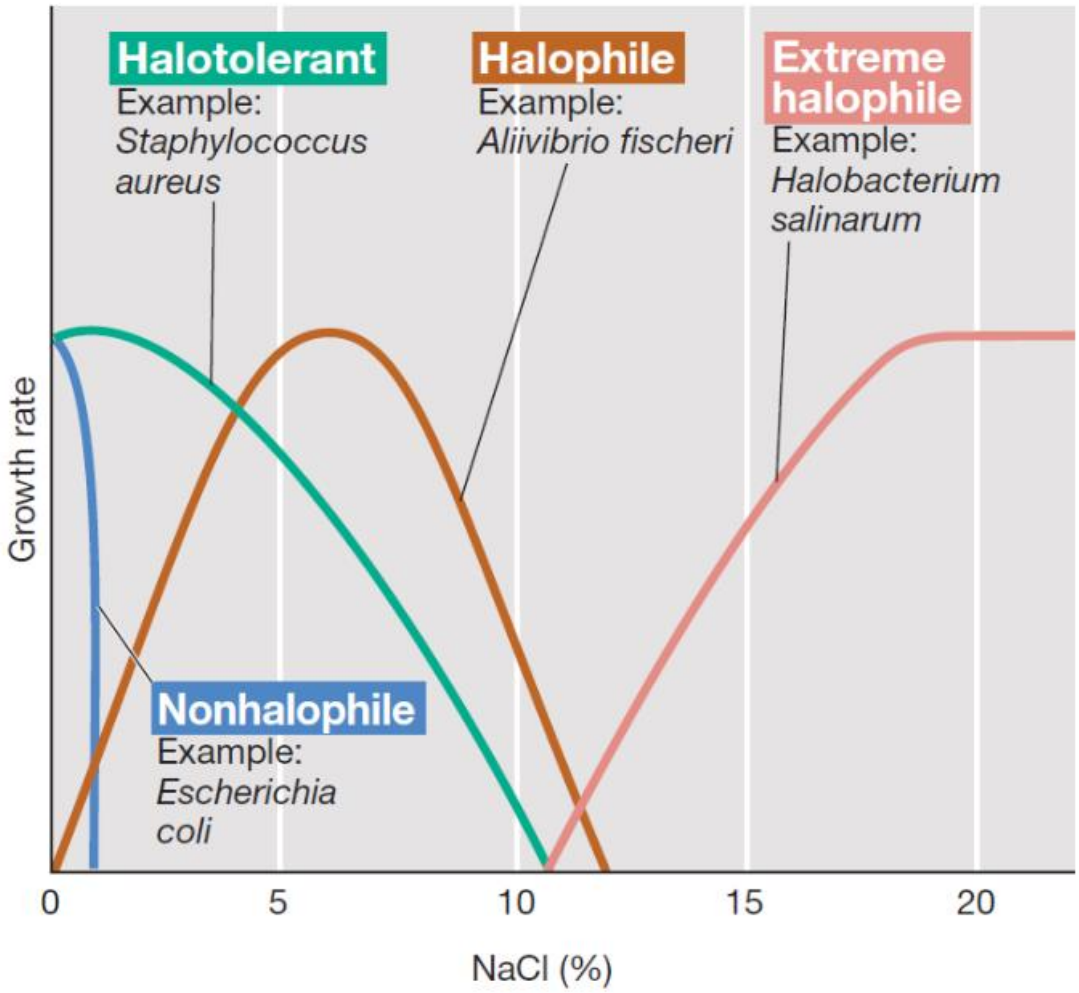

Figure 1.9 - Growth of organisms of varying halotolerance at different salt concentrations (Madigan et al., 2000)

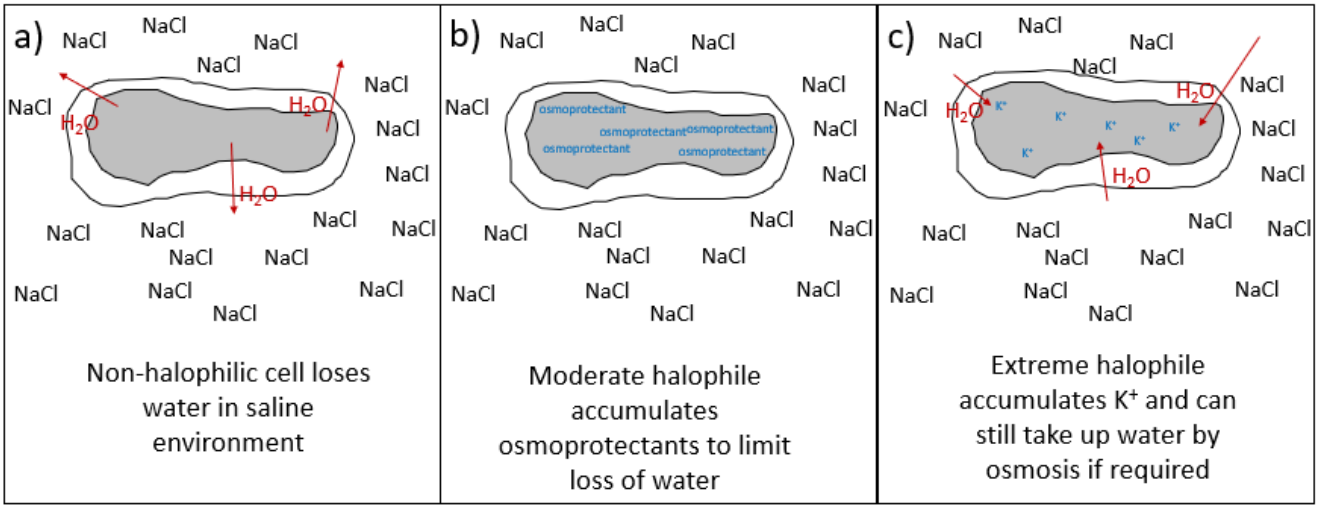

Figure 1.10 - Non-halophilic cells, extreme halophiles and moderate halophiles when exposed to salt rich environments.

a) Osmoprotectant strategy

The "moderate halophiles" (5-20 % NaCl mass by mass) survive by accumulating organic substances called "osmoprotectants" or "compatible solutes" (Grant et al., 1998b) within their cytoplasm (Figure 1.10b). Osmoprotectants primarily protect cells by reducing the damage to internal macromolecules caused by the loss of water from the cell interior (Kempf and Bremer, 1998). The osmoprotectants themselves can be one, or more, of many substances, mainly betaines, sugars and amino acids. Osmoprotectants cannot, however, prevent the loss of water by osmotic pressure, although their impact on the internal water potential does slow the process slightly (Grant et al., 1998b). As a result, this method cannot protect cells from the most saline environments hence the classification of most cells that use this method as "moderate halophiles". Osmoprotection is the method used by the vast majority of halophilic bacteria which explains why halophiles in this domain tend to only be moderate halophiles (Canovas et al., 1996).

b) Salt-in strategy

"Extreme halophiles," primarily the haloarchaea, employ the "salt-in" strategy, which involves accumulating high concentrations of ions within the cell (Figure 1.10c). This results in a lower internal water potential and thus lower osmotic gradient (Grant et al., 1998b). Despite the high abundance of NaCl in most halophilic environments, terrestrial cells avoid high internal Na^+ concentrations because of its toxicity, therefore, the cells instead fill themselves with K^+ (Gunde-Cimerman et al., 2018).

These internal K^+ concentrations can reach as high as 5 M (Deole et al., 2013). K^+ uptake is typically a passive process, utilising diffusion through membrane channels based

upon proton-gradients that the cell already generates (Gunde-Cimerman et al., 2018) *via* respiration and in some archaea the action of bacterioruberin (see Section 1.3.4a). Despite the passive nature of K^+ uptake, there is evidence that halophiles can modulate and control it: the internal K^+ concentration correlates neatly with external NaCl even with rapid artificial modulation in the external concentrations (Deole et al., 2013). An ATP-driven K^+ pump, kdp, has been detected but only in the genera *Halobacteria* (Kixmüller and Greie, 2012).

c) Comparison between the two strategies

The "salt in" method is considerably more effective than the osmoprotectant method and therefore, can support survival in over 3.4 M NaCl (20% mass by mass), hence the halophiles that employ this strategy are classified as "extreme halophiles" (Figure 1.9) (Grant et al., 1998b). The salt-in strategy is also considerably less energy intensive (Yancey et al., 1982), but it is not without its drawbacks. High K^+ levels significantly raise the internal charge of the cell, which impacts the three-dimensional structure of cellular components, such as protein and DNA (Yancey et al., 1982). To compensate for this, the internal components of extreme halophiles have become highly negatively charged in order to retain their shape in the highly positively charged internal environment (Yancey et al., 1982). This has resulted in extremely halophilic cells becoming dependent on high internal concentrations of K^+ ions. A lower internal charge would disrupt the structure of DNA and internal proteins. This means that in low-salt environments the cells cannot excrete the K^+ ions. The intense osmotic pressure results in the cell taking up too much water and bursting (Grant et al., 1998b). For this reason, the extreme halophiles are also described as "obligate halophiles" (DasSarma and DasSarma, 2006).

The list of organic solutes used as osmoprotectants is incredibly large and diverse (Kempf and Bremer, 1998). This diversity of osmoprotectants is also reflected in their positioning across the phylogenetic tree, suggesting that this strategy has numerous independent origins (Oren, 2008). This in turn goes to explain the large diversity of moderately halophilic organisms. There is, however, evidence to suggest that the "salt-in" strategy has only ever evolved once, and is primarily limited to the class of archaea known as the *Halobacteria* (Wright, 2006). In more recent years, the salt-in strategy has been detected within the bacterial phyla *Firmicutes* (Oren, 1986) and *Bacteroidetes (*Anton et al., 2002), but there is strong evidence to suggest that this is a result of horizontal gene transfer with the *Halobacteria* rather than an independent origin (Oren, 2008).

1.3.3 - Entombment of halophiles

Many terrestrial brines are formed in areas where the rate of water influx is less than the rate of evaporation, resulting in salts becoming concentrated (McGenity et al., 2000). This is not a stable system, and eventually leads to complete evaporation of the brine as salt crystals precipitate (McGenity et al., 2000).

When salt crystals form, they contain microscopic pockets - fluid inclusions - of the original brine (Norton and Grant, 1988). Examples of fluid inclusions are shown in Figure 1.11. When halophiles are present in evaporating brines, the size and abundance of these inclusions is increased (Adamski et al., 2006) and halophiles are preferentially entombed within these inclusions (Figure 1.12) rather than within the crystalline matrix (Fendrihan et al., 2009a). These effects have also been observed as occurring in the presence of organic nanoparticles, instead of intact cells (Pasteris et al., 2006),

which implies that entombment is a physico-chemical process rather than biological. It seems that particles, or cells, act as seeds in a process similar to ice nucleation in water (Pasteris et al., 2006).

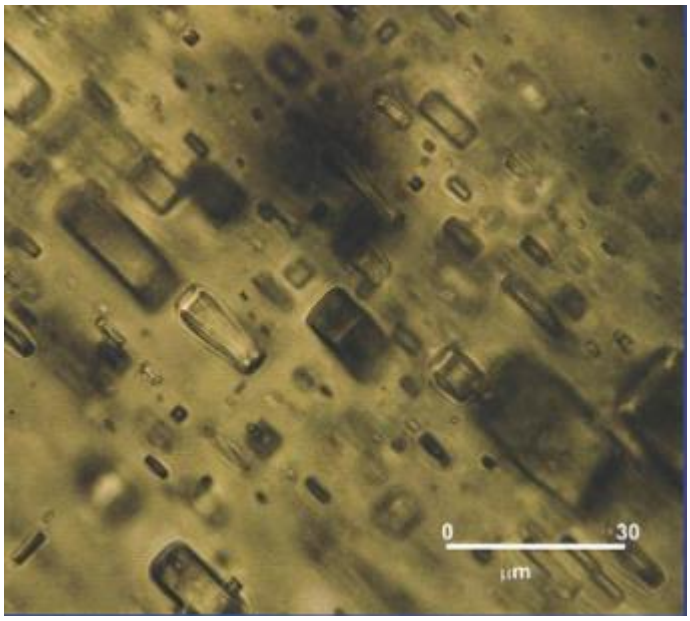

Figure 1.11 - Fluid inclusions imaged in laboratory-grown halite crystals under phase-contrast microscopy. Adapted from Adamski et al., (2006)

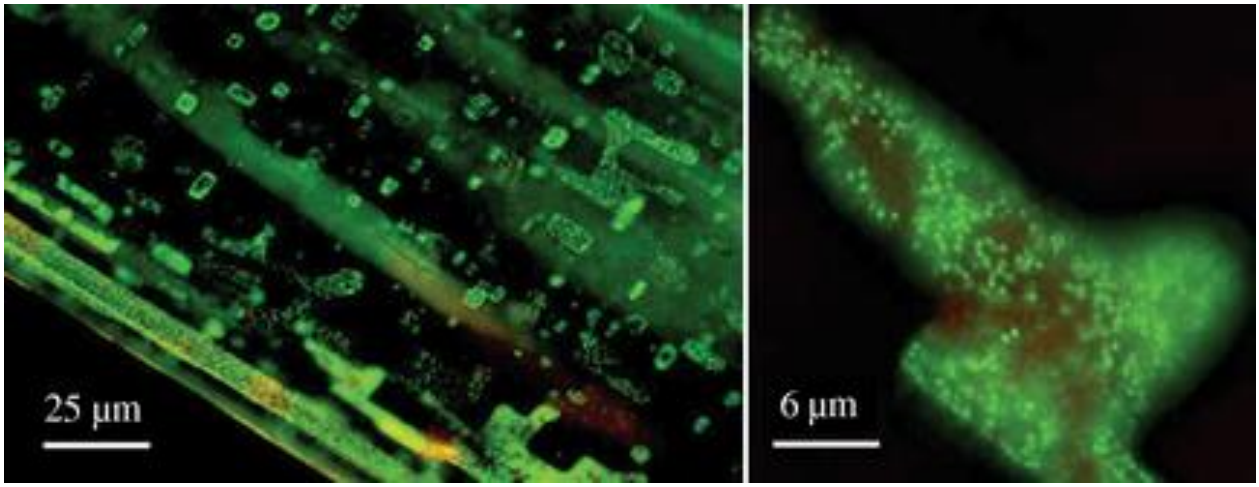

Figure 1.12 - Location of pre-stained cells of Halobacterium salinarum *NRC-1 in laboratory-grown fluid inclusions. Cells are stained using the LIVE/DEAD ® BacLight™ bacterial viability kit, live cells are green and dead cells are red, It can be seen (left) that the green dye is primarily localised within the fluid inclusions, and that (right) within the inclusions, the dye is localised within the cells (Fendrihan et al., 2012)*

Subsequent dissolution of these salt crystals releases the still-viable halophiles into the aqueous environment (McGenity et al., 2000) where they can be dispersed. It has also

been postulated that entombed halophiles can be distributed around the Earth within salt grains blown upon the wind (McGenity et al., 2000). This could potentially explain how obligate halophiles have been able to colonise brines from around the world, despite them being separated by vast regions that are inhospitable to them (Roux et al., 2016)

a) Surviving entombment

There is a tendency in the literature to describe entombed halophilic cells as "dormant" (Fendrihan et al., 2012, Rosenzweig et al., 2000, Graur and Pupko, 2001, McGenity et al., 2000, Norton et al., 1993). In microbiology, however, dormancy refers to a very specific process in which microbes become spores; the available genomic evidence suggests that halophilic archaea lack the necessary genetic pathways to undergo spore formation (Fendrihan et al., 2012, Grant et al., 1998a) and so the term "dormancy" should not be used. Halophiles do, however, appear to undergo large physiological changes when entombed in fluid inclusions that are visually similar to those of dormant cells.

Spherical particles, smaller than a typical halophilic archaeal cell (< 1 μM diameter, compared to approximately 2 μM) , have been observed in ancient fluid inclusions from which halophiles have later been cultured (Schubert et al., 2009). Further work has shown that rod-shaped halophiles could be induced to form similar, miniaturised-spherical shapes (Figure 1.13) in conditions of low water potential, corresponding with those found within inclusions (Fendrihan et al., 2012).

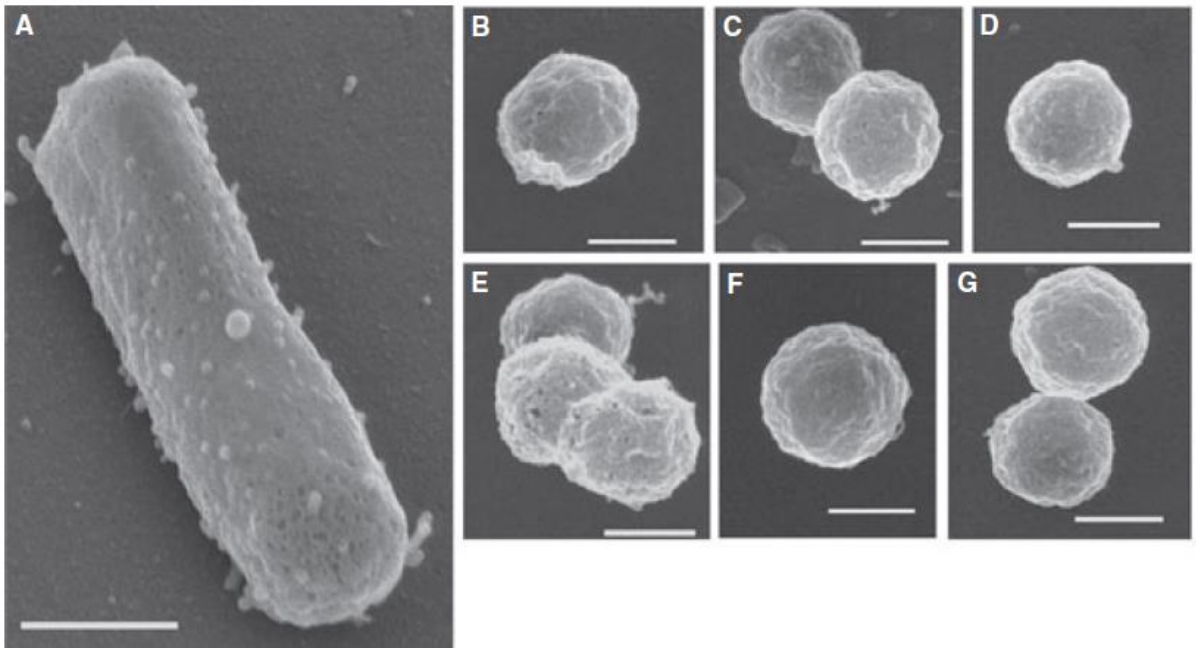

Figure 1.13 - Scanning electron micrographs of Halobacterium salinarum NRC-1 in its normal rod form (A) and as spheres formed in low water potential conditions (B-G). Scale bar is 600 nm in A and 270 nm in B-G. Image from Fendrihan et al. (2012).

Halophiles typically possess an S-layer, a tightly packed hexagonal layer of glycoprotein, as the final exterior layer of the cell (Fendrihan et al., 2006). This layer is believed to be responsible for maintaining the shape of the halophilic cell under different salt conditions (Fendrihan et al., 2006). When the cells form spheres, they appear to completely lose their S-layer (Fendrihan et al., 2012). These spheres also contained significantly less ATP (12.4 ng/mg of biomass) than the rod-shaped form (620 ng/mg of biomass). Loss of ATP and the S-layer are both features of dormant microbes, implying that while they lack the ability to form true spores (Fendrihan et al., 2012, Grant et al., 1998a), the halophilic ability to survive entombment may involve a similar process (Fendrihan et al., 2012).

While the formation of spherical particles with dormancy-like traits suggests that halophiles become inactive to survive entombment, there is also conflicting evidence. For example, microscope observations of laboratory-grown salt crystals suggests that

entombed halophiles do not immediately become inactive, but instead slow their movement over the course of a year of observation (Adamski et al., 2006). It is uncertain whether they eventually cease this movement over longer timescales (Adamski et al., 2006).

Recent studies have also suggested that the ATP driven K^+ pump, kdp, which is unique to the *Halobacterium* genera (Kixmüller and Greie, 2012), may improve survivability of entombment in this genera compared to other haloarchaea (Huby, 2017). The *Halobacterium* genera is also the most abundant archaea to be successfully isolated from both ancient rock salts (McGenity et al., 2000) and modern salterns with a known diverse community. It has been shown that knock out mutants of this pump have considerably reduced survival within crystals (Kixmüller and Greie, 2012), which provides early insights into how this "sphericalisation" process operates and is regulated.

b) Long term survivability in halite

There are a plethora of experimental studies to suggest that it is possible to recover ancient halophiles from salt crystals hundreds of millions of years old (Satterfield et al., 2005, Jaakkola et al., 2014, Gibtan et al., 2017, Rubin et al., 2017, Jaakkola et al., 2016a). Contamination of laboratory equipment and more recent microbial re-colonisation of the salts (Sankaranarayanan et al., 2014) have, however, been suggested as alternative explanations for the presence of such organisms. In many natural environments, viable cells cannot be extracted from salts older than 30,000 years (Schubert et al., 2009, Hebsgaard et al., 2005), implying that this might be a hard limit for long-term microbial survival while entombed.

Owing to the uncertainty of the biological processes halophiles undergo while entombed, it is unknown whether a halophile trapped within a salt crystal is capable of metabolic activity and DNA repair (Schubert et al., 2009). Schubert et. al (2009b) suggested that the greater success rate of inoculating haloarchaea from fluid inclusions containing dead, glycerol-rich algae, might imply that entombed haloarchaea are capable of metabolising the remains of cells that cannot survive entombment. If so, then it was calculated that the carbon content of a single algae cell would be able to support DNA repair of a single *Halobacteria* cell for 12 million years (Schubert et al., 2009). As the glycerol was initially produced by the algae to act as an osmoprotectant in the saline environment prior to salt formation (Kageyama et al., 2017), it also seems plausible that the glycerol-rich algae were being used by the halophile in some way as an osmoprotectant.

1.3.4 - Polyextreme halophiles

Many extremophiles can be classified as "polyextremophiles" - they can survive more than one environmental extreme (Srivastava, 2014). This is often a result of either frequently co-occurring environmental extremes, for example Antarctic extremophiles need to be both cold and desiccation resistant (Pfaff et al., 2016), or because of different environmental stresses inducing the same negative effect on a cell, for example both radiation and desiccation cause DNA damage which can be repaired using the same pathways (Mattimore and Battista, 1996).

Most halophiles are polyextremeophiles and are able to survive, and grow, in saline environments with additional stresses. The tolerance of halophiles to these other stresses makes them a good candidate for use in astrobiology, as many of these

environmental stresses are ones that are also found on the martian surface (though admittedly at lesser extremes). The following sections outline how polyextremophilic halophiles are able to tolerate some of the extreme conditions found on the present-day martian surface outlined in Section 1.2.1.

a) UV-resistance and autotrophy

In areas with extreme amounts of sunlight (e.g. the Dead Sea), brines form in lakes and salterns where the rate of evaporation of water is greater than the rate of water influx, causing a high concentration of the dissolved salts (McGenity et al., 2000). The microorganisms that grow within these environments have adapted to survive exposure to extreme amounts of solar UV radiation in addition to high salt concentrations (Oren, 2009).

Halophilic UV-resistant archaea commonly possess pigments, such as bacterioruberin, that are evident as pink colouration visible to the naked eye (Oren, 2009) as shown in Figure 1.14. Bacterioruberin, and potentially the high internal K^+ concentrations (used to modulate internal water potential, see Section 1.3.2b), provide protection from UV by scavenging the free radicals formed within the cell under high UV conditions (Shahmohammadi et al., 1998). Another pigment, bacteriorhodopsin, also provides protection from UV by absorbing the energy of high wavelengths of light (Oren, 2009). This absorbed energy is used to pump protons out of the cell, and the resulting proton gradient is then used to generate ATP (Oren and Shilo, 1981), the source of all biological energy. It has been proposed that this primitive form of photosynthesis could predate the more commonly used form (Blankenship, 1992).

Figure 1.14 - A saltern near San Francisco. The high salt concentration water appears pink, due to the high concentrations of Halobacterium (DasSarma and DasSarma, 2006).

Despite the UV-resistance of many halophiles, the radiation dosage on the martian surface is still more extreme than a terrestrial halophile could survive in a brine. Even the more radiation-tolerant halophiles typically have 90 % of a population killed when exposed to approximately 10 kJ/m^2 of UV (Leuko et al., 2015), whereas the martian surface typically receives approximately 1,500 kJ/m^2/day (Cockell et al., 2000). There is, however, experimental evidence to suggest that entombment within salt crystals could significantly raise UV-resistance and potentially allow survival even in under the present-day martian radiation environment (Fendrihan et al., 2009a, Fernández-Remolar et al., 2013).

b) Cold tolerance

Brines are also found in cold terrestrial environments. Many subsurface Antarctic lakes are below freezing temperature and the water can only exist as a liquid due to the high salt concentrations (Mikucki et al., 2015), as is hypothesised on present-day Mars (Jones, 2018). Investigations of many terrestrial subsurface hypersaline cold environments, such as Lost Hammer (Niederberger et al., 2010), the lake that feeds Blood Falls (Mikucki and Priscu, 2007), or the lake under Axel Heiberg island in Canada (Sapers et al., 2017), have all shown the presence of microbial communities.

Relatively little research has been carried out into the cold tolerance of halophiles (Oren, 2014), but they seem to consistently be found in samples of Antarctic subsurface hypersaline ice lakes (Yakimov et al., 2015, Oren, 2014, Tregoning et al., 2015, Williams et al., 2014). There is even evidence to suggest that in some sub-zero hypersaline environments, methanogenesis, a commonly proposed energy generation mechanism for potential martian organisms, as discussed in Section 1.1.3 (Mickol and Kral, 2017, Oehler and Etiope, 2017, Fries et al., 2015, Sinha and Kral, 2015), is capable of occurring (Niederberger et al., 2010).

c) pH tolerance

The Earth possess many hypersaline salt lakes, formed by a variety of processes such as the dissolution of carbonates, (Patrick et al., 1981), hydrothermal and volcanic systems (Bowen and Benison, 2009) and even by human pollutants (Tolonen and Jaakola, 1983). Investigations into such lakes have found them to have communities of halophilic microorganisms (Bowen and Benison, 2009). While not as widespread amongst the halophiles as UV-resistance and cold tolerance, acid-tolerant halophiles can be found

across the phylogenetic tree in both the Bacteria and Archaea domains (Zammit and Watkin, 2016). Both acid tolerance and halotolerance require specialised systems to maintain the internal ionic concentration. It is, therefore, believed that acid tolerant halophiles gained acid tolerance as a result of modifications to the already existing halotolerance systems (Zammit and Watkin, 2016).

By analysing the composition and distribution of aqueous alteration features in Gale Crater, constraints can be placed on the chemistry of the water that produced them (Tosca et al., 2011). This evidence suggests that the pH of the brines in Gale Crater were highly variable, both spatially and temporarily, with strong evidence found for both circumneutral and acidic (pH of 3.4-5.2) water (Rampe et al., 2017, Phillips-Lander et al., 2017, Peretyazhko et al., 2016, Tosca et al., 2011). The fact that terrestrial halophiles have been able to adapt the salt-tolerance mechanisms to survive low pH increases the potential range of habitats within Gale Crater

d) Desiccation resistance

Halophiles are often described in the literature as desiccation resistant (Kottemann et al., 2005, Shirsalimian et al., 2017, Leuko et al., 2015). Desiccation resistance in halophilic and non-halophilic microorganisms is routinely examined by evaporating growth medium containing cells (Kottemann et al., 2005, Shirsalimian et al., 2017, Leuko et al., 2015). By necessity, the halophilic growth medium contains high salt concentrations and, as a result, these salts precipitate forming fluid inclusions, with the microorganisms entombed inside. This is, therefore, not a true test of desiccation as the cells remain in the hyper-saline aqueous environment within the fluid inclusions rather than in a desiccated state.

Despite the lack of studies investigating the desiccation resistance of halophiles outside salt crystals, there are some suggestions that haloarchaea could possess true desiccation resistance. Haloarchaeal genomes possess sequences and protein domains, analogous to compounds such as mucins, known to be involved in desiccation resistance in other non-halophilic organisms (Stan-Lotter and Fendrihan, 2015) and these stress response pathways are activated when halophiles are grown on partially desiccated agar plates (Kixmüller and Greie, 2012). Furthermore, haloarchaea tend to possess multiple copies of the genome per cell, a common desiccation resistance tactic as it provides a template for DNA repair (Soppa, 2013). While there is circumstantial evidence that halophiles are desiccation resistant, it has yet to be adequately proven.

It seems unlikely that, in the natural environment on either Earth or Mars, a halophile would ever be exposed to truly desiccating conditions. Evaporation of a halophilic habitat would cause cells to become entombed within salt crystals, as in the above studies. Alternatively, in a natural environment, conditions within the surrounding brine would become too inhospitable to life before the water completely evaporated (McGenity, 2017).

1.4 - Halophiles and martian salts

1.4.1 - Potential entombment on Mars

Halophiles are often used as analogues for potential martian life (Payler et al., 2016, Fendrihan et al., 2009a, Orwig, 2014, Barbieri and Stivaletta, 2011, Fernández-Remolar et al., 2013, Srivastava, 2014, Rolfe et al., 2017, Matsubara et al., 2017). They have been shown, as described above, to be resistance to a wide variety of environmental stresses, which are associated with the martian surface. More crucially, any potential martian

water, either in the present day in the near subsurface or in the distant past as the temperatures and air pressures lowered (see Section 1.2.2), would require a high salt content to remain liquid (Catling, 2014, Massé et al., 2016, Stillman and Grimm, 2018). Interest in terrestrial halophiles as analogues for potential martian life is also likely to increase, given the recent suggestion of a large salt-lake under the martian South Polar glaciers (Orosei et al., 2018 and Section 1.2.1d).

The ability of halophiles to become entombed in salt crystals is of special interest to martian astrobiology for a variety of reasons; it has already been mentioned (Section 1.2.1c) that entombment could provide protection from today's martian radiation environment (Leuko et al., 2015, Fendrihan et al., 2009a, Fernández-Remolar et al., 2013). Entombment is also of relevance because it has been suggested that in the past, if life ever existed on Mars, it might have been geographically isolated and limited to small habitable regions (Westall et al., 2015). If life did ever become established on the martian surface, the changing environmental conditions (see Section 1.2.2) would have meant that surface habitable regions would become increasingly short lived and too geographically dispersed for life to easily travel between them (Cockell et al., 2012); life may not have been able to establish a firm foothold on the surface (Westall et al., 2015). Entombed halophiles blown on the wind, however, have been shown to be able to travel large distances between terrestrial environments habitable to them, as outlined above (McGenity et al., 2000).

Evidence of ancient martian life could be potentially entombed and preserved within martian salt crystals. The Southern Highland chloride deposits (see Section 1.2.2b) are of particular interest in this regard, because it is believed that their formation occurred at the tail end of the presence of large-scale bodies of water on the martian surface

(Osterloo and Hynek, 2015). Once these salts formed, water became considerably more short-lived and rarer. If the lakes that formed these deposits contained life, then these deposits might possess the youngest remaining evidence of past life on Mars (Srivastava, 2014).

The time since these deposits formed (3.65 Ga, Osterloo and Hynek, 2015) is orders of magnitude longer than even the most radical of claims of long-term survival of entombed halophiles (250 Ma, Satterfield et al., 2005). Even if organisms themselves could not survive these timescales, fluid inclusions could be targeted to look for ancient biomolecules. Even compared to the terrestrial environment, biomolecules (including normally short-lived ones such as DNA, Fernández-Remolar et al., 2013) are relatively stable within halite due to the fact that they are airtight, geologically stable, anaerobic and have a high ionic strength and low water activity (Parnell et al., 2007, Grant et al., 1998a).

In the martian radiation environment, where most organic molecules have a half-life that can be measured in months (Poch et al., 2014), the radiation shielding effects of halite would be highly advantageous for the long term preservation of biomolecules (Fernández-Remolar et al., 2013, Parnell et al., 2007). The pigments possessed by halophilic archaea (see Section 1.3.5a) are often proposed as potential biomarkers for detecting evidence of ancient martian life since they can persist in the geological record for millions of years (Parnell et al., 2007), are very clearly of biological origin (Parnell et al., 2007) and give a very distinctive signature under a Raman spectrometer, such as the one that will be included on the ExoMars 2020 rover (Fendrihan et al., 2009b).

While it cannot be definitively stated that evidence of ancient life could survive preservation within martian salt deposits, if biomarkers are preserved anywhere, then salt deposits are one of the better places to look.

1.4.2 - Halophiles and different salt compositions

Martian salt deposits are proposed as locations to look for evidence of ancient martian life (Payler et al., 2016, Tosca et al., 2008, Fendrihan et al., 2009b, Fendrihan et al., 2009a, Orwig, 2014, Barbieri and Stivaletta, 2011, Fernández-Remolar et al., 2013).

There is evidence to suggest that the Southern Highland chlorides might be NaCl (Osterloo et al., 2010), but two factors cast doubt on this: Firstly, all attempts to identify the spectra of martian salt deposits are based on library data from terrestrial deposits. This library data is overwhelmingly skewed in composition towards NaCl-rich deposits and ones formed under very different terrestrial temperature regimes to those likely on Mars (Hanley et al., 2010). Secondly the interpretation of spectra suggests that they are so NaCl-rich (Osterloo et al., 2010) that their purity is far in excess of any terrestrial deposit (Osterloo et al., 2010). This contradicts evidence that (as outlined in Section 1.2.1d) martian brines themselves are not NaCl-rich but instead rich in Mg, sulfates and perchlorates (Tosca et al., 2011).

There is evidence to suggest that extreme obligate halophiles cannot tolerate low water potentials induced by compounds other than NaCl (Grant, 2004); growth of obligate halophiles in brines made by other salts of comparable salinity and water activity is often heavily inhibited (Fox-Powell et al., 2016, Brown and Gibbons, 1955, Mullakhanbhai and Larsen, 1975, Oren and Bekhor, 1989). Hence, based on the likely composition of the salts, potential martian brines could possess a salinity and water

potential suitable for halophilic growth and still not be habitable to halophiles (Fox-Powell et al., 2016).

A greater understanding is needed of the way that salts of different compositions effect cells of both halophiles and non-halophiles, when compared to the effects induced by NaCl. The primary aim of this Thesis, therefore, is to investigate the tolerance of halophiles to a variety of different salts, including Mars relevant ones, in order to determine whether halophiles are capable of withstanding conditions similar to the ones found on Mars.

a) Effect of salt composition on halophiles

The extremely halophilic archaea use high internal K^+ concentrations in order to equalise water potential on either side of their membranes (Wright, 2006). This would imply that they should be able to withstand high dissolved KCl concentrations, since this demonstrates tolerance to K^+ ions and Cl^- ions, present in high concentrations in the vicinity of the cell membrane (though on different sides) This does not, however, appear to be the case; alteration of the NaCl: KCl ratios in liquid culture can have a significant negative impact on their growth (Brown and Gibbons, 1955). That said, there is some positive effects, since supplementation of media with high concentrations of KCl will allow growth of obligate halophiles at lower concentrations of NaCl than they could otherwise tolerate (Brown and Gibbons, 1955). Similar results have been observed independently with $MgCl_2$ (Mullakhanbhai and Larsen, 1975) and NaBr (Oren and Bekhor, 1989), suggesting that this effect is linked not just to cation changes.

Moderate halophiles have also shown different responses to identical water potentials induced by different salts. NaCl and $MgSO_4$ have significantly different effects on the

metabolome (the total number of metabolites produced by an organism) of moderately halophilic bacteria. While in both cases the production of osmoprotectants is upregulated, in $MgSO_4$ brine there is a significant increase in carbohydrate metabolism that is not present during growth in NaCl brine (Schwendner et al., 2018). There was also a significant difference in the amino acid metabolism employed between the two salts (Schwendner et al., 2018). The mechanisms and reasons for these differences are unclear, but indicate that while both salts induce osmotic pressure, they also induce different (but as yet unknown) stresses (Schwendner et al., 2018).

b) Potential mechanisms behind different responses to different salts

There are a number of different chemical factors that can vary between salt solutions of the same salinity. Some of these factors are interlinked, whereas others are independent of each other. Many of these factors, while identified, have yet to be fully understood:

Water activity

Bivalent salts (e.g. NaCl, KCl, NaBr) exert less of an effect on water activity than divalent salts (e.g. $MgCl_2$, $CaCl_2$.), due to the amount of ions in the solution (Hallsworth et al., 2007a). Furthermore, differences in the ion size and electron affinity also mean that ions from the same group in the periodic table, such as Na and K, can have different effects on the water potential (Williams, 1970).

Chaotropicity and kosmotropicity

Another possible explanation is chaotropicity. Although not well understood (Fox-Powell et al., 2016), in the simplest terms, it is known that some substances (such as NaBr, $MgCl_2$ and $CaCl_2$, Cray et al., 2013), termed 'chaotropes', increase the solubility

and stability of hydrophobic biomolecules when co-dissolved in solution. In contrast, other substances, termed kosmotropes, such as NaCl and KCl (Cray et al., 2013) reduce their solubility and stability (Ball and Hallsworth, 2015).

This alteration of the stability of biomolecules by salts can have a profound effect on biological systems, in particular on membranes and proteins. This can be demonstrated *via* agar gels, where chaotropes decrease the gel-point temperature while kosmotropes increase it (Cray et al., 2013). There is also evidence to suggest that, to some extent, kosmotropic effects can be counterbalanced by addition of chaotropic agents, but these effects do not seem to directly cancel each other out on a one-to-one basis (Oren, 2013).

The total impact of chaotropicity within a brine is likely to have a major impact upon its habitability. While it is often stated that, on Earth, wherever water is detected there is life, evidence for life in hypersaline $MgCl_2$ rich deep-sea brines is contradictory at best, despite the billions of years of selection pressure for organisms to adapt to a large, but gradual Mg gradient. This is believed to be a result of the high chaotropicity of $MgCl_2$ (Figure 1.15 and Hallsworth et al., 2017). Terrestrial brines typically become highly chaotropic following precipitation of halite. It is speculated that avoidance of these chaotropic "bitterns" is one of the reason why halophiles preferentially entomb themselves within the halite as it forms (McGenity, 2017).

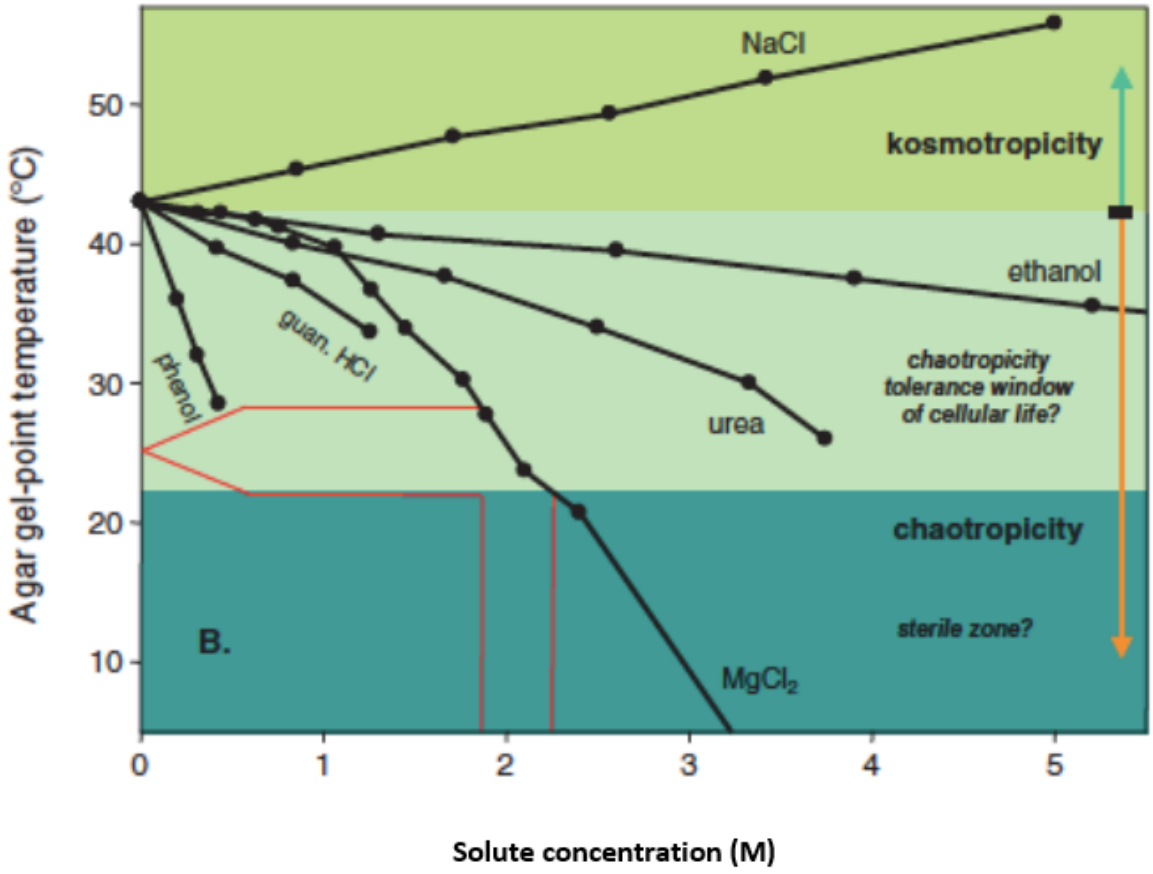

Figure 1.15 - Effect on gel-point temperature (as a proxy for chaotropicity and kosmotripicity) of increasing concentrations of various substances. The middle and top bands represent ranges at which life has been observed to undergo metabolic activity whereas metabolic activity has never been observed in the bottom band. Adapted from Hallsworth et al. (2007).

Chaotropicity seems to be significantly more harmful to microorganisms than kosmotripicity, but the reason for this is unknown (Oren, 2013). The effects of chaotropicity and kosmotropicity are not always detrimental to life. It has been speculated that the effects these have on solubility, if balanced suitably with other environmental extremes, could potentially allow microorganisms to grow in higher or lower temperature environments than they could not otherwise survive (Stevenson et al., 2015a).

Ionic strength and charge

Variations in ionic strength and ionic charge between different salts are also likely to have different impacts upon microbes. Ionic charge and ionic strength are not the same, because different ions can carry different charge. For example, a solution of $MgSO_4$ ($Mg^{2+} + SO_4^{2-}$) with the same ionic strength as a solution of NaCl ($Na^+ + Cl^-$) will have double the charge.

Monovalent salts are known to induce changes in the stability of dissolved proteins in accordance with the Hofmeister series (Dominy et al., 2002). Halophiles, in particular, are known to be sensitive to variations in the charge of their surroundings, because the negative charges accumulated by their proteins and DNA in order to remain stable in high K^+ concentrations can repel each other if the environmental charge changes too much (Elcock and McCammon, 1998).

Despite the fact that previous studies of martian analogue brines indicate that the total concentration of ions, and the charge they carry, may cause separate effects on habitability (Clark and Van Hart, 1981), very little research has yet to be carried out in disentangling these effects, especially in the context of martian rather than terrestrial brines (Fox-Powell et al., 2016).

c) Relevance to this thesis

If martian salts are not NaCl, then it becomes vitally important to investigate the ability of halophiles to survive in different salts. Halophiles clearly possess tolerance to the above factors as they are all present, to some extent, within terrestrial NaCl-rich brines. However, the ability of halophiles to tolerate these factors independent of NaCl concentration is poorly understood. In this Thesis, halophilic tolerance to a variety of

different salts, both in brines and entombed within crystals, are investigated in order to determine whether halophiles are indeed of value to martian astrobiology.

1.5 - Boulby Mine

In order to investigate the tolerance of halophiles to salts other than NaCl, the deposits from Boulby Mine have been utilised. Boulby Mine cuts through 250 million year old Zechstein evaporite deposits, including halite (NaCl), sylvite (KCl within 'potash') and anhydrite ($CaSO_4$) (Woods, 1979).

Microbial research of the mine has, in recent years, tended to focus on the community of NaCl-rich brines formed from dissolution of the evaporites (Fox-Powell et al., 2016, Cockell et al., 2017, Cockell et al., 2018), but past research has demonstrated the presence of culturable halophilic microbes within both the halite and the sylvite-rich deposits (Norton et al., 1993). Prior to this project, however, no work had been undertaken to investigate community differences between the salts. The Boulby Potash-Boulby Halite interface, in particular, provides an opportunity to study a naturally occurring gradient in salt composition, and the microbial communities entombed within.

1.5.1 - The deposits at Boulby

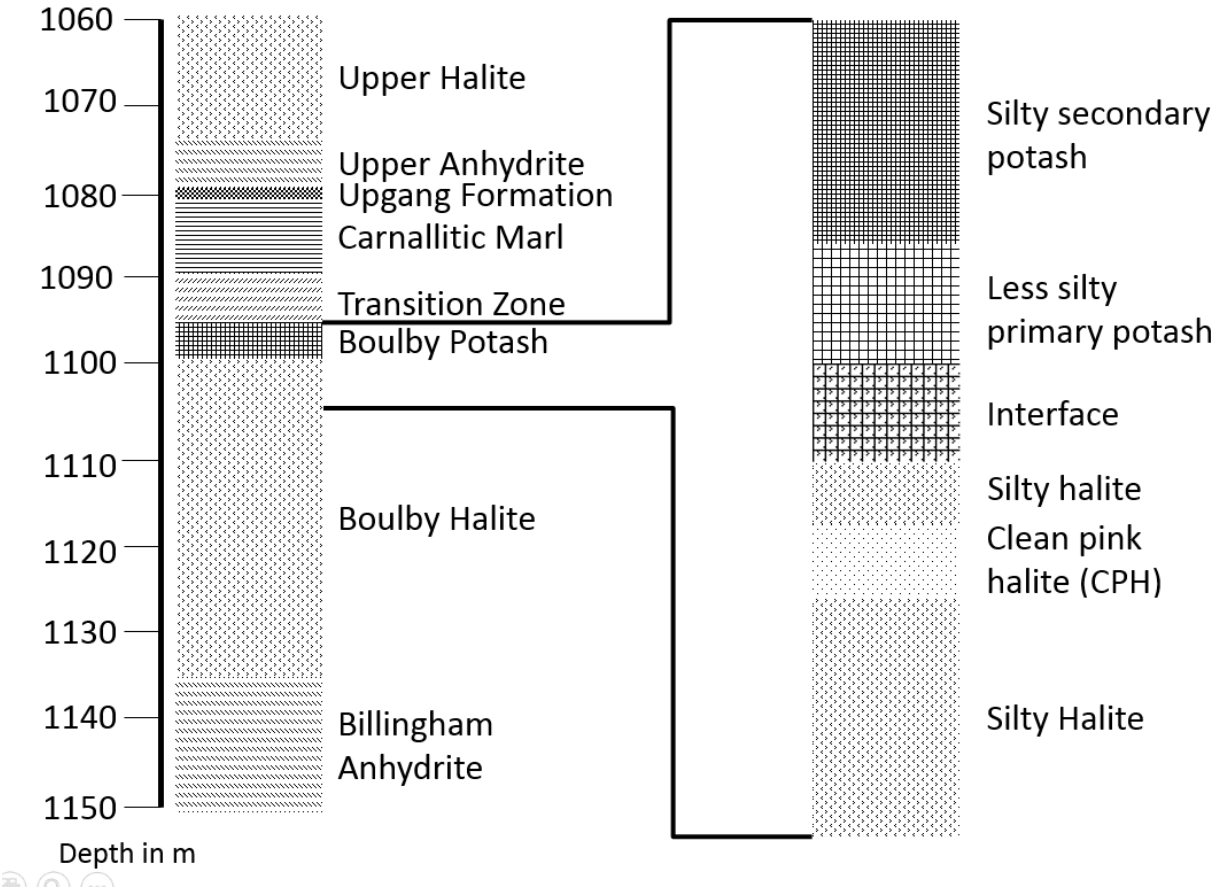

Figure 1.16 - The stratigraphy of Boulby Mine, based on data from Woods, (1979). Cutaway shows the areas of the mine being focused on for this project as described by Thomas Edwards, Senior Exploration Geologist of Boulby Mine

Boulby Mine is a commercial site, with the Boulby Potash its primary commodity (Edwards, 2015). Although "potash" is often used to describe various deposits containing potassium, in this thesis "potash" is used to refer to rock samples that contain both NaCl and KCl. "Sylvite" will be used to specify KCl crystals within potash samples, but "halite" will be used to refer to both the beds in the mine of predominantly NaCl composition (e.g. Boulby Halite) and individual crystals of NaCl within other beds.

The Boulby Potash is categorised according to its commercial viability, which is determined by its composition: the "primary potash" (KCl and NaCl in roughly 50:50 proportions, Woods, 1979) is the most commercially viable, with "secondary potash"

(potash with silt) less so (Hebblewhite, 1977). Typically, the secondary potash overlays the primary potash (Figure 1.16).

To reach the Boulby Potash beds requires excavation through the Boulby Halite below it, presenting an opportunity to sample both of these beds (Woods, 1979). The interface between the two beds varies from a sharp contact at some sites to a gradual merging of the beds over a height of one meter (Edwards, 2015).

The Boulby Halite itself has commercial value and is predominantly NaCl mixed with silt. As with the Boulby Potash, the Boulby Halite is split into two categories for commercial purposes. Grey halite is referred to as "silty halite" (Edwards, 2015), although Woods (1979) identifies this as shale. Pink coloured halite is referred to as "clean pink halite" or "CPH" (Woods, 1979, Edwards, 2015) and represents the purest halite in the mine. As a general rule, most of the halite is silty with occasional regions of CPH throughout it. A narrow band of CPH is also found running through the Boulby Halite below the interface between this bed and the Boulby Potash throughout much of the mine, although the depth of this band varies (Woods, 1979).

The beds of interest are both underlain and overlain by beds of anhydrite (Figure 1.16). The Boulby Halite lies directly above the Billingham Anhydrite, but the Upper Anhydrite is separated from the Boulby Potash *via* the shale-rich Upgang Formation and the Carnallitic Marl (a salt-rich clay, not a marl, Woods, 1979). These beds were not sampled for this study.

1.5.2 - Viability of Boulby Mine as a sampling site

The geology of Boulby Mine represents subsurface chloride deposits, however there have not yet been any subsurface chlorides yet detected on Mars because of lack of

access to the subsurface. The existence of martian chloride deposits on the surface suggests subsurface deposits may exist (Payler et al., 2016), but nothing is known about their composition or distribution. For this reason, there are some limitations in comparing between life within Boulby Mine's deposits and potential life on Mars.

No terrestrial surface deposit, however, can truly represent a martian surface deposit because of the existence of Earth's hydrological cycle. While surface salt deposits exist on Earth in areas where rain is rare, it does still occur (Schulze-Makuch et al., 2018, Jordan et al., 2017). This induces significant aqueous alteration to the top layers of the deposit, as well as delivering new microbes. On Mars, the surface deposits are unlikely to have undergone much, if any, aqueous alteration from surface processes for millions of years (Parnell et al., 2007). The most recent evidence of aqueous alteration on Mars is found in the Stimson Formation, which has a minimum age of 2,000 Ma (Frydenvang et al., 2017). Furthermore, the large martian chloride deposits formed as a result of the cessation of wide-spread surface water (Osterloo and Hynek, 2015). Subsurface terrestrial deposits are therefore more likely to resemble the martian surface deposits, than surface terrestrial deposits and so Boulby Mine provides a viable comparator.

The Boulby deposits do still differ significantly from those on the martian surface. For example, they are also exposed to considerably higher oxygen levels than on Mars. Furthermore, Boulby is a working mine, which means that the deposits are constantly exposed to contamination. This Thesis will attempt to mitigate these factors by means of acid-bleach sterilising the crystals in order to try and investigate only those microbes sealed within the crystals and not exposed to the terrestrial environment (Chapter 2). Perhaps of greater concern is the fact that, while 250 Ma old, the deposits at Boulby Mine are still significantly younger (Woods, 1979) than any that could be expected to

exist on Mars, given how long ago the last martian large bodies of water evaporated (Osterloo and Hynek, 2015). Cells and biomarkers entombed within crystals in Boulby Mine deposits would be younger and entombed for much shorter timescales than any that might exist on Mars today.

Despite these drawbacks, the processes being examined, namely impact of salt concentration on the entombed community, should be comparable regardless of whether the deposit lies on the surface or in the subsurface and is valid regardless of the differences in the age of the deposits, provided these limitations are considered in any interpretation.

1.6 - Outline of this thesis

The overarching aim of this thesis is to investigate entombment and growth of microorganisms in salts other than NaCl, including magnesium salts and sulfates, both of which are abundant on the martian surface (Section 1.2.1d). To do so, this Thesis will address the following objectives:

1. To investigate the effect of variation in Boulby evaporite composition on entombed microbial diversity.
2. To isolate and identify microorganisms from the compositionally-varied evaporite deposits found in Boulby Mine.
3. To characterise the novel microorganisms (isolated in objective 2) with particular focus on their tolerance to salts, both NaCl and others.
4. To investigate the ability of one of these isolates to survive entombment in brines containing high concentrations of non-NaCl salts

5. To investigate whether the composition of the salt crystals effects the survival of the entombed isolates under UV.

These objectives are addressed as follows:

Chapter 2, describes the collection and characterisation of evaporite deposits from Boulby Mine.

Chapter 3 presents a culture-independent study investigating the effect of the composition of the evaporate deposits on the microbial community structure.

Chapter 4 outlines the growth and isolation of microorganisms from the Boulby samples. They are characterised based upon the carbon sources they can utilise, the agars they can grow on, their morphology, halotolerance, and their ability to use salts other than NaCl to make up their minimum salt requirements.

Chapter 5 describes the entombment of one of these isolates, *Halobacterium noricense* FEM1, within laboratory-grown crystals of different salt compositions and the results of experiments that subject these crystals containing cells to Mars-relevant UV conditions.

The Thesis concludes (Chapter 6) with a summary of the key results and suggestions for how this study could be extended and used to inform future martian astrobiological studies, including life detection missions.

Chapter 2: Characterisation of Boulby Mine's evaporite deposits

2.1 - Introduction

The aims of this chapter are as follows:

- To describe the protocols used to obtain, process and store samples from Boulby Mine, North Yorkshire, UK
- To determine those samples' mineralogy and geochemistry, in order for this to inform the planning of, and interpretation of results from, microbiological experiments in Chapters 3 and 4.

A previous study (Norton, et al., 1993) demonstrated the presence of microorganisms within the evaporite deposits of Boulby Mine, UK (see Section 1.5). Using a combination of culturing and lipid analysis, Norton et al., (1993) isolated and identified halophilic archaea (but not bacteria) from both the Boulby Halite and Boulby Potash deposits. Norton's study, however, did not investigate whether there was any variation in community diversity or community composition between these deposits. Indeed, there has generally been an absence of research into whether evaporite deposits of different chemical compositions can support different microbial communities. The work that has been carried out has focused, not on ancient evaporitic deposits such as those in Boulby Mine, but precipitates formed in modern commercial salterns (e.g. Oren, 2005). The details of these studies will be outlined in Chapter 3. There have also not been any studies directly comparing the community composition of evaporites of different chemical compositions, independent of environmental factors, such as changing salinity and chaotropicity, within the brine that formed them. There is, however, abundant evidence that demonstrates that, in non-evaporite geological settings, the chemical

composition of different lithologies can have a significant impact on community structure (Uroz et al., 2009, Skidmore et al., 2005, Reith et al., 2015, Nyyssönen et al., 2014); Na concentration, for example, has been shown to significantly impact the community composition of granite rocks (Gleeson et al., 2006).

As demonstrated in Section 1.5.2, Boulby Mine presents a unique opportunity to investigate the effect of the geochemical composition of salts on microorganisms. The geological sequence exposed in Boulby Mine consists of the Boulby Halite (NaCl) overlain directly by the Boulby Potash (NaCl and KCl in roughly equal concentration, Woods, 1979). This enables a comparison between lithologies (and microbial communities) that have experienced similar geological histories and environmental conditions within the mine (e.g., temperature, humidity and exposure to contamination), but vary only in their cationic composition. This is in contrast to prior papers looking at salts within salterns (Oren, 2005, Javor, 2012, Baati et al., 2011) where these factors have not been kept consistent.

Microorganisms detected within these deposits are expected to either inhabit the surface of crystals (in deliquesced micro-brines, as observed in the Atacama desert, Davila et al., 2013a, Stivaletta et al., 2012) or be entombed within fluid inclusions (Lowenstein et al., 2011, Schubert et al., 2009, McGenity et al., 2000, Gramain et al., 2011). Entombed microorganisms represent communities that have been preserved for significant periods of time, either from the time the salt was precipitated, or from when an influx occurred at a later date. For the purposes of this study, it is assumed that any microorganisms that are entombed predate the excavation of the mine. Those not entombed represent younger communities that have pervaded the beds during exposure to the active mine or that have developed because of secondary alteration of

the lithological units. This assumption has helped to direct the methodology used to prepare and analyse the samples taken.

To allow any relationship between salt composition and microbiology to be determined, samples needed to be collected from Boulby Mine and characterised for their microbiology (outlined in Chapter 3), mineralogy and geochemistry. Understanding the mineralogy and geochemistry is important for two reasons. Firstly, it is important to confirm that the samples are of the lithology expected when sampled from the mine; the sampling itself was based upon characterisation conducted by prior studies (Payler et al., 2016, Woods, 1979, Parnell and Blamey, 2017) and the experience of the mine staff who assisted in the sample collection (Edwards, 2015). Secondly, geochemical and mineralogical characterisation of the samples would allow precise quantification of their composition. This, in turn, would allow better comparisons with microbiological data both within each lithology and throughout the stratigraphic column.

This first data chapter, therefore, describes the excavation of samples from Boulby Mine, and the geochemical and mineralogical analyses undertaken to characterise them. This is then followed, in the next chapter, by a thorough investigation into the microbial community within the samples. Together, these Chapters will shed light on the question of whether martian deposits of compositions other than NaCl would be able to entomb a community of ancient microorganisms.

2.2 - Materials and methods

The following sections describe the methods used to obtain and characterise the geological and biological samples needed to further the aims of this Chapter.

2.2.1 - Sample collection and processing

a) Boulby Mine

Boulby Mine in Saltburn, Cleveland, Yorkshire (54°33'19.1"N, 0°49'20.4"W) is run by Cleveland Potash Limited: a subsidiary of Israel Chemicals Ltd (ICL). The mine is 1.4 km deep and has permission to excavate an area of 820 km^2 (ICL-UK, 2017). In order to access the deposits, a 1,000 km network of underground tunnels has been built (Figure 2.1), although only some of these tunnels are currently accessible (Edwards, 2015). To collect samples for this study, Boulby Mine was visited on two separate occasions (18th November 2014 and 27th October 2015) under the supervision of Thomas Edwards, the Senior Exploration Geologist. The details of both expeditions are provided below.

Despite some scientific endeavours, including astrobiological studies of the subsurface brines (Payler et al., 2017) and dark matter detection experiments (Scovell et al., 2018, Hart and Collaboration, 2002, Smith et al., 1998), Boulby Mine is primarily a commercial operation and so, whilst scientific literature on the mine does exist (Woods, 1979, Norton et al., 1993, Talbot et al., 1982, Parnell and Blamey, 2017), information is often commercially sensitive and not publicly available. For this project, an overview of the mine, as well as descriptions of its environmental conditions, were made available by Thomas Edwards. An idealised stratigraphy of the lithologies excavated within the mine was shown in Figure 1.16 (Chapter 1).

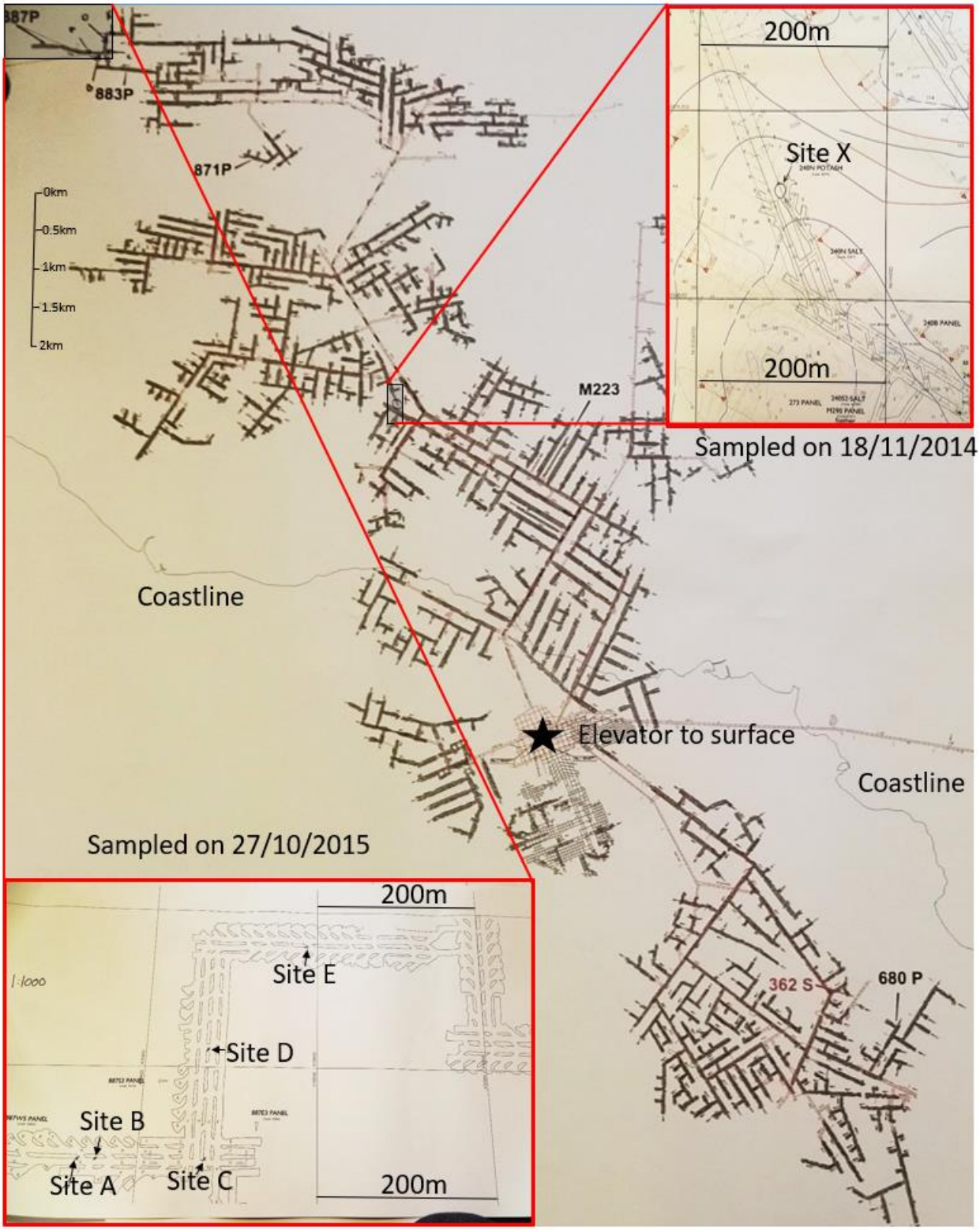

Figure 2.1 - Map of the roadways of Boulby Mine as of November 2015. Cutaways show the locations of the five sampling sites investigated in this project, as well as sixth site (Site C) that was sampled but not used in this project.

b) Sampling procedure

On both expeditions, samples were excavated from the walls of the mine shaft using a chisel and a geological hammer. They were handled using nitrile gloves (Kimtech, Science) that had been sterilised with isopropyl alcohol wipes (Azowipe), then transferred to sterile sample bags (Whirlpak, Fischer Scientific).

The samples were kept at ambient (mine) temperature (38 °C) during field work and, within 24 hours, transported to the Open University laboratories within a thermally insulated container. The samples were kept at the laboratory's ambient temperature, 22 ±2 °C, until further analysis was undertaken.

c) Initial sampling expedition

An initial sampling expedition was carried out on 18th November 2014. This was in the early stages of this project and its goal was to obtain samples for use in pilot experiments that would optimise techniques. As a result, the samples obtained on this occasion were used purely for biological experiments and were not geochemically characterised. Most experiments in which these samples were used were later repeated using samples obtained on the second sampling expedition (described below, Section 2.2.1b). In general, it is the data obtained from this second expedition that is presented in this thesis, but cultures of microorganisms inoculated by samples from this initial sampling expedition, were retained for investigation in Chapter 4.

Site X

The majority of samples obtained from the initial sampling expedition came from a single location within Boulby Mine, designated Site X (Figure 2.1). This site featured the

Boulby Halite and the Boulby Potash, with a well-defined interface region between them.

At Site X, five samples were obtained of the Boulby Potash and four of the Boulby Halite. In both instances, the samples were taken from a distance >1 m from the interface. Five samples from immediately either side of this interface were also collected. Site X featured veins of sylvite, high purity KCl (Woods, 1979, Edwards, 2015), running through the Boulby Potash bed. Three samples of this sylvite were obtained.

No record was made of whether the samples of the Boulby Potash obtained from Site X were of the primary or secondary type (See Section 1.5.1 and also below, 2.2.1d), but the Boulby Halite can be assumed to be of the "silty" variety (see Section 1.5.1 and also below, 2.2.1d) based upon its colouration.

Non-chloride samples

On this initial sampling expedition, four samples were also obtained of anhydrite ($CaSO_4$) and two of polyhalite ($K_2Ca_2Mg(SO_4)_4{\cdot}2(H_2O)$), as identified in the field by Thomas Edwards. These samples were obtained from a conveyor belt transferring product to the surface. As a result, their provenance is uncertain, but it is known that they are sourced from below Boulby Halite in the stratigraphic column (Edwards, 2015).

d) Second sampling expedition - Sites A-E

Following biological investigation into samples obtained on the initial expedition (included in Chapter 4), the decision was made to return to the mine to obtain samples of the Boulby Potash, the Boulby Halite and the interface region, from multiple sites to

enable comparisons and validations to be made. These would be subject to both microbial and geochemical characterisation and be better constrained in terms of their provenance within the mine and the stratigraphic column. For this reason, this second expedition put a greater emphasis on recording details at each sample site including the *in-situ* geology of the samples prior to excavation.

Sample sites for this second expedition were selected based on three criteria:

1) the presence of the Boulby Halite, the Boulby Potash and an interface region between them

2) the presence of both beds with sufficient vertical depth to enable samples to be taken through each stratigraphy

3) ease of accessibility within the working mine.

Thomas Edwards identified, in advance, a tunnel that would best suit the three criteria. This was a relatively new shaft, compared to that of Site X: the tunnel had taken 4.5 months to excavate, and this work had ceased 6 months prior to the field visit. This tunnel, therefore, had the least potential for surface contamination compared to other accessible shafts within the mine. The tunnel was located 4 km north of the British coastline, where the interface between the Boulby Halite and Boulby Potash was approximately 720 m below sea level (Edwards, 2015).

Sites A-E

On the sampling expedition, initially five sample sites were identified within this tunnel (A-E, Figure 2.2). On closer inspection, however, Site C did not excavate the Boulby

Halite and therefore, although samples were taken from Site C, only samples from Sites A, B, D and E were used in the analyses for this Thesis.

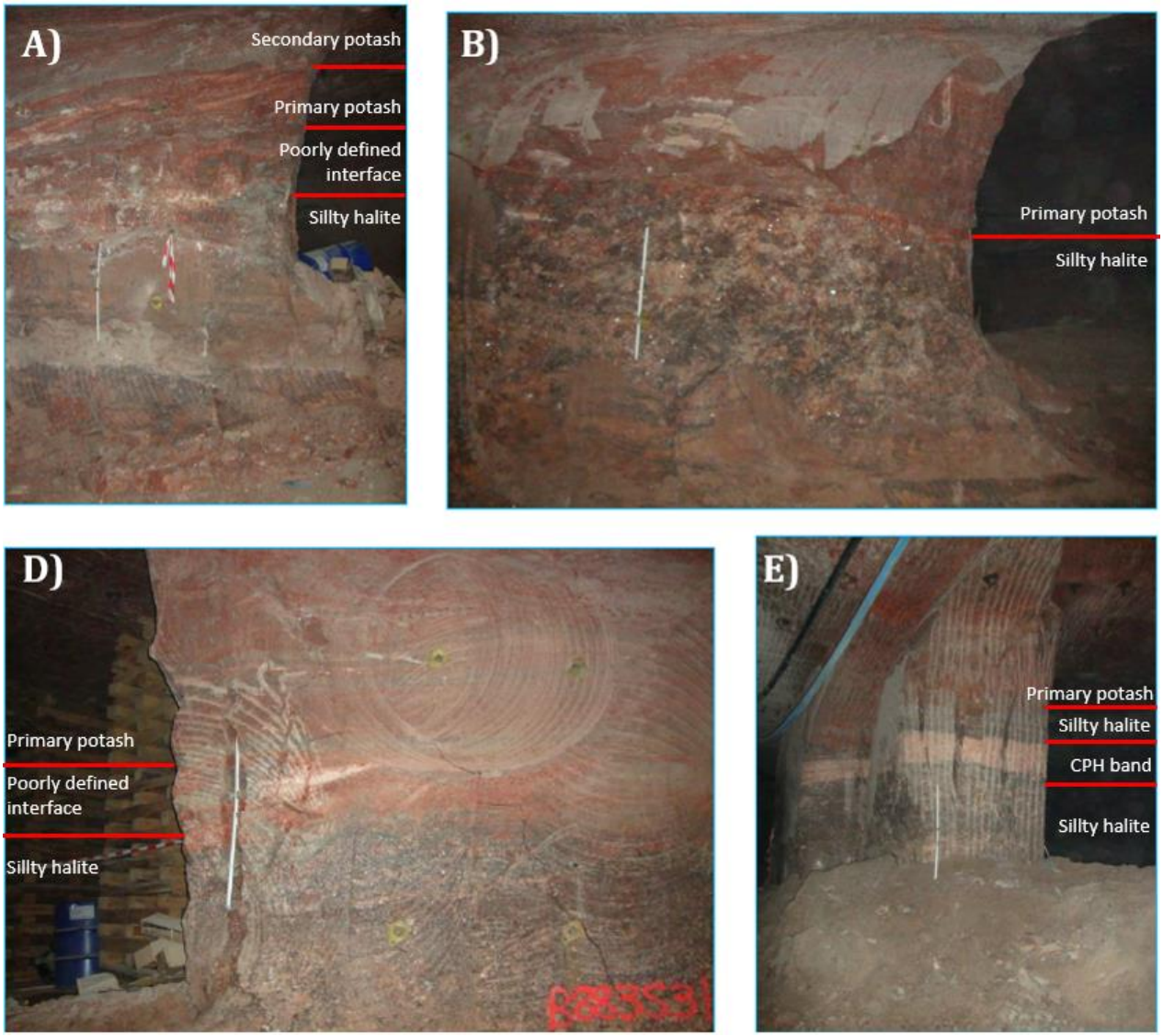

Figure 2.2 - Sampling Sites A, B, D & E showing the stratigraphy that was evident. There is no Site C. Each photo includes a meter ruler for scale

At Sites A, B, D & E, the floor was composed of Boulby Halite and it extended roughly halfway up the walls of the shafts. The Boulby Halite is between 35-40 m thick (Woods, 1979, Edwards, 2015), however the depth of each bed and the location of the potash-halite interface region relative to the shaft floor, varied between sample sites. This is a

result of the variable direction of the mine excavation. Figure 2.2 shows photographs of each sample site with the stratigraphy labelled.

At Sites A, B, D & E, the Boulby Halite was typically a dark grey colour (Figure 2.2), a result of high concentrations of "silt" (described as shale by Woods, 1979). At Site A, however, Clean Pink Halite (CPH), i.e., halite lacking in silt, was also observed, and a thin band of this was also seen at Site E, consistent with the description of Woods (1979).

Above the halite was the interface region, which varied between sites. While at Sites B and E, the interface was sharp and clearly visible to the naked eye (Figure 2.2) as it had been at Site X, the interface was less clear at sites A and D where the two beds appeared to merge. This 'transition zone' is comparable with that identified by Woods (1979).

Above the transition zone/interface was the Boulby Potash, which was between 8 and 10 m thick (Edwards, 2015), extending from the transition zone to the shaft roof. The Boulby Potash is classified according to its commercial viability: silt-poor primary potash is typically found lower down the stratigraphy, closer to the Boulby Halite, whereas silt-rich secondary potash is found higher up (Figure 2.2). At sites B, D & E, only primary potash was evident; however, at Site A, the tunnel's depth was such that the bottom of the secondary potash was accessible.

Samples

A total of 20 samples were obtained from the second sampling expedition (Table 2.1). At each site, one sample of the Boulby Halite and one sample of the Boulby Potash (selecting primary potash, where possible, to minimise excessive silt content) were taken from >1 m from the Boulby Potash-Boulby Halite boundary to avoid the interface/transition zone.

Table 2.1 - List of the samples obtained on the second sampling expedition, and the analysis they were subjected to

Sample location	Petrological analysis of thin sections	EMPA analysis	XRD Analysis	ICP-MS Analysis	TOC and LOI analysis	Community Analysis
Site A						
Secondary potash	✗	✗	✓	✓	✓	✓
Primary potash	✓	✓	✓	✓	✓	✓
Halite from within the Primary potash	✗	✗	✓	✓	✗	✗
Top of the interface	✗	✗	✓	✓	✓	✓
Bottom of the interface	✗	✗	✓	✓	✓	✓
Boulby Halite (silty halite)	✓	✗	✓	✓	✗	✗
Boulby Halite (CPH)	✓	✗	✓	✓	✓	✓
Site B						
Primary potash	✓	✗	✓	✓	✓	✓
Top of the interface	✗	✗	✓	✓	✓	✓
Bottom of the interface	✗	✗	✓	✓	✓	✓
Boulby Halite (silty Halite)	✓	✗	✓	✓	✗	✗
Site D						
Primary potash	✓	✗	✓	✓	✓	✓
Top of the interface	✗	✗	✓	✓	✓	✓
Bottom of the interface	✗	✗	✓	✓	✓	✓
Boulby Halite (silty Halite)	✓	✗	✓	✓	✓	✓
Site E						
Primary potash	✓	✓	✓	✓	✓	✓
Top of the interface	✗	✗	✓	✓	✓	✓
Bottom of the interface	✗	✗	✓	✓	✓	✓
Boulby Halite (silty Halite)	✓	✓	✓	✓	✗	✗
Boulby Halite (CPH)	✓	✗	✓	✓	✓	✓

Samples were also collected from within the interface regions. Where this was a gradual transition, samples were collected both from the top, where it was closer to the Boulby Potash, and the base, where it was closer to the Boulby Halite. Where the interface was more defined, samples were collected from immediately above and immediately below the sharp transition.

Samples of CPH and silty halite were also taken, where available. Furthermore, at Site A, a sample of the secondary potash and a sample of halite from within the primary potash were collected.

e) Sub-sampling

To undertake geochemical analyses alongside the biological, sub-samples were created of the samples from Sites A, B, D & E by splitting them using a rock chisel (Figure 2.3). Although there was no means of carrying this out under sterile conditions, the chisel was sterilised with ethanol before each use, to minimise the risk of cross-contamination.

Figure 2.3 - A selection of sub-samples stored prior to sterilisation

One sub-sample from each sample then underwent surface sterilisation, crushing and homogenisation for use in the microbiology, molecular biology and geochemical analyses described below. The remaining sub-samples were used to create thin sections that could be used to investigate the mineralogy further.

All samples and sub-samples were stored at room temperature within Whirlpak, Fischer Scientific sample bags until further analysis.

f) Sample sterilisation and homogenisation

The molecular and microbiological analyses of the samples was concerned primarily with the microbes entombed within the samples. As a result, whole samples from the first sampling expedition and the selected sub-samples from the second expedition underwent sterilisation to eliminate contamination caused by activity within the mine, for example: human and machine working, the constant airflow through the tunnels from the surface and any contamination that occurred during the sub-sampling process in the lab.

Sub-samples were surface sterilised according to the methodology of Sankaranarayanan et al. (2011), which involves washing the samples in acid and bleach in order to kill surface microbes and degrade DNA.

Solutions of 1M HCl (stock solution 36 %), 1M $NaCO_3$ (stock solution 15 %) and 1M NaClO were prepared by diluting or dissolving in autoclaved NaCl solutions (400 g l^{-1}, which is above the saturation limit of 360 g l^{-1}) thus ensuring the presence of undissolved NaCl in the bottle prior to mixing in the acid, bleach or NaClO. This ensured the final solution remained NaCl-saturated. The principle behind this sterilisation procedure was that the HCl and the NaClO killed the surface microorganisms as well as

those in any pores open to the environment, whilst the NaClO neutralised any traces of the acid and bleach left on the samples that could interfere with later analysis.

The solutions were prepared in saturated NaCl solution, rather than water, to limit the dissolution of the water-soluble samples. Undissolved NaCl was removed from the solutions prior to the sterilisation procedure by allowing the salt to settle at the bottom of the bottle and transferring the solution at the top to fresh sterile bottles.

The sub-samples were washed in 500 ml beakers, which contained 330 ml of the solutions (Figure 2.4). Owing to the potential for HCl and $NaCO_3$ to react to form mustard gas (Evans, 2005), the processes were carried out within a fume cupboard. Sub-samples were transferred between the solutions using a pair of tongs that were flame and ethanol sterilised prior to use.

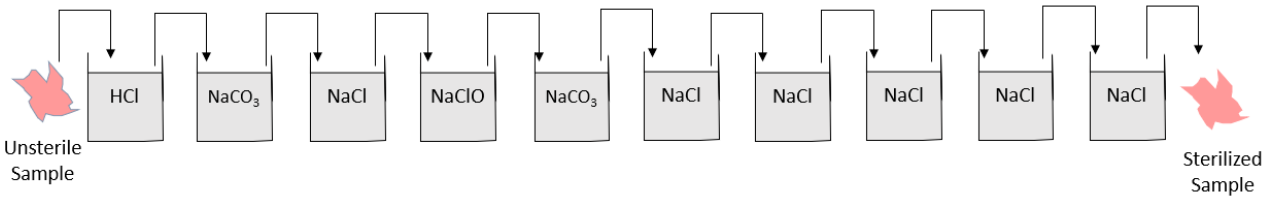

Figure 2.4 - Surface sterilization procedure based on the methodology of Sankaranarayanan et al. (2011)

Figure 2.4 illustrates the process used. The first step was to submerge samples in the HCl solution for 15 minutes, such that the entire volume of it was below the surface of the liquid. The samples were then transferred to the first beaker containing $NaCO_3$ solution (Figure 2.4) and likewise submerged for 15 minutes, in order to neutralise the acid. To remove any traces of the previous solutions, the samples were next washed in a beaker of saturated NaCl solution, again for 15 minutes.

Following acid sterilisation, the samples were bleach sterilized by submerging in the NaClO solution for 15 minutes, followed by neutralisation in fresh $NaCO_3$ solution for 15 minutes. As NaClO can degrade DNA (Sankaranarayanan et al., 2011), and DNA extraction was planned for these samples, any remaining traces of bleach were washed off *via* 15 minute submersions in 5 separate saturated NaCl solutions.

Following sterilisation, the samples were triple-bagged in transparent sterile sampling bags (Whirlpak, Fischer Scientific) and crushed gently between two planks of wood using a rock hammer to facilitate crushing. The end product had a grain size of approximately 1 cm diameter. These grains were mixed, by shaking the bags, to form homogenous samples. For all geochemical and molecular analyses, unless otherwise stated, 2 g of the homogenous mixes were used, with three replicates of each.

g) Thin section preparation

In order to examine the distribution of minerals and fluid inclusions within the samples by petrologic means (see below), thin sections were prepared of the Boulby Halite and primary potash by Michelle Higgins, in the Open University Thin Section laboratory.

Since halite and potash are fragile, water-soluble minerals, care had to be taken during thin section preparation to avoid the use of water, so sections were not polished. Their thickness was made to roughly 30 μm. Finished thin sections were mounted on glass slides using an epoxy resin but were not covered.

2.2.2 - Geological characterisation

Although samples were collected from defined beds, confirmation of their broad mineralogy and an investigation of their detailed chemistry was necessary. In the field

and in the laboratory, this was undertaken by initially examining the hand specimens. Subsequently, a more detailed characterisation was carried out using a variety of techniques.

a) Petrological examination

Thin sections were examined *via* petrologic microscopy. Low magnification photos of each thin section were taken with a Leica-Wild M28 petrological microscope, capable of magnification between ×0.63 and ×5**.** More detailed examination of areas within the thin section were made with a different petrological microscope, allowing magnification at ×5, ×10, ×40 and ×60. Both microscopes were capable of allowing observation under plane and cross-polarised light. Detailed notes and photographs were taken of each section.

b) Electron Microprobe Analysis (EMPA)

Sylvite (KCl) and halite (NaCl), the main components of Boulby Potash, are isomorphic and look similar under both plane and cross-polarised light (Deer et al., 1992) so are difficult to distinguish with a petrological microscope. A Cameca SX100 was used to carry out Electron Microprobe Analysis (EMPA) that could indicate the presence, and distribution, of sylvite and halite crystals within individual samples and provide quantitative information about the samples' compositions.

The thin sections were carbon coated (25 - 30 nm thick) and analysed under standard analytical conditions for this instrument: 20kV, 20 nA and a beam diameter of 10 μm. These conditions had previously been used to investigate halite and sylvite using a similar instrument (Altigani et al., 2016). The probe was set to measure signals from K, Fe, Mn, Si, Mg, Ca, Na, Al, Cl and S. The probe had been previously calibrated to

standards of haematite, bustamite, for-BM4, jad-BM4, sylv BM4 and barite. Between them, these standards contain all the element being investigated at a wide range of concentrations. Detection limits of the instrument are stated by the manufacturer to be in the order of 100 ppm, however, instrument drift means that in practice this varies by element and on a daily basis. Detection limits at the time of measurement, were calculated based on measurement of the standards and are described in Table 2.2.

Table 2.2 - Detection limits of each element in the EMPA

Element	Detection Limit (ppm)
Na	323
Al	176
Si	101
Mg	186
Fe	368
Mn	303
K	129
Ca	182
Cl	568
S	449

c) X Ray Diffraction (XRD)

To determine the precise mineralogy of each sample, they were also analysed *via* X-Ray Diffraction (XRD) at the Natural History Museum (NHM), London, using a Nonius PDS 120 powder diffraction system with an Inel curved, position sensitive detector as described previously (Schofield et al., 2002). Sterilised and homogenised samples were further crushed to a fine powder within an automated tungsten carbide mill for 30 seconds. Samples were then sent to Dr Paul Schofield (NHM) for preparation and analysis.

There, the samples were mixed with acetone to form a slurry and spread evenly upon a circular sapphire substrate. An X-ray tube operating at 45 kV and 32 mA and a

germanium 111 monochromator crystal was used to generate a monochromatic cobalt Kα1 X-ray beam with a height of 0.14 mm and a length of 5.00 mm. The samples were spun in the plane of the sample's surface for 60 minutes while measurements were made in reflection geometry. The sample surface was at an angle of 4 ° to the incident beam.

NIST silicon powder SRM640 and silver behenate were used as calibration standards. Phases were identified via comparison with the International Centre for Diffraction Data (ICDD) Powder Diffraction File (PDF) database and historical data from samples within the NHM mineral collection.

The detection limit of XRD for any given phase, in general, is commonly stated to be 2 % of a sample by volume (Bunaciu et al., 2015).

d) Inductively Coupled Plasma Mass Spectrometry (ICP-MS)

Elemental composition (n = 3) of the samples was measured using Inductively Coupled Plasma Mass Spectrometry (Agilent 7500s ICP-MS with New Wave 213 laser system). Samples were prepared and analysed by Dr Sam Hammond (Open University).

Sterilised, homogenised samples (2 g) were dissolved in 2 % nitric acid to a concentration of 0.005 % w/w. The low final concentration was used because of the potential for the high concentration of chloride ions to damage the instrument. The detection limits varied between elements, however, the standards had been created based on prior ICP-MS studies of halite composition (Titler and Curry, 2009), making the assumption that the highest K concentration in the potash would not exceed the Na in the halite. The list of ions the instrument was calibrated to detect is shown in Table 2.3, along with the detection limits within the 0.005 % solutions.

Table 2.3 - Detection limits of ions measured by the Agilent 7500s ICP-MS

Ion	Detection limit (ppm)
Na	3.21
K	2.02
Ca	0.14
Si	0.033
Mg	0.025
Fe	0.013
Al	0.013
Sr	0.0012
Ba	0.0007
Mn	0.0007

2.2.3 - Organics and volatiles

It was assumed that, because of the detection of microbes in prior studies (Norton et al., 1993), that there must be carbon within the samples. Carbon cannot be detected by ICP-MS since it is not easily ionised. XRD is also unlikely to detect carbon, aside from crystalline components.

Therefore, two methods were employed to measure the carbon content of the samples. The first was by measurement of Total Organic Carbon (TOC) and the second was by measuring Loss on Ignition (LOI). LOI and TOC are often correlated and used in conjunction to confirm findings in low carbon content studies (Labuza, 1980), such as this one.

a) Total Organic Carbon (TOC)

Samples were crushed to a fine powder using an agate pestle and mortar that had been washed with deionised water and dried in a laminar flow hood between each use. The samples (0.1 g) were added to ceramic "TOC boats" (miniature crucibles), which had been pre-weighed. An accurate weight at this stage could not be ascertained, because, once a sample was crushed the mass gradually increased over time as new crystal faces

absorbed more water from the atmosphere. To eliminate the water, the samples were heated for 12 hours at 105 ℃. Once heated, samples were transferred to a desiccator and allowed to cool to room temperature. Samples were briefly removed from the desiccator and the "dry-mass" of the samples were calculated.

Once cooled and weighed, the samples were covered with ceramic wool and transferred to a Shimadzu SSM-5000A- TOC machine. The chamber within the instrument was heated to 900 ℃ and the carbon within the samples combusted to form CO_2. The CO_2 released was measured using a Shimadzu TOC-V. A glucose and a Leco soil calibration standard containing 2.42 % carbon were both used to calibrate the instrument. The detection limit of the instrument was 0.01 %, with a margin of error of ±1 %. The instrument was operated by Timothy Barton (Open University).

b) Loss on Ignition (LOI)

It was anticipated that the carbon content of the samples would be low, potentially lower than the detection limits of the Shimadzu SSM-5000A instrument (0.01%), therefore, the LOI was also measured. While LOI provides the mass of all volatiles (not just organics), LOI and TOC are often strongly correlated (Labuza, 1980). The aim was to obtain LOI values and use them to extrapolate the TOC of those samples that were below the limit of detection of the Shimadzu TOC-V.

Owing to how low the carbon within the samples was expected to be, a sample concentration technique was developed for the LOI analyses. This method was based on the assumption that the majority of the volatiles present would be non-soluble. This assumption was supported by the ICP-MS and XRD data, which showed that the soluble components of the samples were dominated by Na, K and Cl (Sections 2.3.1c & d).

Samples were measured and dissolved in 45 ml ddH_2O within a 50 ml falcon tube. The exact mass varied between samples, but was roughly 10 g ± 0.2 g. The initial mass was chosen to keep the volume of sample well below potential saturation of the solution.

The samples were heated at 40 ℃ and observed regularly until the samples appeared to have completed dissolution. During this process, the lid of the falcon tube was sealed to prevent evaporation of water. The samples were centrifuged at 6,000 x *g* for 15 minutes to concentrate the insoluble components at the base of the tubes. The supernatant was then carefully removed using a pipette, ensuring that the insoluble components of the samples gathered at the bottom of the tube were not disturbed. These insoluble components were then resuspended in 5 ml of ddH_2O to form a slurry. This slurry was split roughly evenly between three crucibles (of known mass) using a pipette with the tip cut off to allow larger particles to be taken up.

The crucibles of slurry were then heated for 12 hours at 105 ℃ to remove the water. The dry-weight of the resulting grey-coloured salt crystals was calculated as for the TOC. By comparing the mass of the original sample, the mass of the water added to the sample and the mass of the sample after the water and soluble components had been removed, the concentration factor for each sample could be calculated. This was typically an order of magnitude, although it varied based upon the amount of non-soluble component left in the sample after evaporation. The exact mass of the samples and water added, and removed, was precisely measured throughout, which allowed a more accurate value for this concentration factor to be calculated for each sample.

Once the dry-weight of these crystals, with concentrated non-soluble components, were calculated, the samples were heated for a further 12 hours at 600 ℃ in order to combust the volatiles. The samples were then cooled to room temperature in the desiccators. The

samples' new mass was then measured and the change in mass calculated. This was then back-calculated to give values for the samples if they had not been concentrated.

c) Thermogravimetric Analysis (TGA)

During data analyses, the LOI data showed unexpected, large variance. In order to attempt to explain this, thermogravimetric analysis (TGA) was employed using a Netzsch Jupiter STA 449C Thermo-microbalance, operated by Pete Landsberg (Open University). This method was similar to LOI, in that it involved heating a sample from room temperature to 600 ℃. As it was heated, the temperatures were held stable for 1 hr at 105 ℃, 150 ℃ and 300 ℃, in order to monitor whether changes in mass would stabilise or continue to change with prolonged heating. The mass of the sample was measured throughout the heating process, allowing a more accurate determination of the volatiles that were being combusted at each temperature.

To prepare the samples for TGA analysis, they were powdered in a pestle and mortar. Samples that had been concentrated and samples that had not been concentrated (as in the LOI experiment, Section 2.2.3b) were investigated, in order to determine whether the concentration process was responsible for the variation seen in the LOI data.

The TGA profiles of chloride salts are not readily available within the scientific literature, and it was uncertain what effect, if any, the concentration technique would have. As a result, standards of 99.9% purity NaCl purchased from Sigma Aldrich were analysed in triplicate (again both concentrated and not concentrated), before analysis of the suite of Boulby samples.

2.2.4 - Fluid inclusions

Morphology and distribution of the fluid inclusions within the crystals was carried out by viewing the thin sections (see Section 2.2.2a) under plane polarised light using a standard petrological microscope.

The thin sections were observed at ×60 magnification (to get an overview of the samples and to identify areas with groups of fluid inclusions) and at ×5 magnification (to attempt to detect lone fluid inclusions not detectable at ×60 and investigate groups of inclusions further). Since lone fluid inclusions would not be visible at lower magnification, this potentially introduces a sampling bias; however, searches for lone inclusions at the high magnifications failed to detect any.

2.2.5 - Statistical analyses

Compositional data were analysed using the statistics software R (Team, 2013). Compositional data from samples of the same bed, but different sites were tested for variance using one-way Analysis of variance (ANOVA) tests (*n* was always > 3). For comparing between beds, Student's t-tests (for two beds) or two-way ANOVA tests (for more than two beds). ANOVA tests were carried out using the aov() function included in R (Team, 2013), whereas Student's t-tests were carried out using the appropriate function in Microsoft Excel. Where variation was detected, post-hoc Tukey HSD tests were carried out to determine whether specific samples differed from each other. This was carried out with the TukeyHD() function included in R (Team, 2013).

2.3 - Results

2.3.1 - Sample characterisation

Before the composition of the microbial community could be investigated, the geology of the samples was fully characterised. The methods that were used to characterise the samples included: visual investigation of hand specimens; petrographic analysis; XRD and ICP-MS (outlined in Section 2.2). The results from each of these methods are discussed below.

a) Hand specimens

Samples from Sites A-E

Visually, the Boulby Halite samples presented a spectrum between the silty halite (dark grey) and the CPH (pink) as displayed in Figure 2.5. Both CPH and silty halite were semi-opaque; crystals on the edges of the samples would allow light to pass through.

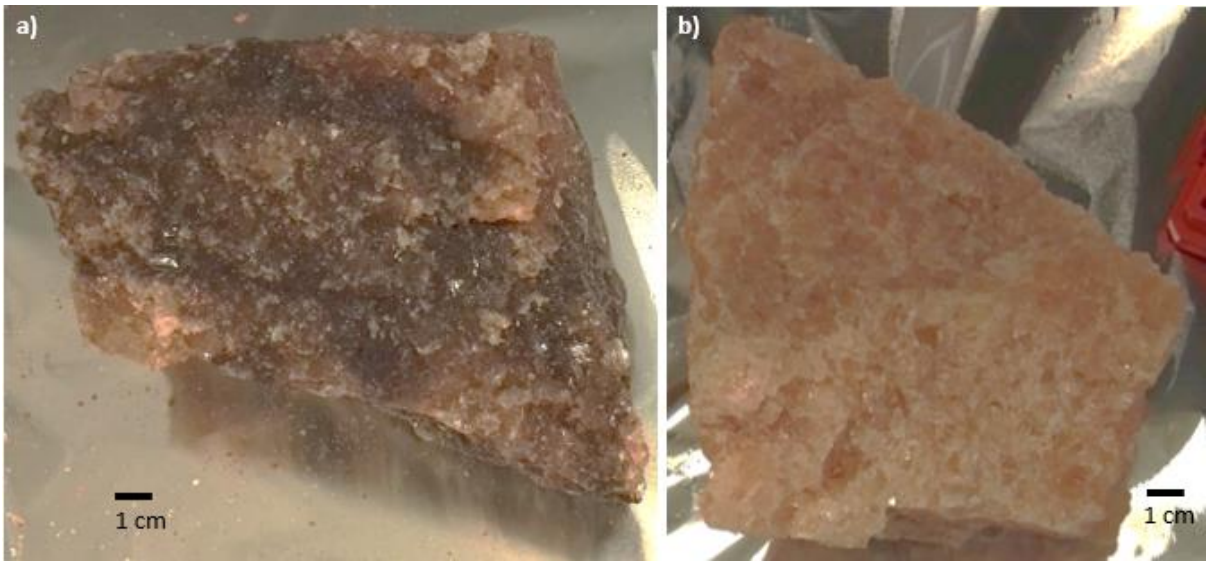

Figure 2.5 - Representative samples of a) the silty halite (from Site A) and b) CPH (from Site E). Both photos are at the same scale.

All four samples of primary potash exhibited red colouration and displayed grey deposits of silt that ran parallel to the bedding planes (Figure 2.6a). There was no observed difference in the distribution of the silt deposits between samples. Boulby Potash was more opaque than Boulby Halite; even at the edges of the sample, light could not pass through.

As expected, secondary potash (from Site A) contained a higher abundance of silt than samples of primary potash. This was expected, since the silt is the reason for the devaluing of the secondary potash from a commercial perspective.

Samples from the interface region varied in visual appearance depending on whether the interface had been clearly or poorly defined (transition zone). Poorly-defined interface (PDI) samples resembled a mixture of the two beds throughout, with the semi-opaqueness of the Boulby Halite, but the deep red colour of Boulby Potash (Figure 2.6b). The well-defined interface (WDI) samples displayed a clear visual contrast between the beds, with samples as described above (Figure 2.6c).

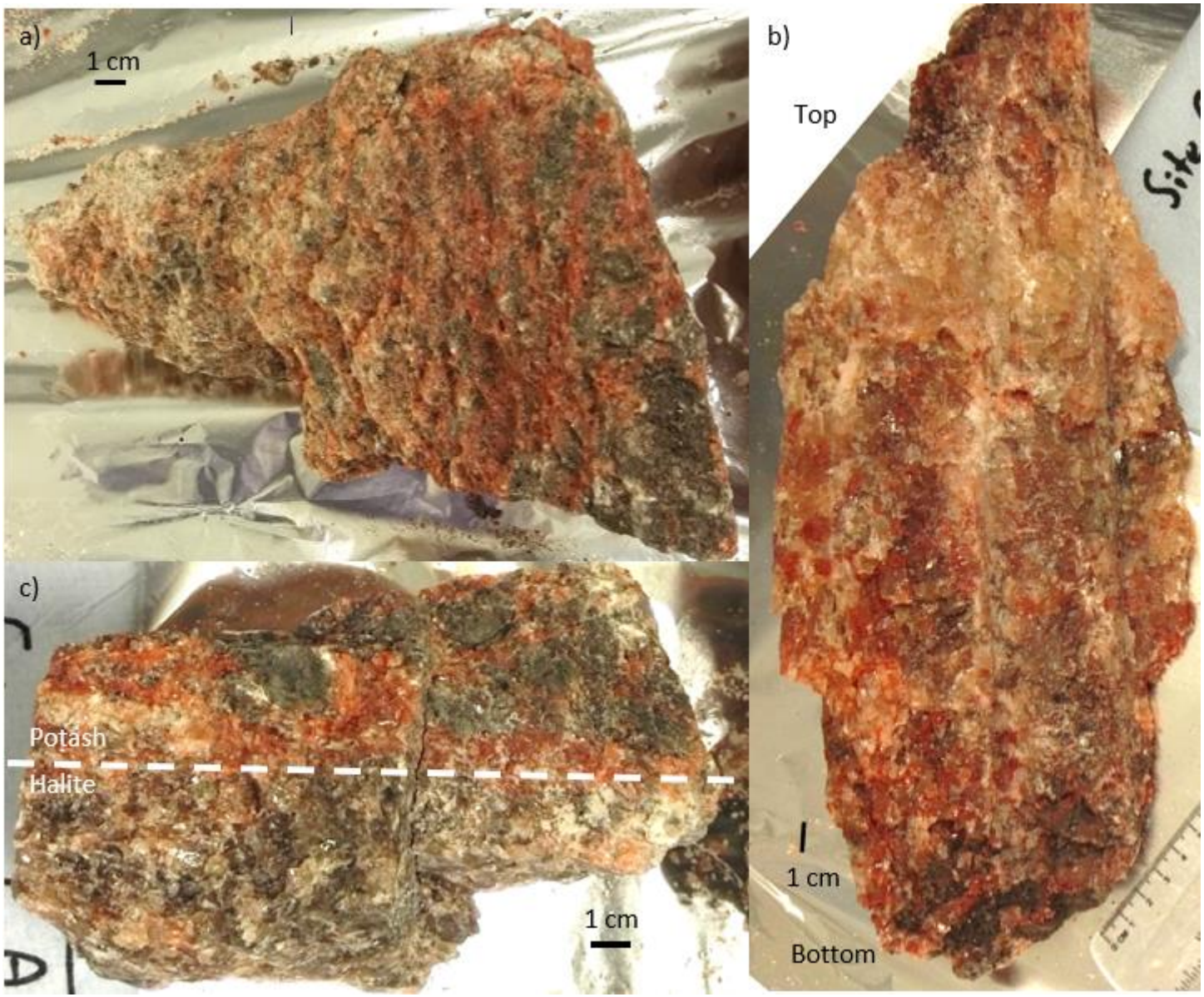

Figure 2.6 - Representative samples of a) primary potash (from Site E), b) poorly-defined interface (from Site A) and c) well-defined interface (from Site E) between Boulby Halite and primary potash

Samples from Site X/first expedition

Samples of three lithologies that did not undergo further geological characterisation were obtained on the first sampling expedition: sylvite, anhydrite and polyhalite. The sylvite samples possessed a crystalline structure similar to that of the Boulby Potash and Boulby Halite, but these crystals were opaque and coloured pure white (Figure 2.7). Both anhydrite and polyhalite appeared a uniform grey colour (Figure 2.7). It was observed that the polyhalite and anhydrite samples were considerably less friable than the samples of the chloride deposits when they were struck with the rock hammer for homogenisation (Section 2.2.1f).

Figure 2.7 - Representatives of the three types of sample that were not present at Sites A-E, a) sylvite, b) anhydrite, c) polyhalite. All images taken at the same scale

b) Mineralogical composition - petrography

Prior research (Woods, 1979) indicated that the Boulby Potash contained sylvite and halite, in comparison to the Boulby Halite, which was mostly halite. While it was known that the Boulby Potash would contain halite and sylvite, it was uncertain how homogenous the samples would be. This was investigated by examining the mineralogy of the samples using petrological microscopy and EMPA.

Halite

Halite crystals, displaying the characteristic distinctive cubic habit under plane-polarised light (as evidenced by the distinct cross hatched cleavage planes; Figure 2.8a), were identified in all thin sections of Boulby Halite, as expected (Deer et al., 1992). In the samples of halite with a high "silt" content, minor (<5 %) opaque phases were also evident.

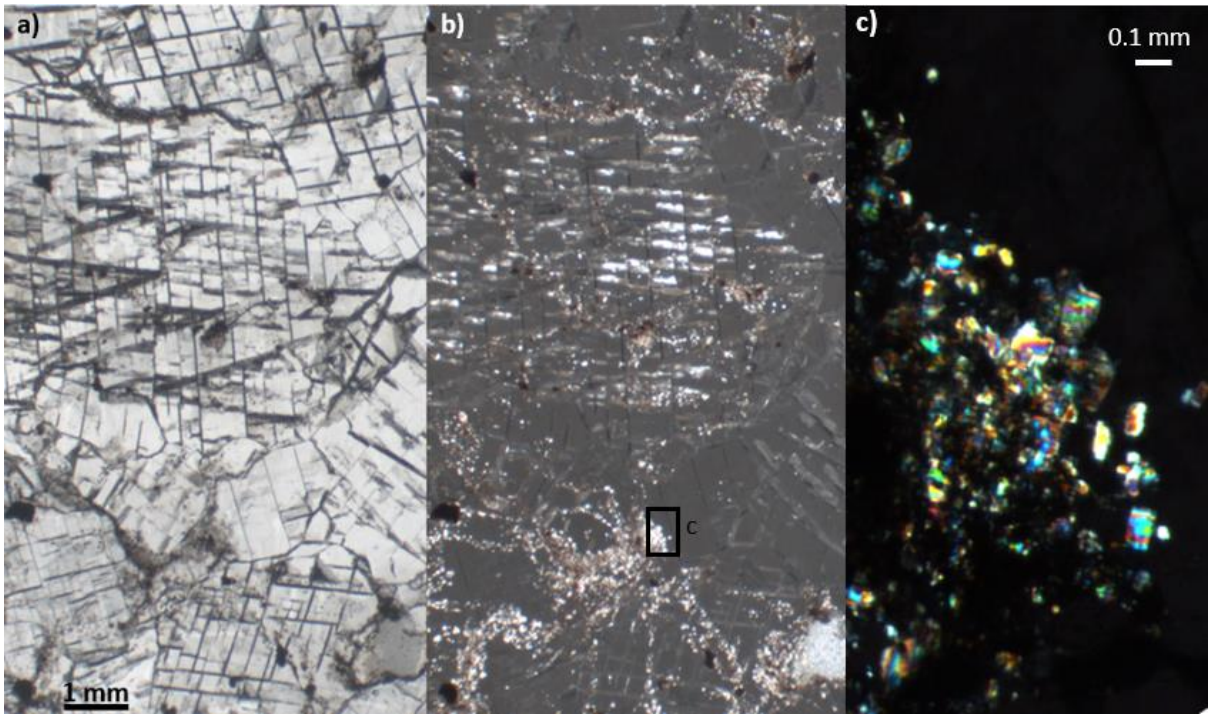

Figure 2.8 - Thin section of halite (from Site E) viewed under a) plane and b) cross-polarised light using lenses of 0.5 × magnification. Smaller, opaque crystals displaying interference colours are visible in the cross-polarised light at the bottom of the image. c) Sections of these veins are expanded at a higher magnification (×40)

Under cross-polarised light, halite is opaque, but the cubic habit remained evident (Figure 2.8b). A phase with blue, green and yellow interference colours was also seen (Figure 2.8c) in some of the Boulby Halite samples. At higher magnification (×40), these phases could be seen to consist of small (0.1mm diameter), irregular crystals. Based on the crystal shape, birefringence and published literature (Deer et al., 1992), these crystals were tentatively identified as anhydrite ($CaSO_4$). Further investigation by ICP-

MS and XRD (Sections 2.3.1d and 2.3.1c) confirmed this identification. The abundance of these crystals varied between the samples. The absence of other minerals in these thin sections confirmed the samples as halite, with only minor additional phases. There were no obvious differences in mineralogy between any of the Boulby Halite samples other than in the abundance of the opaque phases.

Primary potash

The petrography of primary potash samples was also investigated. Potash from Boulby Mine (Section 1.5.1) is a mixture of halite (NaCl) and sylvite (KCl). These minerals are often described as isomorphic (Deer et al., 1992), which would make it difficult to distinguish between them in plane-polarised light. When the thin sections of primary potash were observed under plane-polarised light, halite could be identified (as detailed above), but large areas with a deep red colouration were evident (Figure 2.8a) taking up around 50% of the sample. This was presumed to be sylvite and showed that there was a heterogeneous distribution of halite and sylvite within the primary potash.

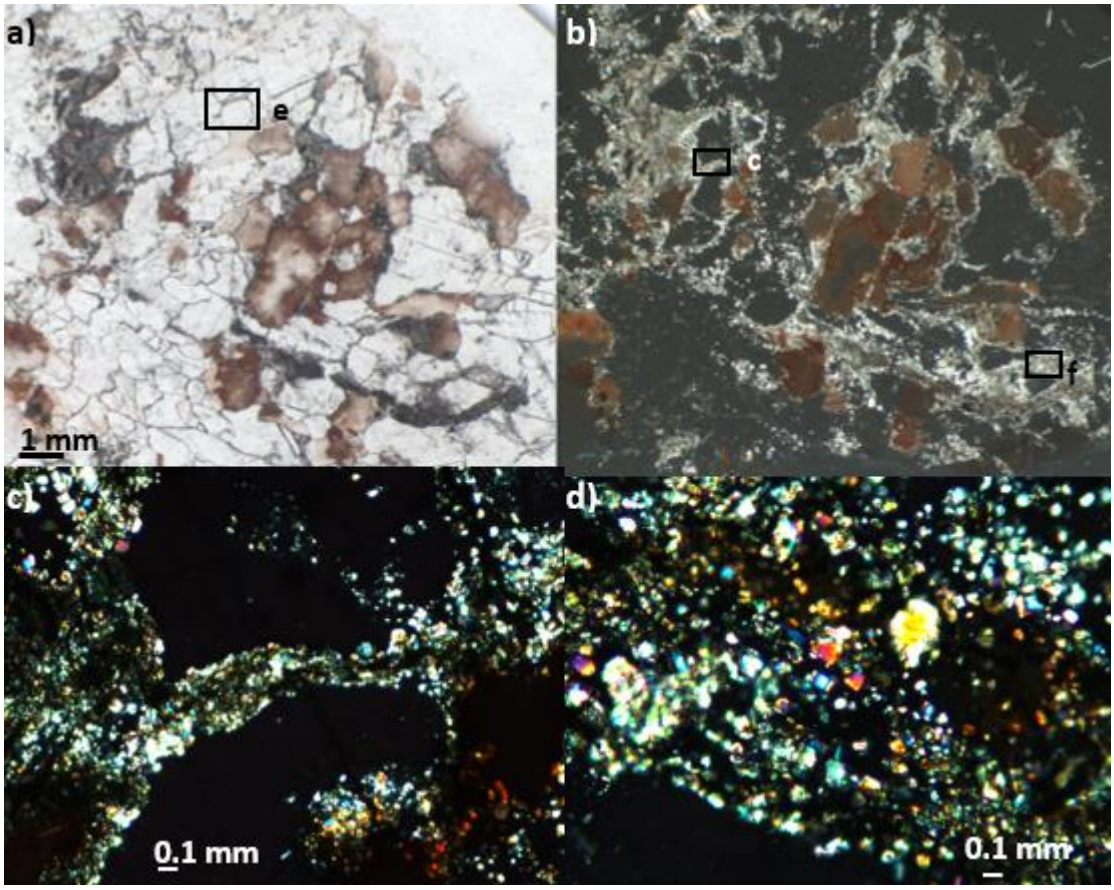

Figure 2.9 - Thin section of primary potash (from Site D) viewed under (a) plane and (b) cross-polarised light. Veins are visible in the cross-polarised light at the bottom of the image. Sections of these veins are expanded at a higher (×40) magnification (c), (d). A particular section of white crystal (e) is labelled here as it is discussed in more detail further on in this Chapter.

As with the Boulby Halite, the primary potash samples were opaque under cross-polarised light, but crystals exhibiting blue, green and yellow interference colours, like those seen in the halite and tentatively identified as anhydrite, were observed but at much greater abundance (Figure 2.9b). These crystals predominantly surrounded the opaque phases but their abundance and distribution were not consistent between samples of primary potash.

c) Mineralogical composition - XRD

The minerology of each of the samples was determined via X-Ray Diffraction (XRD) and the results are displayed on Table 2.4. Halite (NaCl) was a major phase in all the

samples, across all sites and beds (Table 2.4). This was as expected for the samples from the Boulby Halite. It was also expected for the samples of Boulby Potash, as prior studies have shown this bed to contain high amounts of NaCl (Woods, 1979).

Sylvite (KCl) was a major phase in all of the samples of Boulby Potash (Table 2.4). It was also unexpectedly found in some samples of the Boulby Halite from Sites A and B. This would be further investigated *via* ICP-MS analysis.

Woods (1979) identified several calcium deposits ($CaCl_2$, $CaSO_4$ or $CaCO_3$) in Zechstein salts, but here, only $CaSO_4$ (anhydrite) was identified (Table 2.4). Detection of anhydrite corresponded with the appearance of the blue, green and yellow features observed in the thin sections, supporting the conclusion that these were anhydrite crystals. As a general rule, anhydrite tended to be a major phase higher up the stratigraphic column and a minor, or trace, phase lower down. Samples without anhydrite were found in all the beds, so its distribution was heterogeneous.

Cristobalite and quartz were identified in a number of samples, but there was no pattern to the distribution of these minerals. It is presumed, based upon the results of other work which detected quartz in chloride deposits (Har et al., 2010, Har et al., 2006), that they were present specifically within the silt in the primary potash and silty halite.

Table 2.4 - Minerals detected (major, minor or trace phases) by XRD. Phases that were not detected are marked with "n.d."

Sample location	Halite	Sylvite	Anhydrite	Cristobalite	Quartz
Site A					
Secondary potash	Major Phase detected	Major Phase detected	Major Phase detected	n.d	Minor phase detected
Primary potash	Major Phase detected	Major Phase detected	n.d	n.d	n.d
Halite from within the primary potash	Major Phase detected	Major Phase detected	n.d	Trace amounts detected	n.d
Top of the interface	Major Phase detected	Major Phase detected	n.d	n.d	n.d
Bottom of the interface	Major Phase detected	Major Phase detected	Trace amounts detected	n.d	n.d
Boulby halite (silty halite)	Major Phase detected	n.d	Major Phase detected	Trace amounts detected	Trace amounts detected
Boulby halite (CPH)	Major Phase detected	Minor phase detected	Trace amounts detected	Trace amounts detected	n.d
Site B					
Primary potash	Major Phase detected	Major Phase detected	n.d	n.d	n.d
Top of the interface	Major Phase detected	Major Phase detected	Major Phase detected	Trace amounts detected	n.d
Bottom of the interface	Major Phase detected	Major Phase detected	Major Phase detected	n.d	n.d
Boulby halite (silty halite)	Major Phase detected	Major Phase detected	Trace amounts detected	n.d	n.d
Site D					
Primary potash	Major Phase detected	Major Phase detected	Major Phase detected	n.d	Minor phase detected
Top of the interface	Major Phase detected	Major Phase detected	Major Phase detected	Trace amounts detected	n.d
Bottom of the interface	Major Phase detected	Major Phase detected	Trace amounts detected	Trace amounts detected	n.d
Boulby halite (silty halite)	Major Phase detected	n.d	Major Phase detected	Trace amounts detected	n.d
Site E					
Primary potash	Major Phase detected	Major Phase detected	Major Phase detected	Trace amounts detected	n.d
Top of the interface	Major Phase detected	Major Phase detected	Major Phase detected	n.d	n.d
Bottom of the interface	Major Phase detected	Trace amounts detected	Minor phase detected	n.d	Minor phase detected
Boulby halite (silty halite)	Major Phase detected	n.d	Trace amounts detected	Trace amounts detected	n.d
Boulby halite (CPH)	Major Phase detected	n.d	Trace amounts detected	Trace amounts detected	n.d

d) Mineralogical composition - EMPA

Having identified the minerals present, the electron microprobe was used to determine where these minerals were located within the samples and obtain precise chemical data for the phases present.

Four representative thin sections were chosen for EMPA analyses such that there was at least one each of primary potash, silty halite and CPH, as well as a sample each of Boulby Potash and Boulby Halite with and without the crystals presumed to be anhydrite (Table 2.5). Raw data from the EPMA are given in Appendix 1 and Table 2.5 presents the percentage composition of each detected phase.

The EMPA data presented in this Chapter can be considered reliable in comparing and contrasting samples of different composition. This should not, however, be taken as accurate measurements of the composition of the samples themselves. The inability to polish the thin sections (due to their brittleness and water solubility) is likely to have added significant and variable disruption to the electron beam which will in turn have affected the quality of the data. Furthermore, while the EMPA instrument itself, and its automated interpretation of the data, makes the assumption that the majority of the composition of a sample is an oxide, the samples used in this Thesis were predominantly chlorides. While the data tables for these analyses presents the data as oxides, past studies (Woods, 1979, Hollingsworth et al., 2013) would indicate that the Na and K detected in this analyses are NaCl and KCl, not Na_2O and K_2O. This is supported by the XRD data (Section 2.3.1c). Interpreting these chlorides as oxides is likely to have introduced further errors into the data, which might explain why the majority of the samples report measurements of over 105 % of the samples' mass.

Boulby Halite - CPH and silty halite

Both types of Boulby Halite (the CPH and silty halite), showed little variation under either cross- or plane-polarised light and this was reflected in the EMPA data (Table 2.5). The composition of the colourless crystals from CPH and silty halite was identical, consisting mostly of Na (55.16 %) and Cl (60.69%), with much smaller amounts of K, Ca, Al_2O3, SiO_3 and SO_3. Student's t-tests showed $p > 0.05$ for all measured components within between the CPH and silty halite, confirming consistent compositions.

Table 2.5 - Percentage weight composition of CPH, silty halite and Boulby (primary) potash. Each sample was measured in excess of three times and data shown is the mean with the standard deviation of the element oxide (with the exception of chlorine). Boulby Potash areas identified as halite via microscopy can be split into two categories (A and B) as described in the text below.

Wt%	Boulby Halite - CPH	Boulby Halite - silty halite (bulk)	Boulby Halite - silty halite (opaques)	Boulby Potash - "sylvite"	Boulby Potash - "halite" category A	Boulby Potash - "halite" category B
Cl	60.98 ± 1.95	60.47 ± 0.76	1.02 ± 0.41	47.34 ± 1.74	60.55 ± 0.59	48.32 ± 0.33
Na_2O	55.22 ± 2.30	55.11 ± 1.29	0.19 ± 0.01	0.73 ± 0.64	56.45 ± 0.32	0.29 ± 0.12
K_2O	0.13 ± 0.03	0.11 ± 0.02	1.66 ± 1.13	59.08 ± 1.03	0.27 ± 0.19	59.93 ± 0.28
MgO	0.00 ± 0.00	0.1 ± 0.12	13.16 ± 6.13	0.01 ± 0.01	0.02 ± 0.03	0.00 ± 0.00
CaO	0.02 ± 0.00	0.05 ± 0.05	0.9 ± 1.01	0.05 ± 0.12	0.13 ± 0.23	0.01 ± 0.01
MnO	0.00 ± 0.00	0.00 ± 0.01	0.01 ± 0.02	0.00 ± 0.01	0.00 ± 001	0.00 ± 0.00
FeO	0.00 ± 0.00	0.01 ± 0.01	2.47 ± 0.55	0.26 ± 0.21	0.02 ± 0.02	0.01 ± 0.01
Al_2O_3	0.00 ± 0.00	0 ± 0	9.37 ± 2.20	0.00 ± 0.00	0.00 ± 0.00	0.00 ± 0.01
SiO_2	0.01 ± 0.01	0.03 ± 0.02	39.80 ± 9.58	0.04 ± 0.05	0.01 ± 0.01	0.01 ± 0.01
SO_3	0.01 ± 0.02	0.01 ± 0.02	1.28 ± 1.94	0.03 ± 0.04	0.16 ± 0.31	0.03 ± 0.05
Total	116.37 ± 4.22	115.84 ± 0.82	69.86 ± 5.16	107.53 ± 2.81	117.59 ± 0.67	108.60 ± 0.38

As observed under the microscope, the sample of silty halite contained many opaque phases. The EMPA results showed that these opaque phases had a significantly different composition to the halite crystals ($p < 0.001$ for all components except Mn). Opaque phases exhibited lower abundances of Cl (1.02 %) and Na (0.19 %), higher abundances of Mg, Fe, Al and were dominated (39.82 %) by SiO_2 (Table 2.5 and Appendix 1). Variation within the opaques seemed higher than in the halite crystals, as evidenced by the much larger standard deviations. The XRD data (Section 2.3.1c) had shown the

presence of quartz and cristobalite in the samples and it had been speculated that these were present in the silt rather than in the halite crystal. These EMPA results support this hypothesis.

Boulby Potash

The microscopy and XRD indicated that the primary potash exhibited features consistent with the presence of both halite and sylvite (Section 2.3.1b), distributed heterogeneously. The red features, presumed to be sylvite, were targeted by EPMA and were similar in composition to one another (ANOVA tests showed $p > 0.05$ for all measured components), with elevated K abundances (47.31 %) consistent with their identification as sylvite. EMPA measurements of the Na, K and Cl concentrations of these areas differed significantly to those of the Boulby Halite (Student's t-tests showed $p < 0.00001$), but the concentrations of the other components did not. Thus, it could be concluded that these areas represented sylvite within the primary potash.

The remaining crystals within the primary potash had been assumed to be halite, as they had visually resembled the samples of Boulby Halite under the petrological microscope, and there was no observed variation within and between these crystals. The EMPA measurements of these crystals, however, could be split into two categories (A and B, Table 2.5) based upon whether the K concentration was low (in the range 0.05 - 0.5 %) or high (in the range 59.8 - 60.4 %), there were no K values in between these categories.

Category A crystals had a statistically similar composition to the Boulby Halite itself (Student's t-tests showed $p > 0.05$ in all case). Category B crystals had the same composition as the sylvite in the primary potash (Student's t-tests showed $p > 0.05$ for

all measured components), with statistically different Na, K and Cl concentrations to both category A crystals and the Boulby Halite (Student's t-tests showed $p < 0.00001$).

These results indicate that only EPMA analysis could confirm lithologies on the basis of Na and K concentrations, and the results supported the identifications made by the microscopy. Halite crystals, however, had a higher Cl concentration than sylvite (51% compared to 44%, $p < 0.05$). In the absence of other Cl-bearing phases (at the detection limits of the EMPA and XRD), the source of this variation remains unknown.

Anhydrite

The samples investigated by EMPA had been chosen such that there was a sample each of Boulby Halite and Boulby Potash with and without the crystals proposed to be anhydrite (as identified using microscopy and XRD). A Student's t-test showed that crystals identified as potentially anhydrite by microscopy had higher concentrations (as seen in Table 2.5) of Ca and SO_4 compared to the surrounding Boulby Halite or Boulby Potash ($p < 0.05$), further supporting the hypothesis that they were anhydrite. The presence or absence of anhydrite within the thin section, however, made no difference to the overall Boulby Halite or Boulby Potash composition (Student's t-tests showed $p > 0.05$ for all components).

The composition of these (presumed) anhydrite crystals varied within samples from the same site and between sites (Table 2.6) (for all components an ANOVA test shows $p > 0.05$). The variable presence of other components, such as Mg, Al_2O_3 and SiO_2, indicates that they are not pure $CaSO_4$ and that the concentration and composition of these impurities is highly variable.

Table 2.6 - Percentage weight composition of areas of Boulby Halite and Boulby Potash samples that possessed birefringent crystals under cross-polarised light

Wt%	Boulby Halite	Boulby Halite	Boulby Halite	Boulby Halite	Boulby Halite	Boulby Potash	Boulby Potash	Boulby Potash	Boulby Potash	Boulby Potash
Cl	0.35	54.64	0.51	0.71	23.27	0.26	0.95	0.35	39.20	8.07
Na_2O	0.16	47.76	0.75	0.53	24.91	0.31	1.19	0.57	43.36	0.15
K_2O	0.08	0.1	0.65	0.13	0.97	0.71	0.29	0.20	0.96	0.01
MgO	0.48	0.01	7.32	0.50	4.47	0.84	0.08	0.10	0.84	10.82
CaO	38.24	5.9	21.58	36.50	2.96	35.50	38.43	38.86	9.86	0.04
MnO	0	0	0.01	0.00	0.00	0.01	0.00	0.00	0.00	2.65
FeO	0.02	0	1.62	0.06	1.09	0.43	0.01	0.04	0.16	27.05
Al_2O_3	0.02	0	2.84	0.11	1.42	1.61	0.01	0.02	3.47	0.07
SiO_2	0.32	0.03	10.89	0.49	30.28	5.96	0.12	0.24	4.74	0.08
SO_3	44.14	8.75	22.76	43.79	3.66	39.33	57.81	54.49	14.19	0.07
Total	83.81	117.19	68.93	82.82	93.03	84.96	98.89	94.87	116.78	49.01

e) ICP-MS

Chemical characterisation was further investigated using Inductively Coupled Plasma Mass Spectrometry (ICP-MS), as described in Section 2.2.2d. Without knowing the precise density of the samples prior to dissolution, it was not possible to accurately back-calculate the molar concentration of the initial samples. Results are, therefore, left in the form of parts per million (ppm) of the rock samples.

Boulby Halite

The composition of the samples of Boulby Halite (CPH, silty halite and a sample with the visual appearance of CPH found within the Boulby Potash bed) was investigated (Table 2.7). As expected, Na was the dominant element detected ranging in concentration from 2.43×10^5 to 3.85×10^5 ppm.

Table 2.7 - Elemental concentration (ppm) of each of the Boulby Halite samples analysed, as determined by ICP-MS. Error represents standard deviation of that element across 3 replicates. This table extends onto the next page

Site	Sample type	Na	K	Ca	Mg	Si
A	Silty halite	3.85×10^{5} ± 1.88×10^{3}	1.62×10^{3} ± 1.54×10^{1}	2.12×10^{3} ± 2.06×10^{2}	2.42×10^{2} ± 3.69	1.70×10^{3} ± 1.39×10^{2}
A	CPH	3.84×10^{5} ± 3.11×10^{3}	2.12×10^{3} ± 1.83×10^{1}	1.54×10^{3} ± 3.00×10^{2}	3.84×10^{2} ± 1.10×10^{1}	3.28×10^{3} ± 2.84×10^{2}
B	Silty halite	2.43×10^{5} ± 3.24×10^{3}	1.88×10^{5} ± 4.20×10^{3}	0 ± 0	4.57 ± 5.6	2.76×10^{3} ± 7.63×10^{2}
D	Silty halite	3.71×10^{5} ± 4.94×10^{3}	2.95×10^{3} ± 3.18×10^{1}	2.45×10^{3} ± 2.73×10^{2}	3.62×10^{2} ± 5.98	2.01×10^{3} ± 2.00×10^{2}
E	CPH	3.33×10^{5} ± 4.78×10^{3}	8.60×10^{2} ± 2.72×10^{1}	8.70×10^{2} ± 5.53×10^{2}	0 ± 0	2.42×10^{3} ± 1.56×10^{2}
E	Silty halite	3.75×10^{5} ± 1.53×10^{3}	1.19×10^{3} ± 1.33×10^{1}	3.31×10^{3} ± 3.03×10^{2}	3.49×10^{2} ± 1.38×10^{1}	2.93×10^{3} ± 3.43×10^{2}
A	CPH from within potash bed	3.85×10^{5} ± 4.60×10^{3}	1.51×10^{4} ± 3.82×10^{2}	0 ± 0	5.52 ± 2.40	2.32×10^{3} ± 2.90×10^{2}

Site	Sample type	Mn	Fe	Sr	Ba	Al
A	**Silty halite**	2 ± 0	1.07×10^2 ± 13	25 ± 6	8 ± 1	75 ± 4
A	**CPH**	2 ± 0	0 ± 0	22 ± 4	18 ± 2	30 ± 8
B	**Silty halite**	0 ± 0	0 ± 0	1 ± 0	0 ± 0	63 ± 6
D	**Silty halite**	2 ± 0	49 ± 7	28 ± 2	0 ± 0	91 ± 7
E	**CPH**	0 ± 0	0 ± 0	14 ± 32	0 ± 0	1.08×10^2 ± 28
E	**Silty halite**	1 ± 0	42 ± 3	45 ± 10	0 ± 0	1.20×10^2 ± 6
A	**CPH from within potash bed**	0 ± 0	0 ± 0	9 ± 0	13 ± 1	0 ± 0

Variation in Na and K within the Boulby Halite

An initial one-way ANOVA test, investigating variation between all seven samples, showed highly significant variation in Na concentrations between the samples of Boulby Halite ($p < 0.005$). Post-hoc Tukey tests, however, revealed that this variation was entirely the result of the sample from Site B (which was silty halite) which showed lower Na concentrations than the other samples (discussed further below). ANOVA tests ran without this sample were no longer significant ($p = 0.53$). There was no other variation in Na concentration of Boulby Halite between sample sites ($p < 0.05$), meaning an average Na concentration (with the sample from Site B excluded) could be calculated of $3.72\times10^5 \pm 2.00\times10^4$ ppm.

The Boulby Halite sample from Site B had a statistically significantly lower Na concentration than the other samples (2.43×10^5 ppm compared to a mean of 3.7×10^5 ppm). Likewise, this sample showed the highest K concentration by an order of magnitude ($1.88\text{x}10^5$ ppm). However, the ANOVA tests showed that, even with this sample excluded, all samples of Boulby Halite varied significantly in their K concentration ($p < 0.05$) and that this variation was not related to sample site ($p > 0.05$). The sample from Site B had previously been shown by XRD to contain sylvite as a major phase (see Section 2.3.1c). It was therefore concluded that, despite being collected from the Boulby Halite bed, this sample was not representative of Boulby Halite. It was, therefore, excluded from further analyses.

Although sylvite had been detected by XRD as a minor phase in the sample of CPH from Site A (see Section 2.3.1c), this same sample did not contain elevated concentrations of K according to the ICP-MS (statistically compared using post-hoc Tukey tests), so it was retained for further analyses.

Variation in other elements

ANOVA tests had showed no significant variation in the concentration of Na between samples of Boulby Halite, with the exception of the sample from Site B. There was, however, statistically significant variation in the concentration of other measured elements between all the samples (in all instances $p < 0.05$).

For Ca, Si and Sr, the ANOVA tests showed the variations were down to differences between sample sites ($p < 0.005$), whereas for K, Mg, Mn, Fe, Be and Al they did not ($p > 0.05$). This would indicate that K, Mg, Mn, Fe, Be and Al had inter-site variation, but were relatively consistent within a site, whereas Ca, Si and Sr were highly variable even within the same site.

Comparison of silty halite and CPH

Student's t-tests showed that there was no statistically significant difference between the concentrations of any of the elements within the CPH and the silty halite ($p > 0.05$). This would imply, in concordance with the EMPA data, that the presence or absence of silt within a sample has no significant impact on the bulk composition of these samples.

Identification of the samples

Woods (1979) does not go into detail about the composition of the Boulby Halite, instead focusing on the Boulby Potash, but does describe inconsistent leaching of K minerals into the Boulby Halite. This leaching could explain the variable K concentrations between these samples. Woods also describes variable Ca concentrations as high as "*up to 10 percent".* All Ca concentrations observed in the Boulby Halite in this Chapter fit within this roughly described range.

With the exception of the sample from Site B described above, none of the samples of Boulby Halite investigated in this Chapter have a composition that would contradict the descriptions of Woods (1979). As such, it can be assumed that these samples were correctly identified.

Interface

The composition of the samples from the interface region between the Boulby Halite and the Boulby Potash was investigated (Table 2.8). As discussed earlier (Section 2.2.1c), at each site a sample was taken from the top and the bottom of the interface. The definition of the interface varied within the mine, with Sites A and D having a poorly defined interface, and B and E having a well-defined one. This might have implied differences in composition across the interface region. An initial ANOVA test, without taking into account sample site or position within the interface, showed highly significant variation ($p < 0.0001$) in the concentration of all the elements between all nine of these samples (from all sample sites). The next task, therefore, was to investigate what was responsible for this variation.

Variation between the top or bottom of the interface.

It was initially thought that this variation would be a result of position within the interface, with samples from near the Boulby Potash having a composition more similar to this lithology than the samples from near the Boulby Halite, and *vice versa*. However, paired Student's t-tests comparing composition of samples from the top and bottom of the interface at each site showed no significant difference in the concentration of any of the elements (in all cases $p > 0.05$). This would imply that there was little compositional variation between the top and bottom of the interface region.

Table 2.8 - Elemental concentration (ppm) of each of the interface samples analysed, as determined by ICP-MS. Error represents standard deviation of that element across 3 replicates. Table continues onto the next page

Site	Location within the interface	Interface definition	Na	K	Ca	Mg	Si
A	Top	Poorly defined	$3.53\times10^{5} \pm 3.77\times10^{3}$	$2.64\times10^{4} \pm 3.41\times10^{2}$	0 ± 0	9 ± 2	$2.54\times10^{3} \pm 4.16\times10^{2}$
A	Top	Poorly defined	$3.63\times10^{5} \pm 4.45\times10^{3}$	$1.48\times10^{4} \pm 3.13\times10^{2}$	$1.37\times10^{3} \pm 1.92\times10^{2}$	$6.08\times10^{2} \pm 7$	$1.83\times10^{3} \pm 4.05\times10^{2}$
A	Bottom	Poorly defined	$3.84\times10^{5} \pm 4.59\times10^{3}$	$1.51\times10^{4} \pm 3.82\times10^{2}$	0 ± 0	6 ± 2	$2.32\times10^{3} \pm 2.90\times10^{2}$
B	Top	Well defined	$3.18\times10^{5} \pm 2.27\times10^{3}$	$3.54\times10^{4} \pm 9.66\times10^{2}$	$6.88\times10^{3} \pm 5.71\times10^{2}$	$7.18\times10^{2} \pm 11$	$3.06\times10^{3} \pm 4.74\times10^{2}$
B	Bottom	Well defined	$3.37\times10^{5} \pm 9.26\times10^{3}$	$4.68\times10^{4} \pm 1.02\times10^{3}$	$1.06\times10^{3} \pm 2.87\times10^{2}$	$2.19\times10^{2} \pm 7$	$1.75\times10^{3} \pm 4.03\times10^{2}$
D	Top	Poorly defined	$3.77\times10^{5} \pm 5.63\times10^{3}$	$2.95\times10^{4} \pm 1.41\times10^{2}$	$3.68\times10^{3} \pm 3.47\times10^{2}$	35 ± 3	$1.75\times10^{3} \pm 2.25\times10^{2}$
D	Bottom	Poorly defined	$3.60\times10^{5} \pm 3.62\times10^{3}$	$9.60\times10^{3} \pm 1.43\times10^{2}$	$5.95\times10^{3} \pm 5.96\times10^{2}$	$3.25\times10^{2} \pm 12$	$1.83\times10^{3} \pm 4.70\times10^{2}$
E	Top	Well defined	$3.02\times10^{5} \pm 3.66\times10^{3}$	$1.55\times10^{4} \pm 1.85\times10^{2}$	$2.09\times10^{4} \pm 9.84\times10^{2}$	$6.96\times10^{2} \pm 5$	$1.48\times10^{3} \pm 2.64\times10^{2}$
E	Bottom	Well defined	$3.43\times10^{5} \pm 5.13\times10^{3}$	$2.80\times10^{4} \pm 2.40\times10^{2}$	$8.07\times10^{3} \pm 4.06\times10^{2}$	$7.20\times10^{2} \pm 9$	$1.48\times10^{3} \pm 4.53\times10^{2}$

Site	Location within the interface	Interface definition	Mn	Fe	Sr	Ba	Al
A	Top	Poorly defined	1 ± 0	10 ± 10	10 ± 3	15 ± 2	1.07×10^2 ± 33
A	Top	Poorly defined	8 ± 0	1.27×10^2 ± 8	15 ± 1	0 ± 0	88 ± 7
A	Bottom	Poorly defined	0 ± 0	0 ± 0	9 ± 0	13 ± 1	0 ± 0
B	Top	Well defined	18 ± 1	3.65×10^2 ± 18	66 ± 3	20 ± 2	3.04×10^2 ± 25
B	Bottom	Well defined	2 ± 0	55 ± 7	19 ± 2	15 ± 1	1.27×10^2 ± 5
D	Top	Poorly defined	0 ± 0	0 ± 0	32 ± 0	10 ± 1	26 ± 4
D	Bottom	Poorly defined	2 ± 0	92 ± 6	49 ± 3	0 ± 0	1.51×10^2 ± 10
E	Top	Well defined	4 ± 0	2.42×10^2 ± 3	133 ± 5	0 ± 0	2.40×10^2 ± 10
E	Bottom	Well defined	6 ± 0	2.70×10^2 ± 6	58 ± 3	0 ± 0	3.62×10^2 ± 14

Variation between sites and interface type

ANOVA tests showed significant variation in the concentration of Na, Fe and Al between sites ($p < 0.05$). Post-hoc Tukey tests implied that this variation was a result of differences between those sites where the interface was well defined (Sites B and E) compared to those sites where it was poorly defined (Sites A and D). In order to confirm this was the case, Student's t-tests were carried out, which showed significant difference ($p < 0.05$) in the concentration of these elements (Figure 2.10) between samples from where the interface was well-defined and where it was poorly-defined. Poorly defined interface samples had on average more Na than the well-defined ($3.62\times10^5 \pm 1.00\times10^4$ ppm compared to $3.26\times10^5 \pm 1.14\times10^4$ ppm), but lower concentrations of Fe (46 PPM ±15, compared to 233 ±21 ppm) and Al (74 ± 35 ppm compared to 258 ± 31 ppm).

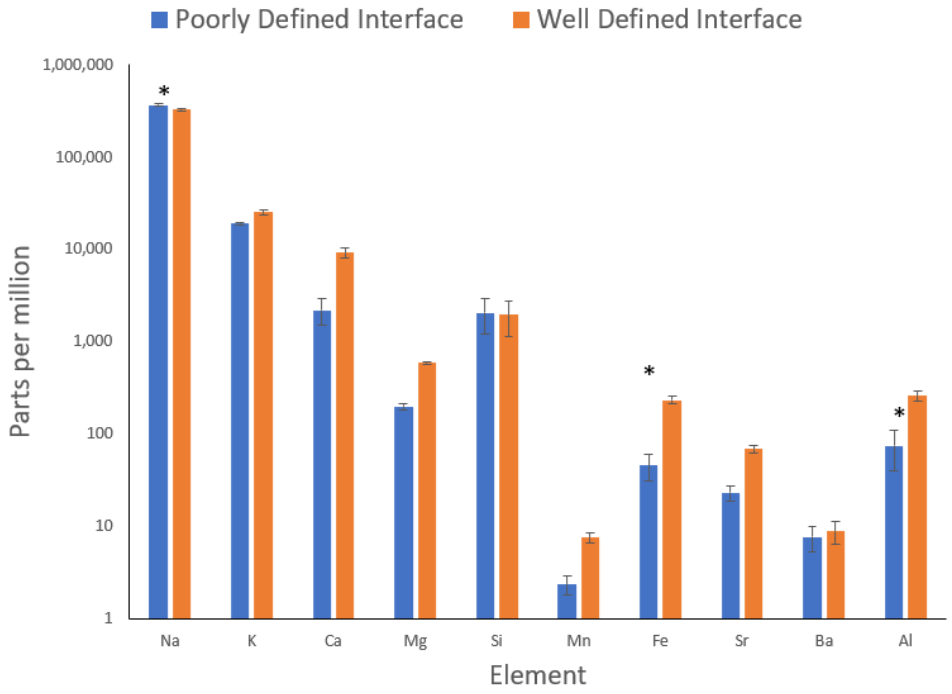

*Figure 2.10 - Variation in elemental composition between poorly-defined interface and well-defined interface. The y-axis presents concentration in parts per million (ppm) plotted on a logarithmic scale. Elements where concentration exhibited a significant difference between the definition types, as determined via Student's t-tests, are marked with *.*

Boulby Potash

ANOVA tests showed significant compositional variation between all samples of Boulby Potash ($p > 0.05$) for all measured elements. This was the case even for Na and K and is reflected in the large range of values for these elements (Table 2.9). Na ranged from 1.59×10^5 to 3.07×10^5 ppm, while K ranged from 5.61×10^4 to 2.41×10^5 ppm. Since there was only one sample of primary potash per site, variation within sites could not be distinguished from variation between sites and thus no cause of this variation could be determined.

The single sample of secondary potash was the only sample, of any lithology, in which the K concentration exceeded the Na concentration.

Woods (1979) described general trends in the composition of the Boulby Potash as follows: "[the] *main constituent minerals are sylvite and halite with minor clay and anhydrite and trace magnesite, pyrite and quartz*". No previous quantitative characterisation is available.

The samples of the Boulby Potash obtained within this study fit Woods' description; the main measured elements were Na and K, indicative of halite and sylvite with Ca (presumed, on the basis of XRD results, to be anhydrite) the next most common element. Woods (1979) does not describe what the "minor clay" consists of, but it seems reasonable to presume this is equivalent to 'silt' within the samples, and is responsible for the measurements of Si that fall between 8.06×10^3 and 3.00×10^2 ppm. This means that all the samples of Boulby Potash obtained on this sampling expedition are likely to have been correctly identified.

Table 2.9 - Elemental concentration (ppm) of each of the potash samples analysed, as determined by ICP-MS. Error represents standard deviation of that element across 3 replicates

Site	Sample characterisation	Na	K	Ca	Mg	Si
A	Secondary Potash	$1.59\times10^{5} \pm 2.38\times10^{3}$	$2.71\times10^{5} \pm 3.98\times10^{3}$	$3.21\times10^{4} \pm 9.05\times10^{2}$	$7.58\times10^{2} \pm 9$	$3.00\times10^{3} \pm 7.09\times10^{2}$
A	Primary Potash	$2.34\times10^{5} \pm 1.92\times10^{3}$	$2.41\times10^{5} \pm 5.24\times10^{3}$	0 ± 0	16 ± 2	$2.40\times10^{3} \pm 5.39\times10^{2}$
B	Primary Potash	$3.07\times10^{5} \pm 2.74\times10^{3}$	$5.61\times10^{4} \pm 8.45\times10^{2}$	$1.92\times10^{3} \pm 3.25\times10^{2}$	$1.50\times10^{2} \pm 5$	$8.08\times10^{2} \pm 5.31\times10^{2}$
D	Primary Potash	$2.17\times10^{5} \pm 2.84\times10^{3}$	$1.79\times10^{5} \pm 2.34\times10^{3}$	$1.58\times10^{4} \pm 9.28\times10^{2}$	$7.99\times10^{2} \pm 15$	$2.06\times10^{3} \pm 3.34\times10^{2}$
E	Primary Potash	$2.67\times10^{5} \pm 3.70\times10^{3}$	$1.39\times10^{5} \pm 2.19\times10^{3}$	$6.43\times10^{3} \pm 6.38\times10^{2}$	$5.41\times10^{2} \pm 11$	$2.52\times10^{3} \pm 2.78\times10^{2}$

Site	Sample characterisation	Mn	Fe	Sr	Ba	Al
A	Secondary Potash	14 ± 0	$2.29\times10^{2} \pm 41$	$2.33\times10^{2} \pm 8$	17 ± 2	$2.10\times10^{2} \pm 16$
A	Primary Potash	0 ± 0	0 ± 0	8 ± 0	12 ± 1	7 ± 6
B	Primary Potash	2 ± 0	45 ± 3	22 ± 1	9 ± 1	74 ± 5
D	Primary Potash	10 ± 0	$3.98\times10^{2} \pm 38$	$1.03\times10^{2} \pm 5$	15 ± 2	$4.01\times10^{2} \pm 37$
E	Primary Potash	4 ± 0	$3.03\times10^{2} \pm 36$	50 ± 3	0 ± 1	$3.26\times10^{2} \pm 11$

Compositional trends across the stratigraphy

Having investigated the composition of the various beds, and variation within them, the data was combined in order to determine trends and patterns throughout the stratigraphy.

Na, K and Cl

As expected, the Boulby Halite and the primary Boulby Potash show significantly different ($p > 0.05$) concentrations of the two major cations (Na and K), and these cations were strongly negatively correlated across all the samples (Figure 2.11), with a Pearson coefficient of -0.94. This means the samples represent a wide variety of Na:K ratios, which can be used to investigate the effect variations in this ratio might have on microbial community structure (Chapter 3 and 4).

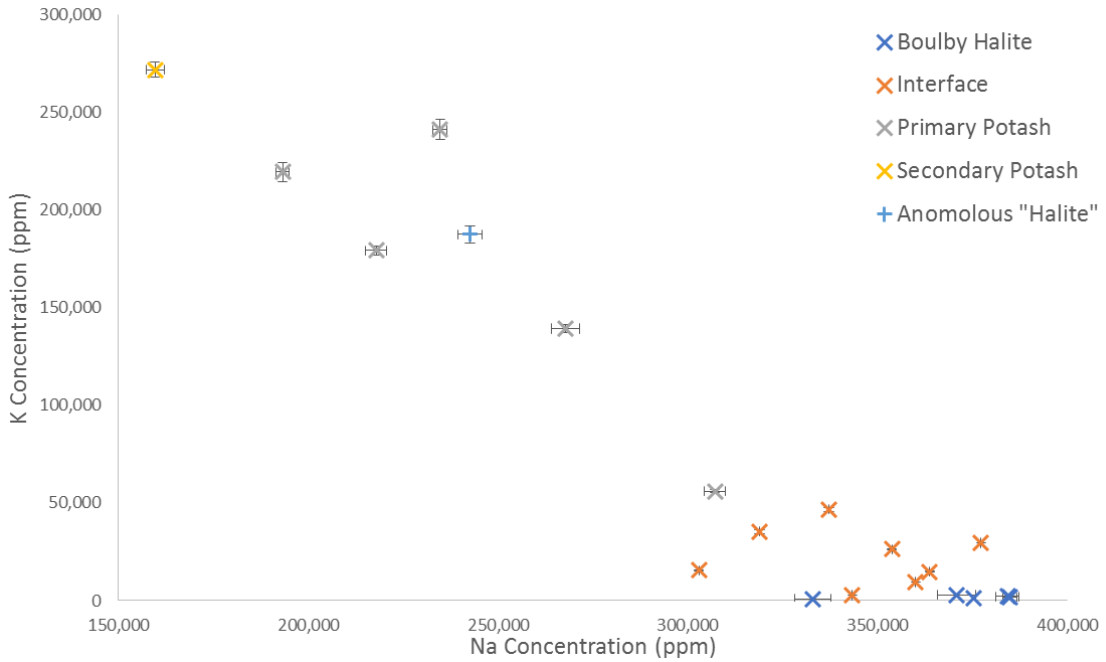

Figure 2.11 - Na and K concentration of each of the samples plotted against each other. Data shown is the mean of each sample run in triplicate while the error bars represent the standard deviation. Anomalous "halite" refers to the sample from site B that had anomalous ICP-MS and XRD data

ICP-MS could not measure the Cl concentration of these samples, but on the basis of the XRD data, it was assumed to be the sum of Na and K (Table 2.10). Since, in each lithology (with the exception of Na, in the Boulby Halite) the concentration of Na and K varied significantly according to ANOVA tests, it is not unexpected that the concentration of this presumed Cl also varied significantly in each of these beds (in all instances the ANOVA tests showed $p < 0.05$). No significant difference was found, however, in the presumed Cl concentration between the Boulby Halite and Boulby Potash (Student's t-test, $p > 0.05$), yet, as described above, significant difference was found in the individual cations. This suggests that the anion concentration remained constant throughout the stratigraphy, while the concentration of each of the two cations varied. Based upon the combined Na and K concentrations observed across all samples (Table 2.10), the mean predicted Cl concentration across all lithologies was $3.83\times10^5 \pm 3.44\times10^4$ ppm.

*Table 2.10 - Mean and standard deviation of the Na, K and presumed Cl concentrations in each bed (*n *varies between lithology but is always > 4).*

	Mean Na concentration	**Mean K concentration**	**Mean presumed Cl concentration**
Boulby Potash	$2.37\times10^5 \pm 5.53\times10^4$	$1.78\times10^5 \pm 8.54\times10^4$	$4.15\times10^5 \pm 4.20\times10^4$
Interface	$3.49\times10^5 \pm 2.65\times10^4$	$2.18\times10^4 \pm 1.39\times10^4$	$3.71\times10^5 \pm 2.76\times10^4$
Boulby Halite (excluding Site B)	$3.72\times10^5 \pm 2.01\times10^4$	$3.98\times10^3 \pm 5.52\times10^3$	$3.76\times10^5 \pm 2.27\times10^4$

Other elements

Sr, Mg, Mn, Fe, Ba and Al were detected in the samples but at low concentrations and their host minerals could not be confirmed via the XRD. None of these elements correlated with either Na or K, and no significant difference was found in their concentration between lithologies (in all cases $p > 0.05$).

It was observed that Ca concentration was at its highest in those samples presumed to contain anhydrite (see Section 2.2.2a, b & c), supporting this suggestion. At each site, Ca concentration decreased with depth, although there was intra-bed variations. There was a strong positive correlation between Ca and Sr (Pearson coefficient = 0.99). This is expected as Sr is often used as a proxy for Ca. They are similar sized atoms, which form minerals in similar ways, and over geological periods of time Ca can be substituted by Sr (Capo et al., 1998).

Ca was also observed to correlate with Mg, Mn, Fe and Al, although this correlation was not strong (Pearson coefficients are 0.71, 0.65, 0.66 and 0.62, respectively). All samples without Fe were in the lower quartile of Ca values (< 3,000 ppm).

There was no correlation observed for Ba and Si with any of the other elements.

2.3.2 - Volatile content and organic carbon

Previous work (Norton et al., 1993) that identified the presence of microbes in Boulby samples supported the assumption that the samples would contain organic carbon. TOC and LOI measurements were taken for the 16 samples that had been chosen for community characterisation.

a) Total organic carbon (TOC)

Initial attempts to assess the carbon content of the samples were carried out *via* a TOC machine. Although organic carbon was detected in all but one of the samples (Table 2.11) its abundance was <0.1 % w/w in all samples except the secondary potash where it was 0.1166 %. The detection limit of this instrument is 0.01 %, the accuracy is ±1 %, and the standard deviation of many of the samples was similar to, or exceeded, the

mean (Table 2.11). These uncertainties on the data means that no statistical analysis of these results could be carried out.

Table 2.11 - Total organic carbon (mean and standard deviation, n *= 3) detected in each sample*

Site	Sample	Total Organic Carbon (as percentage of sample's mass)
A	**Secondary Potash**	0.1166 ± 0.0196
A	**Primary Potash**	0.0258 ± 0.044
A	**Interface top**	0.0515 ± 0.0449
A	**Interface bottom**	0.0564 ± 0.0155
A	**Halite**	0.0399 ± 0.0148
B	**Primary Potash**	0.0152 ± 0.0011
B	**Interface top**	0.0201 ± 0.0181
B	**Interface bottom**	0.0204 ± 0.004
D	**Primary Potash**	0.6230 ± 0.0157
D	**Interface top**	0.0044 ± 0.0019
D	**Interface bottom**	0.0122 ± 0.0068
D	**Halite**	0.0007 ± 0.0011
E	**Primary Potash**	0.0098 ± 0.0139
E	**Interface top**	0.0117 ± 0.0087
E	**Interface bottom**	0.0149 ± 0.0096
E	**Halite**	0.0000 ± 0.0000

b) Loss on Ignition (LOI)

Owing to the low carbon content, the non-soluble components of the samples were concentrated and the LOI measured as described in Section 2.2.3b. Raw data for the concentration factor for each sample, and their initial and final mass, can be found in Appendix 2.

Two-way ANOVA tests showed that the percentage change in mass ($p > 0.05$) was not related to lithology but may be related to sample sites since there were significant differences between them ($p < 0.05$). Tukey post-hoc tests indicated that the samples from Site E differed from the other sites, which is apparent in Figure 2.12, since this site

had the smallest loss of mass and, in the case of the halite, a gain in mass in all three replicates (Figure 2.12).

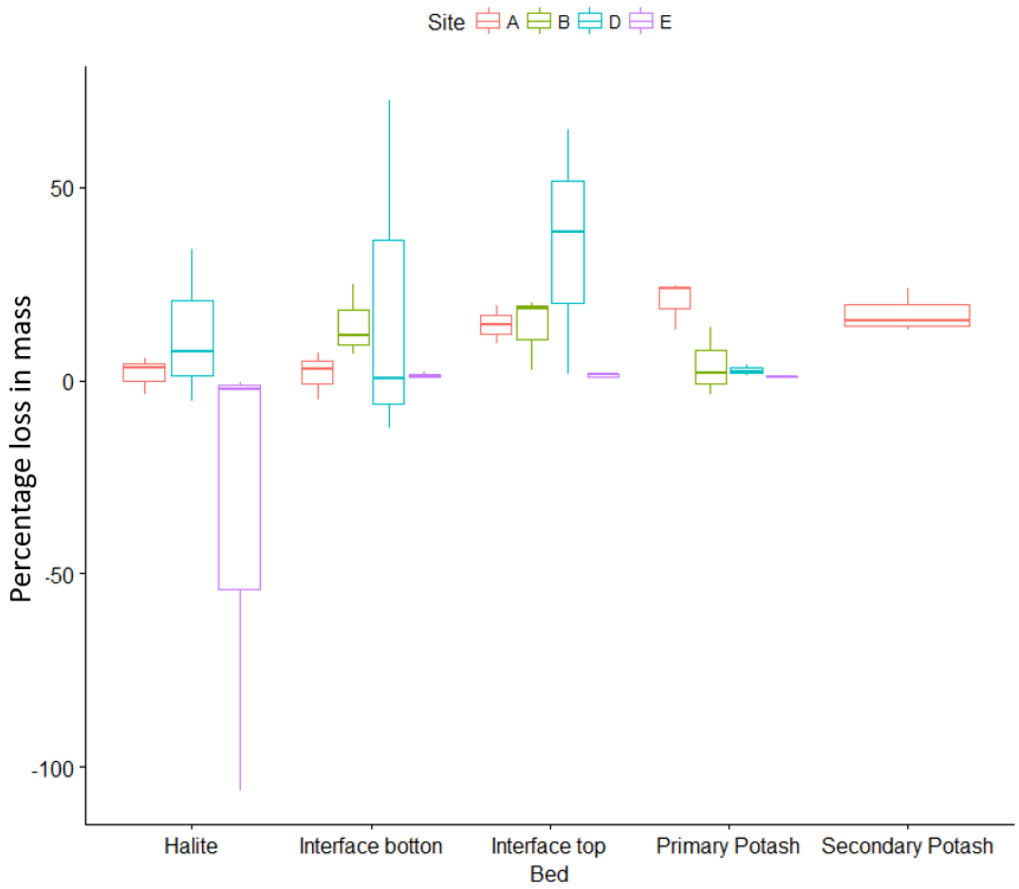

*Figure 2.12 - Box plot showing percentage change in mass upon heating samples from each bed at each site (*n = *3).*

However, this data is problematic. Heating samples to 600 °C did cause the samples to change mass, but this change was inconsistent between replicates. Each sample was run in triplicate, and in general, one of the three replicates would show a gain in mass rather than a loss. Even in cases when all three replicates lost mass, this loss was variable, as evidenced by Figure 2.12. A discussion of these issues accompanies the TGA data in the following section.

c) Thermogravimetric Analysis (TGA)

TOC indicated low abundances of carbon and the percentage change in mass identified by LOI was highly variable (even between replicates of the same sample); some of the replicates gained mass. It was hypothesised that the oxidation of compounds of the minor ions (such as Fe and Mg) might be responsible for this change, although no correlation could be found between the LOI results and samples with a higher abundance of these ions (Section 2.3.1e).

In order to investigate the potential causes of this change of mass, Thermogravimetric Analysis (TGA) was employed, as described in Section 2.2.3c.

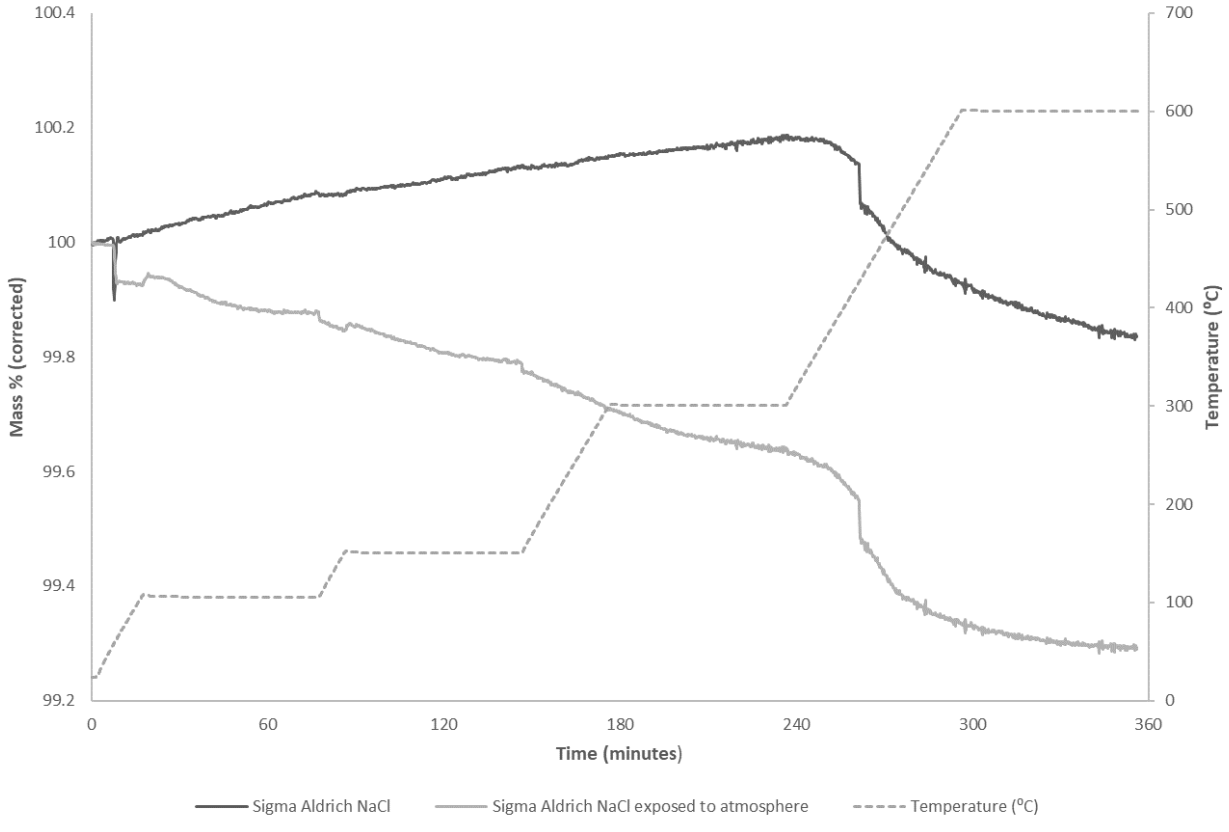

Figure 2.13 - Representative TGA profiles of commercially acquired NaCl that had undergone the concentration technique outlined in Section 2.2.3b. An initial experiment (solid black line) was carried immediately after the sample was removed from the desiccating environment. The second analysis (solid grey line) was carried out after the sample had been exposed to atmospheric conditions at room temperature for 24 hours.

Analyses were initially carried out, not on a sample from Boulby Mine, but of 99.9% purity NaCl (Sigma Aldrich). This was in order to determine whether the unexpected and variable changes in masses measured by LOI were a result of impurities within the samples or were a property inherent to salt. The NaCl was concentrated and analysed using the TGA (Figure 2.13), one sample was analysed immediately following removal from the desiccator and another analysed after exposure to atmospheric conditions for 24 hours.

The NaCl analysed immediately after desiccation was initially heated to 100 ℃, then 150 ℃ and then 300 ℃, leaving the samples for one hour between each temperature step. During each hour, the samples continued to gradually gain in mass at a consistent rate (Figure 2.13). Mass loss began at 311 ℃, while the temperature was being increased to 600 ℃.

The melting point of NaCl is 801 ℃ (Anwar et al., 2003) and it does not combust (Lewis, 2016), so it seems unlikely that chemical reaction or changes in the state of the NaCl were responsible for these changes in mass. With this in mind, the only other potential source of these changes in mass is the amount of absorbed water present within the sample.

In order to confirm this, the experiment was repeated with a sample of commercial NaCl that had been removed from the desiccated environment and allowed to take up atmospheric water over a period of 24 hours. In this sample, there was no gain in mass (Figure 2.13), and the mass gradually decreased until, again, a large drop occurred at 311℃.

Each of these two experiments were carried out in triplicate. While there was always a loss of mass at 311 ℃, below this temperature the profiles were highly variable, but a gain in mass was always seen with dehydrated samples and a loss of mass in those exposed to the atmosphere. This experiment was also repeated using samples that had not undergone the concentration procedure, and it produced the same results.

All TOC and LOI measurements had been based on "dry-weights" obtained by heating to 105 ℃ for 12 hours. These TGA results indicate that heating to 105 ℃ was not sufficient to remove all the water from the samples, and that the water content within replicates of the same sample were inconsistent. This would, therefore, explain the large amounts of variation in the LOI data.

It does not seem feasible to obtain a dry-weight of salt crystals without heating a sample to over 311 ℃. In doing so, however, the temperature of the samples would be increased above the point at which many organic volatiles would combust, for example, wood combusts at 260 ℃ (Ramdahl, 1983). It therefore does not seem feasible to obtain true values for TOC or LOI of hygroscopic salt samples, as they cannot be heated to desiccation without combustion of some of the carbon.

2.3.3 - Detection of fluid inclusions

a) Morphology of inclusions

Previous studies (Lowenstein et al., 2011, Schubert et al., 2009, Gramain et al., 2011, Sankaranarayanan et al., 2011, Adamski et al., 2006) suggest that, if microbes were present within these samples they would be found within fluid inclusions. The presence, morphology and distribution of fluid inclusions within the thin sections were therefore investigated.

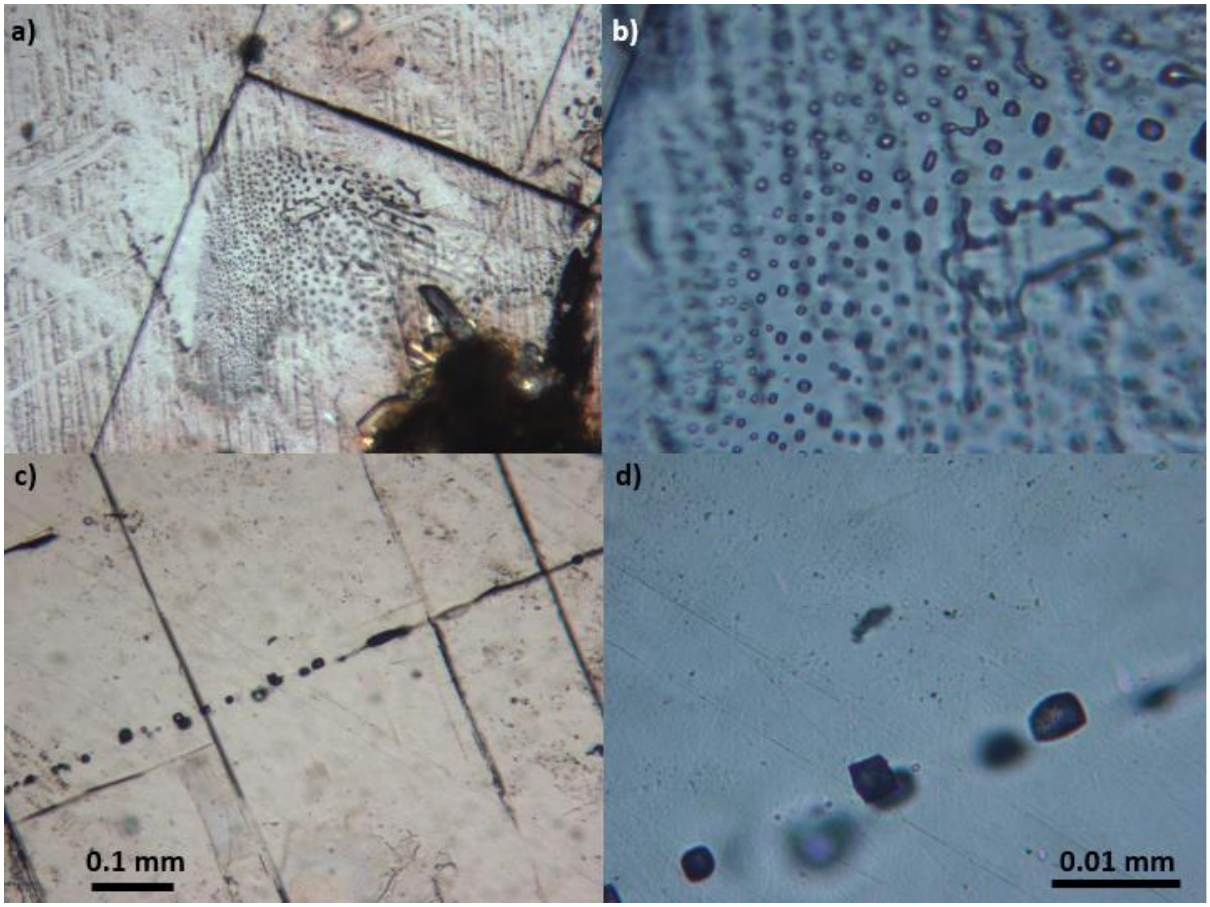

Figure 2.14 - Examples of the two morphologies of fluid inclusions: observed in a sample of CPH from Site E. a) and b) show fluid inclusions forming at high abundance within single crystals (magnification ×60). c) and d) show inclusions forming a straight-line that cuts across multiple crystals (magnification ×15). a) and c) correspond to b) and d) respectively.

Using the technique of searching for large groups of inclusions outlined in Section 2.2.4, fluid inclusions were observed to be present in all thin sections (two of CPH, one of silty halite and three of primary potash). These groups of inclusions had two morphologies: groups of inclusions within a single crystal, or arranged in straight lines, a single inclusion wide, that crossed crystal boundaries (Figure 2.14). There was no difference in the distribution of these fluid inclusions or their morphologies between primary potash, CPH and silty halite.

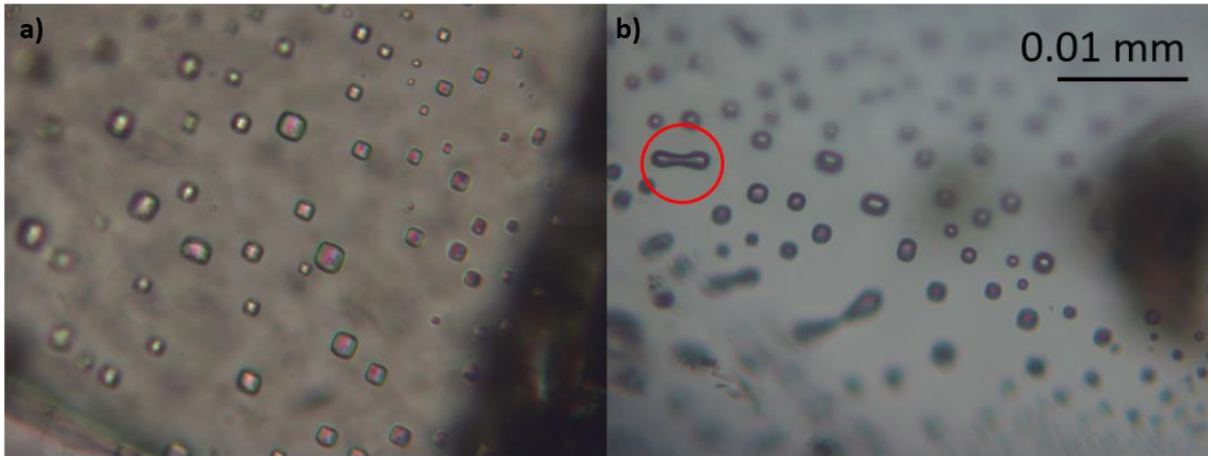

Figure 2.15 - a) Typical morphology and size of fluid inclusions observed in a sample of Boulby Halite from Site A. b) A similar group of fluid inclusions, with a rare "dumbbell" shape (highlighted). Both images taken at ×60 magnification

The majority of the fluid inclusions were square (Figure 2.15), although the occasional dumbbell shape (Carter and Hansen, 1983) was also visible where two inclusions merged. The majority of the squares-shaped inclusions had sides of approximately 20 μm, although smaller sizes were also seen.

b) Composition of inclusions

When using the microprobe to investigate the distribution of minerals with the thin sections (Section 2.3.1d), a group of fluid inclusions was observed within a section of category B (presumably sylvite) crystals from the Boulby Potash (Figure 2.16). This area corresponds to the one labelled in Figure 2.9e in Section 2.3.1b.

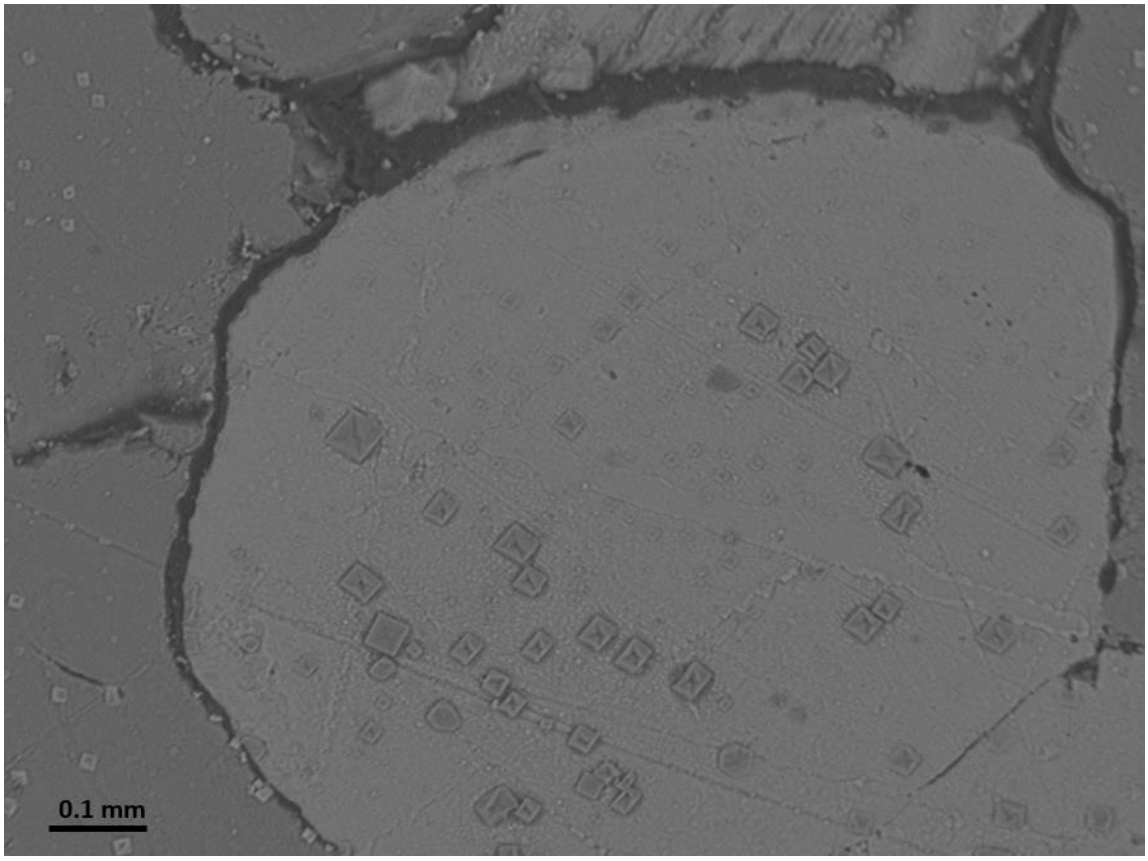

Figure 2.16 - Backscatter electron image from the electron microprobe of an area from a sample of primary potash. This area of crystal contains a high density of fluid inclusions.

Compositional data of four of these inclusions was investigated, but it should be acknowledged that that results would have been affected by the fact that these thin sections had not been polished (Section 2.2.1g) and that the beam had to pass through layers of sylvite before and after hitting the inclusions. Despite these drawbacks, the results show a clear difference in inclusion composition compared to the surrounding sylvite (Figure 2.17). There was no significant difference ($p > 0.05$) in the Cl concentration (52.23 %), but Na was only present at 0.35 % in the sylvite and was significantly higher in the inclusions ($p < 0.05$). For three of the inclusions, Na had a concentration of approximately 50 %, but the final inclusion was much lower at 25%.

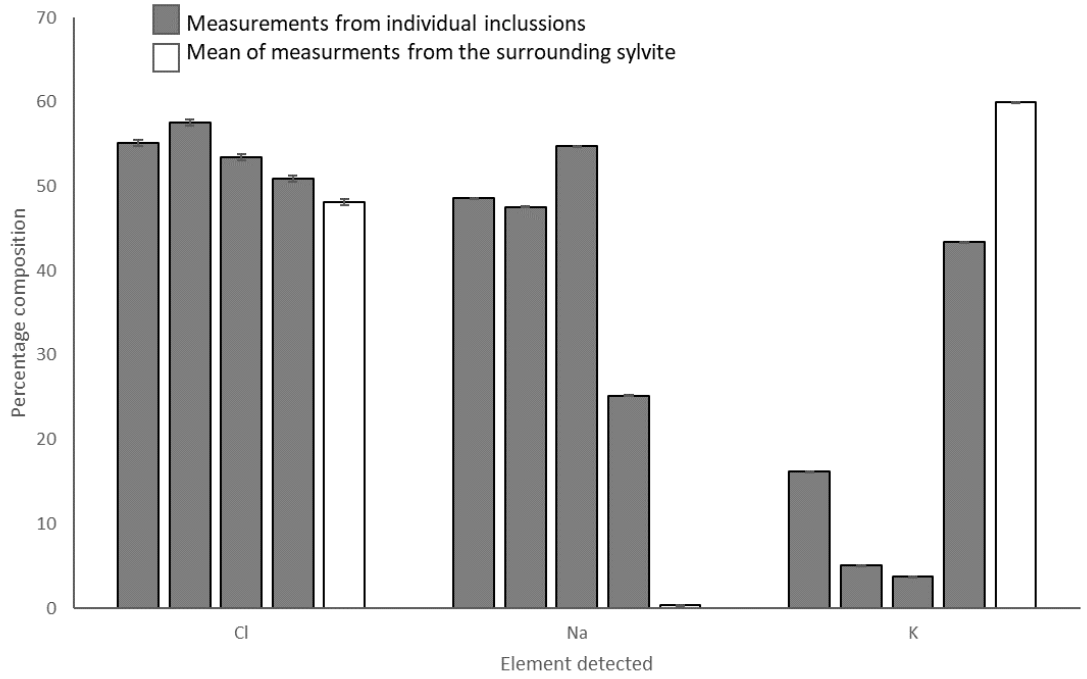

Figure 2.17 - EMPA compositional data from 4 fluid inclusions in close proximity to each other, compared to the mean values from the surrounding sylvite (sylvite n *= 3). Errors bars are standard deviations from within the sylvite*

There was likewise a significant difference in the K concentration of these inclusions compared to the surrounding sylvite ($p < 0.05$). The K concentration varied more between inclusions than the Na did, but in all four inclusions was much lower than the 60% observed in the surrounding sylvite. The EMPA was calibrated to also detect Fe, Mn, Si, Mg, Ca, Al and S (Section 2.2.2b), but these were not detected in either these inclusions or the surrounding sylvite.

Owing to the problems outlined above, care must be taken in over-interpreting these data. For example, the lower Na concentration in one inclusion might represent a difference in its composition, but it might also represent thicker sylvite in this area of the unpolished section. Nevertheless, this is valuable circumstantial evidence to imply that within the K-rich, Na-poor sylvite, the fluid inclusions contain more Na and less K.

2.4 - Discussion

2.4.1 - Sample identification

The samples taken from the Boulby Potash on the second sampling expedition had their composition confirmed to be potash (as defined in the Introduction to this thesis, Section 1.5.1). All but one of the samples of the Boulby Halite from this expedition had their composition confirmed to be halite. The exception was the sample from Site B, which was closer in geochemical composition to the Boulby Potash. The origin of this sample remains uncertain, and it was excluded from further statistical analysis of the samples and the microbiological characterisation in the next chapter. While samples from Site X on the first expedition did not undergo geochemical characterisation, the high rate of successful identification of potash and halite from sites A, B, D & E implies that the samples from Site X are likely to also have been correctly identified.

2.4.2 - Sample composition

Geochemical analysis of the samples had shown that the concentration of Na within the Boulby Halite was relatively consistent throughout the bed, though other elements (K, Ca, Mg, etc.) varied. The Boulby Potash, in comparison, was highly variable in composition for all elements. From a commercial perspective the Boulby Potash is divided into primary and secondary varieties based on their silt content, but Woods (1979) instead described variations based upon the ratios of halite, sylvite and silt within the samples and classified the potash into five categories (A-E, Table 2.12).

Table 2.12 - Descriptions of the five categories of Boulby Potash as defined by Woods (1979)

	A	**B**	**C**	**D**	**E**
Colour	Grey	Grey	Grey	Grey or Red	Grey or Red
Sylvite	Long horizontal crystals	Long horizontal crystals. Excess of 50% of the sample	Long horizontal crystals.	High concentrations. Sometimes in excess of 40% of the sample	Low concentrations. Sometimes below 25% of the sample
Halite	High in $CaSO_4$	High in $CaSO_4$	Sometimes can make up a very large amount of the sample	No description provided	High concentrations. Sometimes in excess of 75% of the sample
"Silt" content	Low concentration	Low concentration	High concentration	Low concentration	Low concentration

Woods (1979) described these categories as highly localised, with a sharp transition between them. No evidence of transition between these categories was observed on the sampling expedition but, with the exception of their colour, many of the differences between categories would not be detectable by eye. The maximum size of an area of a specific category was stated to be a kilometre squared (Woods, 1979), much larger than the distance between the sites in this project, and no minimum size was given. It is, therefore, plausible that some of the sites might have contained different categories of Boulby Potash that went unnoticed at the time of sampling.

All the samples of Boulby Potash obtained in this study were red indicating that they are likely to belong to either category D or E (Table 2.12). The samples from Site A and Site D, both had KCl concentrations in excess of 35% of the sample, indicating that these samples were likely to be of type D, whereas the samples from sites B and E had KCl concentrations below 28 % of the sample, implying that these might have been of Type E.

Woods' (1979) description of Boulby Mine does not feature much discussion of the interface region between the Boulby Halite and the Boulby Potash. It is, however,

described as highly variable, although this variation is primarily considered in terms of different locations within the mine rather than in terms of the stratigraphy as a whole or the lateral variation observed in these results. The hypothesis had been made that vertical variation would be seen, such that samples from nearer the Boulby Potash would have higher K concentrations than samples from nearer the Boulby Halite. This was not observed, and no significant difference was observed in any of the compositional elements of samples from the top or bottom of the interface at the same site. The intention had been to investigate whether the microbial community within the interface differed across the transition from Boulby Halite to Boulby Potash, but these results indicate that this is not possible as chemically this transition does not appear to occur.

The geochemical data across all the samples does, however, presents a range of Na and K concentrations in order to investigate how the changes in the composition of the samples effects community, but this cannot be investigated on a site by site basis. By continuing to include two samples from the interface at each site in the microbial analysis, however, a statistically valid number of samples of both interface type (well defined and poorly defined) can still be investigated (n = 4 of each). This, therefore, can allow investigation into community differences between the various lithologies independent of the overall chemical composition.

2.4.3 - Evidence for alteration

There was an abundance of evidence that some aqueous alteration had occurred since the Permian origin of the samples. For example, the morphology of fluid inclusions cutting across crystals in a straight line (as observed in Figure 2.14c) is typically formed

by secondary alteration, as water moves through the crystals leaving the inclusions behind (Schubert et al., 2009a, Fish et al., 2002).

The XRD data also provides evidence of secondary alteration: the only Ca phase detected was $CaSO_4$, although prior studies indicated the presence of primary $CaCl_2$ within Boulby Mine (Woods, 1979). $CaSO_4$ on the other hand, represents a secondary mineral formed *via* aqueous alteration later in the beds' geological history (Woods, 1979). The $CaSO_4$ may originate from the dissolution and mobilisation by groundwater of Ca^+ and SO_4^- from one of the two nearby (Figure 2.18) anhydrite beds (Woods, 1979).

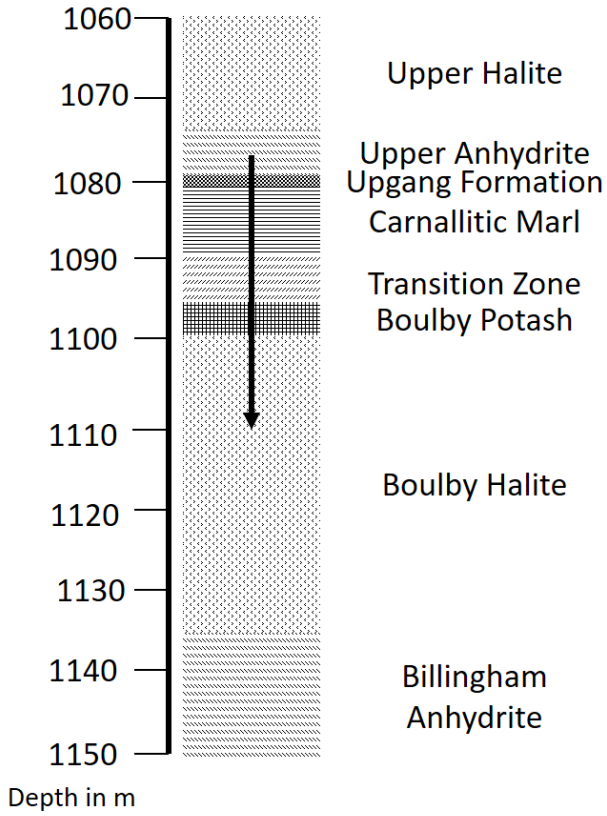

Figure 2.18 - Postulated movement of $CaSO_4$ through the stratigraphic column to the samples

Woods (1979) suggested that fluid flow through the mine had been upwards (Woods, 1979), but there are two pieces of evidence to support the proposal that the aqueous alteration seen in the present study had occurred *via* downward movement of fluid.

Firstly the “foam structure” of halite and sylvite crystals (Figure 2.9), which is characteristic of chlorides that have undergone post-burial recrystallization (Hardie et al., 1985), was only visible in the Boulby Potash thin sections, and never in the Boulby Halite. This implies that the samples from higher beds had undergone more alteration than those from the lower ones. Secondly, the ICP-MS and XRD showed that Ca concentrations decreased with depth at each sample site, which implies downward movement of water. This, in turn, implies that the $CaSO_4$ had been delivered to the rocks by fluid that had moved through the upper anhydrite, presumably passing through the Upgang Formation, Canalitic Marl and Transition Zone along the way (Figure 2.18).

If the Ca was representative of aqueous alteration of the rocks, then this would also explain why the concentrations of many of the minor elements in the samples correlated with Ca, rather than Na or K. They, presumably, also precipitated at the same time as the Ca in the same aqueous alteration event.

2.4.4 - Summary and conclusions

The sampling expedition to Boulby Mine retrieved a variety of samples of both the Boulby Halite, and the Boulby Potash as well as the interface between them.

The confirmation and characterisation of the samples’ compositions will allow a comparison with their community composition in the next chapter. The analysis presented in this Chapter revealed significant intra-lithology variation in composition, as well as potential downwards movement of water through the samples, as evidenced by the presence of $CaSO_4$, that had not been expected in advance. Chapter 3 outlines the community composition of these samples, and the observations in this Chapter need to

be considered in the interpretation of the microbial community and its relationship with salt composition.

Further, the carbon content of all the samples was below the detection limits of the TOC instrument, which implied that the biomass of the samples must be very low and a low-yield of DNA should be expected and planned for. The approach to this is outlined in the next chapter.

Chapter 3: Effect of salt composition on the microbial community in Boulby Mine's deposits

3.1 - Introduction

The aims of this chapter are twofold:

- To determine the microbial diversity within the Boulby Mine evaporites that were characterised in Chapter 2
- To determine whether the cationic composition of these evaporites influences the microbial community structure.

In Chapter 2, samples of Boulby Potash and Boulby Halite from four locations within Boulby Mine were collected and their composition determined. The results showed that these samples represented a range of Na and K compositions, but had relatively consistent Cl concentrations (approximately 3.83×10^5 ppm). This, therefore, allows investigation into whether the cationic composition of the evaporates influences the composition of the microbial community.

Prior work investigating microbial communities that form within evaporites with different compositions from the same saltern showed that gypsum deposits ($CaSO_4.2H_2O$) were dominated by photosynthetic algae, whereas halite (NaCl) was dominated by obligate halophilic archaea (Oren, 2005). These differences are unlikely to be a result of the different evaporite's ability to support different microorganisms, but are more likely to be a result of the changing microbial community of the saltern itself over time (Oren, 2005). This is likely to be driven by the changing salinity of the brine as the evaporites precipitate, first gypsum and then halite (Oren, 2005). The initial

salinity of a saltern is relatively low, supporting photosynthetic algae, which become entombed in gypsum. With increasing evaporation, the salinity increases, resulting in a saltern community composition dominated by obligate halophilic archaea, which become entombed in the later-precipitating halite.

Further studies of salterns have indicated that, once halite precipitation is complete and K salts have started to precipitate (Grant et al., 1998a), the microbial community of a saltern will again change in structure (Javor, 2012, Baati et al., 2011). Although the community composition of the K salts in these settings has not been investigated, it is expected that once K salts start to precipitate, the $MgCl_2$ concentration of the remaining brine becomes elevated, which drives extreme changes of the saltern's chaotropicity and pH (Javor, 2012, Baati et al., 2011), and may encourage a change to the microbial community composition.

Evidence from liquid culture studies also suggests that differences in microbial community might be observed between NaCl- and KCl-rich evaporites (Brown and Gibbons, 1955). Brines of optimum halophile salinity (3.42 M) in a greater than 2:2 KCl:NaCl ratio will not support the growth of obligate halophiles, and growth is still heavily inhibited at below 2:2 ratios (Brown and Gibbons, 1955). Other studies have shown the same effect is induced by $MgCl_2$ and NaBr (Mullakhanbhai and Larsen, 1975, Oren and Bekhor, 1989). These previous studies might, therefore, imply that communities in salts with a low NaCl content may not be dominated by the obligate halophilic archaea which dominate all previously studied NaCl-rich deposits (Schubert et al., 2010, Vreeland et al., 2007, Park et al., 2009).

This Chapter therefore presents culture-independent techniques used to investigate entombed community composition across the lithological transition from Boulby Potash

to Boulby Halite and across the range of compositions determined in Chapter 2. The aim is to investigate whether communities differ between NaCl-rich salts and salts of other compositions, and if so, what possible reasons might be behind this. This will, in turn, shed light on whether potential martian deposits of compositions other than NaCl (see Chapters 1 and 2) would be able to entomb microorganisms.

3.2 - Materials and Methods

3.2.1 - Sample selection

Chapter 2 described the excavation and characterisation of samples from Boulby Mine. The samples had been surface sterilised in order to investigate only microorganisms entombed within the samples and not those on the surface. Sixteen samples were chosen for microbiological investigation and they are listed in Table 3.1. Samples of primary potash, the top of the interface, the bottom of the interface and the Boulby Halite were used from each site (with the exception of Site B where the sample of "halite" had anomalous composition) and the sample of Secondary Potash from Site A. These samples showed a range of Na concentrations from 1.60×10^5 - 3.85×10^5 ppm, K concentrations from 8.60×10^2 - 2.72×10^5 and Ca concentrations from 0 - 3.21×10^4 ppm (Chapter 2), allowing an investigation into how the microbial community changed with composition. The community structure of these samples was ascertained, for the most part using culture-independent techniques, as described below.

Table 3.1 - Samples investigated for community analyses in this Chapter. Table shows the site and lithology of each sample, as well as the concentrations of the main components as determined via ICP-MS in the previous chapter (Section 2.3.1e) and the presumed Cl concentration based upon combining the Na and K concentration

Site	Lithology	Na	K	Ca	Si	Presumed Cl
A	**Secondary Potash**	$1.60\times10^{5} \pm 2.38\times10^{3}$	$2.72\times10^{5} \pm 3.98\times10^{3}$	$3.21\times10^{4} \pm 9.05\times102$	$3.01\times10^{3} \pm 7.09\times10^{2}$	4.32×10^{5}
A	**Primary Potash**	$2.35\times10^{5} \pm 1.93\times10^{3}$	$2.41\times10^{5} \pm 5.24\times10^{3}$	0 ± 0	$2.40\times10^{3} \pm 5.39\times10^{2}$	4.76×10^{5}
A	**Top of the interface**	$3.54\times10^{5} \pm 3.78\times10^{3}$	$2.64\times10^{4} \pm 3.41\times102$	0 ± 0	$2.55\times10^{3} \pm 4.16\times10^{2}$	3.80×10^{5}
A	**Bottom of the interface**	$3.37\times10^{5} \pm 9.26\times10^{3}$	$4.69\times10^{4} \pm 1.02\times10^{3}$	$1.06\times10^{3} \pm 2.87\times10^{2}$	$1.75\times10^{3} \pm 4.03\times10^{2}$	3.84×10^{5}
A	**Boulby Halite**	$3.85\times10^{5} \pm 1.88\times10^{3}$	$1.62\times10^{3} \pm 1.54\times101$	$2.12\times10^{3} \pm 2.06\times10^{2}$	$1.70\times10^{3} \pm 1.39\times10^{2}$	3.86×10^{5}
B	**Primary Potash**	$1.93\times10^{5} \pm 1.72\times10^{3}$	$2.19\times10^{5} \pm 5.12\times10^{3}$	$1.69\times10^{4} \pm 6.20\times10^{2}$	$5.22\times10^{3} \pm 8.13\times10^{2}$	4.13×10^{5}
B	**Top of the interface**	$3.19\times10^{5} \pm 2.28\times10^{3}$	$3.55\times10^{4} \pm 9.66\times102$	$6.89\times10^{3} \pm 5.71\times10^{2}$	$3.07\times10^{3} \pm 4.74\times10^{2}$	3.54×10^{5}
B	**Bottom of the interface**	$3.37\times10^{5} \pm 9.26\times10^{3}$	$4.69\times10^{4} \pm 1.02\times10^{3}$	$1.06\times10^{3} \pm 2.87\times10^{2}$	$1.75\times10^{3} \pm 4.03\times10^{2}$	3.84×10^{5}
D	**Primary Potash**	$2.18\times10^{5} \pm 2.85\times10^{3}$	$1.79\times10^{5} \pm 2.34\times10^{3}$	$1.58\times10^{4} \pm 9.28\times10^{2}$	$2.65\times10^{3} \pm 3.34\times10^{2}$	3.97×10^{5}
D	**Top of the interface**	$3.77\times10^{5} \pm 5.64\times10^{3}$	$2.95\times10^{4} \pm 1.41\times10^{2}$	$3.68\times10^{3} \pm 3.47\times10^{2}$	$1.76\times10^{3} \pm 2.25\times10^{2}$	4.07×10^{5}
D	**Bottom of the interface**	$3.60\times10^{5} \pm 3.63\times10^{3}$	$9.61\times10^{3} \pm 1.43\times10^{2}$	$5.96\times10^{3} \pm 5.96\times10^{2}$	$1.84\times10^{3} \pm 4.70\times10^{2}$	3.70×10^{5}
D	**Boulby Halite**	$3.71\times10^{5} \pm 4.94\times10^{3}$	$2.95\times10^{3} \pm 3.18\times101$	$2.45\times10^{3} \pm 2.73\times10^{2}$	$2.01\times10^{3} \pm 2.00\times10^{2}$	3.74×10^{5}
E	**Primary Potash**	$2.68\times10^{5} \pm 3.70\times10^{3}$	$1.39\times10^{5} \pm 2.19\times10^{3}$	$6.43\times10^{3} \pm 6.38\times10^{2}$	$2.52\times10^{3} \pm 2.78\times10^{2}$	4.07×10^{5}
E	**Top of the interface**	$3.03\times10^{5} \pm 3.66\times10^{3}$	$1.56\times10^{4} \pm 1.85\times10^{2}$	$2.10\times10^{4} \pm 9.84\times10^{2}$	$1.48\times10^{3} \pm 2.64\times10^{2}$	3.18×10^{5}
E	**Bottom of the interface**	$3.43\times10^{5} \pm 5.14\times10^{3}$	$2.82\times10^{3} \pm 2.44\times101$	$8.07\times10^{3} \pm 4.06\times10^{2}$	$1.49\times10^{3} \pm 4.53\times10^{2}$	3.46×10^{5}
E	**Boulby Halite**	$3.33\times10^{5} \pm 4.78\times10^{3}$	$8.60\times10^{2} \pm 2.72\times101$	$8.70\times10^{2} \pm 5.53\times10^{2}$	$2.42\times10^{3} \pm 1.56\times10^{3}$	3.34×10^{5}

3.2.2 - Initial DNA extraction

The first step in community characterisation was to extract genomic DNA from the samples. DNA was extracted from each sample (16 samples, *n* = 3, therefore a total of 48 DNA extracts), in a randomised order, using a modified version of the desalting method described by Sankaranarayanan et al., (2011). The modifications were employed because Leuko et al., (2008) had shown that desalting methods such as this produce a lower yield of some genera of archaea that have a thick cell wall (e.g. *Haloarcula)*. Prior work culturing microbes from these deposits (Norton et al., 1993, McGenity et al., 2000, Cockell, 2017), had implied that the community would be dominated by archaea. In order to improve the yield of what was presumed to be a large part of the entombed community, a heat shock step was added to encourage lysis of these cell types.

In this modified method, 2 g of homogenised sample (Section 2.2.1f) was dissolved in 10 ml of ddH_2O and heated for 30 min at 80 °C. The dissolved sample was concentrated using a 200 µl Amicon centrifugal filter (Ultra-0.5, 50 kDa pore size, YM-50) *via* centrifugation at 3,000 × *g*, at 4 ℃, for 8 min. Following each round of centrifugation the filter was refilled to 200 µl with dissolved sample. The centrifugation and refilling was repeated 17 times. Centrifugation beyond this point typically resulted in very little solution passing through the filter due to the accumulation of silt.

The salt was then diluted/washed out of the filters by a further seven rounds of centrifugation (as above), this time refilling between spins with ddH_2O instead of sample, as described by Sankaranarayanan et al. (2011). The filters were then inverted placed in sterilised 1 ml centrifuge tubes, and centrifuged a final time for 6 min at 6,000 × *g*. The final volume of solution was 200 µl, but the concentration of DNA was below

the detection limits of the laboratory's ThermoScientific Nanodrop 1000, which were 2 ng/µl (Scientific, 2008). The low concentration made ascertaining the presence of DNA problematic; it could not be proven that these had been successful until the amplification stages of the terminal restriction fragment length polymorphism (tRFLP) analyses**.**

3.2.2 - Terminal Restriction Fragment Length Polymorphism (tRFLP)

a) Overview of the tRFLP process

The microbial community composition was assessed using tRFLP analysis, which is a low cost, high-throughput method for investigating microbial diversity and allows statistical differentiation between the different samples. The method involves partial amplification of the 16S rRNA gene using the polymerase chain reaction (PCR). The forward primers (63F and A341F, Bell, 2010 and Baker et al., 2003) had been created with a 6-carboxyfluorescein (6-FAM) attached to their 5' ends.

The PCR products were then fragmented *via* digestion with a restriction enzyme (MspI, Section 3.2.2c). The size of the terminal restriction fragments (tRF) varied according to the specific microbial group (Habtom et al., 2017). The frequency of each fluorescent fragment size was ascertained during the final stage of tRFLP analysis.

Using a combination of Illumina MiSeq and tRFLP analysis, it was possible to identify the taxa that were most likely to contribute to each of the sizes of fluorescent fragments in the tRFLP profile, and thus identify the taxa that change in abundance between samples.

b) PCR with fluorescent primers

For this study, the hypervariable V2 region of the bacterial and archaeal 16S rRNA gene was amplified. The 50 µl PCR mixtures for both bacteria and archaea were identical and contained 10 µM of both forward and reverse primers, 5 µl of PCR Buffer, 1 µl of 2 mM dNTP mix and 0.5 µl of 5 U/µl Taq polymerase. To this, 33.5 µl of the DNA extracts obtained using the Amicon filters, as described above (Section 3.2.2), was added. The bacterial primers (Bell, 2010) were 63F (5′-CAGGCCTAACACATGCAA GTC-3′) and 530R (5′-GTATTACCGCGGCTGCTG-3′) while the archaeal primers (Baker et al., 2003) were A341F (5′-CCTAIGGGGIGCAICAG-3′) and A1204R (5'- TTMGGGGCATRCIKACCT-3′). The PCR programs were as follows:

- Bacteria: initial denaturation at 94 °C for 10 min, followed by 35 cycles of denaturing for 45 secs at 94 °C, annealing for 1 min at 56 °C, elongation for 3 min at 72 °C, followed by a final elongation for 10 min.
- Archaea: initial denaturation at 94 °C for 5 min, followed by 35 cycles of denaturing for 1 min at 94 °C, annealing at 55 °C for 1 min and extension at 72 °C for 1 min, followed by a final extension for 10 min.

The DNA concentration of both the DNA extracts and the completed PCRs were too low to visualise using gel electrophoresis. The DNA concentration of the PCR reactions could not be ascertained *via* nanodrop because the PCR mixture included DNA (dNTP mix and primers) that could not be distinguished from PCR product. The success of the PCR was determined using a positive control. The Discussion section of this Chapter (Section 3.4.5b) will, therefore, include discussion of whether the data is indicative of tRFLP carried out on a successful extract or not. For the archaea, DNA extracted from

Halobacterium noricense (obtained in Chapter 4, Section 4.3.2) was used as a positive control, while the bacterial positive control came from a mixed culture of bacteria inoculated from the River Dee by a fellow student (Curtis-Harper, 2017). Both positive control DNA extracts had a concentration of 10 ng/µl. The selection of samples for further downstream analyses, using the tRFLP approach, was dictated by the presence of a successful positive control during the PCR amplification stage.

c) Restriction digest

The combination of low DNA concentrations and volumes led to the decision not to purify PCR products, as this would cause unacceptable loss of sample. PCR products were digested with the restriction enzyme MspI, which fragments DNA at the sequence CCGG (Waalwijk and Flavell, 1978). This digestion was carried out in a 10 µl reaction, containing 8.6 µl of PCR product, 1 µl of Cutsmart Enzyme Buffer and 0.3 µl of 30 U/µL MspI, for 12 hrs at 37 °C. Samples were then stored at -4 ℃ until they were shipped to Macrogen, Seoul, for analysis.

d) Fragment analyses

Fragment analysis was carried out by Macrogen using a 3730XL DNA analyser. Analysis of the electropherographs were carried out with the commercial software GeneMarker v2.6.4 (Hulce et al., 2011). tRF profiles were analysed in the same random order that they been used for DNA extractions. GeneMarker was used to group fluorescent (start of the PCR product) fragment sizes into manually created bins. Individual peaks presenting less than 50 nucleotides were not included in subsequent analysis as they could not be distinguished from primer dimers, which caused significant noise. Peaks that were separated from each other by two, or less, base pairs, and never occurred

within the same profile, were assumed to be the same peak with slippage of the size ladder. These merged peaks were assigned the mean size of the peaks, rounded to the nearest whole number. In general, the profiles had a relatively stable baseline, and there were relatively few peaks, so no peaks were discounted due to their small size. The relative fluorescence of each peak within each tRFLP profile was determined.

3.2.3 - MiSeq analyses

To facilitate the identification of the tRFLP fragments, MiSeq analyses was carried out on the DNA extracts. The aim of the MiSeq analyses was not to necessarily produce a detailed breakdown of the community structure of the evaporites (though it could shed some light on it), but to provide a list of sequences and their associated taxa which could be used to infer taxonomic identities to the tRFLP data. In order to maximise the efficacy of the tRF identification, the illumina sequencing was conducted on all 48 DNA extracts (Section 3.2.2), pooled together, regardless of their lithology or sample site.

Illumina MiSeq analyses of the pooled DNA extracts were carried out via RTL genomics in Texas using Illumina MiSeq 2x300 flow cell at 10pM. This required a DNA concentration of at least 10 ng/µl, whereas the DNA extracts that had been pooled all had a DNA concentration too low to be determined. A concentration step was therefore required.

The DNA was concentrated using the phenol:chloroform/isopropanol protocol (Sambrook and Russell, 2006). In brief, an equal volume of phenol:chloroform was added to the pooled DNA extract. The DNA and phenol:chloroform were mixed via inversion and centrifuged at 16,000 × *g* for 4 min. The top layer, containing the DNA dissolved in chloroform, was transferred to a sterile Eppendorf tube. The DNA was

precipitated by adding an equal volume of -20 ℃ isopropanol (100 %) and incubating at room temperature for 6 hrs. The precipitate was pelleted by centrifugation at 16,000 × *g* for 5 min. The pellet was washed twice with 70 % -20 ℃ ethanol and centrifuged again. ddH_2O was then added in 20 µl volumes until the pellet had fully dissolved.

The concentration of the new DNA solution was quantified using a ThermoScientific Nanodrop 1000 and was found to be 110 ng/µl. The final concentration was adjusted to 15 ng/µl using ddH_2O. This final concentration of DNA was re-confirmed, again using the Nanodrop (ThermoScientific). This process was accompanied by the same process being carried out on an equal volume of autoclave sterilised ddH_2O. No pellet formed in this negative control, and the nanodrop could not detect any DNA. This implied that the DNA found in the concentrated pooled sample had come from the DNA extraction and that the extractions had been successful.

The pooled and concentrated DNA extract was sequenced using the Illumina MiSeq platform (Caporaso et al., 2011) by RTL genomics, Texas. Sequencing was carried out using the primers 28F (GAGTTTGATCNTGGCTCAG) and 388R (TGCTGCCTCCCGTAGGAGT) for bacteria (Aquino, 2017) and Arch341F (CCTACGGGAGGCAGCAG) and Arch806r (GGACTACVSGGGTATCTAAT) for archaea (Mesa et al., 2017). The unedited datasets provided by RTL genomics can be found within the CD attached to this Thesis, in the folder named “MiSeq Raw Data”.

Quality filtering and identification of the sequences was conducted with the open source program *Mothur* v1.39 (Schloss et al., 2009). Sequences were aligned against the Silva database of 16s genes (Oksanen et al., 2007). Identical sequences were grouped together and those that were too long, too short, appeared chimeric or contained

obvious sequencing errors, such as long strings of repeated bases (homopolymers), were removed. Taxonomy was generated using the BLAST algorithm against the RDP Training set v14 database of archaeal and bacterial 16S rRNA genes (Callahan, 2016). The sequences, their taxonomy and their abundances can also be found in the CD attached to this Thesis, in the folder named "MiSeq as analysed by Mothur".

3.2.4 - Synthesis of MiSeq and tRFLP data

In silico digestions were carried out *via* online Restriction Mapping software (Stothard, 2000) at http://www.bioinformatics.org/sms2/rest_map.html as part of The Sequence Manipulation Suite using the MspI restriction endonuclease. The small number of potential peaks, and relatively low diversity of the MiSeq data meant that Microsoft Excel could be used to manually compare fragment sizes from the tRFLP data with predicted fragment sizes in the MiSeq and thus identify the peaks. Fragment sizes produced by the most abundant sequences in the MiSeq data corresponded to the largest peaks in the tRFLP data, plus or minus 4 bp. The tall peaks of similar fragment size within the MiSeq and the tRFLP were assumed to represent the same nucleic acid sequences. Once these tall peaks had been identified, smaller, less distinctive ones could be identified by examining which peaks predicted by the MiSeq fell between those already identified. Where multiple taxa could contribute a peak, a note was made in the relevant part of the results section.

3.2.5 - Other DNA extraction methods

Following concentration of the pooled DNA extracts, the samples were sent to RTL Genomics for sequencing. Whilst these pooled extracts contained sufficient DNA for sequencing with the bacterial primers, this was not the case for the archaea. RTL

genomics attempted sequencing using multiple archaeal primer pairs, but without success. The low concentration of archaeal DNA was further demonstrated by carrying out PCR on the remains of this extract using the tRFLP primers alongside the positive controls. PCR using bacterial primers was successful, but no bands appeared when PCR was carried out on this extract using the archaea primers.

a) Trouble shooting

When the DNA extracts were pooled to produce the sample for MiSeq (see Section 2.2.5c), isopropanol was used to precipitate the DNA from the solution. The amount of precipitate that was produced was considerably larger than would be expected given the eventual final concentration of DNA measured.

Upon further inspection, and comparison to DNA extractions carried out on cultures of microorganisms (for the work in Chapter 4), it was realised that this precipitate was not DNA. The DNA precipitate appeared as small powdery particles of bright white colouration; whilst in contrast, the narrow, off-white strands (e.g., DNA) was seen when the DNA was precipitated from the pure cultures.

The composition of the small powdery precipitate was investigated using a Zeiss Supra 55VP, Field Electron Gun - Scanning Electron Microscope (FEG-SEM). Three samples of the pellet were fully dissolved in ddH_2O, transferred to microscope slides and dried overnight in a laminar flow hood. The precipitate formed as a viscous substance that adhered to the slide. The slide was then carbon coated (15-20 nm thickness) and mounted within the chamber of the FEG-SEM instrument at an accelerating voltage of 20.00 kV and a 7-10 mm working distance.

Under the FEG-SEM, the precipitate in all three samples appeared to have a similar structure, with irregular shapes typically 5 µm wide (Figure 3.1). Analysis using Energy Dispersive Scattering (EDS) was undertaken to establish the composition of the precipitate. The primary components of all nine spectra were Ca, O and S (Figure 3.1). While these results cannot be fully quantified due to the lack of a polished flat surface, or comparison with standards, the co-detection and high abundance of these three elements would imply that the precipitate is primarily $CaSO_4$. Na and Cl were also detected in lesser amounts in all samples, which was not unexpected given the source of the samples.

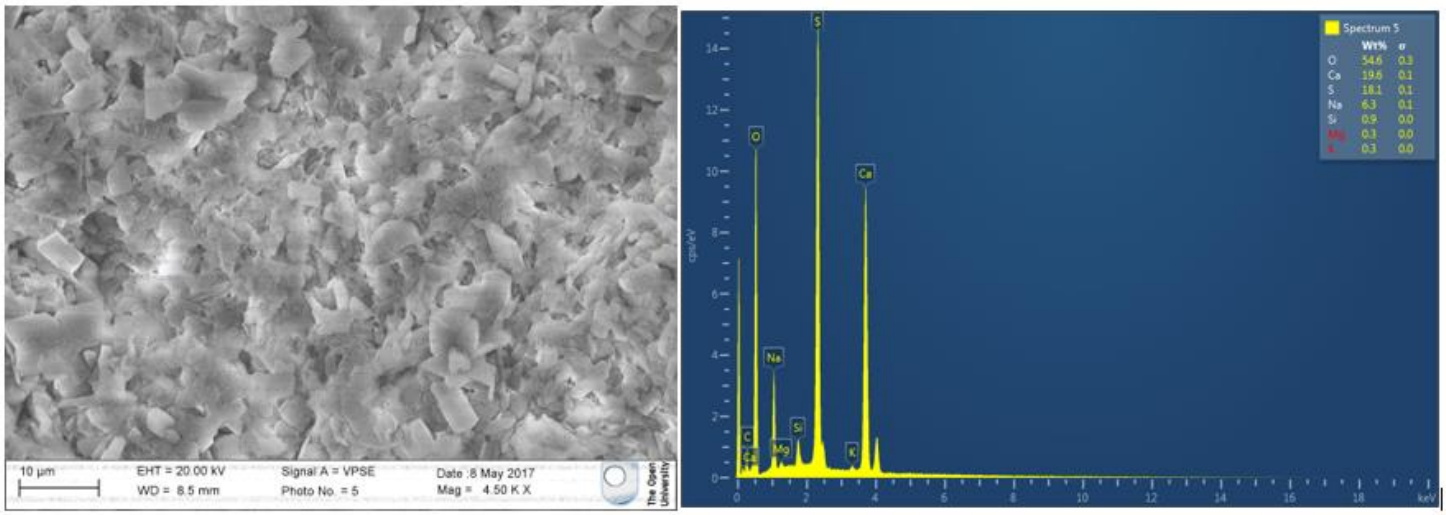

Figure 3.1 - Representative FEG-SEM secondary electron image of the precipitate and accompanying EDS spectra

The ICP-MS analyses of the geological samples had shown they contain $CaSO_4$ (Section 2.3.1d), but always less than 2 % of the concentration of Na or Cl, whereas FEG-SEM analyses of the precipitate following DNA extraction showed the $CaSO_4$ exceeded NaCl. This would imply that, while the washing step in the DNA extraction had removed the main salts, the $CaSO_4$ had been concentrated within the filters along with the DNA. As this does not occur with the Cl^- ions, this might be a result of the larger size of SO_4^{-2} ions,

or a result of the filter potentially possessing a greater affinity to ions with a higher charge.

As it could now be assumed that the majority of the pellet was $CaSO_4$, rather than DNA, attempts were made to add low volumes of water to the precipitate such that the $CaSO_4$ would not be fully dissolved, but the DNA would. When the $CaSO_4$ was not fully re-dissolved, however, PCR (both archaeal and bacterial) was not successful; either the undissolved $CaSO_4$ was inhibiting the PCR reaction or DNA would not enter solution if the $CaSO_4$ was not dissolved. The DNA could not be separated from the $CaSO_4$ or concentrated. As a result, it was concluded that the DNA extracts obtained using the original desalting method was unsuitable for carrying out MiSeq analyses on the archaea due to the low concentration of DNA.

This investigation into the precipitate formed by the phenol:chloroform/isopropanol protocol demonstrated that the concentration of the DNA solution could not be further increased without also raising the $CaSO_4$ concentration in such a way as to prevent downstream use of the DNA. A variety of techniques were employed to attempt to extract sufficient DNA using culture-independent techniques but were not successful. All of these techniques were paired with DNA extraction from a culture of archaea grown in salt-rich media, to act as a positive control. These techniques are listed below, with further details available in Appendix 3:

- Attempts to re-optimise the phenol purification step
- Incubation with Proteinase K between the heat shock and filtration stages of the filter DNA extraction protocol

- Addition of a beat beating step between the heat shock and filtration stages of the filter DNA extraction protocol
- Attempting to purify DNA from the filter DNA extraction protocol by means of a commercially available Zymo Genomic DNA Clean & Concentrator kit
- Use of a CTAB-based DNA extraction protocol, previously used to extract archaeal DNA from solid salt samples (Leuko et al., 2008)
- Use of a bead beating DNA extraction protocol, previously used to extract archaeal DNA from solid salt samples (Leuko et al., 2008)
- Use of a commercially available MP Biomedicals FastDNA™ SPIN Kit.

b) DNA Extraction from culturable archaea

None of the techniques listed above produced sufficient concentrations of archaeal DNA for MiSeq. As a last resort, a culture-based technique was employed to produce a larger microbial biomass for DNA extraction. However, there were limitations to this. The vast majority of microbes within an environmental sample are considered "unculturable" as they will not grow in laboratory conditions. A DNA extract obtained this way would contain only microorganisms suited for growth in the laboratory and, while three different media (that had shown the ability to allow growth of halophilic archaea, see Chapter 4) were used, this would not represent the diversity or distribution of the archaea in the natural environment. This method would, however, provide information regarding some members of the archaeal community, which could be used as a starting point for interpreting the tRFLP data.

Growth media used in this study were optimised for Chapter 4 and are covered in greater detail in Section 4.2.1; however, in brief they are described here:

- **100% Modified Payne's Media** (Norton et al., 1993): A litre of media contained 10 g of Difco yeast extract, 7.5 g of casein hydrolysate, 2 g of KCl, 3 g of trisodium citrate, 200 g l^{-1} NaCl, 20 g l^{-1} $MgSO_4$, 1 ml of 50 g l^{-1} $FeSO_4.7H_2O$ solution and 1 ml of 0.36 g l^{-1} $MnCl_2.4H_2O$ solution. This was made in two parts: an 800 ml part containing the NaCl and $MgSO_4$ and a 200 ml part containing the rest of the ingredients. Both parts had their pH adjusted to between 7 and 7.5, were autoclaved separately and combined in a laminar flow hood.
- **10% Modified Payne's Media:** 100% Modified Payne's Media had been diluted ten-fold in 200 g l^{-1} NaCl that had been pH adjusted to between 7 and 7.5.
- **200 g l^{-1} NaCl:** Saline solution with no nutrients.

In this experiment, 1 g of each of the sterilised, homogenised samples were pooled to a final mass of 16 g. The sample was then dissolved in 160 ml of a 100 g l^{-1} NaCl, 10 g l^{-1} $MgSO_4.7H_2O$ buffer developed by Gramain et al. (2011) to a final concentration of 200 g l^{-1} of salt (halite and potash). The crystals were dissolved in this buffer to ensure that any entombed obligate halophiles were not exposed to osmotic shock.

For dissolution, the suspension was heated at 32 ℃, 180 rpm for 3 hrs. Once the salt was dissolved, 3 ml of the suspension was used as an inoculum into 22 ml of media such that the final concentration of the inoculum solution within each culture was 12 %.

For each of the media types, 15 cultures were set up in 50 ml falcon tubes, with a 25 ml headspace. These falcon tubes were incubated in the dark at 38 ℃. After 1 month, DNA was extracted from the cultures using a modified version of the CTAB method employed by Leuko et al., (2008). For this, 2 ml of each successful culture was centrifuged in sterile Eppendorf tubes at 4,000 x *g* for 8 min at room temperature and resuspended in

576 µl of TE buffer (10 mM Tris-HCl pH 8.0, 1 mM EDTA). For cell lysis, 30 µl of 10 % SDS and 9 µl of proteinase K (10 mg/ml) were added to the tubes prior to incubation at 40 °C, with continuous mixing at 150 rpm. After 3 hrs, 100µl of 5M NaCl was added along with 80 µl of CTAB solution (41 g l^{-1} NaCl and 100 g l^{-1} CTAB). The samples were then heated at 65 °C for 20 min in a heat block. These were allowed to cool to room temperature, before they were pooled and purified using the same phenol:chloroform/isopropanol method used to concentrate the pooled samples (Section 3.2.5c).

3.2.6 - Statistical analyses

tRFLP ordination analyses were carried out using the vegan (Oksanen et al., 2007) and ecodist packages (Goslee and Urban, 2007) for the statistics software R Studio. The dissimilarity of the tRF profiles between rocks of different chemical compositions was tested using analysis of similarity (ANOSIM) tests. The data is displayed graphically using nonmetric multidimensional scaling (NMDS). In these plots, data points near each other represent communities with a similar structure, whereas data points far apart have a dissimilar structure. Groupings and patterns of the distribution of these points can therefore show variation within the community and shed light on clusters of samples with a similar community compared to the total dataset. For both ANOSIMS and NMDS analyses, the tRFLP data needed to be converted into a distance matrix. This was carried out using analyses of Bray-Curtis dissimilarity and the same distance matrix was used for both analyses. A separate distance matrix generated using a binary conversion factor was used to compare the frequency of peaks between profiles, independent of abundance.

Microbial diversity between groups of samples was examined by generating rarefaction curves using the rarecurve function in the vegan package for R. Rarefaction curves required all values to be integers, whereas tRFLP data was typically presented as a percentage of the total community. Some fragments and families contributed as little as 0.001 % of the community. As a result, all values were multiplied by 1,000 to convert them into integers for rarefaction analyses.

Once tRFs could be matched up with taxa, SIMPER statistical tests were carried out using the ecological statistics program Primer (Clarke and Warwick, 1994), in order to determine which microbial families were most affected by the differences in chemical composition.

3.3 - Results

In order to investigate whether the evaporites of different composition contained different microbial communities, the data from the tRFLP analyses presented in this Chapter is considered in the context of the geological and geochemical setting described in Chapter 2.

3.3.1 - Bacterial community

Owing to the use of different primers (Section 3.2.2) the archaeal and bacterial data had to be considered separately. The bacterial data is presented first.

a) Fragment distribution

The bacterial communities from each of the rock samples (16 samples in triplicate producing 48 profiles) were examined using community fingerprinting to provide a

measure of the relative abundance of the various terminal restrictions fragments (tRFs) produced by each sample. Although 48 DNA extracts were analysed, only 46 were successfully amplified to produce tRF profiles.

Across all 46 tRF profiles there were 70 distinct peaks observed. These peaks represented different fragments lengths, varying in size from 53 - 164 bp. Universally present in all of the samples were peaks of 57 bp, 97 bp and 164 bp (Figure 3.2).

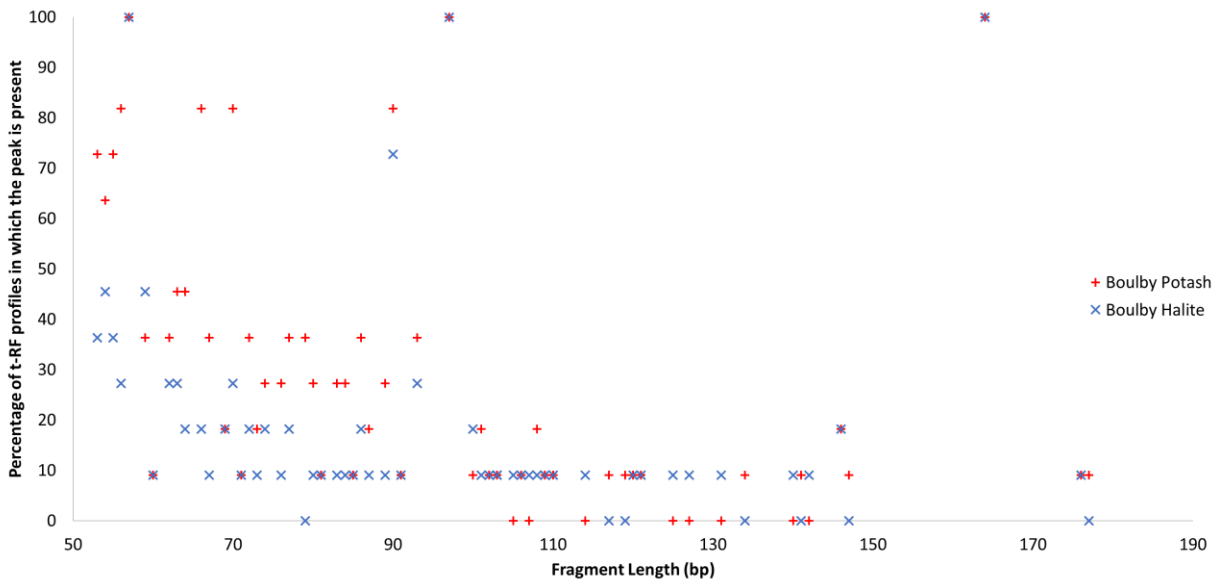

Figure 3.2 - Plot showing variation in the frequency of the peaks between the Boulby Potash and the Boulby Halite

An ANOSIM statistical test was carried out investigating the frequency of the peaks occurring between samples, independent of the heights of the peaks. This showed that the likelihood of a peak being present in a sample was statistically different depending on which bed the sample came from ($p > 0.05$). As a general rule, the peaks with a smaller fragment size were more common within the Boulby Potash than in the Boulby Halite (Figure 3.2). There were seven peaks unique to the Boulby Halite (peak size 79, 117, 119, 134, 141, 146 and 177 bp) and eight peaks unique (peak size 105, 107, 114, 125, 127, 131, 140 and 142 bp) to the Boulby Potash, although in all cases they only

appeared in a relatively small number of T-RFLP profiles, approximately 9% of the samples of the lithology they appeared in).

b) Overall composition of the community

MiSeq analyses

The different fragment sizes reported in the tRFLP analyses correspond to different numbers of bases within strands of DNA. MiSeq analysis was carried out on pooled DNA, from the 48 extracts used for tRFLP analyses. This maximised the chances that all the DNA strands which produced fragments in the tRFLP analysis would be represented in the MiSeq data.

The data from the MiSeq analysis resulted in 38,331 raw reads. These reads ranged in size from 35 to 500 bp, with a mean length of 347 bp and a median of 345 bp. Following quality filtering using the *Mothur* v1.39 software, the number of sequences were reduced to 33,738 reads of 2,813 unique sequences. These sequences ranged in length from 273 to 349 bp, with a median length of 306 bp and a mean of 307 bp. They can be found in the CD attached to this Thesis, in the folder named "MiSeq as analysed by Mothur".

The 16S rRNA genes collected from this sequencing operation were compared to the RDP taxonomy database (as described in Section 3.2.4) and a taxon was assigned to each sequence. All sequences could be identified to the family level with a confidence of 80 % or higher.

The bacterial community contained seven known bacterial phyla (Figure 3.3), which represented 95 % of the obtained sequences. The remaining 5 % of the sequences were those that could not be classified within a known phylum. The three most abundant

phyla were *Proteobacteria* (36.33 %) *Actinobacteria* (25.04 %) and *Firmicutes* (20.64 %), as shown in Figure 3.3. The remaining 13 % of the community consisted of the candidate phyla *Saccharibacteria* (7.32 %), *Fusobacteria* (2.81 %), *Bacteroidetes* (2.77 %) and *Acidobacteria* (0.12 %).

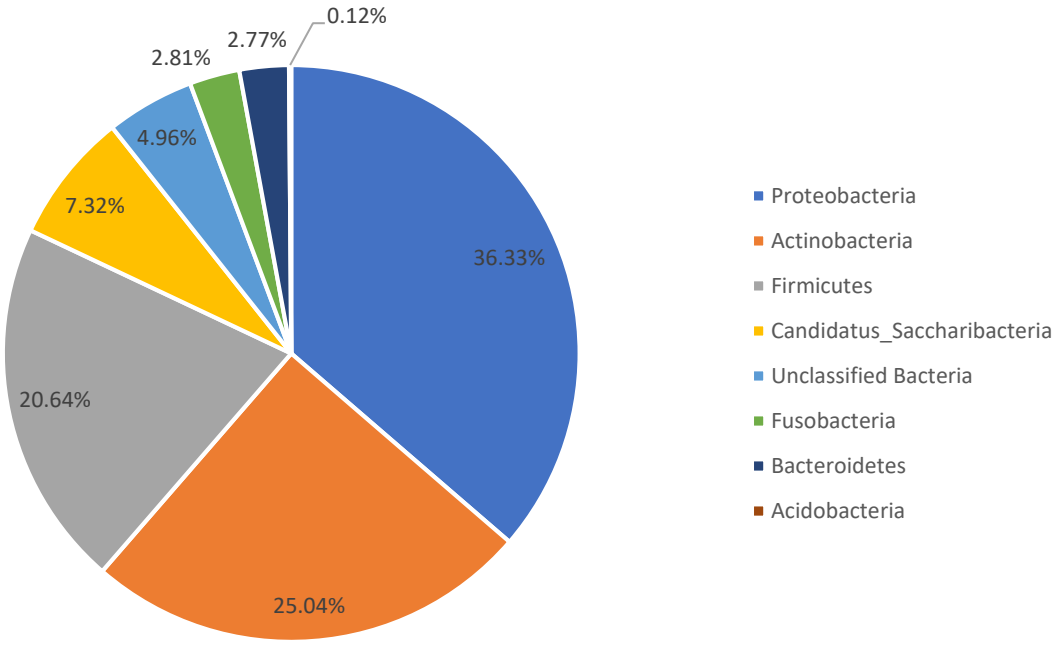

Figure 3.3 - Phyla detected within the MiSeq analyses

There was relatively low diversity within these seven phyla within the MiSeq analysis. The *Actinobacteria*, *Saccharibacteria*, *Fusobacteria* and *Acidobacteria* were each represented by only a single class. The *Bacteroidetes* were represented by five classes but were dominated by just two: the *Cytophagia* and *Flavobacteria.* The *Proteobacteria* were also represented by five classes but were mostly *Alphaproteobacteria* and a smaller amount of *Gammaproteobacteria.* The *Firmicutes* were represented by four classes but the *Clostridia* dominated followed by the *Bacilli* and *Negativicutes.* A detailed breakdown of the classes detected in the other phyla, and the contribution of individual classes to the total community, can be found in Table 3.2.

Table 3.2 - Classes detected in the bacterial community via MiSeq analyses

Phylum	**Class**	**Percentage of total community**
Acidobacteria	Subgroup Gp6	0.12
Actinobacteria	*Actinobacteria*	52.04
Bacteroidetes	Unclassified	0.62
Bacteroidetes	*Bacteroidia*	0.06
Bacteroidetes	*Cytophagia*	1.18
Bacteroidetes	*Flavobacteria*	0.91
Bacteroidetes	*Sphingobacteria*	3.09×10^{-3}
Saccharibacteria	Unclassified	7.32
Firmicutes	*Bacilli*	4.52
Firmicutes	*Clostridia*	14.31
Firmicutes	Unclassified	0.06
Firmicutes	*Negativicutes*	1.76
Fusobacteria	*Fusobacteria*	2.81
Proteobacteria	*Alphaproteobacteria*	21.96
Proteobacteria	*Betaproteobacteria*	1.64
Proteobacteria	*Deltaproteobacteria*	0.01
Proteobacteria	*Gammaproteobacteria*	9.43
Proteobacteria	Unclassified	3.28
Unclassified	Unclassified	4.96

In total, 53 families were detected within the MiSeq analyses (Table 3.3). The identification of all of these families had a confidence level of 80 % or higher. Of these 53 families, the only one with a relative abundance greater than 10 % of the total community was the *Lachnospiraceae* from the phylum *Firmicutes.* This family accounted for 14.3 % of all the sequences. The next most abundant families were the *Propionibacteriaceae* (9.2 %) and *Micrococcaceae* (7.7 %), which both belong to the *Actinobacteria* phylum.

Table 3.3 - Families detected within the MiSeq analyses, and their taxonomy. Continues onto next page

Phyla	**Class**	**Order**	**Family**	**Percentage of total community**
Acidobacteria	*Subgroup Gp6*	*Gp6*	Unclassified	0.123
Actinobacteria	*Actinobacteria*	*Acidimicrobiales*	*Iamiaceae*	0.062
			Actinomycetaceae	0.139
			Corynebacteriaceae	0.225
			Intrasporangiaceae	1.512
			Microbacteriaceae	2.200
			Micrococcaceae	7.743
			Nocardioidaceae	3.919
			Propionibacteriaceae	9.175
			Unclassified	0.068
Bacteroidetes	*Bacteroidia*	*Bacteroidales*	*Bacteroidaceae*	0.046
			Unclassified	0.009
	Cytophagia	*Cytophagales*	*Cytophagaceae*	1.179
	Flavobacteriia	*Flavobacteriales*	*Flavobacteriaceae*	0.913
	Sphingobacteriia	*Sphingobacteriales*	*Chitinophagaceae*	0.003
	Unclassified	Unclassified	Unclassified	0.617
Firmicutes	*Bacilli*	*Bacillales*	*Bacillaceae_1*	0.321
			Staphylococcaceae	0.537
			Unclassified	0.015
		Lactobacillales	*Aerococcaceae*	0.744
			Enterococcaceae	1.392
			Lactobacillaceae	0.130
			Streptococcaceae	1.299
			Unclassified	0.083
	Clostridia	*Clostridiales*	*Lachnospiraceae*	14.298
			Unclassified	0.012
	Negativicutes	*Selenomonadales*	Unclassified	1.756
	Unclassified	Unclassified	Unclassified	0.056

Phyla	Class	Order	Family	Percentage of total community
Fusobacteria	*Fusobacteriia*	*Fusobacteriales*	*Fusobacteriaceae*	2.815
Proteobacteria	*Alphaproteobacteria*	*Caulobacterales*	*Caulobacteraceae*	0.173
		Rhizobiales	*Bradyrhizobiaceae*	1.978
			Hyphomicrobiaceae	0.951
			Rhizobiaceae	3.682
			Unclassified	0.472
		Rhodobacterales	*Rhodobacteraceae*	7.459
			Rhodospirillaceae	5.663
			Unclassified	0.670
		Sphingomonadales	*Sphingomonadaceae*	0.873
		Unclassified	Unclassified	0.043
	Betaproteobacteria	*Burkholderiales*	*Comamonadaceae*	0.667
			Unclassified	0.787
		Unclassified	Unclassified	0.188
	Deltaproteobacteria	*Desulfovibrionales*	*Desulfovibrionaceae*	0.009
	Gammaproteobacteria	*Enterobacteriaceae*	*Enterobacteriaceae*	1.105
		Legionellales	*Coxiellaceae*	2.222
		Pasteurellales	*Pasteurellaceae*	1.241
		Pseudomonadales	*Moraxellaceae*	2.312
			Pseudomonadaceae	2.219
		Unclassified	Unclassified	0.025
		Xanthomonadales	*Xanthomonadaceae*	0.315
	Unclassified	Unclassified	Unclassified	3.281
Saccharibacteria	Unclassified	Unclassified	Unclassified	7.317
Unclassified	Unclassified	Unclassified	Unclassified	4.956

A rarefaction curve was plotted. This curve forms a plateau (Figure 3.4), indicating that this was a relatively accurate representation of the community within the samples.

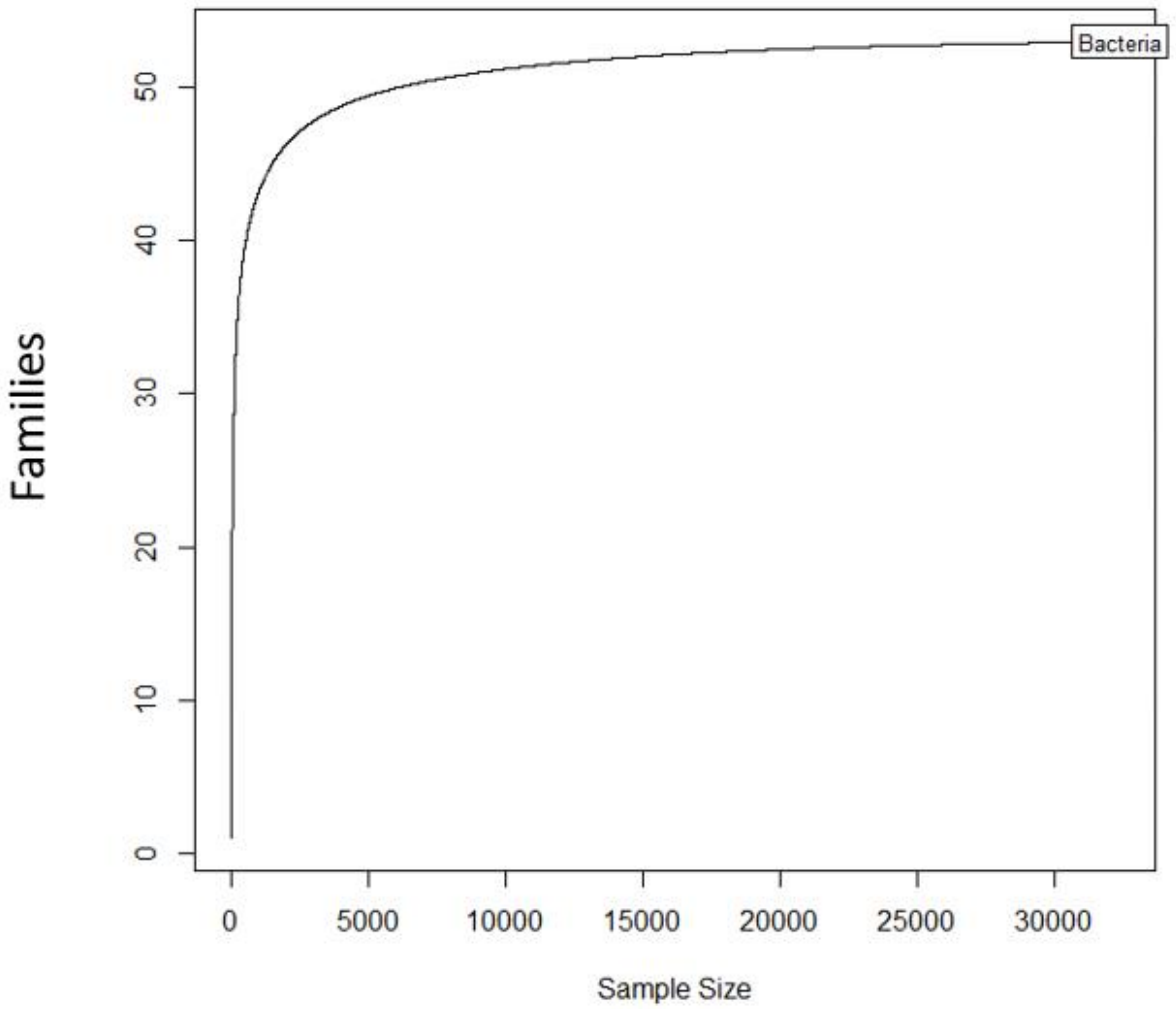

Figure 3.4 - Rarefaction curve of the families detected within the MiSeq analyses.

tRFLP Analyses

In-silico digestion of the MiSeq fragments using the same cleavage site, as used in the tRFLP analyses, permitted taxonomic identification of the tRFs (Table 3.4). The majority of the peaks were generated by only a single family, which allowed them to be identified with relative ease. Some peaks, however, had more than one family contributing. Where this was the case, the fragments were assigned to the taxonomy of the family that

contributed the most fragments of this length (Table 3.4). For all fragment lengths that could be formed by more than one family, one family would typically produce in excess of 88 % of these fragments (Table 3.4). The only exception to this was the 107 bp long fragment that consisted of 67 % *Actinobacteria* (with a 91 % confidence in the sequence identification) and 33 % *Firmicutes* (with a 100 % confidence in the sequence identification). Following the methodology outlined above, for the purposes of this work, this peak was designated as *Actinobacteria* (Table 3.4). The confidence in the assignment of sequences to families was always > 85 % (Table 3.4).

Table 3.4 - Identification of fragments found in tRFLP using MiSeq. Where a fragment could have more than one family contribute to it, all families that contribute > 5% are shown. Fragments sizes are assigned the taxa that contributes the most to the abundance of the fragment (marked in bold). Table continues onto next page

Fragment Size (bp)	Percentage contribution to fragment abundance	Phylum	Class	Order	Family	Mean confidence of sequence identification
53	**100**	***Bacteroidetes***	***Flavobacteriia***	***Flavobacteriales***	***Flavobacteriaceae***	**100**
54	**99**	***Bacteroidetes***	**Unclassified**	**Unclassified**	**Unclassified**	**87**
55	**100**	***Firmicutes***	***Bacilli***	***Lactobacilliales***	***Enterococcaceae***	**100**
56	**100**	***Proteobacteria***	***Gammaproteobacteria***	***Pasteurellales***	***Pasteurellaceae***	**100**
57-60	**100**	**Unclassified**	**Unclassified**	***Unclassified***	***Unclassified***	**100**
62	**100**	***Bacteroidetes***	***Sphingobacteriia***	***Sphingobacteriales***	***Chitinophagaceae***	**99**
63	**88**	***Bacteroidetes***	***Bacteroidia***	***Bacteroidales***	***Bacteroidaceae***	**86**
63	12	*Bacteroidetes*	*Bacteroidia*	*Bacteroidales*	Unclassified	92
64	**100**	***Proteobacteria***	***Betaproteobacteria***	***Burkholderiales***	***Unclassified***	**100**
66	**100**	***Saccharibaceria***	**Unclassified**	***Unclassified***	***Unclassified***	**91**
67-69	**100**	***Proteobacteria***	***Alphaproteobacteria***	***Rhodobacterales***	***Rhodobacteraceae***	**100**
70-90	**93**	***Proteobacteria***	***Alphaproteobacteria***	***Rhizobiales***	***Rhizobiaceae***	**99**
70-90	7	*Proteobacteria*	*Alphaproteobacteria*	*Rhizobiales*	Unclassified	96
91	**100**	***Proteobacteria***	***Gammaproteobacteria***	***Enterobacteriales***	***Enterobacteriaceae***	**99**
93	**100**	***Actinobacteria***	***Actinobacteria***	***Actinomycetales***	***Nocardioidaceae***	**97**
97	**100**	***Firmicutes***	***Bacilli***	***Bacillales***	***Bacillaceae_1***	**100**
100	**100**	***Proteobacteria***	***Alphaproteobacteria***	***Rhodobacterales***	***Rhodobacteraceae***	**100**
101-103	**89**	***Proteobacteria***	**Unclassified**	***Unclassified***	***Unclassified***	**100**
101-103	5	*Proteobacteria*	*Betaproteobacteria*	Unclassified	Unclassified	86
101-103	5	*Actinobacteria*	*Betaproteobacteria*	*Actinomycetales*	4 different families	100
104-105	**94**	***Actinobacteria***	***Actinobacteria***	***Actinomycetales***	***Nocardioidaceae***	**99**
104-105	6	*Proteobacteria*	Unclassified	Unclassified	Unclassified	100
106	**100**	***Actinobacteria***	***Actinobacteria***	***Actinomycetales***	***Intrasporangiaceae***	**100**

Fragment Size (bp)	Percentage contribution to fragment abundance	Phylum	Class	Order	Family	Mean confidence of sequence identification
107	**67**	***Actinobacteria***	***Actinobacteria***	***Actinomycetales***	***Micrococcaceae***	**91**
107	33	*Firmicutes*	*Bacilli*	*Bacillales*	*Staphylococcaceae*	100
108	**83**	***Proteobacteria***	***Alphaproteobacteria***	***Rhizobiales***	***Bradyrhizobiaceae***	**100**
108	7	*Proteobacteria*	*Alphaproteobacteria*	*Caulobacterales*	*Caulobacteraceae*	100
108	6	*Proteobacteria*	*Alphaproteobacteria*	*Sphingomonadales*	*Sphingomonadaceae*	100
109	**100**	***Actinobacteria***	***Actinobacteria***	***Actinomycetales***	***Micrococcaceae***	**99**
110	**1**	***Proteobacteria***	***Alphaproteobacteria***	***Rhizobiales***	***Bradyrhizobiaceae***	**100**
112	**92**	***Firmicutes***	***Bacilli***	***Bacillales***	***Bacillaceae_1***	**93**
112	8	*Actinobacteria*	*Actinobacteria*	*Actinomycetales*	*Propionibacteriaceae*	99
114	**100**	***Firmicutes***	***Bacilli***	***Bacillales***	***Staphylococcaceae***	**100**
115-118	**100**	**Unclassified**	**Unclassified**	***Unclassified***	***Unclassified***	**100**
119	**100**	***Actinobacteria***	***Actinobacteria***	***Actinomycetales***	***Microbacteriaceae***	**100**
120	**100**	***Proteobacteria***	***Gammaproteobacteria***	***Legionellales***	***Coxiellaceae***	**89**
121	**100**	***Unclassified***	**Unclassified**	**Unclassified**	**Unclassified**	**98**
121-129	**100**	***Actinobacteria***	***Actinobacteria***	***Actinomycetales***	***Propionibacteriaceae***	**100**
129	**100**	***Unclassified***	**Unclassified**	**Unclassified**	**Unclassified**	**100**
132	**100**	***Acidonacteria***	***Subgroup Gp6***	***Gp6***	**Unclassified**	**98**
134-141	**100**	***Actinobacteria***	***Actinobacteria***	***Actinomycetales***	***Actinomycetaceae***	**100**
142	**100**	***Bacteriodetes***	***Cytophagia***	***Cytophagales***	***Cytophagaceae***	**96**
146	**100**	***Proteobacteria***	***Alphaproteobacteria***	***Rhodobacteriales***	***Rhodobacteraceae***	**96**
147	**100**	***Proteobacteria***	***Gammaproteobacteria***	***Pseudomanadales***	**Unclassified**	**100**
164	**100**	***Actinobacteria***	***Actinobacteria***	***Actinomycetales***	***Nocardioidaceae***	**100**
165	**100**	***Firmicutes***	***Clostridia***	***Clostridiales***	***Lachnospiraceae***	**97**
176	**100**	***Proteobacteria***	***Unclassified***	**Unclassified**	**Unclassified**	**100**
177	**100**	***Firmicutes***	***Clostridia***	***Clostridiales***	***Lachnospiraceae***	**100**

c) Community differences between samples

Having identified the fragments, a Bray-Curtis dissimilarity matrix was generated to compare the relative abundance of each of the families between each of the tRFLP profiles. ANOSIM statistical tests were then carried out on this matrix.

An initial test was conducted investigating all samples regardless of source (lithology or sample site). This showed that there were statistically significant differences in community between the different samples ($p < 0.001$), but not between replicates of the same sample. With this in mind, further investigation was carried out to determine the source of these differences.

Comparing lithologies

The results of an ANOSIM test showed that there was no significant difference ($p > 0.05$) in the relative abundance of the families between the different lithologies (regardless of sample site): secondary potash ($n = 1$ in triplicate), primary potash ($n = 4$ in triplicate), top of the interface ($n = 4$ in triplicate), bottom of the interface ($n = 4$ in triplicate) or Boulby Halite ($n = 3$ in triplicate).

As had previously been shown (Section 3.3.1a), when the presence or absence of a fragment within a sample, rather than its actual relative abundance, was considered using a binary distance matrix, a statistically significant difference was observed between the Boulby Potash and the Boulby Halite. However, once these fragments were analysed using the taxonomic identities allotted to them from the MiSeq *in-silico* digestion no statistically significant difference was observed.

The lowest taxonomic level which could be identified *via* the MiSeq analyses was family, so this might indicate variation between the treatments on a taxonomic level below family. This difference in where a statistically significant result was observed could, therefore, imply that the Boulby Potash and Boulby Halite contained different strains or species, but the same families in the same ratios.

Comparing sample sites

ANOSIM tests showed no significant difference in the community composition between samples from different sites (Site A $n = 5$ in triplicate, Site B $n = 3$ in triplicate, Site D $n = 4$ in triplicate, Site E $n = 4$ in triplicate). Also, no significant difference was observed in a two-way test comparing samples of the same lithology from different sites (in both cases, $p > 0.05$).

Relationship with Na and K

The samples displayed a wide range of chemical compositions (see Table 3.1 and Chapter 2), so it was investigated whether the variation in chemical composition of the samples was linked to the variation detected in the tRFLP profiles.

ANOSIM statistical tests cannot investigate variation in community compared to the actual measured values of the elemental concentrations, because this test works by comparing between groups. As a result, in order to investigate whether differences in community composition and chemical composition were linked, the samples had to be sorted into groups based upon their composition.

This was initially carried out using groups based on the samples' K and Na concentrations (as determined *via* ICP-MS, Section 2.2.3e, Tables 2.7 - 2.10) as these

major cations were the compositional elements that differed the most between samples; K and Na concentration had been strongly negatively correlated (Section 2.3.1e). Initially, four groups were investigated:

- K < 0.5 %
- 1 % < K < 5 % (there were no samples where K fell between 0.5 % and 1 %)
- 10 % < K <20 % (there were no samples where K fell between 5 and 10 %)
- 20 % < K <30 %

An ANOSIM statistical test was carried out, which showed that there was no statistically significant difference in community composition between these four groupings (p > 0.05). Modifications were made to the grouping criteria, such that there were fewer larger groups, or more smaller groups, but the ANOSIM did not reveal significant differences between them either (in all instances p > 0.05).

A two-way ANOSIM was also carried out, investigating the combined effect of Na/K concentration and the sample site they came from as simultaneous, but independent variables. Again, there was no significant difference in the community structure between these different groups (p > 0.05).

An NMDS ordination was plotted (Figure 3.5), which confirmed that Na and K concentration did not correspond to differences in community composition; there is significant overlap on the plot between profiles from the low K and high K samples. The NMDS also confirmed the results of the initial ANOSIM comparing replicates of individual samples, showing that the community is not uniform; the data points are well distributed across the plot.

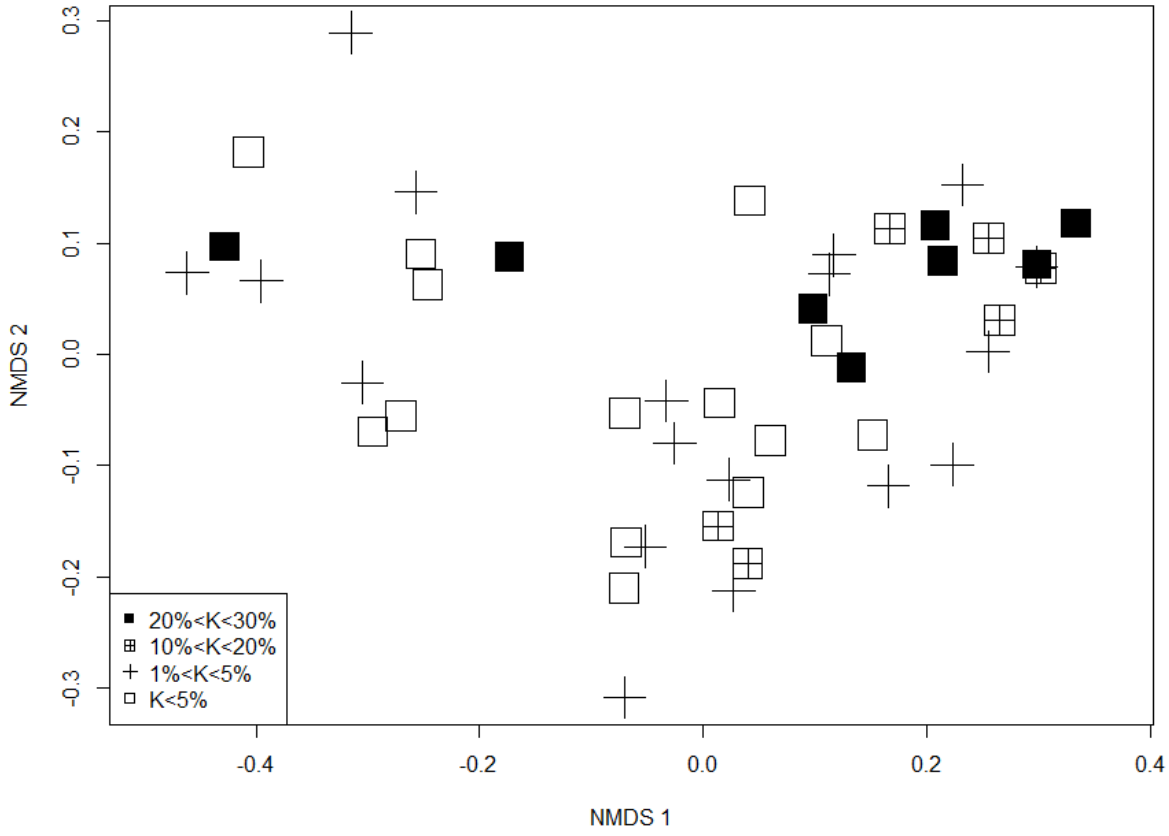

Figure 3.5 - NMDS ordination showing that potassium concentration does not affect the abundance of different bacterial fragments

Relationship with Ca

ICP-MS and XRD had shown heterogeneous distribution of Ca between the samples and this had been linked to aqueous alteration (see Section 2.4.3). In order to investigate the effect Ca had on community composition, as had been undertaken for Na and K, the samples were sorted into four groups according to their Ca concentration. The first two groups designated were the extreme outliers of samples: those with no Ca and those with greater than 1 % Ca. A further two groups were then made by splitting into samples where Ca fell between 0 and 0.5%, and those where it fell between 0.5 and 1%.

The four groups were, therefore, as follows:

- 0 % Ca
- Ca < 0.5 %
- 0.5 % < Ca < 1 %
- Ca > 1 %

The ANOSIM test showed significant differences in community structure between the four groupings of Ca concentration ($p < 0.005$). This was also apparent when the NMDS ordination (Figure 3.5) was altered so that Ca concentrations were plotted (Figure 3.6); there was no overlap between low Ca and high Ca samples. The samples with between 0.5 and 1 % Ca tended to be grouped with the samples > 1 % Ca, whereas the samples with between 0 and 0.5 % Ca were spread across the entire plot.

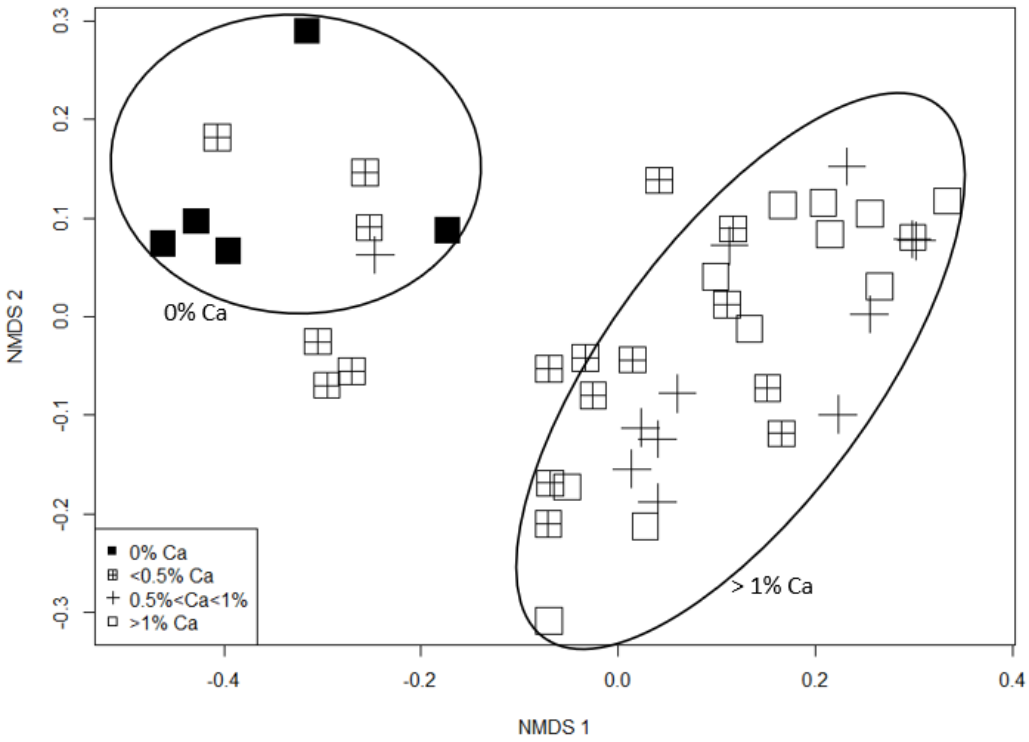

Figure 3.6 - NMDS ordination showing how abundance of bacterial families is affected by calcium concentration.

Relationship with other elements

A significant difference in community structure was also observed when the samples were grouped according to the concentration of some of the elements that had been previously been correlated with Ca concentration: Ba ($p < 0.05$), Sr, Al and Mg ($p < 0.005$). Fe abundances had also been seen to be correlated with Ca abundances, but the ANOSIMS test showed that Fe concentration did not have a statistically significant effect on community composition ($p > 0.05$). This could be a result of the fact that, as discussed in Section 2.3.1e, Fe was absent from many samples that still had small amounts of Ca.

The ANOSIM also showed that Si and Mg had no significant effect on the community composition ($p > 0.05$).

d) Families that differ between samples

The ANOSIM statistical test showed that the only measured factors that influenced the microbial community composition of the samples were the concentrations of Ca and some of the ions that correlated with Ca (Ba, Sr, Al and Mg). With that in mind, the mean abundance of each family was calculated for each of the four Ca groups as defined above (Figure 3.7). It is important to note when considering this data that no conclusions can be drawn about changes in the actual abundance of bacterial cells of each taxa; this data only shows increases and decreases in the relative abundance of each taxa within the total community of unknown (and potentially variable) size. This uncertaintly is discussed in further detail in Section 3.4.3.

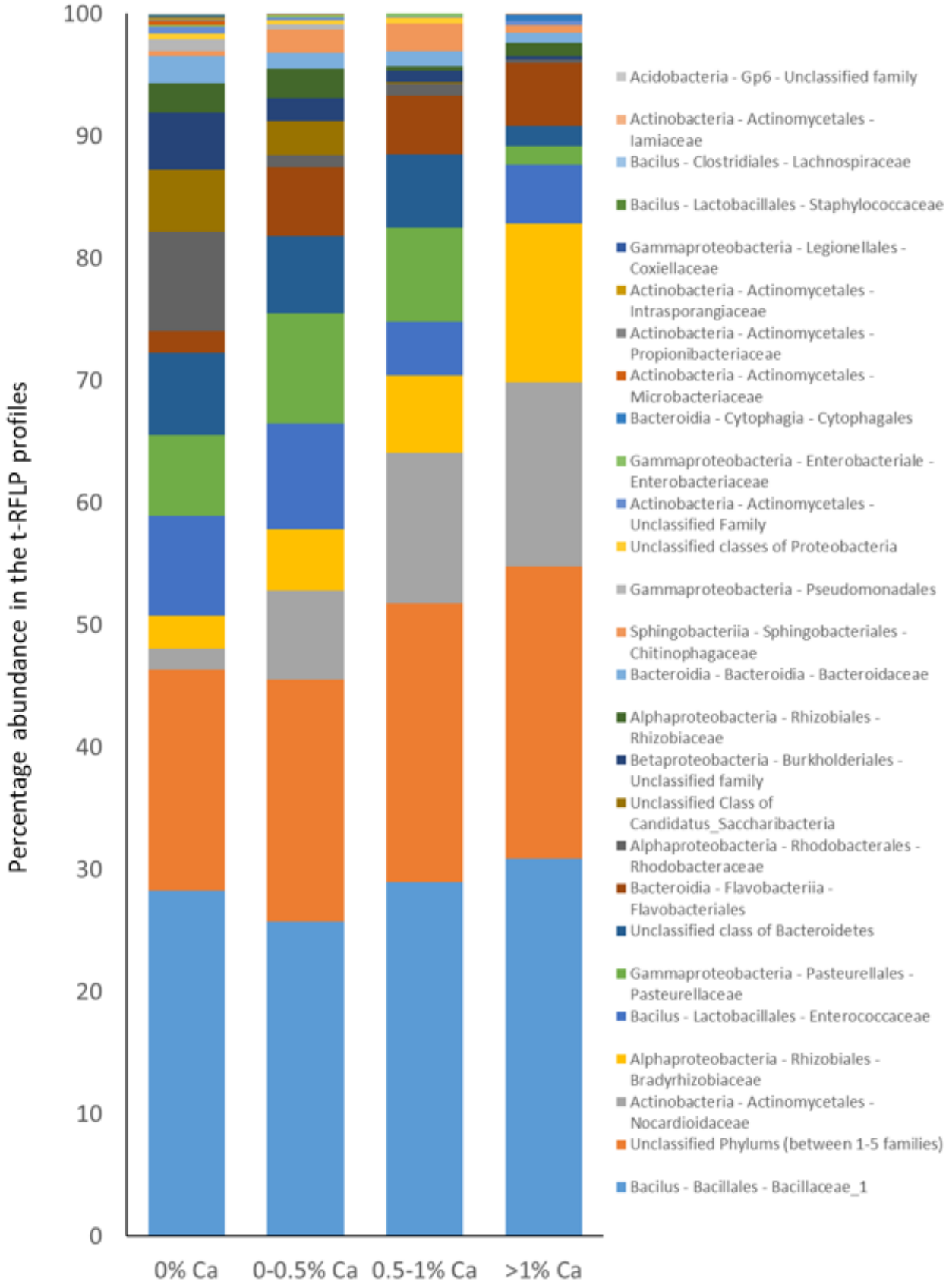

Figure 3.7 - The relative abundance of the taxonomic groupings within samples of different Ca concentration.

A change in community composition with increasing Ca concentration is evident (Figure 3.7). All samples were dominated by the *Bacillacaea_1* and the unclassified phyla. The next two most abundant families, however, the *Nocardioidaceae* and *Bradyrhizobiaceae,* differed significantly in their abundance between samples of different Ca concentration (Student's t-tests where Ca < 0.5 % and > 0.5 %, $p < 0.0001$). There was also a positive correlation between the abundance of both of these families and Ca concentration (Spearman's Rank coefficients = 0.94 and 0.88 respectively).

The *Rhodobacteraceae* showed the most extreme decrease in abundance with increasing Ca concentration. It accounted for 8.1 % of the fragments in the samples with no Ca, but this dropped to 1.0 % in the samples with between 0 and 0.5 % Ca. It then was as low as 0.29 % in the samples with greater than 1 % Ca. The family with the largest increase in abundance with rising Ca were the *Nocardioidaceae*, which went from 1.7 % in the samples with no Ca to 15.0 % in the samples with greater than 1 % Ca

While the *Intrasporangiaceae, Microbacteriaceae, Lachnospiraceae* and *Pseudomonadales* always had low abundances (they were at most 0.1 %, 0.3 %, 0.1 % and 1.0 % respectively), these families were only detected in samples with low Ca concentrations (< 0.5 %), implying that higher concentrations of Ca led to fewer genera in the samples. This was confirmed by comparing the rarefaction curves (Figure 3.8) for each of the four groupings of Ca concentration (again the relative abundances have all been multiplied by 1,000 to ensure they are all integers). While all four curves plateaued, indicating that there were unlikely to be families missed in this analysis, the height of the curves decreased with increasing Ca concentration. Higher Ca concentrations, therefore, corresponded with lower community diversity.

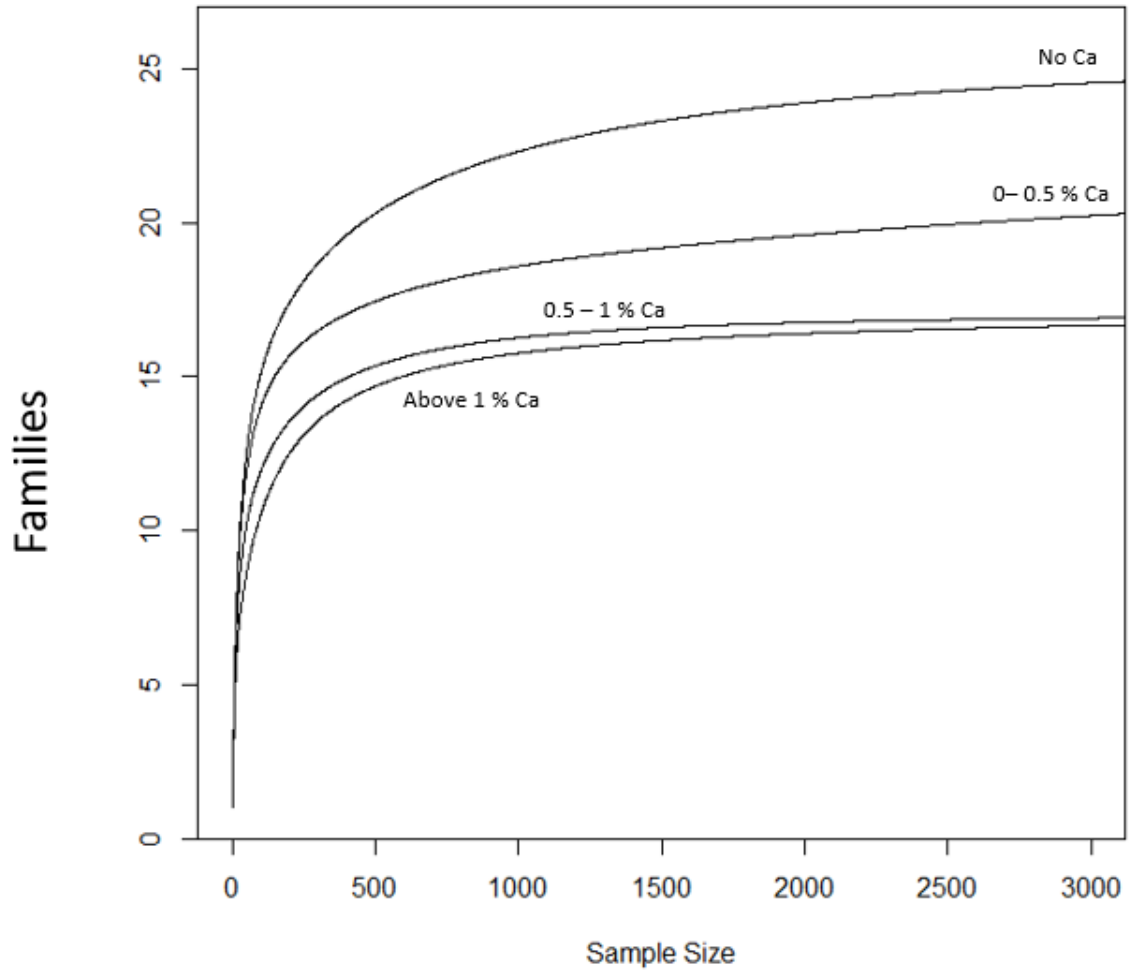

Figure 3.8 - Rarefaction curves, showing species richness within rocks of different elemental composition

A SIMPER statistical test showed the cumulative effect of individual families on bacterial community dissimilarities between samples with different Ca concentrations. Since it was not possible to ascertain the Ca concentration of a sample prior to excavation, there were only two samples with a Ca concentration of 0 %. This was not enough to ensure that the SIMPER test was statistically significant. Therefore, these samples were grouped as those containing 0-0.5 % (inclusive) Ca for this one specific analysis.

Table 3.5 - The taxa most responsible for differences in community structure between different Ca concentrations, as determined by a SIMPER test

Taxa (Class - Order - Family)	**Average abundance in samples below 0.5% Ca**	**Average abundance in samples above 1% Ca**	**Contribution to dissimilarity between two Ca concentrations (%)**	**Cumulative dissimilarity between the two Ca concentrations (%)**
Gammaproteobacteria - Pasteurellales - Pasteurellaceae	7.99	1.45	9.84	9.84
Bacilus - Lactobacillales - Enterococcaceae	8	4.83	9.08	18.92
Bacteroidia - Flavobacteriia - Flavobacteriales	4.52	5.14	8.88	27.8
Alphaproteobacteria - Rhizobiales - Bradyrhizobiaceae	4.27	12.93	8.85	36.65
Unclassified class of *Bacteroidetes*	5.96	1.64	8.74	45.39
Unclassified Class of Candidatus_Saccharibacteria	3.08	0	8.38	53.77
Actinobacteria - Actinomycetales - Nocardioidaceae	5.68	14.91	6.86	60.63
Alphaproteobacteria - Rhizobiales - Rhizobiaceae	2.27	1.11	6.03	66.66
***Betaproteobacteria - Burkholderiales* - Unclassified family**	2.32	0.24	5.65	72.31
Alphaproteobacteria - Rhodobacterales - Rhodobacteraceae	2.35	0.29	5.39	77.7
Bacteroidia - Bacteroidia - Bacteroidaceae	1.38	0.8	4.49	82.19
Sphingobacteriia - Sphingobacteriales - Chitinophagaceae	1.51	0.64	4.14	86.33
Bacilus - Bacillales - Bacillaceae_1	24.63	30.73	2.56	88.89
Unclassified Phyla (Between 1-5 families)	18.24	23.8	2.14	91.03

The SIMPER test showed that 50 % of the difference between samples was a result of six key families. Those that decreased in abundance with rising Ca levels were the *Pasteurellaceae*, *Enterococcaceae*, unclassified class of *Bacteroidetes* and the *Saccharibacteria*, while the *Flavobacteriales* and *Bradyrhizobiaceae* increased in abundance.

3.3.2 - Archaeal community

a) Fragment distribution

Analysis of the tRF profiles of the samples using archaea primers showed 21 peaks, ranging in size from 51 to 192 nucleotides. Of these 21 peaks, seven were relatively common, featuring in at least two of the three replicates of each of the 16 samples analysed. Of the remaining 14 peaks, 12 were unique to individual tRFLP profiles and were not present in replicates of the same sample. Despite the low frequency of these peaks, however, when they were present they were relatively large (the abundance of 13 of these 14 peaks was greater than 0.5 %, the abundance of eight of these 14 peaks was greater than 1 %, and the abundance of two of these 14 peaks was greater than 40 %). Hence, they could not be excluded from the analysis.

As with the bacterial tRFLP data, an ANOSIM test was carried out with the distance matrix only taking into account the presence or absence of the peaks. Unlike with the bacteria, the ANOSIM test showed that there was no significant difference in the presence or absence of peaks between the Boulby Potash or the Boulby Halite. This is probably a result of the large number of peaks with a low frequency between samples, but high relative abundance within individual samples.

b) Overall composition of the community

Attempts were made to carry out partial 16S rRNA gene sequencing using universal archaea primers on the same nucleic acid extracts that had been used to sequence the bacterial community, using the same techniques. RTL genomics in Texas attempted multiple PCR conditions, primers and nested PCRs and hypothesised that this failure was a result of the low DNA concentration of the sample. This would imply that the

archaeal DNA concentration of this sample was below the threshold capable of amplification through PCR techniques.

Multiple attempts were made to extract DNA using methods designed to increase the yield of archaeal DNA. These ranged from modifying the techniques used to successfully extract DNA from the bacteria, to trialling a variety of different techniques (see Appendix 3). None of these attempts were successful.

In order to obtain some sequence data for identification of the archaeal fragments, a mixed community was inoculated from the samples and grown in the laboratory. This community had its DNA extracted and was analysed for MiSeq. This resulted in 81,790 reads of 8,790 unique sequences, ranging in size from 213 to 602 bp, with a mean length of 428 bp and a median of 427. After quality filtering to remove too long, too small or chimeric sequences, as described in Section 2.2.5c, this resulted in 71,695 reads of 1,970 unique sequences. All filtered sequences were 389 bp long and can be found in the CD attached to the back of this Thesis in the folder named "MiSeq as analysed by Mothur".

The 16S rRNA sequences from these cultures were compared with the NCBI Blast database (Johnson et al., 2008). This suggested that, of these 71,695 reads, 71,693 corresponded to *Halobacterium noricense* with 99 % confidence. The remaining two reads corresponded to *Haloarcula* (one with a 99 % confidence and one with 95 %), but they could not be identified to the species level. While the unculturable diversity of the archaea remains uncertain, the culturable diversity is very low. All *Halobacterium noricense* sequences detected in this study would theoretically produce a fragment of 157 bp, which may correspond with a 155 bp long fragment detected in 75 % of the archaeal analyses (mean abundance 5.1 %). The remaining fragments could not be identified.

c) Community differences between samples

As with the bacteria, no significant difference was observed between community composition of samples from different lithologies or sites, or in a two-way test comparing both these factors simultaneously (in all cases $p > 0.05$).

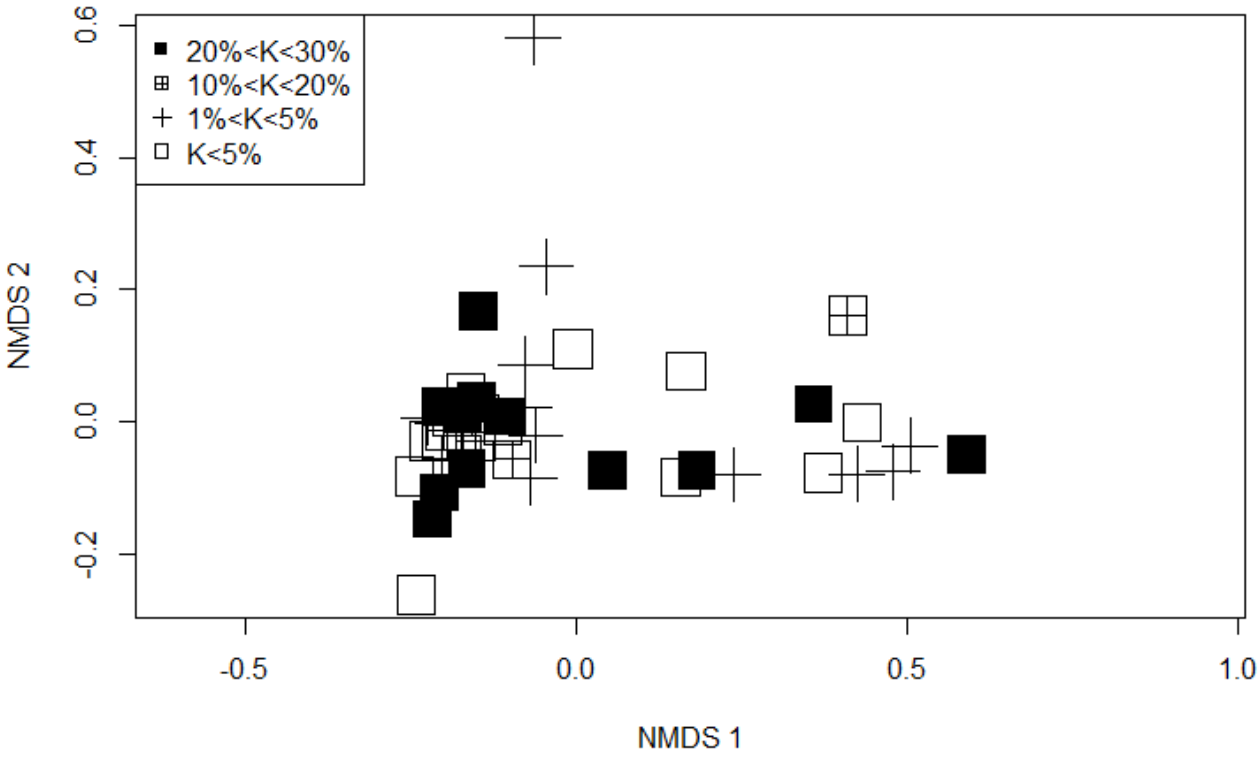

Figure 3.9 - NMDS ordination showing that K concentration does not affect the abundance of different bacterial fragments

For the bacterial analyses, the samples had been grouped according to their composition (Section 3.3.1c) for all the elements detected via ICP-MS (Chapter 2). The same groups were used to analyse the archaeal community. No significant differences in community composition were observed for any of the elements (all ANOISM tests showed, $p > 0.05$). This lack of variation in tRF profiles was supported by the NMDS ordination (Figure 3.9). Unlike in the bacterial NMDS plot, the data was more tightly constrained along the two arbitrary axes with very few outliers. This in turn implied a lack of meaningful difference in community structure.

3.4 - Discussion

3.4.1 - Composition of the microbial community of Boulby Mine

Norton (1993) had isolated microbes from within samples of both the Boulby Potash and the Boulby Halite. This study also showed the presence of DNA within these beds, as well as the interface region between them. The microorganisms identified within this study, however, differed significantly to those in Norton's (1993) results, as discussed below.

a) Archaea

Norton (*ibid.*) had only detected archaea within the mine, namely *Halobacterium saccharovorum* and *salinarium* as well as *Haloarcula vallismortis.* A sufficient yield of archaeal DNA could not be obtained directly from the samples collected in the current study for MiSeq analysis. When mixed cultures were generated using the same media and methodology as Norton, however, only *Halobacterium noricense* and unclassified *Haloarcula* were detected.

Three hypotheses are advanced to explain the differences between this study and the previous one (*ibid*.). The first is that they result from sampling differences. Although this study showed no difference in the composition of the microbial community between different sample sites, this was only over a roughly rectangular area measuring 600 × 400 m. In comparison, Boulby Mine contains over 1,000 km of tunnels and it is uncertain where Norton sampled from. It is therefore possible that over larger or unsampled areas, the archaeal community composition varies despite the fact no evidence of variation was seen in the areas investigated in this study.

This study and Norton's (*ibid*.) also differ in terms of sterilisation techniques. Norton's samples had undergone surface sterilisation by submerging them in ethanol for 5 hrs. More recent studies, however, have called the efficiency of this sterilisation protocol into dispute and suggest that the acid-bleach-based method, employed in this study, is significantly better at removing surface microorganisms (Sankaranarayanan et al., 2011). This might imply that, while the archaea detected in this study came from within the samples, those extracted by Norton may have been on the exterior.

The third hypothesis is that the differences between results of this study and those of Norton (1993) are a result of advancements in the field of taxonomy. Norton's work predated the widespread availability of sequence data, and thus identifications were made based on lipid analysis. It is now known that the extremely charged nature of halophilic, archaeal lipids means that there is less variation between genera than is found in other phyla (Oren, 2012). The advent of 16S rRNA sequencing has led to a significant reordering of the halophilic branches of the taxonomic tree, and the resulting confusion has yet to be fully rectified. Strains that are now believed to be from the same species bear the names of different genera, while strains that are officially nomenclated as *Halobacteria salinarum* can be found to cluster in a variety of different genera instead of the *Halobacteria* (DasSarma and DasSarma, 2008). It is possible that the organisms cultured and identified as *H. saccharovorum, H.salinarium* and *H.vallismortis* by Norton in 1993 would not be recognised *via* sequence data today.

b) Bacteria

While the archaea detected differed from those found previously (*ibid*.), they were, at least, within the same order of the phylogenetic tree. This study, however, also identified 53 families of bacteria, while Norton detected none. Norton's paper describes

the discovery of “eubacteria” in samples from Boulby Mine, but these “eubacteria” are now recognised as archaea.

Studies of the subsurface brines found within Boulby Mine have also shown a community dominated by archaea (McGenity et al., 2000, Cockell, 2017). These brines are formed by fluid flow and dissolution of the evaporites, and it is believed that the communities that inhabit them consist of microbes that have been released from entombment by this dissolution (McGenity et al., 2000, Cockell, 2017). There are no records of bacteria being detected in the Boulby Mine evaporites themselves, however, recently a bacterium has been successfully isolated from these brines (Beblo-Vranesevic et al., 2018). This bacterium, an obligate anaerobe *Halanaerobium* sp. MASE-BB-1, comes from the order *Halanaerobiales* within the phyla *Firmicutes.* This order was not detected in the MiSeq analyses in this study.

Studies of similar evaporite deposits worldwide have also shown communities dominated by archaea rather than bacteria. While bacteria have been successfully isolated from similar halite deposits, they are significantly outnumbered by the archaea (Schubert et al., 2010, Vreeland et al., 2007, Park et al., 2009).

An explanation for why so few bacteria have been detected in prior studies compared to this study, might be because of an influx *via* secondary alteration, as indicated by the presence of $CaSO_4$. This hypothesis will be explored further in Section 3.4.3b. An alternative explanation, however, may be in the techniques used. Prior studies have mainly been culture-dependent and, as such, only viable and culturable microbes were investigated. This Chapter, however, focused on culture-independent techniques that detected DNA sequences not cells. It is possible that the bacterial DNA sequences detected within this study did not represent viable bacteria. The *Proteobacteria*, the

most abundant phyla detected in the illumina MiSeq analyses (36.33 % of the sequences), have not previously been successfully isolated from Permian salt deposits. They have, however, been found at unexpectedly high abundances in another sequence-based culture-independent study which investigated a variety of halite deposits from around the world (Fish et., 2002), both younger (Miocene Badenian Halite from Poland) and older (Silurian Cayugan Halite from Michigan) than the ones investigated in this study.

A comparison of different evaporite deposits, of different ages, formed from different seas and preserved under different conditions is problematic, but on a global scale four of the six bacterial phyla identified *via* MiSeq in Boulby Mine have been identified previously in culture-independent studies of ancient halite: the *Proteobacteria, Actinobacteria, Firmicutes* and *Fusobacteria* (Chen et al., 2007, Fish et al., 2002, Hebsgaard et al., 2005). This leaves only the *Acidobacteria* and the *Saccharibaceria* which have not been discovered in ancient salt deposits prior to this study.

The absence of comparable studies detecting *Saccharibacteria* might be explained by the fact that it is has only recently been classified (He et al., 2015). References in the literature can be found to the identification of *Saccharibacteria,* under its old name of "candidate phyla TM7" (Azua-Bustos et al., 2012), within surface salt deposits in the Atacama desert, where the communities are active and driven by photosynthesis (Davila et al., 2015).

Of the six detected phyla, only the *Acidobacteria* have not been detected inside salt crystals before. The *Acidobacteria* represented a small proportion of the community (0.12 % of the illumina MiSeq) and were only detected within the tRF profiles of a single sample (although in all the replicates). This raises the possibility that this sample had

experienced contamination, either from the working mine environment or in the lab. On the other hand, this sample was visually the purest and uniformly pink coloured sample, and the ICP-MS determined that this sample had no Ca. This sample might, therefore, be the sample that has undergone the least alteration since its formation and thus contain the best preserved ancient community of all the samples.

Entombment within salt crystals exerts environmental stresses on cells. Archaea undergo a variety of physiological changes to withstand this stress (see Chapter 1) and knockout mutants of the K^+ pump system show severely reduced survival (Kixmüller and Greie, 2012). The only bacteria that have been successfully cultured after millennia of entombment are those which can form spores (Vreeland et al., 2000, Willerslev et al., 2004). The two most abundant bacterial families in the tRFLP profiles, *Bacillaceae* and *Nocardioidaceae*, are known to have spore forming varieties, but this is not the case for the majority of bacteria identified in this analysis. It is, therefore, feasible that the vast majority of bacterial families that were trapped in the crystals, and were detected in this study, did not survive over geological time. It has previously been noted (Chapter 1) that entombment within halite is believed to encourage long term preservation of the DNA of deceased organisms due to the sealed, anaerobic, highly charged environment and this may be an explanation for the results observed.

c) Archaeal and bacterial comparison

As noted above, prior culture-dependent studies (Schubert et al., 2010, Vreeland et al., 2007, Park et al., 2009) would indicate that viable archaea within these samples should be both more abundant and more diverse than the viable bacteria. The DNA sequences, however, suggest the contrary - there was higher diversity of bacterial DNA sequences than archaeal.

Excluding the community-dependent nature of the archaea identification process, the tRFLP analyses showed 70 possible bacterial fragment sizes compared to 21 for the archaea. The assumption is made that these communities represent microorganisms that were present in the hyper-saline Zechstein sea as it evaporated and formed these deposits, although this has not been proven. Of the archaeal phyla, only halophiles were detected, while all the bacterial phyla detected possess halophilic members (McGenity and Oren, 2012). These are therefore microorganisms that could have survived the hypersaline conditions of the evaporating Zechstein Sea. Studies of evaporating salterns have shown that, even though communities become weighted towards archaea as salinity increases, the bacterial community remains more diverse (Casamayor et al., 2002), so it seems reasonable to suggest that the same would be true of the evaporating, hyper-saline Zechstein sea. This would fit with the observation in this Chapter of higher bacterial than archaeal diversity.

It was initially intended to use qPCR to quantitatively compare the amount of bacterial and archaeal DNA, but this was not feasible with the low DNA concentrations. It seems reasonable, however, to suggest that the archaeal DNA within the samples was less abundant than that of bacterial origin. Repeated DNA extractions failed to produce a suitable yield of archaeal DNA for later analyses, while bacterial DNA was of sufficient concentrations. While this might be a result of the relative difficulty in breaking the cell walls of halophilic archaea compared to halophilic bacteria (Leuko et al., 2008), the repeated failure of multiple methods, optimised in prior studies to extract DNA from halophilic archaea, implies they have a relatively low biomass.

It has already been speculated above that the bacteria detected within this analysis might not represent viable bacteria, but instead represent deceased cells. It has

previously been hypothesised that one of the ways in which halophilic archaea are able to withstand long-term entombment is by metabolising the remains of long deceased bacteria entombed alongside them (Schubert et al., 2009). If that's the case, then a greater abundance of deceased bacterial cells, previously undetected by culture-dependent studies, within these inclusions might be able to act as an energy source for archaea preserved over geological time periods. This could potentially help to explain reports of ancient (250 Ma) halophiles being revived from both these deposits and others worldwide (Stan-Lotter et al., 1999, Stan-Lotter et al., 2002a, Jaakkola et al., 2016b, Jaakkola et al., 2016a).

3.4.2 - Community composition between beds

One of the goals of this Chapter was to determine whether the cationic composition of samples affected the entombed microbial community. These results indicated that there was no difference in community composition between the Boulby Potash, the Boulby Halite or the interface between them. The geochemical analyses of the samples had shown that there was significant variation in the concentrations of K and Na within the same beds, but this variation was also not linked to any significant differences in the microbial community composition.

The same microorganisms were detected in both the Boulby Halite and the Boulby Potash in the same community structure. Despite the large differences in chemical composition, these samples appear to contain the same genera in the same ratios. Three hypotheses are proposed to explain this result:

The first hypothesis is that halite and potash have similar crystallographies (Deer et al., 1992) and might have the same physiological effects on microorganisms. This structural

similarity might mean that, from a microbial perspective, there is no meaningful difference between the two lithologies as host rocks (Williams, 1970).

The second hypothesis is based upon the observation that the mineralogical composition of each bed is heterogeneous; halite crystals were identified within the Boulby Potash, for example (Section 2.2.2b). It is possible that microbes detected within the samples excavated from the Boulby Potash might have been located exclusively within the halite crystals rather than the sylvite. This seems reasonable since past literature shows that obligate halophiles would not be able to survive the low NaCl-high KCl concentrations of a brine composed of these sylvite crystals dissolved at the cell's optimum salinity (Brown and Gibbons, 1955). Further research, therefore, could investigate differences in the yield of DNA from the Boulby Potash and the Boulby Halite in order to determine whether the lower volume of halite crystals in the Boulby Potash correspond to a lower yield of DNA. The varying silt content of the beds made this impractical to investigate in this study because the different particle sizes and volumes would affect the rate at which DNA could be passed through the filters, and thus the amount of DNA extract obtained from each sample. Chapter 5, however, will present the results of investigations into laboratory-grown crystals that may allow this hypothesis to be investigated further.

The third hypothesis is based on the approximate compositions of fluid inclusions determined by EMPA (Section 2.3.3b); at least some of the fluid inclusions within the sylvite contained high NaCl concentration brines. As it is the fluid inclusions, and the brines contained within, that are the actual location of the cells, not the crystalline matrix of the salt (Fendrihan et al., 2009a), it is possible that the composition of the

surrounding crystal matters little to microbial survival so long as the inclusion itself is habitable.

3.4.3 - The impact of aqueous alteration upon the community

a) Aqueous alteration and diversity

Bacterial community diversity was linked to relatively small variations in Ca concentration (Section 3.3.1c & d). While it might be the case that higher Ca levels were directly responsible for the observed decrease in diversity, Ca was shown in Chapter 2 (Section 2.4.3) to be an indicator that the samples had been aqueously altered. This link between Ca concentration and aqueous alteration makes it difficult to determine how the observed variation in the bacterial community came about.

Aqueous alteration induces a variety of changes to the lithological environment. These changes include, but are not limited to, the precipitation of $CaSO_4$ (and the elements which correlated with it such as Fe, see Section 2.3.3e and Woods, 1979) and the dissolution and recrystallisation of the crystals themselves (Hardie et al., 1985). Any one (or more) of these changes could have been responsible for the observed trends in bacterial community diversity.

It is also important to consider the possibility that fluids moving through the mine might be capable of moving microorganisms as well as dissolved ions. It has often been proposed that so-called "ancient microorganisms" recovered from ancient halite are, in fact, more modern microorganisms inside secondary fluid inclusions created by aqueous alteration (Jaakkola et al., 2016b, Satterfield et al., 2005). The movement of microorganisms in fluids downwards through sample sites A-E might support this hypothesis and explain the trends in bacterial diversity observed in this Chapter.

Cells in lithologies with a higher Ca concentration (presumed to have undergone more aqueous alteration, Section 2.4.3) could have been mobilised and redeposited into lower beds as fluid moved downwards through the stratigraphic column. It is known that events such as these, which decrease population size, also cause a decrease in diversity, because of the likelihood of taxa being completely removed (Herren et al., 2016, Hague and Routman, 2016). These could mean that the decrease in diversity in the more altered lithologies is a result of a reduction in biomass (see Sections 2.2.3 and 3.4.1c for why analysing this was unfeasible). It is important to note that a similar decrease in diversity would be observed, however, if the aqueous alteration did not move cells, but instead caused environmental changes that destroyed DNA.

The observed lower diversity in the more altered samples seems to be limited to the bacteria, with no difference observed in the archaeal community (Section 3.3.2). If this lower bacterial diversity is a result of the movement of cells down the stratigraphic column, it would imply that archaeal cells have a mechanism to prevent them being carried out of their host rock by aqueous alteration. Alternatively, if the lower bacterial diversity is a result of environmental changes within the sample, then this would imply that the archaea are, in general, more resistant to these environmental changes than the bacteria.

b) Aqueous alteration and the detection of bacteria

It is important to bear in mind, that, while the Ca^{2+} and SO_4^{2-} deposited as $CaSO_4$ by evaporation of the fluid seems likely to have originated from the Upper Anhydrite (see Section 2.4.3), the fluid itself could have come from much higher up the stratigraphic column, for example the Upper Halite or even the surface. This means that the fluid

could potentially have transferred microorganisms from any of these locations to the sample sites.

Norton (1993) refers to "*extensive mineralogical change, though there are areas in which little alteration has taken place*" when describing the mine as a whole. However, it is unclear whether the samples investigated in that study were obtained from sites that had been subjected to alteration. This, therefore, introduces an alternative hypothesis to explain the fact that bacteria were observed in this study, but not in Norton's (Section 2.4.1b) - the alteration state of the samples might be different. It could be suggested that fluids may have delivered bacteria to the samples investigated in this project, but not to Norton's samples. Alternatively, Norton's samples may have been subjected to more alteration, removing all bacteria.

Fish (2002), however, identified similar bacterial DNA in a variety of deposits using culture-independent techniques while taking care not to examine aqueously altered samples. This suggests that bacteria which can only be detected *via* culture-independent techniques are relatively common in ancient halite deposits, and aqueous alteration is not required to explain their presence. Occam's razor would suggest that the simplest explanation for the detection of bacteria in this study, and not prior ones, remains the fact that this study was culture-independent, instead of the hypothesis that they can be found in only a relatively small, aqueously altered area of Boulby Mine. Chapter 4 investigates these options further.

Movement of bacteria could impact community diversity

Regardless of the difference between this study and that of Norton (*ibid),* there was a clear difference in bacterial diversity with aqueous alteration, using Ca concentration as a proxy. The greatest diversity of bacteria was found in the samples that had the lowest

Ca concentration (Section 3.3.1d) and were thus assumed to have undergone the least aqueous alteration (Section 2.4.3). The samples subjected to the most alteration (i.e., with the highest Ca concentration), showed the lowest bacterial diversity.

If it is assumed (Section 3.4.3a) that there was already a community of bacteria present in the rocks before aqueous alteration, it implies that fluids removed bacteria and redistributed them elsewhere or that the process led to cell death. This would, in turn, increase the relative diversity of less altered lithologies. If, however, bacteria were introduced into the stratigraphic column *via* this aqueous alteration, then an alternative, as yet undefined, mechanism is required to explain the greater diversity observed in the least altered samples.

Investigation of the fluids

Since the deposits higher up the stratigraphic column were not sampled during the site visit, and could not be sampled later because of health and safety concerns (Edwards, *pers comm.*), it is not possible to determine whether they are the source of bacteria within these samples. Fluids that have passed through these beds, however, have been extensively studied and could give an indication of what microbiology could be mobilised by its movement.

Boulby Mine contains brines. The dissolved salt within these brines is believed to originate from dissolution of the same salt deposits (McGenity et al., 2000, Payler et al., 2017) sampled in this study. The fluid, meanwhile, is believed to originate from aquifers above the salt deposits (Bottrell et al., 1996, Payler et al., 2017) and thus has followed a path similar to the one proposed in Figure 2.18.

As discussed above (Section 3.4.1b), studies of these brines have only ever detected one bacteria, *Halanaerobium* sp. MASE-BB-1(McGenity et al., 2000, Cockell, 2017, Beblo-Vranesevic et al., 2018), and it is not one observed in this study. This implies that the fluids moving through Boulby Mine today do not contain viable bacteria of the families detected in fluid inclusions sampled in this study. This does not rule out the possibilities, however, that the subsurface fluids have changed over time (with respect to the bacteria they carry), or that those fluids which altered the samples in this study delivered non-viable bacteria. As a result, there is no evidence to disprove the hypothesis that the bacteria detected in this study were a result of them being added or modified by aqueous alteration.

3.4.4 - Implications for martian astrobiology

These results imply that large changes in the Na content of chloride deposits do not impact the structure of their microbial community. This raises the possibility that, so long as there is a large amount of NaCl in the salts, that the presence of other salts would not affect the chances of finding evidence of ancient preserved life. The composition of the vast martian chloride deposits remains unknown (Osterloo et al., 2010) and is unlikely to be potash, but these results indicate that a composition as low as 40 % NaCl and 60 % KCl would contain similar microorganisms to one of pure NaCl. Later chapters will investigate this whether this is a property only of NaCl/KCl mixtures of salt, or whether the same survival of microorganisms is seen when NaCl is combined with more Mars relevant salts.

The biggest observed impact on the entombed microbial communities was caused by aqueous alteration. Samples that had undergone more aqueous alteration appeared to

possess a less diverse microbial community. As described above, it is believed that this lower diversity community is a result of the more altered samples having suffered loss of many members of the original ancient community, rather than the less altered samples having an influx of additional microorganisms. The reasons for this were not identified but this has significance for Mars.

Mars is now a dry planet, and it is postulated that formation of the large surface deposits represent the end of large scale liquid water on the planet's surface (Osterloo and Hynek, 2015). It has previously been postulated that martian evaporites are unlikely to have undergone as much aqueous alteration as their terrestrial equivalents (Parnell et al., 2007) and the most recent surface evidence of aqueous alteration on Mars has a minimum age of 2,000 Ma, though it is likely much older (Frydenvang et al., 2017). It has been suggested that this lack of recent aqueous alteration might allow martian salts to better preserve geochemical biosignatures than their terrestrial equivalents (Parnell et al., 2007). The same could be true of community structure. If there was evidence of an ancient martian microbial community entombed within these deposits, then diversity of the original community could be relatively well preserved, at least in comparison to these Zechstein samples.

3.4.5 - Limitations

a) Limitations of the tRFLP technique

Significant differences were observed between the community profile shown by the illumina MiSeq analyses and that shown by the tRFLP analyses, despite both being carried out on the same DNA extracts. One reason for these differences is that the tRFLP profiles only show microorganisms that will form fragments. Of the 2,813 unique

sequences detected via MiSeq, 643 did not contain a restriction site to form a fragment. This accounted for 37% of the MiSeq reads. These sequences were therefore invisible to the tRFLP analyses.

Another reason why some bacteria detected in the MiSeq profile did not appear in the tRFLP profile is that their fragment size was too long. The *Fusobacteria*, for example, comprised 3 % of the community according to MiSeq, but were completely absent in the tRFLP profiles. The restriction mapping software showed that many of the *Fusobacteria* sequences should, theoretically, have produced 233 bp long fragments, but no fragments were detected longer than 164 bp. One of the limitations of tRFLP is that becomes less accurate as fragment size increases (Fredriksson et al., 2014, de Lange and Wijtten, 2010, Sjöberg et al., 2013).

As a result of the above limitations, tRFLP does not show a whole community, but only those elements of the community that would form fragments. Changes in the abundance of specific taxa in different tRFLP profiles did indeed represent changes in the abundance of these taxa in the actual samples (or at least those members of the taxa that produce fragments), but a substantial portion of the community was completely invisible to this technique. It is uncertain how these unobserved members of the community varied between tRFLP profiles. For example, no conclusions can be drawn about the distribution and diversity of the *Fusobacteria* between different samples.

tRFLP also lacks taxonomic accuracy. Multiple sequences from separate families gave rise to the same peak. While in most cases 80 % of the sequences that created a peak came from the same family, it is possible that there were patterns in the distribution of this remaining 20 % of each peak that was not visualised.

b) Archaeal DNA

While the bacterial tRFLP analyses seem relatively robust, the accuracy of the archaeal tRFLP is questionable. The DNA extracts used for this were later discovered to contain insufficient archaeal DNA for MiSeq analyses (Section 3.2.5). The archaeal tRFLP profiles contained many anomalous peaks, present in only one profile across all the samples in triplicate, while the rarefaction curve suggested that a large part of the community went unsampled.

The lack of diversity within the archaeal tRFLP data fits the established literature (Casamayor et al., 2002), but could also be an artefact of a restriction digest being carried out on a PCR with insufficient DNA. The frequent occurrence of peaks larger than a primer dimer would suggest that this is not the case but, in retrospect, a negative control should have been run with the samples.

This situation is less problematic for the bacteria. The fact that there was variation in the tRFLP profiles with elemental abundances (such as Ca), and that the tRF profiles closely resembled those predicted by the MiSeq analyses, means that these are likely to be true results and not an attempt to analyse a negative result.

c) Calcium sulfate interferes with DNA Extraction

Raising the yield of DNA from the extracts proved problematic because of the unexpectedly high concentration of $CaSO_4$ within the extracts. While it was present in the samples, it was at very low concentrations and it was assumed that it would be washed out with the other salts. This does not appear to have occurred and $CaSO_4$ was concentrated within the filters along with the DNA. Once concentrated, DNA and $CaSO_4$ proved difficult to separate. $CaSO_4$ has a similar solubility to DNA: $CaSO_4$ has a

saturation point in water at room temperature of 11.62 mM (Gangolli and Chemistry, 1999). Consistent values for the solubility of DNA in water are not available in the scientific literature, presumably because it can vary with sequence length (Cleaver and Boyer, 1972), many commercial documents from companies that work with DNA estimate the solubility in room temperature water to also be around 10 mM (GeneTools LLC, 2001, Integrated DNA technologies, 2011, Sigma Aldrich, 2016). This could, therefore, help to explain why the DNA and $CaSO_4$ could not be separated by techniques that involved removing one substance from a solution, but not the other.

While in solution, the $CaSO_4$ did not appear to present a problem to the PCR reactions and downstream processing. It appeared, however, that this $CaSO_4$ was in a hypersaturated solution, at a higher concentration than the normal saturation point of $CaSO_4$ (Gangolli and Chemistry, 1999). Most DNA purification techniques require the precipitation of the DNA and resuspension in water. At this stage, a high concentration of $CaSO_4$ would precipitate and could not be re-dissolved unless at significantly higher volumes of water than the volume it was precipitated from. Ironically, this meant that the concentration step of most protocols would result in a higher volume and thus lower concentration of DNA. This has severely impacted the ability to get a clear picture of the archaeal community of Boulby Mine. This should be considered and a solution found during the planning stages of any future attempts to extract DNA from Zechstein environments.

3.4.6 - Further work

a) Work included in this thesis

The work presented in Chapter 1 and this Chapter investigated the microbial community of the Boulby Mine evaporites and found it was dominated by bacteria, in contrast to prior studies (Norton et al., 1993, McGenity et al., 2000). One possibility (Section 3.4.1a) is that this is a result of the culture-independent nature of this study compared to previous studies that have relied on culturing viable microorganisms. Chapter 4 investigates this further by repeating previously used culture-dependent experiments, in order to ascertain whether techniques used in the past would have been capable of detecting the bacteria within them. A wider range of culture conditions was also employed in an attempt to determine whether the large numbers of bacteria detected within these samples were still viable and whether they could be grown in the laboratory.

The community composition of samples of Boulby Halite and Boulby Potash appeared to be identical, despite the large differences in chloride composition. It was discussed in Section 3.4.2 that this might imply that microorganisms can undergo entombment in sylvite crystals, either due to a) structural and chemical similarity to halite or b) the composition of the fluid inclusions being similar within both crystal types. An alternate hypothesis was that the microorganisms detected within the Boulby Potash were located exclusively within the heterogeneously distributed halite crystals within this bed. Attempts are made to investigate the ability of halophiles to entomb themselves within salts of different compositions, including ones similar to the samples from Boulby Mine, in Chapter 5.

b) Proposed further work

The archaeal tRFLP detected a variety of different fragments. Most of these, however, could not be identified because the archaeal biomass within the samples was too low for MiSeq analyses (Section 3.3.2). A variety of alternate DNA extraction methods were attempted, but all failed (Section 3.2.5). It should, however, be noted that the initial DNA extraction probably did produce archaeal DNA (Section 3.4.5b), although the high concentration of $CaSO_4$ prevented this concentration being increased (Section 3.2.5 and 3.4.5c). Replicating this DNA, instead of concentrating it, might, therefore, be a more successful avenue for future research. DNA replication techniques are flawed in that sequences are not replicated at the same rate and this results in highly inaccurate values for relative abundances (Marine et al., 2014). If compared to the tRFLP data obtained in this Chapter, however, then it would be the sequences, and not the relative abundance data, that would be used to identify the fragments. Accuracy of the relative abundances in a MiSeq analysis on a replicated sample would, therefore, not be strictly necessary. Too much inaccuracy, however, could greatly inhibit the ability to line up hypothetical tRF profiles against actual ones for identification purposes.

3.5 - Conclusions

In this Chapter, the microbial community of Boulby Mine was investigated using culture-independent techniques. These techniques appeared to show a higher diversity and abundance of bacteria than archaea, in contrast to previous studies of both Boulby Mine and evaporite deposits worldwide. It is suggested that this is a result of the presence of a large number of deceased bacteria within the samples which has not been detected in previous studies because they focused only on culturable microorganisms.

This Chapter shows that the microbial community of Boulby Mine does not vary between lithologies or Na and K ratios. This implies that the microbial communities found within terrestrial NaCl beds can be used as an analogue for the communities within chloride beds of other cation compositions.

There is strong evidence to suggest that aqueous alteration of the samples has had a negative impact on the bacterial community entombed within. This effect does not appear to impact all the observed taxa equally.

Chapter 4: Isolation and characterisation of microorganisms from Boulby Mine

4.1 - Introduction

The aims of this Chapter are as follows:

- To isolate novel microorganisms from Boulby Mine
- To investigate whether the viable microorganisms vary between the compositionally-varied Boulby evaporites
- To investigate the tolerance of the isolates to salts of diverse compositions.

The results presented in Chapters 2 and 3 provide early evidence to suggest that the Boulby Potash and the Boulby Halite might contain the same viable microorganisms; petrological analyses had shown their crystallography to be similar (see Section 2.3.1b) and no differences were observed in the morphology or distribution of the microbe-containing fluid inclusions (see Section 2.3.3). Additionally, the EMPA analysis suggested that the inclusions within the Boulby Potash contained a brine composition more similar to the salt chemistry of the Boulby Halite (NaCl) than the host KCl (see Section 2.3.3). The molecular data also showed there was no difference in the entombed community between beds or between samples with large differences in Na and K concentration (Section 3.4.2). This implies that the composition of the evaporites does not affect the diversity or distribution of the entombed microorganisms.

It was uncertain, however, whether these microorganisms remained viable, or whether the viability of the microorganisms would be affected by the different evaporite compositions. The viability of these organisms is called into question because the

culture-independent techniques used in Chapter 3 suggest that the majority of the DNA within the samples was bacterial rather than archaeal. However, previous culture-dependent studies of the deposits have shown the viable members of the community to be almost exclusively archaea (Norton and Grant, 1988, Norton et al., 1993, Grant et al., 1998a), a trend shared by evaporite deposits worldwide (Schubert et al., 2010, Vreeland et al., 2007, Park et al., 2009).

Although these differences might be explained by the bacteria no longer being viable (Section 3.4.1c), they might also be a result of the methodologies previously employed (Section 3.1.4b). The culture-dependent studies of both Boulby Mine (Norton et al., 1993), and similar halite deposits worldwide (Schubert et al., 2010, Vreeland et al., 2007, Park et al., 2009), all started from the assumption that the communities consist mostly of halophilic archaea, and, as such, used highly saline media (Norton et al., 1993). The detection of large numbers of bacterial sequences in Chapter 3 (*via* MiSeq, Section 3.3.1), however, calls this assumption into doubt.

Whilst halophiles are known to exist in bacterial genera (McGenity and Oren, 2012), it is also possible that some could survive the saline environment of the samples in the form of non-halophilic spores (Section 3.4.1b). If so, they would not have grown in the highly saline media employed in previous studies. While it is difficult to prove the hypothesis that the bacteria are not viable, culture-dependent detection of bacteria (either halophilic bacteria or revived spores) in these samples would disprove it. Determining which viable microorganisms can be grown from the Boulby deposits is, therefore, the primary topic investigated in this chapter.

Determining whether the viability of microorganisms varies between the Boulby Potash and the Boulby Halite has implications for determining whether life could potentially

survive in martian non-halite salt deposits. Additionally, microorganisms from the Boulby Potash are of further value to the field of martian astrobiology, as these microorganisms must, by definition, have a tolerance to salts that are not dominated by NaCl (at least in the solid, non-aqueous form) given the high concentrations of KCl within this lithology. Hypothesised (aqueous) brines on the martian surface, both in the present day and on early Mars, present a variety of different chemistries, but are often not dominated by NaCl (Tosca et al., 2011). In order to investigate the viability of the isolates obtained in this Chapter for use as analogues for potential martian life, their ability to withstand a variety of salts (Na_2SO_4, KCl, K_2SO_4, $MgSO_4$, $MgCl_2$ and $CaSO_4$) was also investigated. These salts were chosen either because previous studies have shown they will allow the growth of obligate halophiles (as summarised in Section 1.4.2), they have been detected within the Boulby Mine environment where the microorganisms were found (Section 2.3), or they are of relevance to the martian surface (Clark and Van Hart, 1981, Ojha et al., 2015, Davila et al., 2013b, Kerr, 2013).

This Chapter therefore seeks to: a) determine whether microorganisms other than those detected by Norton (1993) can be grown from the samples investigated in the Chapter 3 and whether these differ between the lithologies and b) determine the range of salt compositions that can be tolerated by these viable microorganisms. This will, in turn, shed light on the ability of non-halite evaporites to support life, which has implications for the non-NaCl-based salts found on Mars.

4.2 - Materials and Methods

4.2.1 - Inoculation

a) Samples

Microbial enrichment cultures were prepared by dissolving samples from Boulby Mine in growth media and incubating them for three months. These samples included those which had previously been investigated in Chapter 3 (from Sites A, B, D & E: the Boulby Potash, the Boulby Halite and from the top and bottom of the interface between them), as well as the samples collected on the earlier expedition (from Site X and the samples of anhydrite and polyhalite from deeper in the mine, Section 2.2.1c).

b) Inoculation protocol

The focus of this work was the microorganisms entombed within Boulby's salts, and not those on the samples' surfaces. Therefore, sterilisation was carried out as described in Section 2.2.1f. Once sterilised, 2 g of homogenised sample was incubated in 50 ml conical flasks containing 25 ml of media as described below (this dissolved the rock to release the cells). Inoculation was performed in a laminar flow hood to minimise further risk of contamination. Once inoculated, flasks were sealed with both cotton wool and aluminium foil, in order to allow influx of air and moisture but prevent influx of microorganisms (Amadi et al., 2016, Ukpaka, 2016, Norris and Darbre, 1956, Jagessar et al., 2008).The incubation conditions were designed to replicate, where possible, the environmental conditions from the mine (Section 2.2.1b): in the dark, and at 38 °C.

Halophilic growth medium

A variety of growth media were used to optimise the number of microorganisms isolated. Modified Payne's Medium (MPM) had previously been used to culture microorganisms from Boulby Mine (Norton et al., 1993) and was therefore used in this study. The medium contained (l^{-1}): 10 g of Difco yeast extract; 7.5 g of casein hydrolysate; 2 g of KCl; 3 g of trisodium citrate; 200 g of NaCl; 20 g of $MgSO_4$; 0.0009 g of $FeSO_4.7H_2O$ and 0.00009 g of $MnCl_2.4H_2O$.

MPM was prepared by making two solutions (A and B), which were mixed together after autoclaving. Part A contained 200 g NaCl and 20 g $MgSO_4$, (final volume 800 ml). Part B contained the 10 g of Difco yeast extract; 7.5 g of casein hydrolysate; 2 g of KCl; 3 g of trisodium citrate; 0.0009 g of $FeSO_4.7H_2O$ and 0.00009 g of $MnCl_2.4H_2O$ (final volume 200 ml). The pH of Part A and B were adjusted to between 7 and 7.5 using either 1 M NaOH or 1 M HCl solution. After autoclaving, the solutions were combined aseptically in the laminar flow hood.

In addition, a 10 % strength variant of MPM was prepared, by adding 100 ml of MPM to 900 ml of a 200 g l^{-1} NaCl solution (pH was adjusted to 7-7.5 prior to autoclaving). Samples were also inoculated in the 200 g l^{-1} NaCl solution without additional nutrient media (meaning the only nutrients available for cells would have to come from the dissolved evaporite sample).

MPM was also prepared as an agar, for use in the isolation experiments (Section 4.2.2). This was achieved by creating both 100 % MPM and 10 % MPM with all the ingredients at double their normal concentrations. These were then mixed with an equal volume of

40 g l^{-1} bacteriological agar which had been autoclaved separately, in order to create MPM (of both nutrient strengths) with a final agar concentration of 20 g l^{-1}.

Non-halophilic media

In order to investigate the possibility of non-halophilic bacterial spores present in the salts, a non-saline media was used. This was glucose-yeast-peptose media. This is referred to in this text as GYP, but is also known elsewhere by the name ATCC medium 1049 (Schipper et al., 1996).

GYP contained (l^{-1}): 5 g of Difco yeast extract; 5g of glucose; 5 g of peptose; 5g of sodium acetate; 5 g of pyruvic acid. The pH was adjusted to 7.0 using 1 M HCl and 1 M NaOH and then autoclaved. 50 ml of medium was dispensed into sterilised 50 ml conical flasks in the laminar flow hood. As with the saline media MPM, a 10 % strength GYP was prepared.

The GYP medium was prepared without salts, however, the addition of 2 g of sample increased the salinity of the medium to 80 g l^{-1} (with NaCl to KCl ratio varying between samples). This is more than twice the 35 g l^{-1} NaCl found in sea water (Takagi and Yoshida, 2006), and thus would select for the growth of moderately halophilic microorganisms (Grant et al., 1998b).

In order to also select for the growth of non-halophilic microorganisms, a dilution step was included. For this, the samples were dissolved in GYP medium and after 1 hr, 1 ml was transferred (in the laminar flow hood) to a clean flask containing 24 ml of fresh GYP medium. The final salt concentration of the medium was 3.2 g l^{-1}. As with the saline media, all flasks of GYP medium were incubated at 38 °C in the dark.

c) Visualising the cells

Cell enumeration

Sybr ® Green I microscopy

Cell enumeration was carried out using a modified version of the Sybr ® Green I protocol. For non-saline samples, the manufacturers of this dye recommend an incubation step (Noble and Fuhrman, 1998). In this project, however, it was found that the dye's fluorescence in high salinity media faded in seconds once exposed to the microscope's UV beam. The length of time the fluorescence persisted could be extended to ten seconds if the dye-sample mix was immediately visualised, with little to no incubation time.

Sybr ® Green I DNA dye (10 µl) was added to 10 µl of culture on a microscope slide. The solutions were gently mixed with a sterilised pipette tip and a coverslip was placed on top. The slide was then observed with an epifluorescent Leica DMRP microscope at 100× magnification with an excitation wavelength of 450 - 490 nm and a long band cut-off filter of >515 nm. To optimise visibility, this was carried out in a dark room. It was observed that fluorescence persisted several seconds longer in 100 % MPM than 10 % MPM, while no fluorescence was observed in 200 g l^{-1} NaCl known to contain cells. This implied that one of the components of MPM had a stabilising effect upon the fluorescence. Even in the 100 % MPM, however, this fluorescence was still considerably shorter-lived compared to cultures grown in non-halophilic media (typical salinity < 25 g l^{-1}), where the fluorescence would persist for minutes at a time.

For cell enumeration, a serial dilution was carried out to 10,000× dilution within 100 % MPM. 10 µl of sample was pipetted onto a microscope slide and examined, as described

above. Cell counts were carried out where possible, i.e., when cell numbers were less than 20 per field of view, since rapid fading of fluorescence made counting more cells unreliable. Ten fields of view were selected to collect data from representative areas of the slide and the mean cells per field of view was calculated.

This mean was multiplied by the dilution factor of the sample and a conversion factor. The conversion factor (1,541,401.274) had been previously calculated for this technique using this laboratory's specific microscope, by Dr Stephen Summers (*pers comm*).

Absorbance

In order to monitor microbial growth in numerous cultures simultaneously, an ELx808™ Absorbance Microplate Reader was used. 200 µl aliquots of culture was transferred into a sterile 96 well plate and the absorbance at 590 nm was measured. Cell density and absorbance of light have a strong, positive, linear correlation. This means that changes in absorbance values over time could be used as a proxy for cell growth, without physically counting hundreds of cultures at a time (Jensen et al., 2015, Govantes, 2018, Kutschera and Lamb, 2018).

Cellular morphology - crystal violet staining

To investigate cellular morphology, cells were fixed and dyed with crystal violet. Approximately 1×10^9 cells were centrifuged at 4,000 × *g* at room temperature for 4 min and resuspended in 0.9 ml of 200 g l^{-1} NaCl. This was then mixed with 0.1 ml of 25 % glutaraldehyde and incubated at room temperature for 1 hr. Following incubation, the mixture was chilled for 23 hr, at 4 °C in order to fix the cells. Following fixation, cells were centrifuged (as above) and washed twice in 1 ml of sterile ddH_2O in order to

remove excess salt. 100 µl of fixed sample was transferred to a sterile microscope slide and dried at room temperature overnight.

To stain the cells, the microscope slides were flooded with 0.25 % crystal violet solution for 1 min. The excess stain was removed from the slides and left to dry in a laminar flow hood for a period of 1 hr. A drop of dibutyl phthalate xylene (DPX) was added to the dried samples in order to: a) immobilise the cells and b) seal in place a cover slip which was gently placed on top leaving no air bubbles. After the DPX had dried, samples were observed using a Leica DM RP microscope under visible light using 100× magnification.

4.2.2 - Isolation

Isolation from the microbial enrichments was carried out once growth was confirmed using the Sybr ® Green I method, as described in Section 4.2.1c. Three techniques were used to obtain pure isolates from these samples: a) spread and streak plating on agar; b) serial dilutions in liquid media, and c) floating filters. Each of these methods are described below.

a) Isolation on agar

Spread plates

To obtain single colonies, a 10× dilution series was prepared (from 10^9 cells ml^{-1} to 1×10^3 cells ml^{-1}) from each mixed culture in their relevant media. Both 200 µl and 1 ml volumes of each dilution were spread across agar plates of 100 % and 10 % MPM agar (described in Section 4.2.1b), using a sterilised L shaped spreader. This produced plates containing a wide range of cell numbers ($2x10^2$ - $1x10^9$).

The plates were incubated in the dark at 38 °C to mimic the conditions of the liquid cultures the cells had previously been grown in. The plates were stored in the incubator within sterile plastic bags alongside plates that contained Kimtech wipes dampened with ddH_2O instead of inoculated agar. At this temperature, the damp wipes raised the humidity within the bags and slowed the drying out of the highly saline plates (Leuko, 2016).

Approximately 150 plates of each strength of MPM were inoculated; however, cells were only observed on two of the 100 % MPM agar plates and a single 10 % MPM agar plate. Therefore, 10 g l^{-1} sodium pyruvate was added to the agar, and fresh plates prepared. Sodium pyruvate has previously been used to improve the growth of halophilic archaea on agar (Oren, 2016a), but here it still did not improve the yield. As a result, the following compositions of agar plates were also used, which have previously been used to successfully isolate halophiles:

- **Modified *Halorubrum chaoviator* agar** (Mancinelli et al., 2009) contained (l^{-1}): 200 g of NaCl; 2 g of KCl; 0.2g of $CaCl_2.2H_2O$; 20 g of $MgCl_2.6H_2O$; 5g of Difco yeast extract; 5 g of Casamino acids; 20 g of agar. The final pH was adjusted to 7.4 using NaOH and HCl.
- **Modified CASO Agar** (Leuko, 2016): CASO agar was purchased from Sigma Aldrich and diluted as per the manufacturer's instructions. Prior to autoclaving, the following was added (l^{-1}): 200 g of NaCl; 2g of KCl; 20 g of $MgSO_4$; 2 g of bentonite.
- **Artificial Sea Water (ASW) agar** (Wolf and Oliver, 1992) contained (l^{-1}): 95 g of NaCl; 34.6 g of $MgCl.6H_2O$; 49.5 g of $MgSO_4.7H_20$; 1.25 g of $CaCl.2H_2O$; 5 g of KCl;

0.25 g of $NaHCO_3$; 0.62 g of NaBr; 1 g of Difco yeast extract; 20 g of agar. The pH was neutral and was not adjusted.

After inoculation, the plates were incubated in humid bags as described above. Once colonies were visible, they were streaked onto fresh plates for isolation, as described below.

Streak plates

To obtain pure isolates the streak plate method (Sanders, 2012) was used. This method involves using a quadrant streak technique to facilitate sequential dilution of the original inoculum (Figure 4.1).

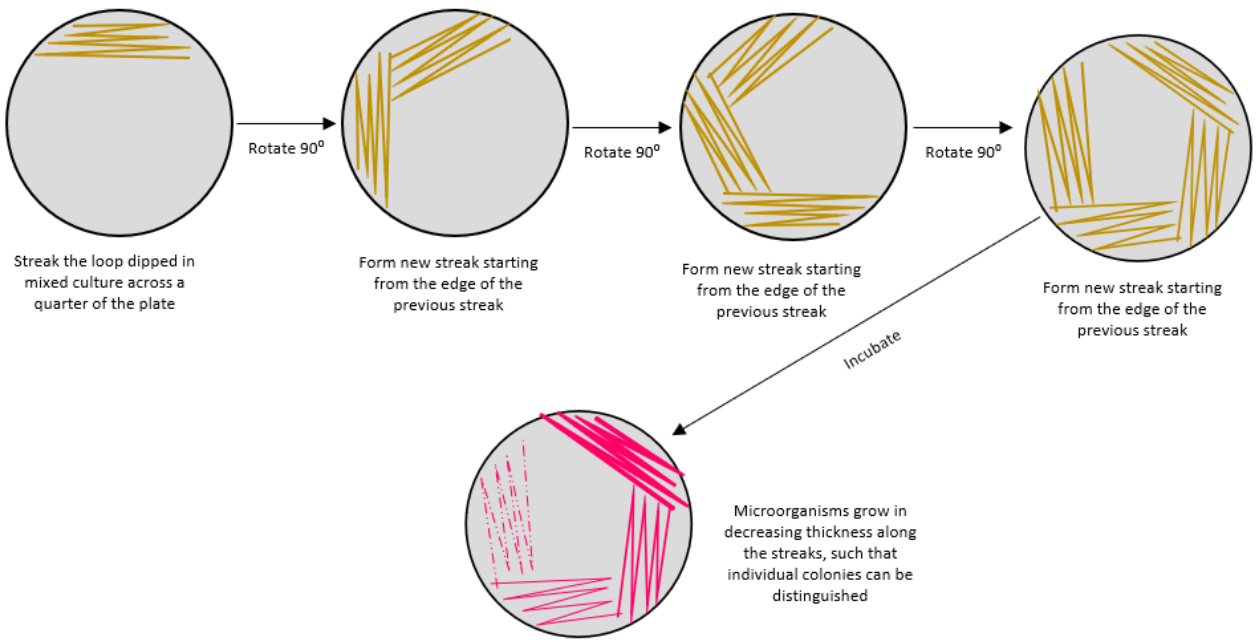

Figure 4.1 -Streak plate isolation technique

A sterile inoculation loop was used to pick cells from a mixed community, and streak them onto a fresh plate, as shown in Figure 4.1. The plates were then incubated in humid bags at 38 °C, as described above. Individual colonies were selected for

molecular analysis, which will be described in Section 4.2.3, and reinoculated (using a sterile plastic loop) into fresh liquid media (as described in Section 4.2.1b).

b) Dilution series using liquid medium

Halophiles have previously been isolated from mixed cultures by means of a dilution series (Sorokin, 2015). This involved a geometric progression of the inoculum in a logarithmic fashion in liquid medium, with the aim being to produce a pure culture.

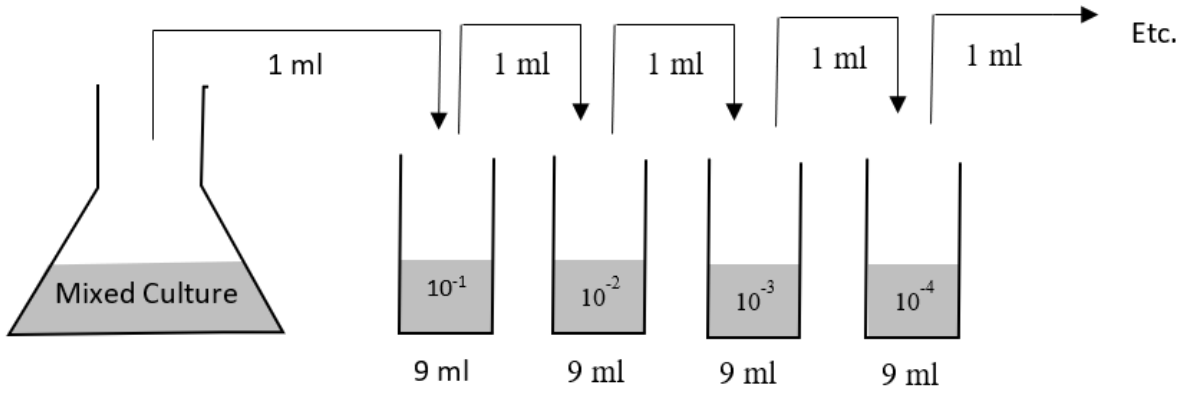

Figure 4.2 - Dilution Series Methodology

For this, 1 ml of inoculum was added to 9 ml of growth media in a 15 ml Falcon tube and mixed *via* inversion for 1 min to establish a homogenous culture (Figure 4.2). This process was further repeated until a 10^{-10} dilution was prepared. All dilutions were then incubated as described in Section 4.2.1b, with the lids slightly unscrewed to allow exchange of air with the atmosphere. After two months, the most diluted culture that could be determined to have undergone growth (as determined *via* fluorescent microscopy, Section 4.2.1c) was used to inoculate two further dilution series, such that each mixed culture underwent three consecutive dilution series in order obtain isolates in pure cultures.

The dilution series was also carried out in MPM with a salinity of either: 150 g l^{-1} NaCl, 100 g l^{-1} NaCl, 50 g l^{-1} NaCl or no NaCl. The aim was to apply selection pressure (higher osmotic stress), in order to select for isolates that could tolerate a wide range of salinities.

The overall goal of the dilution series was to obtain pure cultures. Visual inspection of the cultures could not determine whether this had occurred since all cells in the mixed cultures looked identical under Sybr ® Green I microscopy. As a result, all cultures that had undergone the dilution series were sequenced (as described in Section 4.2.3), without prior knowledge of their purity.

c) Floating Filters

The third isolation technique employed was the "floating filter" technique, initially developed for the isolation of "fastidious" acidophilic bacteria (de Bruyn et al., 1990). This is the first time this method has been used to isolate halophiles. For this method, 1 ml of mixed culture was filtered through a sterile 25 ml Whatman® Nucleopore™ Track-Etched Membrane filter, within a laminar flow hood, using a vacuum pump. All components of the pump apparatus that could potentially come into contact with cells were sterilised with 70 % ethanol before and after filtration. The pore size of the filter was 0.22 µm, which prevented the cells passing through the filter. As a result, they instead formed a layer on the surface of the filter.

The filters were then transferred to a 6 well plate, which contained 10 ml of media. The hydrophobic nature of the filters meant they floated on top of the media, but the cells growing on the surface could still access the nutrients below. Lids were placed on the 6 well plates and they were sealed with parafilm to allow exchange of air with their

surroundings. The plates were then incubated in the dark at 38 °C. Colonies grew on the surface of the filter in a similar manner to on an agar plate.

After a period of approximately two weeks, colonies were visible on the filters. Once this had occurred, the media was gradually pipetted from the wells. This was carried out within the laminar flow hood (to ensure the filters were kept sterile). The colonies were then transferred, using a sterile plastic loop, to 10 ml of media. Colonies with different morphologies were selected for sequencing.

4.2.3 - Identification and characterisation of isolates

DNA was extracted from each of the isolates as described below (Section 4.2.3a). Regions of the 16s rRNA gene were sequenced (Section 4.2.3b) and used for identification.

a) DNA Extraction

The high internal salinity of halophiles means that they tend to burst when submerged in pure water (Grant et al., 1998b). This allowed a relatively simple DNA extraction method to be employed. Aliquots (0.5 ml) of cultures were centrifuged at 4 °C for 4 min at 6,000 × *g* and the salt-rich media removed. The pellet was re-suspended in 0.75 ml sterilised nucleic acid-free ddH_2O in order to burst the cells. To ensure that this had occurred, a freeze-thaw step was employed, in which the samples were frozen at -80 °C and then heated rapidly to 40 °C in a heat-block; this was repeated three times.

The DNA was purified using phenol:chloroform:isoamyl alcohol (25:24:1, v/v) (Sambrook and Russell, 2006). In brief, 0.75 ml of phenol:chloroform:isoamyl alcohol (25:24:1, v/v) was added to the 0.75 ml DNA extract and mixed by inverting the tube

until the contents were visually homogenous. This was then centrifuged at 6,000 × *g* for 4 min, at 4 °C. The top aqueous layer, containing DNA, was transferred into a sterile DNase-free Eppendorf tube. The DNA was precipitated by adding an equal volume of cold isopropanol (4 °C) and incubated at room temperature for 6 hr. The solution was then centrifuged at 6,000 × *g* for 4 min, at 4 °C, and the pellet was washed in cold 70 % ethanol (4 °C). The DNA was resuspended in 200 µl of nucleic acid free water. The final concentration and purity of the DNA was ascertained *via* a Thermo Scientific nanodrop 1000. DNA extracts were stored at -20 °C.

b) PCR

In order to identify the isolates, PCR was used to amplify a region of the 16s rRNA gene for sequencing. This was carried out as outlined below.

PCR reaction mixtures

All PCR amplifications were performed in reaction mixtures with a final volume of 50 µl. These contained: 10 µM each of both forward and reverse primers, 5 µl of PCR Buffer, 0.04 mM dNTP mix, 2.5 U of Taq polymerase and 100 ng of DNA. The final volume was made up to 50 µl using sterile, nucleic-acid free ddH_2O. Success of the PCR was ascertained by running 10 µl of PCR product on a 2 % agarose gels using the DNA binding dye, SybrSafe, to visualise the PCR product.

Primers

The PCR primers that were used are shown in Table 4.1.

Table 4.1 - Primers used for sequencing

Primer Name	Primer Direction	Position	Primer Sequence	Reference
Com1	Forward	519	CAGCAGCCGCGGTAATAC	(Schwieger and Tebbe, 1998)
Com2	Reverse	907	CCGTCAATTCCTTTGAGTTT	(Schwieger and Tebbe, 1998)
A27f	Forward	27	TCCGGTTGATCCTGCCGGAG	(McGenity et al., 1998)
A571f	Forward	571	GCCTAAAGCGTCCGTAGC	(Liao et al., 2009)
A1525r	Reverse	1525	AAGGAGGTGATCCAGCC	(McGenity et al., 1998)
Hb109f	Forward	109	AGCTCAGTAACACGTGGYC	Designed in this study
Hb1354r	Reverse	1354	GTGTGTGCAAGGAGCAGGG	Designed in this study

Com1-Com2

The universal primers Com1 and Com2 were initially used to determine which of the 56 sequences were unique (Schwieger and Tebbe 1998). The PCR reaction for the Com1 and Com2 primers was as follows: initial denaturation at 94 °C for 3 min, followed by 25 cycles of denaturing for 1 min at 94 °C, annealing for 1 min at 45 °C, elongation for 90 sec at 72 °C, followed by a final elongation for 4 min at 72 °C (Schwieger and Tebbe 1998).

The Com1 and Com2 primers allowed sequencing of the V4 and V5 regions of the 16S rRNA gene. The primer binding sites are located in highly conserved regions across both bacteria and archaea (Dohrmann and Tebbe, 2006). Thus, they could be used as primers for PCR reactions when the domain of each isolate was uncertain. While the primer binding sites are stable, the V4 and V5 regions between these primers are highly variable, and thus would allow preliminary identification.

Both the NCBI BLAST program (Johnson et al., 2008) and the Naïve Bayesian rRNA Classifier v1.0 analysis tool within the Ribosomal Database Project II (Wang et al., 2007) identified all the of the isolates as being halophilic archaea.

Use of existing primers

Initial identification of the isolates had been carried out by sequencing the Com1-Com2 region, but more detailed identification required sequencing of a larger region of the gene. Since the isolates had all been identified as haloarchaea, existing haloarchaea specific primers could be used for this larger region, instead of unreliable "universal" primers (Wang et al., 2007, Yu et al., 2008).

The haloarchaeal primers A27f, A571f and A1525r (Table 4.1, McGenity et al., 1998, Liao et al., 2009) did not work as expected. For example, when A571f was used as the forward primer, a PCR product approximately 800 bp shorter than expected was observed, while the primer pair A571f-A1525r produced no visible PCR product.

Therefore, initial identification could only be based on the 300 bp product of the Com1 and Com2 primers. These short sequences were compared with the NCBI database, through the NCBI BLAST algorithm (Johnson et al., 2008). This revealed 18 complete 16S rRNA sequences (>1,300 bp) each of which had in excess of 96 % similarity to at least two of the isolates. These sequences were imported into BioEdit, and aligned against the short sequences from the isolates using the ClustalW plugin (Thompson et al., 2002).

Investigating the failure of existing primers

The archaeal primers A27f, A571f and A1525r, which had resulted in unsuccessful PCR, were aligned with the complete 16S genes obtained from the NCBI database. This alignment showed that, while the forward primers A27f and A571f were located within the 16S genes of organisms closely related to the isolates (Figure 4.3), the primer binding site for A1525r (the antisense of the sequence) was located near position 480 (Figure 4.3) instead of near position 1,525. This explains the unsuccessful PCRs when using the A1525r primer.

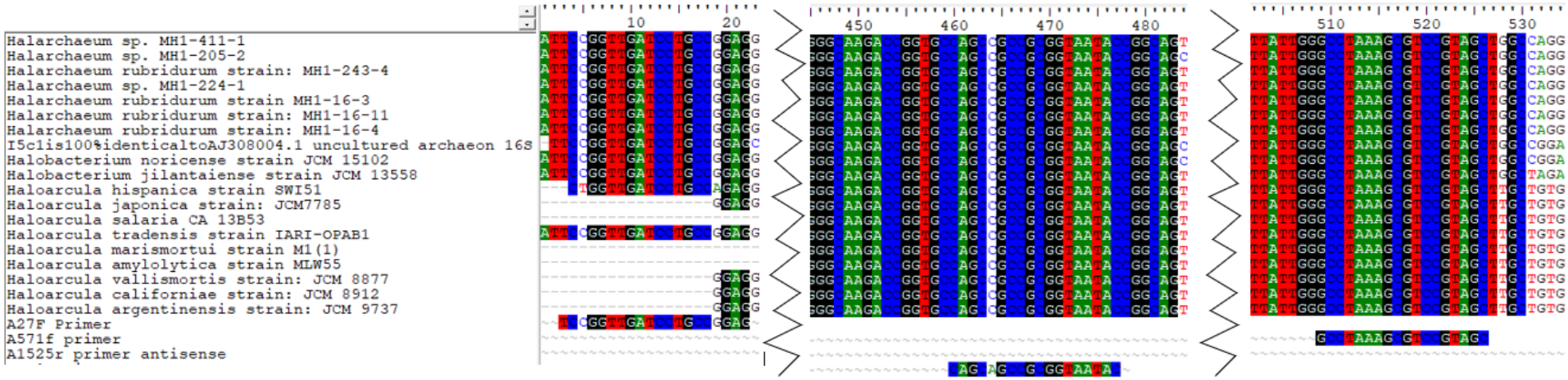

Figure 4.3 - Alignment of the haloarchaeal primers used previously against the top BLAST results for the isolates. A1525r is a reverse primer, so the antisense is aligned instead of the sense. Alignment is shown as a screenshot of the software BioEdit (Hall, 1999) using the ClustalW plugin (Thompson et al., 2002). Sequence position (at the top of the image) represents the position on the longest sequence being aligned and not the actual position on the 16s gene. Position on the sequence is approximately 10bp less than the position on the gene because the library sequences do not include the ends of the 16S rRNA gene.

Primer design

Based on the ClustalW alignment with haloarchaeal16S rRNA sequences similar to those of the isolates, two conserved regions were identified and new PCR primers designed. The forward primer, Hb109f (Figure 4.4), was designed for a region of 19 conserved bases just after the V1 region. Base 18 was variable - it could be a thymine or cytosine - so a degenerate primer was used. This meant that the primers contained one of the two possible bases at this position in equal concentration.

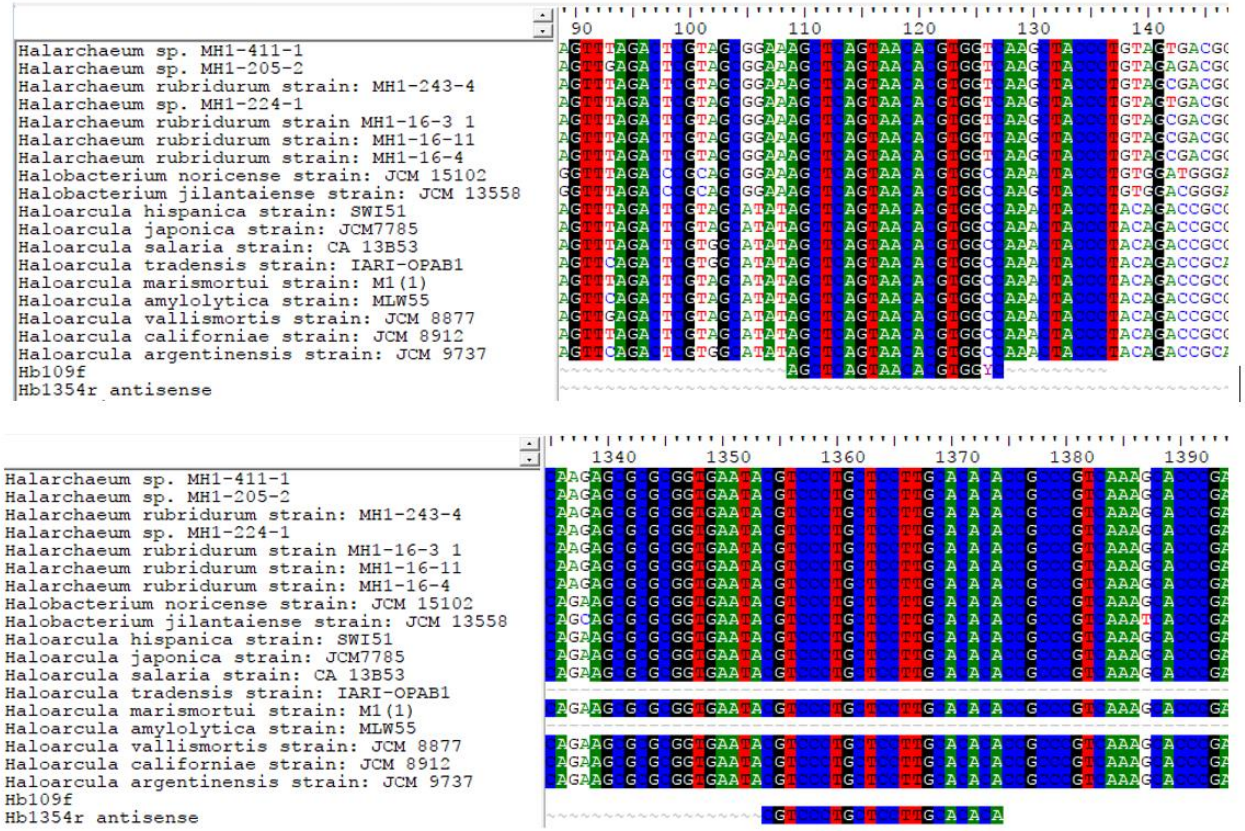

Figure 4.4 Highly conserved regions in 18 sequences and primers based on those sequences. Hb1354r is a reverse primer, so the primer used was the antisense of the conserved region. Alignment is shown as a screenshot of the software BioEdit (Hall, 1999) using the ClustalW plugin (Thompson et al., 2002).

For the reverse primer, a group of conserved bases just after the V8 region was selected. This new primer (Hb1354r) was designed based upon 19 highly conserved bases. As this was a reverse primer, the primer sequence was the antisense of the sequence

within the gene (Figure 4.4). These new primers sequences are listed in Table 4.1 and were expected to produce a theoretical PCR product 1,245bp long, containing the hypervariable regions V2-V8.

Once the primers were designed, the online program OligoCalc (Kibbe, 2007) was used to check that the annealing temperatures of the primers were within 5 °C of each other and that there were no hairpin loops where the sequences would self-complementary.

OligoCalc (Kibbe, 2007) was also used to estimate the PCR conditions for the PCR reaction. While this estimated protocol was successful, the PCR products tended to smear when run on a gel. Therefore, the conditions were modified using trial and error. It was found that lowering the annealing temperature from the predicted temperature of 57 °C to 55 °C produced clear bands of the correct size (Figure 4.5). The final PCR program was, therefore: an initial denaturisation at 94 °C for 5 min, followed by 30 cycles of denaturing at 94 °C for 40 sec, annealing for 30 sec at 55 °C and extension at 72 °C for 1 min, followed by a final extension of 10 min at 72 °C.

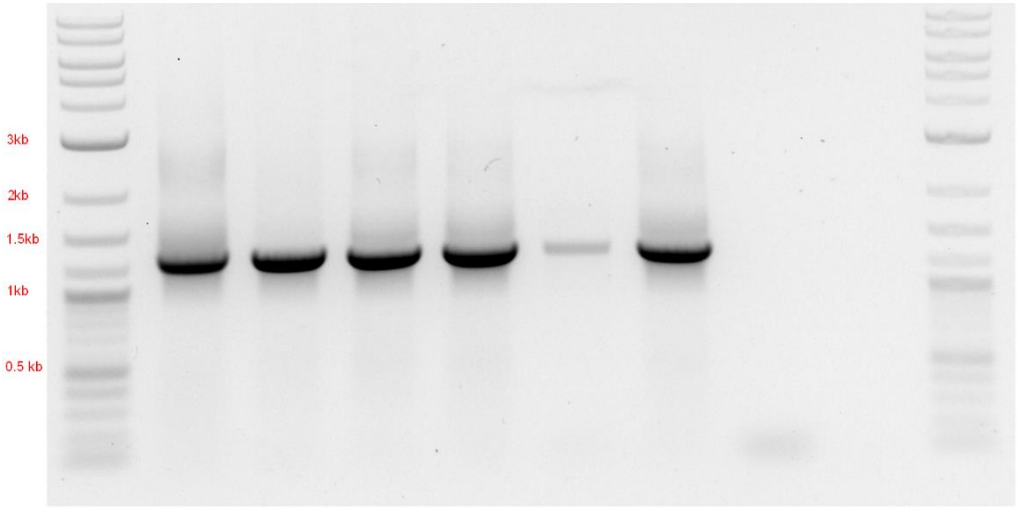

Figure 4.5 Image of successful PCR of the Hb109f and Hb1525r primers designed in this study. Left and right lanes show DNA ladder. Lanes 2-7 (from left to right) show PCR products of roughly 1,200 bp. Lanes 8 and 9 show no PCR product in the negative control

PCR clean up

The PCR products were purified using a QIAquick PCR Purification Kit according to the manufacturer's instructions. Following PCR purification, the concentration of PCR product was ascertained *via* a Thermo Scientific nanodrop 1000.

c) Sequence analysis

The purified PCR products were shipped to Macrogen, Seoul, where they were sequenced using a 3730xl DNA Analyser. Sequencing was carried out in both a forward and reverse direction.

Sequence and quality data was returned from Macrogen in the .ab1 file format. These files were analysed using the software BioEdit v7.2.6 (Hall, 1999). Regions of high quality DNA were identified in each of the DNA electropherograms by the clarity of individual peaks. Using BioEdit (Hall, 1999), a contig (overlapping DNA fragments that in combination represent a consensus region of DNA) was prepared based upon the sequences for the Com1-Com2 and Hb109f-Hb1354r reactions in both forward and reverse directions. Where there was a mismatch in the overlapping sequence data, the quality of the sequencing was investigated by comparing the raw electropherograms and determining which sequence had the clearest and higher quality peaks

The contigs were assigned taxa by means of the Naïve Bayesian rRNA Classifier v1.0 analysis tool within the Ribosomal Database Project II (Wang et al., 2007). The NCBI Blast program (Johnson et al., 2008) was also used to identify the most closely related species to each isolate.

Phylogenetic trees were generated using the software MEGA7 (Kumar et al., 2016). The trees were constructed using type strains of all known species within a genera that an isolate had been assigned to. The trees also included the type strains of species within closely related genera as identified *via* previously drawn phylogenetic trees of the halophilic archaea (Gupta et al., 2015). Type strains of species were identified by means of the online database "List of prokaryotic names with standing in nomenclature" (Parte, 2013). MEGA7 constructed trees using the maximum likelihood method based on the Tamura-Nei model (Tamura and Nei, 1993) and a bootstrap value of 100.

4.2.4 - Carbon utilisation of the isolates

The utilisation of different carbon sources was ascertained by two techniques, as described below.

a) Biolog plates

The first method was the use of Technopath Biolog Ecoplates. These 96 well plates contain 31 different organic carbon sources, selected for their applicability to soil microbial community analysis (Insam, 1997). The carbon sources were dried with essential nutrients, in triplicate, along with negative controls (containing no carbon source, Gryta et al., 2014), as shown in Table 4.2.

Table 4.2 -Layout of the carbon sources within the Biolog Ecoplates. Table is copied from the manufacturer's instruction booklet (Murphy, 2008)

A1 Water	A2 β-Methyl-D-Glucoside	A3 D-Galactonic Acid γ-Lactone	A4 L-Arginine	A1 Water	A2 β-Methyl-D-Glucoside	A3 D-Galactonic Acid γ-Lactone	A4 L-Arginine	A1 Water	A2 β-Methyl-D-Glucoside	A3 D-Galactonic Acid γ-Lactone	A4 L-Arginine
B1 Pyruvic Acid Methyl Ester	B2 D-Xylose	B3 D-Galacturonic Acid	B4 L-Asparagine	B1 Pyruvic Acid Methyl Ester	B2 D-Xylose	B3 D-Galacturonic Acid	B4 L-Asparagine	B1 Pyruvic Acid Methyl Ester	B2 D-Xylose	B3 D-Galacturonic Acid	B4 L-Asparagine
C1 Tween 40	C2 i-Erythritol	C3 2-Hydroxy Benzoic Acid	C4 L-Phenylalanine	C1 Tween 40	C2 i-Erythritol	C3 2-Hydroxy Benzoic Acid	C4 L-Phenylalanine	C1 Tween 40	C2 i-Erythritol	C3 2-Hydroxy Benzoic Acid	C4 L-Phenylalanine
D1 Tween 80	D2 D-Mannitol	D3 4-Hydroxy Benzoic Acid	D4 L-Serine	D1 Tween 80	D2 D-Mannitol	D3 4-Hydroxy Benzoic Acid	D4 L-Serine	D1 Tween 80	D2 D-Mannitol	D3 4-Hydroxy Benzoic Acid	D4 L-Serine
E1 α-Cyclodextrin	E2 N-Acetyl-D-Glucosamine	E3 γ-Hydroxybutyric Acid	E4 L-Threonine	E1 α-Cyclodextrin	E2 N-Acetyl-D-Glucosamine	E3 γ-Hydroxybutyric Acid	E4 L-Threonine	E1 α-Cyclodextrin	E2 N-Acetyl-D-Glucosamine	E3 γ-Hydroxybutyric Acid	E4 L-Threonine
F1 Glycogen	F2 D-Glucosaminic Acid	F3 Itaconic Acid	F4 Glycyl-L-Glutamic Acid	F1 Glycogen	F2 D-Glucosaminic Acid	F3 Itaconic Acid	F4 Glycyl-L-Glutamic Acid	F1 Glycogen	F2 D-Glucosaminic Acid	F3 Itaconic Acid	F4 Glycyl-L-Glutamic Acid
G1 D-Cellobiose	G2 Glucose-1-Phosphate	G3 α-Ketobutyric Acid	G4 Phenylethyl-amine	G1 D-Cellobiose	G2 Glucose-1-Phosphate	G3 α-Ketobutyric Acid	G4 Phenylethyl-amine	G1 D-Cellobiose	G2 Glucose-1-Phosphate	G3 α-Ketobutyric Acid	G4 Phenylethyl-amine
H1 α-D-Lactose	H2 D,L-α-Glycerol Phosphate	H3 D-Malic Acid	H4 Putrescine	H1 α-D-Lactose	H2 D,L-α-Glycerol Phosphate	H3 D-Malic Acid	H4 Putrescine	H1 α-D-Lactose	H2 D,L-α-Glycerol Phosphate	H3 D-Malic Acid	H4 Putrescine

A tetrazolium dye was included in each well and, as the organic carbon was metabolised, the dye was reduced causing a colour change (Gryta et al., 2014). The low carbon content of the rock samples (Section 2.3.2) prevented characterisation of any organic species in the environmental samples, so it is uncertain whether the carbon sources on the plates were representative of those available to the microbes in Boulby Mine. They did, however, represent a wide range of potential carbon sources, important since the ability to metabolise them is highly variable between species of microorganisms (Insam, 1997). This was, therefore, a relatively simple way to carry out preliminary analyses of the carbon sources that these isolates can utilise.

Cells were washed in 200 g l^{-1} NaCl solution to remove traces of their previous media, and then transferred to the Biolog Ecoplates, such that each well contained 200 µl of media and 1×10^8 cells. Plates were sealed with parafilm and incubated at 38 °C in the dark for a period of one month. An abiotic control plate was prepared in parallel, this was in order to ascertain whether the 200 g l^{-1} NaCl was capable of inducing colour change in the wells without microbial activity.

Typically, Biolog Ecoplate experiments are analysed using a plate reader (Insam et al., 2001, Westergaard et al., 2001, Feigl et al., 2017). This was not feasible in this Chapter, because of the highly saline solutions required for growth of the isolates. The high salinity caused the small volumes within the wells to evaporate rapidly and unevenly across the plate, precipitating solid NaCl crystals at the base of the wells; these interfered with absorbance readings. As the plate reader could therefore not be used, after one month the plates were assessed *via* a visual inspection, and the wells where the colour change had occurred were noted.

In order to prevent the plates drying out, they were examined by eye every three days. If the volume of liquid within a well dropped below 100 µl, it was topped up with a mildly saline dissolution buffer (100 g l^{-1} NaCl, 10 g l^{-1} $MgSO_4.7H_2O$) developed by Gramain et al. (2011) and used in Section 2.2.5e.

b) Further carbon characterisation

Biolog carbon plates have not been used with halophilic microorganisms before, so it was uncertain how successful this technique would be. As a result, additional experiments were carried out in parallel using a minimal growth media that had previously been developed for halophiles (Kauri et al., 1990, Dyall-Smith, 2009), designed specifically so that the carbon source can be easily changed.

This media contained (l^{-1}): 200 g of NaCl; 50 g of $MgCl_2.6H_2O$; 5 g of K_2SO_4; 0.26g $CaCl_2.2H_2O$. The pH of the medium was adjusted to 7.5 prior to autoclaving. After sterilisation, 5 ml of filter sterilised 1M NH_4Cl, 2ml of phosphate buffer (Dyall-Smith, 2009) and 1 ml of trace elements solution (Dyall-Smith, 2009) were added to the medium in a sterile laminar flow-hood. The medium (9.75 ml) was dispensed into sterile 15 ml falcon tubes.

Carbon sources were added to the medium to give a final concentration of 5 g l^{-1}. Stock solutions (200 g l^{-1}) were prepared containing the following: Difco Yeast Extract (to act as a positive control), malic acid, ammonium acetate, citric acid, ascorbic acid, ethanol, ferric citrate, D-glucose, glycerol, lactic acid, sodium acetate, tri-sodium citrate, glutamic acid and water with no carbon (to act as a negative control). Where 200 g l^{-1} solutions could not be made because of saturation limits (as was the case for ammonium acetate,

ascorbic acid, ferric citrate and glutamic acid), saturated solutions were prepared. For sterilisation, these solutions were filtered through a 0.22 μm filter.

For inoculation, cells were washed in 200 g l^{-1} NaCl, in order to remove any carbon left over from the growth media, and resuspended in the media to a final density of 1×10^{8} cells ml^{-1}. Cultures were incubated at the dark at 38 °C for a period of 1 month and aerated by hand-shaking twice a week. Each experiment was carried out in triplicate.

After a month, growth was determined using Sybr ® Green I DNA, as previously described (Section 4.2.1.c).

4.2.5 - Salt tolerance of the isolates

The isolation method used in this Chapter selected for a wide range of halotolerances, from 200 - 3.2 g l^{-1}. Therefore, the halotolerance for each of the isolates was determined, as was the ability of the isolates to tolerate salts other than NaCl.

a) Halotolerance

Halotolerance was determined by investigating growth in 10 % MPM with NaCl concentrations of 3.42 M (the unaltered concentration in both 100 % and 10 % MPM), 2.56 M, 1.71 M, 0.87 M and 0 M. Preliminary experiments carried out only on *Haloarcula Sp.* JPW1 and *H.noricense* FEM1 & FEM2 (data presented in Appendix 9a) indicated that when these isolates were transferred to media of this salt concentration and growth occurred, the stationary phase would be reached within a month.

Sudden osmotic shock upon addition to a new media can have significant impact on growth curves (Cheroutre-Vialette et al., 1998). In order to minimise this effect from these experiments, before the growth curve experiments were conducted, the cells were

washed and transferred to a "acclimatisation culture" culture of each of the salt concentrations (at a density of 1×10^8 cells ml^{-1}) and allowed to adjust to these NaCl concentrations for a period of one month.

These acclimatisation cultures were used as an inoculum for the cultures where the growth curve was monitored. To ensure consistency between experiments the same number of cells (1×10^8 cells ml^{-1}) was added to each medium. Growth was monitored for a period of one month, using the plate reader method described above (Section 4.2.1c). To ensure consistency in aeration, which is known to impact microbial growth (Rei, 1959, Winslow et al., 1932) the cultures were continually shaken at 190 rpm during incubation.

Specific growth rates were calculated using the Growthcurver package for the statistics software R (Sprouffske and Wagner, 2016). Each experiment was carried out in quadruplet. Where growth was not detected, the experiment was repeated to a total of eight times.

b) Tolerance to non-halite salts

The tolerance of the isolates to a variety of non-halite salts (in the presence and absence of NaCl) was also determined. The rational for the salts tested was as follows:

- KCl (Brown and Gibbons, 1955) and $MgCl_2$ (Mullakhanbhai and Larsen, 1975) - for comparison with historical data on the survival of halophiles
- KCl and $CaSO_4$ - for comparison with the salts detected in Boulby Mine (Chapter 2)
- Na_2SO_4, KCl, K_2SO_4, $MgCl_2$ and $MgSO_4$ - to investigate any differences between chlorides and sulfates

- $MgCl_2$, $MgSO_4$ and $CaSO_4$ - with relevance to the martian surface (Ojha et al., 2015, Massé et al., 2014, Clark and Van Hart, 1981).

Media preparation

"Stock media" of 10 % MPM containing one of the above salts were prepared, substituting NaCl for the desired salt. The KCl stock medium was created at an equimolar (3.42 M) concentration to the normal NaCl-based MPM. The concentration of the $MgCl_2$ stock medium was 1.71 M in order to give an equimolar Cl concentration to the normal NaCl-based MPM; whilst the Na_2SO_4 stock medium was made at 1.71 M in order to keep an equimolar Na concentration. The $MgSO_4$ stock medium was also made at a concentration of 1.71 M in order to keep Mg and SO_4 concentrations consistent with the $MgCl_2$ and Na_2SO_4 media. K_2SO_4 and $CaSO_4$ based media could not be prepared at 1.71 M as these salts are highly insoluble (NCBI Resource Coordinators, 2018). These stock media were, therefore, prepared as saturated solutions. The concentrations of the stock media are shown in Table 4.3.

Table 4.3 - Final concentrations of salts replacing NaCl in the 10 % MPM Stock Media.

Salt	**Concentration (M)**
NaCl	3.42 M
KCl	3.42 M
$MgCl_2$	1.71 M
Na_2SO_4	1.71 M
$MgSO_4$	1.71 M
K_2SO_4	Saturated = 0.69 M (NCBI Resource Coordinators, 2018)
$CaSO_4$	Saturated = 0.0139 M (NCBI Resource Coordinators, 2018)

Growth experiments

Although the stock media containing high concentrations of non-NaCl salt (Table 4.3) were tested for their ability to support growth, historic data indicated that growth was

unlikely to occur. This is because prior research (Brown and Gibbons, 1955, Mullakhanbhai and Larsen, 1975) indicates that, while the presence of other salts can lower the NaCl-dependency of obligate halophiles, it cannot completely remove it. The stock media were mixed, in a laminar floor hood, with "normal" 10 % MPM (containing NaCl) in the ratios 3:1, 2:2 and 1:3 to create media across a range of salt concentrations, as listed in Table 4.4. The media were then inoculated with 1×10^{8} cells ml^{-1}, and growth was monitored, as described in Section 4.2.4a. Again, the specific growth rate was calculated using the Growthcurver package (Section 4.2.5a).

c) Water activity

In order to determine the water activity of the different media, a Novasina LabMaster AW was used at 38 ℃. The instrument chamber was loaded with 5 ml of medium. 10 % of the media (in an order selected by a random number generator) were prepared and measured in triplicate. In all cases the measurement variation was within the accuracy of the instrument (± 0.003) as stated by the manufacturer (Vandeputte et al., 2017). The remaining 90 % of the readings were only made once, but are, therefore, assumed to be accurate to within ± 0.003.

Table 4.4 - NaCl and ion concentrations when 10 % MPM was mixed with "stock media" of varying compositions.

Ratio of 10 % MPM containing NaCl to stock media with another salt	**NaCl Concentration (M)**	**Cation concentration: Na^+, K^+, Mg^{2+} or Ca^{2+} (M)**	**Anion Concentration: Cl^- or SO_4^{2-} (M)**	**Total Ion Concentration (M)**
4:0	3.42	3.42	3.42	6.84
3:1 No Salt	2.57	2.57	2.57	5.13
3:1 Na_2SO_4	2.57	3.42	2.99	6.41
3:1 $MgSO_4$	2.57	2.99	2.99	5.99
3:1 $MgCl_2$	2.57	2.99	3.42	6.41
3:1 KCl	2.57	3.42	3.42	6.84
3:1 K_2SO_4	2.57	2.91	2.74	5.65
3:1 $CaSO_4$	2.57	2.57	2.57	5.14
2:2 No Salt	1.71	1.71	1.71	3.42
2:2 Na_2SO_4	1.71	3.42	2.57	5.99
2:2 $MgSO_4$	1.71	2.57	2.57	5.13
2:2 $MgCl_2$	1.71	2.57	3.42	5.99
2:2 KCl	1.71	3.42	3.42	6.84
2:2 K_2SO_4	1.71	2.40	2.06	4.46
2:2 $CaSO_4$	1.71	1.72	1.72	3.43
1:3 No Salt	0.86	0.86	0.86	1.71
1:3 Na_2SO_4	0.86	3.42	2.13	5.56
1:3 $MgSO_4$	0.86	2.14	2.14	4.28
1:3 $MgCl_2$	0.86	2.14	3.42	5.56
1:3 KCl	0.86	3.42	3.42	6.84
1:3 K_2SO_4	0.86	1.89	1.37	3.26
1:3 $CaSO_4$	0.86	0.87	0.87	1.73
0:4 No Salt	0.00	0.00	0.00	0.00
0:4 Na_2SO_4	0.00	3.42	3.42	5.13
0:4 $MgSO_4$	0.00	1.71	1.71	3.42
0:4 $MgCl_2$	0.00	1.71	3.42	5.13
0:4 KCl	0.00	3.42	3.42	6.84
0:4 K_2SO_4	0.00	1.38	0.69	2.07
0:4 $CaSO_4$	0.00	0.01	0.01	0.03

4.3 - Results

4.3.1 - Enrichments

In total, 48 samples of surface-sterilised salts were used to prepare microbial enrichments. These included: Boulby Halite; Boulby Potash; the top and bottom of the interface between them from Sites A, B, D, E & X; the sylvite from Site X; and the polyhalite and anhydrite of unknown provenance from deeper in the mine (see Section 2.2.1). After three months, microbial growth was investigated using Sybr ® Green I (Section 4.2.1c). In flasks where growth had occurred, the cell density was between 1×10^{9} and 2×10^{10} cells ml^{-1}. In flasks where no growth was observed, the enrichments were re-examined after another six months, but no further growth was seen. It is assumed, based on the work in Section 3.3.2b, that these were mixed cultures, consisting of a variety of different strains of microorganisms.

Until isolation could be attempted from these mixed cultures (Section 4.3.2), no conclusions could be drawn about the distribution of specific viable microorganisms between lithologies. However, it has previously been proposed that when multiple samples of a lithology are inoculated in separate enrichment cultures, the number of cultures where growth is observed is indicative of the number of viable cells within this lithology (McGenity et al., 2000). This assumption has been employed in this Thesis, in order to investigate potential variation in the number of viable cells between the different lithologies in Boulby Mine.

In order to compare the different number of samples which demonstrated positive growth between the different lithologies with different overall number of samples, a "success rate" for the generation of growing cultures was calculated. The success rate

was the number of cultures where growth was observed after a period of three months, expressed as a percentage of the total number of sample-media mixtures created for that lithology or media composition. For ease of interpretation, calculations of success rates for media (in Section 4.3.1a) are based only on lithologies that had been shown to be capable of producing growth (in Section 4.3.1b). Conversely, calculations of success rates of lithologies (in Section 4.3.1b) are based only on media compositions where growth could be shown to occur (in Section 4.3.1a).

a) Comparison between growth media

Growth was only detected in the 10 % MPM (success rate of 41.6 %), 100 % MPM and the 200 g l^{-1} NaCl media (both had a success rate of 6.25 %). Growth was not detected in the non-saline GYP medium (Section 4.2.1a). Although growth was observed in the 200 g l^{-1} NaCl (containing no additional nutrients), the cultures were incapable of further growth when subbed into fresh 200 g l^{-1} NaCl medium. In order to maintain these cultures long-term, the cultures were therefore re-inoculated into 10 % MPM.

b) Comparison between lithologies

Of the 48 samples used to inoculate the media, 12 were Boulby Halite, 13 were from the bottom of the Boulby Potash-Boulby Halite interface (see Section 2.2.2d), 12 were from the top of this interface and 11 were from the Boulby Potash.

The 12 samples of Boulby Halite were dissolved in flasks of each of the five media compositions (Section 4.2.1) to a total of 60 flasks. Microbial growth was only observed in the 100 % MPM (one culture) and the 10 % MPM (three cultures). No growth was detected with the Boulby Halite samples in any of the other growth media.

The 13 samples from the bottom of the Boulby Potash-Boulby Halite interface were also dissolved in flasks of each of the five media (75 flasks). Here, microbial growth was detected in all three of the saline media: 100 % MPM (one culture), 10 % MPM (eight cultures) and 200 g l^{-1} NaCl (three cultures).

The 12 samples from the top of the interface region were also subjected to the same approach (to a total of 60 flasks), but growth was detected only in the 100 % MPM (one culture) and the 10 % MPM (two cultures); no growth was detected in 200 g l^{-1} NaCl.

For the 11 Boulby Potash samples (55 flasks), growth was only detected in the 10 % MPM (eight cultures).

No growth was detected in the sylvite, polyhalite or anhydrite enrichments. This could be a result of low biomass within the samples, an inability to maintain viable cells, a lack of cells that could grow within the inoculation media or a result of the relatively small number of samples investigated compared to the other sample types (four of sylvite, three of anhydrite and two of polyhalite).

Although it could not be demonstrated statistically, the most growth was observed when Boulby Potash was used as the inoculum (24.2 % success rate), followed by the Boulby Halite (11.1 % success rate). As shown in Section 2.2.2d, the Boulby Potash had a significantly higher K and lower Na concentration than the Boulby Halite. This could suggest that the higher K concentration of the Boulby Potash might influence the chances of viable microorganisms being extracted from the samples. No statistically significant inter-or intra-lithological difference was found, however, between the K or Na concentrations of the samples that produced growth (Student's t-Tests, $p > 0.05$). Chapter 2 had shown significant inter-lithological differences in the Ca, Fe and Mn

concentrations between the samples (Section 2.2.2d), but Student's t-Tests showed no significant difference in the concentration of any of the measured ions between samples that did and did not produce growth ($p > 0.05$ for both inter- and intra-lithological tests).

4.3.2 - Isolation

a) Isolate sequences

Microorganisms were isolated using the methods outlined in Section 4.2.2. Using these methods, DNA was extracted from 56 potential pure cultures for sequencing (Section 4.2.3). Of these 56 potential isolates, 12 were not pure, which was evidenced by an absence of clear peaks in the sequencing electropherograms. These impure cultures had all resulted from the dilution series procedure (Section 4.2.2.b). This indicates that, despite the low diversity of the mixed cultures (as evidenced by the MiSeq data in the previous chapter, Section 3.3.2b, and the small number of sequences observed across 56 potential isolates), it was difficult to obtain pure cultures using the dilution method.

The remaining 44 isolates were represented by six unique sequences (Table 4.5). Four of these sequences were assigned to the genus *Haloarcula* with a 100 % confidence, using the RDP database, and were named JPW1-4. Two of the isolates were identified as members of the genus *Halobacterium* with 100 % confidence and were named FEM1-2. This, therefore, would imply that all six sequences were members of the order *Halobacteriales* in the class *Halobacteria* and the domain *Archaea*. All sequence data for these isolates can be found in FASTA format in Appendix 6.

Table 4.5 -The 48 isolates that produced good quality sequence data contained one of 6 sequences between the Com1-Com2 regions or were an impure sequence. Based on analysis later in this chapter, the four sequences are named FEM1-2 and JPW1-4.

Isolation method	**Sample type**	**Sequence**
100% MPM agar	Boulby Halite	FEM1
Dilution series in 100 g/l NaCl	Boulby Potash	FEM1
Floating filter	Bottom of well-defined interface region	FEM1
Floating filter	Bottom of well-defined interface region	FEM1
Floating filter	Bottom of well-defined interface region	FEM1
Floating filter	Boulby Halite	FEM1
Floating filter	Boulby Halite	FEM1
Floating filter	Boulby Potash	FEM1
Dilution series in 100 g/l NaCl media	Boulby Potash	FEM2
Dilution series in 100 g/l NaCl media	Boulby Potash	FEM2
Dilution series in media of normal salinity	Boulby Potash	FEM2
Dilution series in media of normal salinity	Halite	FEM2
Dilution series in media of normal salinity	Boulby Potash	FEM2
Floating filter	Boulby Potash	FEM2
100% MPM agar	Top of the well-defined interface region	JPW1
100% MPM agar	Top of the well-defined interface region	JPW1
100% MPM agar	Top of the well-defined interface region	JPW1
100% MPM agar	Top of the well-defined interface region	JPW1
Floating filter	Bottom of well-defined interface region	JPW2
Floating filter	Bottom of well-defined interface region	JPW2
Floating filter	Bottom of well-defined interface region	JPW2
Floating filter	Bottom of well-defined interface region	JPW2
Floating filter	Bottom of well-defined interface region	JPW2
10% MPM agar	Boulby Potash	JPW3
10% MPM agar	Boulby Potash	JPW3
10% MPM agar	Boulby Potash	JPW3
10% MPM agar	Boulby Potash	JPW3
Floating filter	Boulby Potash	JPW3
Floating filter	Boulby Halite	JPW3
Floating filter	Boulby Potash	JPW3
Floating filter	Boulby Potash	JPW3
Floating filter	Top of the well-defined interface region	JPW3
Floating filter	Top of the well-defined interface region	JPW3
Floating filter	Top of the well-defined interface region	JPW3
Floating filter	Boulby Potash	JPW3
Floating filter	Boulby Potash	JPW3
Floating filter	Boulby Halite	JPW3
Floating filter	Boulby Halite	JPW3
Floating filter	Top of the well-defined interface region	JPW3
Halorubrum chaoviator agar	Boulby Potash	JPW3
ASW agar	Boulby Potash	JPW3
Modified CASO agar	Boulby Halite	JPW3
Modified CASO agar	Boulby Potash	JPW4
Modified CASO agar	Boulby Potash	JPW4

Strains FEM1, FEM2 & JPW3 were isolated from both the Boulby Halite and the Boulby Potash (Table 4.5), indicating that the presence of *Haloarcula* and *Halobacterium* appeared to be unaffected by geochemical composition. The JPW4 strain was isolated

only twice, in both occasions from the Boulby Potash. Despite the relatively large number of times JPW1 and JPW2 were isolated (four and five times respectively), each isolate was only isolated from a single mixed culture, which means they may have been unique to the specific samples that inoculated these cultures.

b) Taxonomy of the isolates

The Halobacterium isolates

As discussed above (Section 4.3.2a), the isolates FEM1 and FEM2 were identified *via* the RDP classifier as members of the genus *Halobacterium.* Comparison with the NCBI database using the BLAST algorithm (Johnson et al., 2008) showed that the two isolates were closely related to *Halobacterium* sequences (from both isolates and uncultured sequences detected in environmental samples) found in Chinese salt mines (Table 4.6), so their presence here is not unexpected.

Table 4.6 - Taxonomical identification of the Halobacterium isolates identified with the sequence length and identity of the most closely related cultured and uncultured organisms within the NCBI database

Strain	Sequence length (BP)	Similarity to cultured organisms	Similarity to uncultured organisms
FEM1	1105	99% similarity to *Halobacterium salifodinae* strain: JCM 18548 isolated from a Chinese salt mine	99% similarity to *Halobacterium* genes identified in Chinese salt mines
FEM2	1054	99% similarity to *Halobacterium salifodinae* strain: JCM 18548 isolated from a Chinese salt mine	99% similarity to *Halobacterium* genes identified in Chinese salt mines

The high rate of horizontal gene transfer across the class *Halobacterium* (not just within the genus of the same name) means that there is relatively little genetic diversity between organisms regarded as different species (Fullmer et al., 2014). It was, therefore, the case that when the sequences from the genus *Halobacterium* (FEM1 and FEM2) were compared to previously cultured microorganisms (which exist in culture collections and have had more stringent identification carried out than just 16s rRNA

sequencing) using the BLAST algorithm, the results showed a 99 % similarity to multiple different species e.g., *H.noricense, hubeinse* and *salifodinae* (Figure 4.6).

Alignments Download GenBank Graphics Distance tree of results

Description	Max score	Total score	Query cover	E value	Ident	Accession
Halobacterium sp. YZY-6 16S ribosomal RNA gene, partial sequence	2013	2013	100%	0.0	99%	KJ644270.1
Halobacterium sp. QJL-11 16S ribosomal RNA gene, partial sequence	2013	2013	100%	0.0	99%	KJ644256.1
Halobacterium sp. Q37 16S ribosomal RNA gene, partial sequence	2013	2013	100%	0.0	99%	KJ644181.1
Halolamina salifodinae gene for 16S ribosomal RNA, partial sequence, strain: JCM 18548	2013	2013	100%	0.0	99%	AB935417.1
Halobacterium sp. 2-24-7 partial 16S rRNA gene, isolate 2-24-7	2013	2013	100%	0.0	99%	AJ878083.1
Halobacterium sp. 2-24-5 partial 16S rRNA gene, isolate 2-24-5	2013	2013	100%	0.0	99%	AJ878081.1
Halobacterium sp. DCP-2 16S ribosomal RNA gene, partial sequence	2008	2008	100%	0.0	99%	KJ644310.1
Halobacterium hubeiense strain JI20-1 genome assembly, chromosome: I	2008	2008	100%	0.0	99%	LN831302.1
Halobacterium sp. YI80-2 16S ribosomal RNA gene, partial sequence	2008	2008	100%	0.0	99%	KJ917624.1
Halobacterium sp. YI80-1 16S ribosomal RNA gene, partial sequence	2008	2008	100%	0.0	99%	KJ917623.1
Halobacterium noricense strain JCM 15102 16S ribosomal RNA gene, complete sequence	2008	2008	100%	0.0	99%	NR_113426.1
Halobacterium noricense strain A1 16S ribosomal RNA gene, partial sequence	2008	2008	100%	0.0	99%	NR_028187.1
Halobacterium sp. BIHGY150/14 partial 16S rRNA gene, strain BIHGY150/14	2008	2008	100%	0.0	99%	AM902591.1
Halobacterium sp. BIHSTY150/18 partial 16S rRNA gene, strain BIHSTY150/18	2008	2008	100%	0.0	99%	AM902590.1

Figure 4.6 - Screenshot of the BLAST output of isolate FEM1 against the NCBI database. The figure shows the top hits for FEM1 including members of H.salifodinae, H.hubeinse and H.noricense, an expanded image would show other species of Halobacterium which also had 99% similarity. A similar result was observed with FEM2

A phylogenetic tree was constructed for the *Halobacterium* isolates using the program MEGA7 (Section 4.2.3.b). The tree contained the type strains of all members of the *Halobacterium* genus and the closely related genus *Halarcheum* (Figure 4.7). Both FEM1 and FEM2 were seen to be more closely related to the species *Halobacterium noricense* than any of the other species type strains. As a result, the isolates were assigned to the species *Halobacterium noricense.* The two strains of *H.noricense* obtained in this project had very similar 16S rRNA genes (>99 % accuracy), with only five differences observed along the 1,000 bp long contig (Figure 4.8).

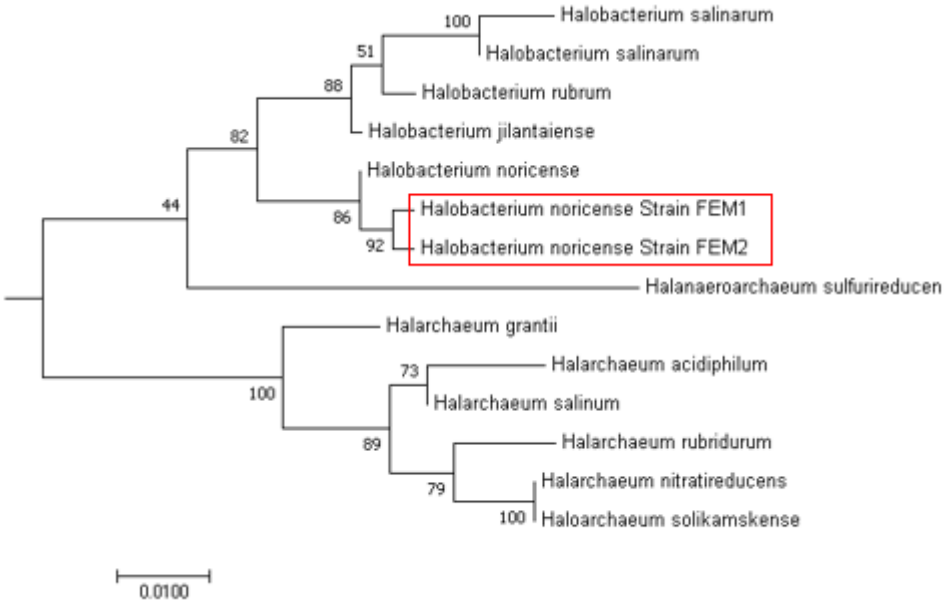

Figure 4.7 - Phylogenetic tree showing relationships between two of the isolates (marked with a red box) *and the genera* Halobacterium, Halarchaeum *and* Halanaeroachaeum. The *percentage of trees in which the associated taxa clustered together is shown next to the branches. The tree is drawn to scale, with branch lengths measured in the number of substitutions per site.*

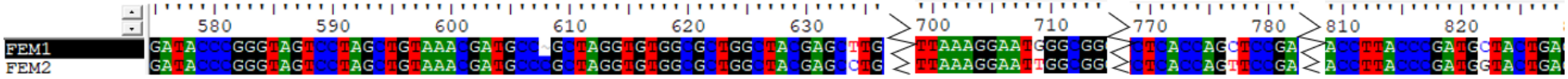

Figure 4.8 - When the Halobacterium *sequences were aligned, only five differences were observed across the entire 1,000 bp long contigs, Alignment shown as a screenshot of the software BioEdit (Hall, 1999) using the ClustalW plugin (Thompson et al., 2002).*

The Haloarcula isolates

As discussed in Section 4.3.2a, the isolates JPW1-4 were identified *via* the RDP classifier as members of the genus *Haloarcula.* Comparison with the NCBI database using the BLAST algorithm showed that three of the isolates had 99 % similarity to previously identified or cultured *Haloarcula* species. However, JPW1's similarity was only 97 % (Table 4.7).

Table 4.7 - Taxonomical identification of the Haloarcula isolates identified with the sequence length and identity of the most closely related cultured and uncultured organisms within the NCBI database

Strain	Sequence Length (bp)	Similarity to cultured organisms	Similarity to uncultured organisms
JPW1	1114	97% similarity to *Haloarcula salaria* isolate CA_13B5 grown in salterns	97% similarity to various uncultured halophiles from salt-lakes
JPW2	1015	99% similarity to *Haloarcula salaria* isolate CA_13B5 grown in salterns	99% similarity to various uncultured halophiles from salt-lakes
JPW3	1135	99% similarity to *Haloarcula salaria* isolate CA_13B5 grown in salterns	99% similarity to various uncultured halophiles from salt-lakes
JPW4	961	99% similarity to *Haloarcula salaria* isolate CA_13B5 grown in salterns	99% similarity to various uncultured halophiles from salt-lakes

As with the *Halobacterium* isolates, the *Haloarcula* isolates showed the same degree of similarity to multiple species within the same genera. In this case, the species were: *H.salaria, H.amylolitica, H.vallismortis,* and *H.hispanica.* As with the *Halobacterium,* a phylogenetic tree was constructed containing the type strains of all members of the *Haloarcula* as well as the closely related genera *Halomicrobium* and *Halomicroarcula* (Figure 4.9). The *Halobacterium* isolates had clustered with one species in particular, which allowed identification, but the JPW isolates clustered far more closely with each other than any previously identified species. This could imply that these isolates represent a species not previously identified; however, as discussed in Section 4.4.6b, proving this is beyond the scope of this PhD.

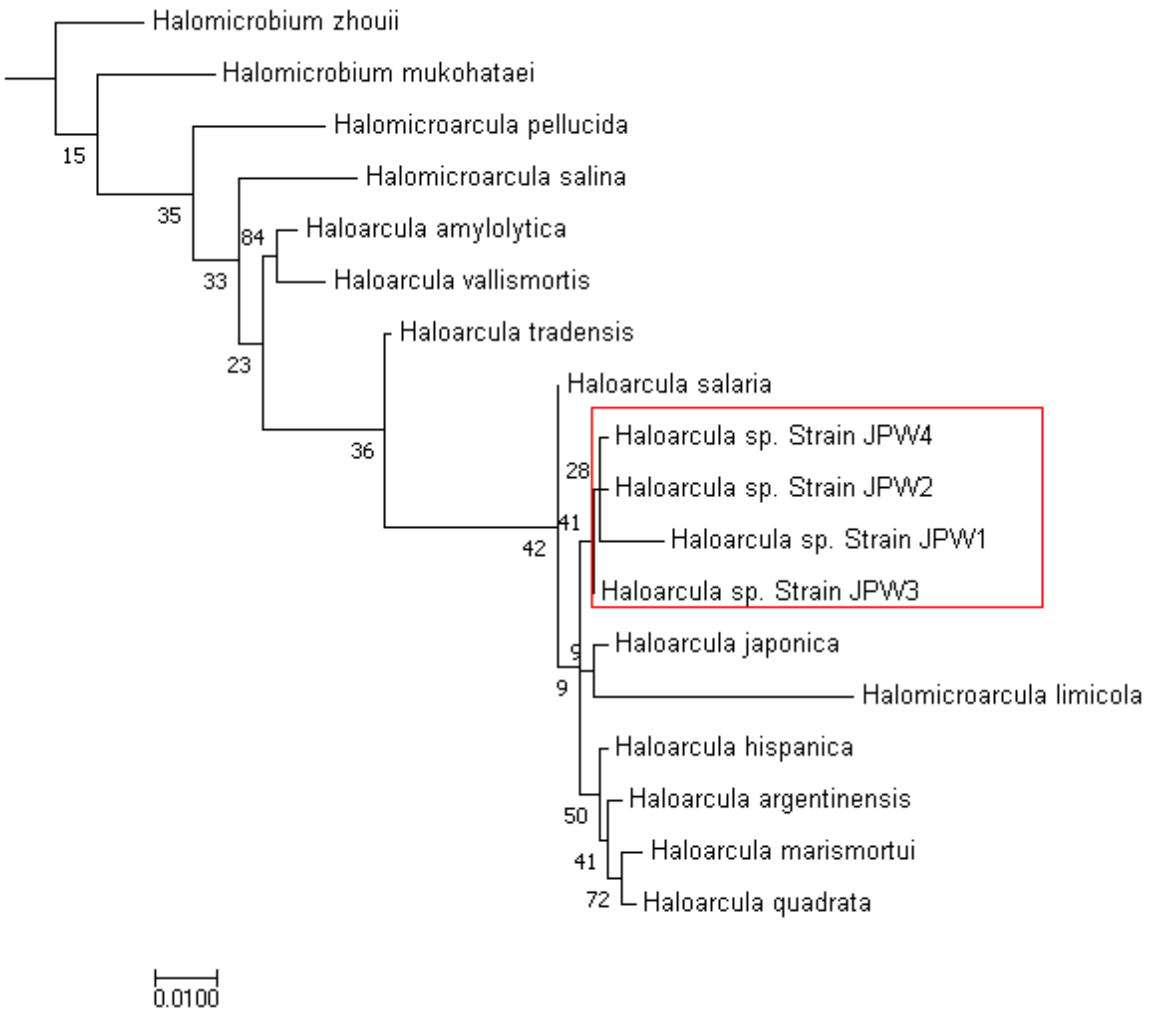

Figure 4.9 - Phylogenetic tree showing relationships between four of the isolates (marked with a red box) and the genera Halomicrobium, Halomicroarcula and Haloarcula. The percentage of trees in which the associated taxa clustered together is shown next to the branches. The tree is drawn to scale, with branch lengths measured in the number of substitutions per site.

c) - Characterisation of the isolates

Cellular appearance and morphology in liquid media

When initially inoculated into fresh media, the cells were a creamy white colour. During mid log phase, however, the cells became a deep pink colour, assumed to be the result of the pigment bacterioruberin (Naziri et al., 2014). Possible reasons for this change in the expression of pigmentation are discussed in Section 4.4.3d.

The cells were examined using both light and UV microscopy. The salinity of the media prevented cells from retaining their fluorescence using the Sybr ® Green I dye long enough for photos to be taken (see Section 4.2.1c), therefore light photomicroscopy was carried out using a different dye: crystal violet. No variation was observed between strains from the same genera. The strains of *Haloarcula* appeared to take up more of the crystal violet stain than the *Halobacterium noricense* strains and thus appeared a darker colour. All six isolates appeared as evenly distributed, unicellular coccoids with a diameter of ~0.5 μM.

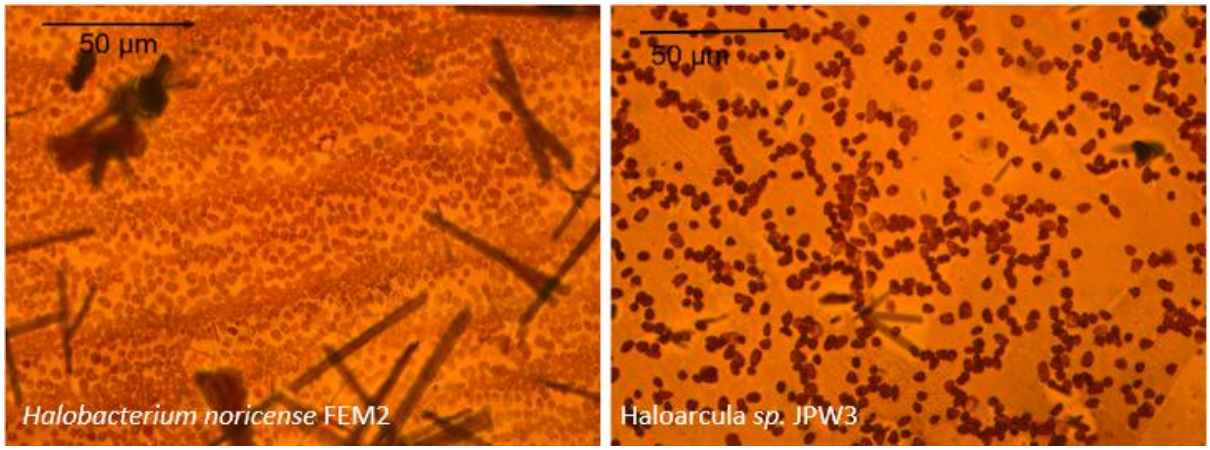

Figure 4.10 - Representative images of a strain of the Halobacterium *isolates and a strain of the* Haloarcula *isolates. Images show fixed cells stained with crystal violet grown in 10 % MPM. Large dark coloured rod-shaped objects are crystal violet crystals that have been improperly dissolved*

Growth on agar

The six isolates were grown on different agars, all containing 200 g l^{-1} NaCl, with the exception of ASW, which contained 95 g l^{-1} (see Section 4.2.2a). They typically formed thick biofilms rather than distinct colonies (Figure 4.11). It was anticipated that reducing the number of cells added to the plates would cause cells to grow at a lower density and thus form individual colonies, but instead this decreased the likelihood of growth occurring; when it did occur, it was still in the form of a biofilm.

Regardless of which agar the isolates had been initially isolated upon (Section 4.3.2a), once purified they all were capable of growth on 100 % MPM agar and the *H.chaoviator* medium agar. In addition, JPW2, JPW4 and JPW3 could grow on 10 % MPM agar, CASO agar and ASW agar, respectively (Table 4.8).

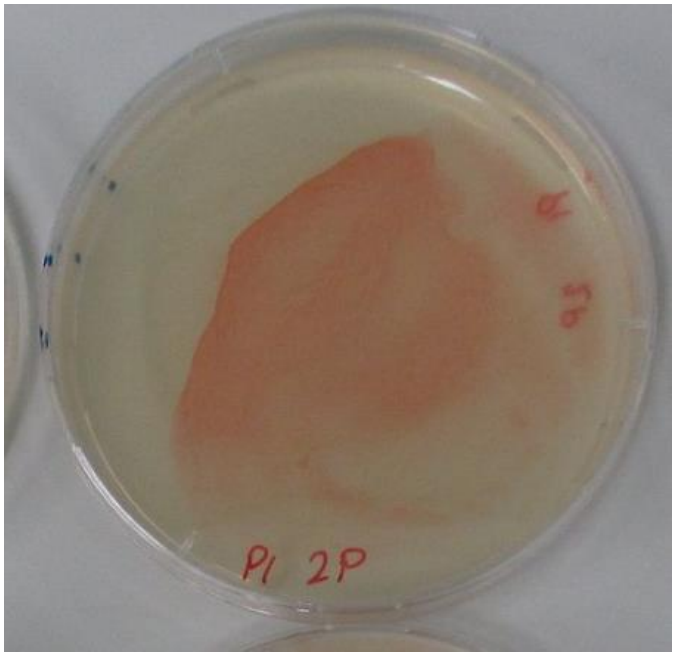

Figure 4.11 - The pink biofilm phenotype was the most common result of growth on agar. Image shows Haloarcula Sp. strain JPW3 on H.chaoviator agar

Table 4.8 - Ability of the isolates to grow on each of the agar compositions used in this project. A tick represents an isolate-agar combination where growth is possible, while a cross represents a combination where it is not.

Species	**Strain**	**100 % MPM**	**10 % MPM**	**CASO agar**	***H.chaoviator* agar**	**ASW**	**Phenotype**
Halobacterium noricense	**FEM1**	✓	×	×	✓	×	Pink biofilm
	FEM2	✓	×	×	✓	×	Pale pink biofilm
Haloarcula sp.	**JPW1**	✓	×	×	✓	×	Pink biofilm
	JPW2	✓	✓	×	✓	×	Pink biofilm
	JPW3	✓	×	×	✓	✓	Pink biofilm on 100% MPM and ASW, orange on CASO agar
	JPW4	✓	×	✓	✓	×	Colourless biofilm

In liquid culture, all of the isolates displayed the same pink pigmentation, but on agar, slight differences in the intensity of this pigmentation were observed. JPW4, in particular, did not express any pigments when grown on agar. As a general rule, an isolate would display the same pigmentation regardless of which agar it was grown on, with the exception of JPW3, which produced an orange pigment on CASO agar. As this was the only isolate that would grow on this agar, it is undetermined whether this is attributable to the agar or of the isolate.

4.3.3 - Carbon utilisation

a) Biolog Plates

96 well Biolog plate were used to investigate the carbon utilisation capability of each of the isolates. Due to the uneven evaporation and precipitation of crystals between wells within a plate, changes in absorbance could not be quantified. Therefore, each well was manually monitored for changes in colour of the tetrazolium dye, which would be indicative of metabolic activity (Gryta et al., 2014).

This experiment did not work as planned. While no colour change was observed in any of the wells of the abiotic negative control plate, the colour changes within the biotic plates were inconsistent. Often the dye changed colour in only one or two of the replicates. The biotic plates also precipitated salts at a much higher rate than the abiotic, which is consistent with the speculation of Adamski et al. (2006) that cells can act as seeds for crystal formation. The biotic plates, therefore, needed more frequent redissolution using Gramain's buffer.

It is speculated that the inconsistency in colour change was a result of repeated crystallisation, dissolution and recrystallisation within the wells. This is evidenced by

the fact that there were repeated occurrences of colour change in the negative control wells (without carbon), indicating that the colour change could be induced in the biotic wells by an effect other than metabolism. As a result, it is highly uncertain if any conclusions can be drawn from this data.

A table of results from the Biolog experiment can be found in Appendix 5.

b) Growth in minimal media

Owing to the inconsistency of results with the Biolog plates, a more simplistic method was employed to investigate carbon utilisation. For this, each isolate was grown in minimal medium containing 5 g l^{-1} of a carbon source (listed in Table 4.9). After a month of incubation, microbial growth was observed in these cultures using the Sybr ® Green I technique outlined in Section 4.2.1c. For each carbon source, either no cells were observed (indicating cell death) or a cell density of between 1-2×10^{10} cells ml^{-1} was measured, which was a 100-fold increase from initial inoculation. Since it was uncertain whether these observations of high cell density occurred during the log, death or stationary phase, it was not possible to calculate specific growth rates. As a result, this data is expressed only in a binary form. The increase in cell number indicates that the isolates were capable of utilising a carbon source, while the absence of cells indicates either that the carbon source is harmful to cells or that it could not be utilised.

No variation was observed between the isolates. Each of the isolates were able to utilise yeast, ferric citrate, glucose, glycerol, sodium acetate, tri-sodium citrate and glutamic acid, as a carbon source. No cells were observed in media containing malic acid, ammonium acetate, citric acid, ascorbic acid, ethanol, lactic acid or no carbon source, though whether this is a result of starvation brought on by an inability to metabolise

this carbon, or a result of a lethal property of a carbon source is uncertain (Table 4.9). For example, ethanol can be both a carbon source and a sterilising agent (Dai et al., 2016).

Table 4.9 - Growth of three replicates of each isolate in minimal medium containing various carbon sources

	Haloarcula Sp.				***Halobacterium noricense***	
	JPW1	**JPW2**	**JPW3**	**JPW4**	**FEM1**	**FEM2**
Positive control (Difco Yeast Extract)	✔	✔	✔	✔	✔	✔
Malic acid	✕	✕	✕	✕	✕	✕
Ammonium acetate	✕	✕	✕	✕	✕	✕
Citric acid	✕	✕	✕	✕	✕	✕
Ascorbic acid	✕	✕	✕	✕	✕	✕
Ethanol	✕	✕	✕	✕	✕	✕
Ferric citrate	✔	✔	✔	✔	✔	✔
D-Glucose	✔	✔	✔	✔	✔	✔
Glycerol	✔	✔	✔	✔	✔	✔
Lactic acid	✕	✕	✕	✕	✕	✕
Sodium acetate	✔	✔	✔	✔	✔	✔
Tri-sodium citrate	✔	✔	✔	✔	✔	✔
Glutamic Acid	✔	✔	✔	✔	✔	✔
Negative control (no carbon source)	✕	✕	✕	✕	✕	✕

4.3.4 - Salt tolerance of the isolates

a) Control experiments

Microbial growth over time was monitored for each isolate in 10 % MPM (3.42 M NaCl) using a plate reader, as described in Section 4.2.1c. Growth was then plotted, as shown in Figure 4.12, and the specific growth rate determined. The R package Growthcurver was used to calculate the mean specific growth of each of the isolates in 10 % MPM. This data is presented Table 4.10.

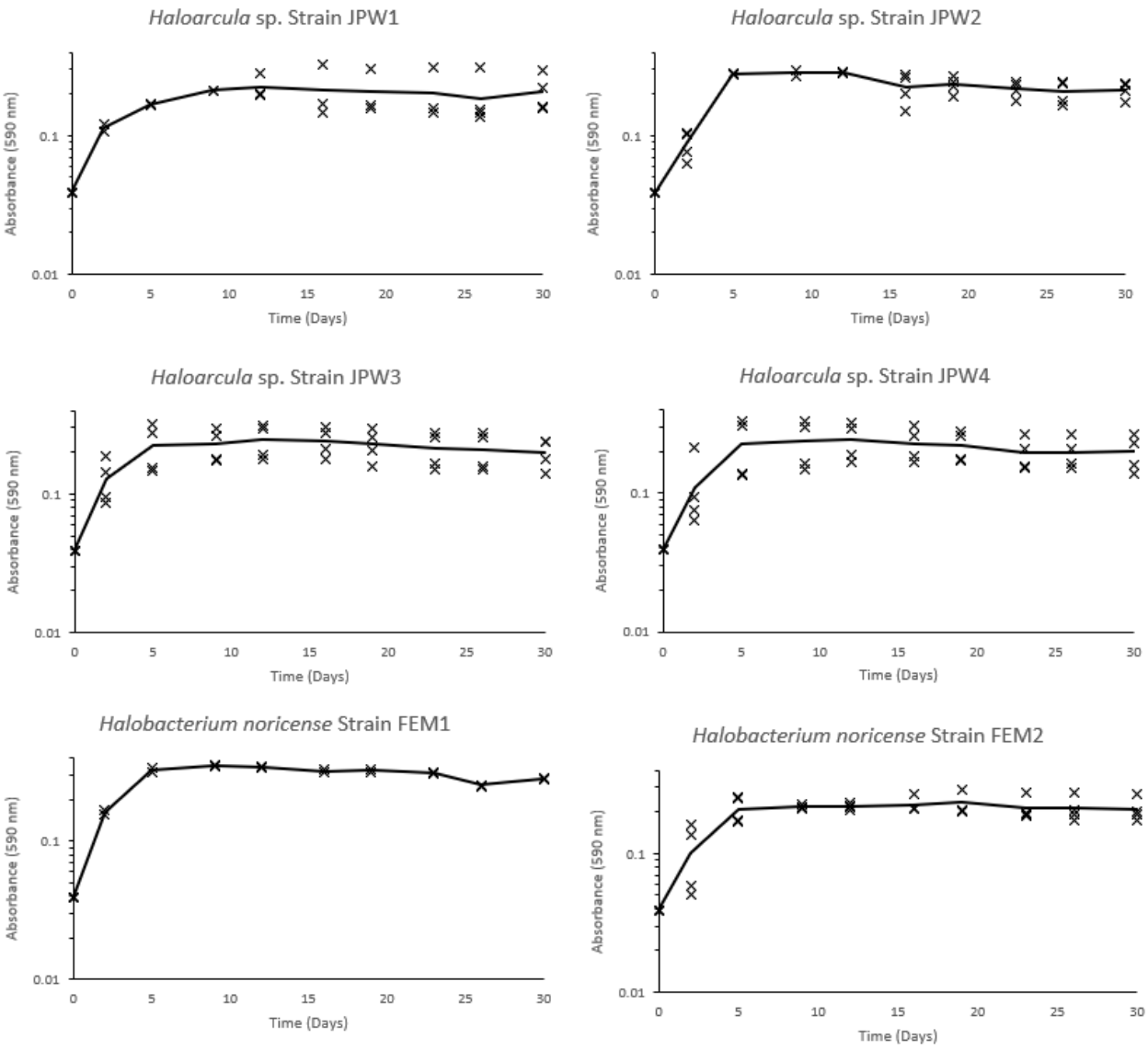

*Figure 4.12 - Growth curve of all 6 isolates grown in 10 % MPM with no modifications to the salt concentration. Black crosses represent data points (*n = *4), while the lines show the mean of the data points. Data is not background subtracted, so as to allow the logarithmic scale to show data at time zero when the cells did not raise absorbance above background levels*

For all isolates other than JPW1, the log phase occurred before day 5 (Figure 4.12), but for JPW1 the log phase extended to at least day 10 (and day 12 in one of the replicates).

*Table 4.10 - Mean specific growth rate and maximum growth of the 6 isolates in 10 % MPM (*n = *4)*

		Mean specific growth rate
Haloarcula Sp.	**JPW1**	0.774
	JPW2	0.971
	JPW3	0.870
	JPW4	1.680
Halobacterium noricense	**FEM1**	1.091
	FEM2	0.830

b) NaCl tolerance

In order to investigate salt tolerance, growth was monitored over a range of NaCl concentrations. In order to obtain cells that had been acclimatised to these salt concentrations (Saros and Fritz, 2000, Aguilera and Amils, 2005) for use in the growth curve experiments, cells were initially inoculated in these media and left to grow for a month in "acclimatisation cultures" (see Section 4.2.5a).

After a month, cells were observed to be present for all isolates at 3.42 M and 2.56 M NaCl. Furthermore, for all isolates, with the exception of *Haloarcula Sp.* JPW1, cells were observed at 1.71 M NaCl. No cells were observed for any of the isolates at 0.86 M or 0.00 M NaCl. This indicates that all the isolates were obligate halophiles, as they could not grow at low concentrations of NaCl. *Haloarcula Sp.* JPW1, however, is more of an obligate halophile than the other five isolates, as the range of NaCl concentrations it could tolerate was smaller.

After this initial acclimatisation step, new cultures were established and the specific growth rates determined using Growthcurver (Table 4.11). For those combinations of isolates and salt concentrations where the acclimatisation cultures did not support cells, the specific growth rates were taken to be 0.

*Table 4.11 - Specific growth rates of the isolates across a range of salinities (*n = *4). Shaded cells indicate experiments where cells were observed in the acclimatisation cultures, but no growth occurred when these cells were inoculated into fresh media*

Species	**Strain**	**3.42 M**	**2.56 M**	**1.71 M**	**0.86 M**	**0.00 M**
Haloarcula Sp.	JPW1	0.774	0.000	0.000	0.000	0.000
	JPW2	0.971	0.530	0.000	0.000	0.000
	JPW3	0.870	0.461	0.000	0.000	0.000
	JPW4	1.680	0.138	0.000	0.000	0.000
Halobacterium noricense	FEM1	1.091	7.455	0.954	0.000	0.000
	FEM2	0.830	0.200	0.000	0.000	0.000

Although the acclimatisation cultures showed that five of the six isolates (all except *H.noricense* JPW1) could survive (i.e., after one month, cells capable of taking up Sybr ® Green I dye were still observed) in NaCl concentrations of between 3.42 M to 1.71 M, when these cells were transferred to fresh media they were incapable of further growth (i.e., there was no change in absorbance and after one week no cells could be seen *via* Sybr ® Green I microscopy) at 1.71 M. The only exception to this was *Halobacterium noricense* FEM1, which had a higher specific growth rate at 2.56 M NaCl than under normal conditions (Table 4.11). *Haloarcula* Sp. JPW1 from the acclimatisation cultures also failed to grow in fresh media at a NaCl concentration as high as 2.56 M.

The harmful effects of NaCl concentrations much lower than the 3.42 M optimum (for example, 0.86 M or 0.00 M) appeared to cause relatively rapid cell death, as no cells were observed a month after inoculation in the acclimatisation cultures. The harmful effects of NaCl concentrations that were only slightly lower than 3.42 M (for example 2.56 M for JPW1, 1.71 M for the remaining isolates) were much slower acting, with cells being able to survive the 30 days of the acclimatisation culture, before cell death occurred within a week in the new cultures.

For the most part, the growth rates decreased with increasing salinity (Table 4.11 and Figure 4.13a). *Halobacterium noricense* FEM1, however, had its highest growth rates in

2.56 M NaCl. It was also the only isolate that could grow at 1.71 M NaCl. This implies that this isolate, while still an obligate halophile, has a lower optimum salinity than the other isolates.

c) Effects of other salts

The above growth curve experiments were repeated, but this time, when the medium had less than 3.42 M NaCl, the salt was replaced with either Na_2SO_4, KCl, K_2SO_4, $MgCl_2$, $MgSO_4$ or $CaSO_4$ as described in Section 4.2.5b. The specific growth rates, calculated by Growthcurver, for each of the isolates in these salt media can be found in Appendix 6 and on Figure 4.13**.**

In accordance with historic data (Mullakhanbhai and Larsen, 1975, Brown and Gibbons, 1955, Oren, 1983), no growth was observed when NaCl was entirely replaced by another salt. The results also confirm the prior observation (*ibid.*) that the NaCl requirement of halophiles can, to some extent, be lowered by the presence of other salts. No growth was detected for many of the isolates at NaCl concentrations of 1.71 M in the absence of other salts, when subbed from the acclimatisation, but the addition of 1.71 M KCl, 0.01 M $CaSO_4$ or 0.86 M $MgSO_4$, $MgCl_2$ or Na_2SO_4, to media would allow cells of all isolates to grow at 1.71 M NaCl (Figure 4.13). Unlike the other salts, however, K_2SO_4, would not allow growth to occur at 1.71 M NaCl (Figure 4.13f).

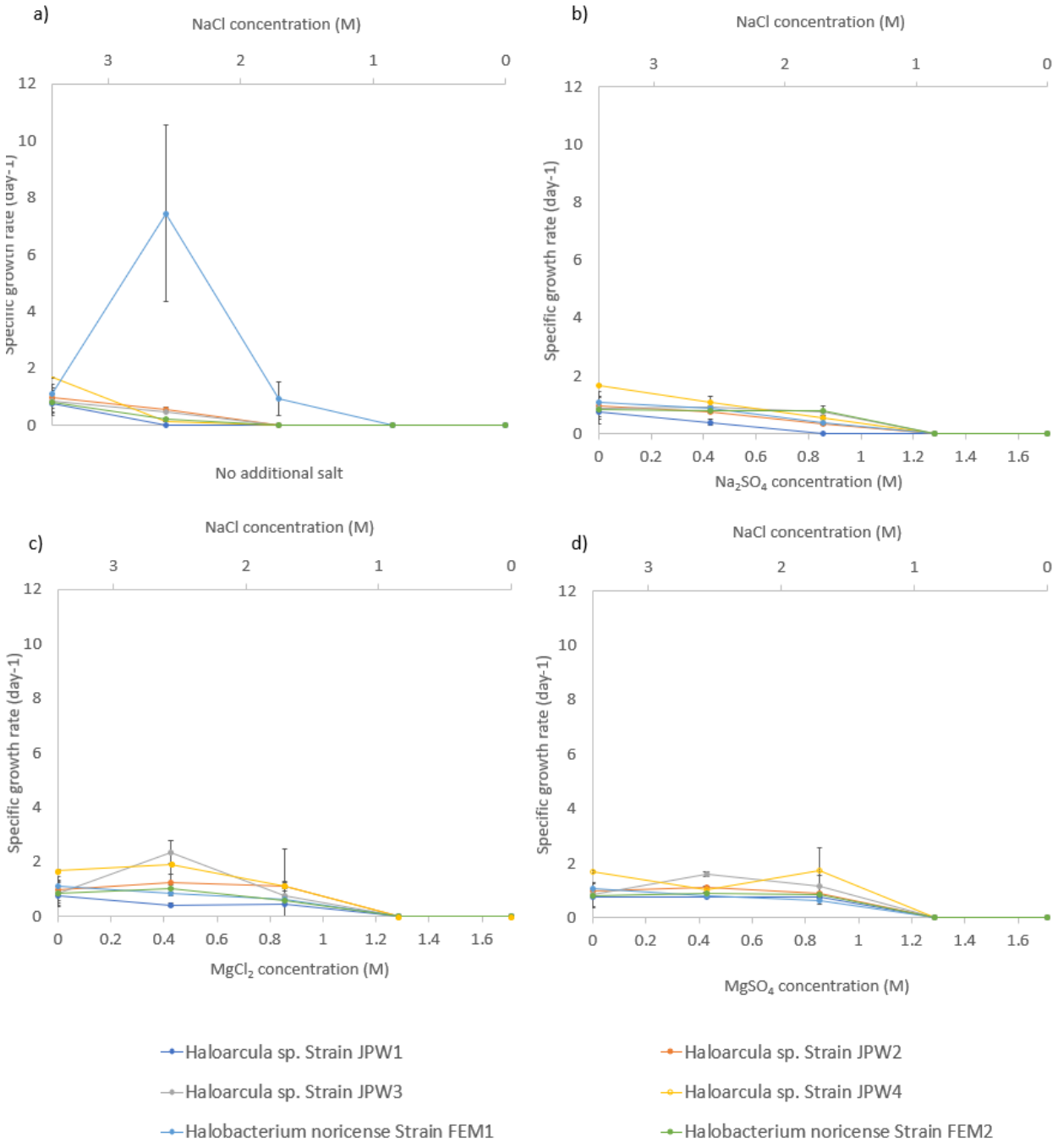

The figure extends onto the next page.

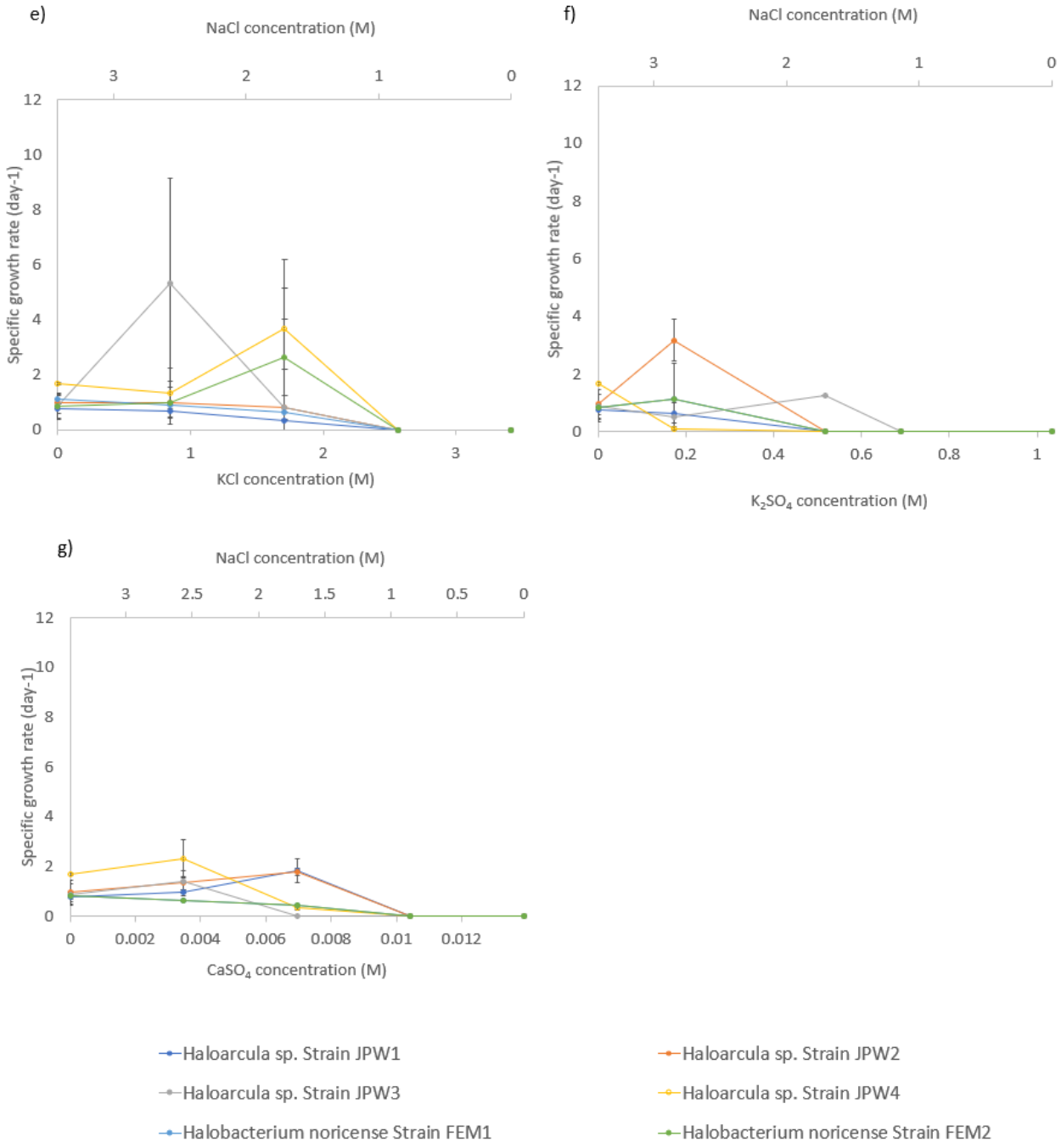

Figure 4.13 - Specific growth rates of the isolates (calculated by Growthcurver) in media containing different salt compositions. The secondary (top) x axis in each graph always represents NaCl concentration (M). The primary (bottom) X axis represents the corresponding concentration of another salt added to replace the NaCl. Each dataset is based on at least three successful growth curves with the error bars representing standard deviation, as calculated by Growthcurver. Where growth did not occur, this was tested eight times and the growth rate was defined as 0. The raw data used to generate these graphs can be found in Appendix 6

The 3.42 M NaCl of unaltered 10 % MPM (Norton et al., 1993) was suitable for the growth of all six isolates. In these experiments, however, it was found that reducing the

NaCl and replacing it with another salt could sometimes result in a higher specific growth rate. Instances in which this occurred included:

- At 2.56 M NaCl and 0.86 M KCl for isolate *Haloarcula Sp.* JPW4 (Figure 4.13e)
- At equimolar NaCl and KCl concentrations of 1.71 M for *Haloarcula Sp.* JPW3 and *H.noricense* FEM 1 (Figure 4.13e)
- At 2.56 M NaCl and 0.0035 M $CaSO_4$ for all four *Haloarcula* isolates (Figure 4.13g)
- At 1.71 M NaCl and 0.007 M $CaSO_4$ for isolates *Haloarcula Sp.* JPW 1 and 2 (Figure 4.13g)
- At 1.71 M NaCl and 0.172 M K_2SO_4 for both *H.noricense* isolates and *Haloarcula* Sp. JPW2 (Figure 4.13f)

The optimum combinations of salts for growth was, therefore, highly variable, even between isolates of the same species.

Water activity

All of the isolates were obligate halophiles (Sections 4.3.4b). Historically the strong osmotic pressure induced by low water activities has been viewed as the reason for the lack of growth of obligate halophiles in high NaCl concentrations (Grant et al., 1998b, DasSarma and DasSarma, 2006). In order to investigate the effect of water activity, the water activity of the different media was determined as described in Section 4.2.5c. The individual data points can be found in Appendix 6.

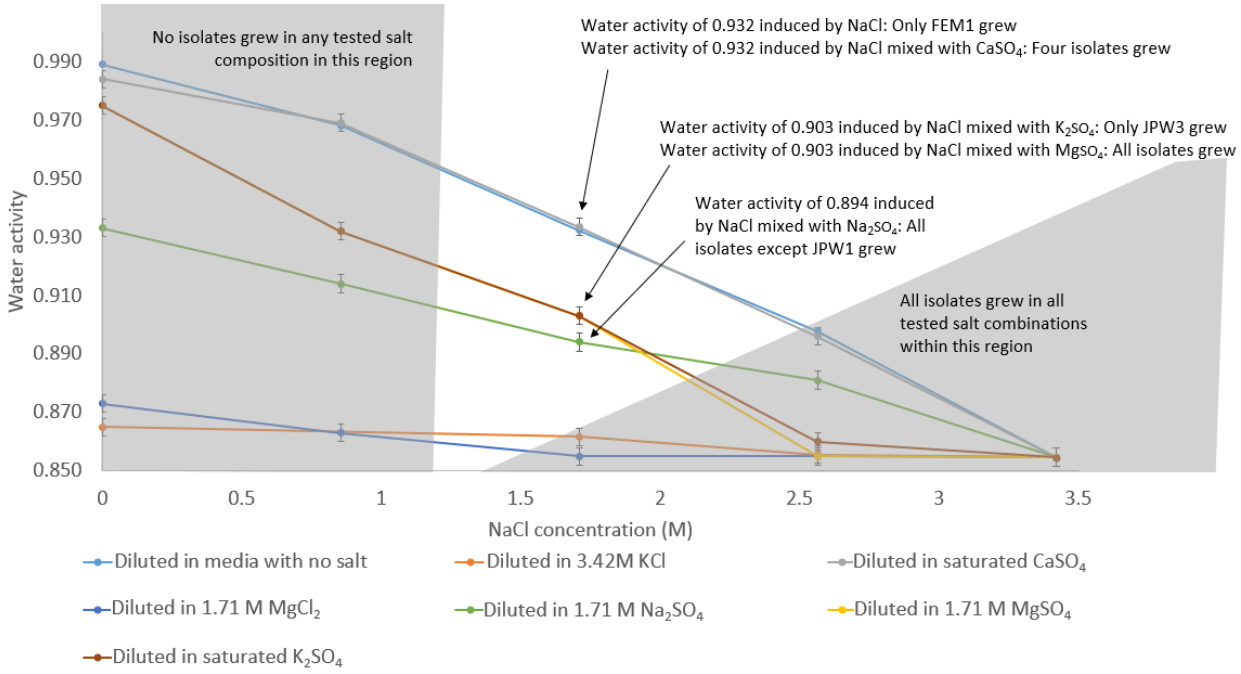

Figure 4.14 - Water activity of 10 % MPM (3.42 M NaCl) diluted in 10 % MPM containing other salts and the growth of the isolates at these salt combinations.

The isolates are assumed to be obligate halophiles since growth was not possible in low NaCl concentrations (Section 4.3.4b). It was assumed that these isolates would also be xerophilies, capable of tolerating low water activities (<0.800, Stevenson et al., 2015a, Tapia et al., 2008) induced by NaCl. This is considered to be the 'normal' environment that halophiles are adapted for (Grant, 2004). The water activities where growth was observed, however, fell within the range 0.855 - 0.932 (Figure 4.14), which is above the point (0.800) at which only extremely halophilic and xerophilic organisms can survive (Stevenson et al., 2015b, Tapia et al., 2008). On the basis of this data, therefore it cannot be determined whether these isolates are both halophilic and xerophilic.

No significant difference in water activity (paired Student's t-test, $p < 0.05$) was observed between 10 % MPM media diluted in MPM without salt and containing 0.0139 M $CaSO_4$ (Figure 4.14). However, the 2:2 dilution in media without salt could only support the growth of *H.noricense* FEM1, whereas dilution in $CaSO_4$ would support

Haloarcula Sp. JPW1, 2 & 4 and *H.noricense* FEM2. This implies that the raised water activity (Figure 4.14) caused by dilution in media without salt was not responsible for the failure of many of the isolates to grow in 1.71 M NaCl (Section 4.3.4b). This is in contrast to conclusions drawn by previous studies of obligate halophiles (Grant, 2004, Grant et al., 1998b, DasSarma and DasSarma, 2006) and might, therefore, suggest that this past work has been misinterpreted.

No growth was observed in any mixture of salts where the water activity exceeded 0.932, and it assumed, in accordance, with prior literature (Grant, 2004, Grant et al., 1998b, DasSarma and DasSarma, 2006) that this is because of the high water activity of the media.

No growth was observed for any of the isolates when the media contained <1.71 M NaCl mixed with KCl or $MgCl_2$. In these cases, the water activity remained within the range 0.855 - 0.873 (Figure 4.14). As all the isolates had been shown to be capable of surviving water activities as low as 0.855 (the unaltered MPM) and as high as 0.932 (in 1.71 M NaCl mixed with 0.866 M $MgSO_4$, Figure 4.14) it can be assumed that the activity of this media cannot be responsible for the lack of growth. Other explanations for the lack of growth are considered in Section 4.4.4b.

Pigmentation

As outlined in Section 4.3.2c, when the isolates were grown in liquid media the cells were initially cream colour, then transitioned to pink in the middle of log phase. Cells grown in the presence of $MgCl_2$ and $MgSO_4$, however remained cream even in the early stages of growth (see Section 4.3.2b).

4.4 - Discussion

4.4.1 - Viable cells

a) Lithologies with viable cells

Viable microorganisms were grown from all of the lithologies that had been shown to contain in excess of 40 % NaCl (Boulby Potash, the Boulby Halite and the interface between them, Sections 2.3.1c & e). This is in line with the results of Norton (1993), although it is uncertain whether that study had sampled the interface region used in this study. Further, these results are comparable with the culture-dependent work found in Chapter 3. Section 3.4.1a discussed the similarities in the mixed culture obtained with those of Norton (*ibid*); the isolates obtained within this Chapter (*Halobacterium* and *Haloarcula,* Section 4.3.2) do not contradict those results. However, Norton did not investigate variations in viability, whereas this Chapter showed a higher success rate for producing cultures when inoculating with Boulby Potash than with Boulby Halite (24 % compared to 11 %, across all three saline media, Section 4.3.1b).

This implies that, while the composition of the microbial community does not differ between the deposits (Section 3.4.2), the Boulby Potash might contain a greater number of cells capable of inoculating saline media than the Boulby Halite. Chapter 2 showed differences in composition even within a lithology, with some indication of heterogeneity introduced by aqueous alteration. Chapter 3 showed that this alteration could be linked to changes in the microbial community (Ca was linked to community diversity, Section 3.3.1c & d). In this Chapter, however, no statistically significant effect was observed between the abundance of these alteration-linked elements and the ability to produce growth when inoculated in saline media (Section 4.3.1b).

Statistics cannot be carried out to compare the number of viable mixed cultures produced from each lithology, because the samples do not represent true replicates. It is therefore possible that the observed difference in the number of mixed cultures obtained from the Boulby Potash and the Boulby Halite was a result of natural variation in the ability of different samples to produce viable cultures rather than any inherent difference between the samples. Section 3.3.2 showed intra-lithological similarities in the archaeal sequences present, but these results might suggest that there is intra-lithological variation in the viability of the organisms that these sequences represent.

Natural variation in the ability of samples from within the same lithology to produce growth could also explain the different numbers of viable cultures produced by samples from the top and from the bottom of the interface region (28 % compared to 8 %, Section 4.3.1b), despite there being no statistically significant difference in the composition of these samples (Section 2.3.1e). If there is, however, a true difference between the number of viable cells within the Boulby Potash and the Boulby Halite, then the mechanism behind why the Boulby Potash might preserve more viable cells is uncertain. Investigating this is part of the study presented in Chapter 5.

Previous studies have reported the number of viable cells within the "rock salt" of Boulby Mine as 2 cells/kg (McGenity et al. 2000, calculations based on data from Norton, 1993). The calculation used to determine this remains uncertain, but it is assumed to involve dividing the number of cultures produced by the total mass of samples investigated, under the assumption that each culture was inoculated by a single cell.

Applying the same calculation to the results of this Chapter shows that, within the NaCl-containing salts of Boulby Mine (Section 4.3.1a) there was a mean of 285 viable cells/kg.

If there is, indeed, a significant difference in the number of viable cells between beds, then this number is likely to be much higher in the Boulby Potash. The difference, of two orders of magnitude, in the density of viable cells, might indicate that the samples investigated in this Thesis differed in an, as yet unidentified, way from those used in the prior study (Norton et al., 1993). However, it could also indicate that the ability to establish viable cultures is highly variable between samples. It is difficult to determine which possibility is the case without further, statistically-rigorous experiments being carried out. Section 4.4.6a considers possible methodologies that could investigate this further.

b) Lithologies which failed to produce growth

Sylvite

While the composition of sylvite (rock) samples from Site X was not investigated, Chapter 2 showed the presence of fluid inclusions within the sylvite mineral of the Boulby Potash (see Section 2.3.3). It therefore seemed reasonable to assume that the sylvite samples from Site X would also possess fluid inclusions containing cells. When these samples were inoculated into media and observed using Sybr ® Green I and light microscopy, however, no cells were observed after either three, six or nine months. The prevalence of so-called "unculturable" microorganisms in environmental samples (Berdy et al., 2017, Pande and Kost, 2017) makes proving the absence of viable cells within the sylvite problematic, as it is plausible that inoculation using different techniques or media might still be capable of producing growth. At the very least, however, this data implies that the six strains of *Haloarcula* and *Halobacterium* isolated in this Chapter are not present within the high-KCl sylvite samples as they have been shown capable of inoculating MPM.

It is important to note that the addition of the sylvite salts raised the KCl concentration of the medium, but this is unlikely to have prevented growth of these isolates if they were present. While the sylvite did contain higher KCl concentrations and lower NaCl concentrations than the Boulby Potash, the growth of the isolates from Boulby Potash samples demonstrated that they could tolerate the ionic strengths generated by dissolution of sylvite samples (Section 4.3.1). The growth curve experiments (Section 4.3.4c) indicated that these isolates could grow in MPM under the NaCl:KCl ratios generated by dissolution of the sylvite samples.

Non-chloride salts

No viable microorganisms were obtained in media inoculated with either polyhalite or anhydrite. Anhydrite (Hawthorne and Ferguson, 1975) and polyhalite (Weck et al., 2014) lack the distinctive cubic, crystalline structures of halite and sylvite (Deer et al., 1992), which means that they may not be conducive to entombment of microorganisms. $MgSO_4$, however, also lacks this structure (Ruiz-Agudo et al., 2007), but has previously been shown to be capable of entombing microorganisms within fluid inclusions in much the same way as chloride salts (Foster et al., 2010).

Alternative explanations as to why viable cultures could not be formed from these minerals include the fact that they experienced very little dissolution; viable cells might not have been exposed to the media in the same way the microorganism within the chloride samples were. The lack of growth might also be down to their provenance from a different area of the mine to Sites A-X (see Section 2.2.1c), or their geological history; these samples were from beds older than those from sites A-E & X and may have been subjected to different conditions since their precipitation.

c) Growth in the different media compositions

MPM

Samples from Boulby Mine produced cultures of viable microorganisms in both nutrient strengths of MPM. The 10 % MPM produced more cultures of viable cells than the 100 % MPM from the same samples, supporting prior findings that high concentrations of nutrients are detrimental to the revival of entombed microorganisms (Vreeland and Powers, 1999).

GYP media

No growth was observed when samples from Boulby Mine were inoculated into non-saline GYP media. The only microorganism that could be cultured from these samples were, therefore, extreme halophiles (growing in 3.42 M NaCl or above, Madigan et al., 2000). When initially dissolved in GYP, the Boulby samples created a moderately halophilic environment (80 g l^{-1}, Madigan et al., 2000, Grant et al., 1998b), but further cultures were prepared by diluting the medium to produce cultures that contained negligible salinity (3.2 g l^{-1}). As discussed in Section 4.4.1b, however, the large number of unculturable microorganisms in any given environment (Berdy et al., 2017, Pande and Kost, 2017) makes it difficult to state conclusively that only viable cells within the samples were halophilic. It is possible that if a larger variety of growth media were used, bacteria (detected using molecular techniques, Section 3.3.1) may have been shown to be viable (Section 3.4.1b).

Saline solution

Cultures were produced by samples dissolved in salt water with no added nutrients, but these cultures would not produce further growth when inoculated in fresh saline media

unless nutrients were added. As discussed above, based upon the number of mixed cultures which experienced growth, there is evidence to suggest a minimum of 285 viable cells/kg of Boulby chloride salts (Section 4.4.1a). If all the cells observed within the cultures had been entombed within the crystals, however, then the observed cell densities of 1×10^{9} - 2×10^{10} cells ml^{-1} (Section 4.3.1) would imply that the crystals contained a minimum of 5×10^{11} cells/kg. While 285 cell/kg was an estimate at the minimum number of cells, the vast difference between these two values implies that cell growth and division had occurred in between release of the entombed cells and observation of the cultures three months later. While this was expected in the cultures containing nutrients, this also occurred in the flasks of saline solution containing no nutrients.

Cells within saline solution inoculated with samples from Boulby Mine would have had access to some of the so-called CHNOPS elements (see Section 1.1.3) essential for life: hydrogen and oxygen are present in the water, while sulfur is known to be present in samples in the form of $CaSO_4$ (see Chapter 2).

In order for growth to occur, the cells must have had access to sources of carbon, nitrogen and phosphorus. Carbon had proved problematic to detect (Chapter 2), and no attempts were made to characterise nitrates or phosphates. These elements might have come either from a source external to the cultures (i.e., the atmosphere) or from within the samples of Boulby Mine dissolved within the saline solution. These two possibilities are explored below, starting with the least likely scenario, that of uptake from the atmosphere.

Nitrogen is found in the terrestrial atmosphere in the form of N_2 (Rayner et al., 1999). Microorganisms are capable of fixing this nitrogen into more biologically exploitable

forms using nitrogenase enzymes (Rees and Howard, 2000). While nitrogenases have been detected in salt-rich environments, they appear to be limited to halophilic bacteria (Argandoña et al., 2005) yet only archaea were grown in this Chapter. Haloarchaea are capable of fixing inorganic nitrogen, but this nitrogen needs to be in the form of nitrate (NO_3^-), rather than molecular N_2 found in the atmosphere (Bonete et al., 2008, Esclapez et al., 2016). It therefore seems unlikely that the microorganisms isolated from the mixed cultures (Section 4.3.2), or present within the community of mixed cultures obtained from many of the same samples in the same media (Section 3.3.2b), would have been capable of atmospheric nitrogen-fixation. Atmospheric nitrogen is, therefore, unlikely to have been the nitrogen source employed by organisms in this nutrient-limiting media. This could be tested using the acetylene reaction (Husen, 2016, Tejada-Jimenez et al., 2017, Hunt and Layzell, 1993), but was beyond the scope of the current work.

Carbon is also found in the terrestrial atmosphere, in the form of CO_2 (Rayner et al., 1999). While there is no mention within the scientific literature of atmospheric carbon uptake by either *Halobacterium noricense* or from the genera *Haloarcula*, this process is known to occur within the haloarchaea. Many haloarchaea contain pigments which act as light-driven proton pumps in order to drive a primitive form of photosynthesis (Oren and Shilo, 1981, Blankenship, 1992). The colouration of the isolates implied the presence of a pigment (Section 4.3.2b), therefore, it is possible that these isolates might be capable of fixing abiotic atmospheric carbon. It is uncertain whether halophilic pigments are capable of providing enough carbon fixation to support an entire community (Oren and Shilo, 1981, Oren, 2016b). It therefore remains possible that the microorganisms obtained from the Boulby samples might be capable of obtaining

enough atmospheric carbon for growth under different conditions than those investigated here. It can, however, be stated that light-driven atmospheric carbon uptake did not occur in these nutrient-free cultures, since they were grown in the dark.

Another common method of carbon-fixation, methanogenesis from atmospheric CO_2, can also be ruled out. While methanogenic halophilic archaea are known to exist, they do not belong to the class *Halobacteria* and instead form their own class, the *Methanonatronarchaeia.* This class exists, from a phylogenetic perspective, between the methanogens and the halophiles (Spang and Ettema, 2017, Sorokin et al., 2017) and is not closely related to the microbes found within this study.

Perhaps more crucially, if primary production was occurring *via* fixation of carbon or nitrogen from a source that was external to the cultures (e.g., atmospheric CO_2), it could not explain why there was no growth when the cells were inoculated into fresh flasks of saline solution containing the same carbon source. Furthermore, while atmospheric uptake of carbon and nitrate is theoretically possible, this does not resolve the source of phosphate, since phosphates are not found in the terrestrial atmosphere (Vardavas et al., 2007).

The lack of growth in the nutrient-free saline solutions, when transferred to fresh medium, implies that an essential element(s) was depleted or diluted out (Pol et al., 2014). Combined with the above discussion this means that the source of carbon, sulfur and phosphorus was likely, but not confirmed, to be the Boulby Mine samples.

Abiotic carbon is assumed to be present within the samples due to the “silt” or shale (Woods, 1979, Edwards, 2015). It is possible to fix abiotic carbon into biologically available forms in a process called chemolithoautotrophy (Section 1.3.2a).

Chemolithoautotrophy, is known to exist within halophilic environments (Mori and Suzuki, 2014, Götz et al., 2018). It is therefore possible that the halophiles in the saline solution culture were metabolising this "silt" released from dissolution of the samples. However, as with nitrogen fixation, the literature would suggest that halophilic chemolithoautotrophy is limited to bacteria (Banciu and Muntyan, 2015, Mori and Suzuki, 2008, Sorokin et al., 2013) yet only archaea were detected in these cultures.

No literature can be found to suggest that abiotic phosphates or nitrates are abundant within Zechstein halite or potash deposits. Phosphates and nitrates can sometimes be found in low concentrations within potash (Warren, 2010) and, therefore, might be present in the Boulby Potash. However, phosphates are more common in potash formed from lake environments than potash from seas (Eckstrand et al., 1995).

The above discussion suggests that abiotic fixation of CHNOPS elements within either the terrestrial atmosphere or the Boulby Mine samples is unlikely to have driven the observed growth of halophilic archaea in the saline solutions without nutrients. There is, however, a known biotic source of all six CHNOPS element within these samples. Chapter 3 showed that many of these samples contained the DNA of 53 families of bacteria, potentially at a greater abundance than the archaea (Section 3.4.1c), but none of them were successfully cultured to indicate their viability. It has previously been speculated that halophilic archaea can undergo long term survival within evaporites by metabolising deceased bacteria heterotrophically (Schubert et al., 2009). If so, this might also occur in these saline solutions. A decline in the concentration of CHNOPS elements as the bacteria were consumed by the viable archaea or as they were diluted out across multiple cultures, would also explain the lack of growth in later cultures where there was no fresh nutrient source supplied.

4.4.2 - Isolation

a) Growth of *Halobacterium* and *Haloarcula*

The isolation protocols employed in this Chapter (Section 4.2.2) resulted in the generation of 48 pure cultures. These represented six strains from two species of separate genera. In Chapter 3, illumina MiSeq was carried out on an enrichment that had been prepared from pooled samples (including many of the samples investigated in this Chapter) that had been grown in the same saline media used in this Chapter (Section 3.3.2b). That work focused on archaea, and the molecular analysis demonstrated that the enrichment was dominated by *Halobacterium noricense* (identified with 99 % confidence) and a *Haloarcula* sp. (with sequence identification varying in confidence between 95-99 %). This in agreement with the results of this Chapter, where only *H. noricense* (identified with 99 % confidence) and an unknown *Haloarcula* (identified with between 97-99 % confidence) were isolated. This implies that members of the *Halobacteria* and *Haloarcula* dominate the viable community. These isolates were found in enrichment cultures of MPM of varying nutrient strength, and nutrient-free saline solution, but it is possible that a greater diversity of viable microorganism could be obtained through the use of different growth media.

Previous studies of Boulby mine using MPM identified the viable microorganisms based upon their lipid profiles. Norton (1993) isolated microorganisms and suggested that they were members of the *Halobacteria* and an unidentified *Haloarcula.* In contrast to this study, Norton's *Halobacteria* belonged to the species *saccharovorum* and *vallismortis* (Norton et al., 1993), rather than *noricense*. *Halobacterium noricense* itself is a species of halophile that was first identified in Permian, Zechstein deposits (Gruber et al., 2004). Section 3.4.1a discussed how changes in the taxonomic structure of the tree

of life mean that species-level historic identifications of halophilic microbes do not always match modern identifications of the same organism. This is especially relevant when, as with Norton's study, the prior identification has been determined based upon lipid analysis and morphology without access to 16s rRNA data.

b) Comparisons of viable microorganisms between lithologies

There did not appear to be any difference in the culturable diversity between the Boulby Potash and the Boulby Halite; there was no difference in which species could be isolated from each bed (Section 4.3.2a). This agrees with the findings in Chapter 3 that indicated that there was no statistically significant variation in the communities between the various lithologies.

On the strain level, three of the isolates (*H.noricense* FEM1 and FEM2, and *Haloarcula Sp.* JPW3) were found in multiple samples of both the Boulby Halite and the Boulby Potash, indicating their presence in both lithologies. Two of the isolates (*Haloarcula Sp.* JPW1 and JPW2) were only detected in individual samples so it cannot be ascertained whether they were unique to a given lithology. *Haloarcula sp.* JPW4 was only detected in two samples of Boulby Potash but may be present only at relatively low abundances rather than being unique to this lithology. Section 4.4.6a discusses how this could be confirmed.

c) Taxonomy of the isolates

The class *Halobacteria* consists of three orders, each of which contains a single family (Gupta et al., 2015). All six isolates, however, belong to the same order: *Halobacteriales.*

In this Chapter, two strains (FEM1 and FEM2) were isolated and shown, *via* the RDP Classifier and the NCBI BLAST algorithm (Section 4.3.2.b), to belong to the genus *Halobacterium.* Comparison of the sequences of FEM1 and FEM2 to other members of this genus showed that they most closely resembled *H.noricense*. A further four strains were isolated, which were members of the genera *Haloarcula.* These *Haloarcula* strains appeared to cluster more with each other than with the other *Haloarcula* species. This suggests that they could belong to a novel species. Further work is needed to confirm this by sequencing the complete genome of one of these JPW strains, characterising its response to a range of different environmental conditions and classifying it.

d) Pigmentation of the isolates

All of the isolates contained a pink pigment, tentatively identified as bacterioruberin (Section 4.3.2c), based on its colouration. Bacterioruberin is typically expressed by halophiles as a response to light and/or low oxygen concentrations (Dummer et al., 2011, Shand and Betlach, 1991). Given that the isolates were grown in the dark and in an aerobic environment, it was unexpected that this pigment was expressed. It is possible that low oxygen conditions could be induced during growth in the incubators if the cells used all the oxygen dissolved in the media. This pigment was, however, also seen when cells were grown in a shaking incubator, where oxygen depletion should not occur (Duetz et al., 2000), but these cells were exposed to the laboratory's ambient lighting conditions when in the shaking incubator. It also remains possible that this pigment has been incorrectly identified. Alternatively, expression of this pigment might be induced as a general stress response to cultivation conditions instead of a specific response to light or anaerobicity.

It was noted that expression of this pigment appeared to be inhibited in all the isolates by Mg salts and was not expressed by *Haloarcula Sp.* JPW4 when grown on agar. Comparison of instances when this pigment was, and was not, expressed could potentially be a pathway to further experiments investigating what this pigment is and why it appeared in the stationary cultures grown in the dark (see Section 4.4.6b).

While it might be unexpected that the cells would express a large photosynthetic, UV-protecting pigment (Oren, 2009, Oren and Shilo, 1981, Blankenship, 1992) when grown in the dark, its presence within subsurface microorganisms is not uncommon. Pigments have been detected in halophiles from subsurface brines across the world including those in Boulby Mine (Vreeland and Huval, 1991, Norton et al., 1993, Thomas et al., 2014), perhaps indicating an evolutionary cost to losing the pigments, even though they are no longer required for their original purpose.

4.4.3 - Bacteria

Chapter 3 investigated the total (viable and non-viable) community entombed within samples from Boulby Mine. Those results, obtained using culture-independent methods, had indicated the presence of a large amount of bacterial DNA that had not been found in previous, culture-dependent studies of Boulby Mine (Norton et al., 1993, Beblo-Vranesevic et al., 2017). Three explanations were proposed in Chapter 3 to explain this discrepancy:

1. The bacteria detected in Chapter 3 were non-viable bacteria that went undetected in prior culture-dependent studies.
2. Downward movement of fluids through the samples had delivered bacteria to them that were not found elsewhere in the mine.

3. The methods used in past studies were unsuitable for encouraging growth of the still-viable bacteria.

One of the goals of this Chapter was to investigate the validity of these three hypotheses. Despite the large number of bacteria identified in Chapter 3 using culture-independent techniques, only archaea were isolated using the culture-dependent methods employed by Norton et al. (1993). While this does not disprove the hypothesis that bacteria were absent from Norton's samples, replicating Norton's methods failed to grow bacteria even when they were known to be present within a sample. This suggests that Norton's (1993) culture-dependent work would have been incapable of detecting bacteria and this suggests hypothesis 1 is true over hypothesis 2.

In order to investigate hypothesis 3, a number of different of inoculation media were used, including moderately saline and low salinity variants, but still bacteria were unable to grow. It remains possible that, with different media, a more diverse selection of isolates could be obtained. Section 4.4.6a also discusses further experiments that could be carried out to investigate the abundance of non-viable cells within Boulby samples.

4.4.4 - Salt tolerances

a) Halotolerance

All of the isolates are obligate halophiles; no growth was observed at a concentration of 0.85 M NaCl or below. All of the isolates were capable of growth at 3.42 M NaCl and are therefore classified as "extreme halophiles" (Madigan et al., 2000).

Halobacterium noricense FEM1 had its highest growth rate observed at 2.55 M and was the only isolate capable of prolonged growth at 1.71 M NaCl (Section 4.3.4b). This would indicate that its optimum growth occurs in conditions that would be considered "moderately" halophilic (Madigan et al., 2000) and, while the other isolates were obligate extreme halophiles, this was a facultative extreme halophile. *Haloarcula* Sp. JPW1, on the other hand, was incapable of prolonged growth at 2.56 M NaCl, indicating that this halophile was less tolerant to low NaCl concentrations than the others, and is, therefore, the most extreme halophile cultured in these experiments.

b) Impact of salt composition

There is historic data to show that the presence of KCl can lower the minimum NaCl requirement for growth of *Halobacterium salinarum* (Brown and Gibbons, 1955), and the presence of $MgCl_2$ can lower the minimum NaCl requirement of *Halobacterium volcanii* (Mullakhanbhai and Larsen, 1975). The work in this Chapter extends these findings by showing that these effects are applicable to other *Halobacterium* species (specifically *Halobacterium noricense*), and members of the *Haloarcula.*

This data also shows that the survival of obligate halophiles at low NaCl concentrations can be induced by a variety of salts, many of which have not previously been investigated. Growth of obligate halophiles in 1.7 M NaCl was possible in the presence of some sulfates (e.g., $MgSO_4$, Na_2SO_4 and $CaSO_4$), but not others (e.g., K_2SO_4). None of these salts, however, could completely replace NaCl and there was never any growth observed when NaCl concentration fell below 1.71 M. Possible reasons for this are explored in the sections below.

Growth in chlorides

These results still cannot provide an adequate explanation for why obligate halophiles were unable to grow in media with a NaCl concentration of 1.71 M or below, when the Cl concentration was maintained at 3.42 M through the addition of KCl or $MgCl_2$ (Section 4.3.4c). Measurements of the water activity in these instances showed that these solutions were within the range of water activities where growth was possible (Figure 4.14). While historic work investigating the tolerance of halophiles to other salts focused on a specific tolerance for NaCl (Brown and Gibbons, 1955, Mullakhanbhai and Larsen, 1975), more recent work (Grant, 2004, Fox-Powell et al., 2016) has suggested halophiles may be optimised to tolerate multiple environmental extremes simultaneously, in particular high salinity and low water activity. Non-NaCl salts affect these environmental extremes in different ways and can also induce other environmental extremes, such as chaotropicity or ionic charge (Fox-Powell et al., 2016, Hallsworth et al., 2007b), which are not induced by NaCl.

This mindset of considering salts in terms of their impact upon environmental extremes can help to explain the failure of the isolates to grow when the $MgCl_2$ concentration exceeded that of NaCl. $MgCl_2$ contains one cation for every two anions, which means that, despite the constant Cl concentration, the cation concentration was variable across the various media compositions (Table 4.4). Furthermore, prior work has shown that salts which contain unequal amounts of cations and anions appear to be more toxic to life than ones with equal concentrations of ions (Fox-Powell et al., 2016). Perhaps most importantly, $MgCl_2$ is highly chaotropic (Hallsworth et al., 2007b) and this is likely to have severely impacted the habitability of the salt media when $MgCl_2$ concentrations exceeded 0.86 M.

It is more difficult however to explain why growth of the isolates was not possible when KCl exceeded NaCl. These KCl-containing media had a similar kosmotropicity to NaCl (Cray et al., 2013), did not induce an extreme water activity (Figure 4.14), and had the same ionic charge and ionic strength as the NaCl-based media (Table 4.4).

While it is possible that the lack of growth in 3.42 M KCl was due to an, as yet uncharacterised, environmental stress, it is also possible that it was a result of physicochemical effects. Halophilic cells maintain steep ionic concentration gradients with their surroundings (Section 1.3.2b). These steep gradients are maintained by proteins, known as antiporters, which transport charged ions across the cell membrane (Oren, 1999). Antiporters are typically considered in terms of their ability to transport Na^+ ions, but the ability to transport other ions and the efficiency at which they do so is highly variable between families of antiporters and the ions in question: some families will transport only Na (Kakar et al., 1989), others will transport various ions (including Na, K, Mg and Ca) at different rates (Cheng et al., 2016a, Swartz et al., 2007), while others will transport all alkali ions at the same rate (Kakar et al., 1989). Many antiporter families operate by transporting H^+ ions in the opposite direction of Na^+ (Oren,1999), but some use Mg^{2+} instead (Kakar et al., 1989).

The environment that terrestrial halophiles are adapted to is one which contains high concentrations of NaCl and relatively low concentrations of other salts. It is already known that the survival of halophilic cells depends on the maintenance of steep Na^+ and K^+ concentration gradients across the cell membrane: high concentrations of toxic Na^+ are kept on the outside of the cell, but not on the inside (DasSarma and DasSarma, 2015). Meanwhile, osmoregulation of the cell depends upon high concentrations of K^+ on the inside while there is relatively little on the outside (Gunde-Cimerman et al.,

2018). Without a full genomic or proteomic analysis of these isolates, it is uncertain which families of antiporter are present, and thus which ions are preferentially transported in which direction across the cell membrane. It seems reasonable, however, to conclude that the antiporters that are present are adapted for an environment which contains high Na^+, which must be removed from the cell, low K^+, which must be transported into the cell, and that Mg^{2+} might also be simultaneously transported in an uncertain direction by these processes. In the <0.86 M NaCl environments containing other chloride salts investigated in this Chapter, it seems likely that the external concentrations of Na^+, K^+ and Mg^{2+} would differ significantly from the optimum conditions the cells' antiporters are adapted for. As such their activity is likely to inhibited to an uncertain extent, which means these important concentration gradients are likely to not be maintained as efficiently as they would be in an NaCl environment. The importance of these concentration gradients to a halophilic cells' osmoregulation means that this could well lead to cell death and be responsible for the lack of growth seen in these experiments.

Growth in sulfates

The impact of replacing NaCl with sulfates instead of chlorides was also investigated. Na_2SO_4 and $MgSO_4$ both had similar effects to KCl and $MgCl_2$, with growth no longer possible when the NaCl concentration fell below 1.71 M.

The data obtained using chloride salts indicated that when the Cl concentration was kept at 3.42 M, cell growth was impossible if the Na concentration was below 1.71 M. A similar result was observed when the Na concentration was kept at 3.42 M and the SO_4 concentration was modified using Na_2SO_4: growth was not observed when the NaCl concentration fell below 1.71 M. While the water activity within the pure Na_2SO_4 media

was higher than for many of the other media, it was still lower than the highest measurement at which growth was observed (Figure 4.14), indicating that water activity was not responsible for the lack of growth when the NaCl concentration fell below 1.71 M but the Na concentration remained constant. While the data presented does not directly confirm that NaCl is required for the growth of these halophiles, it does suggest that there is a minimum requirement of 1.71 M for both the component ions of this molecule.

Given that the dilution of NaCl media in either $MgCl_2$ and $MgSO_4$, had the same effect on the growth of microorganisms, it might be tempting to assume that chlorides and sulfates have the same effect on cells. This is not the case, however, as demonstrated by the results of the experiments using K_2SO_4. The impact of this salt varied considerably between the isolates, but it was the only salt investigated that did not appear to allow growth at 1.71 M NaCl. This is unusual because, as discussed previously, other sulfate salts (Na_2SO_4 and $MgSO_4$) would allow growth to occur.

Further research is therefore needed to investigate the environmental conditions of the K_2SO_4 based media (for example, chaotropicity, pH, ionic charge, ionic strength) and how they differ from NaCl-based media before it can be determined why this salt produces a different effect on growth than the others. Alternatively, this could strengthen the theory, outlined above, that the presence of high concentrations of K^+ ions in the extracellular media interferes with the osmoregulation of obligate halophiles, and that, obligate halophiles, therefore, possess a specific intolerance to K salts.

It should be noted that the lack of growth in the sulfate media might be a result of the organisms investigated, rather than the creation of uninhabitable environments. Some

prior investigation has been carried out into the communities of naturally occurring terrestrial brines containing $MgSO_4$ in concentrations between 1-3 M (Fox-Powell and Cockell, 2018, Lindemann et al., 2013). The NaCl concentration tended to vary between these brines, with no correlation with $MgSO_4$ concentration. Investigations of the microorganisms present within these brines would suggest that it is the NaCl concentration, rather than the total salt concentration, that defines the halotolerance of the microorganisms present. In these previous studies, moderate halophiles were found in brines with 0.5 - 1.5 M NaCl and 2.0-6.0 M $MgSO_4$ (Fox-Powell and Cockell, 2018), while halophiles (moderate or otherwise) were absent from brines with negligible NaCl and 0.1-1.5 M $MgSO_4$ (Lindemann et al., 2013). This could imply that tolerance to high concentrations of sulfate salts is a separate mechanism to NaCl tolerance. Therefore, a microorganism capable of growth at 0.85 M NaCl might be able to grow in sulfate media at the concentrations used in this study. The mechanism that allows halophiles to survive in low NaCl-high $MgSO_4$ brines is uncertain but, as observed in this study, the isolates appeared to respond to extracellular Na_2SO_4 and $MgCl_2$ in the same way they did to $MgSO_4$ (Fox-Powell and Cockell, 2018), perhaps indicating a similar defence mechanism.

Growth in the presence of $CaSO_4$

It was initially assumed (Section 4.3.4b) that the failure of most of the isolates to grow at 1.71 M NaCl was a result of the relatively high water activity (0.932) creating strong osmotic pressure and thus cell lysis (Grant et al., 1998b, DasSarma and DasSarma, 2006). When 0.007 M $CaSO_4$ was added, but the water activity was kept constant (Section 4.3.4c, Figure 4.14), growth was possible for an additional three isolates (Section 4.3.4b).This would imply that the isolates are capable of growth in the water

activities present within the 1.71 M NaCl without other salts, which casts into doubt the interpretation of historical data (Grant et al., 1998b, DasSarma and DasSarma, 2006). Further research is therefore needed into why such relatively low concentrations of both $CaSO_4$ and NaCl can enable growth of these isolates, and whether this effect can be demonstrated in previously studied obligate halophiles.

The above discussion adds credence to the theory that, while the lack of growth in low NaCl concentrations was a response to the changing environmental factors within the media, the ability to grow in other salts might be a physiological response that improves organisms' survival mechanisms, rather than it being a result of the other salts restoring more habitable environmental conditions. This is a topic that requires further research (Section 4.4.6c). No physiological mechanism can be proposed that induces such similar reactions to such a wide range of salts of such a wide range of concentrations, but it is important to bear in mind that the data presented in this Chapter is relatively low resolution; each salt was only investigated at four different concentrations, and it is possible that, across a wider range of concentrations, different trends may emerge. While this data generally shows that, at 1.71 M NaCl and above, obligate halophiles can survive in the presence of other salts, more data points would reveal differences between the salts and potentially indicate that the response of the isolates to different salts invokes different mechanisms.

4.4.5 - Implications for martian astrobiology

a) Halophilic survival in martian brines

As outlined in Chapter 1, the present-day martian surface does not contain any large-scale bodies of water. There is, however, abundant evidence that lakes existed in the

distant past (Moore and Wilhelms, 2001, Frydenvang et al., 2017, Parker et al., 1993, Rodriguez et al., 2016a). In the final stages of evaporation of these bodies of water, the fluids were likely to have been highly saline brines (Catling, 2014, Massé et al., 2016, Stillman and Grimm, 2018). The results presented in Section 4.3.4c suggest that the salts abundant on the martian surface ($MgSO_4$, $MgCl_2$ and $CaSO_4$, Clark and Van Hart, 1981, Ojha et al., 2015), and thus presumably within the martian brines, could have allowed obligate halophiles to grow at lower NaCl concentrations than if NaCl was the sole salt.

The exact concentrations of salts in modelled martian brines varies heavily across martian geography and geological history (Rampe et al., 2017, Phillips-Lander et al., 2017, Peretyazhko et al., 2016, Tosca et al., 2011). Previous studies have tried, but failed, to successfully grow microorganisms, halophilic or otherwise, in modelled martian brines containing combinations of non-NaCl salts (Fox-Powell et al., 2016, Fox-Powell, 2017, Stevenson et al., 2015a). However, these studies were unable to determine which aspect of the brines were responsible for the lack of growth. The work within this Chapter therefore provides the first steps to approaching this problem from another angle. By determining which factors affect and drive the habitability of non-NaCl brines, the large array of possible brine compositions can be narrowed down to the ones most conducive to growth of halophiles.

These experiments also reveal that much is still unknown about the factors affecting habitability of brines. It remains uncertain why the isolates were unable to grow in KCl-rich media with clement water activity, ionic strength and kosmotropicty. It also remains uncertain why comparatively small concentrations of $CaSO_4$ increased the range of water activities that these isolates could tolerate. This work also cannot provide an overarching theory to explain why KCl, $MgCl_2$, $MgSO_4$ and Na_2SO_4 can

improve survival in low NaCl concentrations while K_2SO_4 cannot. This, therefore, identifies areas where further research is required, as without a more detailed understanding of factors affecting habitability of brines (to halophiles or otherwise, Section 4.3.4b), it cannot be stated whether the martian surface is, or ever was, potentially habitable.

b) Potential entombment within the Southern Highland chloride deposits

It is unclear whether the vast chloride deposits located in the Southern Highlands of Mars (Hynek et al., 2015, Osterloo et al., 2008) could contain entombed evidence of ancient microorganisms, because there is uncertainty surrounding the composition of these deposits (See Section 1.4.2) and a lack of knowledge as to the entombment capabilities of non-NaCl salts. Chapter 3, therefore, presented the first study to show that variations in the compositions of evaporites, when all other environmental conditions were maintained, had no impact on the relative abundance of DNA sequences entombed within them (Section 3.4.1). The results presented in this Chapter go further and suggest that the compositional differences between Boulby Potash (approximately 40 % NaCl, 60 % KCl) and Boulby Halite (approximately 100 % NaCl) contain the same viable microorganisms. Conversely, if the martian chloride deposits contain less than 40 % NaCl, it now appears uncertain whether they would be capable of entombing viable microorganisms (Section 4.4.1b).

These chloride deposits are assumed to have formed from evaporation of the last large-scale bodies of water on the martian surface (Osterloo and Hynek, 2015). The composition of these bodies remains uncertain, but it can perhaps be assumed, based upon the deposits that formed, that they too were dominated by chlorides. The results presented in Section 4.3.3, indicate that chloride brines where only half the salinity is

provided by NaCl can still be habitable. While the composition of the deposits still remains uncertain, an NaCl concentration of 50 % or higher would suggest that they formed from evaporation of a brine with habitable chemistry. It remains uncertain whether factors such as temperature and radiation would have otherwise rendered the brine uninhabitable.

Even if terrestrial halophiles could survive in martian chloride deposits of variable compositions, their age (3.65 Ga, Osterloo and Hynek, 2015) compared to the oldest terrestrial equivalents from which life has been revived (250 Ma, Satterfield et al., 2005), suggests a low probability of reviving viable cells at least from primary inclusions. Aqueous alteration of the martian chloride deposits might be detrimental to entombed microorganisms as it would reduce diversity (Section 3.4.3a). It is also possible that aqueous alteration could introduce younger cells to the ancient deposits (Section 3.4.3b). It should be noted, however, that as the formation of these deposits marked the last large-scale presence of water on the martian surface (Osterloo and Hynek, 2015), these deposits are likely to have experienced significantly less aqueous alteration than any terrestrial equivalent.

c) Brines formed by small globally abundant crystals

The large Southern Highland chloride deposits are not the only salts found on the martian surface. As discussed in Section 1.2.1d, hydrated Na and Mg sulfates, chlorides and perchlorates have also been detected at the sites of RSL (Ojha et al., 2015). These salts, as well as Fe and K salts, appear to be found in regolith across the planet (Massé et al., 2014, Clark and Van Hart, 1981, Kounaves et al., 2010, Hecht et al., 2009). These represent potentially younger crystals than the vast chloride deposits, as they could have been precipitated by brines formed by deliquescence (Nikolakakos and Whiteway,

2015) or impact-induced heating events (Clark and Van Hart, 1981) rather than evaporation of large lakes and seas (Hynek et al., 2015, Osterloo et al., 2008).

These salts could, therefore, potentially represent evidence of more recent habitable environments. As mentioned above (Section 4.4.4a), the composition of salts varies across the martian surface. These results indicate that addition of water by one or more of the above processes to an area of the martian surface containing a high concentration of non-NaCl salts could still create a habitable chemical environment, provided NaCl is the dominant salt. In the modern day, any such environment is likely to still be exposed to the martian temperature and radiation regime, which is likely to render any surface brine uninhabitable (Section 1.2.3).

Deliquescence is believed to occur daily in the near subsurface of Gale Crater (Martín-Torres et al., 2015), which would be protected from the UV (Ertem et al., 2017), but the brines would be short-lived (Martín-Torres et al., 2015, Dundas et al., 2017). The ability to become entombed within the precipitating salts could, however, improve the survival of potential microorganisms. Unfortunately, the compositions of the salts found in Boulby Mine are less analogous to these martian salts than the large chloride deposits. The results presented in this Chapter cannot shed light on the viability of halophiles entombed by evaporation of these potentially habitable brines, but this is investigated further in Chapter 5.

d) Use of halophiles as an analogue for martian life

While the martian surface is unlikely to be habitable today (Section 1.2.1), the final aqueous surface environments were likely to have been brines (Section 1.4.1). For this reason, halophiles are often used as analogues for potential martian organisms (Payler

et al., 2016, Fendrihan et al., 2009a, Orwig, 2014, Barbieri and Stivaletta, 2011, Fernández-Remolar et al., 2013, Srivastava, 2014, Rolfe et al., 2017, Matsubara et al., 2017). One of the primary goals of this Thesis is to investigate the validity of this practice, given that terrestrial halophiles live in NaCl-rich environments, whereas most modelled martian brines are not dominated by NaCl (Ojha et al., 2015, Tosca et al., 2011, Clark and Van Hart, 1981).

While Section 4.4.5a & b hypothesise that many of the salts present on the martian surface might allow survival of organisms so long as the NaCl concentration remains 50 % or higher, this conclusion is limited to halophiles. While brines that were dominated by Mars relevant salts showed no growth in these experiments, it was speculated (Section 4.4.4b) that some of these brines would have been habitable to organisms that were less extreme obligate halophiles. These results suggest that, while halophiles can, to some extent, survive low NaCl concentrations in the presence of these other salts, a tolerance to high concentrations of NaCl is not necessarily correlated to tolerance of other salts. It might, therefore, be worthwhile to consider non-halophilic organisms as analogues to potential life in martian brines, especially as many DNA sequences that did not belong to viable halophiles remained preserved within ancient salt deposits (Section 3.4.1b).

4.4.6 - Further work

a) Investigating differences in microbiology between lithologies

The data presented in this Chapter suggests that the Boulby Potash contained more viable microorganisms than the Boulby Halite (Section 4.3.1 and 4.4.2a), but this could not be tested statistically. A future experiment could repeat the work in this Chapter

and investigate growth from each individual sample, multiple times within the same medium. Replicates of the same sample in the same medium would then allow statistically valid analysis to be carried out to determine whether some samples are more likely to successfully inoculate cultures, and whether this is linked to a particular lithology.

This experiment would generate a larger number of mixed cultures from the various lithologies, which would provide an opportunity to investigate whether JPW4 was indeed unique to the Boulby Potash (Section 4.3.2). If a large number of mixed cultures were generated from both the Boulby Potash and the Boulby Halite, then community analysis (as used in Chapter 3) could ascertain whether there were differences in the viable microbial community between the two lithologies. This would allow a more detailed investigation of the complete composition of the mixed cultures, instead of merely identifying one or two specific cells from each of them. Since it has been established in this Chapter that the community does not vary at the species level between the two lithologies, this would need to be carried out *via* MiSeq rather than t-RFLP, in order to obtain data at a suitable resolution.

The question of whether the bacterial cells detected in Chapter 3 were viable or not remains unanswered. It was hypothesised in Section 3.4.1b that, unlike the haloarchaea, viable bacteria in ancient salt deposits survive by becoming dormant. It would be possible to use flow cytometry to count cells within a sample and, in doing-so, distinguish between deceased or dormant cells (Caron, 1998). Future research could, therefore, optimise this technique for samples of dissolved Boulby Halite and Boulby Potash in order to determine whether the bacterial DNA, known to be in the samples (Chapter 3), but uncultured in this Chapter, is contained within viable cells. This

approach could also be used to investigate the number of cells, both viable or otherwise, within these different deposits, and thus confirm the results in this Chapter that suggest there are more viable cells within the Boulby Potash than the Boulby Halite (Section 4.4.2a)

The work in the next chapter (Chapter 5), will present an investigation into how many viable cells remain, from a known initial number, following entombment in laboratory-grown crystals that are analogous to the Boulby Halite and the Boulby Potash. This will shed light onto which salt (if any) is better at preserving entombed cells. This, in turn, would allow astrobiologists to target martian salts that are most likely to contain evidence of potential ancient life.

b) Characterisation of the isolates

Further research could also be carried out to characterise the isolate *Haloarcula Sp.* JPW1 in more detail. Sequencing of a region of 1,114 bases, across hypervariable regions of the 16S rRNA gene, showed only 97 % similarity to previously cultured microorganisms (Section 4.3.2b). Construction of phylogenetic trees showed that the *Haloarcula* isolates grown in this study were more similar to each other than any currently known species. This suggests that these *Haloarcula* isolates are representatives of a hitherto undescribed species. In order to determine whether this is the case, further sequencing should be carried out, ideally of the whole genome. Furthermore the major polar lipids of the JPW isolates need to be determined (Sorokin et al., 2016, Naghoni et al., 2017) as these could reveal similarities to a previously described species that genetic data could not. If both the DNA across a larger region and the lipid content shows dissimilarity to previously described *Haloarcula,* then this would imply that the JPW isolates belong to a novel species.

The utilisable carbon sources and variable morphology (Section 4.3.2b) would also need to be characterised and described (Kämpfer et al., 2003) in greater detail than is presented in this thesis. Initial experiments were carried out to show that strains of this potential novel species were obligately halophilic (Section 4.4.4), but further research would be needed to determine the optimum salinity for growth. Such investigation could consist of a repeat of the experiment presented in Section 4.3.4b but across a smaller range with higher resolution than was investigated in this thesis (Naghoni et al., 2017). The optimum growth temperature should also be determined using a similar experiment (Naghoni et al., 2017).

All the isolates obtained in this Chapter appeared to possess a pink pigment. This pigment was tentatively identified as bacterioruberin based upon its colouration (Section 4.3.1c), but the expression of this pigment in the dark conditions of the incubator calls this identification into question (Section 4.4.3d). There are a variety of ways the hypothesis that this pigment is bacterioruberin could be tested, for example investigating the expression of the bacterioruberin mRNA sequence at the point of the growth curve where this pigment first appears (Section 4.3.1c). The fact that this pigment doesn't occur during growth in the presence of Mg salts (Section 4.3.4c) could provide a negative control for comparison. The composition of the pigment could also be investigated using high-pressured liquid chromatography (Dummer et al., 2011, Ronnekleiv and Liaaen-Jensen, 1992, Fiksdahl et al., 1978) and thus allow identification of the pigment.

c) Survival in low-NaCl brines

This Chapter presents a preliminary investigation into the ability of halophiles to survive when NaCl is substituted for salts of other compositions. While salts similar to

the sulfate salts that allowed growth in these experiments are found on the martian surface, Mars is also rich in perchlorate salts (Clark and Van Hart, 1981, Ojha et al., 2015), which were not tested. An obvious follow up experiment is, therefore, to extend this study to include perchlorate salts, particularly those with cations that have had their chloride and sulfates investigated in this Thesis.

Given the unusual growth effects induced by K_2SO_4 and $CaSO_4$ (Section 4.4.4), these salts should also be investigated further in order to establish if the results presented in this Chapter were a result of them being non-chloride salts or because they were sulfates. In order to investigate this, the environmental conditions (chaotropicity, ionic strength, ionic charge, pH) induced by the salts within these growth media should be monitored.

It was observed that relatively small concentrations of $CaSO_4$ were capable of inducing growth at water activities where growth had previously not been recorded (Section 4.4.4b). As discussed above, this suggests that high water activity is not necessarily the cause of the inhibition of growth in low NaCl solutions. To investigate whether this applies to other, better characterised haloarchaea, transcriptomic techniques (Kliemt and Soppa, 2017, Kurt-Kızıldoğan et al., 2017) could be employed. This would allow comparison of stress-response gene expression at low water activity. This could be undertaken in the presence and absence of $CaSO_4$ and using varying concentrations of the various salts.

4.5 - Conclusions

Two strains of *Halobacterium noricense* and four strains of an unidentified species of *Haloarcula* were isolated from the Boulby Potash, the Boulby Halite and the interface between them. Microorganisms were obtained from across the range of Na and K

concentrations investigated in Chapter 3, and there appeared to be no difference in the viable microorganisms contained in samples across this range. Samples from outside this range, however (obtained exclusively on the first sampling trip), showed no viable microorganisms. This might, therefore, be evidence of a minimum NaCl requirement before halophiles can be entombed. Only obligate halophilic archaea could be grown and there was no evidence that the bacterial DNA extracted in Chapter 3 belonged to viable cells.

The tolerance of these six haloarchaea to a variety of different salts in solutions with low NaCl concentrations was investigated. In accordance with historic data, many of these salts were found to allow growth of obligate halophiles at lower NaCl concentrations than was otherwise observed, but this study presents a larger variety of salts and microorganisms than have previously been tested. The addition of K_2SO_4 did not increase the range of tolerable NaCl concentrations but $CaSO_4$ did, even at concentrations that were three orders of magnitude below that of the NaCl. All six isolates required at least 1.71 M NaCl to grow in all experiments, even though it was expected that KCl should provide the same environmental conditions as NaCl, therefore the fact that growth was not possible in this salt remains unexplained. Having characterised the growth of obligate halophiles within brines containing these salts, Chapter 5 will investigate the survival of cells entombed by evaporation of these brines.

Chapter 5: Survival of UV exposed *Halobacterium noricense* FEM1 entombed in non-NaCl salts

5.1 - Introduction

The aims of this Chapter are as follows:

- To devise a methodology for comparing survivability of microorganisms entombed within salts of different compositions
- To determine how salt composition affects the UV-resistance of entombed cells.

Despite NaCl-tolerant halophiles frequently being proposed as organisms analogous to potential martian life (Payler et al., 2016, Fendrihan et al., 2009a, Orwig, 2014, Barbieri and Stivaletta, 2011, Fernández-Remolar et al., 2013, Srivastava, 2014, Rolfe et al., 2017, Matsubara et al., 2017), NaCl is not the most common salt on the martian surface. Indeed, when brines on the martian surface, in the present day or the distant past, are modelled, the NaCl concentrations tend to be relatively low in comparison to terrestrial halophilic environments (Ojha et al., 2015, Massé et al., 2014). To this end, Chapter 4 investigated the impact of various salts (Na_2SO_4, KCl, K_2SO_4, $MgCl_2$, $MgSO_4$ and $CaSO_4$) on halophiles, when in combination with low concentrations of NaCl (Section 4.3.4d). If life was present within surface or sub-surface martian brines with low NaCl concentrations but high concentrations (either in hypothesised modern transient brines or ancient, more stable brines, Chapter 1), then the ability to withstand entombment might allow life, or evidence of its existence, to survive the desiccating conditions abundant on the present-day martian surface.

Few previous studies have investigated the entombment of organisms within Mars-relevant salts (i.e., Mg salts, sulfates and perchlorates common on the martian surface, (Ojha et al., 2015, Davila et al., 2013b, Kerr, 2013)) either in terms of surviving the entombment process, or in terms of the surviving the martian environment. Although there is evidence to suggest that entombment of microorganisms within halite provides protection from comparable amounts of UV to that found on the present-day martian surface (Leuko et al., 2015, Fendrihan et al., 2009a, Fernández-Remolar et al., 2013), it is uncertain whether this shielding could be provided by other salts.

This Chapter, therefore, features an investigation into the viability of *Halobacterium noricense* FEM1 following entombment in salts crystallised from brines containing NaCl in combination with other salts. Subsequently, the UV-shielding effects of these salts are compared to the shielding received when entombed in halite. FEM1 was selected because it was able to tolerate Na_2SO_4, KCl, K_2SO_4, $MgCl_2$, $MgSO_4$ and $CaSO_4$ in aqueous brines (Section 4.3.4c).

Although there is prior evidence (Foster et al., 2010) to suggest that microorganisms can survive entombment within $MgSO_4$ crystals, this is the first study to quantitatively determine the effect of salt chemistry on microbial viability following entombment. This work is important for determining whether Mars-relevant salts (Massé et al., 2014; Ojha et al., 2015; Kerr, 2013) would support, or inhibit, the survival of potential martian organisms, particularly when exposed to a simulated martian UV-environment. The outcomes could guide the selection of sites on Mars for future life-detection missions.

5.2 - Materials and Methods

The protocol used in this Chapter was consistent across a variety of different experiments: 300 µl of brine of known composition, containing 2.8×10^9 cells of *H.noricense* FEM1, was evaporated to form salt crystals. These crystals were then washed and the number of cells removed from the crystal surfaces ascertained. In some experiments, the crystals were then exposed to UV radiation (of varying intensity, Section 5.2.4). Finally, the crystals were re-dissolved and the number of remaining viable cells calculated.

5.2.1 - Cell culture

a) Culture conditions

H.noricense FEM1 was grown in 250 ml of 10 % MPM (as described in Section 4.2.1b), in sterilised 1 l bottles incubated at 38 ℃, and shaken at 280 rpm. Previous studies investigating the viability of entombed microorganisms used cells that were harvested during the log phase (Fendrihan et al., 2009a, Peeters et al., 2008, Adamski et al., 2006, Kottemann et al., 2005, Lopez-Cortes et al., 1994), with the exception of the work by Leuko et al., (2015) which used stationary phase cells. Hence preliminary experiments (displayed in Appendix 9b) used log phase cells. As described in Section 5.3.2, this approach was reviewed and the final experiments used stationary phase cells instead. Therefore, the experiments presented in this Chapter use stationary phase cells, with the exception of the experiment investigating the effect of different growth phases.

b) Assessing culture density

In Chapter 4, microscopy with Sybr ® Green I dye was used for cell enumeration. In this Chapter, Live/Dead staining was employed to investigate the number of cells following entombment, as it allows differentiation of viable and non-viable cells. In order to enable comparison between all aspects of the experiments presented in this Chapter, this protocol was employed for all cell counts, including the ones used to monitor growth in the cell cultures.

Live/Dead staining uses a combination of dyes: green SYTO®9 and red propidium iodide (Boulos et al., 1999). Like Sybr ® Green I (Section 4.2.1c), SYTO®9 binds to DNA within cells, which results in the cells appearing green under UV light. However, the red propidium iodide dye inhibits the binding of SYTO®9 to DNA and can only enter cells with a damaged membrane. Viable cells, therefore, appear green while dead cells appear red (Boulos et al., 1999).

As per the manufacturer's instructions, the two dyes were mixed together in equal volumes and 0.3 µl of the dye mixture was added to 100 µl of the sample in a sterile Eppendorf tube. The sample was mixed *via* inversion and incubated at room temperature in the dark for 10 min. Following incubation, a 10^4 dilution was prepared in 100 % MPM (Section 4.2.1c). For enumeration, 10 µl of sample was placed on a microscope slide and the cells were counted using an epifluorescent Leica DMRP microscope at 100× magnification at excitation wavelengths of 450 - 490 nm and a long band cut off filter of >515 nm, as described in Section 4.2.1c.

5.2.2 - Laboratory growth of salt crystals

a) Stock solutions and evaporation media

The salts investigated in Chapter 4 (NaCl, Na_2SO_4, KCl, K_2SO_4, $MgCl_2$, $MgSO_4$ and $CaSO_4$) were the focus of the entombment experiments. Crystals were prepared by creating suspensions of cells within "evaporation media" and allowing them to precipitate overnight. Solutions containing either single salts or a mixture of salts were used as the evaporation media.

Single salts

Initial attempts were made to entomb *H.noricense* FEM1 in crystals containing only one salt (inclusive of NaCl) under investigation; entombment has previously been observed in crystals of $MgSO_4$ (Cojoc et al., 2009) implying that entombment in non-NaCl crystals is possible. For this work, the stock media, described in detailed in Section 4.2.5b (and summarised below in Table 5.1) was used as the evaporation media.

Mixtures of salts

In Chapter 4 it was shown that cells of *H.noricense* FEM1 were capable of surviving, for at least the 30 days following inoculation, within solutions created by mixing 10 % MPM in an equal volume with a stock media containing a non-NaCl salt (the compositions of which are listed in Table 5.1). Therefore these solutions were used for the entombment of cells. The water activities of these solutions were calculated at 38 °C in a Novasina LabMaster AW instrument as previously described (Section 4.2.5c).

Table 5.1 - Concentration of the stock solution and evaporation media

Salt	**Concentration of stock media**	**Concentration of salt in mixed media**
NaCl	3.42 M	3.42 M
KCl	3.42 M	1.71 M (+1.71 M NaCl)
$MgCl_2$	1.71 M	0.86 M (+1.71 M NaCl)
Na_2SO_4	1.71 M	0.86 M (+1.71 M NaCl)
K_2SO_4	Saturated (0.69 M, Coordinators, 2018)	0.35 M (+1.71 M NaCl)
$CaSO_4$	Saturated (0.0139 M, Coordinators, 2018)	0.00695 M (+1.71 M NaCl)
$MgSO_4$	1.71 M	0.86 M (+1.71 M NaCl)

b) Preliminary tests

Preliminary tests to establish suitable techniques to visualise cells within salt crystals required the production and evaporation of salt crystals upon transparent microscope slides. This work built on that of Fendrihan et al., (2009).

Cells of *Halobacterium noricense* FEM1 were centrifuged at 4,000 × *g* for 8 min at room temperature (approximately 22 ℃), washed in 200 g l^{-1} NaCl and then resuspended in an evaporation media (Section 5.2.2.a) to a final cell density of $9.33x10^9$ cell ml^{-1}. 100 µl of cell suspension was then added to a microscope slide and 0.3 µl of mixed Live/Dead dye (Section 5.2.1b) was added using a pipette. The pipette was used to spread the saline mix across a wide surface area in order to encourage the formation of a layer of crystals thin enough to observe entombed cells inside the semi-transparent crystals. The crystals were then allowed to form by leaving the solution to evaporate overnight in the laminar flow hood. The next morning, the slide was observed using a Leica DMRP microscope at 5× and 10× magnifications, using light with an excitation wavelength of 450 - 490 nm and a long band cut off filter of >515 nm.

It was found that, despite a consistent volume of solution being added to the microscope slides, the surface area of both the brine and resulting crystals was highly variable.

Attempts were made to spread the solution thinly across the microscope slide but, with the exception of the NaCl-only evaporation media, the crystals that formed were overlapping. The relative thickness of overlapping crystals, as well as the high opacity of the crystal edges, meant that entombed cells could not be visualised within them. The process was repeated with solutions of different salinities, different volumes of solution and different surface areas covered by the solution, but this did not resolve the problem. As a result, the decision was made to investigate entombed cells by means of re-dissolving the crystals into solution and applying Live/Dead staining (Section 5.2.3).

Even with the NaCl crystals, it was difficult to standardise the surface area of the evaporating brine upon the microscope slide. This led to the precipitating crystals also having highly variable surface areas, sometimes consisting of few large crystals and other times consisting of many small crystals. It was suspected that the variable surface area of the crystals would be problematic for the experiments that compared the number of viable cells within samples, as this variable surface area impacted the size of the individual crystals. This would introduce additional variables that might impact on the number of entombed cells. As a result, the decision was made to modify the protocol to decrease the variability of the brines' surface areas, as is described below.

c) Crystal growth in discs

In an attempt to control the crystal sizes (Section 5.2.3b) the media were dispensed into containers so as to create a consistent surface area for each evaporating brine. For this, 0.5 cm diameter × 0.5 cm high, titanium "discs" that had been originally designed as caps for transistors, were used (Figure 5.1). These had previously been used as sample holders in Mars simulation experiments because of their highly non-reactive properties

(*pers comm*, Dr Manish Patel). Between experiments, the discs were washed in distilled water, sterilised *via* an autoclave and dried at 40 ℃.

Table 5.2 - Disc used to grow crystals. a) Empty disc prior to use, b) disc after crystal formation

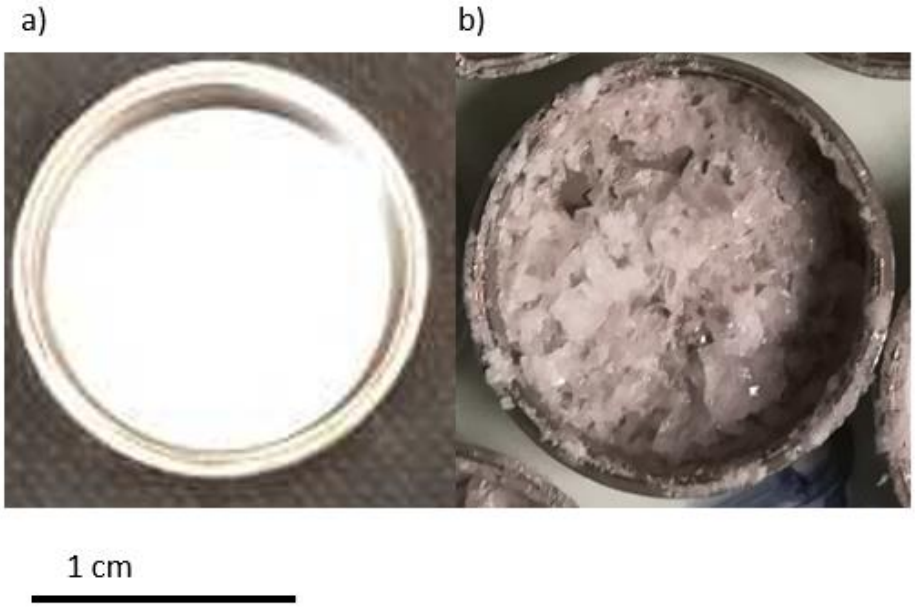

Figure 5.1 - Disc used to grow crystals. a) Empty disc prior to use, b) disc after crystal formation

The mass of each empty disc was measured (to four decimal places) prior to each experiment. Following this, cells of *H.noricense* FEM1 were resuspended (as in Section 5.2.2b) in an evaporation media (Section 5.2.2a) to a final cell density of 9.33×10^9 cell ml^{-1}. In a laminar flow hood, 300 µl of cell suspension was transferred *via* pipette to each disc, with the final number of cells at 2.8×10^9 per disc. The discs were left overnight in the laminar flow hood in order to: a) prohibit microbial contamination during evaporation and b) provide a constant airflow to encourage evaporation and crystal formation.

In all instances, the discs were dry the following morning. The mass of salts formed was calculated by comparing the mass of the disc prior to addition of solution to the mass of the discs containing crystals.

5.2.3 - Determining the viability of cells

a) Surface cells

After crystal formation, it was important to determine whether there were any viable cells on the outside of the crystals, and whether this varied between the different salts. It was also important to remove any viable cells from the outside of the crystals, since these would interfere with the analysis of the entombed cells. The crystals were therefore washed in saturated evaporation media to minimise the loss of salt crystals (Cojoc et al., 2009).

The saturated media were prepared by allowing 50 ml volumes of the evaporation media to evaporate (in the laminar flow-hood) until salts began to precipitate. These were then mixed thoroughly and left in sealed bottles for a further 24 hours to ensure that the crystals did not re-dissolve. A pipette was then used to transfer the saturated media to fresh, sterile bottles while leaving the precipitated salts behind.

400 µl of the relevant saturated media were added to the discs and the discs contents were mixed *via* gentle pipetting. In order to ensure that cells did not remain on the underside of crystals, care was taken to ensure that the mixing mobilised all crystals. Excess saturated media was then removed from the discs, again *via* pipette, and the number of viable cells established using Live/Dead staining (as described in Section 5.2.1b). The water activity of each solution removed was calculated using a Novasina LabMaster AW at 38 ℃ (Section 4.2.5c) and compared with that calculated for each initial evaporation media (Section 5.2.2a) in order to monitor how the environmental condition within the brine changed during the entombment process.

The damp crystals were air dried for 15 min in the laminar flow hood. It was impossible to remove all excess liquid using a pipette, it is therefore presumed that some new salt crystals may have formed, and potentially some cells may have remained on the surface of the salt crystals. Given the low volume of this remaining liquid, relative to the volume of evaporation media that was initially added, and the volume of saturated solution used to wash the cells, it is assumed that the impact of this remaining volume upon the results is negligible.

b) Entombed cells

Determining the number of entombed viable cells required the dissolution of the crystals, since attempting to analyse the cells *in situ* within non-NaCl crystals had proved problematic (Section 5.2.2b). Assessing the viability of entombed cells by dissolving salt crystals is a methodology that is well established within the literature (Rolfe, 2017, Fendrihan et al., 2009a, Leuko et al., 2015, Stan-Lotter et al., 2002b, Kottemann et al., 2005).

Since it is possible that cell death occurred during this process, for example by osmotic shock, the number of 'viable cells' was considered to be those that remained viable after they were released in this way. Although this might be an underestimate of the number that were entombed, the purpose of the Chapter is to establish whether entombment can retain and release viable cells into an aqueous environment; if cells could not survive redissolution they were not considered truly viable.

In order to minimise cell-death by osmotic shock when the cells were released from the crystals, the salt crystals were dissolved in 500µl of a saline buffer. The buffer used for this process consisted of 100 g l^{-1} NaCl, 10 g l^{-1} $MgSO_4.7H_2O$ (Gramain et al. 2011) and

has been previously been used elsewhere in this Thesis (Sections 3.2.5b and 4.2.4a). For ease of explanation, this buffer is designated the gentle dissolution buffer (GDB). Once GDB had been dispensed to each disc, the discs were incubated for 30 mins at 38 ℃ to ensure compete dissolution of the crystals. The solution was then mixed *via* gentle pipetting. Cell counts were carried out using Live/Dead staining (Section 5.2.1b) on a diluted 100 µl aliquot of the sample dissolved in GDB (Section 5.2.3.b).

Initial tests with Live/Dead staining

Although Live/Dead staining has previously been used to investigate the viability of halophilic cells following entombment (Fendrihan et al., 2012, Fendrihan et al., 2009a), initial attempts in this study found that the number of green (live) cells was significantly lower ($p < 0.05$ in Student's t-tests) than the number initially added, but no red (dead) cells were observed. In order to investigate whether the red dye was capable of staining cells under the saline conditions being investigated, a known source of cell death to *H.noricense* FEM1, osmotic shock (Section 4.3.4a), For this, cells were resuspended (Section 5.2.1) in pure water with no salt. The number of live cells did reduce, as expected, but still no dead cells were observed using the Live/Dead staining method. This suggested that, while the green dye was successful in for visualising viable cells, the non-viable cells were not visible.

To test this further, the entombment and dissolution procedures were repeated but the solutions were not diluted to bring the green cells to a density where they could be counted (Sections 4.2.1c & 5.2.1a). Live/dead staining in this instance revealed more red (dead) cells than could be counted, but a repeat using a 10 % dilution resulted in no red cells being observed. Furthermore, dead cells were not observed if the dyes were added to the cells after dilution instead of before it. These resulted implied that the

dilution process may have either destroyed cells or rendered them incapable of being stained.

Dilution was necessary in order to obtain accurate cell counts (as with Sybr ® Green I, Section 4.2.1c) but the fluorescence faded within 15-20 seconds preventing accurate counts of more than 15 cells per field of view. This meant it was impossible to count the dead cells when they were released from entombment; the Live/Dead technique was still used to determine the number of viable cells. Cell survival was instead assessed by comparing the number of viable cells before and after crystal formation.

Investigating variation between replicates

Preliminary experiments (Appendix 9b) using the above methodologies showed significant variation ($p < 0.05$) in the number of viable cells remaining following entombment from discs prepared on different days from different aliquots of cultures, compared with discs prepared at the same time from the same aliquot. It was speculated that this may be because of differences in cell density and growth phase of the culture used to inoculate the discs. In order to investigate whether this was the case, an experiment comparing the growth phase of the cells and survival during entombment was carried out.

For this experiment, 18 × 250 ml cultures were established, using the methods described previously (Section 5.2.1a). The initial density at "Day 0" was 1×10^8 cells ml^{-1}. Every day, cells were enumerated in two cultures using the Live/Dead stain (as described in Section 5.2.1). Six discs of entombed samples were prepared from these two cultures (therefore 12 discs were generated per day). These discs each contained 2.8×10^9 cells in NaCl-based 10 % MPM (Section 5.2.2a). Removing the number of cells

required for these experiments had a significant impact on the remaining volume and headspace of the culture (especially at the early stages of the culture where cell density was low). As a result, each culture could only be used to prepare a single set of discs and, therefore, only provide growth data for a single time point.

After 24 hrs, the number of viable cells remaining within the discs were ascertained using the methodologies outlined above, and a further two cultures were enumerated and used to generate crystals. This continued until data had been obtained for nine days, inclusive of "Day 0". On "Day 0", cells were counted and harvested 6 hrs after inoculation, this allowed cells to acclimatise to their new environment and adjust their growth phase accordingly. Following completion of this experiment, more cultures were set up in order to create a third data point for time points where it was felt that the shape of the growth curve as a whole could be better clarified.

Taking into account the variation between replicates

In order to investigate variation in the number of viable cells entombed in the presence of the salts of various compositions, discs were prepared on four separate occasions from stationary phase cells. These four occasions are referred to in this text as four "repeats." As discussed above, it was likely that there would be significant variation between these repeats. In order to minimise the impact of this variation, the following measures were taken.

In each repeat, three discs were prepared of each salt, with the exception of NaCl, for which six discs were prepared. As it was uncertain what was responsible for the inter-repeat variation, and at what stage of the preparation of crystals it was introduced, the decision was made to keep all cells in the same solution for as long as possible. In order

to do this during the investigation into evaporation of solutions containing NaCl and another salt, the cells were washed and resuspended in 200 g l^{-1} NaCl to a final cell density, which was double that required for the preparation of discs. This suspension was then split into separate aliquots and the stock media added in equal volumes to create suspensions with the composition of the evaporation media outlined in Table 5.1 (the same density as the other experiments in this Chapter).

In order to take into account and investigate the variation between repeats of the same experiment, and the triplicates used, two-way ANOVA tests were employed. Where the two-way ANOVA tests showed only one significant source of variation in an experiment, Students' t-tests could be used to confirm and investigate this. Where the two-way ANOVA tests showed two significant sources of variation, post-hoc Tukey tests were used to further investigate this.

While the number of viable cells inside a crystal appeared to be variable between repeats, UV-radiation should kill the same percentage of cells regardless of how many cells are present (assuming that this variation does not influence the UV-shielding received by individual cells). With this in mind, in the radiation experiments this variation was minimised by considering results in terms of the percentage of cells killed, rather than the actual numbers of cells. When discs of crystals were exposed to UV, at least three discs from the same repeat were kept at the laboratory's ambient UV-conditions. Cell counts were then used to determine the mean number of viable cells within unexposed discs from that repeat (defined as N_0). Cell counts from discs exposed to this UV were then expressed as a percentage of N_0 (defined as N/N_0).

5.2.4 - Survival of entombed *H.noricense* FEM1 under UV light

In order to simulate the high-energy UV conditions on the martian surface, the discs containing entombed cells were exposed to UV, provided by a xenon lamp (LOT-Oriel 150 W). This lamp has been used previously to simulate martian UV conditions for entombed halophiles (Rolfe, 2017), but the conditions for use in these experiments needed to be optimised to take into account the fact the cells were encased within crystals inside discs rather than on a microscope slide, and because it was uncertain how tolerant *H.noricense* FEM1 would be to UV radiation.

a) Characterising output of the UV lamp

In order to determine the energy received by the cells, the lamp was placed in a dark box. A 10×10 grid of 1cm^2 squares was drawn on a sheet of cellulose acetate and this grid was positioned 5 cm below the lamp. An optical cable was clamped in placed below the cellulose acetate grid at its top right corner. The grid was then removed, the box closed, and the lamp turned on. The spectrum of the incident UV at the location of the cable was recorded and analysed by an Avabench 75-ULS2048XL-U2 spectrometer. The lamp was then turned off, the grid replaced, and the optical cable moved to the corner of the next square on the grid. This process was repeated until the UV spectrum received at each point of the grid was measured.

The area under the xenon lamp was divided into four regions (A-D, Figure 5.2), based upon the energy received in the corner of each grid square. The differences between these regions were apparent both by eye and by the spectrometer measurements.

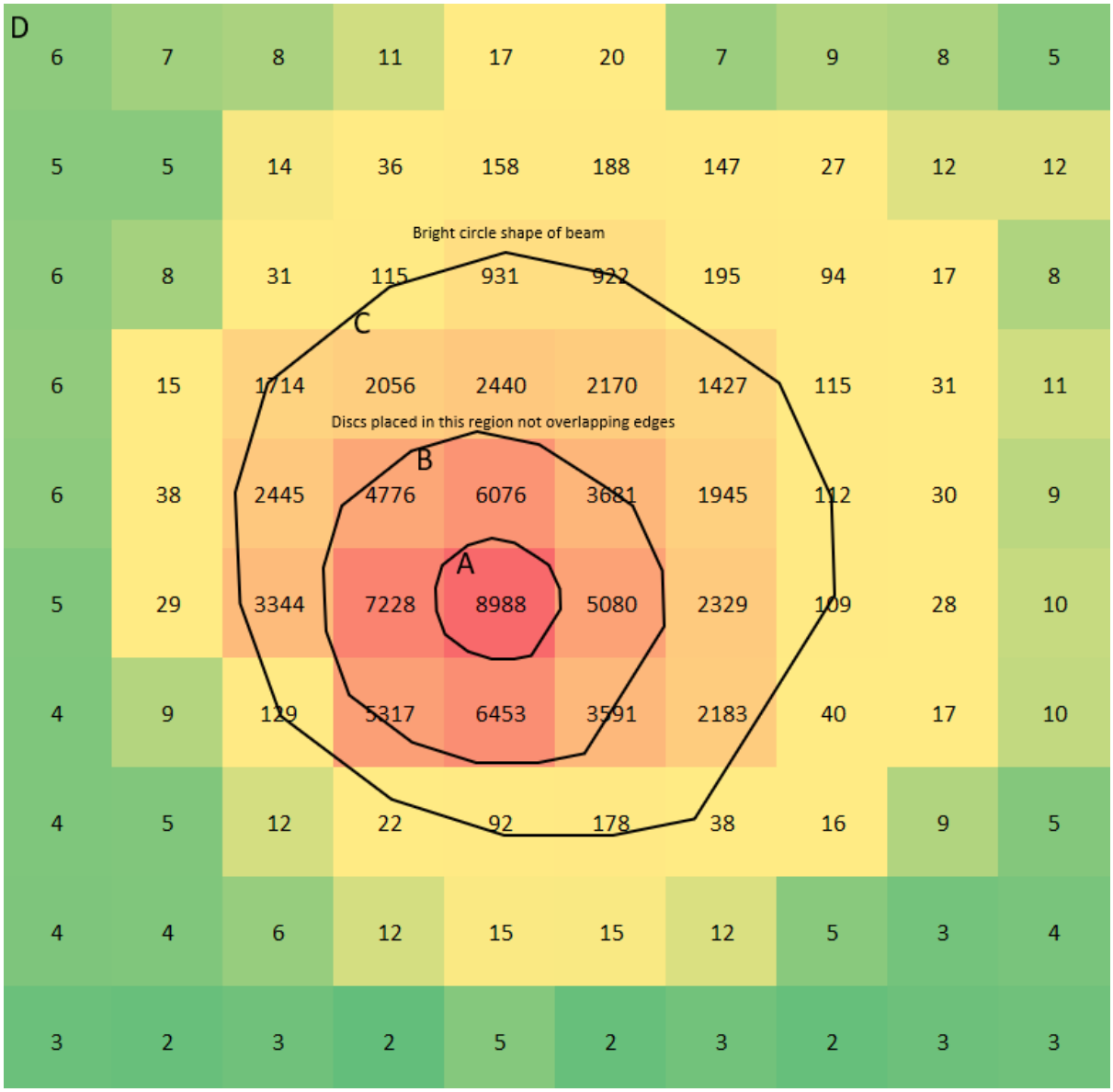

Figure 5.2 - Heatmap of the beam output showing total irradiance measured by the spectrometer in μJcm^{-2}s^{-1} at each location on the grid. When observed by eye, patterns in the distribution of light were also observed, which match those measured those measured by the spectrometer. A is the brightest spot in the centre of the area under the beam. B is a bright circular area. C is a dimly lit area roughly circular in shape, but with more rigidly defined edges at the bottom left than the top right. D is the area not illuminated by the light

Region A (Figure 5.2) was a bright spot, approximately 1 cm in diameter, in the centre of the beam. This spot was visibly brighter than anywhere else under the lamp and had the highest irradiance reading: 8,988 μJcm^{-2}s^{-1}. Region A was in the centre of a larger 3 cm diameter circle, designated Region B. Where one of the grid squares of Region C overlapped the edges of Region B, the irradiance readings were noticeably lower, so those data points were discounted from the calculation of the mean irradiance within

Region B, which was 6,209 $\mu Jcm^{-2}s^{-1}$. Unlike Region B, Region C had a well-defined edge at the bottom left, but at the top right the irradiance faded gradually over a larger area. Within Region C the mean irradiance was 2,260 $\mu Jcm^{-2}s^{-1}$. By eye it did not appear as if the lamp illuminated the area outside of Region C (Region D), but some irradiance was measured (Figure 5.2, <100 $\mu Jcm^{-2}s^{-1}$) around the edges of Region C. As seen within Region C, in Region D there was a sharp drop off in irradiance in the bottom left, and a gradual decrease over a wider area in the top right.

The site chosen to position the discs for the experiments was Region B, as it could be shown that three discs could fit easily within this region, ensuring consistent irradiance.

In each of the measured spectra, the majority of the irradiance was UV-A, though all three types of UV were represented (Figure 5.3).

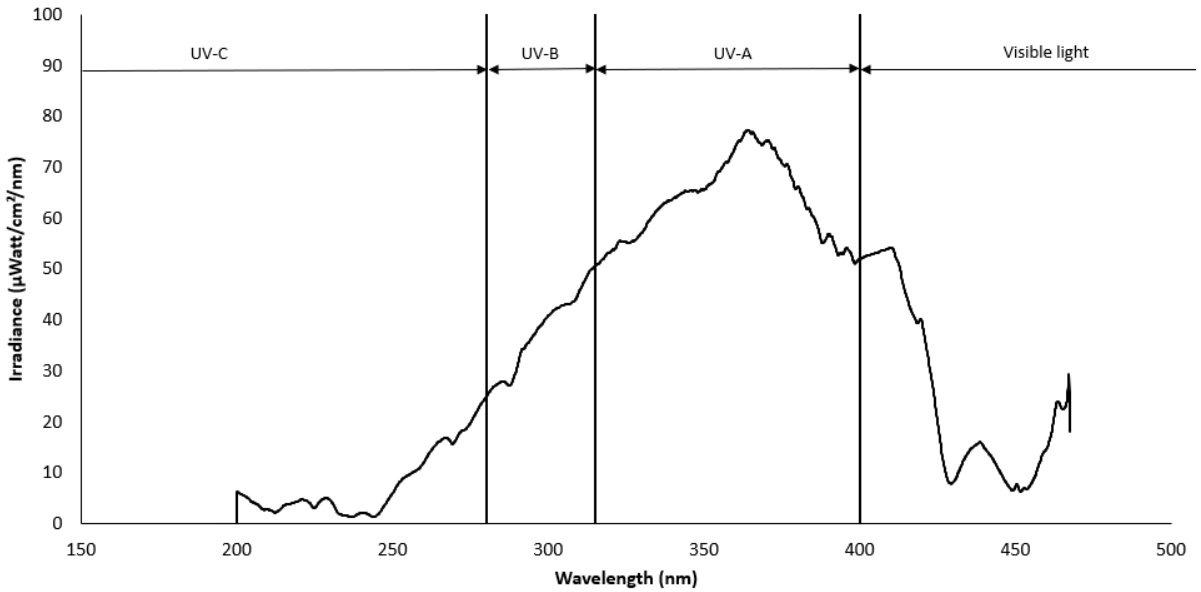

Figure 5.3 - Representative spectra of the xenon lamp. This dataset is from the reading with the highest overall irradiance. Other spectra show the same pattern of peaks in relation to each other, but with a different overall height

b) Survivability of NaCl entombed cells

In order to investigate the ability of entombed *H.noricense* FEM1 to survive under UV radiation, a sample stage was placed under the lamp at a distance of 5 cm, the same distance as the optical cable had been placed at (Section 5.2.4a), and thus the energy received by discs upon this sample stage would be the same as the energy measured at a comparable position on the grid in Section 5.2.4a.

A total of 50 discs were available for use, therefore batches of crystals were prepared from NaCl-based 10 % MPM with cells from the same culture at the same stage of growth, in batches of 24 discs. This number of discs was chosen so as to: a) be a number divisible by three (for the sake of using triplicates for each dosage in each batch), and b) to allow the discs from the previous repeat to undergo washing and sterilisation while the repeat next was on-going. Three discs at a time were placed within Region B (as defined above, Section 5.2.4a, where the mean irradiance was 6,209 $\mu Jcm^{-2}s^{-1}$) and exposed to one of the following dosages of UV radiation: UV (0, 19, 37, 56, 63, 75, 82, 93, 101, 112, 119 and 130 kJ m^{-2}).

Following exposure, the number of surviving cells within each disc was then established *via* dissolution and cell counts (Section 5.2.3b). In each batch, six discs were retained as negative controls (i.e., were not exposed to UV) in order to calculate the N_0 (Section 5.2.3b). N/N_0 (Section 5.2.3b) for each data point was calculated and plotted on a scatter graph to create a kill curve. This was used to determine: a) the UV-dosages that the entombed cells could withstand without significant cell death occurring, and b) the D_{37} value (how much radiation would leave only 37 % of the cells alive (the D_{37} dosage, Safari et al., 2014)).

The D_{37} is used in studies of radiation resistance (Stock and Achey, 2018, Kato, 2016, Yoshino et al., 2018), because statistics show that 63 % cell death corresponds to the point at which there have been the same number of lethal cell-killing events as there were cells to begin with, under the assumption that, once killed, dead cells continue to absorb lethal radiation events that do not impact the number of remaining live cells (Safari et al., 2014).

For each batch of 24 discs prepared, three discs were exposed to each UV dosage (as outlined above). However, the exact dosages investigated between each batch of discs were not identical for two reasons. Firstly, within a batch of 24 discs, 18 samples could be irradiated in groups of triplicates, i.e., 6 different dosages. Secondly, because it was uncertain how this particular strain of *H.noricense* would respond to the UV, initial attempts focused on gathering data from a large range of dosages in order to determine the general shape of the kill curve. Later tests focused on establishing the point at which cell death started occurring and the D_{37}. The results for each dosage represent cell counts from the triplicates of each irradiance, repeated a minimum of three times, i.e., a minimum of 9 individual cell counts.

c) Effect of non-NaCl salts on survival

Having investigated the survival of *H.noricense* FEM1 under UV light when entombed in NaCl crystals, the influence of other salts was investigated. The large variation between repeats (Section 5.2.3b) meant that it was impractical to compare kill curves for each of the evaporation media. As a result, the decision was made to expose cells entombed within these salts to the D_{37} dosage calculated for NaCl, and investigate whether the number of cells killed under this dosage varied significantly between the salts.

Six discs were prepared for each non-NaCl evaporation media, with the exception of the medium which contained NaCl-based media but no other salts, for which nine discs were prepared. Three discs of each were exposed to the D_{37} dosage, while three were left in ambient conditions as negative controls. The tests were repeated four times for each evaporation media.

5.3 - Results

The following sections describe the results of the investigation into how growth phase and salt composition influence the number of viable cells that survive the entombment process, both under ambient terrestrial lighting and under the D_{37} dosage of UV for cells entombed in halite.

5.3.1 - Cell distribution following crystal precipitation

a) Cells on the exterior of the crystals

The focus of this work was the entombed microorganisms; therefore, the laboratory-grown crystals were washed in saturated salt solutions to remove cells from the exterior surface (Section 5.2.3a). Cell counts were carried out on the saturated salt solution after the wash step and no cells were ever detected.

b) Distribution of entombed cells

Before entombment, cells were pre-stained with the Live/Dead stains (Section 5.2.2b). After precipitation of the salt crystals, the shapes of the fluid inclusions could be distinguished at 5× magnification by the high concentration of green SYTO®9 dye (live cells) within the inclusions (Figure 5.4a & c). At 10× magnification, the circular shapes of the dyed cells (as observed in Sections 4.3.2c & e) could be observed. No green cells

were observed on the exterior of the crystals, confirming that all surviving cells detected were entombed.

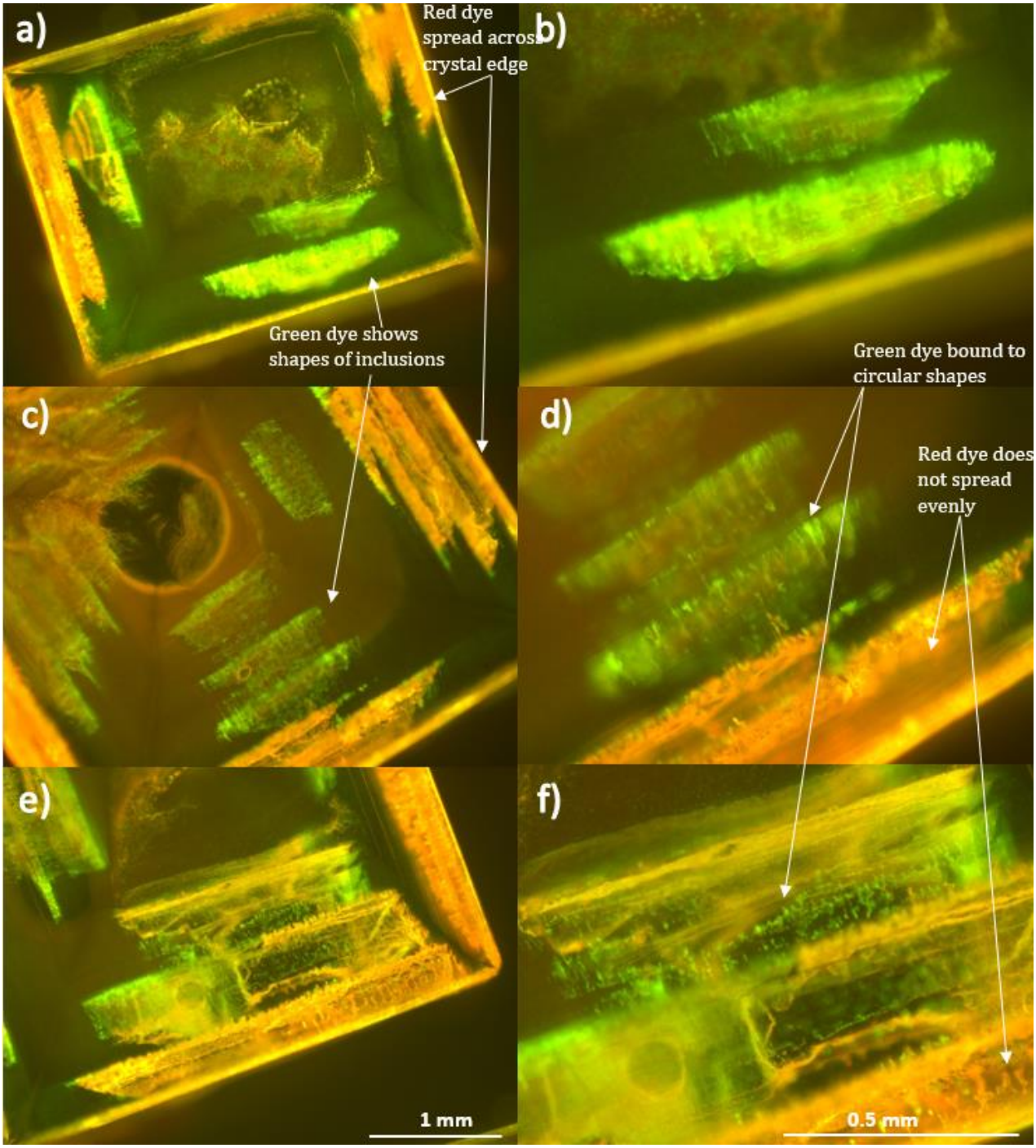

Figure 5.4 - Distribution of the green and red dye in crystals formed from 10% MPM, cells and dye. Fluid inclusions can be visualised by the presence of the green dye, whereas the red dye is localised outside the crystal (a, c & e at 5× magnification). At higher magnifications (10×) of these fluid inclusions, the individual cells can be seen (b, d & f)

There was no evidence of red propidium iodide dye (dead cells) within fluid inclusions or embedded within the crystal interior. While the green dye could be seen to bound to coccoid cellular shapes, the red dye seemed to be attached to the crystal edges rather than cells (Figure 5.4), suggesting either the dye had not bound to dead cells or there were no dead cells present in the crystals.

5.3.2 - Effect of growth phase on survivability

Preliminary experiments (Appendix 9b) indicated significant variation in the number of viable cells that survived entombment from the same initial number of viable cells during "repeats" of the same experiment. Those experiments used the same protocol, and the same cell culture was used to prepare the crystals. It was speculated that the increasing age of the culture was responsible for this variation.

In order to investigate this hypothesis, growth of *H.noricense* FEM1 was monitored under the conditions stated in Sections 5.2.1 and 5.2.3b. Immediately after counting, six discs were prepared of NaCl crystals and 2.8 $x10^9$ cells, which in many cases used most of the cells in a culture. This change to the volume and headspace of the flask would have altered the culture conditions and influenced cell density at later time points (Section 5.2.3b). It should, therefore, be remembered that the growth curve displayed in Figure 5.5 has been compiled by taking a single cell count from 27 different cultures of different ages, rather than the usual method of monitoring the same, much smaller number of, cultures on a daily basis.

The mass of the crystals that formed was higher than the mass of salt that was present within the brines (0.06 g). These results and their implications are discussed in greater detail below (Sections 5.3.2c & 5.4.2) but in order to display this on Figure 5.5, the

masses of crystals are displayed as a percentage of the mass of salt within the brine. For ease of comparing the three variables that were monitored over the nine days of the experiment, the number of cells that survived the entombment process are also displayed as a percentage of the number that were initially added to the brines. The raw data used to make these calculations can be found in Appendix 7.

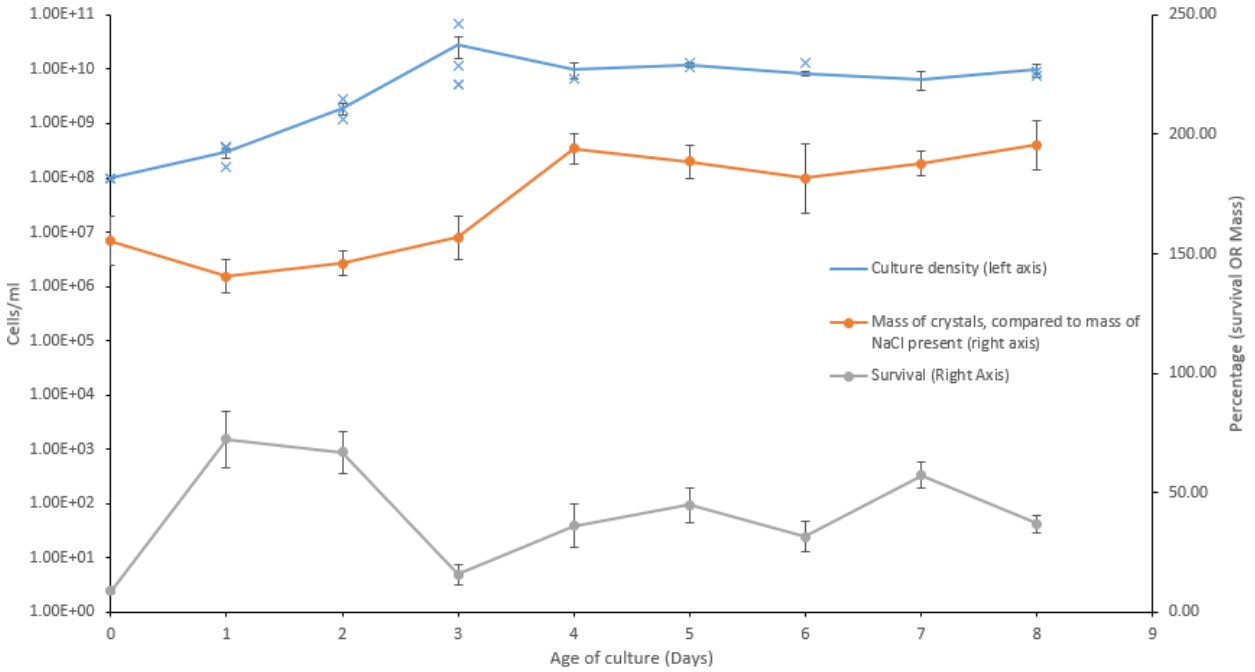

Figure 5.5 - Cell density of cultures of H.noricense FEM1 in the 8 days following inoculation, compared with the percentage of cells that would survive the entombment process and the mass of crystals formed relative to the NaCl present in the disc (0.06 g). Prior to stationary phase there were three measurement of cell density at each incubation period (in stationary phase there was at least two measurements of cell density at each incubation period). Following each measurement of cell density, 6 discs of crystals containing cells were generated incubation period, each of which were used to generate 6 discs.

a) Growth curve

Under these growth conditions, the cells were still in lag phase when measured on day 1 (Figure 5.5). The log phase started at day 2 and late log was reached at day 3 (mean cell density at the peaks of log phase was 2.82×10^{10} cells ml^{-1}). Stationary phase was reached by day 4 and displayed a lower cell density than at day 3 (stationary phase cells had a density of approximately $1x10^{10}$ cells ml^{-1}). As observed in Chapter 4 (Section

4.3.2c), the colour of the cells transitioned from cream to deep pink on day 3, again indicating that log phase was associated with pigmentation changes.

b) Cells surviving entombment

ANOVA tests showed a statistically significant difference in the number of viable cells from crystals prepared from cells of the same growth phase, taken on different days from different cultures, compared to crystals containing cells that were prepared simultaneously from the same culture ($p < 0.00001$).

ANOVA tests also identified further variation between discs containing cells of different growth phases ($p < 0.001$), and post-hoc Tukey tests suggested that this could be because of cells' low survival rates (8.9 % and 15.6 % respectively, Figure 5.5) when entombed on day 0 or day 3. These time points potentially measured cells transitioning between growth phases: on day 0 the cells were entering lag phase after inoculation into the new culture. The relatively large variation in cell densities on day 3 (between 5×10^9 to 6×10^{10} cells ml^{-1}), and the fact that death phase occurred too rapidly to be observed in these time points, makes determining which growth phase day 3 cells were in difficult. At the very least, it can be assumed that day 3 cells, where low numbers of cells survived entombment, were either approaching or had just completed the transition from log phase to death phase. In summary, of these results, although statistical tests proved that variation was always present, greater variation was seen if cells of different growth phases were compared.

The relative shortness of the log phase, and the fact that cells taken from either the beginning or end of it suffered reduced survival during entombment, led to the decision to use cells from five-day old cultures, which were in the stationary phase, for all later

experiments (Sections 5.3.3 and 5.3.4). This would guarantee that all cells in different repeats of the same experiment had come from the same (stationary) growth phase. Although this could not remove the variation in survival rates, it could, at least, remove growth phase-related variation.

c) Crystal mass variation

The mass of the crystals precipitated was in excess of the amount of salt present in the media (0.06 g/disc). Possible sources of this extra mass include the water used in the media and biomolecules within the cells. These are discussed further in Section 5.4.2.

ANOVA tests showed significant variation in the mass of crystals produced from cells in the different growth phases ($p < 0.001$, Figure 5.5) and Student's t-tests showed that crystals generated with cells from the stationary phase (days 4-8 inclusive) weighed significantly more (1.1136 g compared to 0.0897 g) than crystals generated with cells from younger cultures ($p < 0.0001$). Further ANOVA tests, however, showed there were no differences in the masses of crystals produced by stationary phase cells from different cultures or by pre-stationary phase cells from different cultures.

5.3.3 - Effect of salt composition on survivability

The effect of salt composition on survivability of entombed *H.noricense* FEM1 was determined. Initially, solutions of single salts (Na_2SO_4, KCl, K_2SO_4, $MgCl_2$, $MgSO_4$ or $CaSO_4$) were used as the evaporation media (Section 5.2.2a), in order to investigate entombment in the absence of NaCl. When these crystals were dissolved the following day, no cells were observed. The experiment was repeated but this time they were observed after an hour, instead of leaving them to evaporate overnight. Again, no green cells were observed, but undiluted samples showed more cells stained red (dead,

Section 5.2.1a) than could be counted. The experiments in Chapter 4 had indicated that no growth occurred in these solutions in the absence of NaCl (Section 4.3.4c). This experiment supported this, but also indicated that cell death occurred rapidly over the course of an hour.

As a result of the inability of this strain to survive brines without NaCl, the decision was made to use mixtures of salts. This was achieved by mixing the NaCl-based MPM in equal volumes with either the Na_2SO_4, KCl, K_2SO_4, $MgCl_2$, $MgSO_4$ or $CaSO_4$-based MPM stock solutions used in Chapter 4 (Section 5.2.3a), or additional NaCl-based MPM. In order to minimise the effect of variation between crystals prepared from different cultures (Appendix 9b and Section 5.3.2), for each of the four repeats, cells from the same stationary phase culture grown in NaCl-based 10 % MPM were used for entombment in all of the various salt compositions. Each repeat featured three discs of each salt composition (with the exception of NaCl alone, for which six discs were prepared). In all cases, all discs were prepared containing 2.8×10^9 cells.

These data were used to generate a mean and standard error of a) the mass of crystals and b) the number of viable entombed cells for each salt combination from each repeat. Variation between repeats (Section 5.3.2) meant that they needed to be considered independently.

The following sections discuss the appearance of each salt combination as well as the mean and standard error of the mass of crystals and number of viable cells within each salt for each replicate, while the raw data for each individual disc in each replicate can be found in Appendix 8.

a) Morphology of the crystals

In Section 4.3.4d, entombed cells were shown to have a pink pigmentation and, as a result, crystals possessed a faint pink tint (Figure 5.6); the faintness of this tint meant that it did not show up well in digital photographs. The majority of the crystals were transparent to visible light, except in the presence of KCl, K_2SO_4 or Na_2SO_4, where the crystals were more opaque (Figure 5.6). At this stage it is uncertain whether this opacity extends to light in the UV-spectrum. The opaqueness of the crystals correlated negatively with the intensity of the pink colour.

The crystals formed from either NaCl solutions or solutions of NaCl mixed with Na_2SO_4, K_2SO_4 or KCl tended to form thick crystals around the rim of the discs, usually clustered together (Figure 5.6). Brines containing NaCl mixed with $CaSO_4$, however, formed narrow concentric rings of crystals within the discs. Those crystals were thinner and shorter than the crystals formed by other salt combinations. Solutions containing NaCl mixed with $MgSO_4$ or $MgCl_2$ formed irregular, solitary crystals with a diameter of approximately 3 mm, precipitated around the rim of the disc in lower densities than observed for KCl, K_2SO_4 or Na_2SO_4 crystals.

During the washing stage, the more opaque crystals (containing KCl, K_2SO_4 or Na_2SO_4), were less brittle than the more transparent crystals (containing MgCl2, $MgSO_4$, $CaSO_4$ or no salt other than NaCl). These transparent crystals adhered more strongly to the base of the discs, i.e., they required more vigorous movement of the solution and, in some cases, physical force, to detach them from the surface of the disc and ensure the entire surface area was washed.

	Na	K	Ca	Mg
Cl	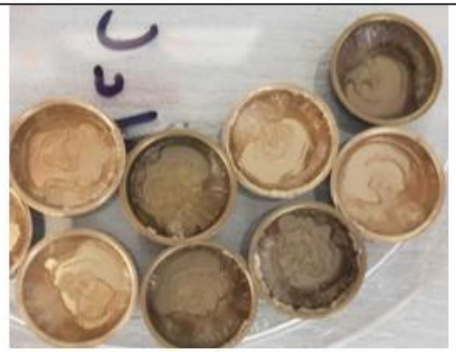		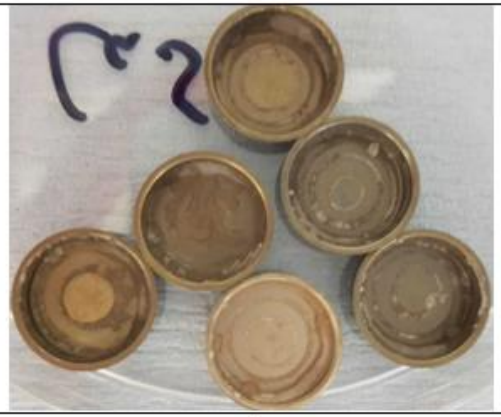	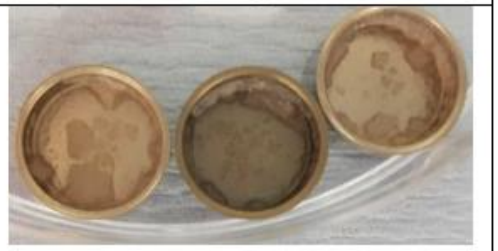
SO_4	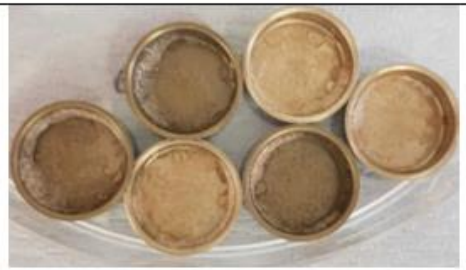		N/A	

Figure 5.6 - Morphology of the crystals formed by brines containing 2.8 x10^9 cells and NaCl mixed with another salt

Although mixed salt solutions were used, this study did not investigate the distribution of the individual salt crystals (as seen, for example, in the Boulby Potash where halite and sylvite formed distinct crystals, Section 2.3.1e). However, there were no differences in crystal morphology within a given disc (Figure 5.6), implying that the salts did not form distinct, separate crystals or there was a compositional homogeneity as a result of the precipitation of a mixed solution.

b) Water activity variation during crystal formation

It was speculated that a variable decrease in water activity during evaporation and saturation of the salt solutions might influence cell survival by creating a xerophilic environment within the evaporating media (Stevenson et al., 2015b). As a result, the water activity of the initial salt solutions, and of their saturated versions (Section 5.2.3a), were measured and are presented in Table 5.3. Evaporation to saturation and precipitation resulted in a decrease in water activity in all cases (Table 5.3).

Table 5.3 - Water activity of the NaCl and other salt combinations upon inoculation of cells and water activity of a saturated solution

	Water activity	
Salt mixed with NaCl	**Initial solution**	**Saturated solution**
$CaSO_4$	0.933	0.752
K_2SO_4	0.903	0.737
KCl	0.862	0.759
$MgCl_2$	0.855	0.732
$MgSO_4$	0.903	0.738
Na_2SO_4	0.894	0.831
NaCl	0.855	0.754

c) Crystal mass

As was undertaken for the NaCl crystals, the crystal masses were measured and are shown in Figure 5.7. The ANOVA tests showed significant variation in the masses of crystals between the four repeats ($p > 0.005$).

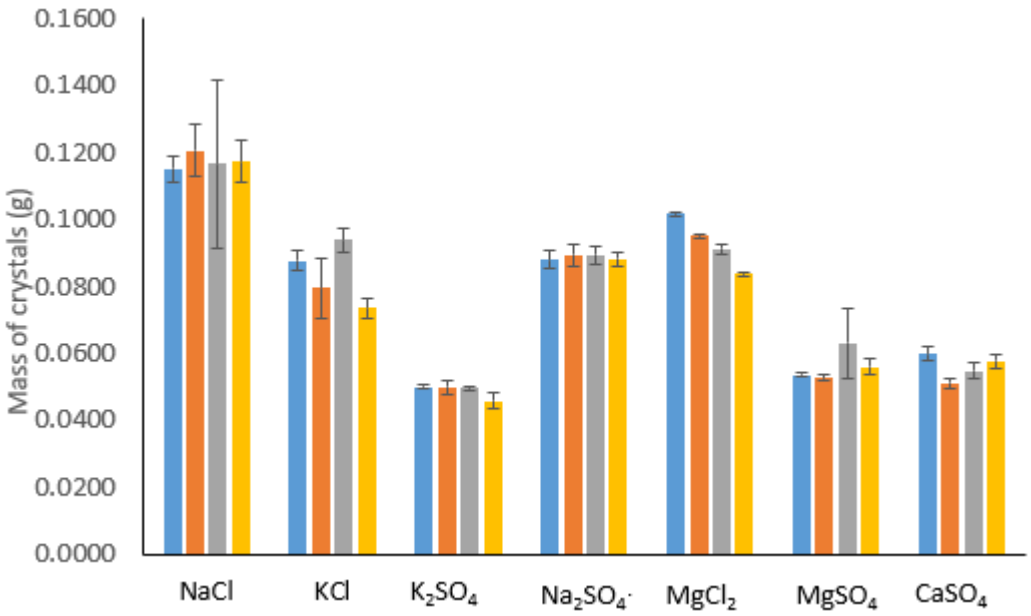

Figure 5.7 - Mass of crystals formed by each of the combinations of NaCl and another salt. The different colours represent four different repeats of this experiment

As expected, the masses varied between the different salt compositions ($p < 0.005$). The largest mass was produced by the solution containing only NaCl (3.42 M), despite the fact that this solution contained the lowest mass of dissolved salt (0.6 g, Table 5.4). The lowest mass was produced by the solution of 1.71 M NaCl mixed with 0.069 M K_2SO_4 (Table 5.4). These results might, therefore, indicate that differences in the crystal mass are a result of them containing different amounts of adsorbed water.

*Table 5.4 - Mass of salts present within the 300 µl brines and mean (*n *= 6 for no other salts, 3 for all other salts) mass of the crystals that formed across the four repeats of the experiment*

Salt mixed with NaCl	Mass of dissolved salt	Mean mass of crystals obtained			
		Experiment 1	Experiment 2	Experiment 3	Experiment 4
NaCl	0.0600	0.1150	0.1206	0.1166	0.1173
KCl	0.0682	0.0877	0.0795	0.0937	0.0734
K_2SO_4	0.0661	0.0500	0.0499	0.0496	0.0457
Na_2SO_4	0.1028	0.0880	0.0893	0.0893	0.0881
$MgCl_2$	0.0788	0.1015	0.0951	0.0913	0.0837
$MgSO_4$	0.0917	0.0535	0.0526	0.0630	0.0560

d) Cells on the exterior of crystals

After the crystals had been weighed, they were washed in saturated brine. No green (live) cells were detected in the discarded saturated solutions, suggesting they were not present on the exterior of the crystals.

e) Viable cells following dissolution of the crystals

The number of viable cells were determined *via* cell counts as described in Section 5.2.1a and displayed in Figure 5.8. As seen elsewhere (Section 5.3.2), the number of viable cells per disc was highly variable between the four different repeats (two-way ANOVA, $p < 0.05$).

Two-way ANOVA tests found significant differences between cells entombed from different salt solutions ($p < 0.00001$). Post-hoc Tukey tests showed that this variation was specifically related to $MgCl_2$ crystals, which contained significantly fewer cells than the other salts ($p < 0.00001$ for all salts in Student's t-Tests).

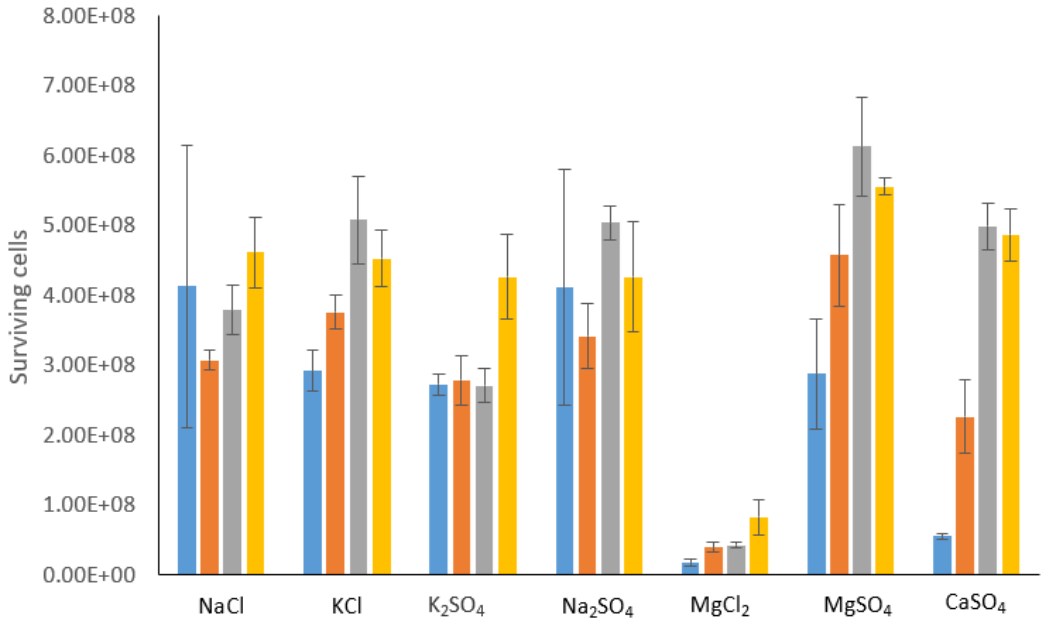

Figure 5.8 - Number of surviving cells following entombment and release from crystals containing NaCl and another salt. The different colours represent four different experiments. Error bars represent standard errors of the mean. In each experiment for NaCl n *=6, all other salts* n *= 3.*

While the number of viable cells entombed within non-NaCl salts varied between repeats in the same way as NaCl, the two-way ANOVA test indicated that this variation was consistent between the salts: there was no significant difference in this variation between different repeats with the different salts ($p > 0.05$). Fewer cells were observed in the first repeat of the $CaSO_4$ solution compared to the other three repeats (Experiment 1;Figure 5.8). Despite this, the post-hoc Tukey tests showed this data point was not significant and it was retained within this dataset. These results, therefore, suggest that only $MgCl_2$ caused a significant change in the number of entombed viable cells.

5.3.4 - Survival of entombed cells under UV

a) Determining the D_{37} within NaCl

Stationary phase cells of *H.noricense* FEM1 were entombed within crystals of NaCl as described in Section 5.2.3b. These were then exposed to varying intensities of UV-

radiation and the number of viable cells remaining (following dissolution of the crystals) was calculated. This was then normalised to the mean number of viable cells calculated for unexposed crystals of the same repeat.

The normalised data points were used to generate a kill curve (Figure 5.9). This showed that UV exposure between 0-40 kJ m^{-2} had a negligible effect on the survival of NaCl-entombed FEM1 (Student's t-test at either 20 or 40 kJ m^{-2} compared to the negative control, unexposed cells, $p > 0.05$, Figure 5.9). Values of 56 kJ m^{-2} and above, however, had a detrimental effect on survival (Student's t-tests showed $p < 0.05$ when N/N_0 values were compared between crystals that received the same > 40 kJ m^{-2} dosage and negative control unexposed cells that received 0 kJm^{-2}).

When comparing the number of cells that survived different dosages to each other, rather than to the negative controls, the general trend was a decrease in N/N_0 values with increasing intensity of UV radiation. The exception to this was at 63 kJ m^{-2} where the mean N/N_0 was 72 %, compared to 63 % at 56 kJ m^{-2} (Figure 5.9). There was, however, no statistically significant difference between values of N/N_0 when data from two successive dosages (Student's t-tests, $p > 0.05$). It is, therefore, assumed that, while there is an overall trend in falling N/N_0, the large variation in the number of viable entombed cells between discs (Section 5.3.2) and the relatively shallow slope of the kill curve makes comparing kill rates for samples that received similar amounts of radiation infeasible. Trends in cell death are only apparent when comparing exposure amounts over a relatively large range.

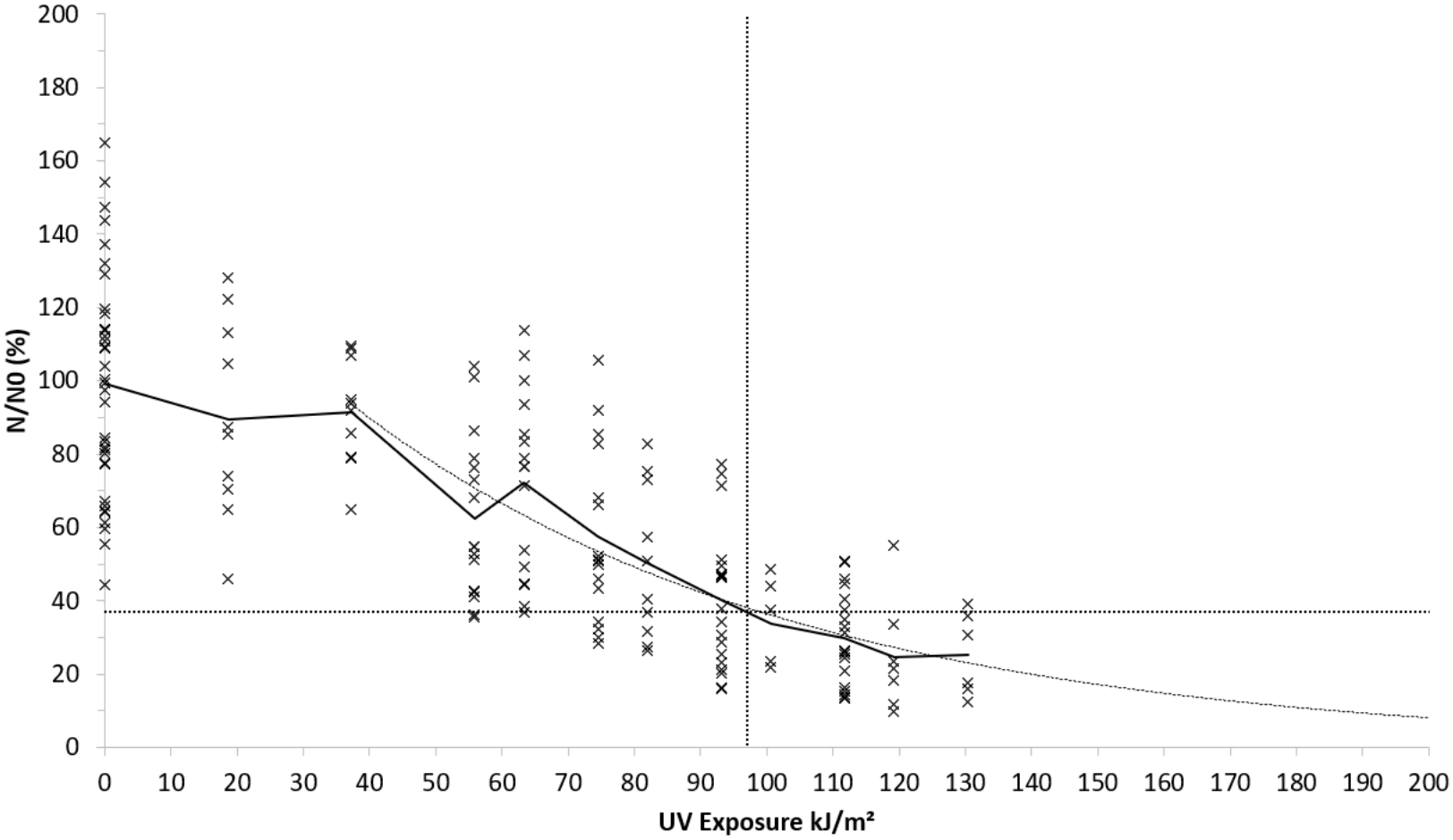

Figure 5.9 - Kill curve of cells of Halobacterium noricense FEM1 under increasing UV when entombed within NaCl crystals. Individual data points are shown, as is the mean at each exposure time. Data points are expressed as a percentage of the mean number of cells that survived in the negative control (exposure of 0 kJ m^{-2}), such that an N/N_0 of 100% is the mean number of cells present in an unexposed crystal (Section 5.2.4b) Representative of data from seven repeats. Each exposure amount is investigated in at least three repeats with three replicates per exposure in each repeat. Dotted straight lines represent the D_{37} value, while the dotted grey line represents the line of best fit for exposures capable of inducing cell death.

The variability in the number of viable cells per disc made judging the D_{37} accurately difficult. The line of best fit for these data points (Figure 5.9) could be calculated to fit the formula $y = 163.93e^{-0.015x}$, which would indicate a D_{37} of 99 kJ m^{-2}. This value is therefore used in the remainder of this Chapter.

b) Comparing UV-shielding of different salts

Direct cell counts

The effect of chemical composition upon the UV shielding effect of salt crystals (Leuko et al., 2015, Fendrihan et al., 2009a, Fernández-Remolar et al., 2013) was investigated. Crystals of the varying compositions, prepared at the same time as the four repeats in Section 5.3.3, were placed under the UV lamp and exposed to 99 kJ m^{-2} of UV radiation (the D_{37}, as determined in Section 5.3.4a). The crystals were then dissolved in GDB and the number of viable cells per disc was determined.

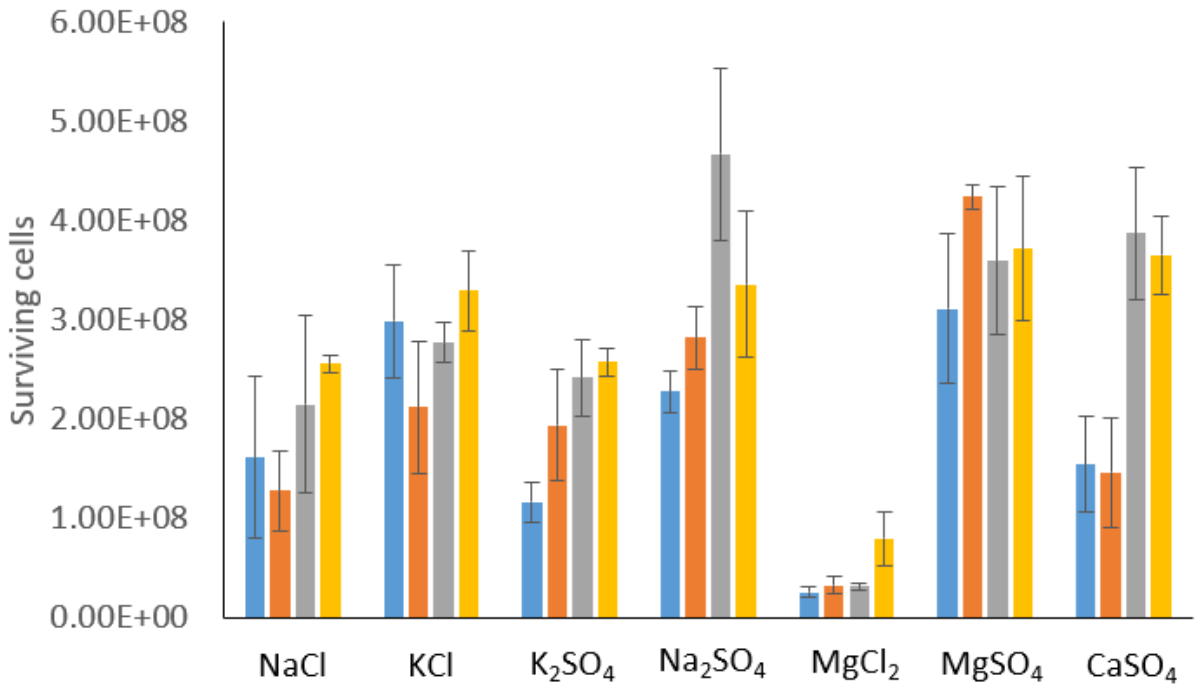

Figure 5.10 - Number of surviving cells following entombment, exposure to 99 kJ m^{-2} of UV radiation and release from crystals containing NaCl and another salt (e.g. NaCl + KCl). The different colours represent four different repeats for each mixed solution. Error bars represent standard errors of the mean. In each experiment n *= 3.*

Two-way ANOVA tests were used to investigate the variation in the number of viable cells between the different salt combinations and their repeats. Significant difference was observed between the repeats ($p < 0.01$) and between the different salts ($p < 0.00001$), but the same was seen for the unexposed discs. The post-hoc Tukey tests suggested that variation between the different repeats was the result of differences across all four experiments (i.e., no single outlier).

As with the unexposed crystals (Section 5.3.3e), the post-hoc Tukey tests showed that the majority of the difference in the number of viable cells extracted from each crystal was a result of the low numbers of cells extracted from the exposed crystals of NaCl combined with $MgCl_2$ ($p < 0.001$ compared to any of the other salt combinations). Significantly more viable cells could also be extracted from the exposed crystals of NaCl combined with Na_2SO_4 or $MgSO_4$ compared to from the exposed crystals containing only NaCl or NaCl combined with K_2SO_4 ($p < 0.05$).

As with the unexposed salts, no significant combined effect on variation was observed between the different salt compositions and the repeats ($p > 0.05$).

Comparison between exposed and unexposed crystals

The number of viable cells extracted from the crystals containing different salts (Section 5.3.3), and from crystals of the same repeat but exposed to 99 kJ m^{-2} of UV radiation (Section 5.2.3b) was measured. By comparing these two values, the relative survival of cells exposed to this radiation could be calculated compared to unexposed cells entombed within the same salt composition and entombed in the same repeat.

ANOVA tests on this data showed statistically significant variation in this relative survival rate between the salts ($p < 0.005$), but not between the repeats ($p > 0.05$). This

means that the data for each salt composition could be expressed as a mean across all four repeats and the repeats did not need to be considered independently. These values of relative survival are displayed in Figure 5.11. Furthermore, this means that while the number of cells that survived the entombment process varied between repeats, the UV killed the same percentage in each one, varying only according to crystal composition.

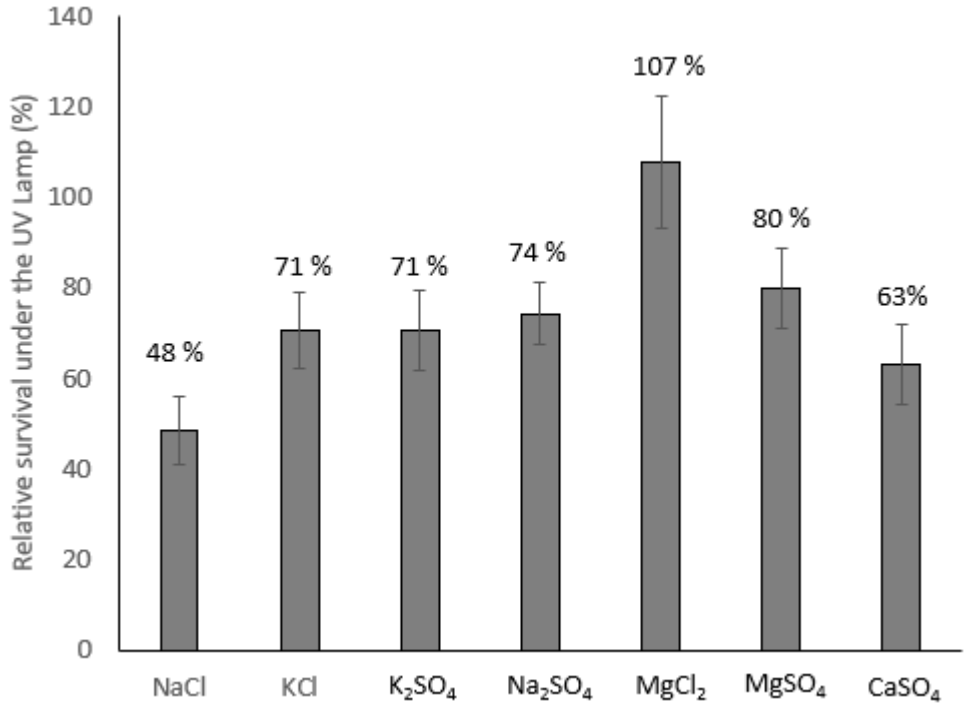

Figure 5.11 - Relative survival of cells in crystals of mixture of NaCl and another salt exposed to 99 kJm^{-2} of UV radiation compared to cells in the same salt prepared at the same time who had not been exposed.

It was found that exposure to 99 kJ m^{-2} of UV radiation only killed 52 % of the cells within NaCl crystals as opposed to the 63 % expected since this was the D_{37} dosage. The value of 48 % survival, obtained using NaCl crystals in the experiment exposing multiple salt compositions to a consistent dosage of radiation (Figure 5.11), was within the range of N/N_0 values observed at the same dosage in the kill curve experiment (Section 5.3.4a). While 48 % survival is higher than might have been expected, this does not contradict the previous findings.

Since normalising the cell survival percentages under UV had removed the inter-repeat variation, the values from each salt could be directly compared to each other using Student's t-tests. The *p* values for these t-tests are displayed in Table 5.5.

Table 5.5 - p *values from Student's t-Tests comparing relative survival in discs containing salts of NaCl mixed with another salt under 99 kJ m^{-2} UV-radiation (*n *= 12 for all salts). Black cells represent comparisons where statistically significant difference (*p *< 0.05) was observed*

	NaCl	**KCl**	**K_2SO_4**	**Na_2SO_4**	**$MgCl_2$**	**$MgSO_4$**	**$CaSO_4$**
NaCl		0.021	0.041	0.010	0.000	0.004	0.091
KCl	0.021		0.973	0.634	0.013	0.307	0.736
K_2SO_4	0.041	0.973		0.704	0.019	0.389	0.754
Na_2SO_4	0.010	0.634	0.704		0.027	0.582	0.474
$MgCl_2$	0.000	0.013	0.019	0.027		0.062	0.023
$MgSO_4$	0.004	0.307	0.389	0.582	0.062		0.249
$CaSO_4$	0.091	0.736	0.754	0.474	0.023	0.249	

H.noricense FEM1 had significantly better survival ($p < 0.05$, Table 5.5) when entombed in NaCl combined with KCl, K_2SO_4, Na_2SO_4, $MgCl_2$ or $MgSO_4$ (71 %, 71 %, 74 %, 107 % and 80 % respectively, Figure 5.11) compared with only NaCl (48 %, Figure 5.11). In fact, entombment in $CaSO_4$ was the only instance that did not improve cell survival rates compared to entombment in NaCl ($p > 0.05$, Table 5.5).

No statistically significant difference was shown in the survival rates between cells entombed in crystals containing KCl, K_2SO_4, $MgSO_4$ or Na_2SO_4 (71%, 71% and 74% respectively, Figure 5.11; $p > 0.05$ in all pairwise comparisons, Table 5.5).

While entombment in crystals containing $MgCl_2$ resulted in significantly fewer viable cells than in any of the other salts (Section 5.3.3e), survival in crystals containing $MgCl_2$ was higher ($p < 0.05$, Table 5.5). These crystals were, in fact, the only ones where no statistically significant difference was observed between the number of cells in unexposed crystals and exposed crystals (Student's t-test, $p > 0.05$). This implies that 99

kJ m^{-2} of UV radiation was incapable of inducing cell death within $MgCl_2$-containing crystals (Figure 5.11).

5.4 - Discussion

5.4.1 - Variation of viable cells after entombment

In this Chapter, the number of viable cells following entombment was highly variable between crystals prepared as part of different repeats of the same experiment (Section 5.3.2b). Investigation showed that the variation could be linked to the growth phase of the culture and, potentially, to the transition between phases. Cells that were entering lag phase, or were harvested at the transition between log phase and stationary phase, had the lowest survival rates (Section 5.2.2b).

Regardless of the growth phase of the cells, entombment always resulted in a significant decrease (Student's t-test, $p < 0.05$) in the number of viable cells. The highest number of viable cells observed in these experiments was 57% of the initial amount. It is assumed that this loss of viable cells is a result of environmental stresses induced during the evaporation process, e.g., decrease in water activity (Section 5.3.3b) or the increase in kosmotropicity, salinity, and ionic charge (Cray et al., 2013, Grant, 2004, Fox-Powell et al., 2016).

Past research indicates that stationary phase cells are more resistant to environmental stresses than phases of growth (Van Rensburg et al., 2004, Jenkins et al., 1991), which explains why cells that were known to be in the stationary phase remained more viable than those believed to be in lag phase or in the transition from lag to stationary phase. It remains uncertain, however, why this relatively high cell survival was also observed in cells that were believed to be in the log phase.

However, even when stationary phase cells of the same age were entombed within crystals, significant variation was observed between repeats of the same experiment. It is plausible that this variation was induced by the experimental protocol: relatively large volumes of cells were placed in the centrifuge to be pelleted and resuspended at much smaller volumes, and it is, therefore, possible that variation in the number of pelleted cells between repeats of the experiments led to slightly different initial numbers of cells were added to the discs in the different repeats. Alternatively, there is evidence in previous literature to suggest high natural variation in the number of viable cells entombed within crystals. Adamski et al., (2006) investigated the number of viable cells within individual fluid inclusions of similar size. They found that the cell density within fluid inclusions of a single crystal can vary by an order of magnitude, and that the number of cells within fluid inclusions of separate crystals grown simultaneously can vary by a further order of magnitude (Adamski et al., 2006). Large, natural variation in the number of viable cells within fluid inclusions might therefore explain the large variation in the number of viable cells within a crystal as a whole.

5.4.2 - Crystal mass

Crystals (Section 5.3.2c) produced from stationary phase cells were significantly heavier (a mean of 0.1136 g) than those formed from earlier growth phases (a mean of 0.0897 g), and yet there was only 0.06 g of salt present within the solutions. There are two potential sources of this excess mass: water and biological components. These are discussed below.

a) Contribution from water towards crystal mass

NaCl is hygroscopic and, as such, readily adsorbs water from the atmosphere (Wise et al., 2007), hence it is expected that the crystals will weigh more than the mass of salts present within the evaporating brine. Indeed, it was this property that prohibited the determination of accurate dry masses of the samples from Boulby Mine (Section 2.3.2) as it was shown that the amount of atmospheric water a sample could absorb was highly variable. This hygroscopic water is unlikely, however, to be responsible for the variation in mass of crystals grown from different growth phases, as no hypothesis can be proposed to explain how cells would influence the ability of a crystal to adsorb water. Not all water in a salt crystal is absorbed hygroscopically from the atmosphere, however, as water is also found within fluid inclusions.

Prior research has shown that the presence of cells will increase the size and abundance of fluid inclusions within a salt crystal as it forms (Norton and Grant, 1988). This excess fluid would presumably increase the mass of the crystal. One hypothesis to explain why stationary phase cells produced heavier crystals, is that these cells resulted in larger and more abundant fluid inclusions than cells from earlier growth phases. This could not be investigated in this Thesis, because of the variation in crystal growth upon microscope slides (Section 5.3.1b), but as discussed in Section 5.4.8a, this is an avenue for further research.

b) Contribution from biological components towards crystal mass

It seems reasonable to suggest that cells in stationary phase would have a greater mass than cells from earlier growth phases, since the older cells have had more time to assemble and accumulate biomolecules. For example, it was observed that the

expression of a pigment (possibly bacterioruberin), an example of a large carotenoid (Yoshimura and Kouyama, 2008), increased during late log phase (Section 4.3.2c). Increased production of heavy biomolecules, such as this large carotenoid, could contribute to the greater mass of crystals formed from older cells.

The washing step during crystal preparation (Section 5.2.2c) would remove any free-floating biomolecules secreted into the media, therefore this mass would need to be contained within, or be anchored to, the cell membrane. The increase in mass between crystals formed from pre- and during stationary phase cells was on average 0.0239 g. If this gain in mass was a result of the presence of heavier biomolecules, then this would correspond to an increase in mass of approximately 0.01 ng per cell. Values for the average mass of a cell vary within the literature, but tend to fall between 0.1-10 ng (Milo et al., 2009), therefore an increase of 0.01 ng between pre-stationary and stationary phase cells is not an infeasible amount of mass for a single cell to accumulate throughout its lifetime. This hypothesis is in contrast to prior studies (Norton and Grant, 1988, Lopez-Cortes et al., 1994) which have doubted the significant contribution of biomass to the overall mass of a crystal. Furthermore, if accumulation of biosynthesised mass was responsible for this increase, then it would be expected that the mass would gradually increase with the age of the culture. Instead the ANOVA tests showed no statistically significant variation over time in the mass of crystals formed by pre-stationary phase cells or in the mass of crystals formed by stationary phase cells.

c) Biomolecules impacting the mass of water present

The actual explanation could be a combination of the above two hypotheses. It has been shown that the increase in abundance and size of fluid inclusions can be induced by organic nanoparticles (Pasteris et al., 2006), not just intact cells. While cells from all

phases of the growth were resuspended to the same density prior to crystal formation, the lag phase of these cells lasted two days, indicating that FEM1 takes time to adjust to changes in the extracellular environment (Section 5.3.2a). Cells taken from the stationary phase might therefore have continued to produce and condition the environment within the disc with stationary phase-specific extracellular molecules that would not be produced by cells in earlier phases. These stationary-phase molecules might trigger the formation of more, or larger, fluid inclusions, trapping more water, and thus resulting in the increase in mass. Investigation into variation into fluid inclusion size and abundance is, therefore, a priority for further research (Section 5.4.8a).

5.4.3 - UV-resistance within NaCl crystals

This study did not compare the survival under UV-light of entombed *H.noricense* FEM1 with FEM1 in liquid media (not entombed), although prior literature suggests that the cells entombed in NaCl may have greater UV resistance than free cells (Leuko et al., 2015, Fendrihan et al., 2009a, Fernández-Remolar et al., 2013, Stan-Lotter et al., 2002b).

It is also not appropriate to compare the values within the kill curve presented in this Chapter (Figure 5.9) with those in the literature because of differences in the entombment, cell counting and data presentation methods used. Independent of the values, however, the shape of the kill curve is similar to published examples (Fendrihan et al., 2009a, Rolfe, 2017, Kottemann et al., 2005, Leuko et al., 2015), with small doses of radiation having little effect and the lack of significant cell death at <40 kJ m^{-2} was also observed in separate experiments where *Halococcus dombrowskii* or various strains of *Halobacterium* were entombed (Fendrihan et al., 2011 and Rolfe, 2017 respectively).

5.4.4 - Effect of salt composition on microbial survival

a) Entombment in non-NaCl salts

Entombment in the absence of NaCl

One of the primary goals of this Chapter, and indeed this Thesis, was to determine whether entombment would be possible within crystals of non-NaCl salts. Investigation into which salts can entomb cells, and which cannot, would allow martian salt deposits to be targeted for future life detection missions. Unfortunately, in this Chapter, viable cells could not be successfully entombed following evaporation of brines without NaCl (Section 5.3.3). This does not mean, however, that only NaCl crystals can entomb cells, but that it is likely that *H.noricense* FEM1 is unable to survive in NaCl-free brines (see Section 4.3.4). This is based upon prior evidence that indicates that entombment of non-halophilic microorganisms is possible in $MgSO_4$ crystals that precipitate from a low NaCl environment (Cojoc et al., 2009). The future work section (Section 5.3.3b), therefore, considers the possible mechanisms by which entombment in non-halite crystals could be investigated.

Entombment in the presence of NaCl

Successful entombment of viable cells required the addition of at least 1.71 M NaCl to the evaporation media. The variation in viable cells prepared from different cultures (Section 5.4.1) meant that, in each repeat, all the cells (Section 5.3.3) were from the same culture. This meant that, regardless of the composition of the evaporating brines, all cells had been grown in NaCl-based 10% MPM. Addition of these cells to the evaporation brines without an equivalent to the acclimatisation cultures (Section 4.2.5a) might have driven changes in the viability of the cells that would be

indistinguishable from changes to viability induced by the entombment in different salts. This does not appear, however, to have occurred, since there was no statistically significant difference in the number of viable cells that could be extracted from crystals formed from salt solutions containing 3.42 M NaCl compared to those containing 1.71 M NaCl when in combination with 1.71 M KCl, 0.87 M $MgSO_4$ or Na_2SO_4, or half saturated $CaSO_4$ or K_2SO_4. This consistency in the viability of cells in the presence of these salts was seemingly unaffected by the significant differences in the masses of these crystals (Section 5.3.3c). The low concentration (0.007 M) of $CaSO_4$ in the evaporating brine meant that it contributed only 1.02 % of the mass of the crystals that precipitated, and yet these crystals contained the same number of viable cells as the ones formed from an evaporation brine containing twice as much NaCl. This could, therefore, imply that the number of cells which survived the entombment process was not governed by the composition or salinity of the brine.

While the number of cells that survived the entombment process could be impacted by the growth phase of the culture they were harvested from (Section 5.4.1), there was no significant variation in the number of viable cells that could be extracted from crystals formed from solutions of the same volume, cell density and pre-evaporation surface area, across a range of salt chemistries and salinities. The only exception was with salt solutions containing $MgCl_2$.

c) Viable cells in $MgCl_2$

$MgCl_2$ was the only salt investigated that displayed a statistically significant difference in the number of viable cells present following the entombment and dissolution process. Allowing for variations between repeats, the mean number of viable cells that could be

extracted from the crystals formed from solutions containing 0.86 M $MgCl_2$ was roughly 11 % of those in crystals that contained only NaCl.

The saturated $MgCl_2$ solution had the lowest water activity of all the solutions investigated in this Chapter (0.732, Table 5.3), outside the range presented in Section 4.3.4d, so it is plausible that exposure to this low water activity during the evaporation process is responsible for the cell death. There is, however, conflicting evidence. Firstly, this low water activity was similar to that reported for the $MgSO_4$ solution (0.735, Table 5.3), where no loss of cells was observed. While not impossible, it seems unlikely that the cells would be able to tolerate a water activity of 0.735 and would experience 88 % cell death at a water activity of 0.732. Finally, while it is the lowest water activity detected in this Thesis, 0.732 is still a higher water activity than the range 0.71 - 0.73 previously stated to be typically tolerable by members of the *Halobacterium* genus (Stevenson et al., 2015b).

Hence, while the low water activity of the evaporating brines containing $MgCl_2$ brines cannot be ruled out as an explanation for the low numbers of viable cells within the resulting crystals, chaotropicity seems a more likely explanation. $MgCl_2$ is considerably more chaotropic than any of the other salts investigated in this chapter (Cray et al., 2013) and evaporation of the brine would have increased the concentration of this salt. Furthermore, precipitation of the NaCl salts would have removed the kosmotropic effects from the solution, which, as discussed in Section 1.2.4d, can act to cancel out chaotropic effects.

5.4.5 - Effect of salt composition on UV survival

a) Differences between salts

As discussed in Section 5.4.3, entombment in NaCl crystals could increase the ability of FEM1 to withstand UV radiation compared to free cells. While the work presented in this Chapter could not prove that *H.noricense* FEM1 entombed within halite crystals had greater UV resistance than non-entombed cells (Section 5.4.3), it has demonstrated that it survival under UV is improved in crystals formed from brines containing NaCl and KCl, K_2SO_4, Na_2SO_4, $MgCl_2$ or $MgSO_4$ (Section 5.3.5a). Variations in the mass of crystals available to absorb the radiation was initially considered as a possible hypothesis to explain this result. However, the heaviest crystals were formed by the brines that contained only NaCl (Section 5.3.3.c) and the resulting NaCl crystals had the lowest relative survival rates when exposed to UV. As discussed in Section 5.4.2, it is believed that the majority of the non-salt mass within a crystal is provided by water, although as these were stationary phase cultures, it is possible that some biomass may have also contributed. Water is capable of absorbing and attenuating UV-radiation (Córdoba-Jabonero et al., 2005, Najita and Carr, 2015), but those crystals believed to possess the most excess water provided the least effective UV protection. This, therefore, suggests that KCl, K_2SO_4, $MgCl_2$ and $MgSO_4$ protect cells from UV in a more effective way than is possible with water.

Including KCl, K_2SO_4 and Na_2SO_4 within the evaporated solutions produced crystals that were more opaque and less fragile than other compositions (Section 5.3.3a). While they produced crystals that provided significantly greater UV protection than crystals of just NaCl (Table 5.5), no significant variation was observed in the relative UV-shielding abilities of these three opaque salts at 99 kJ m^{-2} (Table 5.5), with a mean survival rate of

71.8 % of that of unexposed crystals (Figure 5.11). It is possible that the increased opacity of these crystals to visible light also inhibited penetration of UV (Cockell and Stokes, 2006). However, the presence of $MgCl_2$ or $MgSO_4$ did not alter the opacity or hardness of the resultant crystals and so these factors cannot account for survival rates; the highest relative survival rates were observed for crystals containing these salts (Table 5.5).

While no significant difference was observed for the UV survival rates when cells were entombed in salts containing $MgSO_4$ compared to when entombed in salts containing KCl, K_2SO_4 or Na_2SO_4, $MgSO_4$ was also the only salt that did not induce significant difference in survival (Figure 5.11) compared to $MgCl_2$. This could imply that, independent of the specific effects of $MgCl_2$ (which will be discussed in Section 5.4.5b), Mg salts themselves might have a greater influence on UV protection than opacity through an as-yet undetermined mechanism. Given that the presence of 0.007 M $CaSO_4$ did not have a meaningful impact on the composition of the crystals that formed, it is not unexpected that the crystals formed from brines containing this salt provided the same amount of UV protection as crystals containing only NaCl.

b) $MgCl_2$

Comparing entombment within crystals containing $MgSO_4$ or $MgCl_2$ with crystals containing other salts might imply that that Mg salts provide better UV protection for cells than other compositions (Section 5.4.5a). This effect alone, however, cannot explain the high relative survival of cells entombed in the presence of $MgCl_2$ when subjected to UV. $MgCl_2$ was the only salt investigated that showed no change in the number of viable cells between crystals exposed to 99 kJ m^{-2} of UV radiation and those that were not (Section 5.3.4b). This is unlikely to be a result of a loss of accuracy when

counting low numbers, as the cells had been diluted prior to counting (Section 5.2.1b); in order to count the cells from $MgCl_2$ samples they had to be diluted one less time than the other samples and thus large numbers of cells were still counted. This salt also was the only one where no significant difference was observed in the number of viable cells in crystals exposed to 99 kJ m^{-2} compared with unexposed crystals. It is possible that these two observations are linked.

As discussed above (Section 5.4.4b), it is likely that this low number of viable cells is a result of exposure to highly chaotropic conditions during crystal evaporation. It has also previously been discussed (Section 1.3.4) that many extremophilic defence mechanisms provide protection from more than one environmental extreme, for example cold tolerance and low pressure tolerance appear to be linked (Schuerger and Nicholson, 2016), as does desiccation resistance and radiation resistance (Musilova et al., 2015). It is, therefore, possible that chaotropicity resistance and UV resistance are similarly linked, and that those FEM1 cells most capable of surviving the $MgCl_2$-rich brine were more resistant to the UV radiation.

The lack of knowledge as to how chaotropicity operates (Fox-Powell et al., 2016, Ball and Hallsworth, 2015), and how it might result in resistance to UV, makes proposing a chaotropicity-UV defence mechanism or pathway difficult. It has, however, been postulated that proposed "chaophiles" have extremely rigid plasma membranes containing highly saturated fatty acids, which compensate for the destabilising effects of chaotropes in their natural environments (Leong et al., 2015). If this is the case, then it possible that these saturated fatty acids might also provide UV protection in some way. This chaotropicity defence mechanism still remains unproven, but one experiment to investigate biological mechanisms that may provide protection from chaotropicity is

proposed in Section 5.4.8e, along with a suggested means of investigating a potential correlation between chaotropicity resistance and UV-resistance.

5.4.6 - Implications for natural salts

Experiments from Chapter 2-4 investigated naturally occurring samples of Boulby Potash and Boulby Halite. In the experiments presented in this Chapter, the laboratory-grown crystals of NaCl could be considered analogous to the Boulby Halite samples, while the crystals of NaCl-KCl could be considered analogous to the Boulby Potash (both featured equimolar concentrations of KCl and NaCl). Although the salts are laboratory produced, the results from the experiments (with the exception of those involving UV) can help to shed light on some of the questions raised by earlier chapters. Importantly, the laboratory-grown crystals allowed control of the compositions and number of cells that could be used that natural samples could not provide.

a) Investigating entombment in sylvite crystals

Previous chapters raised the question of whether microorganisms could be entombed within sylvite crystals instead of halite. Chapter 3 had shown no difference in the community composition of samples that were predominantly halite and samples that were a mixture of halite and sylvite. Section 3.4.2 discussed the uncertainties over whether this was because the microorganisms were heterogeneously distributed exclusively within the halite of the Boulby Potash, or whether the same microbial community could be found in crystals of both compositions. In Chapter 4 this was further complicated: more viable microorganisms could be extracted from the sylvite-containing Boulby Potash samples than from the Boulby Halite, but could not be obtained from samples of pure sylvite from Boulby Mine. It was hoped that

investigating the numbers of viable cells within the laboratory-grown crystals could reveal the reasons behind these observations.

For example, if the samples analogous to Boulby Potash contained significantly fewer cells than those analogous to Boulby Halite, it could imply that the cells could only be entombed within the NaCl and not within the KCl. Alternatively, equal numbers of cells within the salts would imply that the cells could be homogenously distributed throughout the crystals regardless of their composition and thus they could be entombed within both sylvite and halite.

The results in this Chapter (Section 5.3.3e) showed equal numbers of cells within crystals analogous to the sylvite and the halite, but the number of viable cells that survived the entombment process was governed by a factor other than composition and brine salinity (Section 5.4.4a). It therefore remains uncertain whether the sylvite crystals investigated in previous chapters were capable of entombing microorganisms. Further means of investigating this are therefore discussed in Sections 5.4.8a & b.

b) Investigating numbers of cells between the Boulby lithologies

As discussed in Chapter 4, the samples of Boulby Potash appeared to contain more viable cells than those of Boulby Halite, although this could not be proven statistically (Section 4.4.1a). In this Chapter, however, when samples analogous to the Boulby Halite and the Boulby Potash were prepared containing the same initial number of cells, the number of viable cells recovered after dissolution was also the same. This raises the possibility that the differences in the number of cells between lithologies from Boulby Mine was either down to chance or a result of the increased secondary alteration to the Boulby Potash, rather than a result of any inherent differences between the primary

lithologies; Section 4.4.7a included discussion of various methods that could be employed to prove this.

5.4.7 - Implications for martian astrobiology

One of the primary goals of this Chapter was to investigate how entombment in Mars-relevant salts would affect the survivability of potential life- on the surface of present-day Mars. This is considered below in two sections, firstly in terms of the salt composition itself, and secondly in terms of protection from the martian environment.

a) Entombment in Mars-relevant salts

This Chapter limited itself to investigation of the crystals formed by evaporation of solutions that contained a minimum of 1.71 M NaCl, as brines with less than this could not be shown to support cell growth (Section 5.4.4a and Chapter 4). It is unclear whether the salts (and cells) were heterogeneously distributed throughout the crystals of mixed compositions (Section 5.4.6), therefore it cannot be determined whether Mars-relevant salts can entomb microorganisms in the absence of NaCl; past research indicates that $MgSO_4$ can (Foster et al., 2010).

What these results do show, however, is that the presence of large concentrations of many of the salts that dominate potential martian brines ($MgSO_4$, $CaSO_4$ and Na_2SO_4, Massé et al., 2014, Ojha et al., 2015, Davila et al., 2013, Kerr, 2013) would not inhibit the survival of entombed halophiles (Section 5.3.3e). Sections 5.4.8a & b propose further research to investigate whether entombment is possible within these additional Mars-relevant salts, or whether microorganisms required the presence of NaCl for entombment to take place.

Of the investigated salts, those containing $MgCl_2$ were the only ones from which fewer viable cells were obtained compared with NaCl alone (Section 5.3.3e). It is uncertain what accounts for this, but it is speculated (Section 5.4.4.c) that this is a result of the physicochemistry of the evaporating brine (specifically its chaotropicity), rather than the chemistry of the crystals. Previous research has indicated that the viability of entombed microorganisms decreases over time (Adamski et al., 2006, Schubert et al., 2009, Kottemann et al., 2005). It remains uncertain whether the presence of different salts would increase or decrease the rate that this occurs, but if the reduced cell viability in the $MgCl_2$ crystals is indeed a result of the chaotropicity of the brine, then there is no evidence to suggest that, once entombed, the viability within these crystals would fall at a greater rate than cells entombed in NaCl. Section 5.4.8c discusses methods that could be used to investigate this further, but if this hypothesis is correct then the data in this Chapter would suggest that the martian $MgCl_2$ and $MgSO_4$ salts might allow entombment of hypothetical martian organisms.

b) Protection from the martian environment

It has been proposed that halite on Mars would be capable of shielding entombed microorganisms from the extreme UV environment (Leuko et al., 2015, Fendrihan et al., 2009a, Fernández-Remolar et al., 2013, Stan-Lotter et al., 2002b). This Chapter shows that non-NaCl salts, including ones present on the martian surface ($MgSO_4$, $CaSO_4$ and Na_2SO_4, Massé et al., 2014, Ojha et al., 2015, Davila et al., 2013, Kerr, 2013), are capable of improving survivability when compared to NaCl.

$MgCl_2$ was unusual in that, while its presence resulted in fewer viable cells being extracted from the crystals, the microorganisms entombed within those crystals did not experience any cell death under 99 kJ m^{-2} of UV radiation. It is uncertain whether this

was a result of $MgCl_2$ providing greater shielding from the UV (Section 4.4.5a) or because the cells most resistant to the presence of $MgCl_2$ were also more UV-resistant (Section 5.4.5b). The former might imply that, while $MgCl_2$ in an aqueous martian environment would be hazardous to potential martian life, once the brine evaporated and crystals precipitated, they could protect cells. The latter hypothesis, however, would suggest that traits that allow microorganisms to survive one extreme of the martian environment also help them to survive another, and thus raises the possibility that a polyextremophilic microorganism might be able to survive in $MgCl_2$ salts.

These results show that many other salts are better at providing UV-protection for microorganisms than the halite they are typically studied in (Section 5.4.3), but this Chapter has investigated only relatively thin layers of crystals. In the large martian chloride deposits (Section 1.4.2), greater thicknesses of the salts - and potentially larger crystals - would presumably increase UV attenuation.

c) Other forms of radiation

The impact of cosmic radiation was not assessed in this Chapter because UV induces the same biological harm and occurs at much higher intensities (Pavlov et al., 2012). Ionising radiation provides negligible energy on the martian surface compared to UV, although more than is delivered to the terrestrial surface (Sato et al., 2017) and it is able to penetrate much deeper than UV (Pavlov et al., 2012, Musilova et al., 2015). If salt crystals such as those on the martian surface do provide protection from UV, then ionising radiation may play a role in cell survival since there is evidence to suggest that halite is unable to protect cells from ionising radiation (Kminek et al., 2003). Further research is required to determine whether any of these more Mars-relevant salts would impart protection against ionising radiation (Section 5.4.8g).

5.4.8 - Further work

This Chapter devised a methodology for investigating the potential of different salts to entomb cells and compared the relative UV-shielding effects of these salts. The results raised a number of questions and possibilities for future work.

a) Investigating fluid inclusions

In this Chapter, crystals were formed within discs. While this allowed greater consistency in cell counts between experiments, it caused the formation of relatively thick crystals on an opaque background, which rendered microscopy difficult. Further research would involve the growth of larger masses of non-overlapping crystals on glass microscope slides (as attempted in Section 5.3.1a, where this was only successful with NaCl crystals) in order to create samples more suitable for light microscopy. These could be used to determine whether the cells taken from different stages of growth altered the size and abundance of fluid inclusions within a given area (as hypothesised in Section 5.4.2) and thus investigate the causes of the greater mass of crystals formed from stationary phase cells.

If the cells were also dyed prior to crystallisation (as in Section 5.3.1b), then light microscopy could be used to determine the distribution of viable cells in the crystals. Following observation of the short-lived dye, the same microscope slide could be examined using EMPA (as in Section 2.3.1d) in order to examine the distribution of the different salts within the crystals. Comparison of these results could then determine whether the microorganisms were homogenously distributed through the crystals or just located within NaCl.

b) Entombment in the absence of NaCl

The experiments in this Chapter focused on the isolate *H.noricense* FEM1 in order to allow comparison with the results obtained from the samples of Boulby Mine (Chapters 3 and 4). This obligate halophile did not survive brines that did not contain NaCl (Section 4.3.4.e and 5.2.6a) and, as such, could not be used to investigate whether crystals of these salts alone (not in combination) were capable of entombing cells. As an alternative, bacterial spores could be used, which are not obligate halophiles and have been revived from fluid inclusions in halite. If a microorganism can be found that can survive the non-NaCl brines (at least for the approximately 0.5 day periods required for evaporation), then it could be determined whether entombment in those salts is possible.

c) Time scales

The experiments in this Chapter only investigated survival over an entombment period of one day. It would be beneficial to repeat these experiments, with a larger number of discs being prepared on the same day but washed and weighed the day after. Unlike the experiments carried out in this Chapter, the dissolution of crystals and the counting of viable cells could be staggered over longer time periods, with some crystals investigated weeks, months or even years later. In this way, it could be determined whether the viability of cells within crystals decreased over time (as suggested by the work of Kotteman et al., 2005) and varied between salts (as discussed in Section 5.4.7a).

Given that this Chapter has identified $MgCl_2$ as the salt that could provide the best protection from the martian UV environment (Section 5.4.5), it should be determined whether the significantly lower number of viable cells entombed within these crystals is

the result of an environmental stress during crystal formation or whether long-term entombment alongside $MgCl_2$ would eventually kill cells even if they were protected from the UV.

d) Further salts

The salts investigated in this Chapter were chosen primarily because Chapter 4 had demonstrated the ability of *H.noricense* FEM1 to survive the brines that formed the crystals (Section 4.3.4e). Significantly, this study has not investigated perchlorate salts, which are abundant on the martian surface. Future work could therefore repeat the experiments of Chapters 4 and 5, investigating the tolerance of *H.noricense* FEM1 to perchlorate brines and crystals of different cationic compositions. If perchlorates could also be shown to be able to entomb microorganisms then this would significantly increase the number of locations on the martian surface where evidence of life (both past or present) could be found.

e) Investigating a link between chaotropicity resistance and UV resistance

In these experiments, the presence of $MgCl_2$ within an evaporating brine caused significant cell death, but when those cells that survived to become entombed were exposed to 99 KJ m^{-2} of UV-radiation, no further cell death was observed. It is hypothesised (Section 5.4.5b) that this might be indicative of a link between chaotropicity resistance and UV-resistance, although the lack of information about the mechanisms that underpin chaotropicity makes this difficult to determine (Fox-Powell et al., 2016, Ball and Hallsworth, 2015).

In order to determine whether this link exists, cells could be exposed to a strain-improvement program. Cultures could be established of a well-characterised strain of

microorganism, and grown in successively more chaotropic environments. This would apply selection pressure to encourage adaptation to this chaotropicity. Once several chaotropicity resistant strains of this organism had been developed, it would then be tested whether their survival under UV-light differs significantly from cultures of the initial microorganism that had not been exposed to chaotropic environments for generations.

Once chaotropic strains of a well-characterised organism had been developed, the genome of these strains could be compared with the wildtype strain, in order to investigate the methods that these mutants used to develop chaotropicity resistance and thus shed light on the relatively unknown biological defences to this environmental extreme.

Many strain-improvement programs pair growth in environments that induce a selection pressure with a mutagenesis protocol (Upendra and Khandelwal, 2016, Cheng et al., 2016b, Rowlands, 1984) to speed up the rate of mutation and adaptation, but that would not be possible in this proposed experiment; mutagenesis would also induce a selection pressure against UV-resistance. This would interfere with attempts to determine whether cells naturally gain UV-resistance as a side effect of chaotropicity resistance. This would, therefore, mean that the strain improvement program would be a slower process than normal and a suitably fast-growing microorganism should be chosen for it.

f) Other environmental factors on Mars

The results presented in this Chapter show that the presence of some Mars-relevant salts (with the exception of $MgCl_2$) do not inhibit the survival of entombed

microorganisms and that many of these salts (including $MgCl_2$) improve the survival of microorganisms under UV radiation. UV is not, however, the only aspect of the martian environment that is hostile to terrestrial life (Section 1.2.1) and the comparative abilities of these salts to protect cells from these other environmental factors should be investigated.

For example, these experiments could be repeated, but instead of exposing half the discs to UV radiation, they could be exposed to -60 °C, the mean martian temperature (McKay, 1999, Ferguson and Lucchitta, 1984), for several days and the survival of viable cells determined. It has already been shown that air pressures as low as 10^{-6} Pa do not affect the survival of *Halobacterium* in NaCl crystals, nor its ability to withstand UV radiation (Kottemann et al., 2005), but it should be determined whether this remains the case for the other salts.

While the intensity of the martian UV environment means that it is the form of radiation most considered, the surface and near sub-surface are exposed to other forms of radiation including cosmic rays and heavy ions (Pavlov et al., 2012, Musilova et al., 2015). These other forms of radiation become more relevant if the Mars-relevant salts are capable of shielding cells from UV (Section 5.4.7c); there is already evidence to indicate that entombment in halite provides no protection from the martian cosmic radiation environment (Kminek et al., 2003), so it should be determined whether this is the case for all of the salts on the martian surface.

Once these factors have been examined individually, the combined environmental pressures should be investigated in a Mars simulation chamber. Ideally, these experiments would work towards the goal of determining which salts on the martian

surface may be the most effective at supporting viable cells under martian conditions and, thus, which could have the greatest astrobiological potential.

5.5 - Conclusions

This Chapter investigated the survival of cells entombed from the salts precipitated from a variety of salt solutions. The same number of viable cells were obtained from crystals of a wide range of salt compositions and salinities, implying the number of viable cells following the entombment process appears to be linked to an, as yet unknown, factor. It was not related to concentration of the salts within the brine. Significantly, fewer viable cells were obtained when NaCl was combined with $MgCl_2$, but this may be because of a loss of cells in the highly chaotropic conditions formed by increasing concentrations of $MgCl_2$ within the brine during salt precipitation.

It was shown that the entombment of microorganisms within salts (with the exception of $CaSO_4$, which had a very low mass) was capable of increasing the survival of cells when exposed to UV radiation. In particular, while the presence of $MgCl_2$ significantly decreased the number of viable entombed cells, no further cell death was observed when these crystals were exposed to the D_{37} dosage of UV. It remains uncertain whether this was a result of increased protection from the cells from the UV environment, or whether the cell death during the initial entombment process had inadvertently selected for polyextremophilic representatives of the cells. These results indicate that the presence of non-NaCl salts within an evaporating brine, as would occur in a martian environment, would increase the amount of protection received by entombed cells from the harsh martian UV.

Chapter 6: Summary and conclusions

This Thesis investigated the microbial community of the ancient evaporite (salt) deposits of Boulby Mine. Initially a culture-independent study of these deposits was carried out, which showed that variation in Na and K composition of the evaporites had no impact on the composition or diversity of the entombed microbial community (Chapter 3). Obligate halophiles were then isolated from these deposits (Chapter 4). Investigations were carried out to determine the ability of these isolates to survive in brines that were not dominated by NaCl, because high salinity but low-NaCl conditions are hypothesised to exist on the martian surface in both the present day and distant past (Chapter 4).

Finally, this Thesis investigated the ability of halophiles to survive entombment during the evaporation of high salinity, low NaCl brines and precipitation of salts of different compositions (Chapter 5). The impact of salt composition on the potential for organisms to be protected from the martian UV environment by entombment (Leuko et al., 2015, Fendrihan et al., 2009a, Fernández-Remolar et al., 2013) was also investigated.

This Chapter, therefore, summarises the key findings, conclusions and implications of this Thesis, both in terms of terrestrial salts and brines, but also hypothesised salts and brines on the martian surface or near subsurface. The limitations of this work, as well as the unanswered questions raised by it, are considered and identified as potential avenues for further research.

6.1 - Characterisation of Boulby Mine

Boulby Mine was initially chosen as a sample site, as it represents a naturally occurring environment featuring a transition from near pure NaCl (Boulby Halite) to NaCl and KCl in roughly equal ratios (Boulby Potash), while all other environmental factors (such as humidity, temperature and human influence) are kept constant. Both these lithologies have previously been shown to contain entombed microorganisms (Norton et al., 1993), but by investigating the communities entombed across the transition between these two lithologies it could be determined whether changes in the (presumably entombed) microbial community composition were driven by changes in the salt composition. This was the first step towards determining whether martian deposits of non-NaCl salts could entomb life, and if so whether commonly used terrestrial halophiles were a suitable analogue for potential martian life.

6.1.1 - Composition of the Boulby evaporites

Samples from Boulby Mine were collected and characterised (Chapter 2). The majority of the samples came from four sites: A, B, D & E. All of these sites featured the Boulby Halite (NaCl), the Boulby Potash (NaCl + KCl) and the interface region between them. A fifth site, Site X, also featured veins of sylvite (KCl) running through it. Sites A-E had their geochemistry and mineralogy characterised in detail.

Investigation of the samples showed that, as expected, the Boulby Halite and the Boulby Potash differed significantly in the concentration of Na^+ and K^+ ions, though not in the concentration of Cl^- ions. There was evidence to suggest that many of the minor elements (Ca, Fe, Mg, Mn and Al) detected within the samples had been delivered to them *via* downwards movement of water through the stratigraphic column.

6.1.2 - Microorganisms entombed within the samples

Initially, the microbial communities entombed within samples from Sites A-E were investigated using culture-independent techniques (Chapter 3). These techniques investigated the relative abundances of the terminal restriction fragment lengths formed when the various copies of the highly variable 16s rRNA genes extracted from the samples were digested with a restriction enzyme. This was the first culture-independent study of the community within the deposits of Boulby Mine, as all prior studies have been culture-dependent (Norton et al., 1993). These experiments were then followed up with attempts to culture microorganisms from the same samples, as well as ones from an additional site (Site X).

a) Variations in community composition

The culture-independent study carried out within this Thesis indicated there was no variation in the abundances of the microbial genera between samples of Boulby Halite and Boulby Potash; no samples of sylvite were analysed because of limited availability. Large variations in the Na (100 - 40 %) or K (0 - 60 %) concentration of the samples had no effect on the composition of the entombed microbial communities (Section 3.4.2). It could be shown, however, that the diversity of genera was significantly lower in the samples that had undergone the most aqueous alteration, as evidenced by the presence of Ca and other minor elements (Section 3.4.3).

Attempts were made to culture microorganisms from the Boulby Potash, Boulby Halite, and the sylvite. Viable cells could be obtained from all lithologies using the culture-independent techniques (Section 4.3.1b), and the same two genera were isolated. There was again no variation between the lithologies (Section 4.4.2b). Culture-dependent

techniques, however, failed to produce viable cells from sylvite, suggesting that viable cells of the genera found within the Boulby Potash and the Boulby Halite were not present within the sylvite. It remains possible that viable cells of other genera could be obtained from the sylvite using a wider variety of media than were investigated in this Project (see Section 4.4.1b for a full discussion of this). The lack of culture-independent DNA data from the sylvite, means that it remains uncertain whether the sylvite would contain the same non-viable cells that were detected in the other lithologies, or whether the sylvite contained cells at all (Section 4.4.5b).

b) Overall community composition

The results of the culture-independent study suggested that the majority of the DNA within the samples belonged to bacteria rather than archaea (Section 3.4.1). This was contrary to the results from previous studies of Boulby Mine's deposits (Norton et al., 1993) that had only detected archaea. The presence of $CaSO_4$ within many of the samples is indicative that the deposits had undergone secondary aqueous alteration (Section 2.4.3), which may have introduced bacteria to the beds at the sites sampled in this study; while Norton's samples were unaltered (Section 3.4.3b). An alternative hypothesis is that ancient halite deposits like those from Boulby typically contain large numbers of unculturable bacteria which can only be detected *via* culture-independent techniques. This hypothesis is suggested by the work of Fish et al., (2002), who used culture-independent techniques to detect many of the same bacteria as were found in this study within ancient salt deposits that had previously only yielded archaea *via* culture-dependent techniques.

To test these theories, Norton's culture-based techniques were replicated (Chapter 4) using the samples in which bacteria had been detected (Chapter 3), and only archaea

could be grown. Therefore, it is proposed that Norton's samples also contained large numbers of bacteria, but the media used by Norton to isolate organisms did not support their growth. This would, in turn, imply that the microbial community that initially entered the precipitating salts 250 Ma was highly diverse, but only the haloarchaea could withstand long-term entombment and remain viable to the present day (Section 3.4.1).

There was evidence to suggest that when the viable haloarchaea within the samples were released from entombment, they were capable of metabolising the deceased bacteria (Section 4.4.1c). These could, therefore, act a source of utilisable CHNOPS elements which might explain the proposal that haloarchaea can withstand entombment for geological time periods (Schubert et al., 2009). It remains uncertain, however, whether these entombed haloarchaea were capable of utilising these CHNOPS elements or had experienced a process similar to dormancy (Section 1.3.3). Section 6.4.2 considers potential methodologies for investigating the metabolism or dormancy of entombed haloarchaea.

6. 2 - Obligate halophiles from Boulby Mine

6.2.1 - Isolation

Six isolates were obtained from the samples of Boulby Mine (Section 4.4.2). Four of these (named FEM1 and FEM2) could be identified as strains of *Halobacterium noricense*, while the remaining four (named JPW1-4) potentially represent a novel species in the genus *Haloarcula* (Section 4.3.2b). All six of these strains were obligate halophiles, although there is evidence to suggest that *H.noricense* FEM1, while still an

obligate halophile (it was incapable of growth at 0.86 M NaCl), grew at a lower optimum NaCl concentration than the others (2.56 M compared to 3.42 M, Section 4.3.4b).

All six of the isolates were characterised by a pink pigment when grown in liquid culture, expressed from mid-log phase onwards. This pink pigment was tentatively identified as bacterioruberin based upon its colouration, although bacterioruberin is typically only expressed by halophiles under conditions of intense light or anaerobic stress (Dummer et al., 2011, Shand and Betlach, 1991), neither of which were present in these cultures (Section 4.4.2d). Experiments to investigate this pigment, and what regulates its expression, were suggested in Section 4.4.6b.

6.2.2 - Survival in brines of different compositions

As mentioned above, all six of these isolates were obligate halophiles: *H.noricense* FEM1 was incapable of successfully inoculating successive cell cultures at NaCl concentrations below 1.71 M (water activities greater than 0.932), while the remaining five could not do so at NaCl concentrations below 2.56 M (water activities greater than 0.898). Prior literature suggests that the inability of halophiles to grow at relatively low NaCl concentrations is a result of an intolerance to the osmotic pressures induced by high water activities (Grant, 2004, Grant et al., 1998b, DasSarma and DasSarma, 2006). This Thesis, however, suggests otherwise: the addition of 0.01 M $CaSO_4$ allowed a further four isolates to grow at 1.71 M NaCl (Section 4.3.4c), but had no significant impact on water activity. The high water activity of the solution is, therefore, unlikely to be the reason why growth was impossible at 1.71 M NaCl in the absence of $CaSO_4$.

The minimum NaCl requirement of the obligate halophiles isolated from Boulby Mine could be lowered by the addition of other salts (including Na_2SO_4, KCl, $MgCl_2$, $MgSO_4$ or

$CaSO_4$). Based upon comparisons with previous studies (Brown and Gibbons, 1955, Mullakhanbhai and Larsen, 1975), it is assumed that this would be the case for all members of the family *Halobacteriaceae* and, potentially, obligate halophiles as a whole.

Despite the fact that the minimum NaCl requirement of the isolates could be lowered by other salts, none of the isolates grew at an NaCl concentration below 1.71 M, even when the Na concentration was kept at a constant 3.42 M by addition of Na_2SO_4, or the Cl concentration was kept at a constant 3.42 M by addition of KCl or $MgCl_2$. This might suggest that the isolates have a specific requirement for NaCl, a hypothesis which can be found in historic literature, but is often neglected in the modern day in favour of the idea that different salts exert different environmental stresses (for example: water activity, chaotropicity and ionic charge) such that halophiles are less adapted to the conditions induced by other salts (Grant, 2004, Fox-Powell et al., 2016, Hallsworth et al., 2007b). The relatively low resolution of this dataset means that it is, as of yet, infeasible to conclude whether the lack of growth at NaCl concentrations below 1.71 M was because of the same stresses in all tested brines, or if they differed depending upon which salt was added (Section 4.4.4b).

Dilution of 3.42 M NaCl in 3.42 M KCl, or 1.71 M $MgCl_2$, Na_2SO_4, or $MgSO_4$ kept the water activity below 0.932, which was the highest water activity at which growth was observed, but it can be suggested that the lack of growth when $MgCl_2$ exceeded 0.86 M was owing to the high chaotropicity of the brine (Cray et al., 2013). No such environmental explanation can be proposed for the lack of growth in the instances when KCl concentration exceeded the NaCl concentration, as NaCl and KCl have highly similar chemical properties (including water activity, ionic charge and kosmotropicty). Given that K_2SO_4 was the only sulfate investigated that could not improve the growth of

obligate halophiles in low NaCl solutions, it is, therefore, possible that there is a specific intolerance to external K^+ ions, and it is speculated that these might interfere with cells' passive osmoregulation mechanisms (Section 4.4.4b).

6.2.3 - Viability of microorganisms entombed in laboratory grown crystals

No difference was observed in the microbial communities entombed within the environmental samples of the Boulby Potash and or Boulby Halite, but more cultures inoculated from the Boulby Potash produced growth than did from the Boulby Halite. In Section 4.4.1a it was suggested that this might indicate a larger number of viable cells within the Boulby Potash compared to the Boulby Halite (although the relative abundances of the genera represented were likely to be the same in both lithologies, Section 6.1.2). In order to investigate this, entombment in salts with compositions analogous to the Boulby Potash and the Boulby Halite was investigated (Chapter 5). The aim was to determine whether the physicochemical properties of the salt crystals would affect the entombment process and hence the number of viable cells.

Interpretation of the results of that investigation was complicated by the fact that there was no significant variation in the number of viable cells that survived the entombment process regardless of salt concentrations, compositions or salinity of the source brine (Section 5.4.4b). By extension, this implies that, regardless of the changing salt composition of the Zechstein Sea when the Boulby salts were precipitated, a similar number of viable microorganisms may have been entombed. If so, the Boulby Potash may have been better at keeping entombed cells viable over geological timescales than the Boulby Halite (Section 5.4.7a), or the differences in the numbers of viable cells

between the two lithologies was a result of random chance. An experiment was proposed in Section 4.4.6a that would allow statistical investigation of these possibilities.

These results also indicate that the presence of KCl, $CaSO_4$, $MgSO_4$, Na_2SO_4 or K_2SO_4 has no impact on the number of viable cells that can survive the entombment process. The presence of $MgCl_2$, however, resulted in an 89 % reduction in the number of viable cells measured, following precipitation and re-dissolution over the course of approximately 1 day. It is assumed that this is a result of this salt's high chaotropicity (Hallsworth et al., 2007a), but is unclear whether this reduction occurs during the aqueous phase, when the brines are evaporating, or increases with the length of time the cells have been entombed (Section 5.4.8c).

6.3 - Implications for Mars

6.3.1 - Halophiles and aqueous martian environments

Saline environments of indeterminate composition have been identified in a variety of extraterrestrial locations including in the subsurfaces of icy moons (Loudon, 2017, Brown et al., 2017), the martian Southern Highlands (Ojha et al., 2015) and underneath the martian ice caps (Eigenbrode et al., 2018). Prior attempts have been made to culture halophilic organisms in brines modelled to exist on the martian surface (i.e., low NaCl), but failed to produce growth (Fox-Powell et al., 2016). This Thesis, therefore, attempted to investigate the factors that determine habitability in low-NaCl brines.

These results indicate that extraterrestrial brine environments do not need to contain as much NaCl as terrestrial brines to be habitable for halophiles, provided that a) there are other salts present that raise the salinity to those of terrestrial halophilic

environments and b) these non-NaCl salts do not induce environmental extremes such as chaotropicity (Section 6.2.2). This widens the range of martian brine compositions that could potentially support halophilic life.

A limitation of this study is that it only investigated habitability when NaCl is replaced by another salt, and this was carried out with only one non-NaCl salt at a time. Modelled martian brines, however, contain a wide variety of salts at different concentrations (Tosca et al., 2011). While this work suggests that NaCl is needed within a brine for halophilic growth (Section 6.2.2), NaCl as a molecule does not exist in saline environments; it dissociates into aqueous Na^+ and Cl^- ions. It is therefore possible that a martian brine containing ions from the dissociation of non-NaCl salts (for example a brine containing high concentrations of $MgCl_2$ and $NaClO_4$), might still contain Na^+ and Cl^- ions at concentrations high enough to allow growth of obligate halophiles. This is dependent, however, upon these chaotropic and toxic salts not otherwise rendering the brine uninhabitable.

6.3.2 - Entombment following evaporation

The presence of brines on the martian surface is believed to have been more common in the distant past (Osterloo and Hynek, 2015) and that there was once large fluvial systems (Section 1.2.2). However, as the surface evolved into the arid, hostile environment found in the present day (Section 1.2.1), the large fluvial systems evaporated, as evidenced by the presence of evaporite deposits (Hynek et al., 2015). If life had ever evolved on early Mars, evidence of this life (Westall et al., 2015) or perhaps even intact or viable cells (Leuko et al., 2015, Fendrihan et al., 2009a, Fernández-Remolar et al., 2013), could be entombed within the evaporite deposits and hence be

protected from the extreme environments associated with the surface of present-day Mars.

The work within this Thesis shows that the presence of some non-NaCl salts within an aqueous environment, including $MgSO_4$ and $CaSO_4$ found on the martian surface (Massé et al., 2014, Clark and Van Hart, 1981, Kounaves et al., 2010, Hecht et al., 2009), do not inhibit microbial survival once the brines evaporate and salt crystals form. This is not the case for all salts however, as $MgCl_2$, which is also abundant on the martian surface (*ibid.*), did cause a decrease in the number of viable cells (Section 5.3.3e). It is speculated that this might not indicate an inability to survive entombment in the presence of this salt, but rather a result of the environmental conditions within the evaporating brine. It is possible that a more chaotropicity-resistant organism (Section 5.4.4c) might have survived in $MgCl_2$-rich brines and become entombed with minimal loss of cell viability.

These results indicate that entombment is possible in the presence of non-NaCl salts, and low-NaCl, high salinity martian brines may be habitable to halophiles. Therefore, future life-detection missions, searching for evidence of life within martian salt crystals, do not need to limit their search to the vast chloride deposits detected in the Southern Highlands (Hynek et al., 2015, Osterloo and Hynek, 2015, Osterloo et al., 2010, Osterloo et al., 2008). Since small salt crystals of a variety of compositions are found across the martian surface (Massé et al., 2014, Clark and Van Hart, 1981, Kounaves et al., 2010, Hecht et al., 2009), these could be targeted as they might be capable of entombing life.

6.3.3 - Environmental extremes

In the present day, the martian surface is exposed to a variety of environmental extremes including cold, desiccating conditions, low atmospheric pressure and harsh radiation (Section 1.2.1). Of these, the biggest obstacle to the survival of life is the radiation environment (Section 1.2.3), which is considerably more extreme than that found on the terrestrial surface. The majority of the radiation received on the martian surface comes in the form of UV (Schuerger et al., 2006), but heavy ionising radiation and cosmic rays are also present at higher intensities than on the terrestrial surface (Matthiä et al., 2016, Pavlov et al., 2012). Entombment within NaCl crystals has been previously demonstrated to provide protection from this UV-radiation (Leuko et al., 2015, Fendrihan et al., 2009a, Fernández-Remolar et al., 2013). This Thesis investigated whether the presence of non-NaCl salts would improve the ability of the entombed microorganisms to survive UV.

In all but one instance ($CaSO_4$), non-NaCl salt crystals led to a higher survival rate of cells when exposed to 99 kJ m^{-2} of UV radiation. The contrary effect with $CaSO_4$ is believed to be the result of its relatively low abundance within the precipitated crystals compared to the other investigated salts (Section 5.4.4a).

While many of the salts tested (KCl, $MgCl_2$, $MgSO_4$, $CaSO_4$ and Na_2SO_4) have been previously detected on the martian surface, $MgSO_4$ and $MgCl_2$ are of particular interest, as they are found in high abundance (Massé et al., 2014, Clark and Van Hart, 1981, Kounaves et al., 2010, Hecht et al., 2009) and are, therefore, likely to be found in high concentrations in any potential evaporating martian brine. Although, significantly fewer cells survived the entombment process in the presence of $MgCl_2$ (presumably due

to chaotropicity, Section 6.3.2), no further loss in viability was observed when these entombed cells were exposed to 99 KJ m^{-2} UV. It remains uncertain whether this was because the $MgCl_2$ provided significantly better UV shielding, or whether those cells that survived the $MgCl_2$ were more suited for UV-survival (these possibilities were considered in greater detail in Section 5.4.5b).

These results indicate that ancient microorganisms, entombed prior to the development of the current radiation environment, might have been better protected from UV in non-NaCl salt crystals. It still remains uncertain, however, what effect, if any, these salts have on protection from the other elements of the modern day martian surface environment (Sections 5.4.7c & 5.4.8f).

6.3.4 - Halophiles compared to non-halophiles as analogues for martian life

Halophiles are often used as analogues for potential martian life (Payler et al., 2016, Fendrihan et al., 2009a, Orwig, 2014, Barbieri and Stivaletta, 2011, Fernández-Remolar et al., 2013, Srivastava, 2014, Rolfe et al., 2017, Matsubara et al., 2017) and, as a result, this Thesis focused primarily on investigating the tolerance of halophiles to non-NaCl salts akin to those found on the martian surface. As discussed above (Section 6.3.1), these results have shown how the NaCl requirements for the growth of obligate halophiles can be reduced by the presence of other, Mars-relevant salts. This has shed valuable light on martian environments that might be habitable to organisms analogous to terrestrial halophiles (Section 6.3.1), but these conclusions are limited purely to halophiles.

The observation that halophiles could not grow in high salinity brines with an NaCl concentration below 1.71 M (Section 4.4.4b) suggests that halophiles are not the best-suited analogue organisms for potential life in low-NaCl martian brines. This suggestion is strengthened by the fact that it remains plausible that terrestrial non-halophilic organisms might undergo entombment following evaporation of low-NaCl brines (or brines where NaCl is absent) but the halophilic organisms investigated in this Thesis could not (Section 5.4.4a). If non-halophilic organisms can survive a wider range of potential martian brine and crystal compositions then halophilic ones, then the use of halophiles as analogues for potential martial life is called into question.

Considering the martian environment as a whole, however, is key. Halophiles are often polyextremophilic (Section 1.3.4), which make them well suited for studies investigating the martian temperature and atmospheric conditions. It is, however, the desiccation-resistance and UV-resistance of halophiles that makes them still relevant to Mars. The current radiation environment is unlikely to allow life to persist on the modern martian surface (Musilova et al., 2015). It could, therefore, be suggested that microorganisms that were entombed prior to the development of the harsh radiation environment might be better protected from the UV than organisms that remained free-living (Section 6.3.3). This, in turn, suggests that life detection missions should prioritise the search for evidence of life in salt crystals that formed before Mars' internal dynamo failed and the radiation environment deteriorated (Arkani-Hamed and Olson, 2010, Weiss et al., 2008).

The results demonstrated in Chapters 3 and 4 suggest that haloarchaea are the terrestrial organisms best adapted for surviving entombment over geological periods of time (Section 6.1.2b). Even if non-halophilic organisms are capable of undergoing

entombment in crystals on the martian surface, this Thesis suggests that organisms analogous to terrestrial halophiles would be more likely to survive the unknown lengths of time required for evidence of them to persist into the present day. Future space missions should prioritise investigations into martian salt crystals of a chemistry which could be tolerated by halophiles which can withstand long-term entombment: ones with NaCl concentrations that exceed 50 %.

6.4 - Further work

The following section considers methods by which the results of this Thesis could be further investigated. The first part of this section, therefore, considers experiments that could be carried out using the protocols designed and optimised already within this Project. Following this, novel experiments are proposed that could attempt to elucidate the underlying biological processes governing entombment in haloarchaea.

6.4.1 - Furthering the experiments presented in this Thesis

a) Further investigation of Boulby Mine

No difference in community composition was observed within samples of Boulby Mine from the Boulby Potash and the Boulby Halite in the culture-independent study. The culture-dependent study, however, could not detect any of the viable haloarchaea found within the Boulby Potash and Boulby Halite within samples of sylvite. Variation in the culturable microorganisms between the Boulby Halite and sylvite suggests that over a larger range of Na and K concentrations than those investigated in the culture-independent study, the community composition might vary. In order to investigate this, another culture-dependent study would need to be carried out comparing samples of

the Boulby Potash and Boulby Halite to samples of sylvite from the same sites at multiple locations throughout Boulby Mine.

b) Protection from other elements of the martian environment

Chapter 5 showed that non-NaCl salts could improve survival of entombed cells under the martian UV-environment. It is, therefore, of vital importance to investigate whether they can also influence survival under other extreme elements of the martian environment. It was proposed (Section 5.4.8e) that the entombment experiments be repeated, but that the crystals containing entombed cells are exposed to other environmental extremes such as low pressure, cold temperatures and ionising radiation

c) Other salts

This Thesis investigated chlorides and sulfates of Na, K and Mg and, in doing so, increased our understanding of environments that can support and entomb halophilic life. These results showed that many non-NaCl salts can lower the NaCl requirement of obligate halophiles (Section 4.4.4b). However, many martian brines are believed to be dominated by perchlorates (Ojha et al., 2015, Massé et al., 2014, Martín-Torres et al., 2015), which were not investigated in this study. It is not known whether perchlorates would also lower the NaCl requirement of halophiles; the results obtained when K_2SO_4 was added to the media indicate that not all salts do so. Even if perchlorates did lower the NaCl requirement of halophiles, it is possible that the cells would not have survived brines containing perchlorate salts. It has already been noted (Sections 4.4.4b and 6.2.2) that non-NaCl salts change the environmental conditions (e.g., ionic charge, water activity and chaotropicity) of a brine in ways that NaCl does not. Perchlorates, in particular, are likely to induce a less habitable environment than many other salts since

they are highly toxic (Davila et al., 2013b) and have a much larger impact on water activity than chloride salts of the equivalent cations (Toner and Catling, 2016). Perchlorates are also highly oxidising (Kerr, 2013) and this effect is worsened by UV radiation, such as that experienced by the martian surface (Wadsworth and Cockell, 2017). However, terrestrial halophiles are amongst the most perchlorate-resistant organisms (Laye and DasSarma, 2018, Oren et al., 2014), and so may exist in perchlorate-rich martian environments even though other organisms could not.

It is also uncertain what impact, if any, the presence of perchlorate salts within a saline martian environment would have upon the entombment of hypothetical martian organisms. It seems likely, however, that, like when $MgCl_2$ was present in the brines, the rising concentrations caused by evaporation of the water would lead to increased toxicity and thus fewer viable cells surviving the process. Once crystals had formed, the presence of any tested (relatively high abundance) non-NaCl salt in the brine improved the ability of entombed cells to survive under UV light, even chaotropic $MgCl_2$ (Section 5.4.5). This might suggest that the presence of perchlorate salts would do the same. However, the fact that perchlorate salts have been shown to become more toxic under UV light (Wadsworth and Cockell, 2017) might mean that cells entombed within perchlorate crystals under martian UV conditions would suffer higher cell death than cells entombed without this salt.

In order to determine which of the above scenarios featuring perchlorate in both saline and evaporite environments are correct, the experiments outlined in Chapters 4 and 5 should be repeated using perchlorate salts of the cations previously investigated. Adding information about how perchlorate salts impact halophilic growth, entombment and UV shielding within crystals, to the data already obtained for chloride and sulfates,

could further expand the range of potential halophilic environments on the martian surface.

6.4.2 - Investigating entombment

There is still much uncertainty as to what the entombment process entails. It is suggested (Section 6.1.2) that the reason haloarchaea are capable of surviving entombment for geological periods of time is that, instead of entering a state akin to dormancy, they remain capable of metabolising deceased bacteria and undergoing DNA repair (Schubert et al., 2009). Two experiments are, therefore proposed in order to further investigate the hypothesis that entombed cells remain active.

a) Entombed cells and metabolism

It is proposed that the ability of entombed cells to carry out metabolic processes could be assessed by means of measuring carbon uptake. This would be done by entombing the cells alongside a radioactive carbon isotope, such as C_{14}. Cells would be removed from crystals at pre-defined time points and the radioactive media washed off. They would then be burst and a scintillation counter used to assess how much C_{14} was incorporated within the cells. If this increased with the age of the crystals, this would be indicative that the cells were continuing metabolic activity during entombment. If the rate of this increase slowed over time, it would indicate that the cells' metabolism was slowing and that they might be gradually entering a state akin to dormancy.

b) Gene regulation during entombment

In order to investigate whether halophilic cells undergo a process similar to dormancy during entombment, mRNA analysis could be employed. Section 4.4.6c, proposed the

use of transcriptomic techniques to investigate halophilic responses to low salt concentrations. Once optimised, however, the same technique could be used to investigate gene regulation during the entombment process. While haloarchaea lack genes responsible for dormancy (Fendrihan et al., 2012, Grant et al., 1998a, Section 1.3.3a), the expression of genes linked to dormancy in other organisms might suggest a similar process occurs during entombment.

Prior work has used miniature drills to extract DNA directly from specific fluid inclusions without damaging the crystal (Vreeland et al., 2000). The same techniques could be used to extract nucleic acids from laboratory grown crystals without dissolving the salt. DNAase could then be used to remove the DNA leaving only the RNA. A transcriptomic analysis of the genes, if any, expressed by entombed cells could shed light on what cellular processes govern entombment and whether cells remain active or not. This could, in turn, help to clarify how long halophiles are capable of surviving entombment, and whether they are capable of surviving the timescales since Mars was a wetter, more habitable world.

6.3 - Conclusions

In this Thesis, microorganisms were detected and grown from the evaporites of Boulby Mine. This revealed there were no significant differences between the microbial communities present within the different lithologies. Furthermore, this Thesis showed that the presence of a variety of non-NaCl salts in an aqueous environment, such as the ones hypothesised to exist on Mars (in both the distant past and the present day), would not inhibit the entombment of life provided that the aqueous environment itself was habitable. It could also be shown that high concentrations of non-NaCl salts within an

evaporating aqueous environment improves the ability of the entombed cells survive to survive UV radiation. As martian salts are likely to contain high concentrations of non-NaCl salts, it could be suggested that they could protect entombed cells from the martian UV environment.

Appendix 1 - Electron microprobe data. Percentage weight compositions of element oxides

Site	Sample Type	Description of the area measured	Cl	Na_2O	K_2O	MgO	CaO	MnO	FeO	Al_2O_3	SiO_2	SO_4	Total
A	CPH	Colourless crystal	61.97	56.33	0.15	0.00	0.02	0.00	0.00	0.00	0.01	0.00	118.48
A	CPH	Colourless crystal	62.23	56.75	0.10	0.00	0.02	0.00	0.00	0.00	0.00	0.03	119.13
A	CPH	Colourless crystal	58.73	52.58	0.15	0.00	0.02	0.00	0.01	0.00	0.02	0.00	111.51
D	Primary Potash	Birefringent crystal	0.35	0.57	0.20	0.10	38.86	0.00	0.04	0.02	0.24	54.49	94.87
D	Primary Potash	Birefringent crystal	39.20	43.36	0.96	0.84	9.86	0.00	0.16	3.47	4.74	14.19	116.78
D	Primary Potash	Birefringent crystal	61.37	55.54	0.19	0.00	0.00	0.01	0.00	0.00	0.01	0.00	117.12
D	Primary Potash	Birefringent crystal	48.79	0.40	59.84	0.00	0.00	0.00	0.03	0.00	0.00	0.00	109.06
D	Primary Potash	Birefringent crystal	59.14	47.93	9.08	0.00	0.01	0.00	0.01	0.00	0.02	0.03	116.22
D	Primary Potash	Birefringent crystal	47.92	0.38	60.00	0.00	0.00	0.00	0.00	0.00	0.02	0.00	108.32
D	Primary Potash	Birefringent crystal	48.41	0.31	59.95	0.00	0.00	0.00	0.01	0.00	0.00	0.00	108.68
D	Primary Potash	Birefringent crystal	61.40	56.02	0.53	0.01	0.02	0.00	0.04	0.00	0.02	0.03	118.07
D	Primary Potash	Birefringent crystal	60.05	56.77	0.25	0.06	0.47	0.00	0.02	0.00	0.01	0.62	118.25
D	Primary Potash	Fluid Inclusion	55.14	48.58	16.16	0.00	0.03	0.00	0.01	0.00	0.02	0.00	119.94
D	Primary Potash	Fluid Inclusion	57.55	47.55	5.07	0.00	0.02	0.00	0.00	0.00	0.02	0.11	110.32
D	Primary Potash	Fluid Inclusion	53.45	54.72	3.78	0.01	0.05	0.02	0.01	0.00	0.05	0.00	112.09
D	Primary Potash	Fluid Inclusion	50.92	25.17	43.39	0.01	0.00	0.00	0.00	0.00	0.02	0.02	119.53
D	Primary Potash	Fluid Inclusion	56.80	34.76	17.07	0.02	0.02	0.00	0.02	0.00	0.02	0.10	108.81
D	Primary Potash	Fluid Inclusion	52.23	25.32	27.94	0.10	1.08	0.00	0.00	0.00	0.06	1.61	108.34
D	Primary Potash	Large birefringent crystal	8.07	0.15	0.01	10.82	0.04	2.65	27.05	0.07	0.08	0.07	49.01
D	Primary Potash	Opaque area	0.26	0.31	0.71	0.84	35.50	0.01	0.43	1.61	5.96	39.33	84.96
D	Primary Potash	Red crystal	45.88	0.47	57.31	0.04	0.39	0.00	0.47	0.00	0.18	0.12	104.86
D	Primary Potash	Red crystal	48.23	0.51	59.00	0.00	0.12	0.01	0.22	0.00	0.09	0.08	108.26
D	Primary Potash	Red crystal	47.96	0.42	60.13	0.00	0.01	0.01	0.01	0.00	0.02	0.00	108.56
D	Primary Potash	Red crystal	47.79	0.36	59.83	0.02	0.00	0.00	0.63	0.00	0.03	0.01	108.67
D	Primary Potash	Red crystal	47.37	1.55	58.89	0.00	0.01	0.00	0.31	0.00	0.03	0.05	108.21

Site	Sample Type	Description of the area measured	Cl	Na_2O	K_2O	MgO	CaO	MnO	FeO	Al_2O_3	SiO_2	SO_4	Total
D	Primary Potash	Red crystal	48.35	0.24	60.08	0.00	0.00	0.01	0.34	0.00	0.01	0.00	109.03
D	Primary Potash	Red crystal	48.61	2.09	59.01	0.00	0.00	0.01	0.38	0.00	0.02	0.00	110.12
E	Silty Halite	Birefringent crystal	0.35	0.16	0.08	0.48	38.24	0.00	0.02	0.02	0.32	44.14	83.81
E	Silty Halite	Birefringent crystal	54.64	47.76	0.10	0.01	5.90	0.00	0.00	0.00	0.03	8.75	117.19
E	Silty Halite	Birefringent crystal	60.78	56.11	0.09	0.01	0.01	0.00	0.02	0.00	0.01	0.00	117.03
E	Primary Potash	Colourless crystal	48.22	0.17	60.32	0.00	0.00	0.00	0.00	0.00	0.01	0.00	108.72
E	Primary Potash	Colourless crystal	48.03	0.37	59.46	0.00	0.03	0.00	0.00	0.00	0.02	0.11	108.02
E	Primary Potash	Colourless crystal	60.33	56.61	0.07	0.00	0.00	0.00	0.01	0.00	0.01	0.00	117.03
E	Primary Potash	Colourless crystal	48.57	0.13	59.99	0.00	0.01	0.01	0.02	0.01	0.01	0.07	108.82
E	Primary Potash	Colourless crystal	48.13	38.84	25.79	0.00	0.14	0.00	0.10	0.00	0.08	0.07	113.15
E	Silty Halite	Colourless crystal	60.20	55.96	0.12	0.03	0.03	0.00	0.00	0.00	0.02	0.00	116.36
E	Silty Halite	Colourless crystal	61.50	53.36	0.10	0.12	0.12	0.00	0.01	0.00	0.05	0.00	115.26
E	Silty Halite	Colourless crystal	59.69	54.94	0.13	0.28	0.02	0.00	0.01	0.00	0.05	0.03	115.15
E	Silty Halite	Colourless crystal	60.50	56.19	0.08	0.01	0.01	0.01	0.01	0.00	0.01	0.00	116.82
E	Silty Halite	Colourless crystal	1.49	0.20	2.93	8.49	0.44	0.00	2.25	10.67	37.25	0.23	63.95
E	Silty Halite	Colourless crystal	0.88	0.18	1.25	20.10	2.05	0.03	3.10	10.61	31.76	3.52	73.48
E	Silty Halite	Colourless crystal	23.27	24.91	0.97	4.47	2.96	0.00	1.09	1.42	30.28	3.66	93.03
E	Silty Halite	Colourless crystal	0.70	0.19	0.79	10.89	0.20	0.00	2.07	6.83	50.40	0.09	72.16
E	Primary Potash	Red crystal	42.89	0.18	57.30	0.00	0.01	0.00	0.11	0.00	0.03	0.00	100.52
E	Primary Potash	Red crystal	47.90	0.39	59.76	0.00	0.00	0.00	0.08	0.00	0.01	0.00	108.14
E	Primary Potash	Red crystal	48.40	1.06	59.44	0.00	0.00	0.00	0.01	0.00	0.00	0.00	108.91

Appendix 2 - Concentration factors applied to samples for LOI analysis, as well as the LOI measurement for each replicate

Site	Bed	Concentration factor	LOI for Replicate 1 %	LOI for Replicate 2 %	LOI for Replicate 3 %	Mean LOI of concentrated samples	Predicted mean LOI from unconcentrated samples	St.Dev of LOI
A	Secondary Potash	14.590	23.822	13.125	15.405	17.451	2.546	0.822
A	Primary Potash	10.086	24.447	23.887	13.100	20.478	2.065	0.645
A	Interface top	16.612	19.194	14.553	9.700	14.483	2.406	0.789
A	Interface bottom	18.586	-4.981	7.324	3.020	1.788	0.332	1.161
A	Halite	24.167	3.392	5.633	-3.652	1.791	0.433	1.171
B	Primary Potash	20.236	13.751	-3.541	2.062	4.090	0.828	1.785
B	Interface top	34.160	18.657	20.123	2.479	13.753	4.698	3.345
B	Interface bottom	36.452	24.940	11.627	6.899	14.489	5.281	3.410
D	Primary Potash	23.636	2.449	4.038	1.413	2.633	0.622	0.312
D	Interface top	32.211	1.655	38.401	64.938	34.998	11.273	10.236
D	Interface bottom	23.784	-12.372	72.424	0.618	20.223	4.810	10.863
D	Halite	19.879	33.928	7.664	-5.324	12.089	2.403	3.975
E	Primary Potash	22.849	0.861	0.790	1.199	0.950	0.217	0.050
E	Interface top	40.936	1.467	2.051	0.697	1.405	0.575	0.278
E	Interface bottom	37.104	1.126	0.920	2.381	1.475	0.547	0.293
E	Halite	25.378	-2.169	-106.134	-0.513	-36.272	-9.205	15.356

Appendix 3 - Attempted methods to extract archaeal DNA from Boulby salts

The concentration of archaeal DNA within the DNA extracts sent to RTL Genomics was not high enough for MiSeq analysis. As a result, a variety of other techniques were trialled in order to produce a DNA extract with a high concentration of archaeal DNA. As discussed in Section 3.2.5a, none of them could produce a successful DNA extract from the environmental samples but would produce successful DNA extracts from a culture of one of the six isolates ran alongside the environmental sample as a positive control. The methods used are as follows:

A3a - Modifications to the existing protocol

It had been discovered that precipitation of DNA from pooled samples created using the Amicon filters caused precipitation of $CaSO_4$ at the same time. This $CaSO_4$ was interfering with re-dissolution of the DNA. The phenol protocol used to concentrate the pooled DNA was, therefore, modified in a variety of ways in an attempt to separate the DNA from the $CaSO_4$. These modifications involved carrying out the precipitation at different temperatures (-80 °C, -4 °C and 4 °C) and using different precipitants (ethanol, PEG and a variety of different ratios of ethanol:isopropanol). Other modifications attempted were intended to increase the yield of DNA extracted by further encouraging the breakdown of cells. These modifications involved addition of Proteinase K to the 40 °C dissolution stage, and addition of a bead beating step following washing of the cells. Further, more complex methods are described below.

A3b - New methodologies

Cetyl Trimethyl Ammonium Bromide (CTAB)

A CTAB-based DNA Extraction protocol (Leuko et al., 2008) was modified to suit the low biomass samples obtained from Boulby Mine. 100 g salt samples were concentrated in Amicon filters as described above (Section 3.2.2). Following the washing step, however, the samples (both pelleted debris and supernatant) were resuspended in 576 µl TE buffer (10 mM Tris-HCl pH 8.0, 1 mM EDTA). To this was added 30 µl of 10 % SDS and 9 µl of proteinase K (10 mg ml^{-1}). The samples were then incubated for 3 hours at 40 °C and mixed at 150 rpm. After this, 100µl of 5M NaCl was added along with 80 µl of CTAB solution (41 g l^{-1} NaCl and 100 l^{-1} CTAB), and it was incubated at 65 °C for 20 minutes. The DNA was then purified using phenol:chloroform as described above.

Bead beating

Another protocol (Leuko et al., 2008) was also modified to suit the Boulby Mine samples. This time the concentrated 100 g samples were resuspended in 500 µl of a different TE-based buffer (100 mM Tris-HCl pH 8.0, 10 mM EDTA, 1 % SDS) in a MP Biomedicals Lysing Matrix E 2 mL bead beating tube. They were vortexed for two minutes and 25 µl of proteinase K (10 mg ml^{-1}) was added. The sample was then incubated for one hour at 37 °C and then boiled for 10 minutes. Following this the sample was vortexed for another two minutes and 500 µl lysis buffer (4 % SDS, 50 mM Tris-HCl, 100 mM EDTA) was added. Following another round of vortexing, samples were incubated at 56 °C for one hour. Finally, samples were freeze/thawed five times at -80 °C and 70 °C. The DNA was then purified using phenol:chloroform as described above.

Commercially available extraction kit

Archaeal DNA has previously been detected in de-salted samples from an evaporite environment using commercially available kits for extracting DNA from soils (Gramain et al., 2011). 0.2 g subsamples were dissolved in GDB (Section 5.2.3b), in order to minimise cells bursting from osmotic shock. The samples were then centrifuged at 10,000 x *g* for 20 minutes at 4 °C before being resuspended in 0.25 ml dd H_2O to burst them. Samples were then processed using a MP Biomedicals FastDNA™ SPIN Kit for Soil, following the manufacturer's instructions.

Zymo

As the bacterial results suggested that DNA was being extracted from the environmental samples, but that it could not be separated from the $CaSO_4$ using the phenol:chloroform method, a Zymo Genomic DNA Clean & Concentrator kit was used to purify 100 g of sample that had undergone concentrating and desalting in the Amicon spin columns.

Appendix 4: FASTA sequences of the isolates obtained in this study

>Haloarcula sp. Strain JPW1
CTGGAGTGCCTAGAGTTAGAAACGTTCCGGCGCTGTAGGATGTGGCTGCGGCCGATTAAGTAGATGGTGGGGTAACGGCCCACCATGCCGATTA
TCGGTACAGGTTGTGAGAGCAAGAACCTGGAGACGGTATCTGAGACAAGATACCGGGCCCTACCGGGCGCAACAGGCGCGAAACCTTTACACTG
CACGACAGTGCGATAGGGGGACTCCCAATGTGAGGGCATATAACCCTCGCTTTTCTGAACCGTAAGGTGGTTCAAGAACAAGGACTGGGCAAGA
CCGGTGCCCGCCGCCGCGGTAATACCGGCAGTCCAAGTGATGGCCGATATTATTGGGCCTAAAGCGTCCGTAACTTGCTGTGTAAGTCCATTGG
GAAATCGACCAGCTCAACTGGTCGGCGTCCGGTGGAAACTACACAGCTTGGGGCCCAGAGACTCAACGGGTACCTCCGGGGTAAGAATGAAATC
CTGTAATCCTGGACGGACCACCAATGGGGAAACCACCTTGAGAGACCGGACCCGACAGTGAGGGACGAAAGCCAGGGTCTCGAACCGGATTAKA
TACCCGGGTAGTCCTGGCTGTAAACAATGCTCGTTAGGTATGTCACGCGCCATGAGCATGTGATGTGCCGTAGTGAAGCCGATAAGCGAGCCGC
TTGGGAAGTACGTCCGCAAGGATGAAATTTAAAGGAATCGGCGGGGGAGCACCACAACCGGAGGAGCTTGCGGTTTAATTGGATTCAACGCCG
GAAATTTCACCGGTCCCGACAGTAGTAATGACAGTCAGGTTGACGACTTTACTGGACGCTACTGAGAGGAGGTGCATGGCCGCCGTCAGCTCGT
ACCGTGAGGCGTCCTGTTAAGTCAGGCAACGAGCGAGACCCGCACTTCTAGTTGCCAGCAATACCCTTGAGGTAGTTGGGTACACTAGGAGGAC
TGCCGTTGCTAAAGCGGAGGAAGGAACGGGCAACGGTAGGTCAGTATGCCCCGAATGGACCGGGCAACACGCGGGCTACAATGGCTCTGACAGT
GGGATGCAACGCCGAGAGGCGAAGCTAATCTCCAAACGGAGTCGTAGTTCGGATTGCGGGCTGAAACCCGCCCGCATAAGC

>Haloarcula sp. Strain JPW2
GCTGGAGTGCCGAGAGTTAGAAACGTTCCGGCGCTGTAGGATGTGGCTGCGGCCGATTAGGTAGATGGTGGGGTAACGGCCCACCATGCCGATA
ATCGGTACAGGTTGTGAGAGCAAGAGCCTGGAGACGGTATCTGAGACAAGATACCGGGCCCTACGGGGCGCAGCAGGCGCGAAACCTTTACACT
GCACGACAGTGCGATAGGGGGACTCCGAGTGTGAGGGCATATAGCCCTCGCTTTTCTGAACCGTAAGGTGGTTCAGGAACAAGGACTGGGCAAG
ACCGGTGCCAGCCGCCGCGGTAATACCGGCAGTCCAAGTGATGGCCGATATTATTGGGCCTAAAGCGTCCGTAGCTTGCTGTGTAAGTCCATTG
GGAAATCGACCAGCTCAACTGGTCGGCGTCCGGTGGAAACTACACAGCTTGGGGCCGAGAGACTCAACGGGTACGTCCGGGGTAGGAGTGAAAT
CCTGTAATCCTGGACGGACCACCAATGGGGAAACCACGTTGAGAGACCGGACCCGACAGTGAGGGACGAAAGCCAGGGTCTCGAACCGGATTAG
ATACCCGGGTAGTCCTGGCTGTAAACAATGCTCGCTAGGTATGTCACGCGCCATGAGCACGTGATGTGCCGTAGTGAAGACGATAAGCGAGCCG
CCTGGGAAGTACGTCCGCAAGGATGAAATTTAAAGGAATTGGCGGGGGAGCACCACAACCGGAGGAGCCTGCGGTTTAATTGGACTCAACGCC
GGAAATCTCACCGGTCCCGACAGTAGTAATGACAGTCAGGTTGACGACTTTACTCGACGCTACTGAGAGGAGGTGCATGGCCGCCGTCAGCTCG
TACCGTGAGGCGTCCTGTTAAGTCAGGCAACGAGCGAGACCCGCACTTCTAGTTGCCAGCAATACCCTTGAGGTAGTTGGGTACACTAGGAGGA
CTGCCGCTGCTAAAGCGGAGGAAGGAACGGGCAACGGTAGGTCAGTATGCCCCGAATGGACCGGGCAACACGCGGG

>Haloarcula sp. Strain JPW3
TAGCGGATATAACTCTCAGGCTGGAGTGCCGAGAGTTAGAAACGTTCCGGCGCTGTAGGATGTGGCTGCGGCCGATTAGGTAGATGGTGGGGT
AACGGCCCACCATGCCGATAATCGGTACAGGTTGTGAGAGCAAGAGCCTGGAGACGGTATCTGAGACAAGATACCGGGCCCTACGGGGCGCAGC
AGGCGCGAAACCTTTACACTGCACGACAGTGCGATAGGGGGACTCCGAGTGTGAGGGCATATAGCCCTCGCTTTTCTGTACCGTAAGGTGGTTC
AGGAACAAGGACTGGGCAAGACCGGTGCCAGCCGCCGCGGTAATACCGGCAGTCCAAGTGATGGCCGATATTATTGGGCCTAAAGCGTCCGTAG
CTTGCTGTGTAAGTCCATTGGGAAATCGACCAGCTCAACTGGTCGGCGTCCGGTGGAAACTACACAGCTTGGGGCCGAGAGACTCAACGGGTAC
GTCCGGGGTAGGAGTGAAATCCTGTAATCCTGGACGGACCACCAATGGGGAAACCACGTTGAGAGACCGGACCCGACAGTGAGGGACGAAAGC
CAGGGTCTCGAACCGGATTAGATACCCGGGTAGTCCTGGCTGTAAACAATGCTCGCTAGGTATGTCACGCGCCATGAGCACGTGATGTGCCGTA
GTGAAGACGATAAGCGAGCCGCCTGGGAAGTACGTCCGCAAGGATGAAACTTAAAGGAATTGGCGGGGGAGCACCACAACCGGAGGAGCCTGC
GGTTTAATTGGACTCAACGCCGGAAATCTCACCGGTCCCGACAGTAGTAATGACAGTCAGGTTGACGACTTTACTCGACGCTACTGAGAGGAGG
TGCATGGCCGCCGTCAGCTCGTACCGTGAGGCGTCCTGTTAAGTCAGGCAACGAGCGAGACCCGCACTTCTAGTTGCCAGCAATACCCTGGAAA
TAGTTGGGTACAGTTGGAGGACTTACGGTGCTAAATCGGATGAAGGAACGGGTATCGGTAGTTCAGTTTTCCCAGAATGTACCGGGCATCACG
AGGGTTACAAGGTATCTCACAGTGGGATGCATCGCCGAGAGGCGAATCTAATCTCCAAAGGGAGTTGTAGTTCGGATTGCGGGCTGAAACCCG
ACCGCATGAAGC

> Haloarcula sp. Strain JPW4
TCTCAGGCTGGAGTGCCGAGAGTTAGAAACGTTCCGGCGCTGTAGGATGTGGCTGCGGCCGATTAGGTAGATGGTGGGGTAACGGCCCACCATG
CCGATAATCGGTACAGGTTGTGAGAGCAAGAGCCTGGAGACGGTATCTGAGACAAGATACCGGGCCCTACGGGGCGCAGCAGGCGCGAAACCTT
TACACTGCACGACAGTGCGATAGGGGGACTCCGAGTGTGAGGGCATATAGCCCTCGCTTTTCTGAACCGTAAGGTGGTTCAGGAACAAGGACTG
GGCAAGACCGGTGCCAGCCGCCGCGGTAATACCGGCAGTCCAAGTGATGGCCGATATTATTGGGCCTAAAGCGTCCGTAGCTTGCTGTGTAAGT
CCATTGGGAAATCGACCAGCTCAACTGGTCGGCGTCCGGTGGAAACTACACAGCTTGGGGCCGAGAGACTCAACGGGTACGTCCGGGGTAGGAG
TGAAATCCTGTAATCCTGGACGGACCACCAATGGGGAAACCACGTTGAGAGACCGGACCCGACAGTGAGGGACGAAAGCCAGGGTCTCGAACCG
GATTAGATACCCGGGTAGTCCTGGCTGTAAACAATGCTCGCTAGGTATGTCACGCGCCATGAGCACGTGATGTGCCGTAGTGAAGACGATAAGC
GAGCCGCCTGGGAAGTACGTCCGCAAGGATGAAACTTAAAGGAATTGGCGGGGGAGCACCACAACCGGAGGAACCCTGCGGTTTAATTGGGAC
TCAACGCCGGAAATCTCACCGGTCCCGACAGTAGTAATGACAGTCAGGTTGACGACTTTACTCGACGCTACTGAGAGGAGGTGCATGGCCGCCG
TCAGCTCGTACCGTGAGGCGTCCTGTTAAGTCAGGCAACGAGCGAGACCCGCACTTCTAGTTGCCAGCAATACCCTTGAGGTAGTTGGGTACAC
TAGGAGGACTGCCGCTGCTAAA

>Halobacterium noricense Strain FEM1
AACGCTCCACCCCTGGAACGGGCGGAGCTGGAAACGCTACGGCGCCACAGGATGTGGCTGCGGTCGATTAGGTAGACGGTGGGGTAACGGCCCA
CCGTGCCAATAATCGGTACGGGTTGTGAGAGCAAGAGCCCGGAGACGGAATCTGAGACAAGATTCCGGGCCCTACGGGGCGCAGCAGGCGCGAA
ACCTTTACACTGTACGCAAGTGCGATAAGGGGACTCCGAGTGTGAAGGCATAGAGCCTTCACTTTTGTACACCGTAAGGTGGTGTACGAATAAG
GGCTGGGCAAGACCGGTGCCAGCCGCCGCGGTAATACCGGCAGCCCGAGTGATGGCCGATATTATTGGGCCTAAAGCGTCCGTAGCTGGCCGGA
CAAGTCCGTTGGGAAATCTGTTCGCTTAACGAGCAGGCGTCCAGCGGAAACTGTTCGGCTTGGGACCGGAAGACCTGAGGGGTACGTCCGGGGT
AGGAGTGAAATCCTGTAATCCTGGACGGACCACCGGTGGCGAAAGCGCCTCAGGAGGACGGATCCGACAGTGAGGGACGAAAGCTAGGGTCTC
GAACCGGATTAGATACCCGGGTAGTCCTAGCTGTAAACGATGCCGCTAGGTGTGGCGCTGGCTACGAGCTTGCGCTGTGCCGTAGGGAAGCCGA
GAAGCGGGCCGCCTGGGAAGTATGTCTGCAAGGATGAAACTTAAAGGAATGGGCGGGGGAGCACTACAACCGGAGGAGCCTGCGGTTTAATTG
GACTCAACGCCGGACATCTCACCAGCTCCGACAGTAGTAATGACGGTCAGGTTGATGACCTTACCCGATGCTACTGAGAGGAGGTGCATGGCCG
CCGTCAGCTCGTACCGTGAGGCGTCCTGTTAAGTCAGGCAACGAGCGAGACCCGCACTCCTAATTGCCAGCAGTACCCTTTGGGTAGCTGGGTA
CATTAGGTGGACTGCCGCTGCTAAAGCGGAGGAAGGAACGGGCAACGGTAGGTCAGTATGCCCCGAATGAGCTGGGCAACACGCGGGCTACAAT
GGTCGAGACAATGGGATGCAACTCCGAGAGGAGGCGCTAATCTCCTAAACTCGATCGTAGTTCGGATTGAGGG

>Halobacterium noricense Strain FEM2
AACGCTCCACCCCTGGAACGGGCGGAGCTGGAAACGCTACGGCGCCACAGGATGTGGCTGCGGTCGATTAGGTAGACGGTGGGGTAACGGCCCA
CCGTGCCAATAATCGGTACGGGTTGTGAGAGCAAGAGCCCGGAGACGGAATCTGAGACAAGATTCCGGGCCCTACGGGGCGCAGCAGGCGCGAA
ACCTTTACACTGTACGCAAGTGCGATAAGGGGACTCCGAGTGTGAAGGCATAGAGCCTTCACTTTTGTACACCGTAAGGTGGTGTACGAATAAG
GGCTGGGCAAGACCGGTGCCAGCCGCCGCGGTAATACCGGCAGCCCGAGTGATGGCCGATATTATTGGGCCTAAAGCGTCCGTAGCTGGCCGGA
CAAGTCCGTTGGGAAATCTGTTCGCTTAACGAGCAGGCGTCCAGCGGAAACTGTTCGGCTTGGGACCGGAAGACCTGAGGGGTACGTCCGGGGT
AGGAGTGAAATCCTGTAATCCTGGACGGACCACCGGTGGCGAAAGCGCCTCARGAGGACGGATCCGACAGTGAGGGACGAAAGCTAGGGTCTC
GAACCGGATTAGATACCCGGGTAGTCCTAGCTGTAAACGATGCCCGCTAGGTGTGGCGCTGGCTACGAGCCTGCGCTGTGCCGTAGGGAAGCCG
AGAAGCGGGCCGCCTGGGAAGTATGTCTGCAAGGATGAAACTTAAAGGAATTGGCGGGGGAGCACTACAACCGGAGGAGCCTGCGGTTTAATT
GGACTCAACGCCGGACATCTCACCAGTTCCGACAGTAGTAATGACGGTCAGGTTGATGACCTTACCCGATGGTACTGAGAGGAGGTGCATGGCC
GCCGTCAGCTCGTACCGTGAGGCGTCCTGTTAAGTCAGGCAACGAGCGAGACCCGCACTCCTAATTGCCAGCAGTACCCTTTGGGTAGCTGGGT
ACATTAGGTGGACTGCCGCTGCTAAAGCGGAGGAAGGAACGGGCAACGGTAGGTCAGTATGCCCCGAATGAGCTGGGCAACACGCGGGCTACA
ATGGTCGAGACAATGGGATGCAA

Appendix 5: Results of the BIOLOG plates.

Each carbon source is included in triplicate, and the number of wells where a colour change occurred for each isolate in carbon source is listed.

	Haloarcula Sp.				*Halobacterium noricense*		Abiotic
Carbon Source	**JPW1**	**JPW2**	**JPW3**	**PW4**	**FEM1**	**FEM2**	
D-Xylose	3	3	3	2	2	3	0
α-D-Lactose	1	2	2	1	3	3	0
D-Galacturonic Acid	1	1	1	1	2	2	0
α-Ketobutyric Acid	1	1	1	1	3	1	0
D,L-α-Glycerol Phosphate	0	2	0	2	3	0	0
D-Cellobiose	1	1	0	0	3	0	0
D-Malic Acid	0	2	0	0	3	0	0
Gylcyl-L-Glutamic Acid	0	1	1	0	3	0	0
L-Serine	0	1	0	1	3	0	0
No carbon	0	1	0	1	3	0	0
Phenylethylamine	1	1	0	0	3	0	0
α-Cyclodextrin	0	2	0	0	3	0	0
β-Methyl D-Glucoside	0	1	0	1	2	1	0
4-Hydroxy Benzoic Acid	1	2	0	0	1	0	0
D-Galactonic Acid γ-Lactone	0	0	1	0	3	0	0
D-Mannitol	0	1	0	0	3	0	0
Glucose-1-Phosphate	0	1	0	0	3	0	0
Glycogen	0	1	0	0	3	0	0
L-Arginine	0	0	0	1	3	0	0
L-Asparagine	0	1	0	0	3	0	0
Putrescine	0	1	0	0	3	0	0
D-Glucosaminic Acid	0	0	0	0	3	0	0
i_Erythritol	0	0	0	0	3	0	0
L-Phenylalanine	0	0	0	0	3	0	0
L-Threonione	0	0	0	0	3	0	0
2-Hydroxy Benzoic Acid	1	0	0	0	1	0	0
N-Acetyl-D-Glucosamine	0	0	0	0	2	0	0
Pyruvic Acid Methyl Ester	0	0	1	0	0	1	0
γ-Hydroxybutyric Acid	0	0	0	0	2	0	0
Tween 40	0	0	0	0	1	0	0
Tween 80	0	0	0	0	1	0	0
Itaconic Acid	0	0	0	0	0	0	0

Appendix 6: Growth of each of the isolates in media of different salt composition.

Data shows mean specific growth rate (*n*=4) and standard error, alongside the ion concentration and measured water activity of each media

Dilution ratio and salt mixed with NaCl-based media	*Haloarcula sp.* Strain JPW1	*Haloarcula sp.* Strain JPW2	*Haloarcula sp.* Strain JPW3	*Haloarcula sp.* Strain JPW4	*Halobacterium noricense* FEM1	*Halobacterium noricense* FEM2	Total Ion Concentration (M)	Water Activity
4:0 diluted in no salt	0.7740 ± 0.1769	0.9706 ± 0.4839	0.8700 ± 0.4425	0.6678 ± 0.0328	1.0913 ± 0.1523	0.8303 ± 0.4752	6.840	0.855
3:1 diluted in no Salt	0.0000 ± 0.0000	0.5629 ± 0.0713	0.4612 ± 0.0000	0.1375 ± 0.0000	7.4549 ± 3.1088	0.2040 ± 0.0598	5.130	0.898
3:1 diluted in Na_2SO_4	0.3940 ± 0.1022	0.7634 ± 0.0489	0.9412 ± 0.4266	1.0939 ± 0.2072	0.8966 ± 0.0823	0.8019 ± 0.0576	6.840	0.881
3:1 diluted in $MgSO_4$	0.7763 ± 0.0642	1.1065 ± 0.1724	1.6082 ± 0.0770	1.0311 ± 0.1185	0.8227 ± 0.0698	0.9137 ± 0.0268	5.985	0.855
3:1 diluted in $MgCl_2$	0.4252 ± 0.0525	1.2561 ± 0.2767	2.3568 ± 0.4280	1.9192 ± 0.8461	0.8268 ± 0.0821	1.0048 ± 0.1361	6.413	0.855
3:1 diluted in KCl	0.6651 ± 0.2615	0.9989 ± 0.1582	5.3339 ± 3.7891	1.3489 ± 0.8716	0.9095 ± 0.1282	0.9848 ± 0.7688	6.840	0.856
3:1 diluted in K_2SO_4	0.6578 ± 0.3664	3.1719 ± 0.7215	0.5059 ± 1.8794	0.1215 ± 0.0510	3.6111 ± 1.2573	1.1500 ± 0.0150	5.648	0.860
3:1 diluted in $CaSO_4$	0.9403 ± 0.1237	1.3198 ± 0.2652	1.3703 ± 0.4356	2.3191 ± 0.7741	0.7816 ± 0.0635	0.6257 ± 0.1338	5.137	0.896
2:2 diluted in No Salt	0.0000 ± 0.0000	0.0000 ± 0.0000	0.0000 ± 0.0000	0.0000 ± 0.0000	0.9537 ± 0.5863	0.0000 ± 0.0000	3.420	0.932
2:2 diluted in Na_2SO_4	0.000 ± 0.000	0.3356 ± 0.0389	0.7519 ± 1.7152	0.5674 ± 0.0476	0.3639 ± 0.0266	0.7851 ± 0.1736	6.840	0.894
2:2 diluted in $MgSO_4$	0.7750 ± 0.0971	0.8939 ± 0.0816	1.1442 ± 0.4264	1.7468 ± 0.8360	0.6261 ± 0.1116	0.8601 ± 0.0674	5.130	0.903
2:2 diluted in $MgCl_2$	0.4469 ± 0.0602	1.1059 ± 0.1815	0.7519 ± 0.5438	1.1328 ± 0.1152	0.6135 ± 0.1581	0.6004 ± 0.1284	5.985	0.855
2:2 diluted in KCl	0.3499 ± 0.0206	0.8231 ± 0.1121	0.8143 ± 5.3613	3.6679 ± 1.4761	0.6411 ± 0.0000	2.6434 ± 1.3879	6.840	0.862
2:2 diluted in K_2SO_4	0.0000 ± 0.000	0.0000 ± 0.0000	1.2460 ± 0.0000	0.000 ± 0.000	0.0000 ± 0.0000	0.0000 ± 0.0000	4.455	0.903
2:2 diluted in $CaSO_4$	1.8233 ± 0.4752	1.7923 ± 0.1460	0.0000 ± 0.0000	0.3169 ± 0.0969	0.0000 ± 0.0000	0.4228 ± 0.0639	3.434	0.933

Dilution ratio and salt mixed with NaCl-based media	***Haloarcula sp.* Strain JPW1**	***Haloarcula sp.* Strain JPW2**	***Haloarcula sp.* Strain JPW3**	***Haloarcula sp.* Strain JPW4**	***Halobacterium noricense* FEM1**	***Halobacterium noricense* FEM2**	**Total Ion Concentration (M)**	**Water Activity**
1:3 diluted in No Salt	0.000 ± 0.000	0.000 ± 0.000	0.000 ± 0.000	0.000 ± 0.000	0.000 ± 0.000	0.000 ± 0.000	1.710	0.968
1:3 diluted in Na_2SO_4	0.000 ± 0.000	0.000 ± 0.000	0.000 ± 0.000	0.000 ± 0.000	0.000 ± 0.000	0.000 ± 0.000	6.840	0.914
1:3 diluted in $MgSO_4$	0.000 ± 0.000	0.000 ± 0.000	0.000 ± 0.000	0.000 ± 0.000	0.000 ± 0.000	0.000 ± 0.000	4.275	0.932
1:3 diluted in $MgCl_2$	0.000 ± 0.000	0.000 ± 0.000	0.000 ± 0.000	0.000 ± 0.000	0.000 ± 0.000	0.000 ± 0.000	5.558	0.863
1:3 diluted in KCl	0.000 ± 0.000	0.000 ± 0.000	0.000 ± 0.000	0.000 ± 0.000	0.000 ± 0.000	0.000 ± 0.000	6.840	0.865
1:3 diluted in K_2SO_4	0.000 ± 0.000	0.000 ± 0.000	0.000 ± 0.000	0.000 ± 0.000	0.000 ± 0.000	0.000 ± 0.000	3.263	0.932
1:3 diluted in $CaSO_4$	0.000 ± 0.000	0.000 ± 0.000	0.000 ± 0.000	0.000 ± 0.000	0.000 ± 0.000	0.000 ± 0.000	1.731	0.969
0:4 diluted in No Salt	0.000 ± 0.000	0.000 ± 0.000	0.000 ± 0.000	0.000 ± 0.000	0.000 ± 0.000	0.000 ± 0.000	0.000	0.989
0:4 diluted in Na_2SO_4	0.000 ± 0.000	0.000 ± 0.000	0.000 ± 0.000	0.000 ± 0.000	0.000 ± 0.000	0.000 ± 0.000	6.840	0.933
0:4 diluted in $MgSO_4$	0.000 ± 0.000	0.000 ± 0.000	0.000 ± 0.000	0.000 ± 0.000	0.000 ± 0.000	0.000 ± 0.000	3.420	0.975
0:4 diluted in $MgCl_2$	0.000 ± 0.000	0.000 ± 0.000	0.000 ± 0.000	0.000 ± 0.000	0.000 ± 0.000	0.000 ± 0.000	5.130	0.873
0:4 diluted in KCl	0.000 ± 0.000	0.000 ± 0.000	0.000 ± 0.000	0.000 ± 0.000	0.000 ± 0.000	0.000 ± 0.000	6.840	0.871
0:4 diluted in K_2SO_4	0.000 ± 0.000	0.000 ± 0.000	0.000 ± 0.000	0.000 ± 0.000	0.000 ± 0.000	0.000 ± 0.000	2.070	0.975
0:4 diluted in $CaSO_4$	0.000 ± 0.000	0.000 ± 0.000	0.000 ± 0.000	0.000 ± 0.000	0.000 ± 0.000	0.000 ± 0.000	0.028	0.984

Appendix 7: Cell density of various cultures of *H.noricense* FEM1 of different ages, alongside the mass of crystals formed and number of viable cells remaining following entombment of $2x10^9$ cells

Age of culture (days)	Density of culture (cells ml^{-1})	Mass of crystals (g)	Viable cells per disc following entombment
0	1.00E+08	0.0747	1.97E+08
		0.0778	3.21E+08
		0.0886	3.08E+08
		0.0825	3.82E+08
		0.0775	2.96E+08
		0.0796	2.03E+08
0	1.00E+08	0.0730	1.71E+08
		0.0725	1.90E+08
		0.0718	2.13E+08
		0.0840	1.57E+08
		0.0722	1.66E+08
		0.0901	1.71E+08
0	1.00E+08	0.1391	4.95E+08
		0.1328	3.93E+08
		0.1348	2.22E+08
		0.1400	3.10E+08
		0.1159	2.22E+08
		0.0720	4.16E+07
1	3.55E+08	0.0775	3.51E+09
		0.0956	2.16E+09
		0.0819	1.05E+09
		0.0795	5.30E+09
		0.0789	3.51E+09
		0.0891	5.61E+09
1	3.70E+08	0.0502	1.43E+08
		0.0599	4.90E+08
		0.0583	2.73E+08
		0.0523	2.08E+08
		0.0520	4.16E+08
		0.0542	4.72E+08
1	1.54E+08	0.0900	3.47E+09
		0.1137	3.61E+09
		0.0932	2.36E+09
		0.1018	5.55E+08
		0.1034	2.87E+09
		0.1100	2.36E+09
1	3.05E+08	0.1067	6.94E+08
		0.0906	1.25E+09
		0.0913	2.59E+09
		0.0935	9.25E+08
		0.0947	2.22E+09
		0.1059	2.50E+09

Age of culture (days)	Density of culture (cells ml^{-1})	Mass of crystals (g)	Viable cells per disc following entombment
2	1.80E+09	0.0904	3.27E+09
		0.0975	2.96E+09
		0.0947	2.90E+09
		0.0831	3.39E+09
		0.0990	2.34E+09
		0.0966	3.33E+09
2	1.22E+09	0.0791	1.11E+09
		0.0827	1.62E+09
		0.0632	7.40E+08
		0.0838	4.16E+08
		0.0692	1.06E+09
		0.0618	6.01E+08
2	2.77E+09	0.0842	2.22E+09
		0.0942	2.22E+09
		0.1123	1.25E+09
		0.0890	2.50E+09
		0.0942	5.09E+08
		0.1002	1.29E+09
3	1.16E+10	0.1069	3.70E+08
		0.1196	5.55E+08
		0.1574	2.59E+08
		0.1101	2.17E+08
		0.1127	1.48E+08
		0.1216	1.43E+08
3	5.09E+09	0.0669	2.54E+08
		0.0683	9.25E+07
		0.0757	2.64E+08
		0.0695	1.53E+08
		0.0588	7.86E+06
		0.0613	2.50E+07
3	6.78E+10	0.0911	3.70E+07
		0.0550	0.00E+00
		0.1150	4.62E+07
		0.0703	1.62E+08
		0.0590	0.00E+00
		0.0949	7.86E+06
3	5.20E+09	0.1210	1.39E+09
		0.1214	1.66E+09
		0.0846	0.00E+00
		0.0878	1.66E+09
		0.1114	1.53E+09
		0.1173	1.48E+09
4	6.78E+09	0.1238	1.25E+09
		0.1273	1.11E+09
		0.1180	5.09E+08
		0.1191	3.05E+09
		0.0911	3.70E+07
4	1.31E+10	0.1287	1.25E+09
		0.0917	2.91E+08
		0.1163	3.70E+08
		0.0971	5.09E+08
		0.1257	1.02E+09
		0.1161	7.40E+08

Age of culture (days)	Density of culture (cells ml^{-1})	Mass of crystals (g)	Viable cells per disc following entombment
5	1.10E+10	0.1172	5.09E+08
		0.0994	6.94E+08
		0.1132	6.01E+08
		0.1072	1.90E+09
		0.1375	1.25E+09
		0.1352	1.39E+09
5	1.31E+10	0.1062	2.08E+09
		0.1281	2.77E+09
		0.1016	1.06E+09
		0.1084	9.25E+08
		0.0915	1.48E+09
		0.1123	3.70E+08
6	7.55E+09	0.0896	2.59E+08
		0.0796	3.79E+08
		0.0820	2.77E+08
		0.0812	4.86E+08
		0.0707	3.65E+08
6	9.09E+09	0.1403	1.34E+09
		0.1311	1.80E+09
		0.1200	7.86E+08
		0.1178	1.11E+09
		0.1400	1.90E+09
		0.1462	1.02E+09
7	1.85E+09	0.1291	1.43E+09
		0.1129	9.25E+08
		0.1250	1.85E+09
		0.1247	1.71E+09
		0.1157	2.82E+09
7	8.90E+09	0.1031	8.32E+08
		0.1198	6.47E+08
		0.0900	1.66E+09
		0.1166	2.03E+09
		0.0878	1.16E+09
		0.0981	9.71E+08
7	8.79E+09	0.1349	1.25E+09
		0.1227	2.77E+09
		0.1092	2.45E+09
		0.1085	1.53E+09
		0.1117	1.29E+09
		0.1054	1.94E+09
8	1.26E+10	0.1127	1.48E+09
		0.1375	5.09E+08
		0.1164	1.06E+09
		0.1088	7.40E+08
		0.1084	9.25E+08
8	7.24E+09	0.1621	1.34E+09
		0.0792	1.43E+09
		0.1170	5.09E+08
		0.1129	8.79E+08
		0.1269	1.16E+09
		0.1099	1.29E+09

Appendix 8: Mass of crystals and number of viable cells obtained from crystals of various compositions initially containing 2.8×10^9 cells.

Crystals were prepared in four separate "repeats," and half the crystals in each repeat were exposed to 99 kJ m-2 of UV radiation

Salt	Repeat number	Exposed to UV?	Mass of salt	Viable cells/disc
NaCl	1	No	0.0957	8.32E+07
NaCl	1	No	0.1075	9.25E+07
NaCl	1	No	0.1105	6.01E+08
NaCl	1	No	0.1172	1.34E+09
NaCl	1	No	0.1199	1.71E+08
NaCl	1	No	0.1232	1.80E+08
NaCl	2	No	0.0958	2.68E+08
NaCl	2	No	0.1120	3.38E+08
NaCl	2	No	0.1143	3.01E+08
NaCl	2	No	0.1184	2.59E+08
NaCl	2	No	0.1315	3.33E+08
NaCl	2	No	0.1522	3.38E+08
NaCl	3	No	0.1211	4.95E+08
NaCl	3	No	0.1290	3.33E+08
NaCl	3	No	0.1317	2.82E+08
NaCl	3	No	0.1345	3.01E+08
NaCl	3	No	0.1352	4.58E+08
NaCl	4	No	0.0881	3.05E+08
NaCl	4	No	0.1090	6.10E+08
NaCl	4	No	0.1138	5.36E+08
NaCl	4	No	0.1229	4.86E+08
NaCl	4	No	0.1254	5.09E+08
NaCl	4	No	0.1303	3.14E+08
NaCl	1	Yes	0.1127	2.96E+08
NaCl	1	Yes	0.1167	1.76E+08
NaCl	1	Yes	0.1315	1.34E+07
NaCl	2	Yes	0.1145	2.08E+08
NaCl	2	Yes	0.1176	7.86E+07
NaCl	2	Yes	0.1293	9.71E+07
NaCl	3	Yes	0.1275	3.70E+08

Salt	Repeat number	Exposed to UV?	Mass of salt	Viable cells/disc
NaCl	3	Yes	0.1398	2.13E+08
NaCl	3	Yes	0.1497	6.20E+07
NaCl	4	Yes	0.1069	2.40E+08
NaCl	4	Yes	0.1256	2.68E+08
NaCl	4	Yes	0.1335	2.59E+08
$NaCl + Na_2SO_4$	1	No	0.0880	3.56E+08
$NaCl + Na_2SO_4$	1	No	0.0937	7.26E+08
$NaCl + Na_2SO_4$	1	No	0.0973	1.48E+08
$NaCl + Na_2SO_4$	2	No	0.0810	4.25E+08
$NaCl + Na_2SO_4$	2	No	0.0839	3.33E+08
$NaCl + Na_2SO_4$	2	No	0.0900	2.64E+08
$NaCl + Na_2SO_4$	3	No	0.0891	5.32E+08
$NaCl + Na_2SO_4$	3	No	0.0969	5.23E+08
$NaCl + Na_2SO_4$	3	No	0.0989	4.53E+08
$NaCl + Na_2SO_4$	4	No	0.0882	5.83E+08
$NaCl + Na_2SO_4$	4	No	0.0916	3.33E+08
$NaCl + Na_2SO_4$	4	No	0.0934	3.61E+08
$NaCl + Na_2SO_4$	1	Yes	0.0792	2.17E+08
$NaCl + Na_2SO_4$	1	Yes	0.0835	2.68E+08
$NaCl + Na_2SO_4$	1	Yes	0.0863	1.99E+08
$NaCl + Na_2SO_4$	2	Yes	0.0823	3.42E+08
$NaCl + Na_2SO_4$	2	Yes	0.0988	2.40E+08
$NaCl + Na_2SO_4$	2	Yes	0.0997	2.64E+08
$NaCl + Na_2SO_4$	3	Yes	0.0819	4.62E+08
$NaCl + Na_2SO_4$	3	Yes	0.0844	6.20E+08
$NaCl + Na_2SO_4$	3	Yes	0.0847	3.19E+08
$NaCl + Na_2SO_4$	4	Yes	0.0803	2.27E+08
$NaCl + Na_2SO_4$	4	Yes	0.0842	3.05E+08
$NaCl + Na_2SO_4$	4	Yes	0.0909	4.76E+08
$NaCl + MgSO_4$	1	No	0.0510	3.65E+08
$NaCl + MgSO_4$	1	No	0.0526	2.08E+08
$NaCl + MgSO_4$	2	No	0.0503	5.55E+08
$NaCl + MgSO_4$	2	No	0.0546	3.14E+08
$NaCl + MgSO_4$	2	No	0.0556	4.99E+08
$NaCl + MgSO_4$	3	No	0.0487	4.76E+08
$NaCl + MgSO_4$	3	No	0.0526	7.17E+08
$NaCl + MgSO_4$	3	No	0.0565	6.43E+08
$NaCl + MgSO_4$	4	No	0.0488	5.46E+08
$NaCl + MgSO_4$	4	No	0.0553	5.78E+08
$NaCl + MgSO_4$	4	No	0.0653	5.41E+08
$NaCl + MgSO_4$	1	Yes	0.0535	1.76E+08
$NaCl + MgSO_4$	1	Yes	0.0539	3.24E+08

Salt	Experiment repeat	Exposed to UV?	Mass of salt	Viable cells/disc
NaCl + $MgSO_4$	1	Yes	0.0553	4.35E+08
NaCl + $MgSO_4$	2	Yes	0.0501	4.44E+08
NaCl + $MgSO_4$	2	Yes	0.0506	4.02E+08
NaCl + $MgSO_4$	2	Yes	0.0544	4.25E+08
NaCl + $MgSO_4$	3	Yes	0.0482	3.33E+08
NaCl + $MgSO_4$	3	Yes	0.0560	4.99E+08
NaCl + $MgSO_4$	3	Yes	0.1157	2.45E+08
NaCl + $MgSO_4$	4	Yes	0.0497	4.90E+08
NaCl + $MgSO_4$	4	Yes	0.0569	3.84E+08
NaCl + $MgSO_4$	4	Yes	0.0597	2.40E+08
NaCl + $MgCl_2$	1	No	0.1015	2.64E+07
NaCl + $MgCl_2$	1	No	0.1016	1.11E+07
NaCl + $MgCl_2$	1	No	0.1031	1.11E+07
NaCl + $MgCl_2$	2	No	0.0950	3.42E+07
NaCl + $MgCl_2$	2	No	0.0966	2.96E+07
NaCl + $MgCl_2$	2	No	0.0968	5.13E+07
NaCl + $MgCl_2$	3	No	0.0922	3.51E+07
NaCl + $MgCl_2$	3	No	0.0948	4.95E+07
NaCl + $MgCl_2$	3	No	0.0949	4.02E+07
NaCl + $MgCl_2$	4	No	0.0823	1.29E+08
NaCl + $MgCl_2$	4	No	0.0824	4.62E+07
NaCl + $MgCl_2$	4	No	0.0857	6.94E+07
NaCl + $MgCl_2$	1	Yes	0.0975	2.08E+07
NaCl + $MgCl_2$	1	Yes	0.1026	3.61E+07
NaCl + $MgCl_2$	1	Yes	0.1028	1.99E+07
NaCl + $MgCl_2$	2	Yes	0.0930	3.93E+07
NaCl + $MgCl_2$	2	Yes	0.0933	4.39E+07
NaCl + $MgCl_2$	2	Yes	0.0960	1.57E+07
NaCl + $MgCl_2$	3	Yes	0.0859	2.50E+07
NaCl + $MgCl_2$	3	Yes	0.0888	3.38E+07
NaCl + $MgCl_2$	3	Yes	0.0909	3.70E+07
NaCl + $MgCl_2$	4	Yes	0.0823	5.09E+07
NaCl + $MgCl_2$	4	Yes	0.0841	5.55E+07
NaCl + $MgCl_2$	4	Yes	0.0852	1.34E+08
NaCl + KCl	1	No	0.0846	3.47E+08
NaCl + KCl	1	No	0.0889	2.77E+08
NaCl + KCl	1	No	0.1027	2.50E+08
NaCl + KCl	2	No	0.0821	3.84E+08
NaCl + KCl	2	No	0.0854	3.28E+08
NaCl + KCl	2	No	0.1063	4.12E+08
NaCl + KCl	3	No	0.0841	3.98E+08
NaCl + KCl	3	No	0.0934	6.15E+08

Salt	Experiment repeat	Exposed to UV?	Mass of salt	Viable cells/disc
NaCl + KCl	1	No	0.0846	3.47E+08
NaCl + KCl	4	No	0.0651	3.70E+08
NaCl + KCl	4	No	0.0722	4.95E+08
NaCl + KCl	4	No	0.0875	4.90E+08
NaCl + KCl	1	Yes	0.0807	2.77E+08
NaCl + KCl	1	Yes	0.0828	2.13E+08
NaCl + KCl	1	Yes	0.0867	4.07E+08
NaCl + KCl	2	Yes	0.0380	1.90E+08
NaCl + KCl	2	Yes	0.0810	1.11E+08
NaCl + KCl	2	Yes	0.0841	3.38E+08
NaCl + KCl	3	Yes	0.0836	3.10E+08
NaCl + KCl	3	Yes	0.0975	2.82E+08
NaCl + KCl	3	Yes	0.1001	2.40E+08
NaCl + KCl	4	Yes	0.0694	2.50E+08
NaCl + KCl	4	Yes	0.0694	3.70E+08
NaCl + KCl	4	Yes	0.0769	3.70E+08
NaCl + K_2SO_4	1	No	0.0499	2.87E+08
NaCl + K_2SO_4	1	No	0.0503	2.40E+08
NaCl + K_2SO_4	1	No	0.0529	2.87E+08
NaCl + K_2SO_4	2	No	0.0436	2.17E+08
NaCl + K_2SO_4	2	No	0.0493	3.38E+08
NaCl + K_2SO_4	2	No	0.0548	2.77E+08
NaCl + K_2SO_4	3	No	0.0472	2.27E+08
NaCl + K_2SO_4	3	No	0.0492	2.73E+08
NaCl + K_2SO_4	3	No	0.0511	3.10E+08
NaCl + K_2SO_4	4	No	0.0374	5.46E+08
NaCl + K_2SO_4	4	No	0.0491	3.65E+08
NaCl + K_2SO_4	4	No	0.0498	3.65E+08
NaCl + K_2SO_4	1	Yes	0.0473	1.16E+08
NaCl + K_2SO_4	1	Yes	0.0491	8.32E+07
NaCl + K_2SO_4	1	Yes	0.0504	1.53E+08
NaCl + K_2SO_4	2	Yes	0.0455	1.94E+08
NaCl + K_2SO_4	2	Yes	0.0503	9.71E+07
NaCl + K_2SO_4	2	Yes	0.0557	2.91E+08
NaCl + K_2SO_4	3	Yes	0.0485	1.66E+08
NaCl + K_2SO_4	3	Yes	0.0505	2.91E+08
NaCl + K_2SO_4	3	Yes	0.0513	2.68E+08
NaCl + K_2SO_4	4	Yes	0.0414	2.31E+08
NaCl + K_2SO_4	4	Yes	0.0457	2.64E+08
NaCl + K_2SO_4	4	Yes	0.0510	2.77E+08
NaCl + $CaSO_4$	1	No	0.0523	5.04E+07
NaCl + $CaSO_4$	1	No	0.0651	5.87E+07

Salt	Experiment repeat	Exposed to UV?	Mass of salt	Viable cells/disc
$NaCl + CaSO_4$	2	No	0.0453	2.73E+08
$NaCl + CaSO_4$	2	No	0.0528	1.20E+08
$NaCl + CaSO_4$	2	No	0.0562	2.82E+08
$NaCl + CaSO_4$	3	No	0.0481	5.46E+08
$NaCl + CaSO_4$	3	No	0.0552	5.13E+08
$NaCl + CaSO_4$	3	No	0.0594	4.35E+08
$NaCl + CaSO_4$	4	No	0.0490	4.12E+08
$NaCl + CaSO_4$	4	No	0.0577	5.23E+08
$NaCl + CaSO_4$	4	No	0.0609	5.23E+08
$NaCl + CaSO_4$	1	Yes	0.0577	1.26E+08
$NaCl + CaSO_4$	1	Yes	0.0601	2.50E+08
$NaCl + CaSO_4$	1	Yes	0.0656	8.88E+07
$NaCl + CaSO_4$	2	Yes	0.0468	2.50E+08
$NaCl + CaSO_4$	2	Yes	0.0510	1.25E+08
$NaCl + CaSO_4$	2	Yes	0.0534	6.47E+07
$NaCl + CaSO_4$	3	Yes	0.0472	4.86E+08
$NaCl + CaSO_4$	3	Yes	0.0554	2.59E+08
$NaCl + CaSO_4$	3	Yes	0.0620	4.16E+08
$NaCl + CaSO_4$	4	Yes	0.0534	2.87E+08
$NaCl + CaSO_4$	4	Yes	0.0617	4.16E+08
$NaCl + CaSO_4$	4	Yes	0.0624	3.93E+08

Appendix 9 - Preliminary experiments

This section describes the methodology employed and data obtained from preliminary experiments. These used different methodologies and featured fewer data points than the actual data sets presented within this thesis, but the results presented below could be used to guide and optimise the actual experiments.

A9a - Pilot growth curve experiments

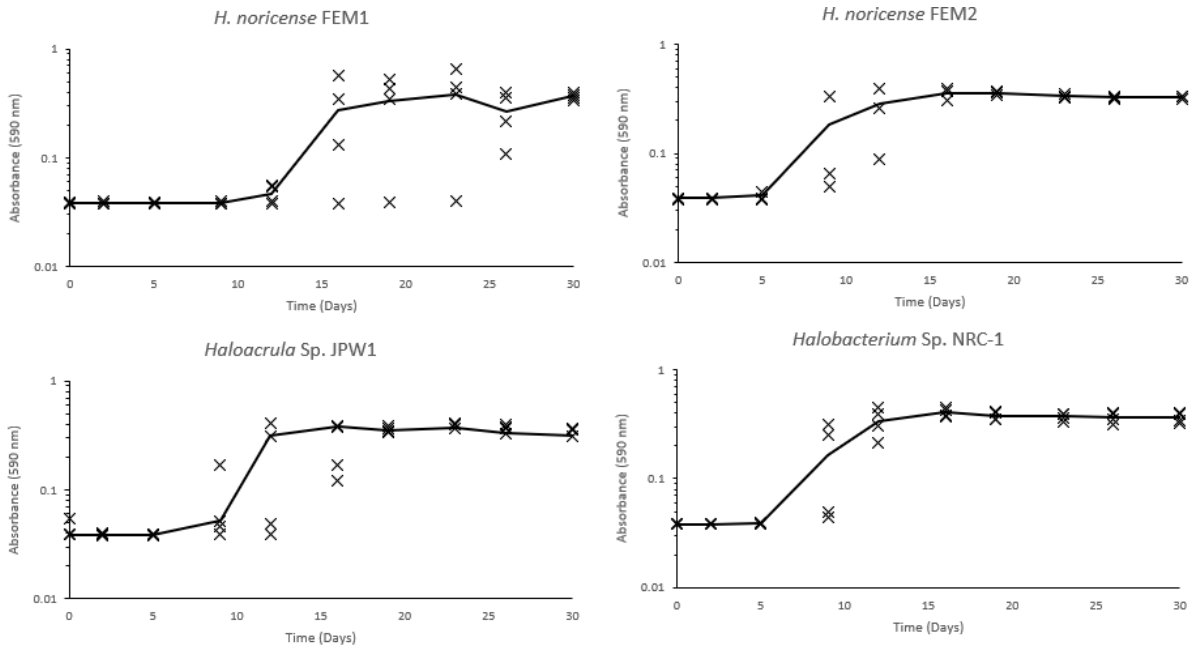

Figure A9.6.1 - Growth of three isolates and a positive control over a period of a month when transferred from 100 % MPM in stationary conical flasks to rotated 10% MPM

These experiments in 10 % MPM containing 3.42 M NaCl were carried out using the methodology outlined in Section 4.2.5, with the following exceptions: Cells were washed and transferred directly from stationary conical flasks of 100 % MPM (as described in Section 4.2.1) to the aerated falcon tubes without an "acclimatisation culture." Only three isolates had been obtained when these experiments were carried out, so growth curves were only drawn of *Haloarcula Sp.* JPW1 and *H.noricense* FEM1 & FEM2. Growth curves of *Halobacterium* Sp. NRC-1, a very well characterised halophile (Bishop et al.,

1959, Kennedy et al., 2001, Ng et al., 2000), were used as a positive control to confirm that growth was possible under these conditions.

A9b - Pilot entombment experiments

Chapter 5 featured entombment of *H.noricense* FEM1 within salt crystals. Initial experiments featuring entombment in crystals containing NaCl did not consider which growth phase cells were in prior to entombment. Nine discs containing crystals with entombed cells were prepared on four separate occasions.

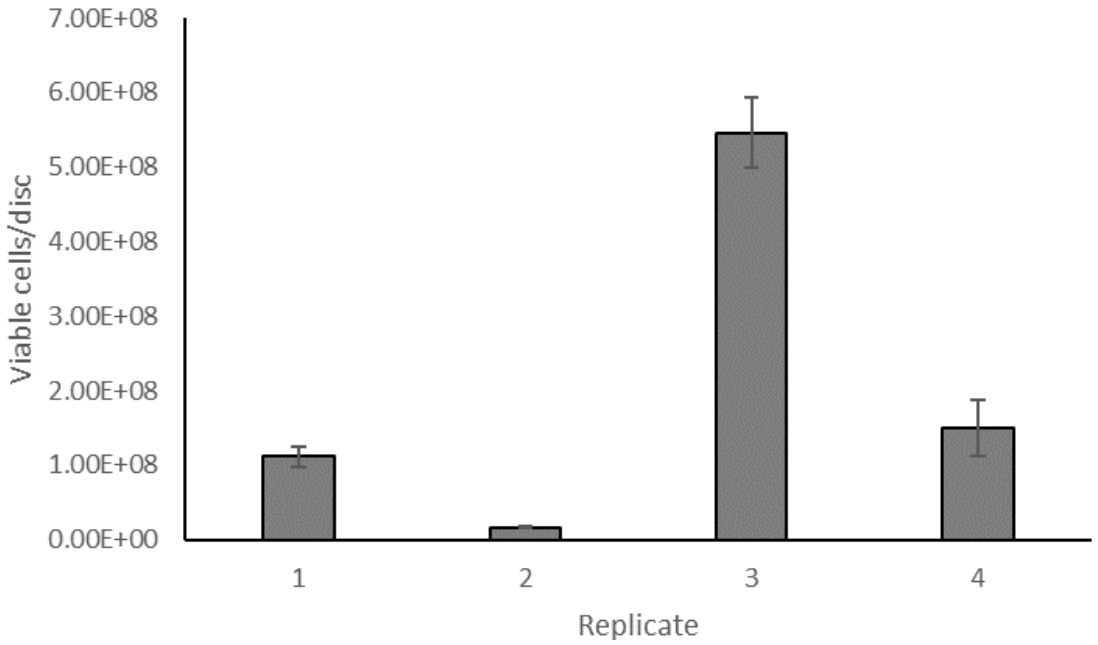

*Figure A9.6.2 - Mean number of viable cells remaining per disc (*n = 9*) when 2.8 ×10⁹ cells of H.noricense FEM1 were entombed in NaCl crystals on four separate occasions without regard to growth phase of the source culture. Errors bars represent standard error of the mean*

There was extreme variability between the number of viable cells observed between discs prepared from the same culture on different days, compared to discs prepared simultaneously (ANOVA, $p < 0.05$). This led to the investigation into possible sources of this variation, as outlined in Section 5.2.3c.

References

ABRAMOV, O. & MOJZSIS, S. J. 2009. Microbial habitability of the Hadean Earth during the late heavy bombardment. *Nature,* 459**,** 419.

ADAMSKI, J. C., ROBERTS, J. A. & GOLDSTEIN, R. H. 2006. Entrapment of bacteria in fluid inclusions in laboratory-grown halite. *Astrobiology,* 6**,** 552.

AGUILERA, A. & AMILS, R. 2005. Tolerance to cadmium in Chlamydomonas sp.(Chlorophyta) strains isolated from an extreme acidic environment, the Tinto River (SW, Spain). *Aquatic toxicology,* 75**,** 316.

ALAIN, K. & QUERELLOU, J. 2009. Cultivating the uncultured: limits, advances and future challenges. *Extremophiles,* 13**,** 583.

ALLEN, J. F. 2016. A Proposal for Formation of Archaean Stromatolites before the Advent of Oxygenic Photosynthesis. *Frontiers in microbiology,* 7**,** 1784.

ALTIGANI, M., MERKLE, R. K. W. & DIXON, R. D. 2016. Geochemical identification of episodes of gold mineralisation in the Barberton Greenstone Belt, South Africa. *Ore Geology Reviews,* 75**,** 186.

AMADI, O., ONYEMA, N., NWAGU, T., MONEKE, A., OKOLO, B. & AGU, R. 2016. Evaluating the Potential of Wild Cocoyam "Caladium Bicolor" for Ethanol Production Using Indigenous Fungal Isolates. *Procedia Environmental Sciences,* 35**,** 809.

ANDREWS-HANNA, J. & BOTTKE, W. 2017. Mars During the Pre-Noachian. *Abstracts from The Fourth International Conference on Early Mars: Geologic, Hydrologic, and Climatic Evolution and the Implications for Life,* 2014.

ANDREWS-HANNA, J. C. & LEWIS, K. W. 2011. Early Mars hydrology: 2. Hydrological evolution in the Noachian and Hesperian epochs. *Journal of Geophysical Research: Planets,* 116**,** E02007.

ANGUITA, F., FERNÁNDEZ, C., CORDERO, G., CARRASQUILLA, S., ANGUITA, J., NÚÑEZ, A., RODRÍGUEZ, S. & GARCÍA, J. 2006. Evidences for a Noachian–Hesperian orogeny in Mars. *Icarus,* 185**,** 331.

ANTON, J., OREN, A., BENLLOCH, S., RODRIGUEZ-VALERA, F., AMANN, R. & ROSSELLO-MORA, R. 2002. Salinibacter ruber gen. nov., sp. nov., a novel, extremely halophilic member of the Bacteria from saltern crystallizer ponds. *Int J Syst Evol Microbiol,* 52**,** 485.

ANWAR, J., FRENKEL, D. & NORO, M. G. 2003. Calculation of the melting point of NaCl by molecular simulation. *The Journal of chemical physics,* 118**,** 728.

AQUINO, M. 2017. *Impacts of Ozone Dose and Empty Bed Contact Time on Bulk Organic Removal and Disinfection Byproduct Mitigation in Ozone-Biofiltration Systems.* Master of Science in Engineering, Universidade Federal do Rio Grande do Norte.

ARGANDOÑA, M., FERNÁNDEZ-CARAZO, R., LLAMAS, I., MARTÍNEZ-CHECA, F., CABA, J. M., QUESADA, E. & MORAL, A. D. 2005. The moderately halophilic bacterium Halomonas maura is a free-living diazotroph. *FEMS Microbiology Letters,* 244**,** 69.

ARKANI-HAMED, J. & OLSON, P. 2010. Giant impacts, core stratification, and failure of the Martian dynamo. *Journal of Geophysical Research: Planets,* 115**,** E07012.

AUJLA, I. S. & PAULITZ, T. C. 2017. An Improved Method for Establishing Accurate Water Potential Levels at Different Temperatures in Growth Media. *Frontiers in microbiology,* 8**,** 1497.

AZUA-BUSTOS, A., URREJOLA, C. & VICUÑA, R. 2012. Life at the dry edge: microorganisms of the Atacama Desert. *FEBS letters,* 586**,** 2939.

AZUA-BUSTOS, A., ZÚÑIGA, J., ARENAS-FAJARDO, C., ORELLANA, M., SALAS, L. & RAFAEL, V. 2014. Gloeocapsopsis AAB1, an extremely desiccation-tolerant cyanobacterium isolated from the Atacama Desert. *Extremophiles,* 18**,** 61.

BAATI, H., JARBOUI, R., GHARSALLAH, N., SGHIR, A. & AMMAR, E. 2011. Molecular community analysis of magnesium-rich bittern brine recovered from a Tunisian solar saltern. *Canadian journal of microbiology,* 57**,** 975.

BAKER, G., SMITH, J. J. & COWAN, D. A. 2003. Review and re-analysis of domain-specific 16S primers. *Journal of microbiological methods,* 55**,** 541.

BAKERMANS, C. 2017a. Determining the Limits of Microbial Life at Subzero Temperatures. *Psychrophiles: From Biodiversity to Biotechnology.* Springer.

BAKERMANS, C. 2017b. Limits for microbial life at subzero temperatures. *Psychrophiles: From Biodiversity to Biotechnology.* Springer.

BALL, P. & HALLSWORTH, J. E. 2015. Water structure and chaotropicity: their uses, abuses and biological implications. *Physical Chemistry Chemical Physics,* 17**,** 8297.

BALME, M., GRINDROD, P., SEFTON-NASH, E., DAVIS, J., GUPTA, S. & FAWDON, P. Aram Dorsum, Candidate ExoMars Rover Landing Site: a Noachian Inverted Fluvial Channel System in Arabia Terra Mars. EGU General Assembly Conference Abstracts, 2016. 14030.

BANCIU, H. L. & MUNTYAN, M. S. 2015. Adaptive strategies in the double-extremophilic prokaryotes inhabiting soda lakes. *Current opinion in microbiology,* 25**,** 73.

BARBIERI, R. & STIVALETTA, N. 2011. Continental evaporites and the search for evidence of life on Mars. *Geological Journal,* 46**,** 513.

BARNS, S. M., DELWICHE, C. F., PALMER, J. D. & PACE, N. R. 1996. Perspectives on archaeal diversity, thermophily and monophyly from environmental rRNA sequences. *Proceedings of the National Academy of Sciences,* 93**,** 9188.

BAUERMEISTER, A., RETTBERG, P. & FLEMMING, H.-C. 2014. Growth of the acidophilic iron–sulfur bacterium Acidithiobacillus ferrooxidans under Mars-like geochemical conditions. *Planetary and Space Science,* 98**,** 205.

BEBLO-VRANESEVIC, K., BOHMEIER, M., PERRAS, A. K., SCHWENDNER, P., RABBOW, E., MOISSL-EICHINGER, C., COCKELL, C. S., PUKALL, R., VANNIER, P. & MARTEINSSON, V. T. 2017. The responses of an anaerobic microorganism, Yersinia intermedia MASE-LG-1 to individual and combined simulated Martian stresses. *PloS one,* 12**,** e0185178.

BEBLO-VRANESEVIC, K., BOHMEIER, M., PERRAS, A. K., SCHWENDNER, P., RABBOW, E., MOISSL-EICHINGER, C., COCKELL, C. S., VANNIER, P., MARTEINSSON, V. T. & MONAGHAN, E. P. 2018. Lack of correlation of desiccation and radiation tolerance in microorganisms from diverse extreme environments tested under anoxic conditions. *FEMS microbiology letters,* 365**,** fny044.

BECKETT, B. S. 1986. 2.7 Osmosis and diffusion in cells. *Biology: A Modern Introduction.* Oxford University Press.

BEKKER, A. 2014. Great oxygenation event. *Encyclopedia of Astrobiology, eds R. Amils, M. Gargaud, J. Cernicharo Quintanilla, JH Cleaves, MW Irvine, D. Pinti, et al.*: Springer.

BELL, E. 2012. Hypersaline environments and halophiles *Life at Extremes: Environments, Organisms, and Strategies for Survival.* CABI.

BELL, T. 2010. Experimental tests of the bacterial distance–decay relationship. *The ISME journal,* 4**,** 1357.

BERDY, B., SPOERING, A. L., LING, L. L. & EPSTEIN, S. S. 2017. In situ cultivation of previously uncultivable microorganisms using the ichip. *Nature protocols,* 12**,** 2232.

BERNAL, J. D. 1951. *The physical basis of life*, Routledge and Paul.

BHARDWAJ, A., SAM, L., MARTÍN-TORRES, F. J., ZORZANO, M.-P. & FONSECA, R. M. 2017. Martian slope streaks as plausible indicators of transient water activity. *Scientific reports,* 7**,** 7074.

BIEMANN, K. 2007. On the ability of the Viking gas chromatograph–mass spectrometer to detect organic matter. *Proceedings of the National Academy of Sciences,* 104**,** 10310.

BIEMANN, K. & BADA, J. L. 2011. Comment on "Reanalysis of the Viking results suggests perchlorate and organics at midlatitudes on Mars" by Rafael Navarro-González et al. *Journal of Geophysical Research: Planets,* 116**,** E12001.

BISHOP, C., ANET, E. & GORHAM, P. 1959. Isolation and identification of the fast-death factor in Microcystis aeruginosa NRC-1. *Canadian Journal of Biochemistry and Physiology,* 37**,** 453.

BLANKENSHIP, R. E. 1992. Origin and early evolution of photosynthesis. *Photosynthesis research,* 33**,** 91.

BLAUSTEIN, R. 2016. The Great Oxidation Event: Evolving understandings of how oxygenic life on Earth began. *BioScience,* 66**,** 189.

BONETE, M. J., MARTÍNEZ-ESPINOSA, R. M., PIRE, C., ZAFRILLA, B. & RICHARDSON, D. J. 2008. Nitrogen metabolism in haloarchaea. *Saline Systems,* 4**,** 9.

BOST, N., WESTALL, F., RAMBOZ, C. & VISO, M. Early Archaean Shallow Water Sediments as Analogues for Noachian Sediments on Mars. First International Conference on Mars Sedimentology and Stratigraphy, 2010. 9.

BOSTOCK, J. 1855. The Natural History. Pliny the Elder, with Copious Notes and Illustrations. Taylor and Francis, Red Lion Court, Fleet Street.

BOTTRELL, S. H., LEOSSON, M. A. & NEWTON, R. 1996. *Origin of brine inflows at Boulby potash mine, Cleveland, England*.

BOULEY, S., BARATOUX, D., PAULIEN, N., MISSENARD, Y. & SAINT-BÉZAR, B. 2018. The revised tectonic history of Tharsis. *Earth and Planetary Science Letters,* 488**,** 126.

BOULOS, L., PREVOST, M., BARBEAU, B., COALLIER, J. & DESJARDINS, R. 1999. LIVE/DEAD® BacLight™: application of a new rapid staining method for direct enumeration of viable and total bacteria in drinking water. *Journal of microbiological Methods,* 37**,** 77.

BOWEN, B. B. & BENISON, K. C. 2009. Geochemical characteristics of naturally acid and alkaline saline lakes in southern Western Australia. *Applied Geochemistry,* 24**,** 268.

BRACK, A. 2002. Water, the spring of life. *Astrobiology. The Quest for the Conditions of Life***,** 79.

BROWN, A. J., CALVIN, W. M., BECERRA, P. & BYRNE, S. 2015. Quantification of summertime water ice deposition on the Martian north polar ice cap. *arXiv preprint arXiv:1501.02040*.

BROWN, H. J. & GIBBONS, N. E. 1955. The effect of magnesium, potassium, and iron on the growth and morphology of red halophilic bacteria. *Can J Microbiol,* 1**,** 486.

BROWN, J., BOLLENGIER, O. & VANCE, S. Experimental Thermodynamics of [Na-Mg-Cl-SO4] Aqueous Solutions at GPa Pressure With Application to Icy Worlds. AGU Fall Meeting Abstracts, 2017. MR31B.

BROŽ, P., HAUBER, E., PLATZ, T. & BALME, M. 2015. Evidence for Amazonian highly viscous lavas in the southern highlands on Mars. *Earth and Planetary Science Letters,* 415**,** 200.

BULAT, S. A. 2016. Microbiology of the subglacial Lake Vostok: first results of borehole-frozen lake water analysis and prospects for searching for lake inhabitants. *Phil. Trans. R. Soc. A,* 374**,** 20140292.

BUNACIU, A. A., UDRIŞTIOIU, E. G. & ABOUL-ENEIN, H. Y. 2015. X-Ray Diffraction: Instrumentation and Applications. *Critical Reviews in Analytical Chemistry,* 45**,** 289.

BURBINE, T. H., MCCOY, T. J., MEIBOM, A., GLADMAN, B. & KEIL, K. 2002. Meteoritic parent bodies: Their number and identification. *Asteroids,* III**,** 653.

CALLAHAN, B. 2016. The RDP and GreenGenes taxonomic training sets formatted for DADA2. Zenodo.

CANOVAS, D., VARGAS, C., CSONKA, L. N., VENTOSA, A. & NIETO, J. J. 1996. Osmoprotectants in Halomonas elongata: high-affinity betaine transport system and choline-betaine pathway. *Journal of bacteriology,* 178**,** 7221.

CAPO, R. C., STEWART, B. W. & CHADWICK, O. A. 1998. Strontium isotopes as tracers of ecosystem processes: theory and methods. *Geoderma,* 82**,** 197.

CAPORASO, J. G., LAUBER, C. L., WALTERS, W. A., BERG-LYONS, D., LOZUPONE, C. A., TURNBAUGH, P. J., FIERER, N. & KNIGHT, R. 2011. Global patterns of 16S rRNA diversity at a depth of millions of sequences per sample. *Proceedings of the National Academy of Sciences of the United States of America,* 108**,** 4516.

CARON, G. N. V. 1998. Assessment of bacterial viability status by flow cytometry and single cell sorting. *Journal of applied microbiology,* 84**,** 988.

CARR, M. H. & BELL, J. F. 2014. Mars: surface and interior. *Encyclopedia of the Solar System (Third Edition).* Elsevier.

CARR, M. H. & HEAD III, J. W. 2010. Geologic history of Mars. *Earth and Planetary Science Letters,* 294**,** 185.

CARR, M. H. & HEAD, J. W. 2010a. Acquisition and history of water on Mars. *Lakes on Mars. Elsevier***,** 31.

CARR, M. H. & HEAD, J. W. 2010b. Geologic history of Mars. *Earth and Planetary Science Letters,* 294**,** 185.

CARTER, N. L. & HANSEN, F. D. 1983. Creep of rocksalt. *Tectonophysics,* 92**,** 275.

CASAMAYOR, E. O., MASSANA, R., BENLLOCH, S., ØVREÅS, L., DÍEZ, B., GODDARD, V. J., GASOL, J. M., JOINT, I., RODRÍGUEZ-VALERA, F. & PEDRÓS-ALIÓ, C. 2002. Changes in archaeal, bacterial and eukaryal assemblages along a salinity gradient by comparison of genetic fingerprinting methods in a multipond solar saltern. *Environmental Microbiology,* 4**,** 338.

CASSANELLI, J. P., HEAD, J. W. & FASTOOK, J. L. 2015. Sources of water for the outflow channels on Mars: Implications of the Late Noachian “icy highlands” model for

melting and groundwater recharge on the Tharsis rise. *Planetary and Space Science,* 108**,** 54.

CASTRO-FERNANDEZ, V., ZAMORA, R., HERRERA-MORANDE, A., VALLEJOS, G., GONZALEZ-ORDENES, F. & GUIXÉ, V. 2017. Evolution, Metabolism and Molecular Mechanisms Underlying Extreme Adaptation of Euryarchaeota and Its Biotechnological Potential. *Archaea-New Biocatalysts, Novel Pharmaceuticals and Various Biotechnological Applications.* InTech.

CATLING, D., CLAIRE, M., ZAHNLE, K., QUINN, R., CLARK, B., HECHT, M. & KOUNAVES, S. 2010. Atmospheric origins of perchlorate on Mars and in the Atacama. *Journal of Geophysical Research: Planets,* 115**,** E00E11.

CATLING, D. C. 2014. Mars atmosphere: History and surface interactions. *Encyclopedia of the Solar System (Third Edition).* Elsevier.

CAVALAZZI, B. & BARBIERI, R. 2016. Emergence and Evolution of Early Life in the Geological Environment. *The Cnidaria, Past, Present and Future.* Springer.

CAVICCHIOLI, R. 2011. Archaea—timeline of the third domain. *Nature Reviews Microbiology,* 9**,** 51.

CHAKRADHAR, T., REDDY, C. M., KANYGIN, A., REDDING, K. & CHANDRASEKHAR, T. 2017. Salt tolerant genes from halophytes are potential key players of salt tolerance in glycophytes. *Environmental and Experimental Botany,* 124**,** 39.

CHATTERJEE, S. 2016. A symbiotic view of the origin of life at hydrothermal impact crater-lakes. *Physical Chemistry Chemical Physics,* 18**,** 20033.

CHEN, Y., LI, H., LI, Q., CHEN, W. & CUI, X. 2007. Phylogenetic diversity of culturable bacteria in the ancient salt deposits of the Yipinglang Salt Mine, PR China]. *Wei sheng wu xue bao= Acta microbiologica Sinica,* 47**,** 571.

CHENG, B., MENG, Y., CUI, Y., LI, C., TAO, F., YIN, H., YANG, C. & XU, P. 2016a. Alkaline response of a halotolerant alkaliphilic halomonas strain and functional diversity of its Na+ (K+)/H+ antiporters. *Journal of Biological Chemistry***,** jbc. M116. 751016.

CHENG, Y.-R., SUN, Z.-J., CUI, G.-Z., SONG, X. & CUI, Q. 2016b. A new strategy for strain improvement of Aurantiochytrium sp. based on heavy-ions mutagenesis and synergistic effects of cold stress and inhibitors of enoyl-ACP reductase. *Enzyme and microbial technology,* 93**,** 182.

CHEROUTRE-VIALETTE, M., LEBERT, I., HEBRAUD, M., LABADIE, J. & LEBERT, A. 1998. Effects of pH or aw stress on growth of Listeria monocytogenes. *International journal of food microbiology,* 42**,** 71.

CHIRIFE, J. & RESNIK, S. L. 1984. Unsaturated solutions of sodium chloride as reference sources of water activity at various temperatures. *Journal of Food Science,* 49**,** 1486.

CHRISTENSEN, P. R. 2006. Water at the poles and in permafrost regions of Mars. *Elements,* 2**,** 151.

CIANCIO, A., PIETERSE, C. M. & MERCADO-BLANCO, J. 2016. Harnessing useful rhizosphere microorganisms for pathogen and pest biocontrol. *Frontiers in microbiology,* 7**,** 1620.

CIARLETTI, V., CLIFFORD, S., PLETTEMEIER, D., LE GALL, A., HERVÉ, Y., DORIZON, S., QUANTIN-NATAF, C., BENEDIX, W.-S., SCHWENZER, S. & PETTINELLI, E. 2017. The WISDOM radar: unveiling the subsurface beneath the ExoMars Rover and identifying the best locations for drilling. *Astrobiology,* 17**,** 565.

ĆIRKOVIĆ, M. M. 2004. Earths: rare in time, not space? *J. Br. Interplan. Soc,* 57**,** 53.

CITRON, R. I. & ZHONG, S. 2012. Constraints on the formation of the Martian crustal dichotomy from remnant crustal magnetism. *Physics of the Earth and Planetary Interiors,* 212**,** 55.

CLARK, B. C. & VAN HART, D. C. 1981. The salts of Mars. *Icarus,* 45**,** 370.

CLARK, D. R., MATHIEU, M., MOUROT, L., DUFOSSÉ, L., UNDERWOOD, G. J., DUMBRELL, A. J. & MCGENITY, T. J. 2017. Biogeography at the limits of life: Do extremophilic microbial communities show biogeographical regionalization? *Global Ecology and Biogeography,* 26**,** 1435.

CLARKE, A., MORRIS, G. J., FONSECA, F., MURRAY, B. J., ACTON, E. & PRICE, H. C. 2013. A Low Temperature Limit for Life on Earth. *PLoS ONE,* 8**,** e66207.

CLARKE, K. R. & WARWICK, R. M. 1994. *Change in Marine Communities: An Approach to Statistical Analysis and Interpretation*, Plymouth marine laboratory, Natural environment research council.

CLEAVER, J. E. & BOYER, H. W. 1972. Solubility and dialysis limits of DNA oligonucleotides. *Biochimica et Biophysica Acta (BBA)-Nucleic Acids and Protein Synthesis,* 262**,** 116.

CLIFFORD, S. & MCCUBBIN, F. 2016. How Well Does the Present Surface Inventory of Water on Mars Constrain the Past? *Abstracts from 47th Lunar and Planetary Science Conference***,** 20160003145

COCKELL, C., SCHWENDNER, P., PERRAS, A., RETTBERG, P., BEBLO-VRANESEVIC, K., BOHMEIER, M., RABBOW, E., MOISSL-EICHINGER, C., WINK, L. & MARTEINSSON, V. 2017. Anaerobic microorganisms in astrobiological analogue environments: from field site to culture collection. *International Journal of Astrobiology,* 17**,** 314.

COCKELL, C. S. 1998. Biological effects of high ultraviolet radiation on early Earth—a theoretical evaluation. *Journal of theoretical biology,* 193**,** 717.

COCKELL, C. S. 2001. 'Astrobiology'and the ethics of new science. *Interdisciplinary Science Reviews,* 26**,** 90.

COCKELL, C. S. 2010. Astrobiology—what can we do on the Moon? *Earth, Moon, and Planets,* 107**,** 3.

COCKELL, C. S. 2014. Trajectories of Martian Habitability. *Astrobiology,* 14**,** 182.

COCKELL, C. S. 20/6/2017 2017. *RE: Personal communication with Charles Cockell, PI of a project investiating the microbial communities inhaiting brine pools within Boulby Mine on 20/6/2017.*

COCKELL, C. S., BALME, M., BRIDGES, J. C., DAVILA, A. & SCHWENZER, S. P. 2012. Uninhabited habitats on Mars. *Icarus,* 217**,** 184.

COCKELL, C. S., BILLER, B., BRYCE, C., COUSINS, C., DIREITO, S., FORGAN, D., FOX-POWELL, M., HARRISON, J., LANDENMARK, H. & NIXON, S. 2018. The UK Centre for Astrobiology: A Virtual Astrobiology Centre. Accomplishments and Lessons Learned, 2011–2016. *Astrobiology,* 18**,** 224.

COCKELL, C. S., BUSH, T., BRYCE, C., DIREITO, S., FOX-POWELL, M., HARRISON, J., LAMMER, H., LANDENMARK, H., MARTIN-TORRES, J. & NICHOLSON, N. 2016. Habitability: a review. *Astrobiology,* 16**,** 89.

COCKELL, C. S., CATLING, D. C., DAVIS, W. L., SNOOK, K., KEPNER, R. L., LEE, P. & MCKAY, C. P. 2000. The ultraviolet environment of Mars: biological implications past, present, and future. *Icarus,* 146**,** 343.

COCKELL, C. S. & STOKES, M. D. 2006. Hypolithic colonization of opaque rocks in the Arctic and Antarctic polar desert. *Arctic, Antarctic, and Alpine Research,* 38**,** 335.

COJOC, R., MERCIU, S., POPESCU, G., DUMITRU, L., KAMEKURA, M. & ENACHE, M. 2009. Extracellular hydrolytic enzymes of halophilic bacteria isolated from a subterranean rock salt crystal. *Rom Biotechnol Lett,* 14**,** 4658.

COLLINS JR, S. 1971. *The Mariner 6 and 7 pictures of Mars*, NASA, Washington, United States.

CONNERNEY, J., ACUNA, M., WASILEWSKI, P., KLETETSCHKA, G., NESS, N., REME, H., LIN, R. & MITCHELL, D. 2001. The global magnetic field of Mars and implications for crustal evolution. *Geophysical Research Letters,* 28**,** 4015.

CÓRDOBA-JABONERO, C., ZORZANO, M.-P., SELSIS, F., PATEL, M. R. & COCKELL, C. S. 2005. Radiative habitable zones in martian polar environments. *Icarus,* 175**,** 360.

CORKREY, R., MCMEEKIN, T. A., BOWMAN, J. P., OLLEY, J., RATKOWSKY, D. & ROSS, T. 2018. The maximum growth rate of life on Earth. *International Journal of Astrobiology,* 17**,** 17.

CRAY, J. A., RUSSELL, J. T., TIMSON, D. J., SINGHAL, R. S. & HALLSWORTH, J. E. 2013. A universal measure of chaotropicity and kosmotropicity. *Environmental Microbiology,* 15**,** 287.

CURTIS-HARPER, E. 2017. *Potential microbial processes in an ancient martian environment, an investigation into bio-signature production and community ecology.* PhD thesis, The Open University.

DA SILVA, A. M. F., BOUKHDOUD, N. & GROS, R. 2016. Distance from the sea as a driving force of microbial communities under water potential stresses in litters of two typical Mediterranean plant species. *Geoderma,* 269**,** 1.

DAI, Z., RONHOLM, J., TIAN, Y., SETHI, B. & CAO, X. 2016. Sterilization techniques for biodegradable scaffolds in tissue engineering applications. *Journal of tissue engineering,* 7**,** 2041731416648810.

DARTNELL, L. R., DESORGHER, L., WARD, J. & COATES, A. 2007. Modelling the surface and subsurface martian radiation environment: implications for astrobiology. *Geophysical research letters,* 34**,** L02207.

DARTNELL, L. R., HUNTER, S. J., LOVELL, K. V., COATES, A. J. & WARD, J. M. 2010. Low-temperature ionizing radiation resistance of Deinococcus radiodurans and Antarctic Dry Valley bacteria. *Astrobiology,* 10**,** 717.

DARTNELL, L. R. & PATEL, M. R. 2014. Degradation of microbial fluorescence biosignatures by solar ultraviolet radiation on Mars. *International Journal of Astrobiology,* 13**,** 112.

DASSARMA, P. & DASSARMA, S. 2008. On the origin of prokaryotic" species": the taxonomy of halophilic Archaea. *Saline Systems,* 4**,** 5.

DASSARMA, S. & DASSARMA, P. 2006. Halophiles. *eLS*.

DASSARMA, S. & DASSARMA, P. 2015. Halophiles and their enzymes: negativity put to good use. *Current opinion in microbiology,* 25**,** 120.

DAVIES, P. C. W. 2003. Does life's rapid appearance imply a Martian origin? *Astrobiology,* 3**,** 673.

DAVILA, A. F., HAWES, I., ASCASO, C. & WIERZCHOS, J. 2013a. Salt deliquescence drives photosynthesis in the hyperarid Atacama Desert. *Environmental microbiology reports,* 5**,** 583.

DAVILA, A. F., HAWES, I., GARCÍA ARAYA, J., GELSINGER, D. R., DIRUGGIERO, J., ASCASO, C., OSANO, A. & WIERZCHOS, J. 2015. In situ metabolism in halite endolithic microbial communities of the hyperarid Atacama Desert. *Frontiers in Microbiology,* 6**,** 1035.

DAVILA, A. F. & SCHULZE-MAKUCH, D. 2016. The Last Possible Outposts for Life on Mars. *Astrobiology,* 16**,** 159.

DAVILA, A. F., WILLSON, D., COATES, J. D. & MCKAY, C. P. 2013b. Perchlorate on Mars: a chemical hazard and a resource for humans. *International Journal of Astrobiology,* 12**,** 321.

DAVIS, J., BALME, M., GRINDROD, P., WILLIAMS, R. & GUPTA, S. 2016. Extensive Noachian fluvial systems in Arabia Terra: Implications for early Martian climate. *Geology,* 44**,** 847.

DAY, M., ANDERSON, W., KOCUREK, G. & MOHRIG, D. 2016. Carving intracrater layered deposits with wind on Mars. *Geophysical Research Letters,* 43**,** 2473.

DE BRUYN, J. C., BOOGERD, F. C., BOS, P. & KUENEN, J. G. 1990. Floating filters, a novel technique for isolation and enumeration of fastidious, acidophilic, iron-oxidizing, autotrophic bacteria. *Applied and environmental microbiology,* 56**,** 2891.

DE LANGE, L. & WIJTTEN, P. MICROBIAL PROFILES IN THE GASTRO-INTESTINAL TRACT OF BROILERS AND ITS RELATION TO FEED EFFICIENCY. 21 st ANNUAL AUSTRALIAN POULTRY SCIENCE SYMPOSIUM, 2010. 191.

DE VERA, J.-P., DULAI, S., KERESZTURI, A., KONCZ, L., LOREK, A., MOHLMANN, D., MARSCHALL, M. & POCS, T. 2014. Results on the survival of cryptobiotic cyanobacteria samples after exposure to Mars-like environmental conditions. *International Journal of Astrobiology,* 13**,** 35.

DEER, W. A., HOWIE, R. A. & ZUSSMAN, J. 1992. PART 5 NON-SILICATES. *An introduction to the rock-forming minerals.* Longman Scientific & Technical.

DEHANT, V., LAMMER, H., KULIKOV, Y. N., GRIEßMEIER, J.-M., BREUER, D., VERHOEVEN, O., KARATEKIN, Ö., VAN HOOLST, T., KORABLEV, O. & LOGNONNÉ, P. 2007. Planetary magnetic dynamo effect on atmospheric protection of early Earth and Mars. *Space Science Reviews,* 129**,** 279.

DEOLE, R., CHALLACOMBE, J., RAIFORD, D. W. & HOFF, W. D. 2013. An Extremely Halophilic Proteobacterium Combines a Highly Acidic Proteome with a Low Cytoplasmic Potassium Content. *The Journal of Biological Chemistry,* 288**,** 581.

DES MARAIS, D. J., NUTH III, J. A., ALLAMANDOLA, L. J., BOSS, A. P., FARMER, J. D., HOEHLER, T. M., JAKOSKY, B. M., MEADOWS, V. S., POHORILLE, A. & RUNNEGAR, B. 2008. The NASA astrobiology roadmap. *Astrobiology,* 8**,** 715.

DIREITO, S. O., MAREES, A. & ROLING, W. F. 2012. Sensitive life detection strategies for low-biomass environments: optimizing extraction of nucleic acids adsorbing to terrestrial and Mars analogue minerals. *FEMS Microbiol Ecol,* 81**,** 111.

DODD, M. S., PAPINEAU, D., GRENNE, T., SLACK, J. F., RITTNER, M., PIRAJNO, F., O'NEIL, J. & LITTLE, C. T. 2017. Evidence for early life in Earth's oldest hydrothermal vent precipitates. *Nature,* 543**,** 60.

DOHRMANN, A. B. & TEBBE, C. C. 2006. Genetic profiling of bacterial communities from the rhizospheres of ozone damaged Malva sylvestris (Malvaceae). *European journal of soil biology,* 42**,** 191.

DOMINY, B. N., PERL, D., SCHMID, F. X. & BROOKS III, C. L. 2002. The effects of ionic strength on protein stability: the cold shock protein family. *Journal of molecular biology,* 319**,** 541.

DONG, X., MILHOLLAND, B. & VIJG, J. 2016. Evidence for a limit to human lifespan. *Nature,* 538**,** 257.

DUETZ, W. A., RÜEDI, L., HERMANN, R., O'CONNOR, K., BÜCHS, J. & WITHOLT, B. 2000. Methods for intense aeration, growth, storage, and replication of bacterial strains in microtiter plates. *Applied and environmental microbiology,* 66**,** 2641.

DUMMER, A. M., BONSALL, J. C., CIHLA, J. B., LAWRY, S. M., JOHNSON, G. C. & PECK, R. F. 2011. Bacterioopsin-mediated regulation of bacterioruberin biosynthesis in Halobacterium salinarum. *Journal of bacteriology,* 193**,** 5658.

DUNDAS, C. M., MCEWEN, A. S., CHOJNACKI, M., MILAZZO, M. P., BYRNE, S., MCELWAINE, J. N. & URSO, A. 2017. Granular flows at recurring slope lineae on Mars indicate a limited role for liquid water. *Nature Geoscience,* 10**,** 903.

DYALL-SMITH, M. 2009. The halohandbook. *Protocols for haloarchaeal genetics. Edited by: Dyall-Smith M. University of Melbourne,* 3010.

DZIECIOL, A. J. & MANN, S. 2012. Designs for life: protocell models in the laboratory. *Chemical Society reviews,* 41**,** 79.

ECKSTRAND, O. R., SINCLAIR, W. & THORPE, R. 1995. *Geology of Canadian mineral deposit types*, Geological Survey of Canada.

EDWARDS, C. D., BARELA, P. R., GLADDEN, R. E., LEE, C. H. & DE PAULA, R. Replenishing the Mars relay network. Aerospace Conference, 2014 IEEE, 2014. IEEE, 1.

EDWARDS, T. 27/10/2015 2015. *RE: Personal communication with Thomas Edwards, Senior Exploration Geologist of Boulby Mine on 27/10/2015.*

EHLMANN, B. L. & EDWARDS, C. S. 2014. Mineralogy of the Martian surface. *Annual Review of Earth and Planetary Sciences,* 42**,** 291.

EIGENBRODE, J. L., SUMMONS, R. E., STEELE, A., FREISSINET, C., MILLAN, M., NAVARRO-GONZÁLEZ, R., SUTTER, B., MCADAM, A. C., FRANZ, H. B. & GLAVIN, D. P. 2018. Organic matter preserved in 3-billion-year-old mudstones at Gale crater, Mars. *Science,* 360**,** 1096.

ELCOCK, A. H. & MCCAMMON, J. A. 1998. Electrostatic contributions to the stability of halophilic proteins1. *Journal of molecular biology,* 280**,** 731.

EMERSON, J. B., THOMAS, B. C., ALVAREZ, W. & BANFIELD, J. F. 2016. Metagenomic analysis of a high carbon dioxide subsurface microbial community populated by chemolithoautotrophs and bacteria and archaea from candidate phyla. *Environmental microbiology,* 18**,** 1686.

ENAY, R. 1993. The Start of Life on Earth and the First Fossils. *Palaeontology of Invertebrates.* Springer.

ERTEM, G., ERTEM, M., MCKAY, C. & HAZEN, R. 2017. Shielding biomolecules from effects of radiation by Mars analogue minerals and soils. *International Journal of Astrobiology,* 16**,** 280.

ESCLAPEZ, J., CAMACHO, M., PIRE, C., BAUTISTA, V., VEGARA, A., PEDRO-ROIG, L., PÉREZ-POMARES, F., MARTÍNEZ-ESPINOSA, R. M. & BONETE, M. J. 2016. Recent Advances in the Nitrogen Metabolism in Haloarchaea and Its Biotechnological Applications. *In:* RAMPELOTTO, P. H. (ed.) *Biotechnology of Extremophiles: Advances and Challenges.* Cham: Springer International Publishing.

EVANS, R. B. 2005. Chlorine: state of the art. *Lung,* 183**,** 151.

FASSETT, C. I. & HEAD III, J. W. 2006. Valleys on Hecates Tholus, Mars: Origin by basal melting of summit snowpack. *Planetary and Space Science,* 54**,** 370.

FASTOOK, J. L., HEAD, J. W., MARCHANT, D. R., FORGET, F. & MADELEINE, J.-B. 2012. Early Mars climate near the Noachian–Hesperian boundary: Independent evidence for cold conditions from basal melting of the south polar ice sheet (Dorsa Argentea Formation) and implications for valley network formation. *Icarus,* 219**,** 25.

FAWDON, P., GUPTA, S., DAVIS, J. M., WARNER, N. H., ADLER, J. B., BALME, M. R., BELL III, J. F., GRINDROD, P. M. & SEFTON-NASH, E. 2018. The Hypanis Valles delta: The last highstand of a sea on early Mars? *Earth and Planetary Science Letters,* 500**,** 225.

FEIGL, V., UJACZKI, É., VASZITA, E. & MOLNÁR, M. 2017. Influence of red mud on soil microbial communities: Application and comprehensive evaluation of the Biolog EcoPlate approach as a tool in soil microbiological studies. *Science of the Total Environment,* 595**,** 903.

FENDRIHAN, S., BÉRCES, A., LAMMER, H., MUSSO, M., RONTÓ, G., POLACSEK, T. K., HOLZINGER, A., KOLB, C. & STAN-LOTTER, H. 2009a. Investigating the Effects of Simulated Martian Ultraviolet Radiation on Halococcus dombrowskii and Other Extremely Halophilic Archaebacteria. *Astrobiology,* 9**,** 104.

FENDRIHAN, S., DORNMAYR-PFAFFENHUEMER, M., GERBL, F. W., HOLZINGER, A., GROSBACHER, M., BRIZA, P., ERLER, A., GRUBER, C., PLATZER, K. & STAN-LOTTER, H. 2012. Spherical particles of halophilic archaea correlate with exposure to low water activity--implications for microbial survival in fluid inclusions of ancient halite. *Geobiology,* 10**,** 424.

FENDRIHAN, S., LEGAT, A., PFAFFENHUEMER, M., GRUBER, C., WEIDLER, G., GERBL, F. & STAN-LOTTER, H. 2006. Extremely halophilic archaea and the issue of long-term microbial survival. *Re/views in environmental science and bio/technology (Online),* 5**,** 203.

FENDRIHAN, S., MUSSO, M. & STAN-LOTTER, H. 2009b. Raman spectroscopy as a potentialmethod for the detection of extremely halophilic archaea embedded in halite in terrestrial and possibly extraterrestrial samples. *Journal of Raman spectroscopy : JRS,* 40**,** 1996.

FERGUSON, H. & LUCCHITTA, B. 1984. Dark streaks on talus slopes, Mars. *NASA Tech. Memo., NASA TM-86246*, 188.

FERNÁNDEZ-REMOLAR, D. C., CHONG-DÍAZ, G., RUÍZ-BERMEJO, M., HARIR, M., SCHMITT-KOPPLIN, P., TZIOTIS, D., GÓMEZ-ORTÍZ, D., GARCÍA-VILLADANGOS, M., MARTÍN-REDONDO, M. P., GÓMEZ, F., RODRÍGUEZ-MANFREDI, J. A., MORENO-PAZ, M., DE DIEGO-CASTILLA, G., ECHEVERRÍA, A., URTUVIA, V. N., BLANCO, Y., RIVAS, L., IZAWA, M. R. M., BANERJEE, N. R., DEMERGASSO, C. & PARRO, V. 2013. Molecular preservation in halite- and perchlorate-rich hypersaline subsurface deposits in the Salar Grande basin (Atacama Desert, Chile): Implications for the search for molecular biomarkers on Mars. *Journal of Geophysical Research: Biogeosciences,* 118, 922.

FERNANDEZ-REMOLAR, D. C., SANCHEZ-ROMAN, M., HILL, A. C., GOMEZ-ORTIZ, D., BALLESTEROS, O. P., ROMANEK, C. S. & AMILS, R. 2011. The environment of early Mars and the missing carbonates. *Meteoritics & Planetary Science,* 46, 1447.

FIKSDAHL, A., MORTENSEN, J. T. & LIAAEN-JENSEN, S. 1978. High-pressured liquid chromatography of carotenoids. *Journal of Chromatography A,* 157, 111.

FISCHER, E., MARTÍNEZ, G. M., ELLIOTT, H. M. & RENNÓ, N. O. 2014. Experimental evidence for the formation of liquid saline water on Mars. *Geophysical Research Letters,* 41, 2014GL060302.

FISCHER, W. W., HEMP, J. & VALENTINE, J. S. 2016. How did life survive Earth's great oxygenation? *Current opinion in chemical biology,* 31, 166.

FISH, S. A., SHEPHERD, T. J., MCGENITY, T. J. & GRANT, W. D. 2002. Recovery of 16S ribosomal RNA gene fragments from ancient halite. *Nature,* 417, 432.

FITOUSSI, C., BOURDON, B. & WANG, X. 2016. The building blocks of Earth and Mars: A close genetic link. *Earth and Planetary Science Letters,* 434, 151.

FORTERRE, P., FILÉE, J. & MYLLYKALLIO, H. 2004. Origin and evolution of DNA and DNA replication machineries. *The genetic code and the origin of life.* Springer.

FOSTER, I. S., KING, P. L., HYDE, B. C. & SOUTHAM, G. 2010. Characterization of halophiles in natural MgSO4 salts and laboratory enrichment samples: Astrobiological implications for Mars. *Planetary and Space Science,* 58, 599.

FOX-POWELL, M. & COCKELL, C. 2018. Building a Geochemical View of Microbial Salt Tolerance: Halophilic Adaptation of Marinococcus in a Natural Magnesium Sulfate Brine. *Frontiers in Microbiology,* 9, 739.

FOX-POWELL, M. G. 2017. *Habitability of aqueous environments on Mars.* PhD Thesis, University of Edinburgh.

FOX-POWELL, M. G., HALLSWORTH, J. E., COUSINS, C. R. & COCKELL, C. S. 2016. Ionic strength is a barrier to the habitability of Mars. *Astrobiology,* 16, 427.

FREDRIKSSON, N. J., HERMANSSON, M. & WILÉN, B.-M. 2014. Impact of T-RFLP data analysis choices on assessments of microbial community structure and dynamics. *BMC bioinformatics,* 15**,** 360.

FRIES, C., STEELE, A. & HYNEK, B. HALITE AS A METHANE SEQUESTRATION HOST: A POSSIBLE EXPLANATION FOR PERIODIC METHANE RELEASE ON MARS, AND A SURFACE-ACCESSIBLE SOURCE OF ANCIENT MARTIAN. Lunar and Planetary Science Conference, 2015. 3017.

FRYDENVANG, J., GASDA, P. J., HUROWITZ, J. A., GROTZINGER, J. P., WIENS, R. C., NEWSOM, H. E., EDGETT, K. S., WATKINS, J., BRIDGES, J. C. & MAURICE, S. 2017. Diagenetic silica enrichment and late-stage groundwater activity in Gale Crater, Mars. *Geophysical Research Letters,* 44**,** 4716.

FULLMER, M. S., SOUCY, S. M., SWITHERS, K. S., MAKKAY, A. M., WHEELER, R., VENTOSA, A., GOGARTEN, J. P. & PAPKE, R. T. 2014. Population and genomic analysis of the genus Halorubrum. *Frontiers in Microbiology,* 5**,** 140.

GANGOLLI, S. & CHEMISTRY, R. S. O. 1999. *The Dictionary of Substances and Their Effects: C*, Royal Society of Chemistry.

GENETOOLS LLC 2001. Morpholino Oligomers Essential Information. http://www.xenbase.org/other/static/methods/antisense-data/GeneToolsInfo9.pdf.

GIBTAN, A., PARK, K., WOO, M., SHIN, J.-K., LEE, D.-W., SOHN, J. H., SONG, M., ROH, S. W., LEE, S.-J. & LEE, H.-S. 2017. Diversity of Extremely Halophilic Archaeal and Bacterial Communities from Commercial Salts. *Frontiers in microbiology,* 8**,** 799.

GLADMAN, B. J., BURNS, J. A., DUNCAN, M., LEE, P. & LEVISON, H. F. 1996. The exchange of impact ejecta between terrestrial planets. *Science,* 271**,** 1387.

GLEESON, D., MCDERMOTT, F. & CLIPSON, N. 2006. Structural diversity of bacterial communities in a heavy metal mineralized granite outcrop. *Environmental microbiology,* 8**,** 383.

GÓMEZ, F., RODRÍGUEZ-MANFREDI, J. A., RODRÍGUEZ, N., FERNÁNDEZ-SAMPEDRO, M., CABALLERO-CASTREJÓN, F. J. & AMILS, R. 2012. Habitability: Where to look for life? Halophilic habitats: Earth analogs to study Mars habitability. *Planetary and Space Science,* 68**,** 48.

GOOSEN, N. & MOOLENAAR, G. F. 2008. Repair of UV damage in bacteria. *DNA repair,* 7**,** 353.

GOSLEE, S. C. & URBAN, D. L. 2007. The ecodist package for dissimilarity-based analysis of ecological data. *Journal of Statistical Software,* 22**,** 1.

GÖTZ, F., LONGNECKER, K., KIDO SOULE, M. C., BECKER, K. W., MCNICHOL, J., KUJAWINSKI, E. B. & SIEVERT, S. M. 2018. Targeted metabolomics reveals proline as a major osmolyte in the chemolithoautotroph Sulfurimonas denitrificans. *MicrobiologyOpen,* 7**,** e00586.

GOUDGE, T. A. & FASSETT, C. I. 2018. Incision of Licus Vallis, Mars from Multiple Lake Overflow Floods. *Journal of Geophysical Research: Planets*.

GOVANTES, F. 2018. Serial Dilution-Based Growth Curves and Growth Curve Synchronization for High-Resolution Time Series of Bacterial Biofilm Growth. *Host-Pathogen Interactions.* Springer.

GRAF, J. E., ZUREK, R. W., EISEN, H. J., JAI, B., JOHNSTON, M. & DEPAULA, R. 2005. The Mars reconnaissance orbiter mission. *Acta Astronautica,* 57**,** 566.

GRAMAIN, A., DÍAZ, G. C., DEMERGASSO, C., LOWENSTEIN, T. K. & MCGENITY, T. J. 2011. Archaeal diversity along a subterranean salt core from the Salar Grande (Chile). *Environmental microbiology,* 13**,** 2105.

GRANT, W. 2004. Life at low water activity. *Philosophical Transactions of the Royal Society of London B: Biological Sciences,* 359**,** 1249.

GRANT, W. D., GEMMELL, R. T. & MCGENITY, T. J. 1998a. Halobacteria: the evidence for longevity. *Extremophiles,* 2**,** 279.

GRANT, W. D., GEMMELL, R. T. & MCGENITY, T. J. 1998b. Halophiles. *In:* HORIKOSHI, K. & GRANT, W. D. (eds.) *Extremophiles: Microbial Life in Extreme Environments.* Wiley.

GRAUR, D. & PUPKO, T. 2001. The Permian bacterium that isn't. *Molecular Biology and Evolution,* 18**,** 1143.

GRIFFIN, D. H. 1996. Chemical Requirements for Growth. *Fungal Physiology.* Wiley.

GRINSPOON, D. H. & BULLOCK, M. A. 2007. Astrobiology and Venus exploration. *Exploring Venus as a Terrestrial Planet***,** 191.

GRONSTAL, A. L. 2013. Extraterrestrial Life in the Microbial Age. *Astrobiology, History, and Society.* Springer.

GROSS, M. 2014. The past and future habitability of planet Mars. *Current Biology,* 24**,** R175.

GROTZINGER, J. 2009. Beyond water on Mars. *Nature Geoscience,* 2**,** 231.

GROTZINGER, J., GUPTA, S., MALIN, M., RUBIN, D., SCHIEBER, J., SIEBACH, K., SUMNER, D., STACK, K., VASAVADA, A. & ARVIDSON, R. 2015. Deposition, exhumation, and paleoclimate of an ancient lake deposit, Gale crater, Mars. *Science,* 350**,** aac7575.

GROTZINGER, J. P., SUMNER, D., KAH, L., STACK, K., GUPTA, S., EDGAR, L., RUBIN, D., LEWIS, K., SCHIEBER, J. & MANGOLD, N. 2014. A habitable fluvio-lacustrine environment at Yellowknife Bay, Gale Crater, Mars. *Science,* 343**,** 1242777.

GRUBER, C., LEGAT, A., PFAFFENHUEMER, M., RADAX, C., WEIDLER, G., BUSSE, H.-J. & STAN-LOTTER, H. 2004. Halobacterium noricense sp. nov., an archaeal isolate from a bore core of an alpine Permian salt deposit, classification of

Halobacterium sp. NRC-1 as a strain of H. salinarum and emended description of H. salinarum. *Extremophiles,* 8**,** 431.

GRYTA, A., FRĄC, M. & OSZUST, K. 2014. The application of the Biolog EcoPlate approach in ecotoxicological evaluation of dairy sewage sludge. *Applied biochemistry and biotechnology,* 174**,** 1434.

GUNDE-CIMERMAN, N., PLEMENITAŠ, A. & OREN, A. 2018. Strategies of adaptation of microorganisms of the three domains of life to high salt concentrations. *FEMS Microbiology Reviews,* 42**,** 353.

GUPTA, R. S., NAUSHAD, S. & BAKER, S. 2015. Phylogenomic analyses and molecular signatures for the class Halobacteria and its two major clades: a proposal for division of the class Halobacteria into an emended order Halobacteriales and two new orders, Haloferacales ord. nov. and Natrialbales ord. nov., containing the novel families Haloferacaceae fam. nov. and Natrialbaceae fam. nov. *International journal of systematic and evolutionary microbiology,* 65**,** 1050.

HABERLE, R. M., CLANCY, R. T., FORGET, F., SMITH, M. D. & ZUREK, R. W. 2017. Thermal Structure and Composition. *The Atmosphere and Climate of Mars.* Cambridge University Press.

HABTOM, H., DEMANÈCHE, S., DAWSON, L., AZULAY, C., MATAN, O., ROBE, P., GAFNY, R., SIMONET, P., JURKEVITCH, E. & PASTERNAK, Z. 2017. Soil characterisation by bacterial community analysis for forensic applications: A quantitative comparison of environmental technologies. *Forensic Science International: Genetics,* 26**,** 21.

HAGUE, M. T. J. & ROUTMAN, E. J. 2016. Does population size affect genetic diversity? A test with sympatric lizard species. *Heredity,* 116**,** 92.

HALL, T. A. BioEdit: a user-friendly biological sequence alignment editor and analysis program for Windows 95/98/NT. Nucleic acids symposium series, 1999. [London]: Information Retrieval Ltd., c1979-c2000., 95.

HALLSWORTH, J. E., YAKIMOV, M. M., GOLYSHIN, P. N., GILLION, J. L., D'AURIA, G., DE LIMA ALVES, F., LA CONO, V., GENOVESE, M., MCKEW, B. A. & HAYES, S. L. 2007a. Limits of life in MgCl2-containing environments: chaotropicity defines the window. *Environmental microbiology,* 9**,** 801.

HALLSWORTH, J. E., YAKIMOV, M. M., GOLYSHIN, P. N., GILLION, J. L., D'AURIA, G., DE LIMA ALVES, F., LA CONO, V., GENOVESE, M., MCKEW, B. A., HAYES, S. L., HARRIS, G., GIULIANO, L., TIMMIS, K. N. & MCGENITY, T. J. 2007b. Limits of life in MgCl2-containing environments: chaotropicity defines the window. *Environ Microbiol,* 9**,** 801.

HANLEY, J., CHEVRIER, V., DAVIS, B., ALTHEIDE, T. & FRANCIS, A. Reflectance spectra of low-temperature chloride and perchlorate hydrates and their relevance to the martian surface. Lunar and Planetary Science Conference, 2010. 1953.

HANSEN, L. H. 2009. Why is there no liquid water on Mars at present?

HAR, N., BARBU, O., CODREA, V. & PETRESCU, I. 2006. New data on the mineralogy of the salt deposit from Slanic Prahova (Romania). *Studia UBB Geologia,* 51**,** 29.

HAR, N., RUSZ, O., CODREA, V. & BARBU, O. 2010. New data on the mineralogy of the salt deposit from Sovata (Mureş County-Romania). *Carpath J Earth Env,* 5**,** 127.

HARDIE, L. A., LOWENSTEIN, T. K. & SPENCER, R. J. The problem of distinguishing between primary and secondary features in evaporites. Sixth international symposium on salt, 1985. Salt Institute Alexandria, 11.

HARPER-OWEN, R., DYMOCK, D., BOOTH, V., WEIGHTMAN, A. & WADE, W. 1999. Detection of unculturable bacteria in periodontal health and disease by PCR. *Journal of clinical microbiology,* 37**,** 1469.

HART, S. & COLLABORATION, B. D. M. 2002. Status of dark matter searches in the boulby mine. *Nuclear Physics B-Proceedings Supplements,* 110**,** 91.

HARTMANN, W. K. & NEUKUM, G. 2001. Cratering chronology and the evolution of Mars. *Chronology and evolution of Mars.* Springer.

HASSLER, D. M., ZEITLIN, C., WIMMER-SCHWEINGRUBER, R. F., EHRESMANN, B., RAFKIN, S., EIGENBRODE, J. L., BRINZA, D. E., WEIGLE, G., BÖTTCHER, S., BÖHM, E., BURMEISTER, S., GUO, J., KÖHLER, J., MARTIN, C., REITZ, G., CUCINOTTA, F. A., KIM, M.-H., GRINSPOON, D., BULLOCK, M. A., POSNER, A., GÓMEZ-ELVIRA, J., VASAVADA, A., GROTZINGER, J. P. & TEAM, M. S. 2014. Mars' Surface Radiation Environment Measured with the Mars Science Laboratory's Curiosity Rover. *Science,* 343**,** 1244797.

HAUBER, E., BROŽ, P., JAGERT, F., JODŁOWSKI, P. & PLATZ, T. 2011. Very recent and wide-spread basaltic volcanism on Mars. *Geophysical Research Letters,* 38**,** L10201.

HAWTHORNE, F. & FERGUSON, R. 1975. Anhydrous sulphates; II, Refinement of the crystal structure of anhydrite. *The Canadian Mineralogist,* 13**,** 289.

HAYS, L. E., GRAHAM, H. V., DES MARAIS, D. J., HAUSRATH, E. M., HORGAN, B., MCCOLLOM, T. M., PARENTEAU, M. N., POTTER-MCINTYRE, S. L., WILLIAMS, A. J. & LYNCH, K. L. 2017. Biosignature preservation and detection in Mars analog environments. *Astrobiology,* 17**,** 363.

HAZEN, R. M. 2017. Chance, necessity and the origins of life: a physical sciences perspective. *Phil. Trans. R. Soc. A,* 375**,** 20160353.

HE, X., MCLEAN, J. S., EDLUND, A., YOOSEPH, S., HALL, A. P., LIU, S. Y., DORRESTEIN, P. C., ESQUENAZI, E., HUNTER, R. C., CHENG, G., NELSON, K. E., LUX, R. & SHI, W. 2015. Cultivation of a human-associated TM7 phylotype reveals a reduced genome and epibiotic parasitic lifestyle. *Proc Natl Acad Sci U S A,* 112**,** 244.

HEBBLEWHITE, B. K. 1977. Underground potash mine design based on rock mechanics principles and measurements.

HEBSGAARD, M. B., PHILLIPS, M. J. & WILLERSLEV, E. 2005. Geologically ancient DNA: fact or artefact? *Trends in microbiology,* 13**,** 212.

HECHT, M., KOUNAVES, S., QUINN, R., WEST, S., YOUNG, S., MING, D., CATLING, D., CLARK, B., BOYNTON, W. & HOFFMAN, J. 2009. Detection of perchlorate and the soluble chemistry of martian soil at the Phoenix lander site. *Science,* 325**,** 64.

HELBERT, J. 2014. Mercury. *Encyclopedia of Astrobiology***,** 1.

HERREN, C. M., WEBERT, K. C. & MCMAHON, K. D. 2016. Environmental Disturbances Decrease the Variability of Microbial Populations within Periphyton. *mSystems,* 1**,** e00013.

HERSCHEL, W. 1784. XIX. On the remarkable appearances at the polar regions of the planet Mars, and its spheroidical figure; with a few hints relating to its real diameter and atmosphere. *Philosophical Transactions of the Royal Society of London,* 74**,** 233.

HERSCHY, B., WHICHER, A., CAMPRUBI, E., WATSON, C., DARTNELL, L., WARD, J., EVANS, J. R. & LANE, N. 2014. An origin-of-life reactor to simulate alkaline hydrothermal vents. *Journal of molecular evolution,* 79**,** 213.

HOLLINGSWORTH, S., COLBECK, S. & AULD, F. 2013. Design of shaft linings to resist time dependent deformation in evaporite rocks. *Mining Technology,* 122**,** 221.

HORNECK, G., STÖFFLER, D., OTT, S., HORNEMANN, U., COCKELL, C. S., MOELLER, R., MEYER, C., DE VERA, J.-P., FRITZ, J. & SCHADE, S. 2008. Microbial rock inhabitants survive hypervelocity impacts on Mars-like host planets: first phase of lithopanspermia experimentally tested. *Astrobiology,* 8**,** 17.

HOU, J. & CUI, H.-L. 2017. In Vitro Antioxidant, Antihemolytic, and Anticancer Activity of the Carotenoids from Halophilic Archaea. *Current microbiology,* 7**,** 266.

HU, R., BLOOM, A. A., GAO, P., MILLER, C. E. & YUNG, Y. L. 2016. Hypotheses for near-surface exchange of methane on Mars. *Astrobiology,* 16**,** 539.

HU, R., KASS, D. M., EHLMANN, B. L. & YUNG, Y. L. 2015. Tracing the fate of carbon and the atmospheric evolution of Mars. *Nature Communications,* 6**,** 10003.

HUBY, T. J. C. C., DAVE R.; MATHEIU, MÉGANE, MOUROT, LÉONIE, DUFOSSÉ, LAURENT; UNDERWOOD, GRAHAM J. C.; DUMBRELL, ALEX J; MCGENITY, TERRY J. The biogeography and survival of haloarchaea inside halite crystals. Microbiology Society, 2017 Edinburgh.

HUGENHOLTZ, P. & TYSON, G. W. 2008. Microbiology: metagenomics. *Nature,* 455**,** 481.

HULCE, D., LI, X., SNYDER-LEIBY, T. & JOHATHAN LIU, C. S. 2011. GeneMarker® Genotyping Software: Tools to Increase the Statistical Power of DNA Fragment Analysis. *Journal of Biomolecular Techniques : JBT,* 22**,** S35.

HUNT, S. & LAYZELL, D. B. 1993. Gas exchange of legume nodules and the regulation of nitrogenase activity. *Annual review of plant biology,* 44**,** 483.

HUSEN, E. 2016. Screening of soil bacteria for plant growth promotion activities in vitro. *Indonesian Journal of Agricultural Science,* 4**,** 27.

HYNEK, B. M., OSTERLOO, M. K. & KIEREIN-YOUNG, K. S. 2015. Late-stage formation of Martian chloride salts through ponding and evaporation. *Geology,* 43**,** 787.

ICL-UK. 2017. *http://www.icl-uk.uk/history/* [Online]. [Accessed 22/12/2017.

INAGAKI, F., HINRICHS, K.-U., KUBO, Y., BOWLES, M. W., HEUER, V. B., HONG, W.-L., HOSHINO, T., IJIRI, A., IMACHI, H. & ITO, M. 2015. Exploring deep microbial life in coal-bearing sediment down to∼ 2.5 km below the ocean floor. *Science,* 349**,** 420.

INSAM, H. 1997. A new set of substrates proposed for community characterization in environmental samples. *Microbial communities: functional versus structural approaches***,** 259.

INSAM, H., FEURLE, J. & RANGGER, A. 2001. Community level physiological profiles (Biolog substrate use tests) of environmental samples. *Molecular Microbial Ecology Manual.* Kluwer Academic Publishers.

INTEGRATED DNA TECHNOLOGIES. 2011. *What is the maximum solubility of DNA in water?* [Online]. Available: http://www.idtdna.com/pages/education/technical-reports/faq-old/application-support/storage/faqs/2011/07/01/what-is-the-maximum-solubility-of-dna-in-water-(weight-unit-volume-unit)- [Accessed 8/12/16 2016].

IRWIN, R. P., WRAY, J. J., MEST, S. C. & MAXWELL, T. A. 2018. Wind-Eroded Crater Floors and Intercrater Plains, Terra Sabaea, Mars. *Journal of Geophysical Research: Planets,* 123**,** 445.

IVARSSON, M. & LINDGREN, P. 2010. The search for sustainable subsurface habitats on Mars, and the sampling of impact ejecta. *Sustainability,* 2**,** 1969.

IZIDORO, A., HAGHIGHIPOUR, N., WINTER, O. & TSUCHIDA, M. 2014. Terrestrial planet formation in a protoplanetary disk with a local mass depletion: A successful scenario for the formation of Mars. *The Astrophysical Journal,* 782**,** 31.

JAAKKOLA, S. T., PFEIFFER, F., RAVANTTI, J. J., GUO, Q., LIU, Y., CHEN, X., MA, H., YANG, C., OKSANEN, H. M. & BAMFORD, D. H. 2016a. The complete genome of a viable archaeum isolated from 123-million-year-old rock salt. *Environmental microbiology,* 18**,** 565.

JAAKKOLA, S. T., RAVANTTI, J. J., OKSANEN, H. M. & BAMFORD, D. H. 2016b. Buried Alive: Microbes from Ancient Halite. *Trends in microbiology,* 24**,** 148.

JAAKKOLA, S. T., ZERULLA, K., GUO, Q., LIU, Y., MA, H., YANG, C., BAMFORD, D. H., CHEN, X., SOPPA, J. & OKSANEN, H. M. 2014. Halophilic archaea cultivated from surface sterilized middle-late Eocene rock salt are polyploid. *PloS one,* 9**,** e110533.

JAGESSAR, R., MARS, A. & GOMES, G. 2008. Selective Antimicrobial properties of Phyllanthus acidus leaf extract against Candida albicans, Escherichia coli and Staphylococcus aureus using Stokes Disc diffusion, Well diffusion, Streak plate and a dilution method. *Nature and Science,* 6**,** 24.

JAKOSKY, B. M. & PHILLIPS, R. J. 2001. Mars' volatile and climate history. *nature,* 412**,** 237.

JAVOR, B. J. 2012. *Hypersaline environments: microbiology and biogeochemistry*, Springer Science & Business Media.

JENKINS, D. E., AUGER, E. A. & MATIN, A. 1991. Role of RpoH, a heat shock regulator protein, in Escherichia coli carbon starvation protein synthesis and survival. *Journal of bacteriology,* 173**,** 1992.

JENSEN, P. A., DOUGHERTY, B. V., MOUTINHO JR, T. J. & PAPIN, J. A. 2015. Miniaturized plate readers for low-cost, high-throughput phenotypic screening. *Journal of laboratory automation,* 20**,** 51.

JOHNSON, M., ZARETSKAYA, I., RAYTSELIS, Y., MEREZHUK, Y., MCGINNIS, S. & MADDEN, T. L. 2008. NCBI BLAST: a better web interface. *Nucleic acids research,* 36**,** W5.

JONES, B. W. 2008. Mars before the space age. *International Journal of Astrobiology,* 7**,** 143.

JONES, E. G. 2018. Shallow transient liquid water environments on present-day mars, and their implications for life. *Acta Astronautica,* 146**,** 144.

JONES, S. E. & LENNON, J. T. 2010. Dormancy contributes to the maintenance of microbial diversity. *Proceedings of the National Academy of Sciences,* 107**,** 5881.

JORDAN, T., SCOTT, C. & LOHMAN, R. InSAR coherence study of unusual rain events in the Atacama Desert. AGU Fall Meeting Abstracts, 2017.

JOSSET, J.-L., WESTALL, F., HOFMANN, B. A., SPRAY, J., COCKELL, C., KEMPE, S., GRIFFITHS, A. D., DE SANCTIS, M. C., COLANGELI, L. & KOSCHNY, D. 2017. The Close-Up Imager onboard the ESA ExoMars Rover: objectives, description, operations, and science validation activities. *Astrobiology,* 17**,** 595.

JOURDAN, F. & EROGLU, E. 2017. 40Ar/39Ar and (U-Th)/He model age signatures of elusive Mercurian and Venusian meteorites. *Meteoritics & Planetary Science,* 52**,** 884.

JUDSON, O. P. 2017. The energy expansions of evolution. *Nature ecology & evolution,* 1**,** 0138.

KAGEYAMA, H., WADITEE-SIRISATTHA, R., TANAKA, Y. & TAKABE, T. 2017. Osmoprotectant and Sunscreen Molecules From Halophilic Algae and Cyanobacteria. *Algal Green Chemistry.* Elsevier.

KAKAR, S., MAHDI, F., LI, X. & GARLID, K. 1989. Reconstitution of the mitochondrial non-selective Na+/H+ (K+/H+) antiporter into proteoliposomes. *Journal of Biological Chemistry,* 264**,** 5846.

KÄMPFER, P., BUCZOLITS, S., ALBRECHT, A., BUSSE, H.-J. & STACKEBRANDT, E. 2003. Towards a standardized format for the description of a novel species (of an established genus): Ochrobactrum gallinifaecis sp. nov. *International journal of systematic and evolutionary microbiology,* 53**,** 893.

KATO, M. 2016. Effect of ionizing radiation on the motility of Escherichia coli. *Microbes in the Spotlight: Recent Progress in the Understanding of Beneficial and Harmful Microorganisms***,** 478.

KAUFFMAN, S. 2007. Question 1: origin of life and the living state. *Origins of Life and Evolution of Biospheres,* 37**,** 315.

KAURI, T., WALLACE, R. & KUSHNER, D. J. 1990. Nutrition of the halophilic archaebacterium, Haloferax volcanii. *Systematic and Applied Microbiology,* 13**,** 14.

KEMPF, B. & BREMER, E. 1998. Stress responses ofBacillus subtilis to high osmolarity environments: Uptake and synthesis of osmoprotectants. *Journal of biosciences,* 23**,** 447.

KENNEDY, S. P., NG, W. V., SALZBERG, S. L., HOOD, L. & DASSARMA, S. 2001. Understanding the adaptation of Halobacterium species NRC-1 to its extreme environment through computational analysis of its genome sequence. *Genome research,* 11**,** 1641.

KERR, R. A. 2013. Pesky Perchlorates All Over Mars. *Science,* 340**,** 138.

KIBBE, W. A. 2007. OligoCalc: an online oligonucleotide properties calculator. *Nucleic acids research,* 35**,** W43.

KINDZIERSKI, V., RASCHKE, S., KNABE, N., SIEDLER, F., SCHEFFER, B., PFLÜGER-GRAU, K., PFEIFFER, F., OESTERHELT, D., MARIN-SANGUINO, A. & KUNTE, H.-J. 2017. Osmoregulation in the halophilic bacterium Halomonas elongata: A case study for integrative systems biology. *PloS one,* 12**,** e0168818.

KIXMÜLLER, D. & GREIE, J. C. 2012. An ATP-driven potassium pump promotes long-term survival of Halobacterium salinarum within salt crystals. *Environmental microbiology reports,* 4**,** 234.

KLIEMT, J. & SOPPA, J. 2017. Diverse Functions of Small RNAs (sRNAs) in Halophilic Archaea: From Non-coding Regulatory sRNAs to Microprotein-Encoding sRNAs. *RNA Metabolism and Gene Expression in Archaea.* Springer.

KLING, A. M., HABERLE, R. M., MCKAY, C. P., BRISTOW, T. F. & RIVERA-HERNANDEZ, F. 2017. The Ice-Covered Lakes Hypothesis in Gale Crater: Implications for the Early Hesperian Climate. *6th International Workshop on the Mars Atmosphere: Modeling and Observations; 17-20 Jan. 2017; Granada; Spain*

KMINEK, G., BADA, J. L., POGLIANO, K. & WARD, J. F. 2003. Radiation-dependent limit for the viability of bacterial spores in halite fluid inclusions and on Mars. *Radiation research,* 159**,** 722.

KNOLL, A. H. & GROTZINGER, J. 2006. Water on Mars and the prospect of martian life. *Elements,* 2**,** 169.

KONG, C. H., HAMID, N., MA, Q., LU, J., WANG, B.-G. & SAROJINI, V. 2017. Antifreeze peptide pretreatment minimizes freeze-thaw damage to cherries: An in-depth investigation. *LWT-Food Science and Technology,* 84**,** 441.

KORABLEV, O., MONTMESSIN, F., TROKHIMOVSKIY, A., FEDOROVA, A., SHAKUN, A., GRIGORIEV, A., MOSHKIN, B., IGNATIEV, N., FORGET, F. & LEFÈVRE, F. 2018. The atmospheric chemistry suite (ACS) of three spectrometers for the ExoMars 2016 Trace Gas Orbiter. *Space Science Reviews,* 214**,** 7.

KOTTEMANN, M., KISH, A., ILOANUSI, C., BJORK, S. & DIRUGGIERO, J. 2005. Physiological responses of the halophilic archaeon Halobacterium sp. strain NRC1 to desiccation and gamma irradiation. *Extremophiles,* 9**,** 219.

KOUNAVES, S. P., HECHT, M. H., KAPIT, J., QUINN, R. C., CATLING, D. C., CLARK, B. C., MING, D. W., GOSPODINOVA, K., HREDZAK, P. & MCELHONEY, K. 2010. Soluble sulfate in the martian soil at the Phoenix landing site. *Geophysical Research Letters,* 37**,** L09201.

KRAMER, E. M. & MYERS, D. R. 2012. Five popular misconceptions about osmosis. *American Journal of Physics,* 80**,** 694.

KRESLAVSKY, M. A. & HEAD, J. W. 2018. Mars Climate History: Insights From Impact Crater Wall Slope Statistics. *Geophysical Research Letters,* 45**,** 1751.

KRESS, A. M. & HEAD, J. W. 2015. Late Noachian and early Hesperian ridge systems in the south circumpolar Dorsa Argentea Formation, Mars: Evidence for two stages of melting of an extensive late Noachian ice sheet. *Planetary and Space Science,* 109**,** 1.

KUANG, W., JIANG, W. & WANG, T. 2008. Sudden termination of Martian dynamo?: Implications from subcritical dynamo simulations. *Geophysical Research Letters,* 35**,** L14204.

KUMAR, S., STECHER, G. & TAMURA, K. 2016. MEGA7: molecular evolutionary genetics analysis version 7.0 for bigger datasets. *Molecular biology and evolution,* 33**,** 1870.

KUPRIYANOVA, E., PRONINA, N. & LOS, D. 2017. Carbonic anhydrase—a universal enzyme of the carbon-based life. *Photosynthetica,* 55**,** 3.

KURT-KıZıLDOĞAN, A., ABANOZ, B. & OKAY, S. 2017. Global transcriptome analysis of Halolamina sp. to decipher the salt tolerance in extremely halophilic archaea. *Gene,* 601**,** 56.

KUTSCHERA, A. & LAMB, J. J. 2018. Cost-Effective Live Cell Density Determination of Liquid Cultured Microorganisms. *Current microbiology,* 75**,** 231.

LABUZA, T. P. 1980. The effect of water activity on reaction kinetics of food deterioration. *Food Technol,* 34**,** 36.

LANE, N. 2017. Proton gradients at the origin of life. *Bioessays,* 39**,** 1600217

LANE, N., ALLEN, J. F. & MARTIN, W. 2010. How did LUCA make a living? Chemiosmosis in the origin of life. *BioEssays,* 32**,** 271.

LAPOTRE, M. G., LAMB, M. P. & WILLIAMS, R. M. 2016. Canyon formation constraints on the discharge of catastrophic outburst floods of Earth and Mars. *Journal of Geophysical Research: Planets,* 121**,** 1232.

LAYE, V. J. & DASSARMA, S. 2018. An Antarctic Extreme Halophile and Its Polyextremophilic Enzyme: Effects of Perchlorate Salts. *Astrobiology,* 18**,** 412.

LEBRE, P. H., DE MAAYER, P. & COWAN, D. A. 2017. Xerotolerant bacteria: surviving through a dry spell. *Nature Reviews Microbiology,* 15**,** 285.

LEIGHTON, R. B., MURRAY, B. C., SHARP, R. P., ALLEN, J. D. & SLOAN, R. K. 1965. Mariner IV photography of Mars: Initial results. *Science,* 149**,** 627.

LEONG, S. L. L., LANTZ, H., PETTERSSON, O. V., FRISVAD, J. C., THRANE, U., HEIPIEPER, H. J., DIJKSTERHUIS, J., GRABHERR, M., PETTERSSON, M. & TELLGREN-ROTH, C. 2015. Genome and physiology of the ascomycete filamentous fungus X eromyces bisporus, the most xerophilic organism isolated to date. *Environmental microbiology,* 17**,** 496.

LEUKO, S. 18/8/16 2016. *RE: Agar recommended by Dr Stefan Leuko of DLR based on his personal experience of isolating halophiles.*

LEUKO, S., DOMINGOS, C., PARPART, A., REITZ, G. & RETTBERG, P. 2015. The survival and resistance of Halobacterium salinarum NRC-1, Halococcus hamelinensis, and Halococcus morrhuae to simulated outer space solar radiation. *Astrobiology,* 15**,** 987.

LEUKO, S., GOH, F., IBANEZ-PERAL, R., BURNS, B. P., WALTER, M. R. & NEILAN, B. A. 2008. Lysis efficiency of standard DNA extraction methods for Halococcus spp. in an organic rich environment. *Extremophiles,* 12**,** 301.

LEVIN, G. V. & STRAAT, P. A. 1981. A search for a nonbiological explanation of the Viking Labeled Release life detection experiment. *Icarus,* 45**,** 494.

LEVIN, G. V. & STRAAT, P. A. 2016. The case for extant life on Mars and its possible detection by the Viking Labeled Release Experiment. *Astrobiology,* 16**,** 798.

LEWIS, R. A. 2016. *Hawley's condensed chemical dictionary*, John Wiley & Sons.

LIAO, L., XU, X.-W., WANG, C.-S., ZHANG, D.-S. & WU, M. 2009. Bacterial and archaeal communities in the surface sediment from the northern slope of the South China Sea. *Journal of Zhejiang University. Science. B,* 10**,** 890.

LINDEMANN, S. R., MORAN, J. J., STEGEN, J. C., RENSLOW, R. S., HUTCHISON, J. R., COLE, J. K., DOHNALKOVA, A. C., TREMBLAY, J., SINGH, K., MALFATTI, S. A., CHEN, F., TRINGE, S. G., BEYENAL, H. & FREDRICKSON, J. K. 2013. The epsomitic phototrophic microbial mat of Hot Lake, Washington: community structural responses to seasonal cycling. *Frontiers in Microbiology,* 4**,** 323.

LOIZEAU, D., QUANTIN-NATAF, C., CARTER, J., FLAHAUT, J., THOLLOT, P., LOZAC'H, L. & MILLOT, C. 2018. Quantifying widespread aqueous surface weathering on Mars: The plateaus south of Coprates Chasma. *Icarus,* 302**,** 451.

LOPEZ-CORTES, A., OCHOA, J. L. & VAZQUEZ-DUHALT, R. 1994. Participation of halobacteria in crystal formation and the crystallization rate of NaCl. *Geomicrobiology journal,* 12**,** 69.

LOUDON, C.-M. Microbial Growth in the Magnesium-Chloride-Sodium-Sulphate Ion System: Implications for Habitability in Terrestrial and Extraterrestrial Salts. AGU Fall Meeting Abstracts, 2017.

LOWELL, P. 1908. *Mars as the Abode of Life*, The Macmillan Company.

LOWENSTEIN, T. K., SCHUBERT, B. A. & TIMOFEEFF, M. N. 2011. Microbial communities in fluid inclusions and long-term survival in halite. *GSA Today,* 21**,** 4.

MA, Y., GALINSKI, E. A., GRANT, W. D., OREN, A. & VENTOSA, A. 2010. Halophiles 2010: life in saline environments. *Appl Environ Microbiol,* 76**,** 6971.

MADIGAN, M. T., MARTINKO, J. M. & BROCK, T. D. 2006. *Brock Biology of Microorganisms*, Pearson Prentice Hall.

MADIGAN, M. T., MARTINKO, J. M. & PARKER, J. 2000. *Brock Biology of Microorganisms*, Prentice Hall.

MANCINELLI, R. L. 2000. Accessing the Martian deep subsurface to search for life. *Planetary and Space Science,* 48**,** 1035.

MANCINELLI, R. L. 2005. Halophiles: A Terrestrial Analog for Life in Brines on Mars. *In:* GUNDE-CIMERMAN, N., OREN, A. & PLEMENITAŠ, A. (eds.) *Adaptation to Life at High Salt Concentrations in Archaea, Bacteria, and Eukarya.* Springer.

MANCINELLI, R. L., FAHLEN, T. F., LANDHEIM, R. & KLOVSTAD, M. R. 2004. Brines and evaporites: analogs for Martian life. *Advances in Space Research,* 33**,** 1244.

MANCINELLI, R. L., LANDHEIM, R., SANCHEZ-PORRO, C., DORNMAYR-PFAFFENHUEMER, M., GRUBER, C., LEGAT, A., VENTOSA, A., RADAX, C., IHARA, K. & WHITE, M. R. 2009. Halorubrum chaoviator sp. nov., a haloarchaeon isolated from sea salt in Baja California, Mexico, Western Australia and Naxos, Greece. *International journal of systematic and evolutionary microbiology,* 59**,** 1908.

MARGULIS, L., MAZUR, P., BARGHOORN, E. S., HALVORSON, H. O., JUKES, T. H. & KAPLAN, I. R. 1979. The Viking mission: Implications for life on Mars. *Journal of Molecular Evolution,* 14**,** 223.

MARINE, R., MCCARREN, C., VORRASANE, V., NASKO, D., CROWGEY, E., POLSON, S. W. & WOMMACK, K. E. 2014. Caught in the middle with multiple displacement amplification: the myth of pooling for avoiding multiple displacement amplification bias in a metagenome. *Microbiome,* 2**,** 3.

MARRA, W. A., HAUBER, E., DE JONG, S. M. & KLEINHANS, M. G. 2015. Pressurized groundwater systems in Lunae and Ophir Plana (Mars): Insights from small-scale morphology and experiments. *GeoResJ,* 8**,** 1.

MARTÍN-TORRES, F. J., ZORZANO, M.-P., VALENTÍN-SERRANO, P., HARRI, A.-M., GENZER, M., KEMPPINEN, O., RIVERA-VALENTIN, E. G., JUN, I., WRAY, J. & MADSEN, M. B. 2015. Transient liquid water and water activity at Gale crater on Mars. *Nature Geoscience,* 8**,** 357.

MARTÍNEZ, G., NEWMAN, C., DE VICENTE-RETORTILLO, A., FISCHER, E., RENNO, N., RICHARDSON, M., FAIRÉN, A., GENZER, M., GUZEWICH, S. & HABERLE, R. 2017. The modern near-surface Martian climate: A review of in-situ meteorological data from Viking to Curiosity. *Space Science Reviews,* 212**,** 295.

MASSÉ, M., BECK, P., SCHMITT, B., POMMEROL, A., MCEWEN, A., CHEVRIER, V., BRISSAUD, O. & SÉJOURNÉ, A. 2014. Spectroscopy and detectability of liquid brines on Mars. *Planetary and space science,* 92**,** 136.

MASSÉ, M., CONWAY, S., GARGANI, J., PATEL, M., PASQUON, K., MCEWEN, A., CARPY, S., CHEVRIER, V., BALME, M. & OJHA, L. 2016. Transport processes induced by metastable boiling water under Martian surface conditions. *Nature Geoscience,* 9**,** 425.

MASTASCUSA, V., ROMANO, I., DI DONATO, P., POLI, A., DELLA CORTE, V., ROTUNDI, A., BUSSOLETTI, E., QUARTO, M., PUGLIESE, M. & NICOLAUS, B. 2014. Extremophiles Survival to Simulated Space Conditions: An Astrobiology Model Study. *Origins of Life and Evolution of the Biosphere,* 44**,** 231.

MATSUBARA, T., FUJISHIMA, K., SALTIKOV, C. W., NAKAMURA, S. & ROTHSCHILD, L. J. 2017. Earth analogues for past and future life on Mars: isolation of perchlorate resistant halophiles from Big Soda Lake. *International Journal of Astrobiology,* 16**,** 218.

MATTHIÄ, D., EHRESMANN, B., LOHF, H., KÖHLER, J., ZEITLIN, C., APPEL, J., SATO, T., SLABA, T., MARTIN, C. & BERGER, T. 2016. The Martian surface radiation environment–a comparison of models and MSL/RAD measurements. *Journal of Space Weather and Space Climate,* 6**,** A13.

MATTIMORE, V. & BATTISTA, J. R. 1996. Radioresistance of Deinococcus radiodurans: functions necessary to survive ionizing radiation are also necessary to survive prolonged desiccation. *J Bacteriol,* 178**,** 633.

MAZUR, P. 1980. Limits to life at low temperatures and at reduced water contents and water activities. *Limits of Life.* Springer.

MCEWEN, A. S., DUNDAS, C. M., MATTSON, S. S., TOIGO, A. D., OJHA, L., WRAY, J. J., CHOJNACKI, M., BYRNE, S., MURCHIE, S. L. & THOMAS, N. 2013. Recurring slope lineae in equatorial regions of Mars. *Nature Geoscience,* 7**,** 53.

MCEWEN, A. S., OJHA, L., DUNDAS, C. M., MATTSON, S. S., BYRNE, S., WRAY, J. J., CULL, S. C., MURCHIE, S. L., THOMAS, N. & GULICK, V. C. 2011. Seasonal flows on warm Martian slopes. *Science,* 333**,** 740.

MCGENITY, T. J. Halophiles at the limit of existence. Microbiology Society Conference 2017, 4/4/17 2017 Edinburgh.

MCGENITY, T. J., GEMMELL, R. T. & GRANT, W. D. 1998. Proposal of a new halobacterial genus Natrinema gen. nov., with two species Natrinema pellirubrum nom. nov. and Natrinema pallidum nom. nov. *International Journal of Systematic and Evolutionary Microbiology,* 48**,** 1187.

MCGENITY, T. J., GEMMELL, R. T., GRANT, W. D. & STAN-LOTTER, H. 2000. Origins of halophilic microorganisms in ancient salt deposits. *Environmental Microbiology,* 2**,** 243.

MCGENITY, T. J. & OREN, A. 2012. Hypersaline Environments. *In:* BELL, E. (ed.) *Life at Extremes: Environments, Organisms and Strategies for Survival.* CABI.

MCKAY, C. P. 1999. Bringing life to Mars. *Scientific American Presents,* 10**,** 52.

MCKAY, C. P. 2016. Titan as the Abode of Life. *Life,* 6**,** 8.

MCSWEEN JR, H. Y. 1984. SNC meteorites: Are they Martian rocks? *Geology,* 12**,** 3.

MESA, V., GALLEGO, J. L., GONZÁLEZ-GIL, R., LAUGA, B., SÁNCHEZ, J., MÉNDEZ-GARCÍA, C. & PELÁEZ, A. I. 2017. Bacterial, Archaeal, and Eukaryotic Diversity across Distinct Microhabitats in an Acid Mine Drainage. *Frontiers in microbiology,* 8**,** 1756.

MICHALSKI, J. R., CUADROS, J., NILES, P. B., PARNELL, J., ROGERS, A. D. & WRIGHT, S. P. 2013. Groundwater activity on Mars and implications for a deep biosphere. *Nature Geoscience,* 6**,** 133.

MICHALSKI, J. R., JEAN, P., POULET, F., LOIZEAU, D., MANGOLD, N., DOBREA, E. N., BISHOP, J. L., WRAY, J. J., MCKEOWN, N. K., PARENTE, M., HAUBER, E., ALTIERI, F., CARROZZO, F. G. & NILES, P. B. 2010. The Mawrth Vallis region of Mars: A potential landing site for the Mars Science Laboratory (MSL) mission. *Astrobiology,* 10**,** 687.

MICHALSKI, J. R., ONSTOTT, T. C., MOJZSIS, S. J., MUSTARD, J., CHAN, Q. H., NILES, P. B. & JOHNSON, S. S. 2018. The Martian subsurface as a potential window into the origin of life. *Nature Geoscience,* 11**,** 21.

MICKOL, R. & KRAL, T. 2017. Low pressure tolerance by methanogens in an aqueous environment: implications for subsurface life on Mars. *Origins of Life and Evolution of Biospheres,* 47**,** 511.

MICKOL, R., TAKAGI, Y. & KRAL, T. 2018a. Survival of non-psychrophilic methanogens exposed to martian diurnal and 48-h temperature cycles. *Planetary and Space Science,* 157**,** 63.

MICKOL, R. L., LAIRD, S. K. & KRAL, T. A. 2018b. Non-Psychrophilic Methanogens Capable of Growth Following Long-Term Extreme Temperature Changes, with Application to Mars. *Microorganisms,* 6**,** 34.

MIKUCKI, J. A., AUKEN, E., TULACZYK, S., VIRGINIA, R. A., SCHAMPER, C., SORENSEN, K. I., DORAN, P. T., DUGAN, H. & FOLEY, N. 2015. Deep groundwater and potential subsurface habitats beneath an Antarctic dry valley. *Nat Commun,* 6**,** 6831.

MIKUCKI, J. A. & PRISCU, J. C. 2007. Bacterial diversity associated with Blood Falls, a subglacial outflow from the Taylor Glacier, Antarctica. *Applied and Environmental Microbiology,* 73**,** 4029.

MILO, R., JORGENSEN, P., MORAN, U., WEBER, G. & SPRINGER, M. 2009. BioNumbers—the database of key numbers in molecular and cell biology. *Nucleic acids research,* 38**,** D750.

MIRINO, M., BALME, M., FAWDON, P., DAVIS, J., BARNES, R., ALLENDER, E. & GRINDROD, P. 2018. Field study of exhumed channels in Green River and Hanksville areas, Utah, and a comparison with inverted channel features on Mars. *Geophysical Research Abstracts,* 20**,** 16047.

MIROSHNICHENKO, M. L. & BONCH-OSMOLOVSKAYA, E. A. 2006. Recent developments in the thermophilic microbiology of deep-sea hydrothermal vents. *Extremophiles,* 10**,** 85.

MITROFANOV, I., ZUBER, M., LITVAK, M., DEMIDOV, N., SANIN, A., BOYNTON, W., GILICHINSKY, D., HAMARA, D., KOZYREV, A. & SAUNDERS, R. 2007. Water ice permafrost on Mars: Layering structure and subsurface distribution according to HEND/Odyssey and MOLA/MGS data. *Geophysical Research Letters,* 34**,** L18102.

MOORE, J. M. & WILHELMS, D. E. 2001. Hellas as a possible site of ancient ice-covered lakes on Mars. *Icarus,* 154**,** 258.

MOORE, W. B., LENARDIC, A., JELLINEK, A., JOHNSON, C., GOLDBLATT, C. & LORENZ, R. 2017. How habitable zones and super-Earths lead us astray. *NATURE,* 1**,** 0043.

MOREIRA, D. & LÓPEZ-GARCÍA, P. 1998. Symbiosis between methanogenic archaea and δ-proteobacteria as the origin of eukaryotes: the syntrophic hypothesis. *Journal of Molecular Evolution,* 47**,** 517.

MORI, K. & SUZUKI, K.-I. 2008. Thiofaba tepidiphila gen. nov., sp. nov., a novel obligately chemolithoautotrophic, sulfur-oxidizing bacterium of the Gammaproteobacteria

isolated from a hot spring. *International journal of systematic and evolutionary microbiology,* 58**,** 1885.

MORI, K. & SUZUKI, K.-I. 2014. The family Thioalkalispiraceae. *The Prokaryotes.* Springer.

MUELLER, G. M., FOSTER, M. S. & BILLS, G. F. 2011. Xerophilic. *Biodiversity of Fungi: Inventory and Monitoring Methods.* Elsevier Science.

MULLAKHANBHAI, M. F. & LARSEN, H. 1975. Halobacterium volcanii spec. nov., a Dead Sea halobacterium with a moderate salt requirement. *Archives of Microbiology,* 104**,** 207.

MURPHY, S. 2008. Microbial Community Analysis EcoPlate™. *In:* BIOLOG INC (ed.). http://www.biolog.com/pdf/milit/00A_012_EcoPlate_Sell_Sheet.pdf.

MURUKESAN, G., LEINO, H., MÄENPÄÄ, P., STÅHLE, K., RAKSAJIT, W., LEHTO, H. J., ALLAHVERDIYEVA-RINNE, Y. & LEHTO, K. 2016. Pressurized Martian-Like Pure CO 2 Atmosphere Supports Strong Growth of Cyanobacteria, and Causes Significant Changes in their Metabolism. *Origins of Life and Evolution of Biospheres,* 46**,** 119.

MUSILOVA, M., WRIGHT, G., WARD, J. M. & DARTNELL, L. R. 2015. Isolation of radiation-resistant bacteria from Mars analog Antarctic Dry Valleys by preselection, and the correlation between radiation and desiccation resistance. *Astrobiology,* 15**,** 1076.

NAGHONI, A., EMTIAZI, G., AMOOZEGAR, M. A., RASOOLI, M., ETEMADIFAR, Z., FAZELI, S. A. S., MINEGISHI, H. & VENTOSA, A. 2017. Natronoarchaeum persicum sp. nov., a haloarchaeon isolated from a hypersaline lake. *International journal of systematic and evolutionary microbiology,* 67**,** 3339.

NAJITA, J. & CARR, J. 2015. Water, UV shielding, and Organic Molecules in the Terrestrial Planet Region of Disks. *IAU General Assembly,* 22**,** 2257800.

NATALICCHIO, M., DELA PIERRE, F., LUGLI, S., LOWENSTEIN, T. K., FEINER, S. J., FERRANDO, S., MANZI, V., ROVERI, M. & CLARI, P. 2014. Did Late Miocene (Messinian) gypsum precipitate from evaporated marine brines? Insights from the Piedmont Basin (Italy). *Geology,* 42**,** 179.

NAVARRO-GONZÁLEZ, R., NAVARRO, K. F., DE LA ROSA, J., IÑIGUEZ, E., MOLINA, P., MIRANDA, L. D., MORALES, P., CIENFUEGOS, E., COLL, P. & RAULIN, F. 2006. The limitations on organic detection in Mars-like soils by thermal volatilization–gas chromatography–MS and their implications for the Viking results. *Proceedings of the National Academy of Sciences,* 103**,** 16089.

NAZIRI, D., HAMIDI, M., HASSANZADEH, S., TARHRIZ, V., MALEKI ZANJANI, B., NAZEMYIEH, H., HEJAZI, M. A. & HEJAZI, M. S. 2014. Analysis of Carotenoid Production by Halorubrum sp. TBZ126; an Extremely Halophilic Archeon from Urmia Lake. *Advanced Pharmaceutical Bulletin,* 4**,** 61.

NCBI RESOURCE COORDINATORS 2018. Database resources of the National Center for Biotechnology Information. *Nucleic acids research,* 46**,** D8.

NELSON, N. & JUNGE, W. 2015. Structure and energy transfer in photosystems of oxygenic photosynthesis. *Annual review of biochemistry,* 84**,** 659.

NG, W. V., KENNEDY, S. P., MAHAIRAS, G. G., BERQUIST, B., PAN, M., SHUKLA, H. D., LASKY, S. R., BALIGA, N. S., THORSSON, V. & SBROGNA, J. 2000. Genome sequence of Halobacterium species NRC-1. *Proceedings of the National Academy of Sciences,* 97**,** 12176.

NICHOLSON, W. L., KRIVUSHIN, K., GILICHINSKY, D. & SCHUERGER, A. C. 2013. Growth of Carnobacterium spp. from permafrost under low pressure, temperature, and anoxic atmosphere has implications for Earth microbes on Mars. *Proceedings of the National Academy of Sciences of the United States of America,* 110**,** 666.

NIEDERBERGER, T. D., PERREAULT, N. N., TILLE, S., LOLLAR, B. S., LACRAMPE-COULOUME, G., ANDERSEN, D., GREER, C. W., POLLARD, W. & WHYTE, L. G. 2010. Microbial characterization of a subzero, hypersaline methane seep in the Canadian High Arctic. *The ISME journal,* 4**,** 1326.

NIER, A., HANSON, W., SEIFF, A., MCELROY, M., SPENCER, N., DUCKETT, R., KNIGHT, T. & COOK, W. 1976. Composition and structure of the Martian atmosphere: Preliminary results from Viking 1. *Science,* 193**,** 786.

NIKOLAKAKOS, G. & WHITEWAY, J. A. 2015. Laboratory investigation of perchlorate deliquescence at the surface of Mars with a Raman scattering lidar. *Geophysical Research Letters,* 42**,** 7899.

NOBLE, R. T. & FUHRMAN, J. A. 1998. Use of SYBR Green I for rapid epifluorescence counts of marine viruses and bacteria. *Aquatic Microbial Ecology,* 14**,** 113.

NORRIS, F. & DARBRE, A. 1956. The microbiological assay of inositol with a strain of Schizosaccharomyces pombe. *Analyst,* 81**,** 394.

NORTON, C. F. & GRANT, W. D. 1988. Survival of Halobacteria Within Fluid Inclusions in Salt Crystals. *Journal of General Microbiology,* 134**,** 1365.

NORTON, C. F., MCGENITY, T. J. & GRANT, W. D. 1993. Archaeal halophiles (halobacteria) from two British salt mines. *Journal of General Microbiology,* 139**,** 1077.

NUTMAN, A. P., BENNETT, V. C., FRIEND, C. R., VAN KRANENDONK, M. J. & CHIVAS, A. R. 2016. Rapid emergence of life shown by discovery of 3,700-million-year-old microbial structures. *Nature,* 537**,** 535.

NYYSSÖNEN, M., HULTMAN, J., AHONEN, L., KUKKONEN, I., PAULIN, L., LAINE, P., ITÄVAARA, M. & AUVINEN, P. 2014. Taxonomically and functionally diverse microbial communities in deep crystalline rocks of the Fennoscandian shield. *The ISME journal,* 8**,** 126.

OAKES, C. S., BODNAR, R. J. & SIMONSON, J. M. 1990. The system NaCl・ CaCl2・ H2O: I. The ice liquidus at 1 atm total pressure. *Geochimica et Cosmochimica Acta,* 54**,** 603.

OEHLER, D. Z. & ETIOPE, G. 2017. Methane seepage on Mars: where to look and why. *Astrobiology,* 17**,** 1233.

OHMOTO, H., RUNNEGAR, B., KUMP, L. R., FOGEL, M. L., KAMBER, B., ANBAR, A. D., KNAUTH, P. L., LOWE, D. R., SUMNER, D. Y. & WATANABE, Y. 2008. Biosignatures in ancient rocks: a summary of discussions at a field workshop on biosignatures in ancient rocks. Mary Ann Liebert, Inc. 140 Huguenot Street, 3rd Floor New Rochelle, NY 10801-5215 USA.

OJHA, L., WILHELM, M., MURCHIE, S. L., MCEWEN, A. S., WRAY, J., HANLEY, J., MASSÉ, M. & CHOJNACKI, M. 2015. Spectral Evidence for Hydrated Salts in Seasonal Brine Flows on Mars. *EPSC Abstracts,* 10.

OKSANEN, J., KINDT, R., LEGENDRE, P., O'HARA, B., STEVENS, M. H. H., OKSANEN, M. J. & SUGGESTS, M. 2007. The vegan package. *Community ecology package,* 10.

OLLIVIER, B., CAUMETTE, P., GARCIA, J. L. & MAH, R. A. 1994. Anaerobic bacteria from hypersaline environments. *Microbiological Reviews,* 58**,** 27.

ONSTOTT, T., MAGNABOSCO, C., AUBREY, A., BURTON, A., DWORKIN, J., ELSILA, J., GRUNSFELD, S., CAO, B., HEIN, J. & GLAVIN, D. 2014. Does aspartic acid racemization constrain the depth limit of the subsurface biosphere? *Geobiology,* 12**,** 1.

OREN, A. 1983. Halobacterium sodomense sp. nov., a Dead Sea halobacterium with an extremely high magnesium requirement. *International Journal of Systematic and Evolutionary Microbiology,* 33**,** 381.

OREN, A. 1986. Intracellular salt concentrations of the anaerobic halophilic eubacteria Haloanaerobium praevalens and Halobacteroides halobius. *Canadian journal of microbiology,* 32**,** 4.

OREN, A. 1999. Bioenergetic aspects of halophilism. *Microbiology and molecular biology reviews,* 63**,** 334.

OREN, A. 2005. Microscopic examination of microbial communities along a salinity gradient in saltern evaporation ponds: a 'halophilic safari'. *Adaptation to Life at High Salt Concentrations in Archaea, Bacteria, and Eukarya.* Springer.

OREN, A. 2008. Microbial life at high salt concentrations: phylogenetic and metabolic diversity. *Saline Systems,* 4**,** 2.

OREN, A. 2009. Microbial diversity and microbial abundance in salt-saturated brines: why are the waters of hypersaline lakes red? *Natural Resources and Environmental Issues,* 15**,** 247.

OREN, A. 2012. Taxonomy of the family Halobacteriaceae: a paradigm for changing concepts in prokaryote systematics. *International journal of systematic and evolutionary microbiology,* 62**,** 263.

OREN, A. 2013. Life in Magnesium and Calcium rich hypersaline environments: salt stress by chaotropic ions. *In:* SECKBACH, J., OREN, A. & STAN-LOTTER, H. (eds.) *Polyextremophiles.* Dordrecht, NETHERLANDS: Springer Netherlands.

OREN, A. 2014. Halophilic archaea on Earth and in space: growth and survival under extreme conditions. *Phil. Trans. R. Soc. A,* 372**,** 20140194.

OREN, A. 24/5/16 2016a. *RE: Personal Communication with the Halophile Expert Aharon Oren at the 2016 Halophiles Conference in Puerto Rico.*

OREN, A. 2016b. Probing Saltern Brines with an Oxygen Electrode: What Can We Learn about the Community Metabolism in Hypersaline Systems? *Life,* 6**,** 23.

OREN, A., BARDAVID, R. E. & MANA, L. 2014. Perchlorate and halophilic prokaryotes: implications for possible halophilic life on Mars. *Extremophiles,* 18**,** 75.

OREN, A. & BEKHOR, D. 1989. Tolerance of extremely halophilic archaebacteria towards bromide. *Current Microbiology,* 19**,** 371.

OREN, A. & SHILO, M. 1981. Bacteriorhodopsin in a bloom of halobacteria in the Dead Sea. *Archives of Microbiology,* 130**,** 185.

OROSEI, R., LAURO, S. E., PETTINELLI, E., CICCHETTI, A., CORADINI, M., COSCIOTTI, B., DI PAOLO, F., FLAMINI, E., MATTEI, E., PAJOLA, M., SOLDOVIERI, F., CARTACCI, M., CASSENTI, F., FRIGERI, A., GIUPPI, S., MARTUFI, R., MASDEA, A., MITRI, G., NENNA, C., NOSCHESE, R., RESTANO, M. & SEU, R. 2018. Radar evidence of subglacial liquid water on Mars. *Science,* 361**,** 490.

ORWIG, J. 2014. Cultivating salt-loving microbes on Mars. *Eos, Transactions American Geophysical Union,* 95**,** 416.

OSTERLOO, M., HAMILTON, V., BANDFIELD, J., GLOTCH, T., BALDRIDGE, A., CHRISTENSEN, P., TORNABENE, L. & ANDERSON, F. 2008. Chloride-bearing materials in the southern highlands of Mars. *Science,* 319**,** 1651.

OSTERLOO, M. & HYNEK, B. Martian chloride deposits: The last gasps of widespread surface water. Lunar and Planetary Science Conference, 2015. 1054.

OSTERLOO, M. M., ANDERSON, F. S., HAMILTON, V. E. & HYNEK, B. M. 2010. Geologic context of proposed chloride-bearing materials on Mars. *Journal of Geophysical Research: Planets,* 115**,** E10012.

PALUCIS, M. C., DIETRICH, W. E., WILLIAMS, R. M. E., HAYES, A. G., PARKER, T., SUMNER, D. Y., MANGOLD, N., LEWIS, K. & NEWSOM, H. 2016. Sequence and relative timing of large lakes in Gale crater (Mars) after the formation of Mount Sharp. *Journal of Geophysical Research: Planets,* 121**,** 472.

PALUMBO, A. M. & HEAD, J. W. 2017. Impact cratering as a cause of climate change, surface alteration, and resurfacing during the early history of Mars. *Meteoritics & Planetary Science*, 1.

PANDE, S. & KOST, C. 2017. Bacterial unculturability and the formation of intercellular metabolic networks. *Trends in microbiology,* 25, 349.

PARK, J., VREELAND, R., CHO, B., LOWENSTEIN, T., TIMOFEEFF, M. & ROSENZWEIG, W. 2009. Haloarchaeal diversity in 23, 121 and 419 MYA salts. *Geobiology,* 7, 515.

PARKER, T. J., GORSLINE, D. S., SAUNDERS, R. S., PIERI, D. C. & SCHNEEBERGER, D. M. 1993. Coastal geomorphology of the Martian northern plains. *Journal of Geophysical Research: Planets,* 98, 11061.

PARNELL, J. & BLAMEY, N. 2017. Hydrogen from Radiolysis of Aqueous Fluid Inclusions during Diagenesis. *Minerals,* 7, 130.

PARNELL, J., CULLEN, D., SIMS, M. R., BOWDEN, S., COCKELL, C. S., COURT, R., EHRENFREUND, P., GAUBERT, F., GRANT, W., PARRO, V., ROHMER, M., SEPHTON, M., STAN-LOTTER, H., STEELE, A., TOPORSKI, J. & VAGO, J. 2007. Searching for life on Mars: selection of molecular targets for ESA's aurora ExoMars mission. *Astrobiology,* 7, 578.

PARSONS, R. A., MOORE, J. M. & HOWARD, A. D. 2013. Evidence for a short period of hydrologic activity in Newton crater, Mars, near the Hesperian-Amazonian transition. *Journal of Geophysical Research: Planets,* 118, 1082.

PARTE, A. C. 2013. LPSN—list of prokaryotic names with standing in nomenclature. *Nucleic acids research,* 42, D613.

PASTERIS, J. D., FREEMAN, J. J., WOPENKA, B., QI, K., MA, Q. & WOOLEY, K. L. 2006. With a grain of salt: what halite has to offer to discussions on the origin of life. *Astrobiology,* 6, 625.

PATRICK, R., BINETTI, V. P. & HALTERMAN, S. G. 1981. Acid Lakes from Natural and Anthropogenic Causes. *Science,* 211, 446.

PAULINO-LIMA, I. G., FUJISHIMA, K., NAVARRETE, J. U., GALANTE, D., RODRIGUES, F., AZUA-BUSTOS, A. & ROTHSCHILD, L. J. 2016. Extremely high UV-C radiation resistant microorganisms from desert environments with different manganese concentrations. *Journal of Photochemistry and Photobiology B: Biology,* 163, 327.

PAVLOV, A., VASILYEV, G., OSTRYAKOV, V., PAVLOV, A. & MAHAFFY, P. 2012. Degradation of the organic molecules in the shallow subsurface of Mars due to irradiation by cosmic rays. *Geophysical research letters,* 39, L13202.

PAVLOV, A. K., SHELEGEDIN, V. N., VDOVINA, M. A. & PAVLOV, A. A. 2010. Growth of microorganisms in Martian-like shallow subsurface conditions: laboratory modelling. *INTERNATIONAL JOURNAL OF ASTROBIOLOGY,* 9, 51.

PAYLER, S. J., BIDDLE, J. F., COATES, A. J., COUSINS, C. R., CROSS, R. E., CULLEN, D. C., DOWNS, M. T., DIREITO, S. O., EDWARDS, T. & GRAY, A. L. 2016. Planetary science and exploration in the deep subsurface: results from the MINAR Program, Boulby Mine, UK. *International Journal of Astrobiology,* 16**,** 114.

PAYLER, S. J., BIDDLE, J. F., COATES, A. J., COUSINS, C. R., CROSS, R. E., CULLEN, D. C., DOWNS, M. T., DIREITO, S. O., EDWARDS, T. & GRAY, A. L. 2017. Planetary science and exploration in the deep subsurface: results from the MINAR Program, Boulby Mine, UK. *International Journal of Astrobiology,* 16**,** 114.

PEETERS, E., NELIS, H. J. & COENYE, T. 2008. Comparison of multiple methods for quantification of microbial biofilms grown in microtiter plates. *Journal of microbiological methods,* 72**,** 157.

PERETÓ, J., LÓPEZ-GARCÍA, P. & MOREIRA, D. 2004. Ancestral lipid biosynthesis and early membrane evolution. *Trends in biochemical sciences,* 29**,** 469.

PERETYAZHKO, T., FOX, A., SUTTER, B., NILES, P., ADAMS, M., MORRIS, R. & MING, D. 2016. Synthesis of akaganeite in the presence of sulfate: Implications for akaganeite formation in Yellowknife Bay, Gale Crater, Mars. *Geochimica et Cosmochimica Acta,* 188**,** 284.

PFAFF, S., BORCHHARDT, N., BOY, J., KARSTEN, U. & GUSTAVS, L. 2016. Desiccation tolerance and growth-temperature requirements of Coccomyxa (Trebouxiophyceae, Chlorophyta) strains from Antarctic biological soil crusts. *Algological Studies,* 151**,** 3.

PHILLIPS-LANDER, C. M., PARNELL, S., MCGRAW, L. & MADDEN, M. E. 2017. Carbonate dissolution rates in high salinity brines: Implications for post-Noachian chemical weathering on Mars. *Icarus,* 307**,** 281.

PIA02031 1999. Maps of Mars Global Topography. *NASA Jet Propulsion Laboratory Photojournal*.

PIERREHUMBERT, R. T. 2010. The big questions. *Principles of planetary climate.* Cambridge University Press.

PINHEIRO, V. B. & HOLLIGER, P. 2012. The XNA world: progress towards replication and evolution of synthetic genetic polymers. *Current opinion in chemical biology,* 16**,** 245.

PLÜMPER, O., KING, H. E., GEISLER, T., LIU, Y., PABST, S., SAVOV, I. P., ROST, D. & ZACK, T. 2017. Subduction zone forearc serpentinites as incubators for deep microbial life. *Proceedings of the National Academy of Sciences,* 114**,** 4324.

POCH, O., KACI, S., STALPORT, F., SZOPA, C. & COLL, P. 2014. Laboratory insights into the chemical and kinetic evolution of several organic molecules under simulated Mars surface UV radiation conditions. *Icarus,* 242**,** 50.

POL, A., BARENDS, T. R., DIETL, A., KHADEM, A. F., EYGENSTEYN, J., JETTEN, M. S. & OP DEN CAMP, H. J. 2014. Rare earth metals are essential for methanotrophic life in volcanic mudpots. *Environ Microbiol,* 16**,** 255.

PROBST, A. J., LADD, B., JARETT, J. K., GELLER-MCGRATH, D. E., SIEBER, C. M. K., EMERSON, J. B., ANANTHARAMAN, K., THOMAS, B. C., MALMSTROM, R. R., STIEGLMEIER, M., KLINGL, A., WOYKE, T., RYAN, M. C. & BANFIELD, J. F. 2018. Differential depth distribution of microbial function and putative symbionts through sediment-hosted aquifers in the deep terrestrial subsurface. *Nature Microbiology,* 3**,** 328.

PRYOR, A. 2018. It's a great big universe: Astrobiology and future trends for an astrotheology. *Dialog,* 57**,** 5.

RAMDAHL, T. 1983. Retene—a molecular marker of wood combustion in ambient air. *Nature,* 306**,** 580.

RAMPE, E. B., MING, D. W., BLAKE, D. F., BRISTOW, T. F., CHIPERA, S. J., GROTZINGER, J. P., MORRIS, R. V., MORRISON, S. M., VANIMAN, D. T., YEN, A. S., ACHILLES, C. N., CRAIG, P. I., DES MARAIS, D. J., DOWNS, R. T., FARMER, J. D., FENDRICH, K. V., GELLERT, R., HAZEN, R. M., KAH, L. C., MOROOKIAN, J. M., PERETYAZHKO, T. S., SARRAZIN, P., TREIMAN, A. H., BERGER, J. A., EIGENBRODE, J., FAIRÉN, A. G., FORNI, O., GUPTA, S., HUROWITZ, J. A., LANZA, N. L., SCHMIDT, M. E., SIEBACH, K., SUTTER, B. & THOMPSON, L. M. 2017. Mineralogy of an ancient lacustrine mudstone succession from the Murray formation, Gale crater, Mars. *Earth and Planetary Science Letters,* 471**,** 172.

RAMPELOTTO, P. H. 2010. Resistance of microorganisms to extreme environmental conditions and its contribution to astrobiology. *Sustainability,* 2**,** 1602.

RASUK, M., FERRER, G., MORENO, J., FARIAS, M. & ALBARRACÍN, V. 2016. 4 The Diversity of Microbial Extremophiles. *Molecular Diversity of Environmental Prokaryotes***,** 87.

RAYNER, P., ENTING, I., FRANCEY, R. & LANGENFELDS, R. 1999. Reconstructing the recent carbon cycle from atmospheric CO2, δ13C and O2/N2 observations. *Tellus B: Chemical and Physical Meteorology,* 51**,** 213.

REES, D. C. & HOWARD, J. B. 2000. Nitrogenase: standing at the crossroads. *Current opinion in chemical biology,* 4**,** 559.

REI, T. S. 1959. The Effect of Rotation Aeration on the Growth of Mycobacterium Tuberculosis. *Japanese Journal of Microbiology,* 3**,** 509.

REITH, F., ZAMMIT, C. M., POHRIB, R., GREGG, A. L. & WAKELIN, S. A. 2015. Geogenic factors as drivers of microbial community diversity in soils overlying polymetallic deposits. *Applied and environmental microbiology,* 81**,** 7822.

RETTBERG, P., ANESIO, A. M., BAKER, V. R., BAROSS, J. A., CADY, S. L., DETSIS, E., FOREMAN, C. M., HAUBER, E., ORI, G. G. & PEARCE, D. A. 2016. Planetary

protection and Mars special regions—a suggestion for updating the definition. 16**,** 119.

RETTBERG, P., BEBLO-VRANESEVIC, K., RABBOW, E., BOHMEIER, M., LEUKO, S., MOELLER, R., BERGER, T., ANTUNES, A., COCKELL, C. & DENG, L. 2017. MEXEM–Mars Exposed Extremophile Mixture–a space experiment to investigate the capability of anaerobic organisms to survive on Mars. *EANA 2017.*

RICHARDSON, M. I. & WILSON, R. J. 2002. Investigation of the nature and stability of the Martian seasonal water cycle with a general circulation model. *Journal of Geophysical Research: Planets,* 107.

RODIONOV, D., KORABLEV, O., ZELENYI, L. & VAGO, J. Mars Atmospheric Measurements Planned at Exomars 2020 Surface Platform. The Sixth International Workshop on the Mars Atmosphere: Modelling and observation was held on January 17-20 2017, in Granada, Spain. Scientific committee: F. Forget, MA Lopez-Valverde, S. Amiri, M.-C. Desjean, F. Gonzalez-Galindo, J. Hollingsworth, B. Jakosky, SR Lewis, D. McCleese, E. Millour, H. Svedhem, D. Titov, M. Wolff., p. 4407, 2017. 4407.

RODRIGUEZ, J. A. P., FAIRÉN, A. G., TANAKA, K. L., ZARROCA, M., LINARES, R., PLATZ, T., KOMATSU, G., MIYAMOTO, H., KARGEL, J. S. & YAN, J. 2016a. Tsunami waves extensively resurfaced the shorelines of an early Martian ocean. *Scientific reports,* 6**,** 25106

RODRIGUEZ, J. A. P., ZARROCA, M., LINARES, R., GULICK, V., WEITZ, C. M., YAN, J., FAIRÉN, A. G., MIYAMOTO, H., PLATZ, T. & BAKER, V. 2016b. Groundwater flow induced collapse and flooding in Noctis Labyrinthus, Mars. *Planetary and Space Science,* 124**,** 1.

ROGERS, A. D., WARNER, N. H., GOLOMBEK, M. P., HEAD, J. W. & COWART, J. C. 2018. Areally extensive surface bedrock exposures on Mars: Many are clastic rocks, not lavas. *Geophysical Research Letters,* 45**,** 1767.

ROLFE, S. 2017. *Characteristic Raman Bands of Amino Acids and Halophiles as Biomarkers in Planetary Exploration.* PhD Thesis, The Open University.

ROLFE, S., PATEL, M., OLSSON-FRANCIS, K., GILMOUR, I., RINGROSE, T. & MCGENITY, T. 2017. Mars simulated exposure and the characteristic Raman biosignatures of amino acids and halophilic microbes. *7th Astrobiology Society of Britain Conference***,** 21.

RONNEKLEIV, M. & LIAAEN-JENSEN, S. 1992. Bacterial carotenoids. 52. C-50-carotenoids. 22. Naturally-occurring geometrical-isomers of bacterioruberin. *Acta Chemica Scandinavica,* 46**,** 1092.

ROSENBERG, E. N. & HEAD III, J. W. 2015. Late Noachian fluvial erosion on Mars: Cumulative water volumes required to carve the valley networks and grain size of bed-sediment. *Planetary and Space Science,* 117**,** 429.

ROSENZWEIG, W. D., PETERSON, J., WOISH, J. & VREELAND, R. H. 2000. Development of a protocol to retrieve microorganisms from ancient salt crystals. *Geomicrobiology Journal,* 17**,** 185.

ROSSI, F., RISTORI, S., MARCHETTINI, N. & PANTANI, O. L. 2014. Functionalized clay microparticles as catalysts for chemical oscillators. *The Journal of Physical Chemistry C,* 118**,** 24389.

ROUX, S., ENAULT, F., RAVET, V., COLOMBET, J., BETTAREL, Y., AUGUET, J. C., BOUVIER, T., LUCAS-STAAT, S., VELLET, A. & PRANGISHVILI, D. 2016. Analysis of metagenomic data reveals common features of halophilic viral communities across continents. *Environmental microbiology,* 18**,** 889.

ROWLANDS, R. 1984. Industrial strain improvement: mutagenesis and random screening procedures. *Enzyme and microbial technology,* 6**,** 3.

RUBIN, S. S., MARÍN, I., GÓMEZ, M. J., MORALES, E. A., ZEKKER, I., SAN MARTÍN, P., RODRÍGUEZ, N. & AMILS, R. 2017. Prokaryotic diversity and community composition in the Salar de Uyuni, a large scale, chaotropic salt flat. *Environmental Microbiology,* 19**,** 3745.

RUIZ-AGUDO, E., MARTÍN-RAMOS, J. D. & RODRIGUEZ-NAVARRO, C. 2007. Mechanism and kinetics of dehydration of epsomite crystals formed in the presence of organic additives. *The Journal of Physical Chemistry B,* 111**,** 41.

SAFARI, A., MORTAZAVI, S. & MOZDARANI, H. 2014. Introducing the RadBioStat Educational Software: Computer-Assisted Teaching of the Random Nature of Cell Killing. *Journal of biomedical physics & engineering,* 4**,** 69.

SAGAN, C. & FOX, P. 1975. The canals of Mars: an assessment after Mariner 9. *Icarus,* 25**,** 602.

SAMBROOK, J. & RUSSELL, D. W. 2006. Purification of nucleic acids by extraction with phenol: chloroform. *Cold Spring Harbor Protocols,* 2006**,** pdb. prot4455.

SANDERS, E. R. 2012. Aseptic laboratory techniques: plating methods. *Journal of visualized experiments: JoVE,* 63**,** 3064.

SANKARANARAYANAN, K., LOWENSTEIN, T. K., TIMOFEEFF, M. N., SCHUBERT, B. A. & LUM, J. K. 2014. Characterization of Ancient DNA Supports Long-Term Survival of Haloarchaea. *Astrobiology,* 14**,** 553.

SANKARANARAYANAN, K., TIMOFEEFF, M. N., SPATHIS, R., LOWENSTEIN, T. K. & LUM, J. K. 2011. Ancient microbes from halite fluid inclusions: optimized surface sterilization and DNA extraction. *PLoS One,* 6**,** e20683.

SAPERS, H. M., RONHOLM, J., RAYMOND-BOUCHARD, I., COMREY, R., OSINSKI, G. R. & WHYTE, L. G. 2017. Biological Characterization of Microenvironments in a Hypersaline Cold Spring Mars Analog. *Frontiers in Microbiology,* 8**,** 2527.

SAPP, A., HUGUET-TAPIA, J. C., SÁNCHEZ-LAMAS, M., ANTELO, G. T., PRIMO, E. D., RINALDI, J., KLINKE, S., GOLDBAUM, F. A., BONOMI, H. R. & CHRISTNER, B. C. 2018. Draft Genome Sequence of Methylobacterium sp. Strain V23, Isolated from Accretion Ice of the Antarctic Subglacial Lake Vostok. *Genome announcements,* 6**,** e00145.

SAROS, J. E. & FRITZ, S. C. 2000. Changes in the growth rates of saline-lake diatoms in response to variation in salinity, brine type and nitrogen form. *Journal of Plankton Research,* 22**,** 1071.

SATO, T., NAGAMATSU, A., UENO, H., KATAOKA, R., MIYAKE, S., TAKEDA, K. & NIITA, K. 2017. Comparison Of Cosmic-ray Environments On Earth, Moon, Mars And In Spacecarft Using Phits. *Radiation Protection Dosimetry,* 180**,** 146.

SATTERFIELD, C. L., LOWENSTEIN, T. K., VREELAND, R. H., ROSENZWEIG, W. D. & POWERS, D. W. 2005. New evidence for 250 Ma age of halotolerant bacterium from a Permian salt crystal. *Geology,* 33**,** 265.

SAUTTER, V., TOPLIS, M. J., BECK, P., MANGOLD, N., WIENS, R., PINET, P., COUSIN, A., MAURICE, S., LEDEIT, L. & HEWINS, R. 2016. Magmatic complexity on early Mars as seen through a combination of orbital, in-situ and meteorite data. *Lithos,* 254**,** 36.

SCHIPPER, M., MASLEN, M., HOGG, G., CHOW, C. & SAMSON, R. 1996. Human infection by Rhizopus azygosporus and the occurrence of azygospores in zygomycetes. *Sabouraudia,* 34**,** 199.

SCHIRMACK, J., ALAWI, M. & WAGNER, D. 2015. Influence of Martian regolith analogs on the activity and growth of methanogenic archaea, with special regard to long-term desiccation. *Frontiers in Microbiology,* 6**,** 210.

SCHLOSS, P. D., WESTCOTT, S. L., RYABIN, T., HALL, J. R., HARTMANN, M., HOLLISTER, E. B., LESNIEWSKI, R. A., OAKLEY, B. B., PARKS, D. H. & ROBINSON, C. J. 2009. Introducing mothur: open-source, platform-independent, community-supported software for describing and comparing microbial communities. *Applied and environmental microbiology,* 75**,** 7537.

SCHMIDT, F., ANDRIEU, F., COSTARD, F., KOCIFAJ, M. & MERESESCU, A. G. 2017. Formation of recurring slope lineae on Mars by rarefied gas-triggered granular flows. *Nature Geoscience,* 10**,** 270.

SCHOFIELD, P., KNIGHT, K., COVEY-CRUMP, S., CRESSEY, G. & STRETTON, I. 2002. Accurate quantification of the modal mineralogy of rocks when image analysis is difficult. *Mineralogical Magazine,* 66**,** 189.

SCHUBERT, B. A., LOWENSTEIN, T. K., TIMOFEEFF, M. N. & PARKER, M. A. 2009. How do prokaryotes survive in fluid inclusions in halite for 30 k.y.? *Geology,* 37**,** 1059.

SCHUBERT, B. A., LOWENSTEIN, T. K., TIMOFEEFF, M. N. & PARKER, M. A. 2010. Halophilic archaea cultured from ancient halite, Death Valley, California. *Environmental microbiology,* 12**,** 440.

SCHUERGER, A. C. & NICHOLSON, W. L. 2016. Twenty Species of Hypobarophilic Bacteria Recovered from Diverse Soils Exhibit Growth under Simulated Martian Conditions at 0.7 kPa. *Astrobiology,* 16**,** 964.

SCHUERGER, A. C., RICHARDS, J. T., NEWCOMBE, D. A. & VENKATESWARAN, K. 2006. Rapid inactivation of seven Bacillus spp. under simulated Mars UV irradiation. *Icarus,* 181**,** 52.

SCHULZE-MAKUCH, D., AIRO, A. & SCHIRMACK, J. 2017. The Adaptability of Life on Earth and the Diversity of Planetary Habitats. *Frontiers in microbiology,* 8**,** 2011.

SCHULZE-MAKUCH, D., WAGNER, D., KOUNAVES, S. P., MANGELSDORF, K., DEVINE, K. G., DE VERA, J.-P., SCHMITT-KOPPLIN, P., GROSSART, H.-P., PARRO, V. & KAUPENJOHANN, M. 2018. Transitory microbial habitat in the hyperarid Atacama Desert. *Proceedings of the National Academy of Sciences,* 115**,** 2670.

SCHUMANN, W. 2016. Regulation of bacterial heat shock stimulons. *Cell Stress & Chaperones,* 21**,** 959.

SCHWARTZMAN, D. W. 2014. Life was thermophilic for the first two-thirds of earth history. *Thermophiles.* CRC Press.

SCHWENDNER, P., BOHMEIER, M., RETTBERG, P., BEBLO-VRANESEVIC, K., GABOYER, F., MOISSL-EICHINGER, C., PERRAS, A. K., VANNIER, P., MARTEINSSON, V. T. & GARCIA-DESCALZO, L. 2018. Beyond chloride brines: Variable metabolomic responses in the anaerobic organism, Yersinia intermedia MASE-LG-1, to NaCl and MgSO4 at identical water activity. *Frontiers in Microbiology,* 9**,** 335.

SCHWIEGER, F. & TEBBE, C. C. 1998. A new approach to utilize PCR-single-strand-conformation polymorphism for 16S rRNA gene-based microbial community analysis. *Appl Environ Microbiol,* 64**,** 4870.

SCIENTIFIC, T. F. 2008. NanoDrop 1000 Spectrophotometer V3. 7 User's Manual. *Thermo Fisher Scientific***,** 1.

SCOVELL, P., MEEHAN, E., ARAÚJO, H., DOBSON, J., GHAG, C., KRAUS, H., KUDRYAVTSEV, V., MAJEWSKI, P., PALING, S. & PREECE, R. 2018. Low-background gamma spectroscopy at the Boulby Underground Laboratory. *Astroparticle Physics,* 97**,** 160.

SEGURA, T. L., TOON, O. B., COLAPRETE, A. & ZAHNLE, K. 2002. Environmental effects of large impacts on Mars. *Science,* 298**,** 1977.

SEYBOLD, H., KITE, E. & KIRCHNER, J. 2017. The role of surface water in the geometry of Mars' valley networks and its climatic implications. *arXiv preprint arXiv:1709.09834*.

SHAHMOHAMMADI, H. R., ASGARANI, E., TERATO, H., SAITO, T., OHYAMA, Y., GEKKO, K., YAMAMOTO, O. & IDE, H. 1998. Protective roles of bacterioruberin and intracellular KCl in the resistance of Halobacterium salinarium against DNA-damaging agents. *J Radiat Res,* 39**,** 251.

SHAND, R. F. & BETLACH, M. C. 1991. Expression of the bop gene cluster of Halobacterium halobium is induced by low oxygen tension and by light. *Journal of bacteriology,* 173**,** 4692.

SHEN, L., LIU, C., WANG, L., HU, Y., HU, M. & FENG, Y. 2017. Degree of brine evaporation and origin of the Mengyejing potash deposit: evidence from fluid inclusions in halite. *Acta Geologica Sinica (English Edition),* 91**,** 175.

SHESHPARI, M., FUJII, Y. & TANI, T. 2017. Underground structures in Mars excavated by tunneling methods for sheltering humans. *Tunnelling and Underground Space Technology,* 64**,** 61.

SHIBATA, A. & JEGGO, P. 2019. A historical reflection on our understanding of radiation-induced DNA double strand break repair in somatic mammalian cells; interfacing the past with the present. *International journal of radiation biology***,** 1.

SHIRSALIMIAN, M., AMOOZEGAR, M., SEPAHY, A. A., KALANTAR, S. & DABBAGH, R. 2017. Isolation of extremely halophilic Archaea from a saline river in the Lut Desert of Iran, moderately resistant to desiccation and gamma radiation. *Microbiology,* 86**,** 403.

SIGMA ALDRICH 2016. Product Information: Deoxyribonucleic Acid (DNA), Sodium Salt from Salmon Testes. https://www.sigmaaldrich.com/content/dam/sigma-aldrich/docs/Sigma/Product_Information_Sheet/d1626pis.pdf.

SINHA, N. & KRAL, T. Growth of Methanogens on Different Mars Regolith Analogues and Stable Carbon Isotope Fractionation During Methanogenesis. Lunar and Planetary Science Conference, 2015. 1628.

SJÖBERG, F., NOWROUZIAN, F., RANGEL, I., HANNOUN, C., MOORE, E., ADLERBERTH, I. & WOLD, A. E. 2013. Comparison between terminal-restriction fragment length polymorphism (T-RFLP) and quantitative culture for analysis of infants' gut microbiota. *Journal of microbiological methods,* 94**,** 37.

SKIDMORE, M., ANDERSON, S. P., SHARP, M., FOGHT, J. & LANOIL, B. D. 2005. Comparison of microbial community compositions of two subglacial environments reveals a possible role for microbes in chemical weathering processes. *Applied and Environmental Microbiology,* 71**,** 6986.

SLEEP, N. H. & ZAHNLE, K. 1998. Refugia from asteroid impacts on early Mars and the early Earth. *Journal of Geophysical Research: Planets,* 103**,** 28529.

SLOAN, D., BATISTA, R. A. & LOEB, A. 2017. The Resilience of Life to Astrophysical Events. *Scientific Reports,* 7**,** 5419.

SMITH, D. E., ZUBER, M. T., FREY, H. V., GARVIN, J. B., HEAD, J. W., MUHLEMAN, D. O., PETTENGILL, G. H., PHILLIPS, R. J., SOLOMON, S. C. & ZWALLY, H. J. 2001. Mars Orbiter Laser Altimeter: Experiment summary after the first year of global mapping of Mars. *Journal of Geophysical Research: Planets,* 106**,** 23689.

SMITH, P., SMITH, N., LEWIN, J., HOMER, G., ALNER, G., ARNISON, G., QUENBY, J., SUMNER, T., BEWICK, A. & ALI, T. 1998. Dark matter experiments at the UK Boulby Mine UK Dark Matter Collaboration. *Physics Reports,* 307**,** 275.

SOJO, V., HERSCHY, B., WHICHER, A., CAMPRUBI, E. & LANE, N. 2016. The origin of life in alkaline hydrothermal vents. *Astrobiology,* 16**,** 181.

SOLOMON, S. C., AHARONSON, O., AURNOU, J. M., BANERDT, W. B., CARR, M. H., DOMBARD, A. J., FREY, H. V., GOLOMBEK, M. P., HAUCK, S. A. & HEAD, J. W. 2005. New perspectives on ancient Mars. *science,* 307**,** 1214.

SOPPA, J. 2013. Evolutionary advantages of polyploidy in halophilic archaea. *Molecular Biology of Archaea.* Portland Press Limited.

SOROKIN, D. Y. 2015. Halo (natrono) archaea isolated from hypersaline lakes utilize cellulose and chitin as growth substrates. *Frontiers in microbiology,* 6**,** 942.

SOROKIN, D. Y., BANCIU, H., ROBERTSON, L. A., KUENEN, J. G., MUNTYAN, M. & MUYZER, G. 2013. Halophilic and haloalkaliphilic sulfur-oxidizing bacteria. *The Prokaryotes.* Springer.

SOROKIN, D. Y., KUBLANOV, I. V., YAKIMOV, M. M., RIJPSTRA, W. I. C. & DAMSTÉ, J. S. S. 2016. Halanaeroarchaeum sulfurireducens gen. nov., sp. nov., the first obligately anaerobic sulfur-respiring haloarchaeon, isolated from a hypersaline lake. *International journal of systematic and evolutionary microbiology,* 66**,** 2377.

SOROKIN, D. Y., MAKAROVA, K. S., ABBAS, B., FERRER, M., GOLYSHIN, P. N., GALINSKI, E. A., CIORDIA, S., MENA, M. C., MERKEL, A. Y. & WOLF, Y. I. 2017. Discovery of extremely halophilic, methyl-reducing euryarchaea provides insights into the evolutionary origin of methanogenesis. *Nature microbiology,* 2**,** 17081.

SPANG, A. & ETTEMA, T. J. 2017. Archaeal evolution: The methanogenic roots of Archaea. *Nature microbiology,* 2**,** 17109.

SPROUFFSKE, K. & WAGNER, A. 2016. Growthcurver: an R package for obtaining interpretable metrics from microbial growth curves. *BMC bioinformatics,* 17**,** 172.

SQUYRES, S., GROTZINGER, J., ARVIDSON, R., BELL, J., CALVIN, W., CHRISTENSEN, P., CLARK, B., CRISP, J., FARRAND, W. & HERKENHOFF, K. E. 2004. In situ evidence for an ancient aqueous environment at Meridiani Planum, Mars. *science,* 306**,** 1709.

SRIVASTAVA, A. Halobacterium Salinarum: Polyextremophile Model for Life Inside Martian Halite. Eighth International Conference on Mars, 2014 Pasadena, California. LPI Contribution, 1477.

STAN-LOTTER, H. & FENDRIHAN, S. 2015. Halophilic archaea: life with desiccation, radiation and oligotrophy over geological times. *Life,* 5**,** 1487.

STAN-LOTTER, H., MCGENITY, T. J., LEGAT, A., DENNER, E. B., GLASER, K., STETTER, K. O. & WANNER, G. 1999. Very similar strains of Halococcus salifodinae are found

in geographically separated permo-triassic salt deposits. *Microbiology,* 145 (Pt 12)**,** 3565.

STAN-LOTTER, H., PFAFFENHUEMER, M., LEGAT, A., BUSSE, H.-J., RADAX, C. & GRUBER, C. 2002a. Halococcus dombrowskii sp. nov., an archaeal isolate from a Permian alpine salt deposit. *International journal of systematic and evolutionary microbiology,* 52**,** 1807.

STAN-LOTTER, H., RADAX, C., GRUBER, C., LEGAT, A., PFAFFENHUEMER, M., WIELAND, H., LEUKO, S., WEIDLER, G., KÖMLE, N. & KARGL, G. 2002b. Astrobiology with haloarchaea from Permo-Triassic rock salt. *International Journal of Astrobiology,* 1**,** 271.

STELMACH, K. B., NEVEU, M., VICK-MAJORS, T. J., MICKOL, R. L., CHOU, L., WEBSTER, K. D., TILLEY, M., ZACCHEI, F., ESCUDERO, C. & FLORES MARTINEZ, C. L. 2018. Secondary Electrons as an Energy Source for Life. *Astrobiology,* 18**,** 1510.

STERN, J. C., SUTTER, B., FREISSINET, C., NAVARRO-GONZÁLEZ, R., MCKAY, C. P., ARCHER, P. D., BUCH, A., BRUNNER, A. E., COLL, P. & EIGENBRODE, J. L. 2015. Evidence for indigenous nitrogen in sedimentary and aeolian deposits from the Curiosity rover investigations at Gale crater, Mars. *Proceedings of the National Academy of Sciences,* 112**,** 4245.

STEVENSON, A., BURKHARDT, J., COCKELL, C. S., CRAY, J. A., DIJKSTERHUIS, J., FOX-POWELL, M., KEE, T. P., KMINEK, G., MCGENITY, T. J., TIMMIS, K. N., TIMSON, D. J., VOYTEK, M. A., WESTALL, F., YAKIMOV, M. M. & HALLSWORTH, J. E. 2015a. Multiplication of microbes below 0.690 water activity: implications for terrestrial and extraterrestrial life. *Environ Microbiol,* 17**,** 257.

STEVENSON, A., CRAY, J. A., WILLIAMS, J. P., SANTOS, R., SAHAY, R., NEUENKIRCHEN, N., MCCLURE, C. D., GRANT, I. R., HOUGHTON, J. D. & QUINN, J. P. 2015b. Is there a common water-activity limit for the three domains of life? *The ISME journal,* 9**,** 1333.

STILLMAN, D. E. & GRIMM, R. E. 2018. Two pulses of seasonal activity in martian southern mid-latitude recurring slope lineae (RSL). *Icarus,* 302**,** 126.

STILLMAN, D. E., MICHAELS, T. I. & GRIMM, R. E. 2017. Characteristics of the numerous and widespread recurring slope lineae (RSL) in Valles Marineris, Mars. *Icarus,* 285**,** 195.

STILLMAN, D. E., MICHAELS, T. I., GRIMM, R. E. & HANLEY, J. 2016. Observations and modeling of northern mid-latitude recurring slope lineae (RSL) suggest recharge by a present-day martian briny aquifer. *Icarus,* 265**,** 125.

STOCK, D. & ACHEY, P. 2018. Repair of Single-Strand Breaks in Dna From Cultured Lepidopteran Cells Exposed to Gamma Radiation. *Invertebrate Cell System Applications.* CRC Press.

STOTHARD, P. 2000. The sequence manipulation suite: JavaScript programs for analyzing and formatting protein and DNA sequences.

SUBRAMANIAM, A. B., WAN, J., GOPINATH, A. & STONE, H. A. 2011. Semi-permeable vesicles composed of natural clay. *Soft Matter,* 7**,** 2600.

SWARTZ, T. H., ITO, M., OHIRA, T., NATSUI, S., HICKS, D. B. & KRULWICH, T. A. 2007. Catalytic Properties of Staphylococcus aureus and Bacillus Members of the Secondary Cation/Proton Antiporter-3 (Mrp) Family Are Revealed by an Optimized Assay in an Escherichia coli Host. *Journal of Bacteriology,* 189**,** 3081.

TAKAGI, M. & YOSHIDA, T. 2006. Effect of salt concentration on intracellular accumulation of lipids and triacylglyceride in marine microalgae Dunaliella cells. *Journal of bioscience and bioengineering,* 101**,** 223.

TALBOT, C., TULLY, C. & WOODS, P. 1982. The structural geology of Boulby (potash) mine, Cleveland, United Kingdom. *Tectonophysics,* 85**,** 167.

TAMURA, K. & NEI, M. 1993. Estimation of the number of nucleotide substitutions in the control region of mitochondrial DNA in humans and chimpanzees. *Molecular biology and evolution,* 10**,** 512.

TANAKA, K., ROBBINS, S., FORTEZZO, C., SKINNER JR, J. & HARE, T. 2014. The digital global geologic map of Mars: Chronostratigraphic ages, topographic and crater morphologic characteristics, and updated resurfacing history. *Planetary and Space Science,* 95**,** 11.

TANAKA, K. L. 1986. The stratigraphy of Mars. *Journal of Geophysical Research: Solid Earth,* 91**,** E139.

TAPIA, M. S., ALZAMORA, S. M. & CHIRIFE, J. 2008. 10 Effects of Water Activity (a w) on Microbial Stability: As a Hurdle in Food Preservation. *Water activity in foods***,** 239.

TEAM, R. C. 2013. R: A language and environment for statistical computing.

TEJADA-JIMENEZ, M., GIL-DIEZ, P., LEON-MEDIAVILLA, J., WEN, J., MYSORE, K., IMPERIAL, J. & GONZALEZ-GUERRERO, M. 2017. Medicago truncatula MOT1. 3 is a plasma membrane molybdenum transporter required for nitrogenase activity in root nodules. *bioRxiv***,** 102517.

THOMAS, C., IONESCU, D., ARIZTEGUI, D. & TEAM, D. S. 2014. Archaeal populations in two distinct sedimentary facies of the subsurface of the Dead Sea. *Marine genomics,* 17**,** 53.

THOMPSON, J. D., GIBSON, T. & HIGGINS, D. G. 2002. Multiple sequence alignment using ClustalW and ClustalX. *Current protocols in bioinformatics,* 00**,** 2.3. 1.

TIRSCH, D., BISHOP, J. L., VOIGT, J., TORNABENE, L. L., ERKELING, G., HIESINGER, H. & JAUMANN, R. Aqueous outcrops at Libya Montes, Mars: A close eye on morphology and mineralogy. EGU General Assembly Conference Abstracts, 2015.

TITLER, R. V. & CURRY, P. 2009. Chemical analysis of major constituents and trace contaminants of rock salt. *Pennsylvania Department of Environmental Protection, Bureau of Water Standards and Facility Regulation Report*, 1.

TOLONEN, K. & JAAKOLA, T. History of lake acidification and air pollution studied on sediments in South Finland. Annales Botanici Fennici, 1983. JSTOR, 57.

TONER, J. D. & CATLING, D. C. 2016. Water activities of NaClO4, Ca(ClO4)2, and Mg(ClO4)2 brines from experimental heat capacities: Water activity >0.6 below 200K. *Geochimica et Cosmochimica Acta,* 181, 164.

TOSCA, N. J., KNOLL, A. H. & MCLENNAN, S. M. 2008. Water activity and the challenge for life on early Mars. *Science,* 320, 1204.

TOSCA, N. J., MCLENNAN, S. M., LAMB, M. P. & GROTZINGER, J. P. 2011. Physicochemical properties of concentrated Martian surface waters. *Journal of Geophysical Research: Planets,* 116, E05004.

TREGONING, G. S., KEMPHER, M. L., JUNG, D. O., SAMARKIN, V. A., JOYE, S. B. & MADIGAN, M. T. 2015. A halophilic bacterium inhabiting the warm, CaCl2-rich brine of the perennially ice-covered Lake Vanda, McMurdo Dry Valleys, Antarctica. *Applied and environmental microbiology,* 81, 1988.

TREIMAN, A. H. 2003. Geologic settings of Martian gullies: Implications for their origins. *Journal of Geophysical Research: Planets,* 108, 12.

TRIPATHY, S., PADHI, S. K., MOHANTY, S., SAMANTA, M. & MAITI, N. K. 2016. Analysis of the metatranscriptome of microbial communities of an alkaline hot sulfur spring revealed different gene encoding pathway enzymes associated with energy metabolism. *Extremophiles,* 20, 525.

TROKHIMOVSKIY, A., FEDOROVA, A., KORABLEV, O., MONTMESSIN, F., BERTAUX, J.-L., RODIN, A. & SMITH, M. D. 2015. Mars' water vapor mapping by the SPICAM IR spectrometer: Five martian years of observations. *Icarus,* 251, 50.

TWING, K. I., BRAZELTON, W. J., KUBO, M. D., HYER, A. J., CARDACE, D., HOEHLER, T. M., MCCOLLOM, T. M. & SCHRENK, M. O. 2017. Serpentinization-influenced groundwater harbors extremely low diversity microbial communities adapted to high pH. *Frontiers in microbiology,* 8, 308.

UKPAKA, C. 2016. Development of model for bioremediation of crude oil using moringa extract. *Chem. Int,* 2, 19.

ULANOWSKI, Z., LUDLOW, I. & WAITES, W. 1987. Water content and size of spore components determined by laser diffractometry. *FEMS microbiology letters,* 40, 229.

UPENDRA, R. & KHANDELWAL, P. 2016. Physical mutagenesis based strain improvement of Aspergillus sp. for enhanced production of lovastatin. *International Journal of Pharmacy and Pharmaceutical Science,* 8, 163.

UROZ, S., CALVARUSO, C., TURPAULT, M. P. & FREY-KLETT, P. 2009. Mineral weathering by bacteria: ecology, actors and mechanisms. *Trends Microbiol,* 17**,** 378.

VAN LONG, N. N., RIGALMA, K., COROLLER, L., DADURE, R., DEBAETS, S., MOUNIER, J. & VASSEUR, V. 2017. Modelling the effect of water activity reduction by sodium chloride or glycerol on conidial germination and radial growth of filamentous fungi encountered in dairy foods. *Food microbiology,* 68**,** 7.

VAN RENSBURG, E., DU PREEZ, J. & KILIAN, S. 2004. Influence of the growth phase and culture medium on the survival of Mannheimia haemolytica during storage at different temperatures. *Journal of applied microbiology,* 96**,** 154.

VANDEPUTTE, D., FALONY, G., D'HOE, K., VIEIRA-SILVA, S. & RAES, J. 2017. Water activity does not shape the microbiota in the human colon. *Gut,* 0**,** 313530.

VARDAVAS, I. M., VARDAVAS, I., TAYLOR, F., TAYLOR, F. W., TAYLOR, A. O. P. P. C. L. F. & PRESS, O. U. 2007. The climate system. *Radiation and Climate.* OUP Oxford.

VIVER, T., CIFUENTES, A., DÍAZ, S., RODRÍGUEZ-VALDECANTOS, G., GONZÁLEZ, B., ANTÓN, J. & ROSSELLÓ-MÓRA, R. 2015. Diversity of extremely halophilic cultivable prokaryotes in Mediterranean, Atlantic and Pacific solar salterns: evidence that unexplored sites constitute sources of cultivable novelty. *Systematic and applied microbiology,* 38**,** 266.

VIVIANO-BECK, C., MURCHIE, S., BECK, A. & DOHM, J. 2017. Compositional and structural constraints on the geologic history of eastern Tharsis Rise, Mars. *Icarus,* 284**,** 43.

VOGT, J. C., ABED, R. M., ALBACH, D. C. & PALINSKA, K. A. 2018. Bacterial and archaeal diversity in hypersaline cyanobacterial mats along a transect in the intertidal flats of the Sultanate of Oman. *Microbial ecology,* 75**,** 331.

VOOSEN, P. 2017. Tougher than hell. *Science,* 358**,** 984.

VREELAND, R., JONES, J., MONSON, A., ROSENZWEIG, W., LOWENSTEIN, T., TIMOFEEFF, M., SATTERFIELD, C., CHO, B., PARK, J. & WALLACE, A. 2007. Isolation of live Cretaceous (121–112 million years old) halophilic Archaea from primary salt crystals. *Geomicrobiology Journal,* 24**,** 275.

VREELAND, R. H. & HUVAL, J. 1991. Phenotypic characterization of halophilic bacteria from ground water sources in the United States. *General and Applied Aspects of Halophilic Microorganisms.* Springer.

VREELAND, R. H. & POWERS, D. W. 1999. *Considerations for microbiological sampling of crystals from ancient salt formations*, CRC Press, Boca Raton, FL.

VREELAND, R. H., ROSENZWEIG, W. D. & POWERS, D. W. 2000. Isolation of a 250 million-year-old halotolerant bacterium from a primary salt crystal. *Nature,* 407**,** 897.

WAALWIJK, C. & FLAVELL, R. A. 1978. MspI, an isoschizomer of HpaII which cleaves both unmethylated and methylated HpaII sites. *Nucleic Acids Research,* 5**,** 3231.

WADSWORTH, J. & COCKELL, C. S. 2017. Perchlorates on Mars enhance the bacteriocidal effects of UV light. *Scientific reports,* 7**,** 4662.

WALKER, S. I. 2017. Origins of life: a problem for physics, a key issues review. *Reports on Progress in Physics,* 80**,** 092601.

WANG, Q., GARRITY, G. M., TIEDJE, J. M. & COLE, J. R. 2007. Naive Bayesian classifier for rapid assignment of rRNA sequences into the new bacterial taxonomy. *Applied and environmental microbiology,* 73**,** 5261.

WARNER, N., GUPTA, S., LIN, S. Y., KIM, J. R., MULLER, J. P. & MORLEY, J. 2010. Late Noachian to Hesperian climate change on Mars: Evidence of episodic warming from transient crater lakes near Ares Vallis. *Journal of Geophysical Research: Planets,* 115**,** E06013.

WARREN, J. K. 2010. Evaporites through time: Tectonic, climatic and eustatic controls in marine and nonmarine deposits. *Earth-Science Reviews,* 98**,** 217.

WASSON, J. & WETHERILL, G. 1979. Dynamical chemical and isotopic evidence regarding the formation locations of asteroids and meteorites. *Asteroids***,** 926.

WAY, M., DEL GENIO, A., AMUNDSEN, D., SOHL, L., KIANG, N., ALEINOV, I. & KELLEY, M. Modeling Venus-like Worlds Through Time and Implications for the Habitable Zone. AGU Fall Meeting Abstracts, 2017.

WEBSTER, C. R., MAHAFFY, P. R., ATREYA, S. K., FLESCH, G. J., MISCHNA, M. A., MESLIN, P.-Y., FARLEY, K. A., CONRAD, P. G., CHRISTENSEN, L. E. & PAVLOV, A. A. 2014. Mars methane detection and variability at Gale crater. *Science,* 347**,** 415.

WECK, P. F., KIM, E., JOVÉ-COLÓN, C. F. & SASSANI, D. C. 2014. First-principles study of anhydrite, polyhalite and carnallite. *Chemical Physics Letters,* 594**,** 1.

WEISS, B. P., FONG, L. E., VALI, H., LIMA, E. A. & BAUDENBACHER, F. J. 2008. Paleointensity of the ancient Martian magnetic field. *Geophysical Research Letters,* 35**,** L23207.

WESTALL, F. 2005. 3 Early Life on Earth and Analogies to Mars. *Water on Mars and life.* Springer.

WESTALL, F. & BRACK, A. 2018. The importance of water for life. *Space Science Reviews,* 214**,** 50.

WESTALL, F., DE RONDE, C. E., SOUTHAM, G., GRASSINEAU, N., COLAS, M., COCKELL, C. & LAMMER, H. 2006. Implications of a 3.472–3.333 Gyr-old subaerial microbial mat from the Barberton greenstone belt, South Africa for the UV environmental conditions on the early Earth. *Philosophical Transactions of the Royal Society of London B: Biological Sciences,* 361**,** 1857.

WESTALL, F., FOUCHER, F., BOST, N., BERTRAND, M., LOIZEAU, D., VAGO, J. L., KMINEK, G., GABOYER, F., CAMPBELL, K. A. & BRÉHERET, J.-G. 2015. Biosignatures on Mars: what, where, and how? Implications for the search for martian life. *Astrobiology,* 15**,** 998.

WESTALL, F., LOIZEAU, D., FOUCHER, F., BOST, N., BETRAND, M., VAGO, J. & KMINEK, G. 2013. Habitability on Mars from a Microbial Point of View. *Astrobiology,* 13**,** 887.

WESTERGAARD, K., MÜLLER, A., CHRISTENSEN, S., BLOEM, J. & SØRENSEN, S. 2001. Effects of tylosin as a disturbance on the soil microbial community. *Soil Biology and Biochemistry,* 33**,** 2061.

WHITMAN, W. B., COLEMAN, D. C. & WIEBE, W. J. 1998. Prokaryotes: the unseen majority. *Proceedings of the National Academy of Sciences,* 95**,** 6578.

WHITMIRE, D. P. & MATESE, J. J. 2009. The distribution of stars most likely to harbor intelligent life. *Astrobiology,* 9**,** 617.

WILHELMS, D. E. & SQUYRES, S. W. 1984. The Martian hemispheric dichotomy may be due to a giant impact. *Nature,* 309**,** 138.

WILLERSLEV, E., HANSEN, A. J., RØNN, R., BRAND, T. B., BARNES, I., WIUF, C., GILICHINSKY, D., MITCHELL, D. & COOPER, A. 2004. Long-term persistence of bacterial DNA. *Current Biology,* 14**,** R9.

WILLIAMS, R. 1970. Tilden Lecture. The biochemistry of sodium, potassium, magnesium, and calcium. *Quarterly Reviews, Chemical Society,* 24**,** 331.

WILLIAMS, T. J., ALLEN, M. A., DEMAERE, M. Z., KYRPIDES, N. C., TRINGE, S. G., WOYKE, T. & CAVICCHIOLI, R. 2014. Microbial ecology of an Antarctic hypersaline lake: genomic assessment of ecophysiology among dominant haloarchaea. *The ISME journal,* 8**,** 1645.

WINSLOW, C.-E., WALKER, H. & SUTERMEISTER, M. 1932. The influence of aeration and of sodium chloride upon the growth curve of bacteria in various media. *Journal of bacteriology,* 24**,** 185.

WISE, M. E., SEMENIUK, T. A., BRUINTJES, R., MARTIN, S. T., RUSSELL, L. M. & BUSECK, P. R. 2007. Hygroscopic behavior of NaCl-bearing natural aerosol particles using environmental transmission electron microscopy. *Journal of Geophysical Research: Atmospheres,* 112**,** D10224.

WOLF, P. W. & OLIVER, J. D. 1992. Temperature effects on the viable but non-culturable state of Vibrio vulnificus. *FEMS Microbiology Letters,* 101**,** 33.

WOOD, C. A. & ASHWAL, L. D. SNC meteorites-Igneous rocks from Mars. Lunar and Planetary Science Conference Proceedings, 1982. 1359.

WOODS, P. 1979. The geology of Boulby Mine. *Economic Geology,* 74**,** 409.

WORDSWORTH, R., FORGET, F., MILLOUR, E., HEAD, J. W., MADELEINE, J. B. & CHARNAY, B. 2013. Global modelling of the early martian climate under a denser CO2 atmosphere: Water cycle and ice evolution. *Icarus,* 222**,** 1.

WORDSWORTH, R. D. 2016. The climate of early Mars. *Annual Review of Earth and Planetary Sciences,* 44**,** 381.

WORDSWORTH, R. D., KERBER, L., PIERREHUMBERT, R. T., FORGET, F. & HEAD, J. W. 2015. Comparison of "warm and wet" and "cold and icy" scenarios for early Mars in a 3-D climate model. *Journal of Geophysical Research: Planets,* 120**,** 1201.

WORTH, R. J., SIGURDSSON, S. & HOUSE, C. H. 2013. Seeding life on the moons of the outer planets via lithopanspermia. *Astrobiology,* 13**,** 1155.

WRIGHT, A. D. 2006. Phylogenetic relationships within the order Halobacteriales inferred from 16*S* rRNA gene sequences. *Int J Syst Evol Microbiol,* 56**,** 1223.

YAKIMOV, M. M., LA CONO, V., SPADA, G. L., BORTOLUZZI, G., MESSINA, E., SMEDILE, F., ARCADI, E., BORGHINI, M., FERRER, M. & SCHMITT-KOPPLIN, P. 2015. Microbial community of the deep-sea brine Lake Kryos seawater–brine interface is active below the chaotropicity limit of life as revealed by recovery of mRNA. *Environmental microbiology,* 17**,** 364.

YAN, N., MARSCHNER, P., CAO, W., ZUO, C. & QIN, W. 2015. Influence of salinity and water content on soil microorganisms. *International Soil and Water Conservation Research,* 3**,** 316.

YANCEY, P., CLARK, M., HAND, S., BOWLUS, R. & SOMERO, G. 1982. Living with water stress: evolution of osmolyte systems. *Science,* 217**,** 1214.

YOSHIMURA, K. & KOUYAMA, T. 2008. Structural role of bacterioruberin in the trimeric structure of archaerhodopsin-2. *Journal of molecular biology,* 375**,** 1267.

YOSHINO, H., IWABUCHI, M., KAZAMA, Y., FURUKAWA, M. & KASHIWAKURA, I. 2018. Effects of retinoic acid-inducible gene-I-like receptors activations and ionizing radiation cotreatment on cytotoxicity against human non-small cell lung cancer in vitro. *Oncology letters,* 15**,** 4697.

YU, L. Z. H., LUO, X. S., LIU, M. & HUANG, Q. 2015. Diversity of ionizing radiation-resistant bacteria obtained from the Taklimakan Desert. *Journal of basic microbiology,* 55**,** 135.

YU, Z., GARCÍA-GONZÁLEZ, R., SCHANBACHER, F. L. & MORRISON, M. 2008. Evaluations of different hypervariable regions of archaeal 16S rRNA genes in profiling of methanogens by Archaea-specific PCR and denaturing gradient gel electrophoresis. *Applied and environmental microbiology,* 74**,** 889.

ZAHNLE, K. 2001. Decline and fall of the Martian empire. *Nature,* 412**,** 209.

ZAMMIT, C. M. & WATKIN, E. L. 2016. Adaptation to extreme acidity and osmotic stress. *Acidophiles: Life in Extremely Acidic Environments***,** 49.

ZHANG, S.-H. & WEI, Y. 2017. Applications of Haloalkaliphilic Fungi in Mycoremediation of Saline-Alkali Soil. *Mycoremediation and Environmental Sustainability.* Springer.